



International Agreement Report

Experimental Study of Narrow Pulse Effects on the Behavior of High Burnup Fuel Rods with Zr-1%Nb Cladding and UO₂ Fuel (VVER Type) under Reactivity-Initiated Accident Conditions:
Test Conditions and Results

Prepared by

L. Yegorova, K. Lioutov, N. Jouravkova
Nuclear Safety Institute of Russian Research Centre "Kurchatov Institute"
Kurchatov Square 1, Moscow 123182, Russian Federation

O. Nechaeva, A. Salatov
A.A. Bochvar All-Russian Research Institute of Inorganic Materials
Rogov Street 5, Moscow 123182, Russian Federation

V. Smirnov, A. Goryachev
State Research Centre "Research Institute of Atomic Reactors"
Dimitrovgrad 433510, Russian Federation

V. Ustinenko, I. Smirnov
Russian Federal Nuclear Centre "All-Russian Research Institute of Experimental Physics"
Sarov 607200, Russian Federation

**Office of Nuclear Regulatory Research
U.S. Nuclear Regulatory Commission
Washington, DC 20555-0001**

March 2006

Prepared for

U.S. Nuclear Regulatory Commission (United States),
Institute for Radiological Protection and Nuclear Safety (France),
and Joint Stock Company "TVEL" (Russian Federation)

Published by

U.S. Nuclear Regulatory Commission

AVAILABILITY OF REFERENCE MATERIALS IN NRC PUBLICATIONS

NRC Reference Material

As of November 1999, you may electronically access NUREG-series publications and other NRC records at NRC's Public Electronic Reading Room at <http://www.nrc.gov/reading-rm.html>. Publicly released records include, to name a few, NUREG-series publications; *Federal Register* notices; applicant, licensee, and vendor documents and correspondence; NRC correspondence and internal memoranda; bulletins and information notices; inspection and investigative reports; licensee event reports; and Commission papers and their attachments.

NRC publications in the NUREG series, NRC regulations, and *Title 10, Energy*, in the Code of *Federal Regulations* may also be purchased from one of these two sources.

1. The Superintendent of Documents
U.S. Government Printing Office
Mail Stop SSOP
Washington, DC 20402-0001
Internet: bookstore.gpo.gov
Telephone: 202-512-1800
Fax: 202-512-2250
2. The National Technical Information Service
Springfield, VA 22161-0002
www.ntis.gov
1-800-553-6847 or, locally, 703-605-6000

A single copy of each NRC draft report for comment is available free, to the extent of supply, upon written request as follows:

Address: Office of the Chief Information Officer,
Reproduction and Distribution
Services Section
U.S. Nuclear Regulatory Commission
Washington, DC 20555-0001
E-mail: DISTRIBUTION@nrc.gov
Facsimile: 301-415-2289

Some publications in the NUREG series that are posted at NRC's Web site address <http://www.nrc.gov/reading-rm/doc-collections/nuregs> are updated periodically and may differ from the last printed version. Although references to material found on a Web site bear the date the material was accessed, the material available on the date cited may subsequently be removed from the site.

Non-NRC Reference Material

Documents available from public and special technical libraries include all open literature items, such as books, journal articles, and transactions, *Federal Register* notices, Federal and State legislation, and congressional reports. Such documents as theses, dissertations, foreign reports and translations, and non-NRC conference proceedings may be purchased from their sponsoring organization.

Copies of industry codes and standards used in a substantive manner in the NRC regulatory process are maintained at—

The NRC Technical Library
Two White Flint North
11545 Rockville Pike
Rockville, MD 20852-2738

These standards are available in the library for reference use by the public. Codes and standards are usually copyrighted and may be purchased from the originating organization or, if they are American National Standards, from—

American National Standards Institute
11 West 42nd Street
New York, NY 10036-8002
www.ansi.org
212-642-4900

Legally binding regulatory requirements are stated only in laws; NRC regulations; licenses, including technical specifications; or orders, not in NUREG-series publications. The views expressed in contractor-prepared publications in this series are not necessarily those of the NRC.

The NUREG series comprises (1) technical and administrative reports and books prepared by the staff (NUREG-XXXX) or agency contractors (NUREG/CR-XXXX), (2) proceedings of conferences (NUREG/CP-XXXX), (3) reports resulting from international agreements (NUREG/IA-XXXX), (4) brochures (NUREG/BR-XXXX), and (5) compilations of legal decisions and orders of the Commission and Atomic and Safety Licensing Boards and of Directors' decisions under Section 2.206 of NRC's regulations (NUREG-0750).

DISCLAIMER: Where the papers in these proceedings have been authored by contractors of the U. S. Government, neither the U.S. Government nor any agency thereof, nor any U.S. employee makes any warranty, expressed or implied, or assumes any legal liability or responsibility for any third party's use or the results of such use, of any information, apparatus, product, or process disclosed in these proceedings, or represents that its use by such third party would not infringe privately owned rights. The views expressed in these proceedings are not necessarily those of the U. S. Regulatory Commission.



NUREG/IA-0213, Vol. 2
IRSN/DPAM 2005-275
NSI RRC KI 3230

International Agreement Report

Experimental Study of Narrow Pulse Effects on the Behavior of High Burnup Fuel Rods with Zr-1%Nb Cladding and UO₂ Fuel (VVER Type) under Reactivity-Initiated Accident Conditions: Test Conditions and Results

Prepared by

L. Yegorova, K. Lioutov, N. Jouravkova
Nuclear Safety Institute of Russian Research Centre "Kurchatov Institute"
Kurchatov Square 1, Moscow 123182, Russian Federation

O. Nechaeva, A. Salatov
A.A. Bochvar All-Russian Research Institute of Inorganic Materials
Rogov Street 5, Moscow 123182, Russian Federation

V. Smirnov, A. Goryachev
State Research Centre "Research Institute of Atomic Reactors"
Dimitrovgrad 433510, Russian Federation

V. Ustinenko, I. Smirnov
Russian Federal Nuclear Centre "All-Russian Research Institute of Experimental Physics"
Sarov 607200, Russian Federation

**Office of Nuclear Regulatory Research
U.S. Nuclear Regulatory Commission
Washington, DC 20555-0001**

March 2006

Prepared for

U.S. Nuclear Regulatory Commission (United States),
Institute for Radiological Protection and Nuclear Safety (France),
and Joint Stock Company "TVEL" (Russian Federation)

Published by

U.S. Nuclear Regulatory Commission

ABSTRACT

This volume of the report contains a detailed description of calculation and test results obtained in the fast-pulse-graphite-reactor (BIGR) tests of twelve fuel rods refabricated from the VVER-440 and VVER-1000 high burnup fuel elements (50, 60 MW d/kg U).

The BIGR data base includes the following types of fuel rod characterization:

- material and geometrical parameters of VVER-440 and VVER-1000 commercial fuel elements before the base irradiation in the nuclear power plant (NPP);
- parameters of fuel cycles and characteristics of commercial fuel elements after the base irradiation;
- characteristics of twelve refabricated fuel rods before the BIGR pulse tests;
- parameters of the BIGR power pulses;
- characteristics of refabricated fuel rods during and after the BIGR tests.

FOREWORD

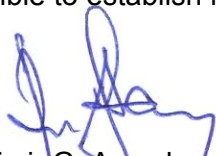
This two-volume report provides results of a cooperative research program involving the Russian Research Center–Kurchatov Institute, the French Institute for Radiological Protection and Nuclear Safety (IRSN), and the United States Nuclear Regulatory Commission (NRC). The research addresses the behavior of high-burnup nuclear fuel under postulated reactivity-initiated accident (RIA) conditions, based on experimental results from the Russian fast-pulse graphite reactor, known as BGR.

The Kurchatov Institute initiated its RIA test program in 1983, several years before the accident at Chernobyl. That accident, which resulted from a rapid increase in reactivity, demonstrated that severe fuel damage may occur too quickly to be easily mitigated. However, the consequences of such an event can be reduced by thorough understanding and design.

Information concerning Russian reactivity insertion experiments in the Impulse Graphite Reactor (IGR) was first revealed to western observers in 1992. Differences between IGR and other fuel behavior tests were initially attributed to differences in Russian fuel designs and the larger pulse width of the IGR test reactor. However, the test rods used in the IGR were taken from zirconium-niobium clad uranium dioxide (UO₂) fuel rods that were commercially irradiated in pressurized, light-water-reactors. This type of cladding material is used throughout the world, and generated great interest. The IRSN and NRC recognized the value of this test program and, in 1995, joined with the Kurchatov Institute in assessing and interpreting the IGR data. Then, in July 1999, the agencies jointly published the results in a three-volume compendium, identified as NUREG/IA-0156, “Data Base on the Behavior of High Burnup Fuel Rods with Zr-1%Nb Cladding and UO₂ Fuel (VVER Type) Under Reactivity Accident Conditions.”

More recently, the Kurchatov Institute addressed the issue of the broad pulse width effects in the IGR with a series of narrow pulse width experiments in the BGR fast-pulse graphite reactor. The work was performed in cooperation with other Russian institutes and support of the Russian fuel vendor (Joint Stock Company “TVEL”). Pulses produced by the two test reactors span an extraordinary range, from 3 milliseconds in BGR to over 700 milliseconds in IGR, and bound the expected pulse widths for postulated RIA events in commercial light-water reactors. Taken together, these test results show that cladding with very light corrosion is remarkably resistant to failure — even under high-burnup conditions.

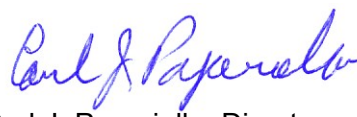
Results of the BGR program, as documented in this report, demonstrate the continued value of the cooperative efforts of the Kurchatov Institute, the IRSN, and the NRC. This collaborative program further allows a comparison of conclusions from other data sources (e.g., France, Japan, and the U.S.). By comparing these results, studying the employed techniques, and creating a common language necessary for the mutual understanding these events, it will be possible to establish more appropriate regulatory limits for reactivity-initiated accidents.



Vladimir G. Asmolov, Director
Research and Development
Russian Research Centre -
“Kurchatov Institute”



Michel Schwarz, Director
Major Accident
Prevention Division
Institut de Radioprotection
et de Sûreté Nucléaire



Carl J. Paperiello, Director
Office of Nuclear
Regulatory Research
U.S. Nuclear Regulatory
Commission

TABLE OF CONTENTS

| | Page |
|---|------|
| ABSTRACT | iii |
| FOREWORD | v |
| TABLE OF CONTENTS | vii |
| LIST OF APPENDICES | ix |
| ACKNOWLEDGEMENTS | xi |
| EXECUTIVE SUMMARY | 1.1 |
| GUIDE TO THE DATA BASE | 2.1 |
| COMMENTS TO APPENDIX A | 2.1 |
| COMMENTS TO APPENDIX B | 2.1 |
| COMMENTS TO APPENDIX C | 2.2 |
| COMMENTS TO APPENDIX D | 2.2 |
| COMMENTS TO APPENDIX E | 2.2 |
| | |
| APPENDIX A Reference Characteristics of VVER-440 and VVER-1000 | |
| Commercial Fuel Elements before the Base Irradiation | A-1 |
| | |
| APPENDIX B Fuel Cycle Parameters and Post-Irradiation | |
| Characteristics of Commercial Fuel Rods | B-1 |
| | |
| APPENDIX C Characteristics of Refabricated Fuel Rods | |
| before the BGR Tests | C-1 |
| | |
| APPENDIX D Characteristics of the BGR Power Pulses | D-1 |
| | |
| APPENDIX E Characteristics of Refabricated Fuel Rods | |
| after the BGR Tests | E-1 |

LIST OF APPENDICES

| | | Page |
|----------------------|---|-------------|
| Appendix A | Reference Characteristics of VVER-440 and VVER-1000 Commercial Fuel Elements before the Base Irradiation | A-1 |
| Appendix B | Fuel Cycle Parameters and Post-Irradiation Characteristics of Commercial Fuel Rods | B-1 |
| Appendix C | Characteristics of Refabricated Fuel Rods before the BGR Tests | C-1 |
| <i>Appendix C-1</i> | <i>Individual Characteristics of Fuel Rod # RT1 before the BGR Test</i> | <i>C-7</i> |
| <i>Appendix C-2</i> | <i>Individual Characteristics of Fuel Rod # RT2 before the BGR Test</i> | <i>C-15</i> |
| <i>Appendix C-3</i> | <i>Individual Characteristics of Fuel Rod # RT3 before the BGR Test</i> | <i>C-23</i> |
| <i>Appendix C-4</i> | <i>Individual Characteristics of Fuel Rod # RT4 before the BGR Test</i> | <i>C-31</i> |
| <i>Appendix C-5</i> | <i>Individual Characteristics of Fuel Rod # RT5 before the BGR Test</i> | <i>C-39</i> |
| <i>Appendix C-6</i> | <i>Individual Characteristics of Fuel Rod # RT6 before the BGR Test</i> | <i>C-47</i> |
| <i>Appendix C-7</i> | <i>Individual Characteristics of Fuel Rod # RT7 before the BGR Test</i> | <i>C-55</i> |
| <i>Appendix C-8</i> | <i>Individual Characteristics of Fuel Rod # RT8 before the BGR Test</i> | <i>C-63</i> |
| <i>Appendix C-9</i> | <i>Individual Characteristics of Fuel Rod # RT9 before the BGR Test</i> | <i>C-71</i> |
| <i>Appendix C-10</i> | <i>Individual Characteristics of Fuel Rod # RT10 before the BGR Test</i> | <i>C-79</i> |
| <i>Appendix C-11</i> | <i>Individual Characteristics of Fuel Rod # RT11 before the BGR Test</i> | <i>C-87</i> |
| <i>Appendix C-12</i> | <i>Individual Characteristics of Fuel Rod # RT12 before the BGR Test</i> | <i>C-95</i> |
| Appendix D | Characteristics of the BGR Power Pulses | D-1 |
| Appendix E | Characteristics of Refabricated Fuel Rods after the BGR Tests | E-1 |
| <i>Appendix E-1</i> | <i>Individual Characteristics of Fuel Rod # RT1 after the BGR Test</i> | <i>E-1</i> |
| <i>Appendix E-2</i> | <i>Individual Characteristics of Fuel Rod # RT2 after the BGR Test</i> | <i>E-15</i> |
| <i>Appendix E-3</i> | <i>Individual Characteristics of Fuel Rod # RT3 after the BGR Test</i> | <i>E-29</i> |
| <i>Appendix E-4</i> | <i>Individual Characteristics of Fuel Rod # RT4 after the BGR Test</i> | <i>E-43</i> |
| <i>Appendix E-5</i> | <i>Individual Characteristics of Fuel Rod # RT5 after the BGR Test</i> | <i>E-59</i> |
| <i>Appendix E-6</i> | <i>Individual Characteristics of Fuel Rod # RT6 after the BGR Test</i> | <i>E-75</i> |
| <i>Appendix E-7</i> | <i>Individual Characteristics of Fuel Rod # RT7 after the BGR Test</i> | <i>E-91</i> |

| | | |
|----------------------|---|--------------|
| <i>Appendix E-8</i> | <i>Individual Characteristics of Fuel Rod # RT8 after the BGR Test</i> | <i>E-105</i> |
| <i>Appendix E-9</i> | <i>Individual Characteristics of Fuel Rod # RT9 after the BGR Test</i> | <i>E-121</i> |
| <i>Appendix E-10</i> | <i>Individual Characteristics of Fuel Rod # RT10 after the BGR Test</i> | <i>E-141</i> |
| <i>Appendix E-11</i> | <i>Individual Characteristics of Fuel Rod # RT11 after the BGR Test</i> | <i>E-157</i> |
| <i>Appendix E-12</i> | <i>Individual Characteristics of Fuel Rod # RT12 after the BGR Test</i> | <i>E-173</i> |
| <i>Appendix E-13</i> | <i>Azimuthal Distribution of Cladding Thickness for Fuel Rods ## RT7–12</i> | <i>E-187</i> |

ACKNOWLEDGEMENTS

The authors are deeply grateful the support and assistance of the following specialists in the Russian Federation:

- V. Sazhnov (Russian Federal Nuclear Centre “All-Russian Research Institute of Experimental Physics”): the performance of the BGR tests with VVER refabricated fuel rods;
- A. Bortash, A. Zvyageen, V. Malofeev, A. Avvakumov, E. Kaplar (Nuclear Safety Institute and Institute of Nuclear Reactors of Russian Research Centre “Kurchatov Institute”): neutronic calculations and energy deposition determination;
- G. Maslov, V. Ilyin (Russian Federal Nuclear Centre “All-Russian Research Institute of Experimental Physics”): experimental measurements and computer calculations of neutronic parameters during the BGR tests;
- A. Shestopalov (Nuclear Safety Institute of Russian Research Centre “Kurchatov Institute”): FRAP-T6/VVER calculations of thermal mechanical parameters of high burnup fuel rods under the BGR test conditions;
- E. Zvir, L. Stupina, A. Svyatkin (State Research Centre “Research Institute of Atomic Reactors”): pre-test and post-test examinations of refabricated fuel rods including metallographic studies and computer processing of obtained data;
- A. Chetvyarikov (State Research Centre “Research Institute of Atomic Reactors”): the management by radio chemical measurements of the fuel isotopic composition;
- A. Konobeev, G. Abyshov (Nuclear Safety Institute of Russian Research Centre “Kurchatov Institute”): the computer processing of some experimental data.

Without the efforts of these individuals, and their willingness to share results of several special investigations, this report would not have been possible.

1. EXECUTIVE SUMMARY

Taking into account that the BGR^a tests were performed under reactivity-initiated-accident (RIA) conditions to widen the VVER^b RIA high burnup fuel data base obtained earlier due to the pulse graphite reactor (IGR^c) tests, it was decided to keep approximately the same format of the test data organization, which was developed during the preparation of the IGR/RIA data base [1]. In accordance with this approach, the Volume 2 of the BGR report contains several types of test data listed in Fig. 1. As it can be observed from this Figure, the high burnup fuel rods tested in the BGR reactor were refabricated from the VVER-440 and VVER-1000 fuel elements irradiated at the NovoVoronezh and Kola nuclear power plants (NV^d NPP and Kola^e NPP). To follow the evolution of the cladding and fuel changes from the beginning of fuel cycles at the NPP to RIA accident conditions at the burnup 50, 60 MW d/kg U, special measurements of fuel rod parameters were performed and presented in several Appendices of this volume of the report. The contents of each Appendix are given in Chapter 2 of this volume.

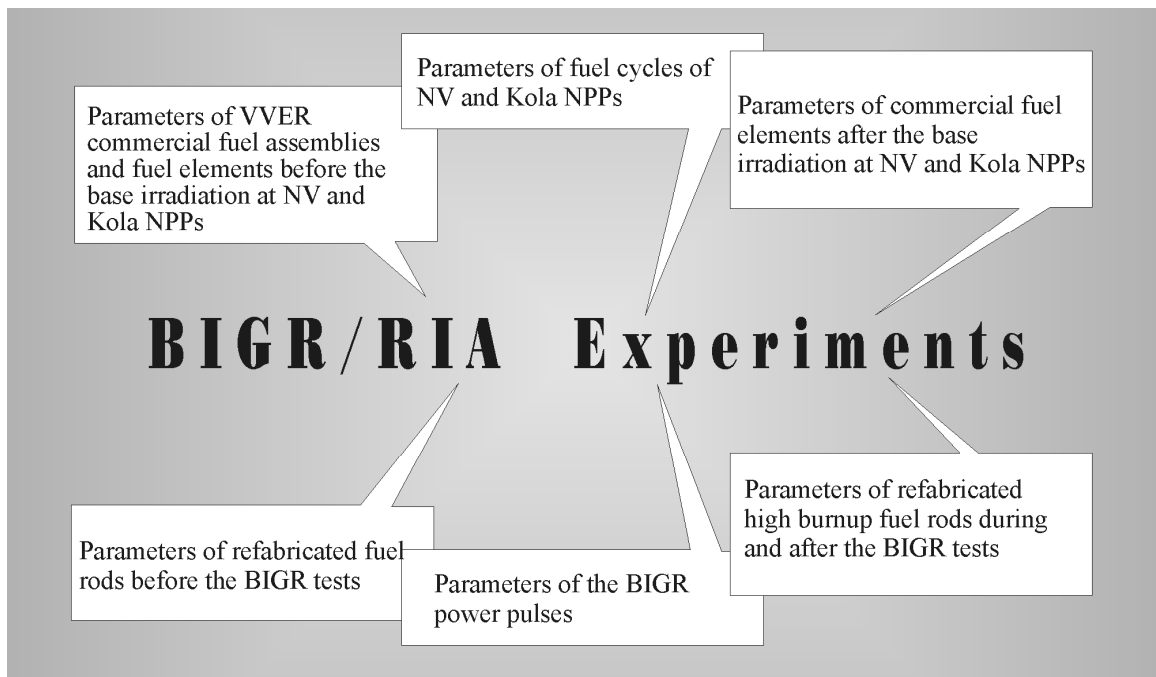


Fig. 1. Arrangement of the BGR/RIA test results

^a BGR – Bystry Impulsnyy Graphitovy Reactor (Fast Pulse Graphite Reactor)

^b VVER – Vodo-Vodyanoy Energetichesky Reactor (Russian type of Pressurized Water Reactor)

^c IGR – Impulsnyy Graphitovy Reactor (Pulse Graphite Reactor)

^d NV – Novovoronezhskay (Nuclear Power Plant)

^e Kola – Kolskay (Nuclear Power Plant)

REFERENCES

[1] Yegorova L., Asmolov V., Abyshov G., Malofeev V., Avvakumov A., Kaplar E., Lioutov K., Shestopalov A., Bortash A., Maiorov L., Mikitiouk K., Polvanov V., Smirnov V., Goryachev A., Prokhorov V., and Vurim A. “Data Base on the Behavior of High Burnup Fuel Rods with Zr-1%Nb Cladding and UO₂ Fuel (VVER Type) under Reactivity Accident Conditions”, RRC "Kurchatov Institute" report NSI RRC 2179, Vol.1-3, 1999 (also USNRC report NUREG/IA-0156 and IPSN report IPSN 99/08–2).

2. GUIDE TO THE DATA BASE

The BIGR/RIA data base is subdivided into five subject sets of data presented in the following Appendices:

| | |
|------------|--|
| Appendix A | Reference Characteristics of VVER-440 and VVER-1000 Commercial Fuel Elements before the Base Irradiation |
| Appendix B | Fuel Cycle Parameters and Post-Irradiation Characteristics of Commercial Fuel Rods |
| Appendix C | Characteristics of Refabricated Fuel Rods before the BGR Tests |
| Appendix D | Characteristics of the BGR Power Pulses |
| Appendix E | Characteristics of Refabricated Fuel Rods after the BGR Tests |

The subsections of this Chapter contain some important comments, which may simplify the work with this data base.

2.1. Comments to Appendix A

In this Appendix reference parameters of three fuel assemblies of the VVER-440 and VVER-1000 types are presented. The most part of these parameters was determined with using the standard documentation of the manufacturer. As for differences in characteristics of these assemblies at the beginning of the base irradiation, the following parameters may be pointed out:

- the initial fill gas pressure in VVER-440 fuel elements (Helium, 0.5–0.7 MPa)^a is lesser significantly than that in VVER-1000 fuel elements (Helium, 1.9–2.6 MPa)^a;
- each of these three fuel assemblies had fuel elements with a central hole, but of a different diameter fuel pellet (1.2, 1.6–1.7, 2.4 mm);
- two types of fuel pellets were used in these fuel assemblies:
 - simple cylindrical pellets;
 - cylindrical pellets with chamfers.

2.2. Comments to Appendix B

This Appendix contains two types of the data:

1. The data characterizing fuel cycles of six fuel elements, which were used for the manufacturing of twelve refabricated fuel rods tested in the BGR reactor.
2. The data characterizing parameters of these six fuel elements in accordance with the post-irradiation-examination (PIE) results.

The first type of the data allowed to perform neutronic calculations of base irradiation histories for these fuel elements. Due to these calculations, radial and axial distributions of the isotopic composition of high burnup fuel was determined in the each fuel element.

The second type of the data characterizes the microstructure of fuel and cladding for six fuel elements, the fission gas release (FGR) at the end of irradiation, fuel burnup, hydrogen content in the irradiated cladding and geometrical sizes of high burnup fuel and irradiated cladding. The analysis of these data allowed to reveal the following important features:

- four fuel elements of the VVER-1000 type had approximately the similar maximum burnup (47.8–50.12 MW d/kg U), geometrical parameters of fuel and cladding, cladding hydrogen content ($5 \cdot 10^{-3}$ % by volume), rim layer thickness (0.05–0.07 mm) and residual value of fuel/cladding gap (0.017–0.032 mm);
- two fuel elements of the VVER-440 type had the similar maximum burnup also (61.6 and 61.7 MW d/kg U). Unfortunately, it was impossible to compare the most part of other characteristics for these fuel elements because the PIE data of one of these elements were very limited;
- nevertheless, the comparison of parameters of fuel elements on two levels of the maximum fuel burnup (47.8–50.12 and 61.6–61.7 MW d/kg U correspondently) allowed to reveal that:

^a This parameter is presented at the room temperature

- the rim layer thickness was increased from 50–70 μm at 50 MW d/kg U up to 150–200 μm at 62 MW d/kg U burnup;
- a radial fuel/cladding gap was not apparent at 62 MW d/kg U burnup;
- the hydrogen content in the irradiated cladding was somewhat increased at 62 MW d/kg U burnup. This fact correlates with the data presented in Table C.1 of Appendix C to characterize the cladding oxidation after the base irradiation. These data showed that at 50 MW d/kg U burnup, the irradiated cladding was covered with the 3–5 μm zirconium dioxide layer on the outer surface only. At 62 MW d/kg U burnup, the oxidation of the cladding internal surface was observed. The thickness of inner ZrO_2 layer was 8–10 μm although the outer oxide layer remained 3–5 μm .

2.3. Comments to Appendix C

This Appendix is devoted to the presentation of measured and calculated parameters of twelve refabricated fuel rods before the BGR tests. The individual characterization of each fuel rod is contained in Appendices C-1 – C-12. Besides, the reference and average representative values of parameters are listed in Tables C.1–C.3 of Appendix C. Design schemes of refabricated fuel rods supplement this data base.

Individual characteristics of fuel rods presented in Appendices C-1 – C-12 include the following graphical and tabular data:

- radial distribution of isotopic nuclear concentrations in four radial fuel layers;
- axial distributions of the cladding average outer diameter, fuel mass, gas flow area, burnup, intensity of Cs and Eu isotopes and results of the eddy current examination.

General differences between initial parameters of these fuel rods were as follows:

- eight fuel rods had burnup in the range 46.9–48.6 MW d/kg U and four fuel rods had the burnup in the range 59.8–60.5 MW d/kg U;
- ten fuel rods had the initial fill gas pressure in the range 2.0–2.1 MPa and two fuel rods had the initial fill gas pressure 0.1 MPa;
- the fuel stack in one fuel rod (#RT3) was damaged at the refabrication. The obtained fuel configuration (along the axis) is presented in the data base.

2.4. Comments to Appendix D

This Appendix consists of the following data characterizing the BGR pulse conditions:

- the BGR power history at the test of each fuel rod;
- pulse half-width for the BGR tests of twelve fuel rods.

The BGR power histories presented in this Appendix have the status of the as-measured parameter. This data base was developed in accordance with the neutron detector recording. The procedure of these experimental data transformation into the input data for the computer codes is described in the Volume 1 of the report.

2.5. Comments to Appendix E

This appendix consists of twelve subappendices with the following types of data:

- appearance of the fuel rod and photographs of fuel and cladding microstructure obtained in the PIE procedures;
- time dependent energy characteristics of the fuel rod during the BGR test (power, number of fissions, energy deposition, fuel enthalpy). It should be noted that two independent procedures were used to determine neutronic parameters of the fuel rod versus time and the fuel enthalpy versus time. In the first case, these two procedures were developed in the Russian Research Centre “Kurchatov Institute” (RRC KI) and Russian Federal Nuclear Centre “All-Russian Research Institute of Experimental Physics” (VNIIEF) (see volume 1 of the report).

In the second case, two different codes (FRAP-T6/VVER and RAPTA-5) were used in the RRC KI and A.A. Bochvar All-Russian Research Institute of Inorganic Materials (VNIINM) to calculate the fuel enthalpy (see volume 1 of the report). Taking into account that results of neutronic calculations performed in accordance with RRC KI and VNIIEF procedures are very similar, the tabular data contain the average values only. The RRC KI and

VNIINM data characterizing the fuel enthalpy are similar in general. But to compare definite differences in these data, results of both calculations are presented in the report:

- to illustrate the specific character of the energy deposition radial distribution in the high burnup fuel, the tabular and graphical data were incorporated into the data base. In addition to these data, the transformation of the fuel enthalpy radial profile as a function of time is presented also in accordance with the FRAP-T6/VVER and RAPTA-5 calculations;
- the interpretation of the fuel rod thermal mechanical behavior during the BGR test is presented in accordance with results of FRAP-T6/VVER and RAPTA-5 calculations;
- PIE results characterizing the cladding and fuel strain, cladding oxidation and FGR are listed in the graphical and tabular forms. Appendix A-13 contains the data base characterizing the azimuthal distribution of cladding thickness in fuel rods ## RT7-12 obtained due to the processing of cross-section images;
- the last position of each subappendix contains the major results of the BGR test in accordance with the calculated and experimental data.

To overcome the difficulties with terminology used in this Appendix, a special glossary is presented in Table 2.1.

Table 2.1. The glossary of neutronics and energy parameters presented in Appendix E

| Term | Meaning of term |
|---|--|
| 1. Relative reactor power vs. time (per-unit) | The reactor power in the place of the VVER fuel rod installation determined in accordance with the procedure presented in Volume 1 of the report |
| 2. Cumulative number of fissions in the fuel rod vs. time (fiss.) | A total number of fissions occurred within the whole fuel mass by the i-time |
| 3. Power of fuel rod vs. time (kW) | Power generated in the total mass of fuel due to the whole set of fissile isotopes by the i-time |
| 4. Energy deposition in the fuel rod vs. time (cal/g fuel) | Energy generated in the whole fuel mass by i-time and normalized for the fuel mass |
| 5. Number of fissions vs. radial fuel layer (fiss.) | A total number of fissions occurred in the undamaged part of a given radial layer of the fuel column within $0-\infty$ s |
| 6. Power vs. radial fuel layer (kW) | The maximum power noted during the BGR test in the radial fuel layer |
| 7. Energy deposition vs. radial fuel layer (cal/g fuel) | Total energy deposition generated in a given radial layer normalized for the fuel mass within time interval $0-\infty$ s |
| 8. Energy deposition vs. radial fuel layer (per-unit) | Energy deposition of a given radial layer of the fuel column normalized for energy deposition in the 4 th radial layer |
| 9. Fuel enthalpy vs. time (cal/g fuel) | Radially averaged fuel enthalpy versus time for any cross-section (the axial peak power factor is 1) |

APPENDIX A

REFERENCE CHARACTERISTICS OF VVER-440 AND

VVER-1000 COMMERCIAL FUEL ELEMENTS

BEFORE THE BASE IRRADIATION

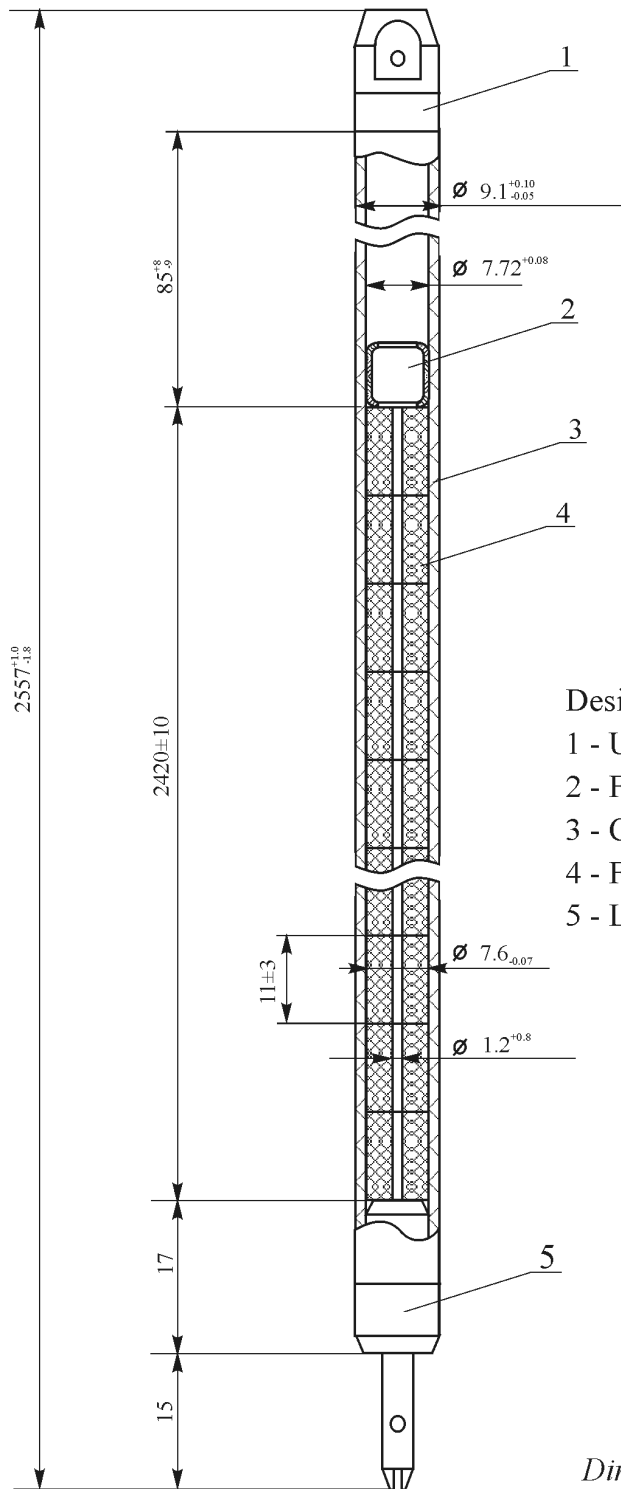
Table A.1. Reference characteristics of VVER commercial fuel element before the irradiation

| Characteristic | Unit | Value | | |
|------------------------------------|-------------------|--------------------------------------|--|--------------------------------------|
| Fuel assembly type | – | VVER-440 | VVER-1000 | VVER-440 |
| Commercial number of fuel assembly | – | 14422222 | ED4108 | 23635228 |
| 1. UO₂ fuel | | | | |
| 1.1. Isotopic composition | | | | |
| U ²³⁵ | % by weight | 4.37* | 4.40 | 3.60 |
| U ²³⁸ | % by weight | 95.57 | 95.54 | – |
| U ²³⁴ | % by weight | 0.03 | 0.03 | – |
| U ²³⁶ | % by weight | 0.03* | 0.03 | – |
| 1.2. Enrichment | % | 4.37* | 4.40 | 3.60 |
| 1.3. Oxygen-to-metal ratio | per-unit | 2.001–2.002* | 2.000–2.015 | – |
| 1.4. Density | g/cm ³ | 10.5–10.7* | 10.5–10.8 | 10.4–10.8 |
| 1.5. Grain size | μm | 6.6* | 4–8 | – |
| 1.6. Pellet shape | – | without chamfers | without chamfers | with chamfers |
| 1.7. Pellet outer diameter | mm | 7.54–7.58* | 7.57 _{-0.04} | 7.60 _{-0.07} |
| 1.8. Diameter of central hole | mm | 1.6–1.7* | 2.4±0.05 | 1.20 ^{+0.8} |
| 1.9. Pellet height | mm | 8–14 | 9–14 | 11±3 |
| 1.10. Fuel mass | g | 1087±22 | 1469±22 | 1041±21 |
| 2. Zr-1%Nb cladding | | | | |
| 2.1. Composition: | | | | |
| Zr | % by weight | 98.67–98.87 | 98.67–98.87 | 98.67–98.87 |
| Nb | % by weight | 0.9–1.1 | 0.9–1.1 | 0.9–1.1 |
| O ₂ | % by weight | < 0.1 | < 0.1 | < 0.1 |
| N, C, Si, Al, Mo, Ni, Fe | % by weight | < 0.13 | < 0.13 | < 0.13 |
| 2.2. Outer diameter | mm | 9.1 ^{+0.1} _{-0.05} | 9.13 ^{+0.06} _{-0.05} | 9.1 ^{+0.1} _{-0.05} |
| 2.3. Inner diameter | mm | 7.72 ^{+0.08} | 7.72 ^{+0.08} | 7.72 ^{+0.08} |
| 3. Fuel rod | | | | |
| 3.1. Design | – | See Fig. A.1 | See Fig. A.2 | See Fig. A.3 |
| 3.2. Upper plenum length | m | 85 ^{+8.0} _{-9.0} | 239 ^{+21.0} _{-4.0} | – |
| 3.3. Fuel stack length | mm | 2420 ⁺¹⁰ ₋₁₀ | 3530 ⁺⁴ ₋₁₂ | 2320 ⁺¹⁰ ₋₁₀ |
| 3.4. Gas pressure** | MPa | 0.5–0.7 | 1.9–2.6 | 0.5–0.7 |
| 3.5. Gas composition | – | He | He | He |
| 3.6. Internal void volume | cm ³ | 13.7 | 14.5 | 38.3 |
| 3.7. Pitch*** | mm | 12.2 | 12.75 | 12.2 |
| 3.8. Hydraulic diameter | mm | 8.93 | 10.5 | 8.93 |

* These values were measured during the fabrication. Other values were determined from specifications of fuel rods

** At the room temperature

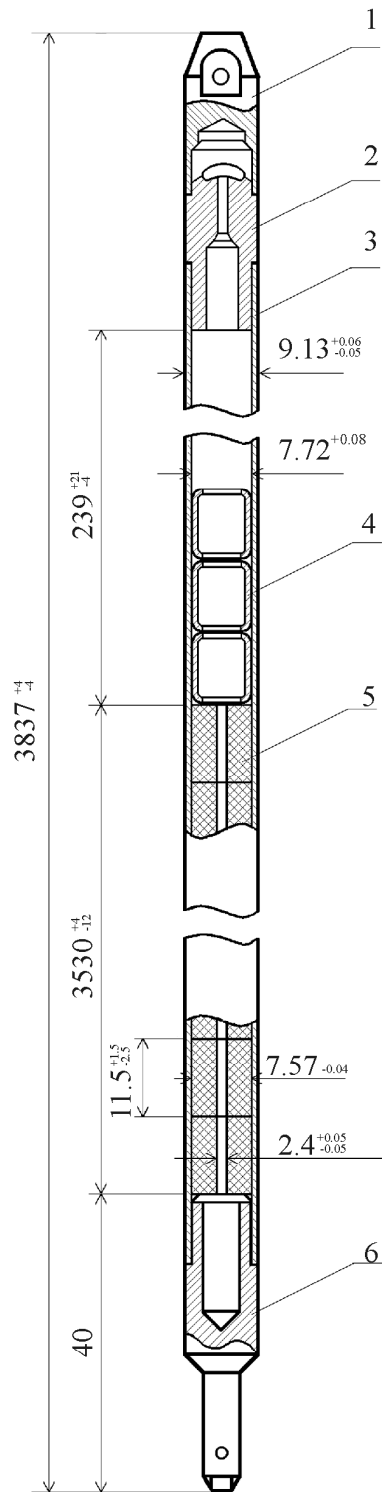
*** The distance between the centers of 2 adjacent rods in the VVER hexagonal geometry



- Design elements:
- 1 - Upper cap;
 - 2 - Fixing ring;
 - 3 - Cladding;
 - 4 - Fuel pellet;
 - 5 - Lower cap

Dimensions are presented in mm

Fig. A.1. Design scheme of VVER-440 commercial fuel rod from the fuel assembly #14422222



Design elements:

- 1 - Upper cap;
- 2 - Plug;
- 3 - Cladding;
- 4 - Fixing ring;
- 5 - Fuel pellet;
- 6 - Lower cap

Dimensions are presented in mm

Fig. A.2. Design scheme of VVER-1000 commercial fuel rod from the fuel assembly #ED4108

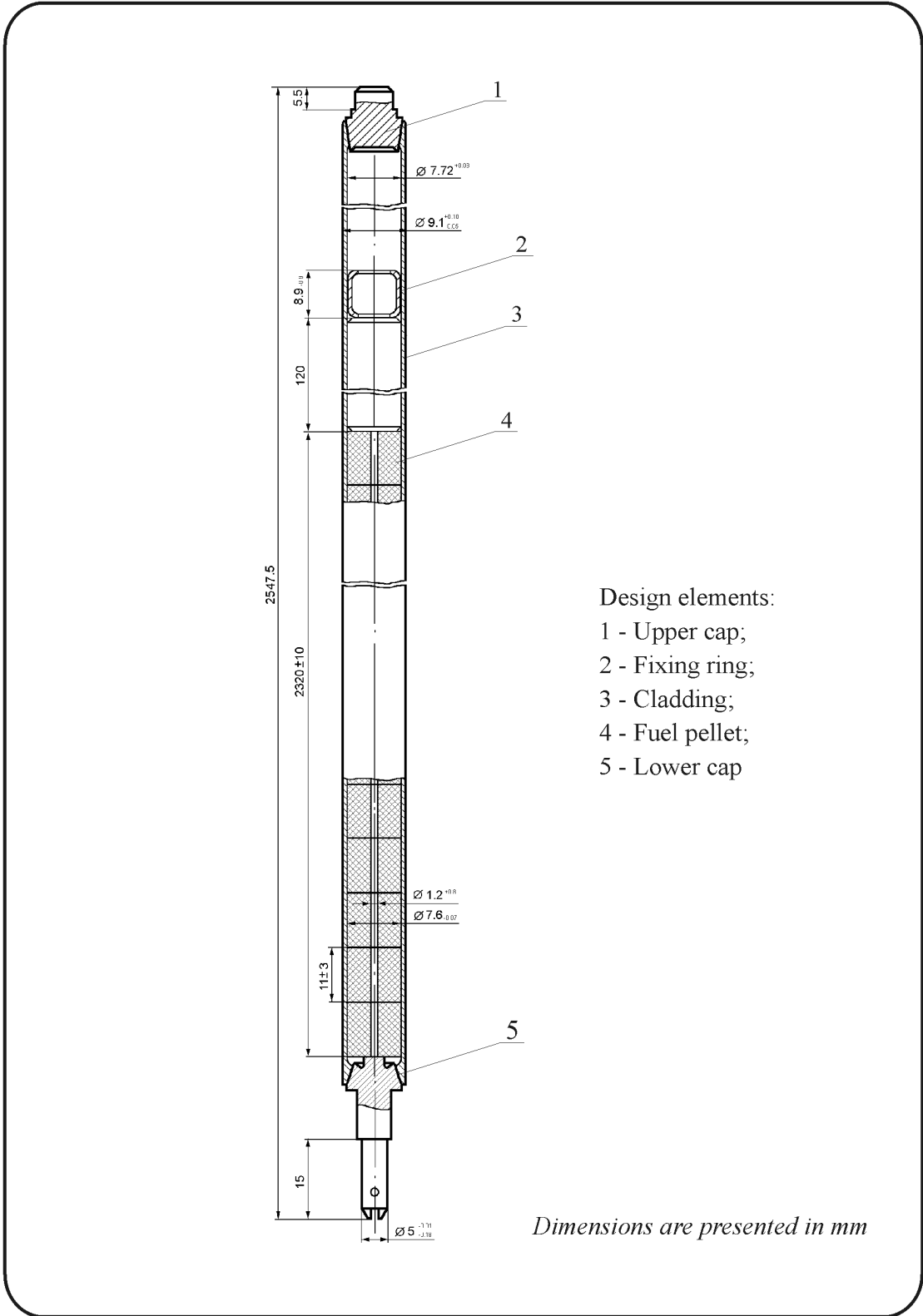


Fig. A.3. Design scheme of VVER-440 commercial fuel rod from the fuel assembly #23635228

APPENDIX B

FUEL CYCLE PARAMETERS AND POST-IRRADIATION CHARACTERISTICS OF COMMERCIAL FUEL RODS

Table B.1. Base irradiation history of fuel assembly #14422222

| Characteristic | Unit | Value |
|--|---------------------|--|
| 1. Number of fuel assembly | – | 14422222 |
| 2. Operation place | – | 3 rd unit of Kola NPP |
| 3. Number of cycles | – | 5 |
| 4. Operation periods | ef.day | 245.6; 336.0; 298.5; 379.7; 305.5 ^a |
| 5. Irradiation beginning | – | 24.09.86 |
| 6. Irradiation end | – | 15.10.91 |
| 7. Reactor thermal power | MW | 1375 |
| 8. Fuel assembly location in the reactor for each fuel cycle | – | See Fig. B.1. |
| 9. The arrangement of fuel rods in the fuel assembly | – | See Fig. B.2 |
| 10. Boric acid concentration for each fuel cycle | g/kg | 5.95; 6.84; 6.71; 7.38; 5.26 |
| 11. Inlet coolant temperature | C | 268 |
| 12. Outlet coolant temperature | C | 298 |
| 13. Coolant pressure | MPa | 12.8 |
| 14. Mass flow rate | kg/m ² s | 4000 |
| 15. Power history ^b | – | see Table B.6 |

Table B.2. Base irradiation history of fuel assembly #ED4108

| Characteristic | Unit | Value |
|--|---------------------|--|
| 1. Number of fuel assembly | – | ED4108 |
| 2. Operation place | – | 5 th unit of NovoVoronezh NPP |
| 3. Number of cycles | – | 3 |
| 4. Operation periods | ef.day | 301.7; 261.7; 317.8 ^a |
| 5. Irradiation beginning | – | 05.06.86 |
| 6. Irradiation end | – | 11.07.90 |
| 7. Reactor thermal power | MW | 3000 |
| 8. Fuel assembly location in the reactor for each fuel cycle | – | See Fig. B.3 |
| 9. The arrangement of fuel rods in the fuel assembly | – | See Fig. B.4 |
| 10. Boric acid concentration for each fuel cycle | g/kg | 6.33; 6.33; 7.15 |
| 11. Inlet coolant temperature | C | 287 |
| 12. Outlet coolant temperature | C | 317 |
| 13. Coolant pressure | MPa | 15.7 |
| 14. Mass flow rate | kg/m ² s | 5000 |
| 15. Power history | – | see Table B.5 |

^a It is the list of durations for each fuel cycle (ef.day)

^b see comments to Table B.3

Table B.3. Base irradiation history of fuel assembly #23635228

| Characteristic | Unit | Value |
|--|---------------------|---|
| 1. Number of fuel assembly | – | 23635228 |
| 2. Operation place | – | 4 th unit of NovoVoronezh NPP |
| 3. Number of cycles | – | 5 |
| 4. Operation periods | ef.day | 98.7; 325.1; 372.1; 350.7; 368.1 ^a |
| 5. Irradiation beginning | – | 17.01.90 |
| 6. Irradiation end | – | 15.02.97 |
| 7. Reactor thermal power | MW | – ^{bb} |
| 8. Fuel assembly location in the reactor for each fuel cycle | – | See Fig. B.5 |
| 9. The arrangement of fuel rods in the fuel assembly | – | See Fig. B.6 |
| 10. Boric acid concentration for each fuel cycle | g/kg | – ^b |
| 11. Inlet coolant temperature | C | – ^b |
| 12. Outlet coolant temperature | C | – ^b |
| 13. Coolant pressure | MPa | – ^b |
| 14. Mass flow rate | kg/m ² s | – ^b |
| 15. Power history ^c | – | – ^b |

^a It is the list of durations for each fuel cycle (ef.day)

^b The data were not open to this research

^c The VVER-440 reactor contains two types of fuel assemblies, operating assemblies and follower (control) assemblies. Assembly #228, from which refabricated rod #RT7 was taken, is the follower type. Therefore, the design of the appropriate fuel elements differs from the design of the operating fuel element (#222), from which other refrabricated rods were taken. The follower assemblies are the part of the reactor control system. In the general case, the follower assemblies are not in the core with their full length. Their positions can change during the operation of the unit. Therefore, the characterization of the power history for such an assembly is a very difficult task and the linear heat rating for refabricated rod #RT7 is not presented in appropriate Table.

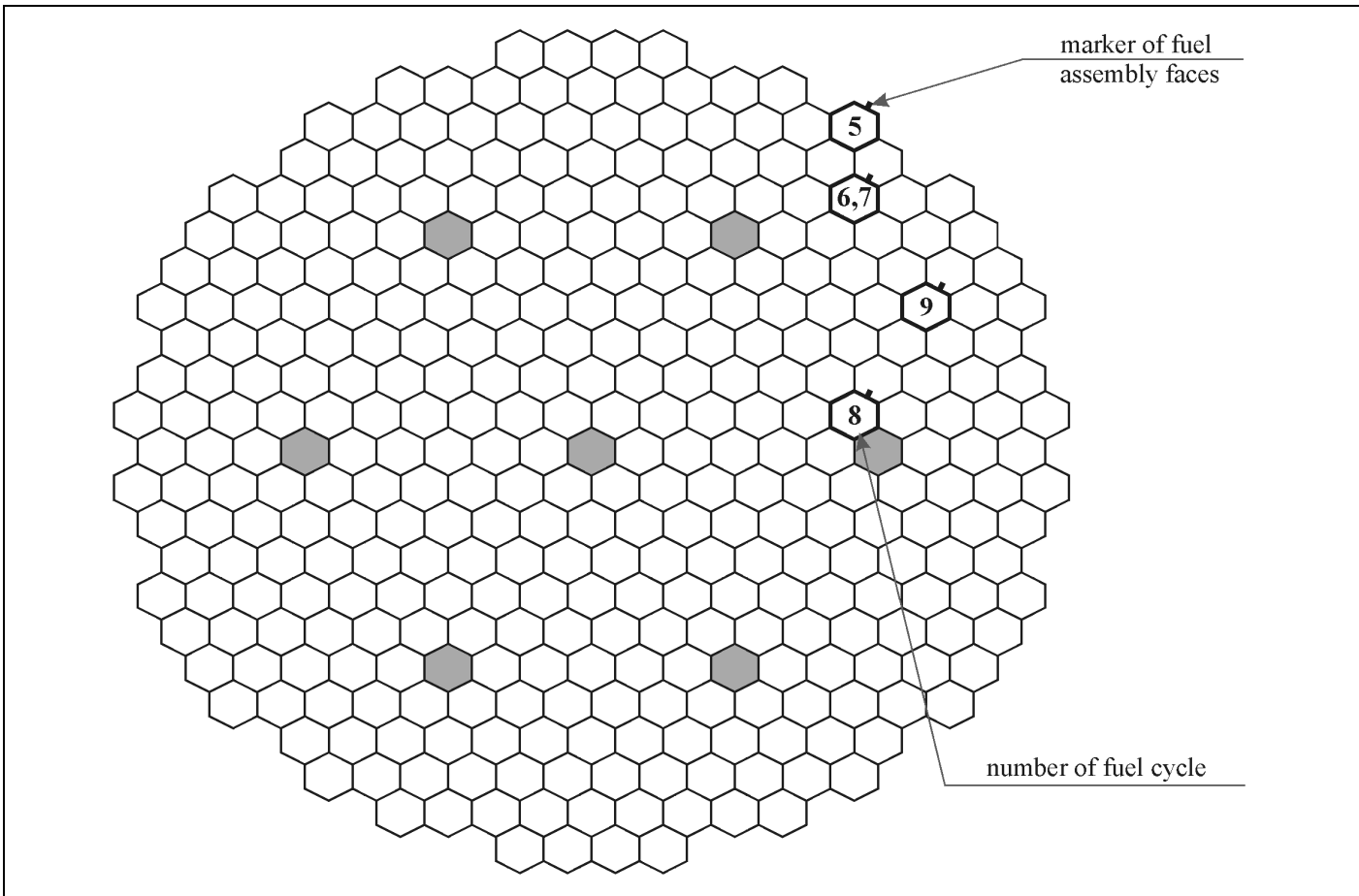


Fig. B.1. Arrangement of fuel assembly #14422222 (222) in the reactor core

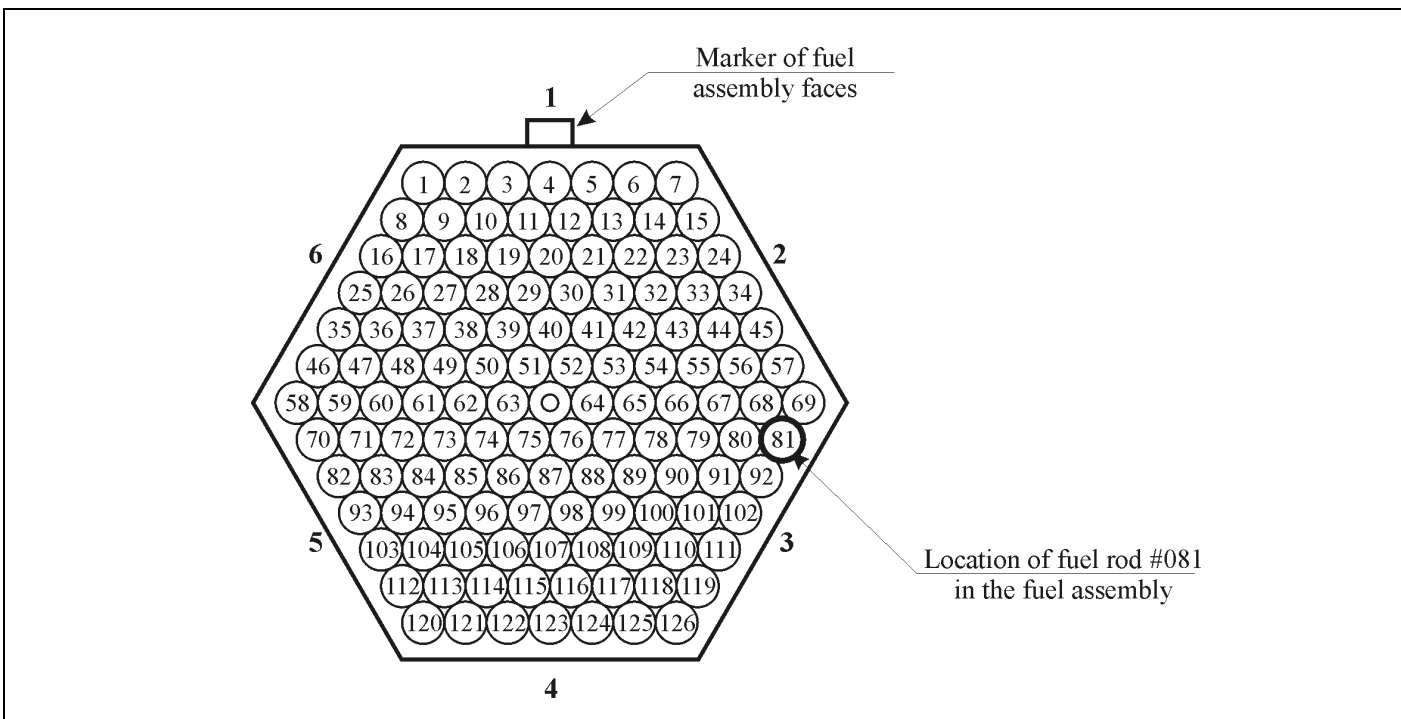


Fig. B.2. Arrangement of fuel rods in the fuel assembly #222

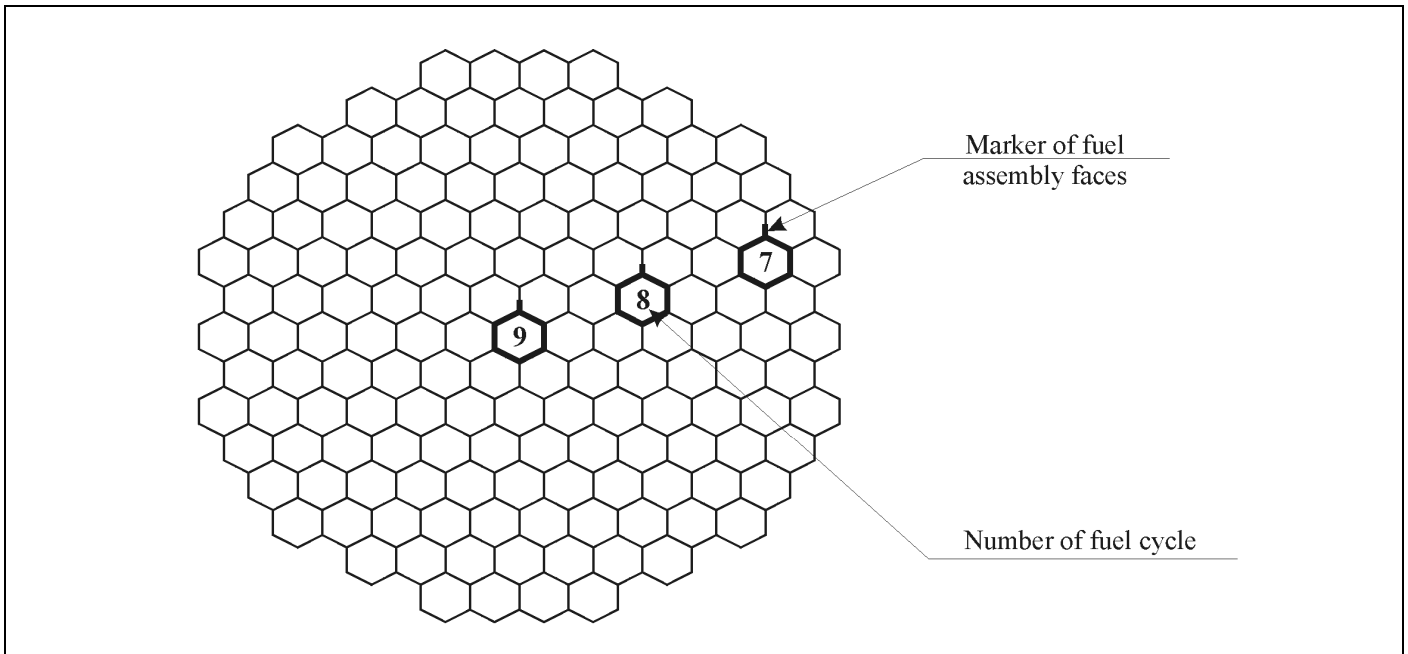


Fig. B.3. Arrangement of fuel assembly #ED4108 (108) in the reactor core

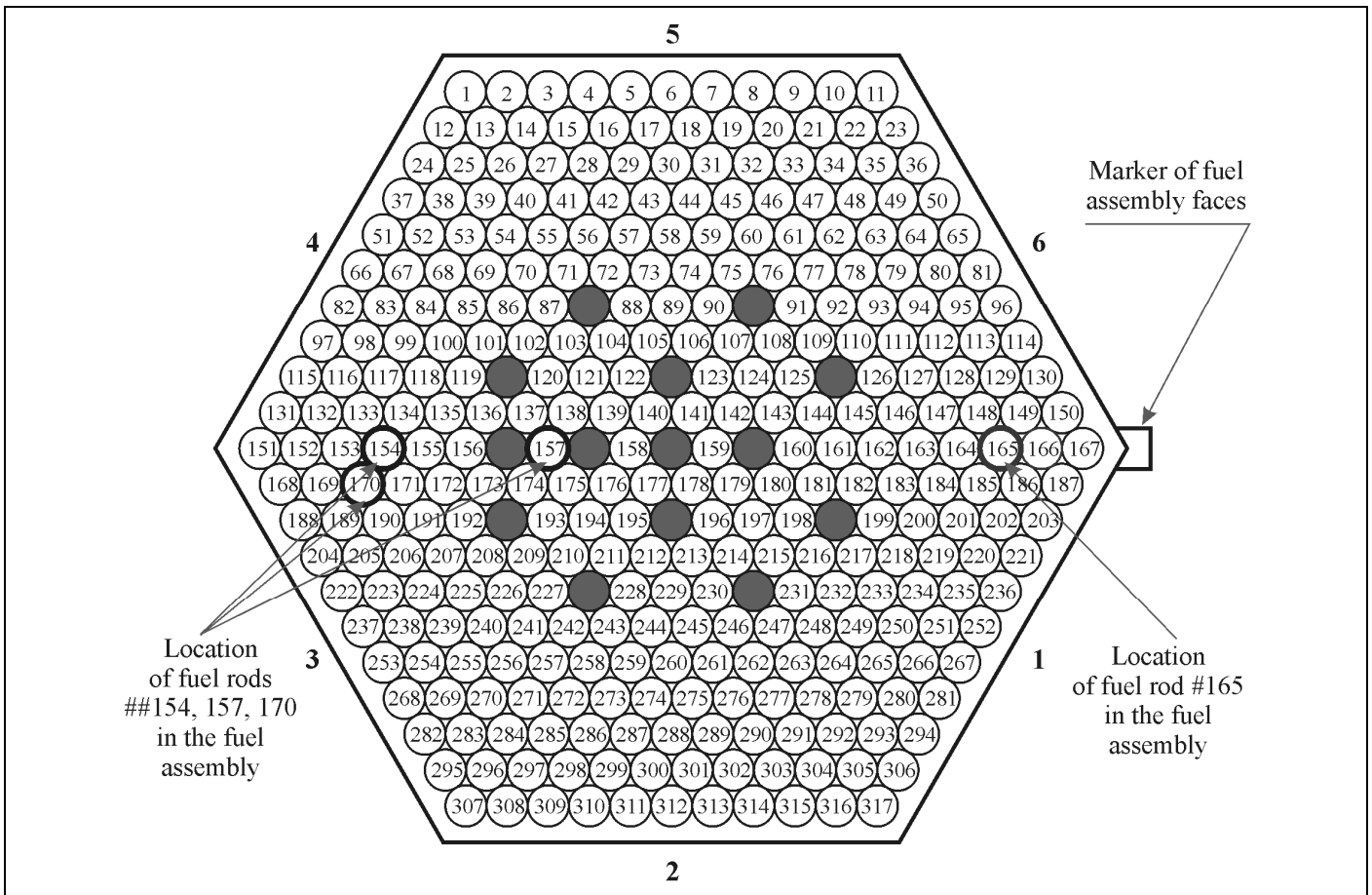


Fig. B.4. Arrangement of fuel rods in the fuel assembly #ED4108 (108)

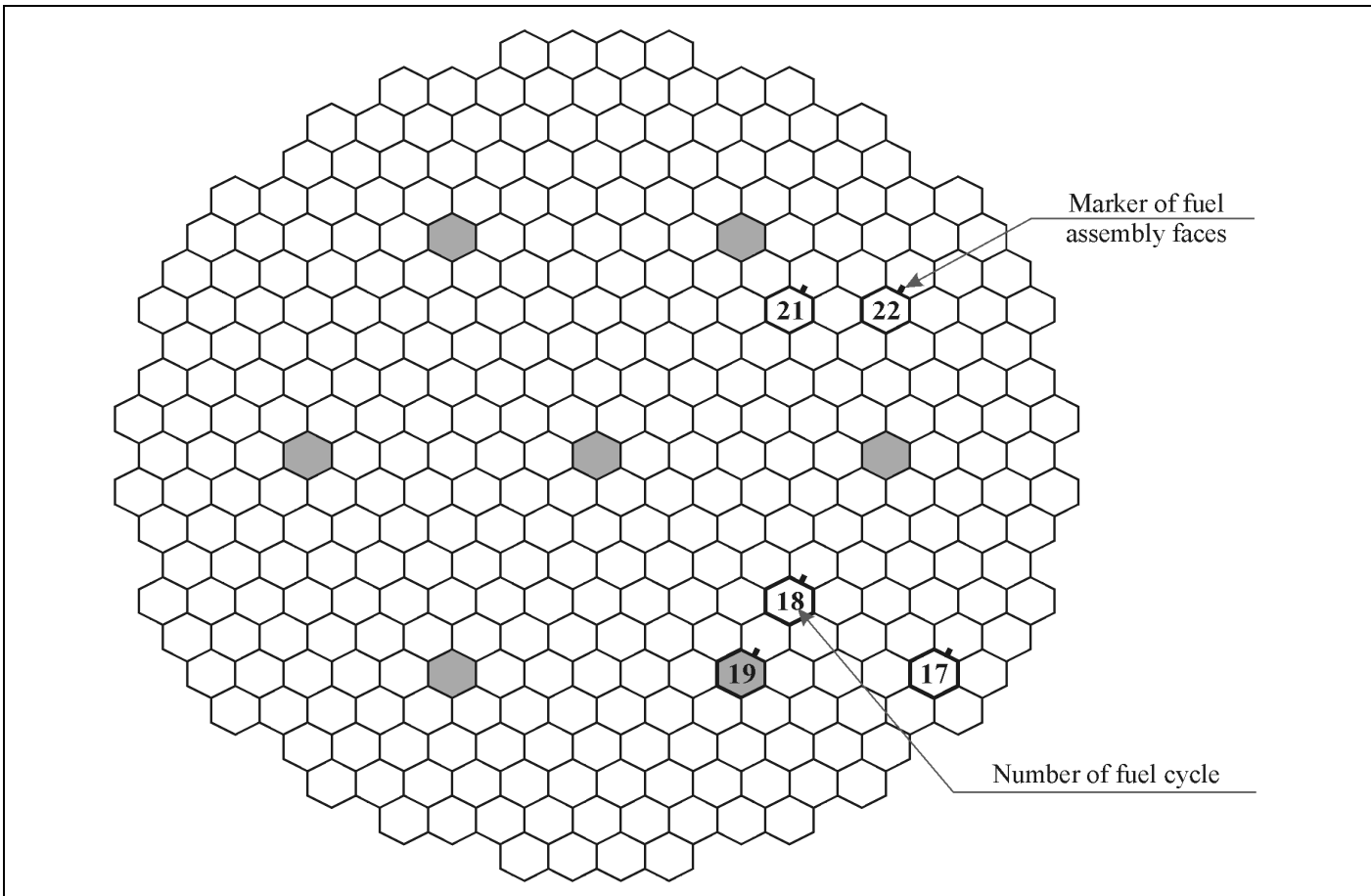


Fig. B.5. Arrangement of fuel assembly #23635228 (228) in the reactor core

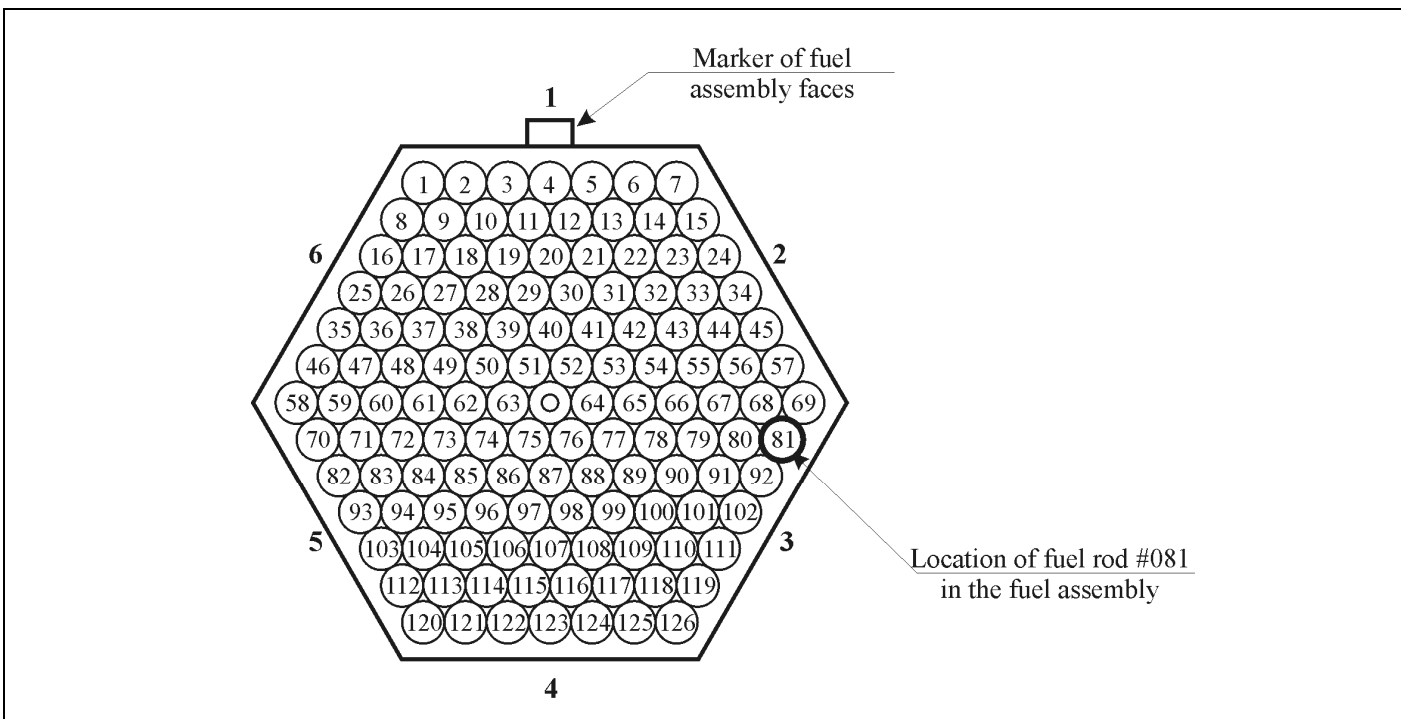


Fig. B.6. Arrangement of fuel rods in the fuel assembly #228

**Table B.4. Characteristics of commercial fuel rods used for the refabrication after the base irradiation
(in accordance with PIE results)**

| Characteristic | Unit | Value | | | | | |
|---|-------------------|----------------------|--------------------|--------------------|--------------------|--------------------|----------|
| Fuel rod type | – | VVER-440 | VVER-1000 | VVER-1000 | VVER-1000 | VVER-1000 | VVER-440 |
| Number of fuel assembly | – | 222 | 108 | 108 | 108 | 108 | 228 |
| Number of fuel rod (see Fig. B.2, Fig. B.4, Fig. B.6) | – | 081 | 154 | 157 | 165 | 170 | 081 |
| Commercial number of fuel rod | – | 18801/75 | E023269 | E023261 | E023267 | E023404 | – |
| <i>Fuel rod</i> | | | | | | | |
| Gas pressure | MPa | 1.26 | 2.64 | 2.93 | 2.86 | 2.87 | 1.08 |
| He content in the gas composition | % by volume | 67.72 | 95.65 | 92.58 | 94.69 | 96.61 | 86.05 |
| Kr and Xe content | % by volume | 28.84 | 4.01 | 6.94 | 4.62 | 3.25 | 13.73 |
| FGR | % by volume | 2.82 | 2.41 | 4.46 | 2.85 | 2.08 | 1.15 |
| Radial fuel/cladding gap* | mm | 0 | 0.032 | 0.017 | 0.025 | – | – |
| Internal void volume | cm ³ | 10.4 | 35.4 | 33.3 | 32.7 | 33.4 | 10.1 |
| <i>Fuel</i> | | | | | | | |
| Average burnup | MW d/kg U | 52.35 | 43.54 | 44.49 | 44.01 | 44.5 | 55.4 |
| Maximum burnup | MW d/kg U | 61.58 | 49.01 | 50.12 | 49.62 | 47.8 | 61.7 |
| Fuel outer diameter | mm | 7.61 | 7.62 | 7.66 | 7.57 | 7.66 | 7.68 |
| Fuel inner diameter | mm | 1.70 | 2.50 | 2.50 | 2.46 | 2.50 | 1.65 |
| Density* | g/cm ³ | 10.1–10.3 | 10.3–10.5 | 10.3–10.5 | 10.3–10.5 | 10.3–10.5 | – |
| Grain size* | µm | 3 | 3–8 | 3–8 | 3–8 | 3–8 | – |
| Rim layer thickness | mm | 0.15–0.20 | 0.05–0.07 | 0.05–0.07 | 0.05–0.07 | 0.05–0.07 | – |
| ZrO ₂ outer thickness* | µm | 3–5 | 3–5 | 3–5 | 3–5 | 3–5 | 3–5 |
| ZrO ₂ inner thickness* | µm | 10 | 0 | 0 | 0 | 0 | 8–10 |
| <i>Cladding</i> | | | | | | | |
| Average diameter along upper plenum | mm | 9.137 | 9.14 | 9.14 | 9.14 | 9.154 | 9.101 |
| Average diameter along fuel stack | mm | 9.07 | 9.08 | 9.08 | 9.07 | 9.083 | 9.045 |
| Average thickness | mm | 0.73 | 0.70 | 0.69 | 0.72 | 0.69 | – |
| H ₂ content | % by weight | 6–8·10 ⁻³ | 5·10 ⁻³ | 5·10 ⁻³ | 5·10 ⁻³ | 5·10 ⁻³ | – |
| ZrO ₂ outer thickness | µm | 3–5 | 3–5 | 3–5 | 3–5 | 3–5 | 3–5 |
| ZrO ₂ inner thickness | µm | 0–10 | 0 | 0 | 0 | 0 | 0–10 |

* This parameter characterizes that part of the fuel element, which was used for the refabrication

Table B.5. The calculated linear heat rating of VVER-1000 fuel elements during the base irradiation at elevations used for the manufacture of refabricated fuel rods

| Number of fuel element* | Elevation (mm) | Number of refabricated fuel rod | Linear heat rating (kW/m) | | | | | |
|-------------------------|----------------|---------------------------------|---------------------------|------|-----------------------|------|-----------------------|------|
| | | | 7 th cycle | | 8 th cycle | | 9 th cycle | |
| | | | B** | E*** | B | E | B | E |
| 154 | 2180 | RT6 | 26.0 | 23.7 | 23.3 | 17.7 | 18.0 | 15.0 |
| 157 | 2410 | RT5 | 24.0 | 22.0 | 25.3 | 19.0 | 18.7 | 15.7 |
| 165 | 1120 | RT1 | 27.0 | 26.0 | 23.3 | 19.0 | 18.3 | 15.0 |
| 165 | 1350 | RT2 | 27.0 | 25.3 | 24.0 | 18.7 | 18.3 | 14.3 |
| 165 | 2410 | RT3 | 24.7 | 24.0 | 23.7 | 18.7 | 18.7 | 15.0 |
| 170 | 2180 | RT10 | 27.0 | 24.2 | 23.3 | 17.7 | 18.3 | 14.7 |
| 170 | 2410 | RT11 | 25.7 | 24.3 | 23.7 | 17.7 | 18.0 | 14.7 |
| 170 | 2650 | RT12 | 25.0 | 24.0 | 23.7 | 18.0 | 18.0 | 15.3 |

* Numbers are presented in accordance with Fig. B.4

** The Beginning (B) of cycle

*** The End (E) of cycle

Table B.6. The calculated linear heat rating of VVER-440 (FA #222) fuel elements during the base irradiation at elevations used for the manufacture of refabricated fuel rods

| Number of fuel element* | Elevation (mm) | Number of refabricated fuel rod | Linear heat rating (kW/m) | | | | | | | | | |
|-------------------------|----------------|---------------------------------|---------------------------|------|-----------------------|------|-----------------------|------|-----------------------|------|-----------------------|------|
| | | | 5 th cycle | | 6 th cycle | | 7 th cycle | | 8 th cycle | | 9 th cycle | |
| | | | B** | E*** | B | E | B | E | B | E | B | E |
| 81 | 860 | RT4 | 15.0 | 13.3 | 20.0 | 16.0 | 17.7 | 15.0 | 15.3 | 13.3 | 12.0 | 10.7 |
| 81 | 970 | RT8 | 15.0 | 13.3 | 20.0 | 16.3 | 18.0 | 15.0 | 15.7 | 13.3 | 12.0 | 10.7 |
| 81 | 1210 | RT9 | 15.7 | 13.3 | 19.3 | 16.7 | 17.0 | 15.0 | 15.0 | 13.7 | 11.3 | 11.0 |

* Numbers are presented in accordance with Fig. B.4

** The Beginning (B) of cycle

*** The End (E) of cycle

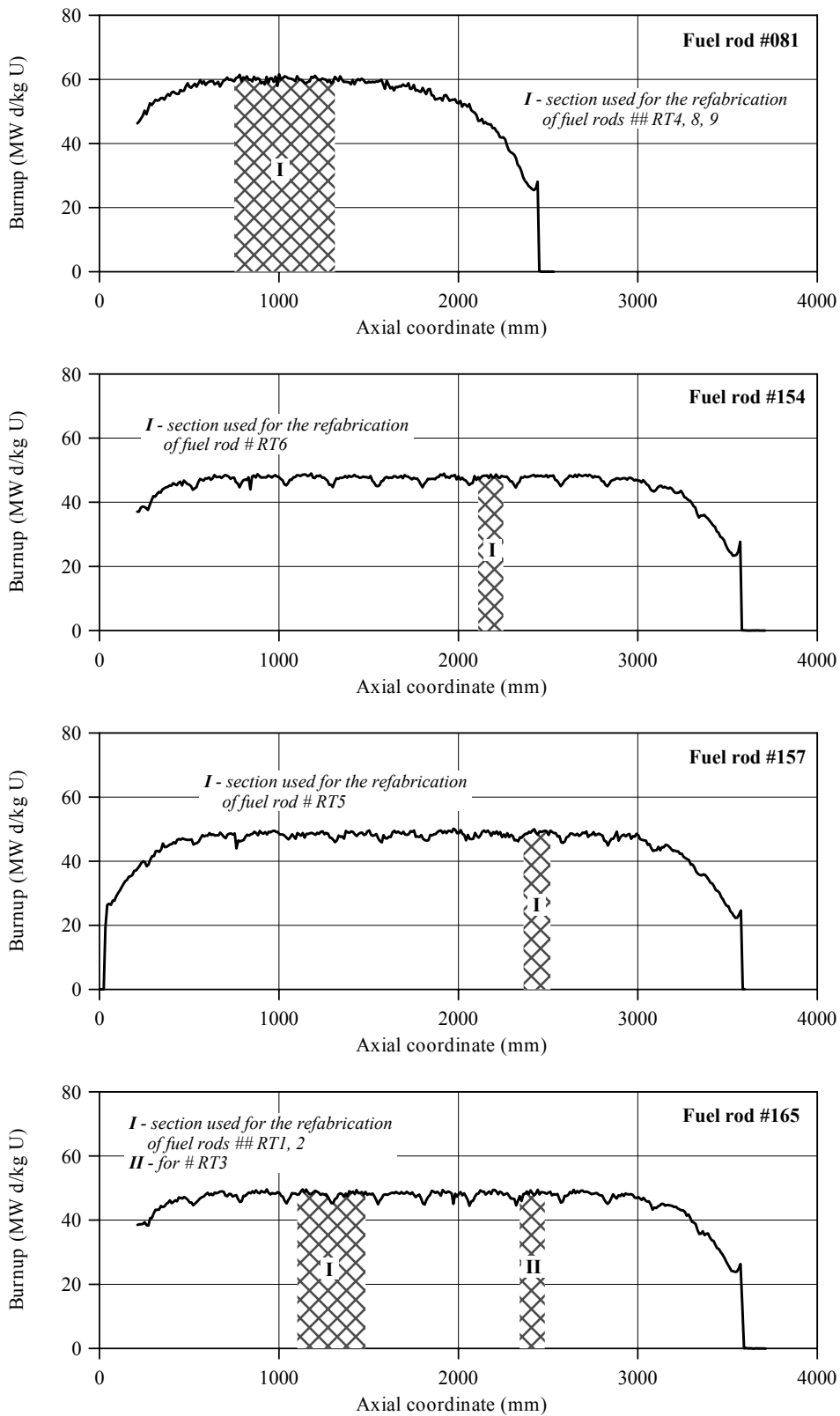


Fig. B.7. Axial distribution of fuel burnup in fuel rods ## 081, 154, 157, 165 of fuel assemblies ##222, 108

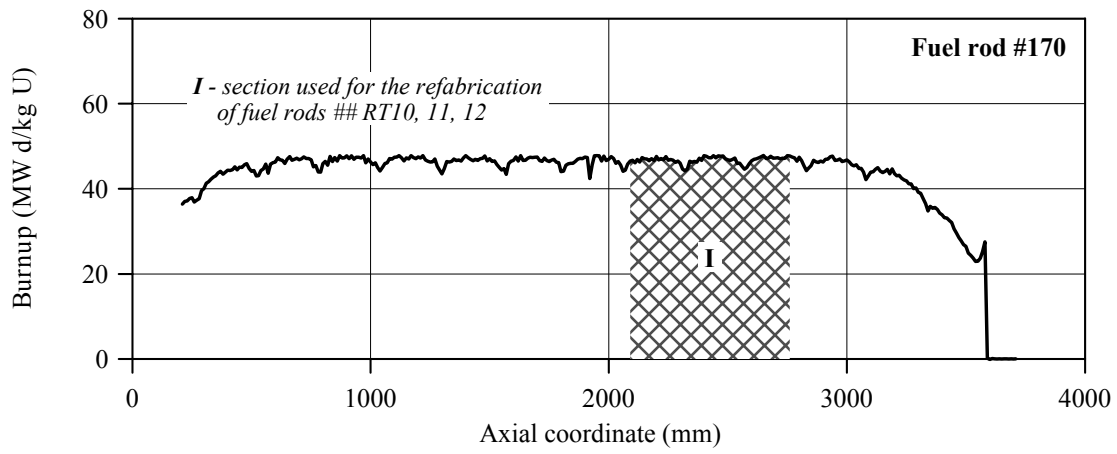
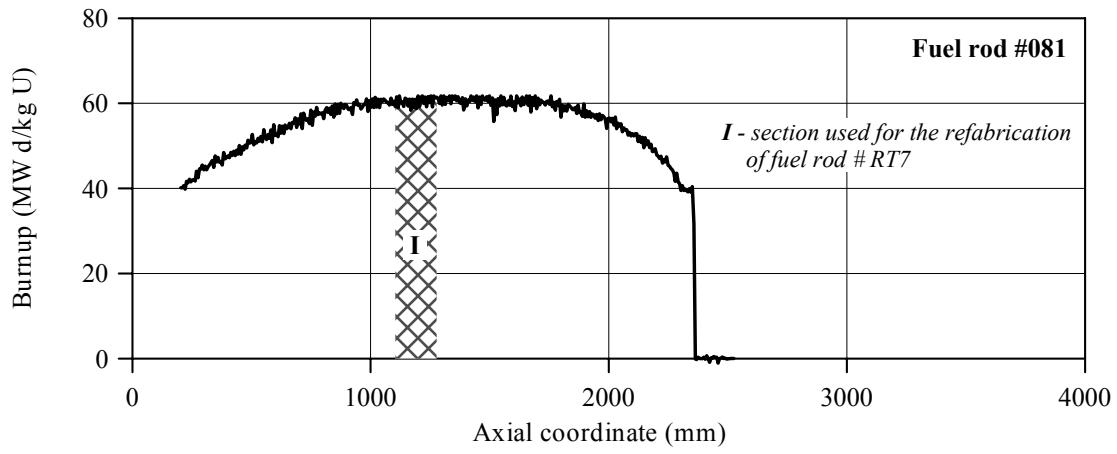


Fig. B.8. Axial distribution of fuel burnup in fuel rods ## 081, 170 of fuel assemblies ##228, 108

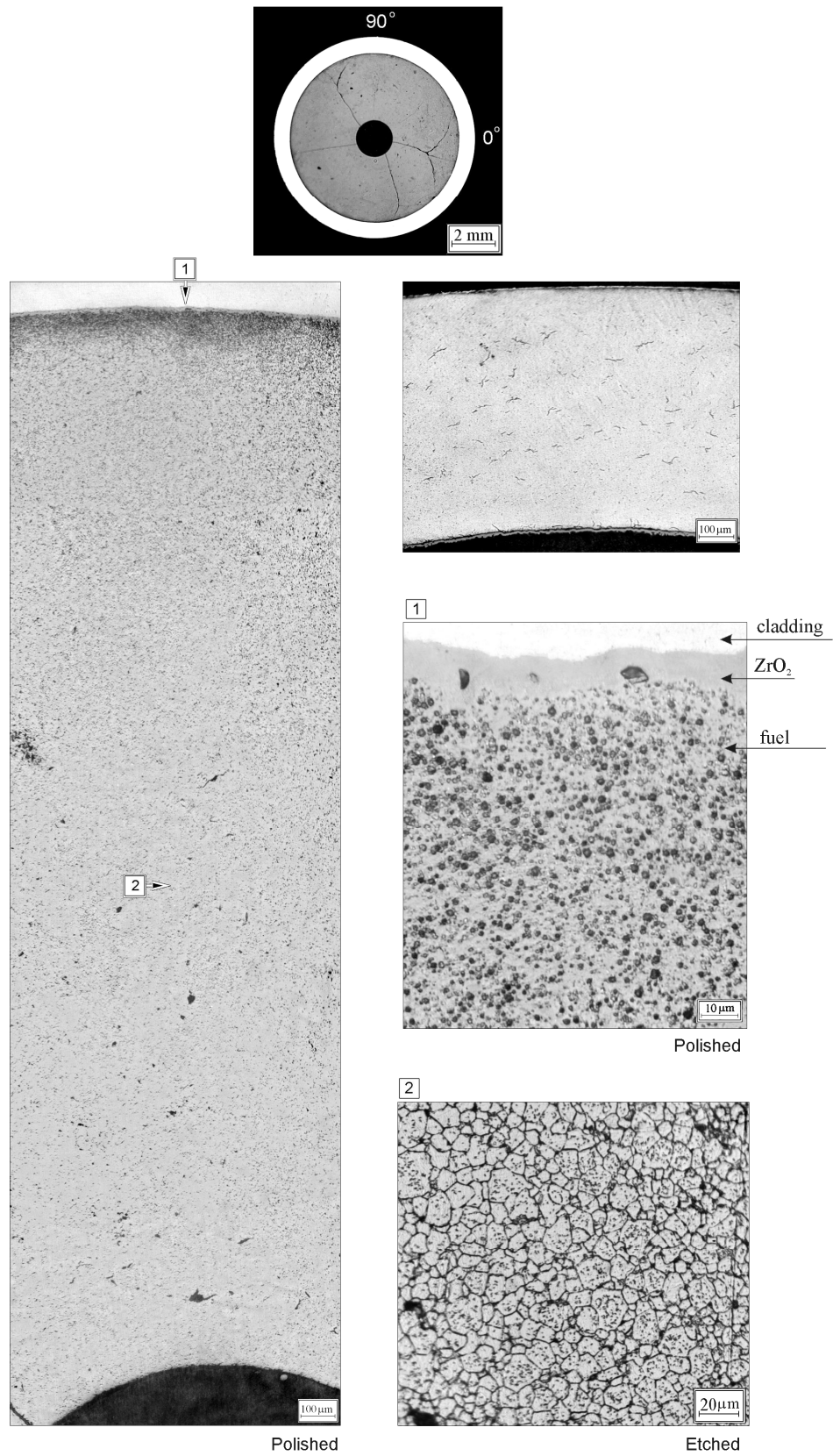


Fig. B.9. Macro- and microstructures of fuel and cladding in commercial fuel rod #081 (VVER-440, fuel assembly #222) at 1110 mm elevation after the base irradiation

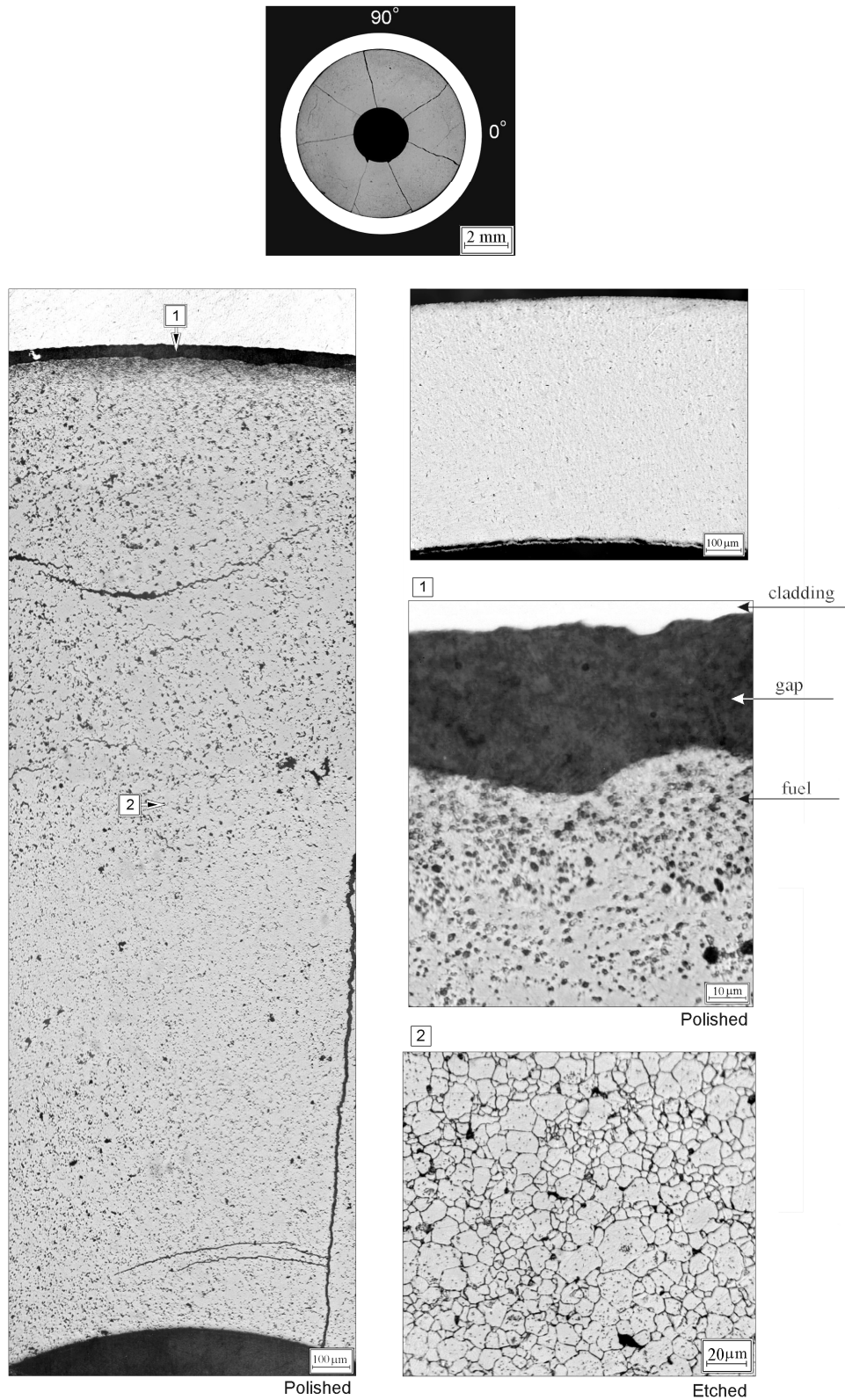


Fig. B.10. Macro- and microstructures of fuel and cladding in commercial fuel rod #154 (VVER-1000, fuel assembly #108) at 2080 mm elevation after the base irradiation

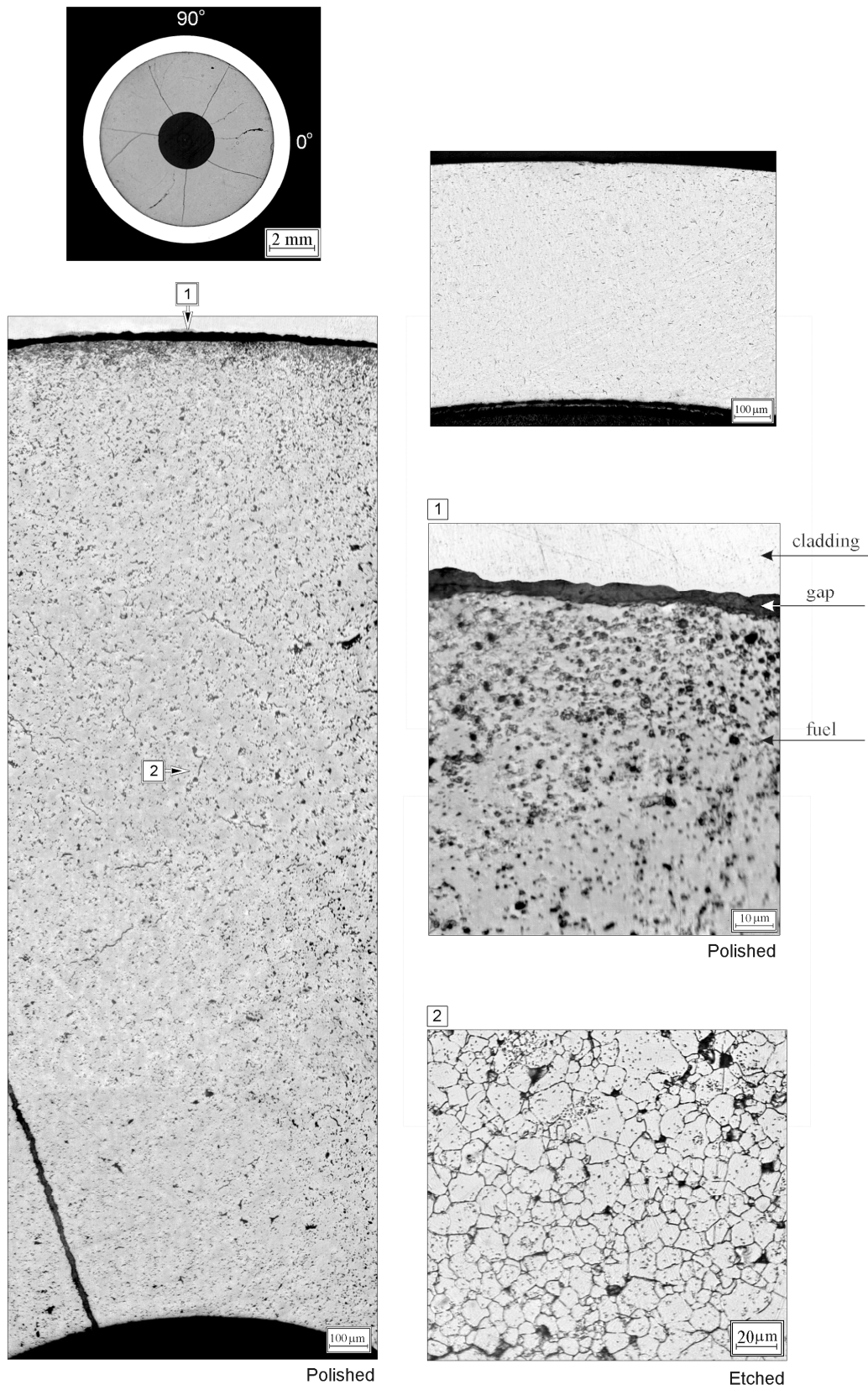


Fig. B.11. Macro- and microstructures of fuel and cladding in commercial fuel rod #157 (VVER-1000, fuel assembly #108) at 2340 mm elevation after the base irradiation

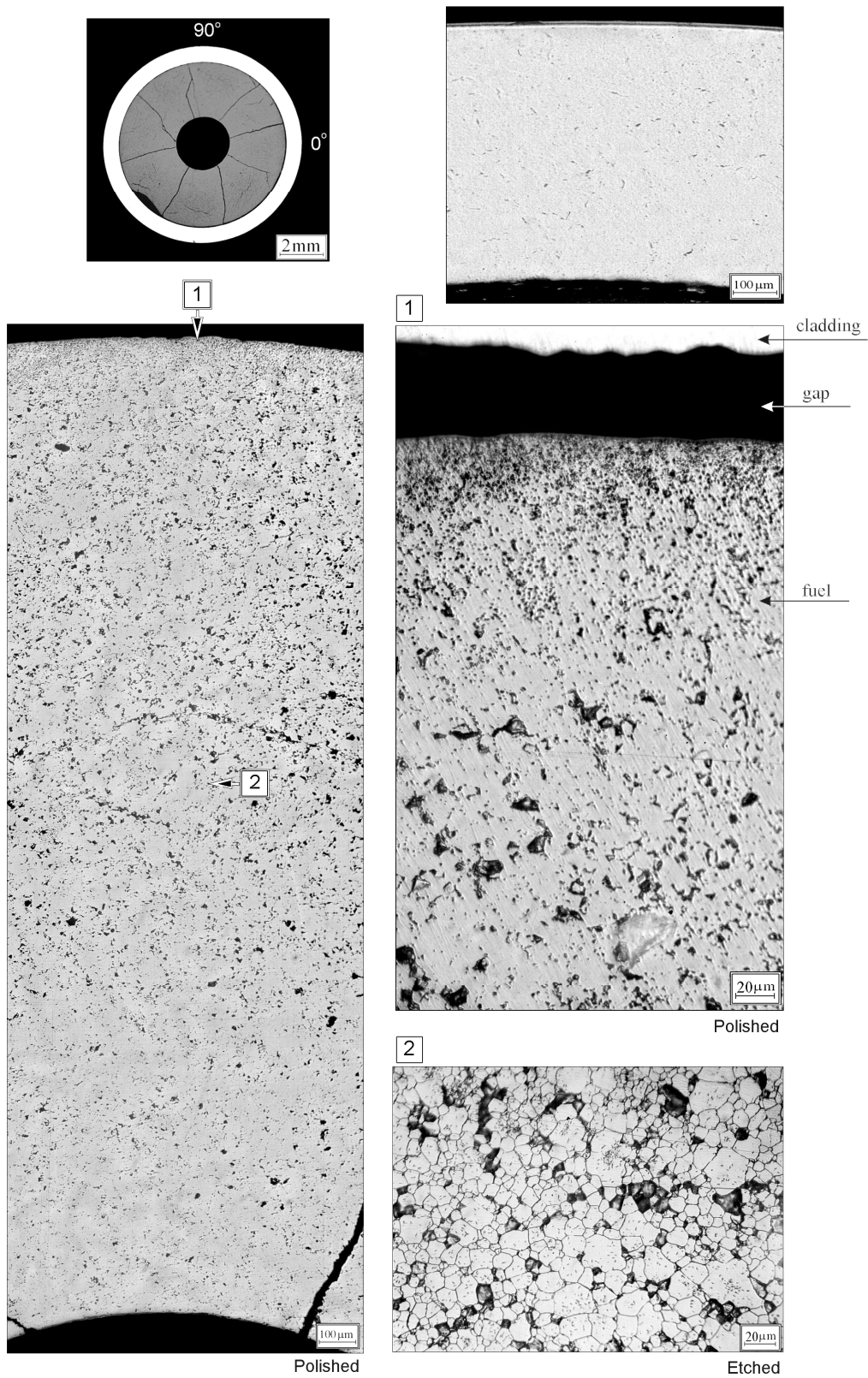


Fig. B.12. Macro- and microstructures of fuel and cladding in commercial fuel rod #165 (VVER-1000, fuel assembly #108) at 1495 mm elevation after the base irradiation

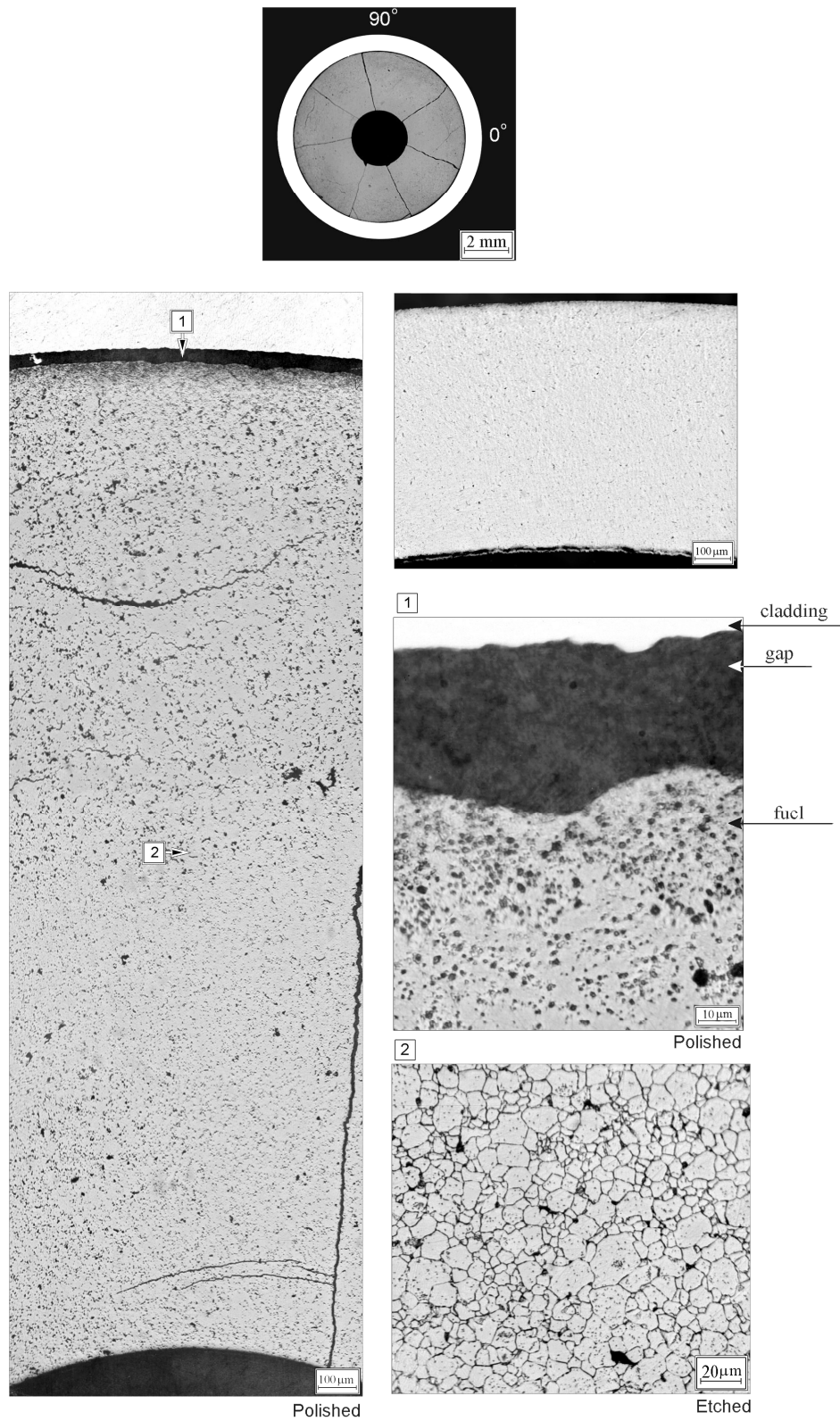


Fig. B.13. Macro- and microstructures of fuel and cladding in commercial fuel rod #170 (VVER-1000, fuel assembly #108) at 2270 mm elevation after the base irradiation

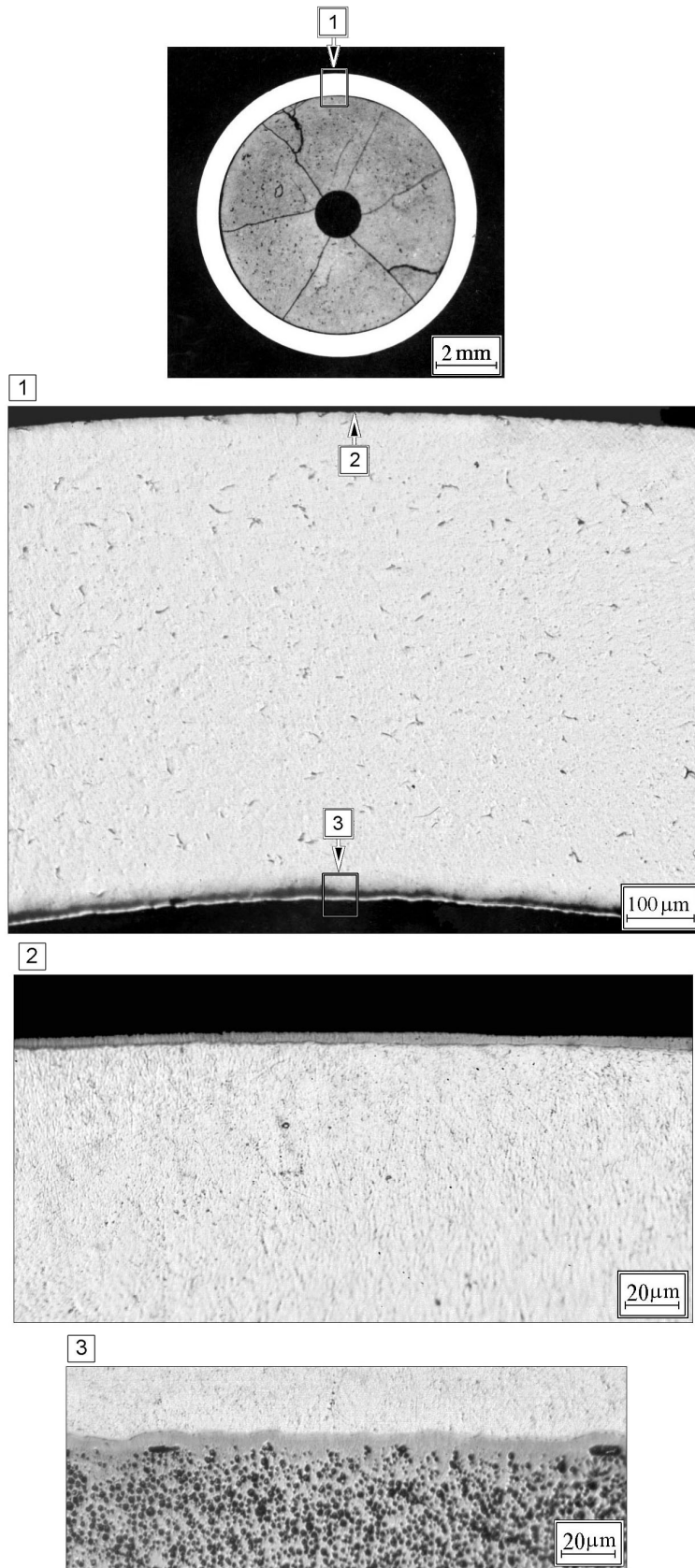
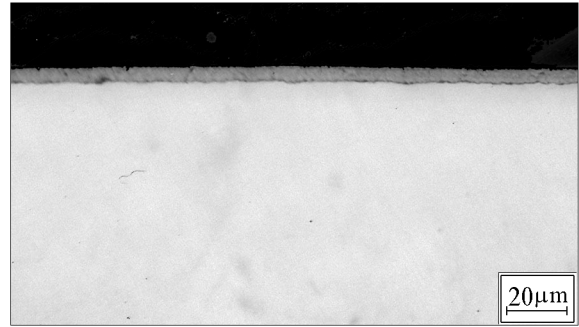
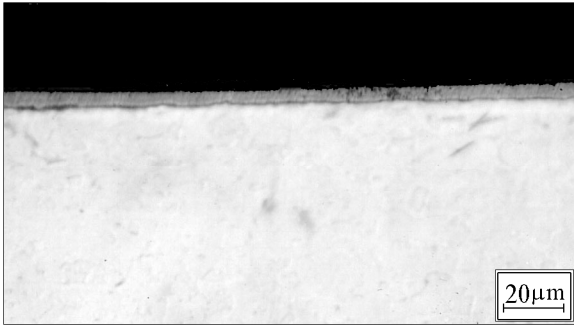


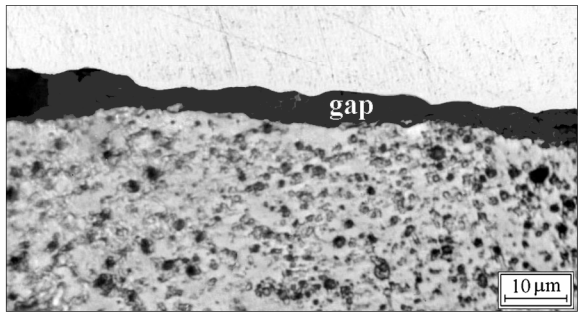
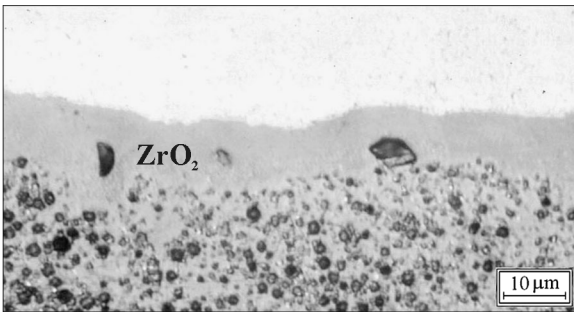
Fig. B.14. Macro- and microstructures of fuel and cladding in commercial fuel rod #081 (VVER-440, fuel assembly #228) at 1300 mm elevation after the base irradiation

Fuel rod #081 at elevation 1110 mm
(fuel assembly #222)
60 MW day/kg U

Fuel rod #157 at elevation 2340 mm
(fuel assembly #108)
50 MW day/kg U



Cladding outer surface



Cladding inner surface

Fig. B.15. Comparative data characterizing the cladding oxidation and fuel/cladding gap at burnup 50 and 60 MW d/kg U

APPENDIX C

**CHARACTERISTICS OF REFABRICATED
FUEL RODS BEFORE THE BIGR TESTS**

Table C.1. Characteristics of fuel rods before BIGR tests: Reference data*

| Characteristic | Unit | Value | | |
|---------------------------------------|-------------------|---|------------------------------|--------------|
| Commercial fuel rod type | – | VVER-440 | VVER-1000 | VVER-440 |
| Number of fuel assembly | – | 222 | 4108 | 228 |
| Number of commercial fuel rod | – | 081 | 154, 157, 165, 170 | 081 |
| Number of refabricated fuel rod | – | RT 4, 8, 9 | RT 1, 2, 3, 5, 6, 10, 11, 12 | RT 7 |
| 1. Fuel | | | | |
| 1.1. Outer diameter | mm | 7.61 | 7.57–7.66 | 7.68 |
| 1.2. Inner diameter | mm | 1.7 | 2.46–2.5 | 1.65 |
| 1.3. Density | g/cm ³ | 10.1–10.3 | 10.3–10.5 | – |
| 1.4. Grain size | μm | 3 | 3–8 | – |
| 2. Cladding | | | | |
| 2.1. Outer diameter | mm | 9.07–9.09 | 9.06–9.08 | 9.06 |
| 2.2. Thickness | mm | 0.73 | 0.69–0.72 | 0.69 |
| 2.3. ZrO ₂ outer thickness | μm | 3–5 | 3–5 | 3–5 |
| 2.4. ZrO ₂ inner thickness | μm | 10 | 0 | 8–10 |
| 2.5. Hydrogen content | % by weight | 6–8·10 ⁻³ | 5·10 ⁻³ | – |
| 3. Refabricated fuel rod | | | | |
| 3.1. Design | – | RT4 see Fig. C.1 RT8, 9 see Fig. C.2 | see Fig. C.1 | see Fig. C.1 |
| 3.2. Gas composition | – | He | He | He |

Table C.2. Individual parameters of refabricated fuel rods ## RT1–6 before BIGR tests**

| Parameter | Number of fuel rod | | | | | |
|---|--------------------|---------------|---------------|------------|--------------|--------------|
| | RT1 | RT2 | RT3 | RT4 | RT5 | RT6 |
| Number of mother fuel rods | 165 | 165 | 165 | 081 | 157 | 154 |
| Coordinates of mother fuel rod section used for refabrication*** (mm) | 1093 1246 | 1331 1482 | 2340 2489 | 745 900 | 2360 2513 | 2103 2254 |
| Pellet stack coordinate*** (mm) | 24 177 | 25.4 176.4 | 23.6 172.6 | 22 177 | 24 177 | 23 174 |
| Coordinates of undamaged section of pellet stack**** (mm) | 24 177 | 25.4 176.4 | 65.5 110.5 | 22 177 | 24 177 | 23 165 |
| Undamaged section length (mm) | 153 | 151 | 45 | 155 | 153 | 142 |
| Average burnup (MW d/kg U) | 48.3 | 48.0 | 47.5 | 60.1 | 48.6 | 47.8 |
| Total fuel mass (g) | 63.5 | 62.1 | 60.4 | 69.5 | 63.1 | 61.9 |
| Mass of undamaged fuel section (g) | 63.5 | 62.1 | 18.36 | 69.5 | 63.1 | 58.4 |
| L ₁ ***** (mm) | 4.6 | 6.0 | 4.2 | 2.6 | 4.6 | 3.6 |
| L ₂ ***** (mm) | 153 | 151 | 149 | 155 | 153 | 151 |
| L ₃ ***** (mm) | 4.5 | 3.1 | 3.4 | 2.5 | 2.5 | 2.5 |
| L ₄ ***** (mm) | 302 | 300 | 296.5 | 300 | 300 | 297 |
| Total gas volume (cm ³) | 6.13 | 6.12 | 6.08 | 5.54 | 6.07 | 6.03 |
| Cladding outer diameter (mm) | 9.06 | 9.06 | 9.06 | 9.08 | 9.06 | 9.07 |
| Fuel-cladding radial gap (mm) | 0.025 | 0.025 | 0.025 | 0.000 | 0.017 | 0.032 |
| Central hole diameter (mm) | 2.46 | 2.46 | 2.46 | 1.65 | 2.50 | 2.50 |
| Internal gas pressure (MPa) | 2.1 | 2.1 | 2.1 | 2.1 | 2.1 | 2.1 |

* Characteristics were developed in accordance with data of Table B.4.

** Parameters were determined using pre-test examination results

*** From lower cap of fuel rod

**** Taking into account the risk of fuel damage at the refabrication procedure, special measurements were performed to estimate the coordinates of that part of fuel stack, which was identified as “undamaged” after the refabrication. The coordinates of undamaged part was determined from lower cap of fuel rod

***** See Fig. C.1

Table C.3. Individual parameters of refabricated fuel rods ## RT7–12 before BGR tests *

| Parameter | Number of fuel rod | | | | | |
|---|--------------------|-------------|--------------|---------------|--------------|---------------|
| | RT7 | RT8 | RT9 | RT10 | RT11 | RT12 |
| Number of mother fuel rods | 081 | 081 | 081 | 170 | 170 | 170 |
| Coordinates of mother fuel rod section used for refabrication ** (mm) | 1100 1278 | 931 1109 | 1133 1311 | 2090 2268 | 2343 2522 | 2590 2769 |
| Pellet stack coordinate ** (mm) | 23 176.1 | 7 157 | 8 157 | 21.4 173.4 | 23 175 | 21.3 173.9 |
| Coordinates of undamaged section of pellet stack *** (mm) | 23 176.1 | 7 157 | 8 157 | 21.4 173.4 | 23 175 | 21.3 173.9 |
| Fuel stack length (mm) | 153.1 | 150 | 149 | 152 | 152 | 152.6 |
| Average burnup (MW d/kg U) | 60.5 | 60.0 | 59.8 | 46.9 | 47.2 | 47.3 |
| Total fuel mass (g) | 66.8 | 66.2 | 66.2 | 62.6 | 62.9 | 63.0 |
| L ₁ **** (mm) | 3.6 | 0.0 | 0.0 | 2.0 | 3.6 | 1.9 |
| L ₂ **** (mm) | 153.1 | 150.0 | 149.0 | 152.0 | 152.0 | 152.6 |
| L ₃ **** (mm) | 2.4 | 9.1 | 10.1 | 5.1 | 3.5 | 5.6 |
| L ₄ **** (mm) | 299 | 299 | 299 | 299 | 299 | 300 |
| Total gas volume (cm ³) | 5.75 | 5.93 | 5.88 | 6.10 | 6.23 | 6.11 |
| Cladding outer diameter (mm) | 9.062 | 9.09 | 9.07 | 9.072 | 9.08 | 9.066 |
| Fuel-cladding radial gap (mm) | 0.003 | 0.003 | 0.001 | 0.023 | 0.018 | 0.012 |
| Central hole diameter (mm) | 1.65 | 1.65 | 1.65 | 2.50 | 2.50 | 2.50 |
| Internal gas pressure (MPa) | 2.0 | 2.0 | 0.1 | 2.0 | 2.0 | 0.1 |

* Parameters were determined using pre-test examination results

** From lower cap of fuel rod

*** Taking into account the risk of fuel damage at the refabrication procedure, special measurements were performed to estimate the coordinates of that part of fuel stack, which was identified as “undamaged” after the refabrication. The coordinates of undamaged part was determined from lower cap of fuel rod

**** See Figs. C.1, C.2

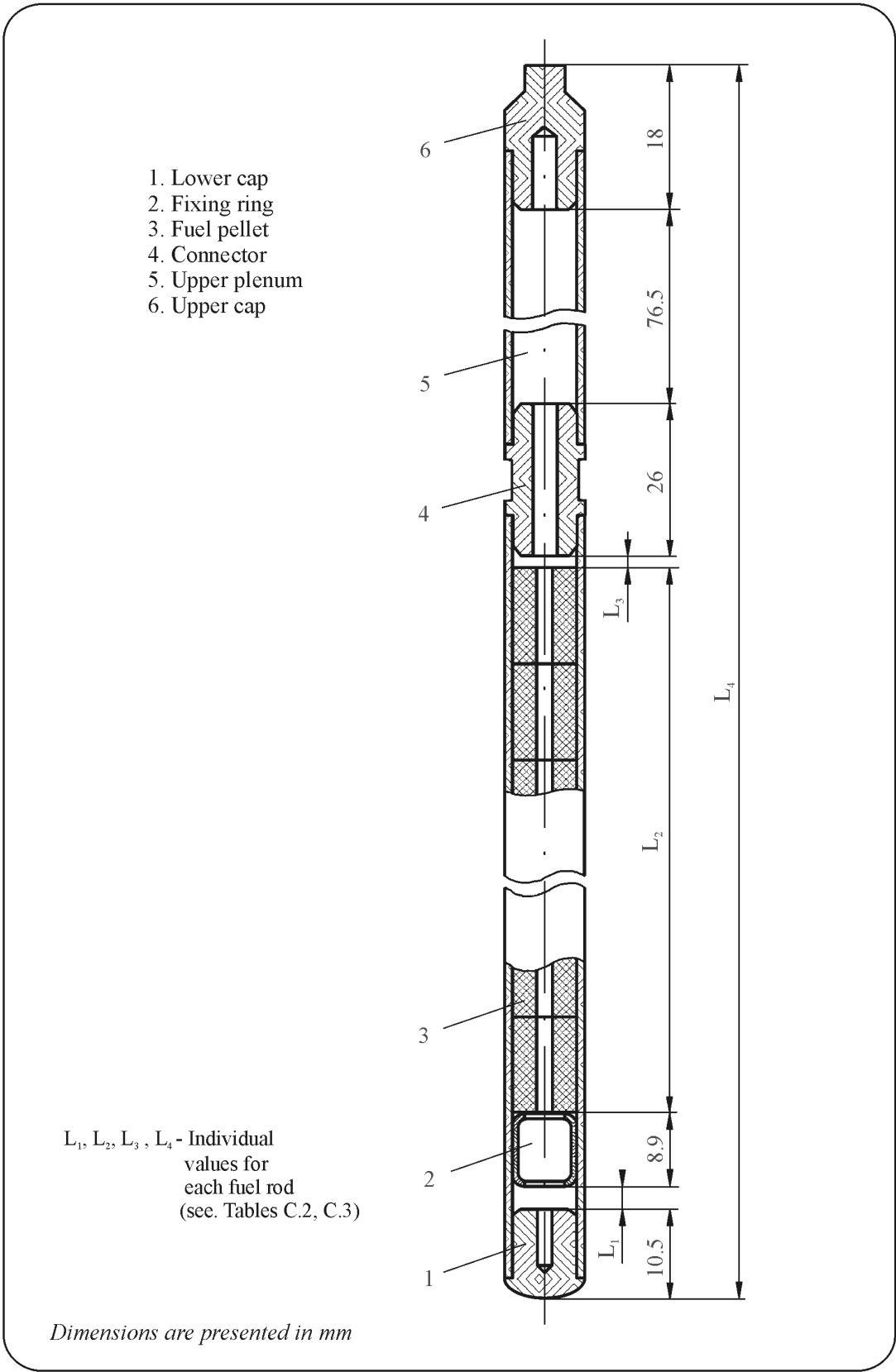


Fig. C.1. Design scheme of refabricated fuel rods ## RT 1–7, 10, 12

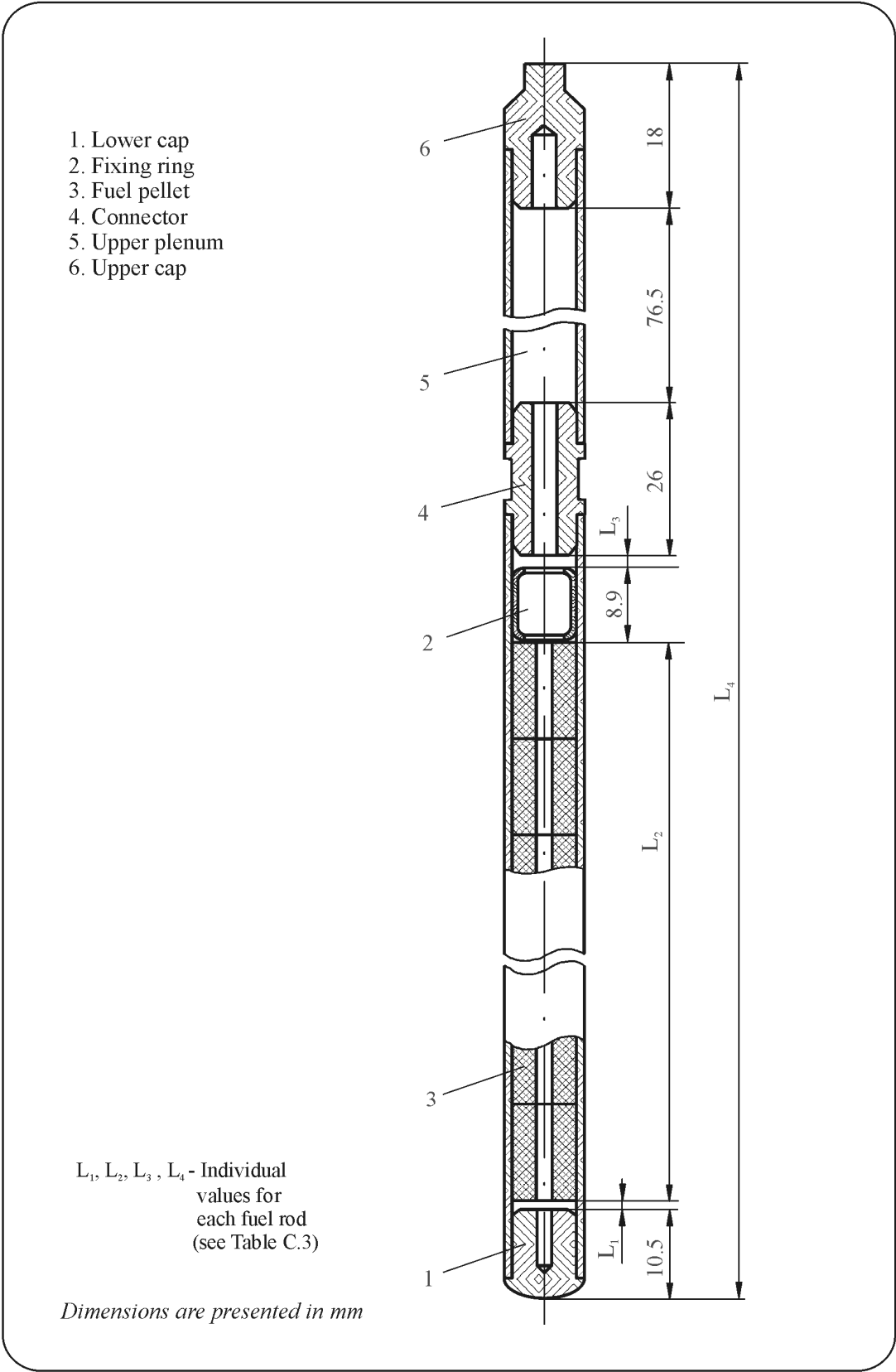


Fig. C.2. Design scheme of refabricated fuel rods ## RT8, 9

Appendix C-1
Individual Characteristics
of Fuel Rod # RT1 before the BGR Test

RT1

**Table C-1.1. Radial distribution of isotope nuclear concentrations for fuel rod #RT1
(values averaged of over the fuel stack length)***

| Isotope | Isotopic concentrations (kg/t U) in four fuel radial layers | | | |
|------------------------|---|--------------|--------------|---------------|
| | 1.23-2.82 mm | 2.82-3.44 mm | 3.44-3.71 mm | 3.71-3.795 mm |
| U ²³⁴ | 0.233 | 0.229 | 0.226 | 0.222 |
| U ²³⁵ | 7.714 | 7.414 | 7.140 | 6.952 |
| U ²³⁶ | 6.401 | 6.413 | 6.425 | 6.440 |
| U ²³⁸ | 928.8 | 925.1 | 913.6 | 882.2 |
| Pu ²³⁸ | 0.361 | 0.381 | 0.412 | 0.468 |
| Pu ²³⁹ | 4.952 | 5.516 | 7.463 | 12.68 |
| Pu ²⁴⁰ | 2.581 | 2.740 | 3.537 | 5.775 |
| Pu ²⁴¹ | 1.037 | 1.217 | 1.738 | 3.134 |
| Pu ²⁴² | 0.751 | 0.905 | 1.332 | 2.480 |
| Np ²³⁷ | 0.606 | 0.625 | 0.644 | 0.657 |
| Am ²⁴¹ | 0.382 | 0.443 | 0.627 | 1.132 |
| Oxygen | 134.5 | 134.5 | 134.5 | 134.5 |
| Other fission products | 47.16 | 50.05 | 58.19 | 79.88 |

* Measured averaged concentrations and calculated relative radial distributions of isotopes (TRIFOB code) were used to develop these data

Table C-1.2. Initial individual characteristics of fuel rod # RT1*

| Axial coordinate (from lower cap) (mm) | Cladding average outer diameter (mm) | Fuel mass ** (g) | Linear fuel mass** (g/cm) | Gas flow area ^{3)**} (mm ²) | Burnup** (MW d/kg U) |
|--|---|---------------------|---------------------------------|--|-------------------------|
| 25 ¹⁾ | - | 1.47 | 4.18 | 4.800 | 48.05 |
| 30 | 9.065 | 2.08 | 4.17 | 4.806 | 47.98 |
| 35 | 9.066 | 2.07 | 4.14 | 5.101 | 47.95 |
| 40 | 9.065 | 2.08 | 4.17 | 4.806 | 47.98 |
| 45 | 9.063 | 2.13 | 4.25 | 4.800 | 47.94 |
| 50 | 9.067 | 2.12 | 4.25 | 4.800 | 47.75 |
| 55 | 9.063 | 2.13 | 4.26 | 4.800 | 47.56 |
| 60 | 9.064 | 2.08 | 4.17 | 4.806 | 47.51 |
| 65 | 9.063 | 2.07 | 4.14 | 5.101 | 47.70 |
| 70 | 9.067 | 2.07 | 4.13 | 5.199 | 48.14 |
| 75 | 9.066 | 2.02 | 4.03 | 6.183 | 48.72 |
| 80 | 9.064 | 2.06 | 4.12 | 5.298 | 49.20 |
| 85 | 9.065 | 2.03 | 4.07 | 5.790 | 49.17 |
| 90 | 9.063 | 2.06 | 4.12 | 5.298 | 48.59 |
| 95 | 9.061 | 2.08 | 4.17 | 4.806 | 48.34 |
| 100 | 9.061 | 2.04 | 4.07 | 5.790 | 48.83 |
| 105 | 9.065 | 2.00 | 3.99 | 6.576 | 49.17 |
| 110 | 9.063 | 2.03 | 4.05 | 5.986 | 48.77 |
| 115 | 9.065 | 2.10 | 4.20 | 4.800 | 48.17 |
| 120 | 9.063 | 2.10 | 4.20 | 4.800 | 47.82 |
| 125 | 9.059 | 2.11 | 4.22 | 4.800 | 47.71 |
| 130 | 9.061 | 2.12 | 4.24 | 4.800 | 47.75 |
| 135 | 9.059 | 2.11 | 4.23 | 4.800 | 47.90 |
| 140 | 9.061 | 2.11 | 4.21 | 4.800 | 48.13 |
| 145 | 9.059 | 2.09 | 4.17 | 4.806 | 48.40 |
| 150 | 9.059 | 2.09 | 4.17 | 4.806 | 48.68 |
| 155 | 9.059 | 2.07 | 4.14 | 5.101 | 48.79 |
| 160 | 9.058 | 2.08 | 4.16 | 4.904 | 48.68 |
| 165 | 9.059 | 2.06 | 4.12 | 5.298 | 48.49 |
| 170 | 9.062 | 2.05 | 4.10 | 5.495 | 48.32 |
| 175 ²⁾ | 9.066 | 1.83 | 4.05 | 5.986 | 48.16 |

* All parameters were determined using results of pre-test examinations

** Average values at the length interval equal to the axial coordinate ± 2.5 mm

¹⁾ Bottom end coordinate of fuel stack is 24 mm;

²⁾ Top end coordinate of fuel stack is 177 mm

³⁾ Gas flow area beyond the fuel stack (mm²):

Bottom: 0.0-3.0mm – 0.00; 3.0-10.5mm – 12.56; 10.5-15.1mm – 45.82; 15.1-24.0mm – 24.97

Top: 177.0-181.5mm – 45.82; 181.5-207.5mm – 28.26; 207.5-284mm – 45.82; 284-293mm – 28.26; 293-302mm – 0.00

RT1

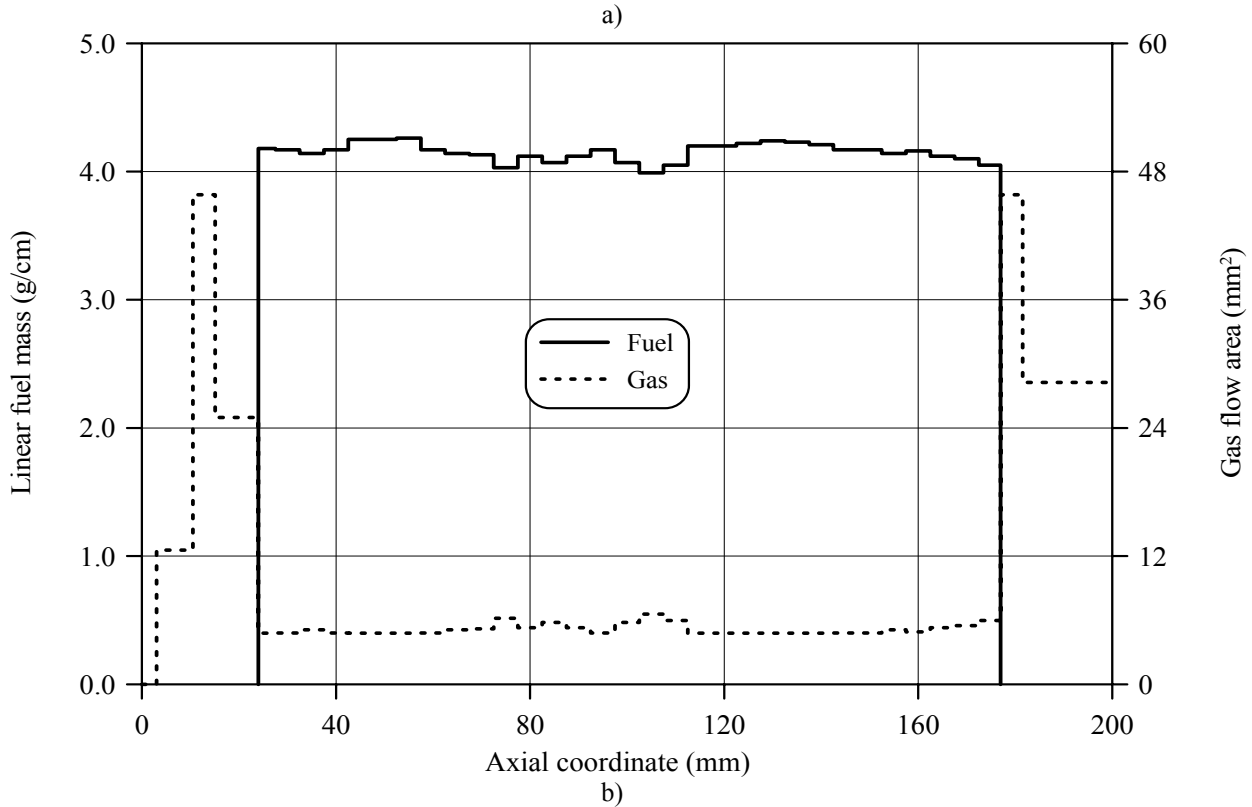
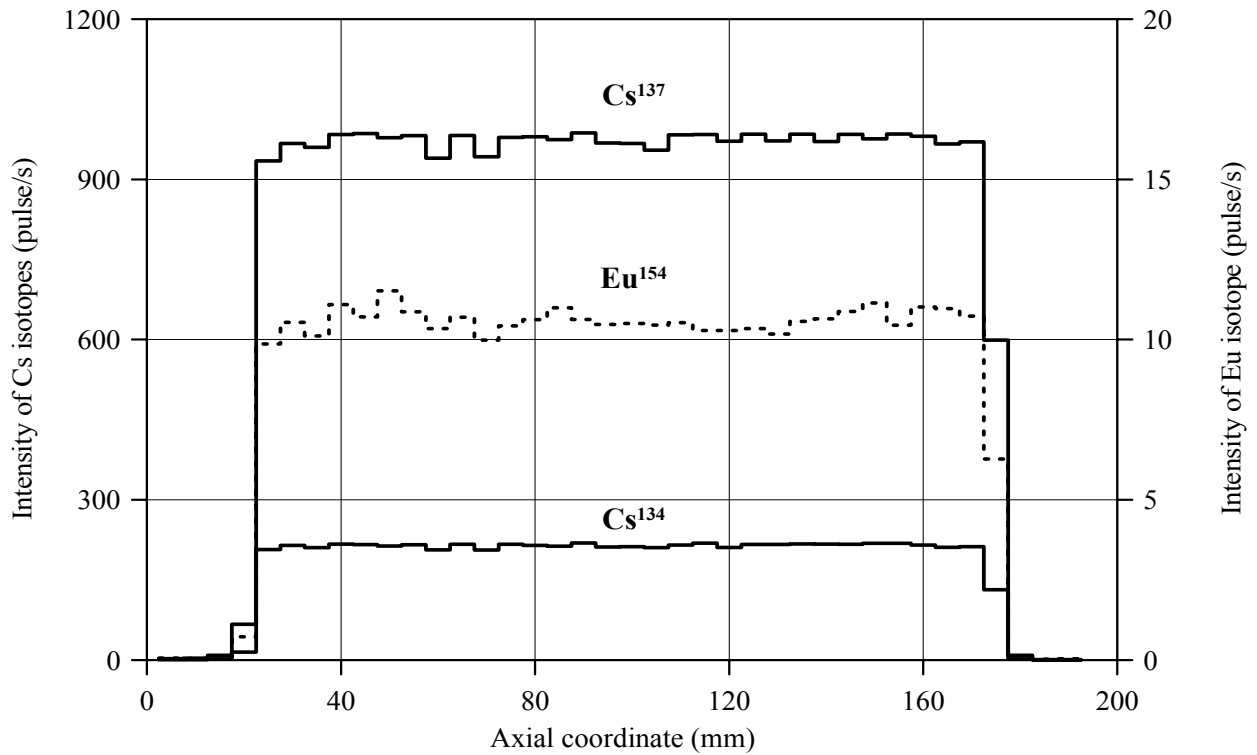
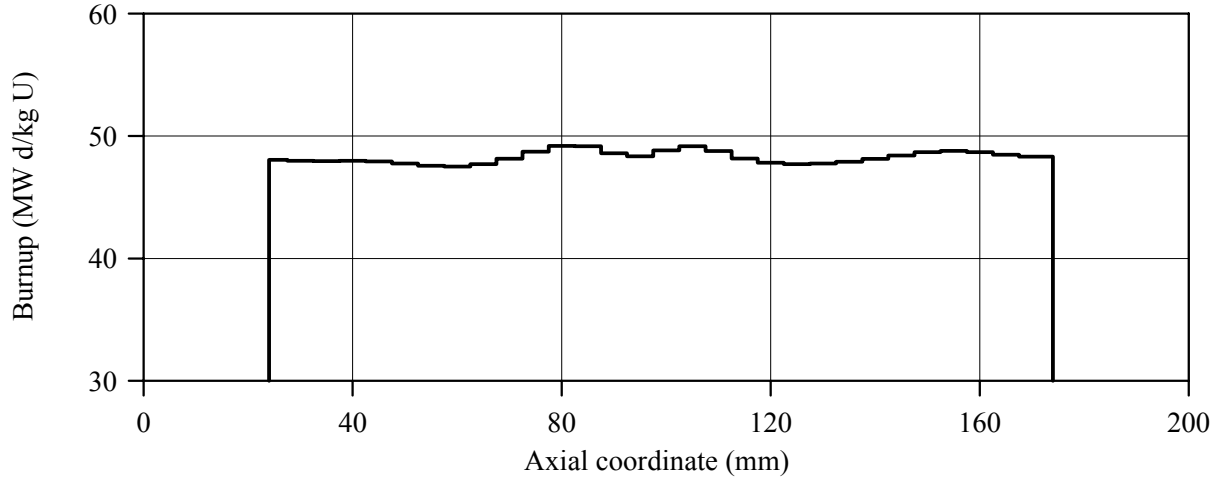
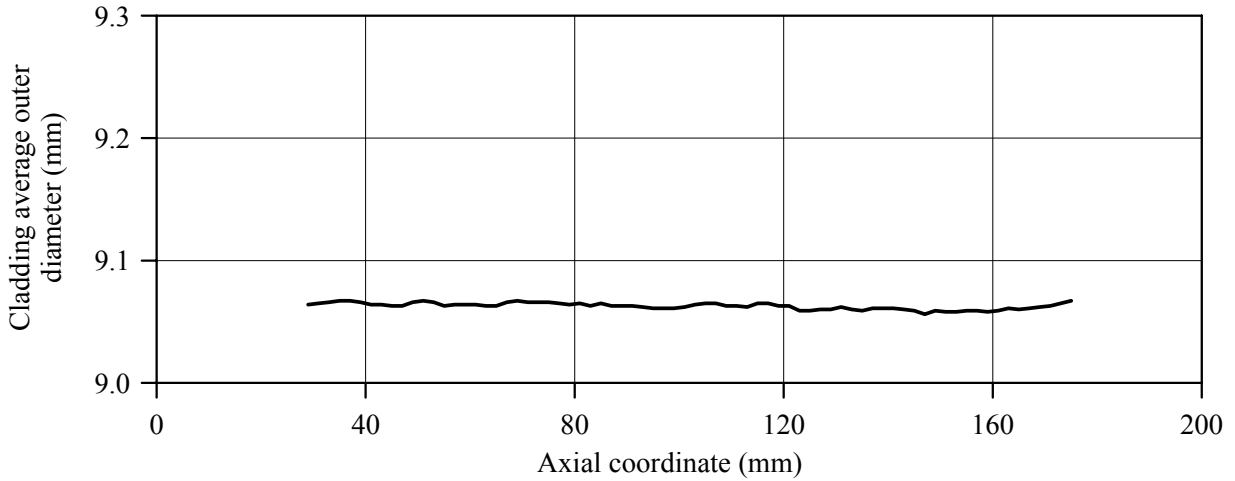


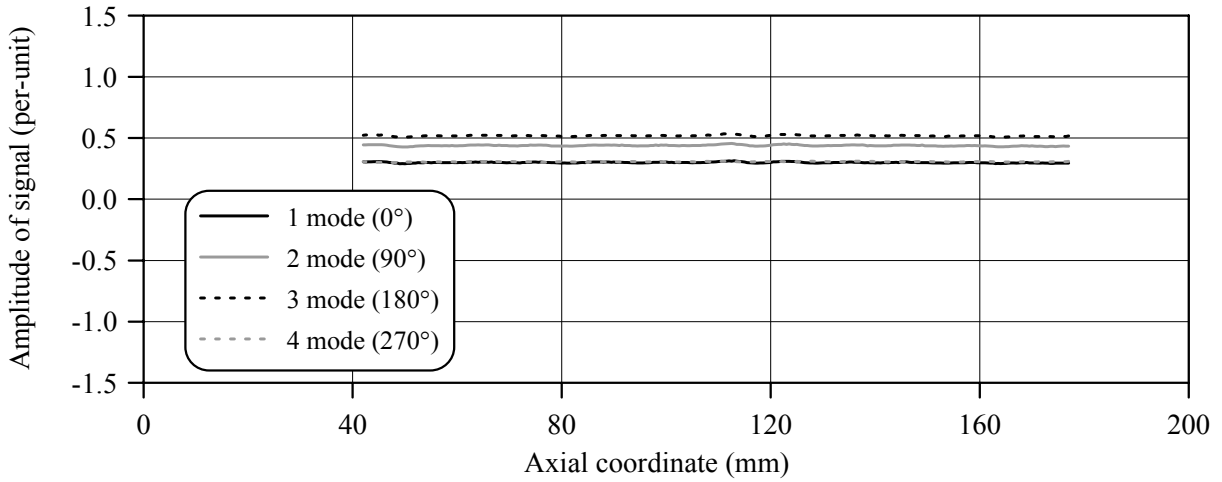
Fig.C-1.1. (a) Results of γ -scanning, (b) Axial fuel mass distribution and axial gas flow area distribution for fuel rod # RT1



a)



b)



c)

Fig.C-1.2. (a) Axial burnup distribution and (b) results of profilometry and (c) eddy-current examination of fuel rod # RT1

RT1

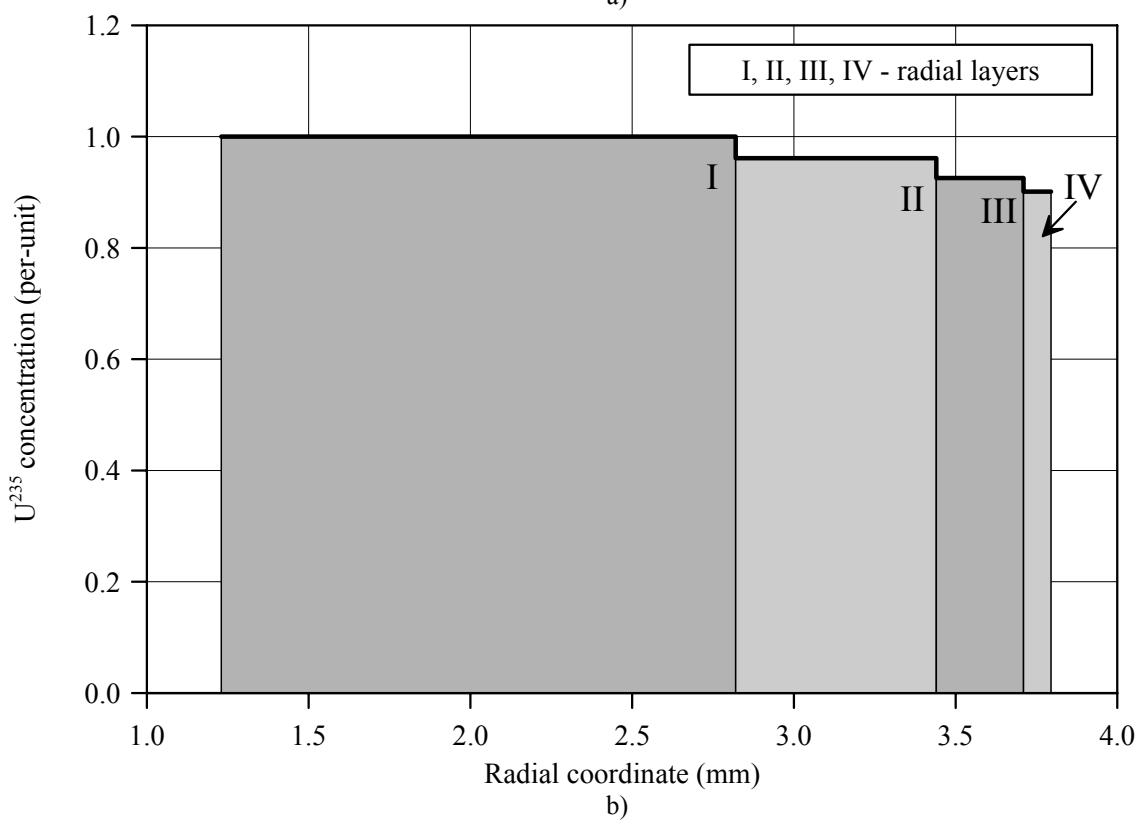
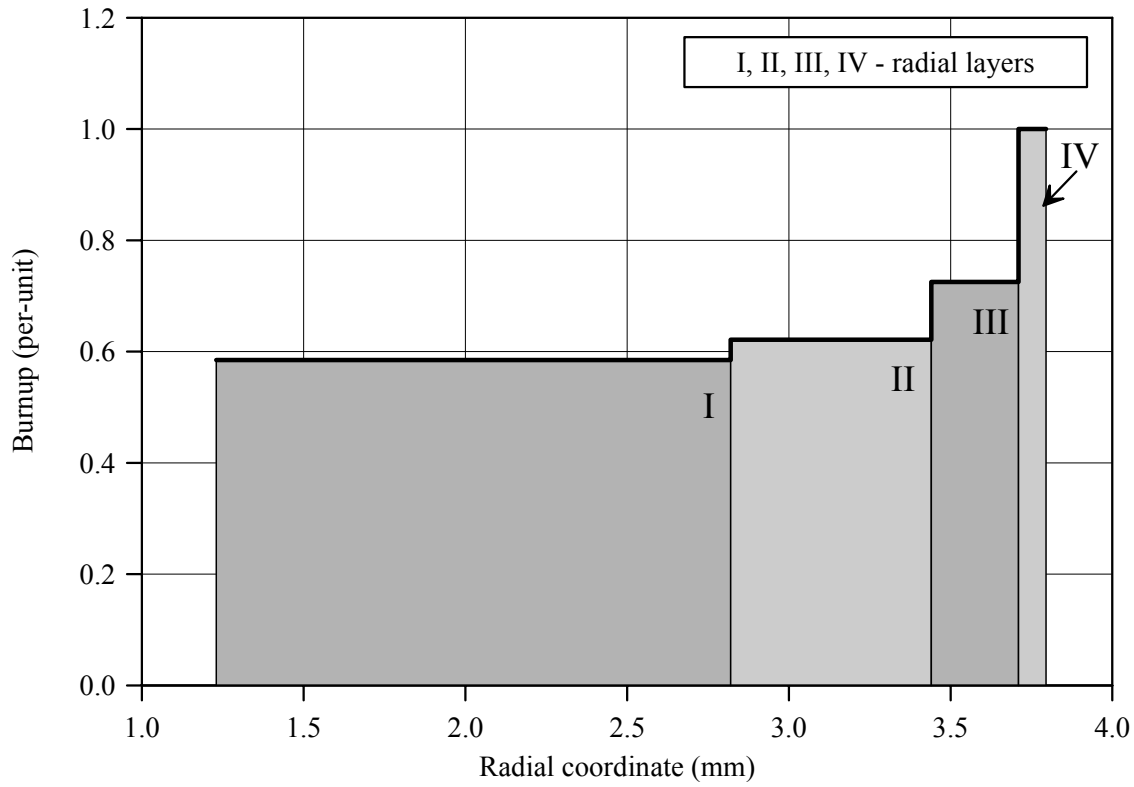


Fig.C-1.3. (a) Burnup radial distribution and (b) U^{235} radial distribution for fuel rod # RT1 (calculated values)

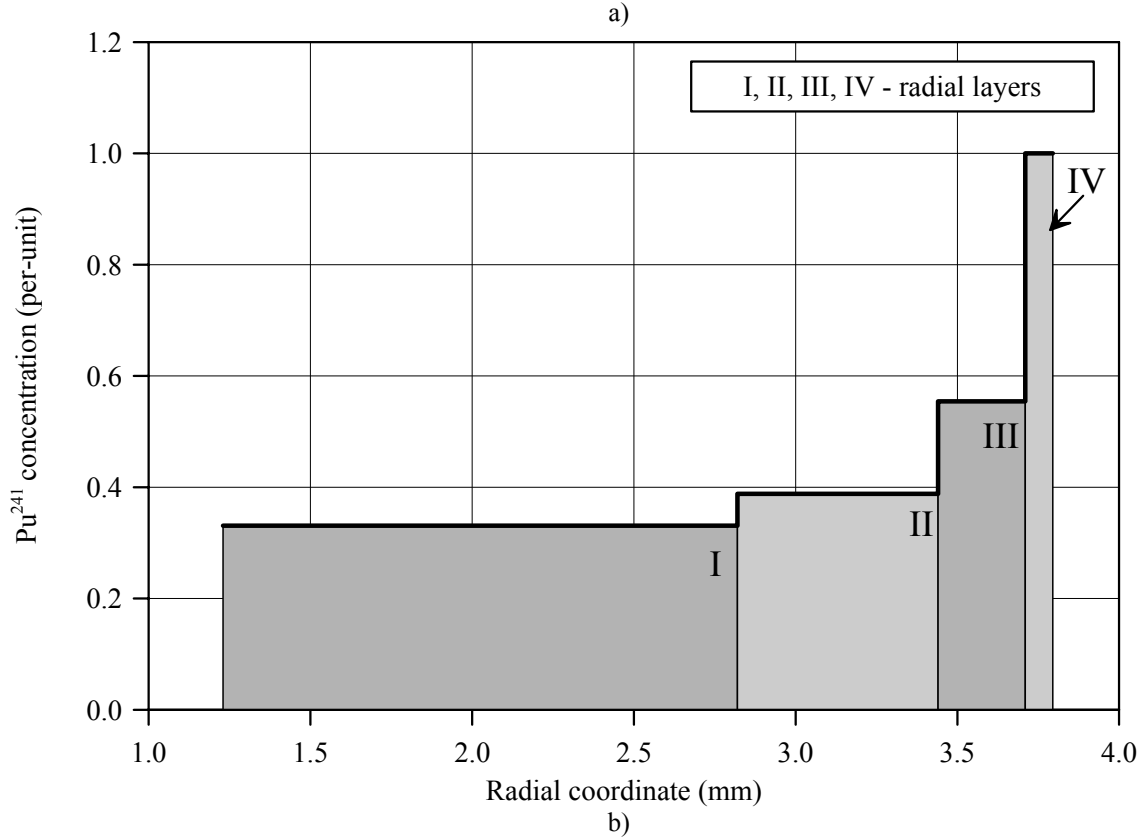
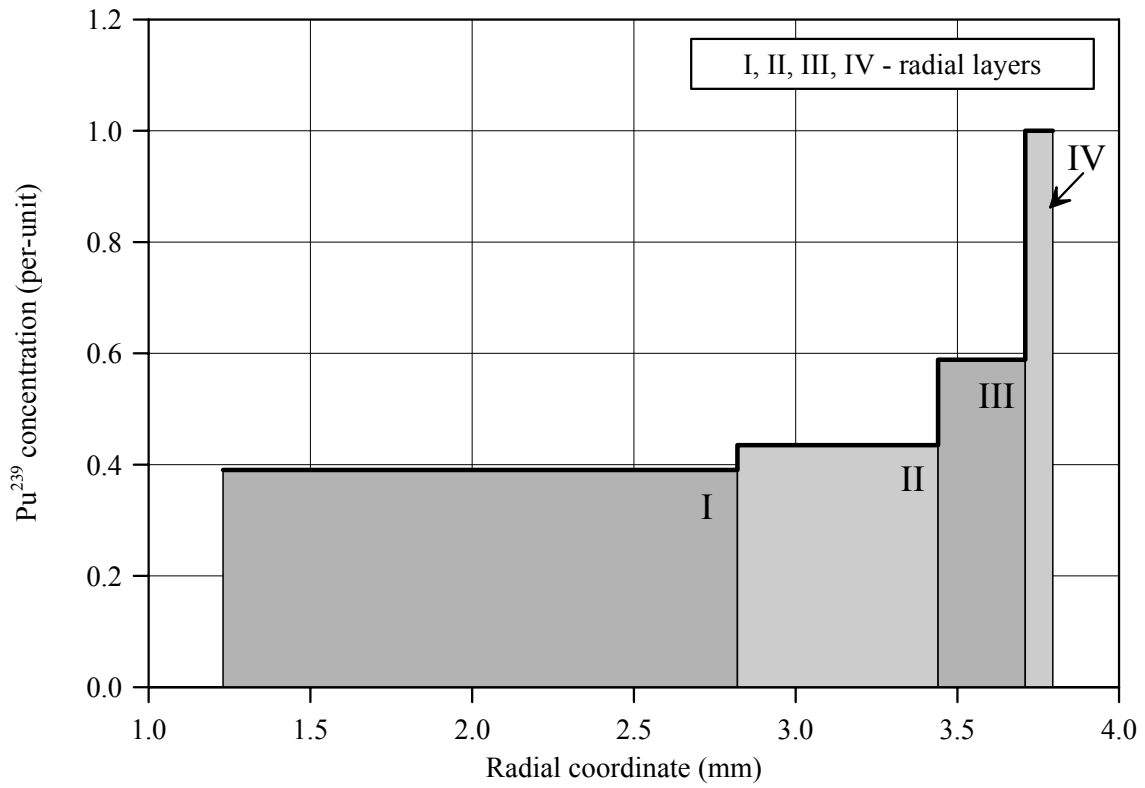


Fig.C-1.4. Radial distribution of (a) Pu^{239} and (b) Pu^{241} for fuel rod # RT1 (calculated values)

Appendix C-2
Individual Characteristics
of Fuel Rod # RT2 before the BGR Test

RT2**Table C-2.1. Radial distribution of isotope nuclear concentrations for fuel rod #RT2
(values averaged of over the fuel stack length)***

| Isotope | Isotopic concentrations (kg/t U) in four fuel radial layers | | | |
|------------------------|---|--------------|--------------|---------------|
| | 1.23-2.82 mm | 2.82-3.44 mm | 3.44-3.71 mm | 3.71-3.795 mm |
| U ²³⁴ | 0.233 | 0.229 | 0.226 | 0.222 |
| U ²³⁵ | 7.796 | 7.493 | 7.216 | 7.026 |
| U ²³⁶ | 6.451 | 6.463 | 6.475 | 6.490 |
| U ²³⁸ | 928.7 | 925.0 | 913.5 | 882.1 |
| Pu ²³⁸ | 0.352 | 0.371 | 0.401 | 0.456 |
| Pu ²³⁹ | 4.766 | 5.310 | 7.184 | 12.20 |
| Pu ²⁴⁰ | 2.466 | 2.618 | 3.380 | 5.519 |
| Pu ²⁴¹ | 0.997 | 1.170 | 1.671 | 3.014 |
| Pu ²⁴² | 0.712 | 0.859 | 1.263 | 2.352 |
| Np ²³⁷ | 0.606 | 0.625 | 0.644 | 0.657 |
| Am ²⁴¹ | 0.366 | 0.424 | 0.601 | 1.084 |
| Oxygen | 134.5 | 134.5 | 134.5 | 134.5 |
| Other fission products | 47.48 | 50.42 | 58.72 | 80.81 |

* Measured averaged concentrations and calculated relative radial distributions of isotopes (TRIFOB code) were used to develop these data

Table C-2.2. Initial individual characteristics of fuel rod # RT2*

| Axial coordinate (from lower cap) (mm) | Cladding average outer diameter (mm) | Fuel mass ** (g) | Linear fuel mass** (g/cm) | Gas flow area ^{3)**} (mm ²) | Burnup** (MW d/kg U) |
|--|---|---------------------|---------------------------------|--|-------------------------|
| 25 ¹⁾ | - | 0.85 | 4.07 | 5.410 | 47.65 |
| 30 | - | 2.04 | 4.08 | 5.310 | 47.82 |
| 35 | 9.067 | 2.03 | 4.06 | 5.509 | 47.97 |
| 40 | 9.067 | 2.02 | 4.05 | 5.608 | 48.03 |
| 45 | 9.064 | 2.04 | 4.08 | 5.310 | 47.81 |
| 50 | 9.066 | 2.05 | 4.10 | 5.112 | 47.23 |
| 55 | 9.063 | 2.09 | 4.19 | 4.800 | 46.90 |
| 60 | 9.064 | 2.09 | 4.18 | 4.800 | 47.41 |
| 65 | 9.063 | 2.10 | 4.20 | 4.800 | 47.93 |
| 70 | 9.065 | 2.05 | 4.11 | 5.013 | 47.53 |
| 75 | 9.066 | 2.12 | 4.23 | 4.800 | 47.11 |
| 80 | 9.063 | 2.10 | 4.20 | 4.800 | 47.76 |
| 85 | 9.063 | 2.06 | 4.13 | 4.814 | 48.63 |
| 90 | 9.063 | 2.04 | 4.08 | 5.310 | 48.58 |
| 95 | 9.063 | 2.01 | 4.02 | 5.906 | 48.21 |
| 100 | 9.063 | 2.06 | 4.13 | 4.814 | 48.36 |
| 105 | 9.062 | 2.04 | 4.08 | 5.310 | 48.53 |
| 110 | 9.062 | 2.06 | 4.12 | 4.913 | 48.09 |
| 115 | 9.061 | 2.04 | 4.09 | 5.211 | 47.73 |
| 120 | 9.063 | 2.07 | 4.15 | 4.800 | 48.29 |
| 125 | 9.061 | 2.06 | 4.11 | 5.013 | 48.96 |
| 130 | 9.063 | 2.01 | 4.03 | 5.807 | 48.74 |
| 135 | 9.060 | 2.06 | 4.12 | 4.913 | 48.13 |
| 140 | 9.060 | 2.06 | 4.12 | 4.913 | 47.93 |
| 145 | 9.058 | 2.08 | 4.16 | 4.800 | 48.12 |
| 150 | 9.058 | 2.07 | 4.13 | 4.814 | 48.40 |
| 155 | 9.059 | 2.09 | 4.19 | 4.800 | 48.43 |
| 160 | 9.058 | 2.08 | 4.16 | 4.800 | 47.99 |
| 165 | 9.061 | 2.03 | 4.06 | 5.509 | 47.61 |
| 170 | 9.062 | 2.00 | 3.99 | 6.204 | 47.86 |
| 175 ²⁾ | - | 1.58 | 4.06 | 5.509 | 48.39 |

* All parameters were determined using results of pre-test examinations

** Average values at the length interval equal to the axial coordinate ± 2.5 mm

¹⁾ Bottom end coordinate of fuel stack is 25.4 mm;

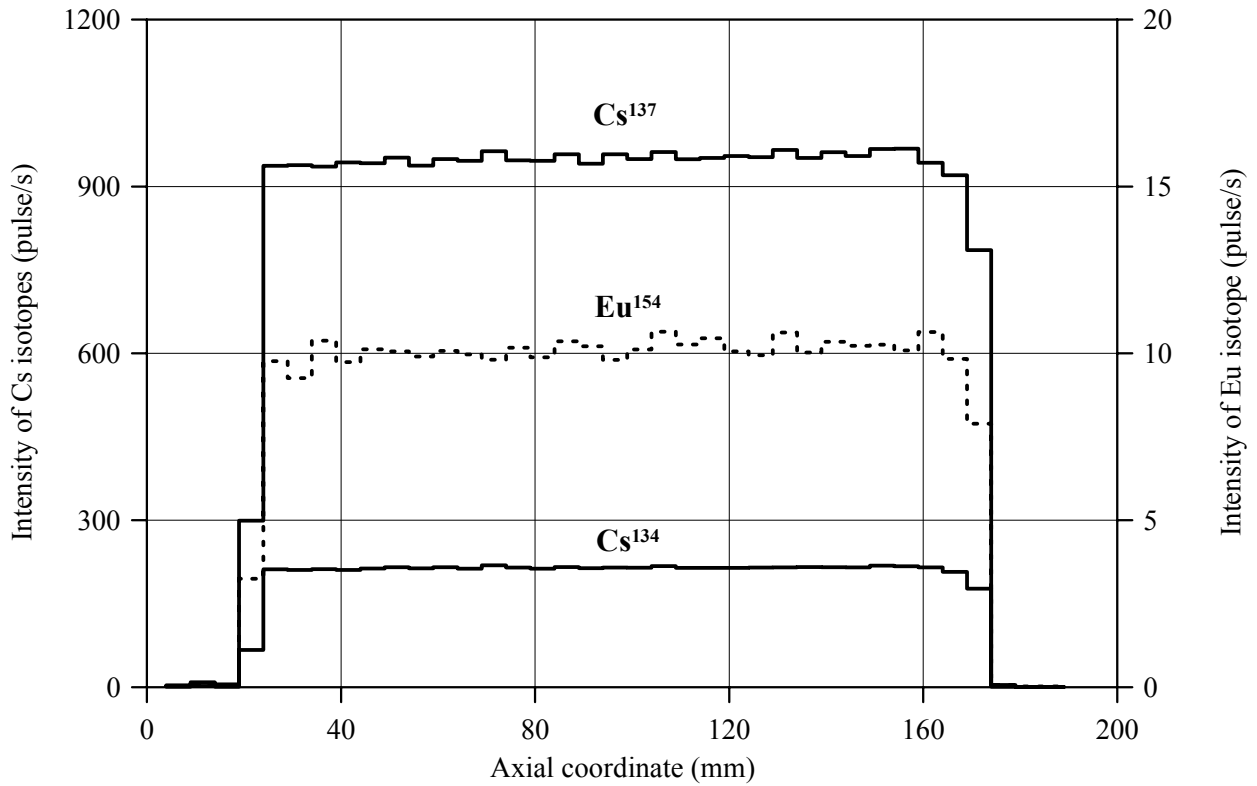
²⁾ Top end coordinate of fuel stack is 176.4 mm

³⁾ Gas flow area beyond the fuel stack (mm²):

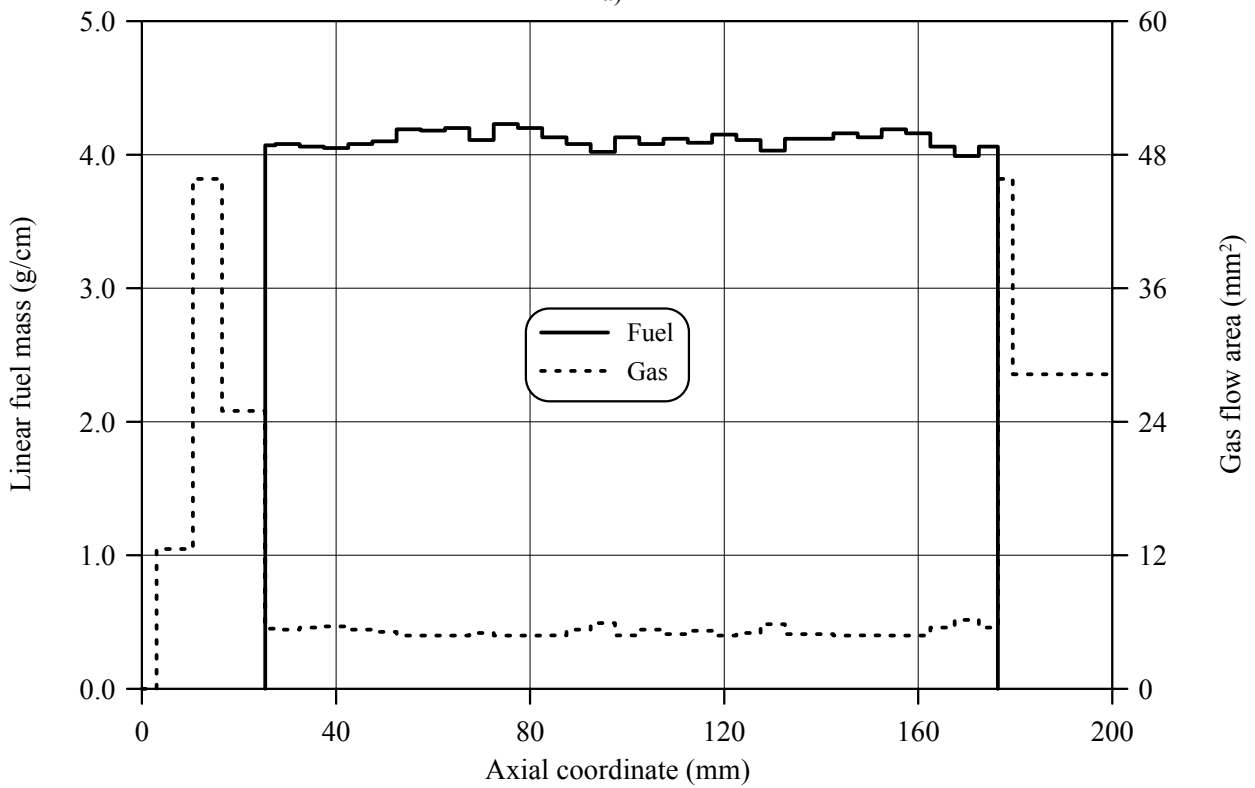
Bottom: 0.0-3.0mm – 0.00; 3.0-10.5mm – 12.56; 10.5-16.5mm – 45.82; 15.1-25.4mm – 24.97

Top: 176.4-179.5mm – 45.82; 179.5-205.5mm – 28.26; 205.5-282mm – 45.82; 282-291mm – 28.26; 291-300mm – 0.00

RT2

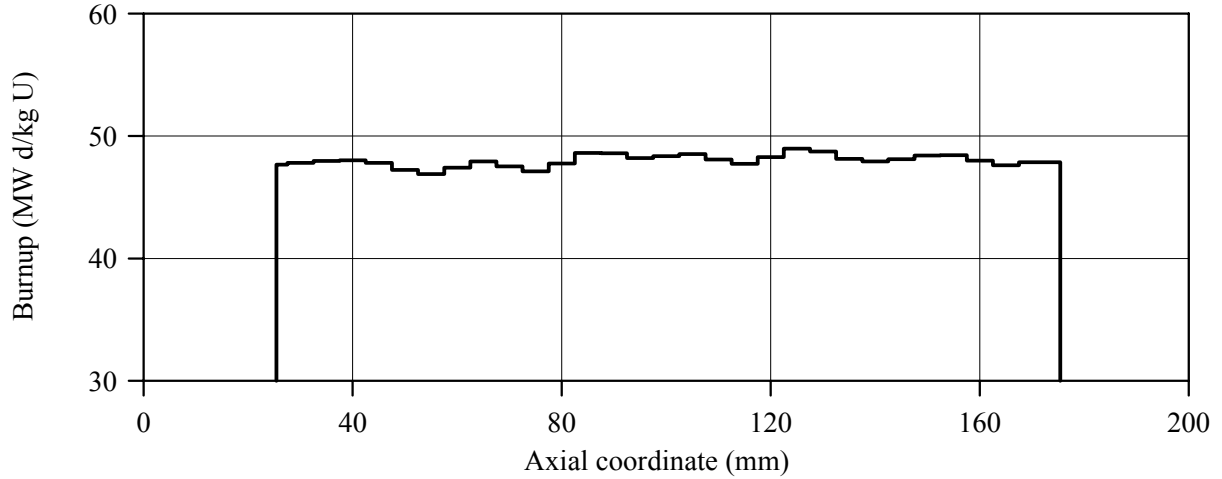


a)

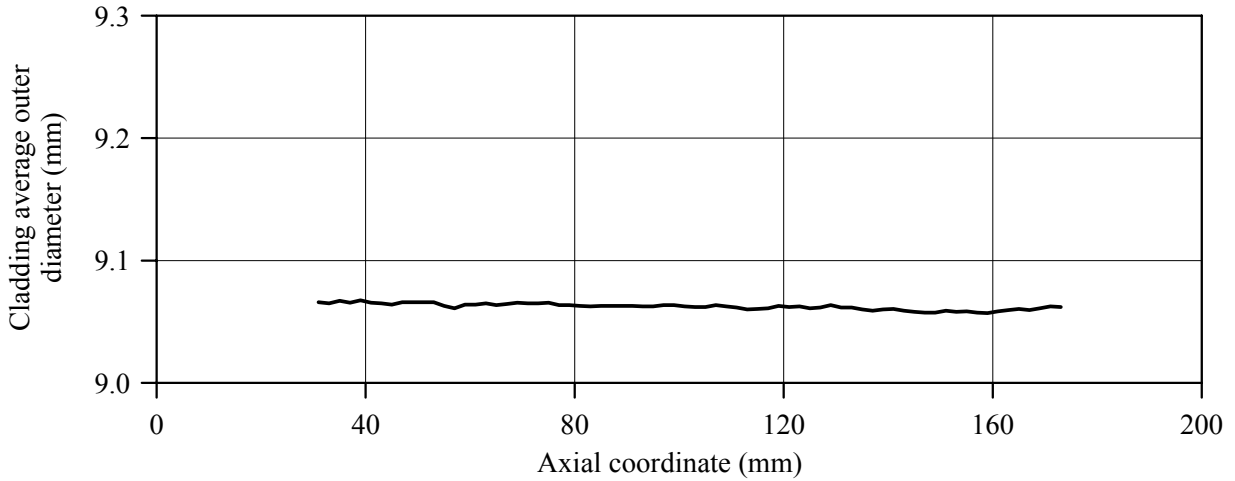


b)

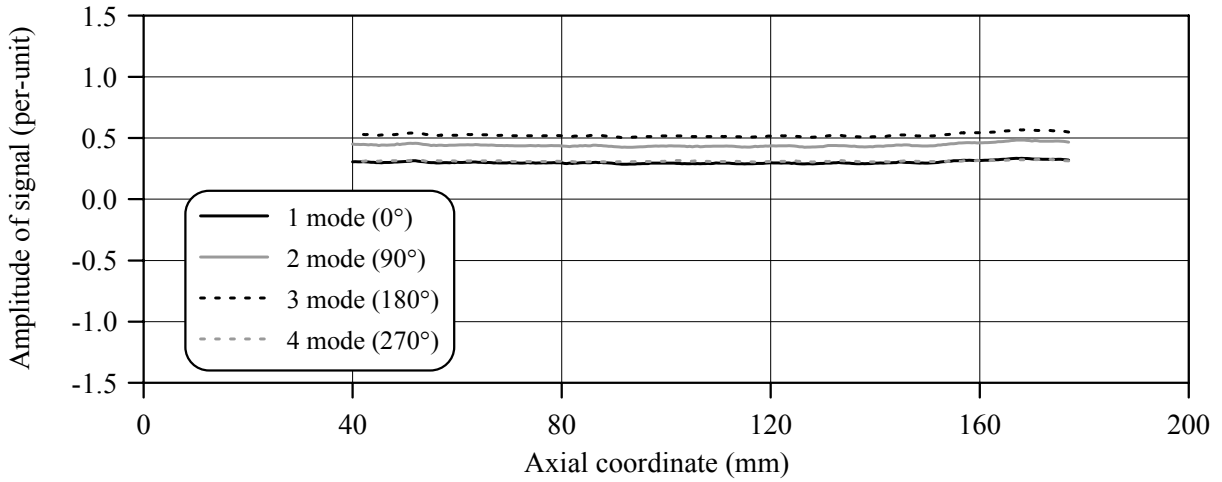
Fig.C-2.1. (a) Results of γ -scanning, (b) Axial fuel mass distribution and axial gas flow area distribution for fuel rod # RT2



a)



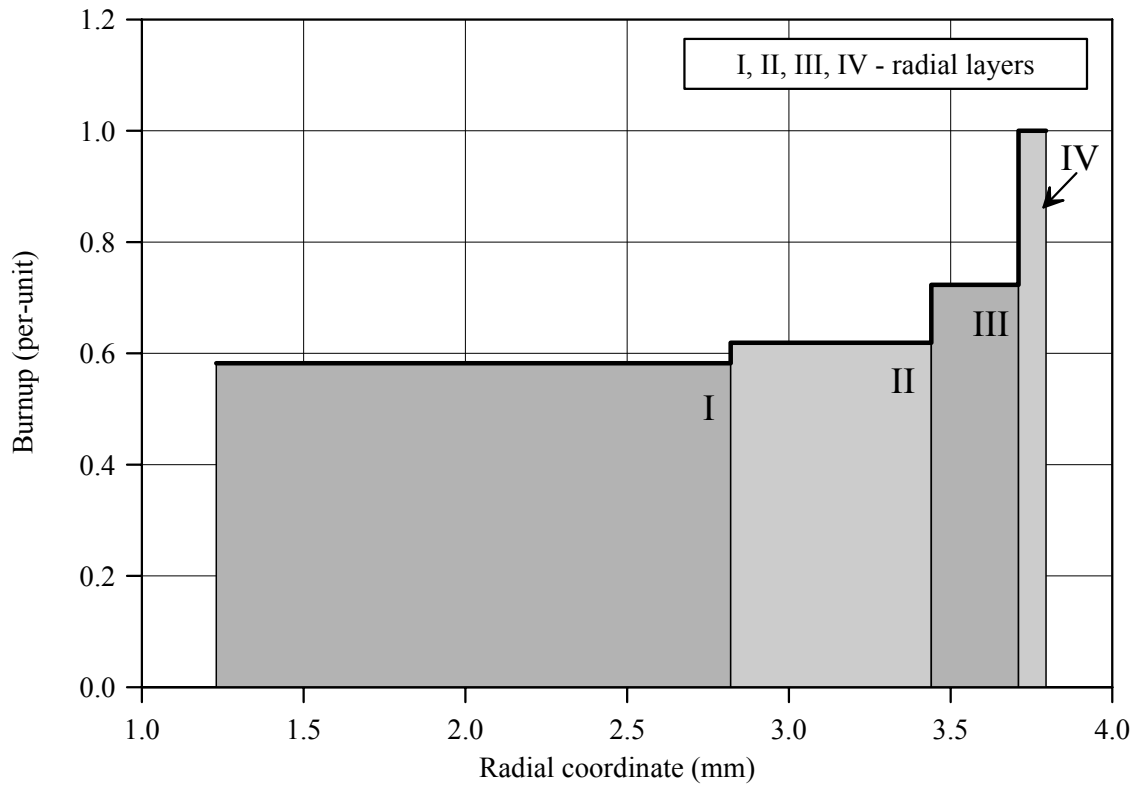
b)



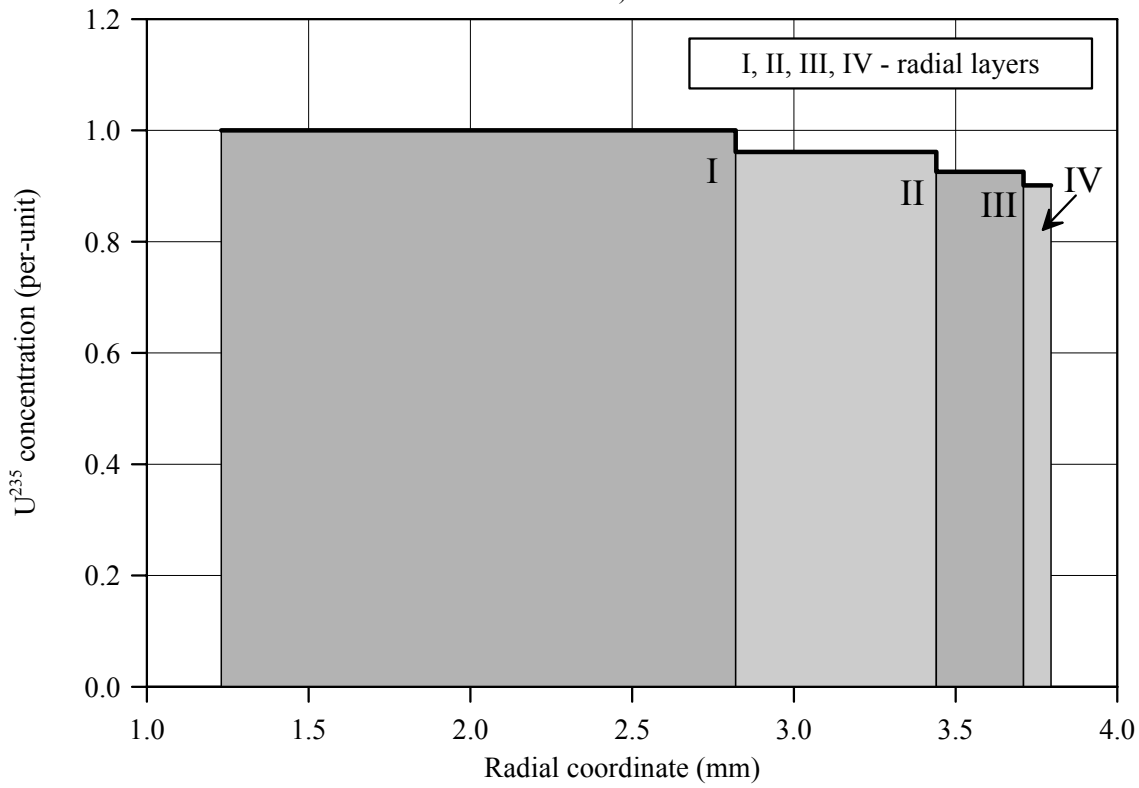
c)

Fig.C-2.2. (a) Axial burnup distribution and (b) results of profilometry and (c) eddy-current examination of fuel rod # RT2

RT2



a)



b)

Fig.C-2.3. (a) Burnup radial distribution and (b) U^{235} radial distribution for fuel rod # RT2 (calculated values)

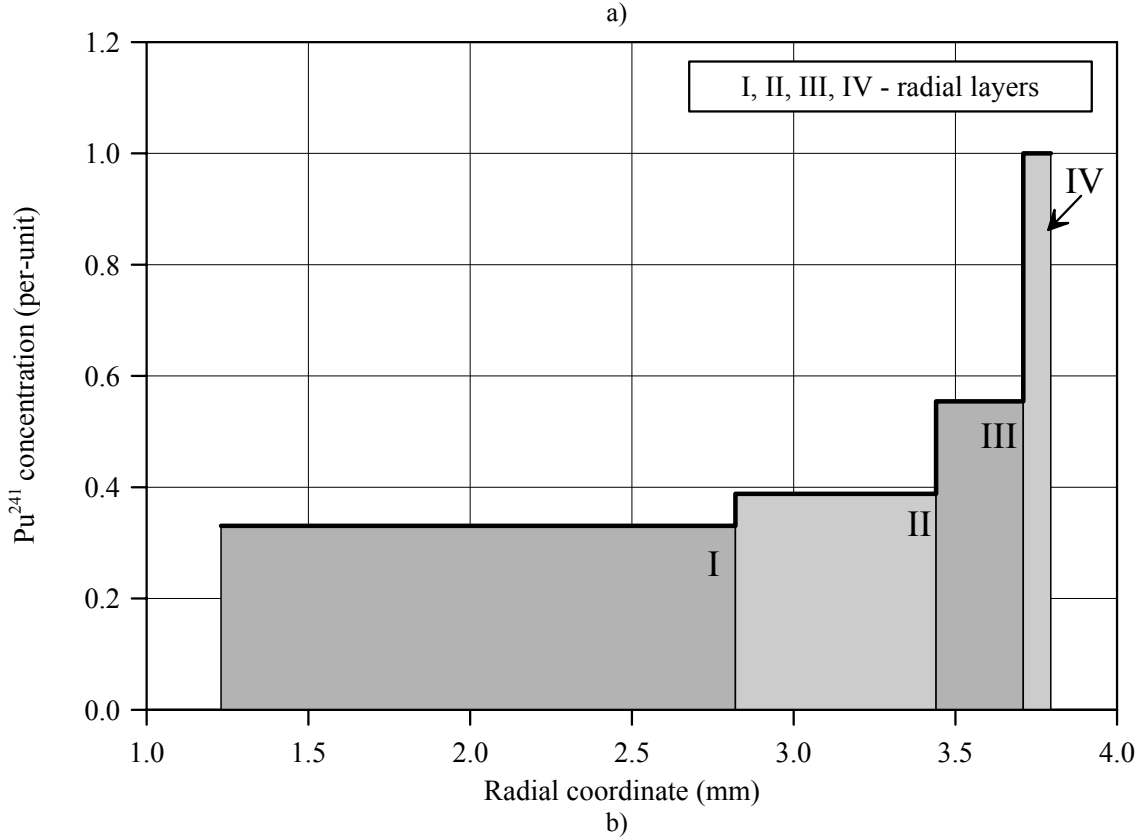
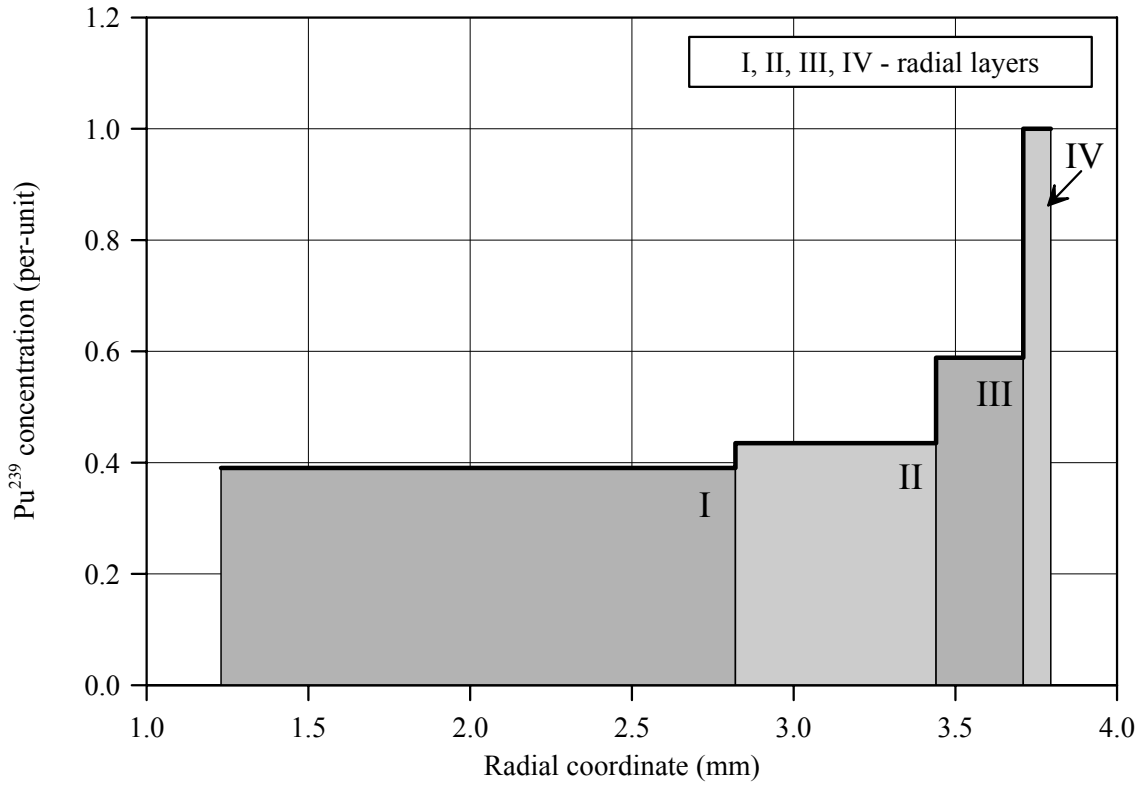


Fig.C-2.4. Radial distribution of (a) Pu^{239} and (b) Pu^{241} for fuel rod # RT2 (calculated values)

Appendix C-3
Individual Characteristics
of Fuel Rod # RT3 before the BGR Test

RT3**Table C-3.1. Radial distribution of isotope nuclear concentrations for fuel rod #RT3
(values averaged of over the fuel stack length)***

| Isotope | Isotopic concentrations (kg/t U) in four fuel radial layers | | | |
|------------------------|---|--------------|--------------|---------------|
| | 1.23-2.82 mm | 2.82-3.44 mm | 3.44-3.71 mm | 3.71-3.795 mm |
| U ²³⁴ | 0.202 | 0.199 | 0.196 | 0.193 |
| U ²³⁵ | 7.828 | 7.537 | 7.269 | 7.085 |
| U ²³⁶ | 6.220 | 6.233 | 6.247 | 6.262 |
| U ²³⁸ | 929.1 | 925.4 | 913.7 | 882.1 |
| Pu ²³⁸ | 0.380 | 0.401 | 0.433 | 0.491 |
| Pu ²³⁹ | 5.029 | 5.601 | 7.576 | 12.85 |
| Pu ²⁴⁰ | 2.565 | 2.722 | 3.511 | 5.718 |
| Pu ²⁴¹ | 1.053 | 1.236 | 1.765 | 3.180 |
| Pu ²⁴² | 0.728 | 0.878 | 1.290 | 2.397 |
| Np ²³⁷ | 0.620 | 0.640 | 0.659 | 0.672 |
| Am ²⁴¹ | 0.393 | 0.455 | 0.643 | 1.158 |
| Oxygen | 134.5 | 134.5 | 134.5 | 134.5 |
| Other fission products | 46.83 | 49.69 | 58.00 | 79.91 |

* Measured averaged concentrations and calculated relative radial distributions of isotopes (TRIFOB code) were used to develop these data

Table C-3.2. Initial individual characteristics of fuel rod # RT3*

| Axial coordinate (from lower cap) (mm) | Cladding average outer diameter (mm) | Fuel mass ** (g) | Linear fuel mass** (g/cm) | Gas flow area ^{3)**} (mm ²) | Burnup** (MW d/kg U) |
|--|---|---------------------|---------------------------------|--|-------------------------|
| 25 ¹⁾ | - | 1.58 | 3.97 | 5.704 | 44.35 |
| 30 | - | 2.01 | 4.03 | 5.098 | 44.41 |
| 35 | 9.061 | 2.05 | 4.09 | 4.800 | 44.59 |
| 40 | 9.063 | 2.02 | 4.04 | 4.997 | 45.19 |
| 45 | 9.063 | 2.01 | 4.01 | 5.300 | 46.06 |
| 50 | 9.061 | 2.00 | 3.99 | 5.502 | 47.09 |
| 55 | 9.062 | 1.90 | 3.81 | 7.321 | 47.14 |
| 60 | 9.062 | 1.76 | 3.51 | 10.352 | 46.10 |
| 65 | 9.057 | 1.87 | 3.73 | 8.129 | 45.83 |
| 70 | 9.060 | 2.03 | 4.06 | 4.795 | 47.06 |
| 75 | 9.066 | 2.02 | 4.04 | 4.997 | 48.09 |
| 80 | 9.062 | 2.05 | 4.10 | 4.800 | 48.08 |
| 85 | 9.059 | 2.02 | 4.03 | 5.098 | 48.06 |
| 90 | 9.063 | 2.01 | 4.02 | 5.199 | 48.54 |
| 95 | 9.059 | 2.04 | 4.08 | 4.800 | 48.64 |
| 100 | 9.064 | 2.09 | 4.18 | 4.800 | 48.09 |
| 105 | 9.062 | 2.08 | 4.16 | 4.800 | 47.97 |
| 110 | 9.070 | 2.02 | 4.05 | 4.896 | 48.65 |
| 115 | 9.061 | 1.93 | 3.86 | 6.816 | 49.05 |
| 120 | 9.056 | 1.93 | 3.86 | 6.816 | 48.60 |
| 125 | 9.058 | 2.05 | 4.10 | 4.800 | 47.94 |
| 130 | 9.054 | 2.10 | 4.19 | 4.800 | 47.57 |
| 135 | 9.059 | 2.11 | 4.21 | 4.800 | 47.51 |
| 140 | 9.056 | 2.11 | 4.21 | 4.800 | 47.75 |
| 145 | 9.052 | 2.05 | 4.11 | 4.800 | 48.36 |
| 150 | 9.053 | 2.02 | 4.04 | 4.997 | 49.08 |
| 155 | 9.050 | 2.08 | 4.16 | 4.800 | 49.09 |
| 160 | 9.049 | 2.13 | 4.25 | 4.800 | 48.25 |
| 165 | 9.048 | 2.09 | 4.19 | 4.800 | 47.75 |
| 170 | 9.049 | 2.07 | 4.14 | 4.800 | 48.14 |
| 175 ²⁾ | 9.054 | 0.04 | 4.11 | 4.800 | 48.51 |

* All parameters were determined using results of pre-test examinations

** Average values at the length interval equal to the axial coordinate ± 2.5 mm

¹⁾ Bottom end coordinate of fuel stack is 23.6 mm;

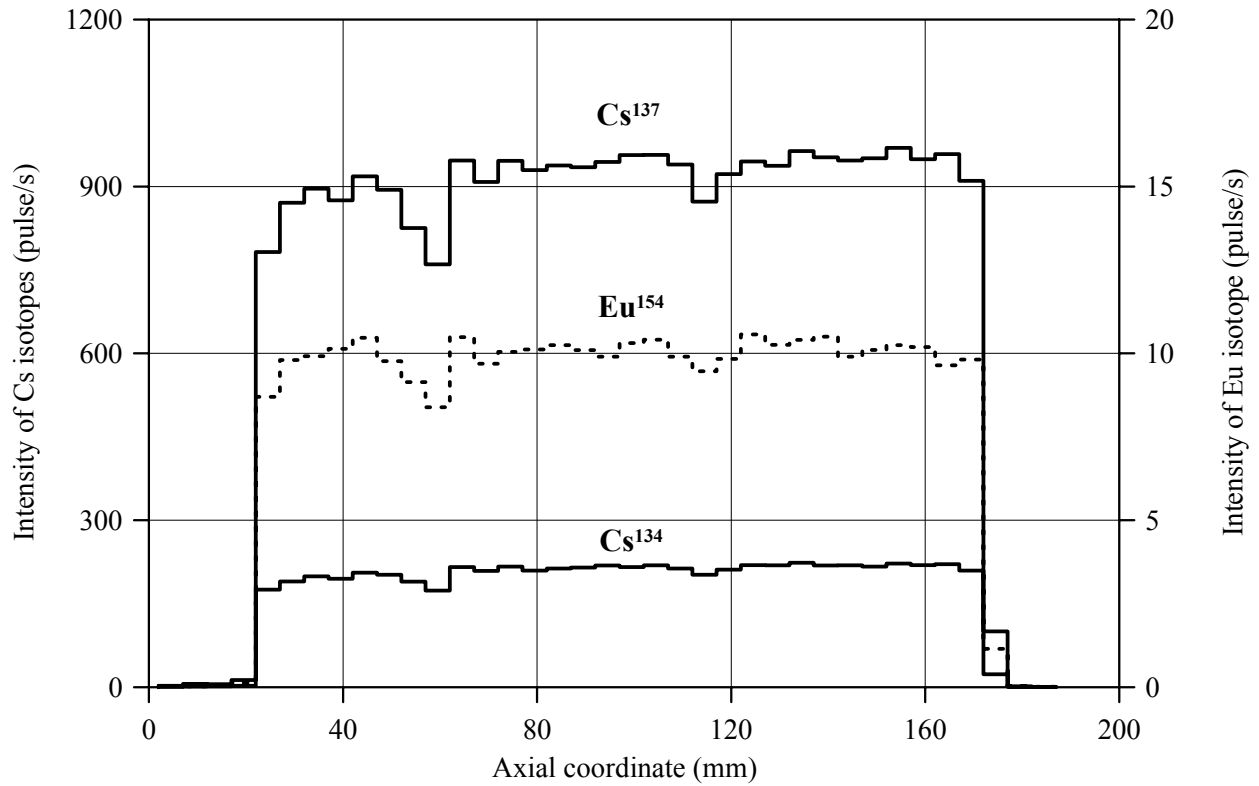
²⁾ Top end coordinate of fuel stack is 172.6 mm

³⁾ Gas flow area beyond the fuel stack (mm²):

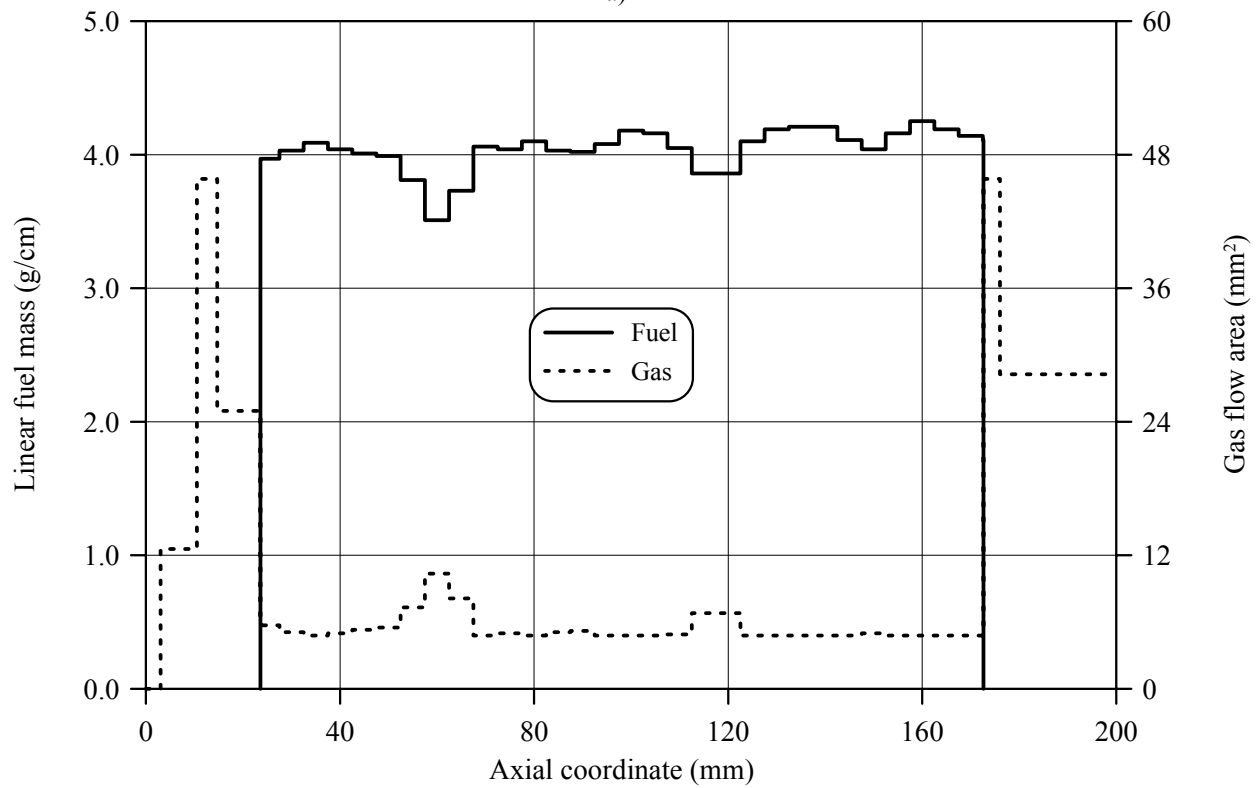
Bottom: 0.0-3.0mm – 0.00; 3.0-10.5mm – 12.56; 10.5-14.7mm – 45.82; 14.7-23.6mm – 24.97

Top: 172.6-176mm – 45.82; 176-202mm – 28.26; 202-278.5mm – 45.82; 278.5-287.5mm – 28.26; 287.5-296.5mm – 0.00

RT3

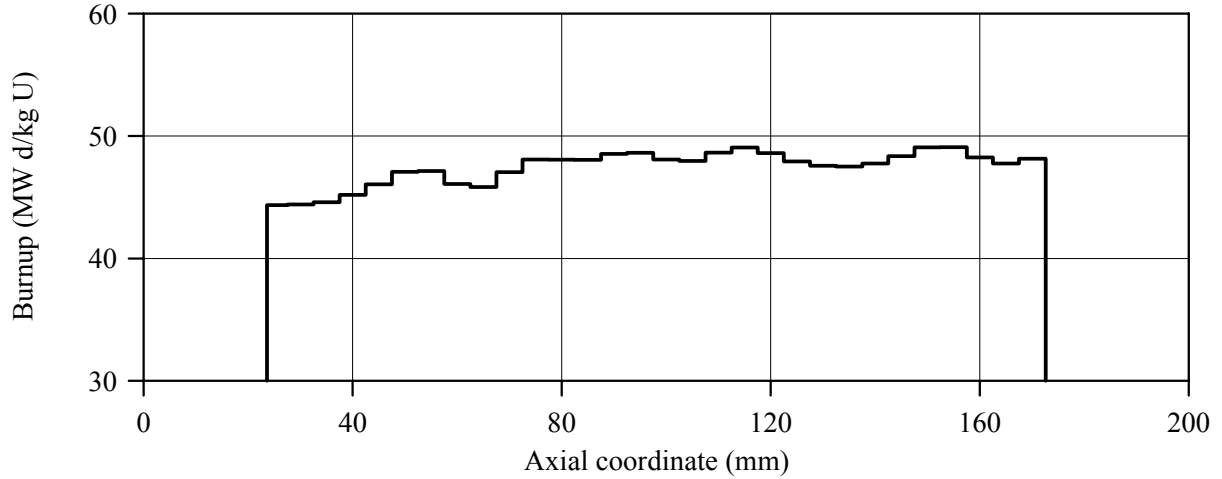


a)

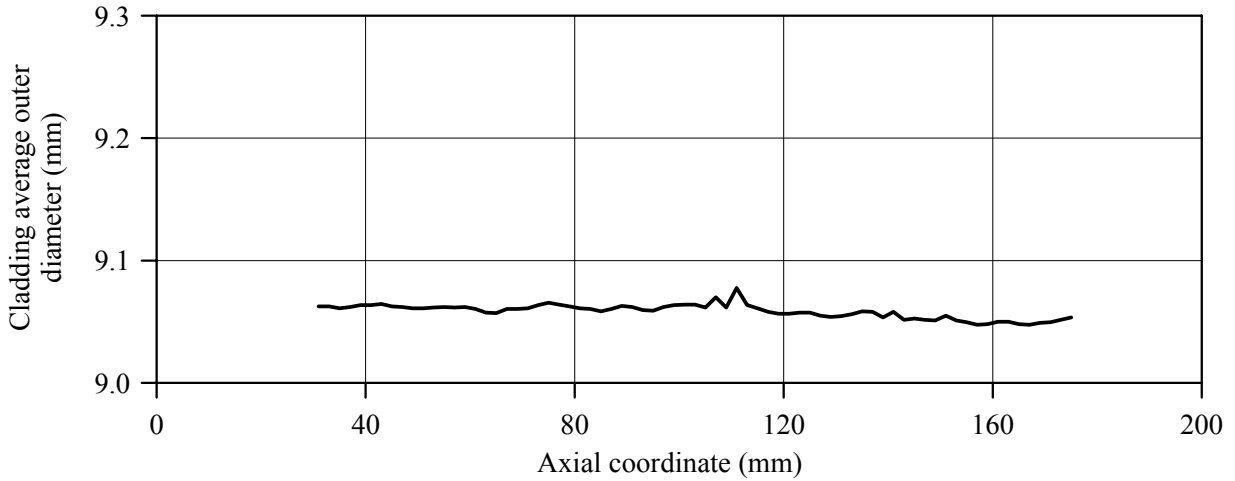


b)

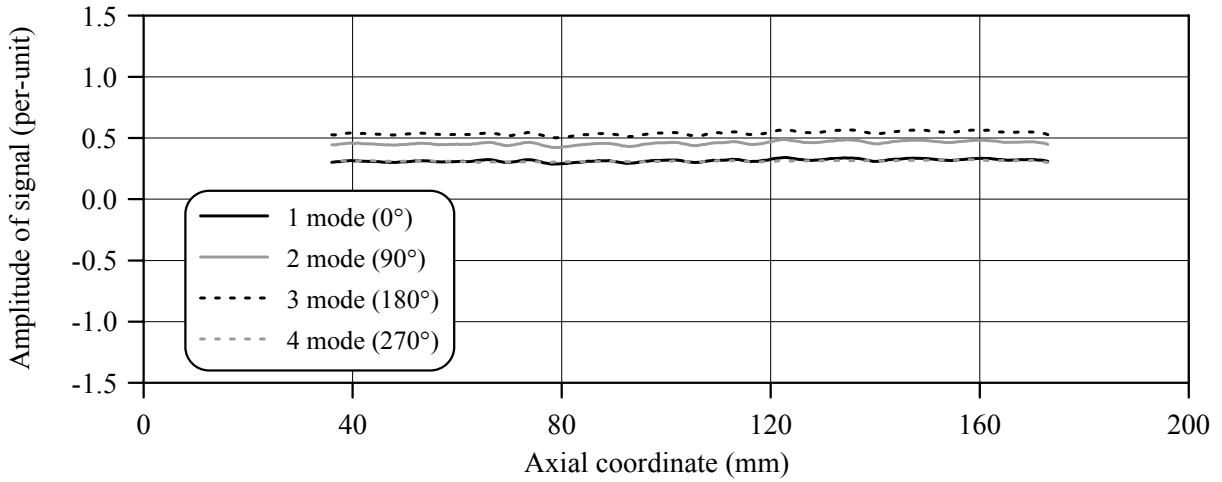
Fig.C-3.1. (a) Results of γ -scanning, (b) Axial fuel mass distribution and axial gas flow area distribution for fuel rod # RT3



a)



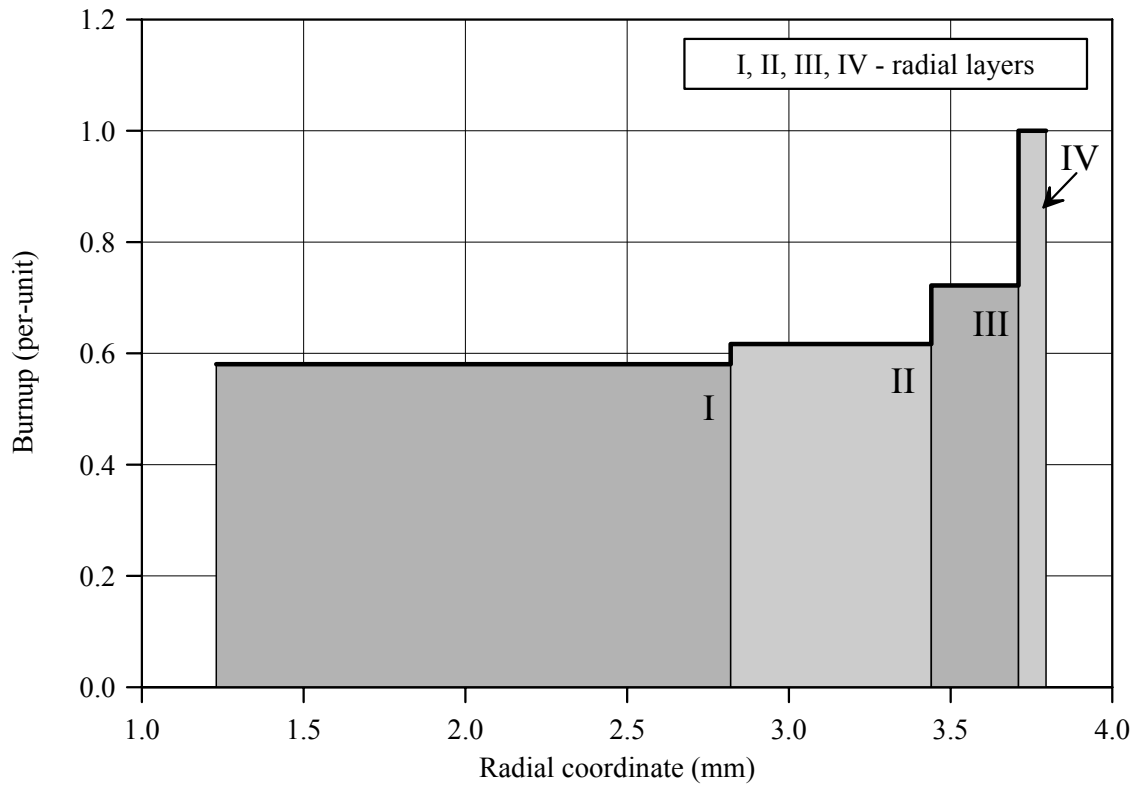
b)



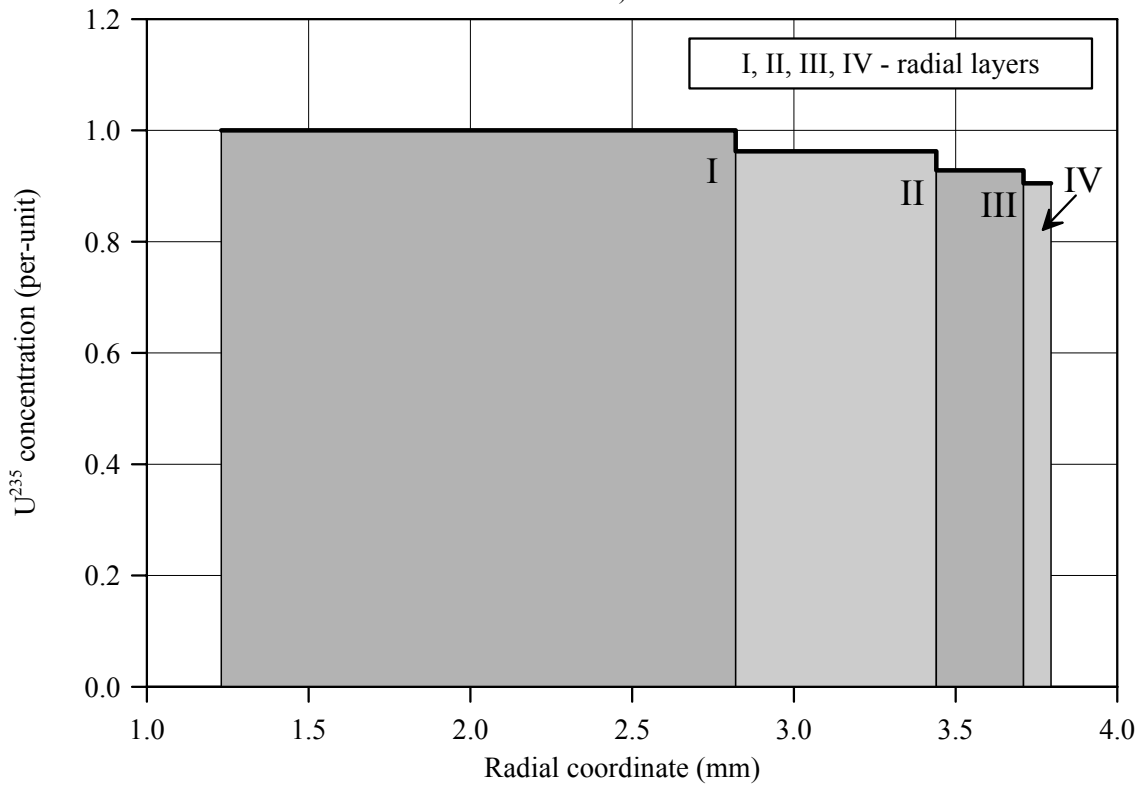
c)

Fig.C-3.2. (a) Axial burnup distribution and (b) results of profilometry and (c) eddy-current examination of fuel rod # RT3

RT3



a)



b)

Fig.C-3.3. (a) Burnup radial distribution and (b) U^{235} radial distribution for fuel rod # RT3 (calculated values)

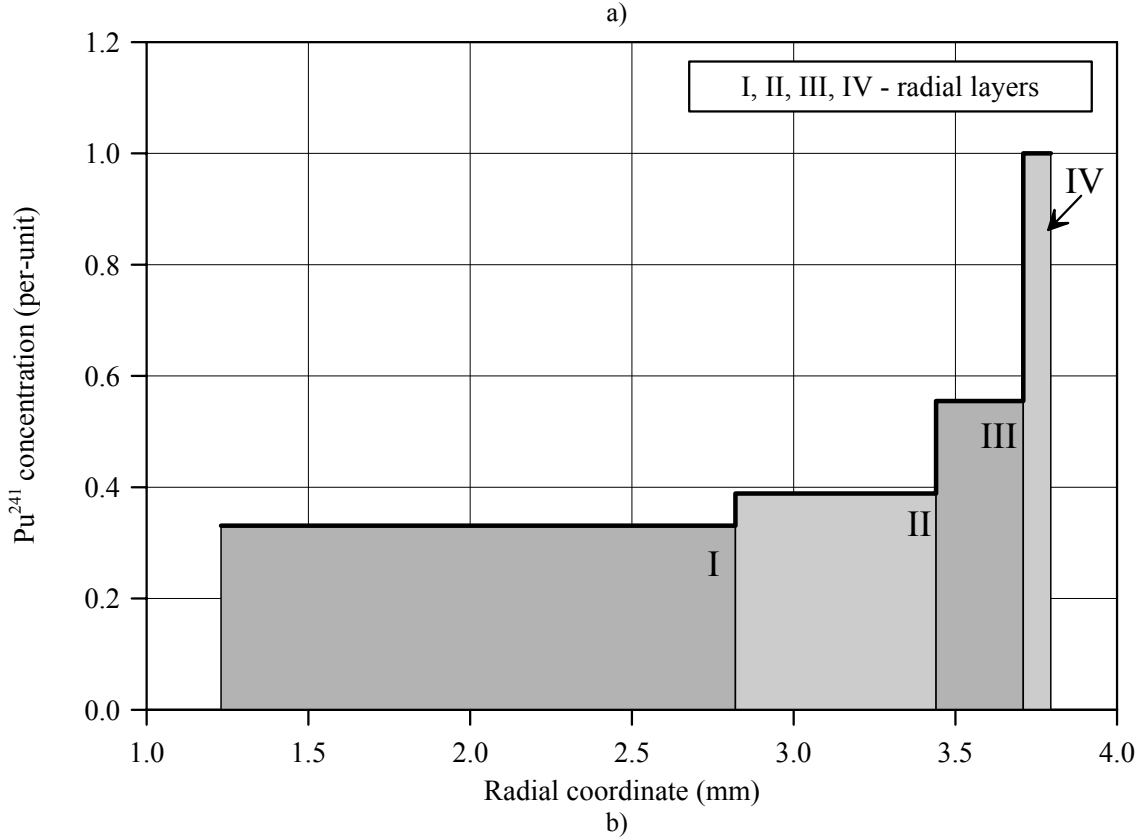
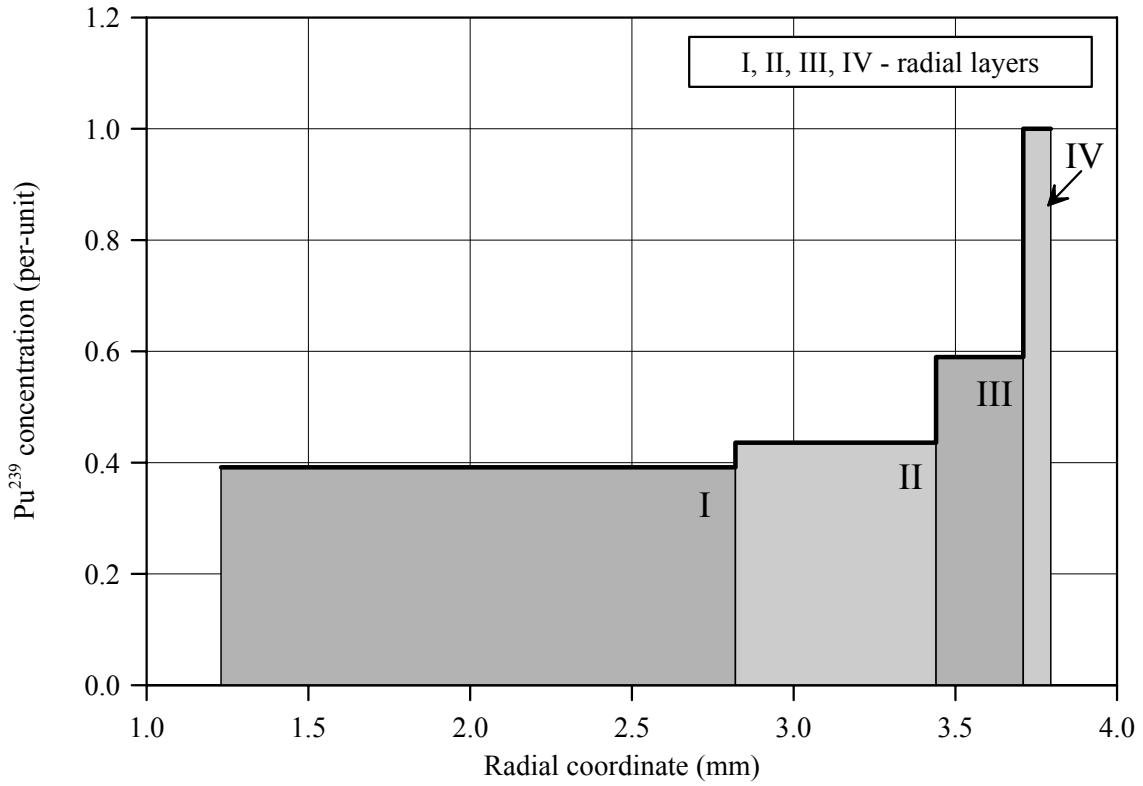


Fig.C-3.4. Radial distribution of (a) Pu^{239} and (b) Pu^{241} for fuel rod # RT3 (calculated values)

Appendix C-4
Individual Characteristics
of Fuel Rod # RT4 before the BGR Test

RT4**Table C-4.1. Radial distribution of isotope nuclear concentrations for fuel rod #RT4
(values averaged of over the fuel stack length)***

| Isotope | Isotopic concentrations (kg/t U) in four fuel radial layers | | | |
|------------------------|---|--------------|--------------|--------------|
| | 0.825-2.77 mm | 2.77-3.45 mm | 3.45-3.75 mm | 3.75-3.84 mm |
| U ²³⁴ | 0.220 | 0.219 | 0.220 | 0.227 |
| U ²³⁵ | 4.900 | 4.626 | 4.403 | 4.255 |
| U ²³⁶ | 6.668 | 6.642 | 6.620 | 6.610 |
| U ²³⁸ | 922.3 | 917.6 | 904.3 | 865.5 |
| Pu ²³⁸ | 0.531 | 0.574 | 0.648 | 0.822 |
| Pu ²³⁹ | 4.923 | 5.421 | 7.106 | 11.97 |
| Pu ²⁴⁰ | 2.757 | 2.839 | 3.487 | 5.564 |
| Pu ²⁴¹ | 1.064 | 1.244 | 1.728 | 3.116 |
| Pu ²⁴² | 0.985 | 1.196 | 1.720 | 3.217 |
| Np ²³⁷ | 0.773 | 0.803 | 0.828 | 0.846 |
| Am ²⁴¹ | 0.903 | 1.054 | 1.463 | 2.639 |
| Oxygen | 134.5 | 134.5 | 134.5 | 134.5 |
| Other fission products | 55.69 | 59.58 | 69.70 | 98.70 |

* Measured averaged concentrations and calculated relative radial distributions of isotopes (TRIFOB code) were used to develop these data

Table C-4.2. Initial individual characteristics of fuel rod # RT4*

| Axial coordinate (from lower cap) (mm) | Cladding average outer diameter (mm) | Fuel mass ** (g) | Linear fuel mass** (g/cm) | Gas flow area ^{3)**} (mm ²) | Burnup** (MW d/kg U) |
|--|---|---------------------|---------------------------------|--|-------------------------|
| 25 ¹⁾ | 9.066 | 2.48 | 4.50 | 2.270 | 58.72 |
| 30 | 9.069 | 2.25 | 4.49 | 2.339 | 59.36 |
| 35 | 9.078 | 2.27 | 4.53 | 2.270 | 60.53 |
| 40 | 9.073 | 2.27 | 4.54 | 2.270 | 60.51 |
| 45 | 9.087 | 2.24 | 4.48 | 2.437 | 60.03 |
| 50 | 9.075 | 2.22 | 4.45 | 2.731 | 59.74 |
| 55 | 9.087 | 2.22 | 4.43 | 2.927 | 60.13 |
| 60 | 9.092 | 2.22 | 4.43 | 2.927 | 60.72 |
| 65 | 9.085 | 2.24 | 4.48 | 2.437 | 60.41 |
| 70 | 9.077 | 2.24 | 4.48 | 2.437 | 59.48 |
| 75 | 9.078 | 2.22 | 4.45 | 2.731 | 59.27 |
| 80 | 9.073 | 2.22 | 4.43 | 2.927 | 59.74 |
| 85 | 9.077 | 2.25 | 4.50 | 2.270 | 59.88 |
| 90 | 9.082 | 2.29 | 4.57 | 2.270 | 59.75 |
| 95 | 9.077 | 2.28 | 4.56 | 2.270 | 60.14 |
| 100 | 9.083 | 2.27 | 4.55 | 2.270 | 60.81 |
| 105 | 9.075 | 2.27 | 4.54 | 2.270 | 60.73 |
| 110 | 9.076 | 2.27 | 4.54 | 2.270 | 60.15 |
| 115 | 9.067 | 2.25 | 4.50 | 2.270 | 60.18 |
| 120 | 9.077 | 2.23 | 4.46 | 2.633 | 60.58 |
| 125 | 9.066 | 2.24 | 4.48 | 2.437 | 60.18 |
| 130 | 9.082 | 2.26 | 4.53 | 2.270 | 59.41 |
| 135 | 9.086 | 2.25 | 4.50 | 2.270 | 59.80 |
| 140 | 9.093 | 2.23 | 4.47 | 2.535 | 61.00 |
| 145 | 9.080 | 2.26 | 4.52 | 2.270 | 61.34 |
| 150 | 9.076 | 2.28 | 4.56 | 2.270 | 60.76 |
| 155 | 9.085 | 2.26 | 4.52 | 2.270 | 60.42 |
| 160 | 9.085 | 2.22 | 4.44 | 2.829 | 60.44 |
| 165 | 9.083 | 2.22 | 4.44 | 2.829 | 60.17 |
| 170 | 9.080 | 2.25 | 4.49 | 2.339 | 59.57 |
| 175 ²⁾ | 9.086 | 1.98 | 4.40 | 3.221 | 59.10 |

* All parameters were determined using results of pre-test examinations

** Average values at the length interval equal to the axial coordinate ± 2.5 mm

¹⁾ Bottom end coordinate of fuel stack is 22 mm;

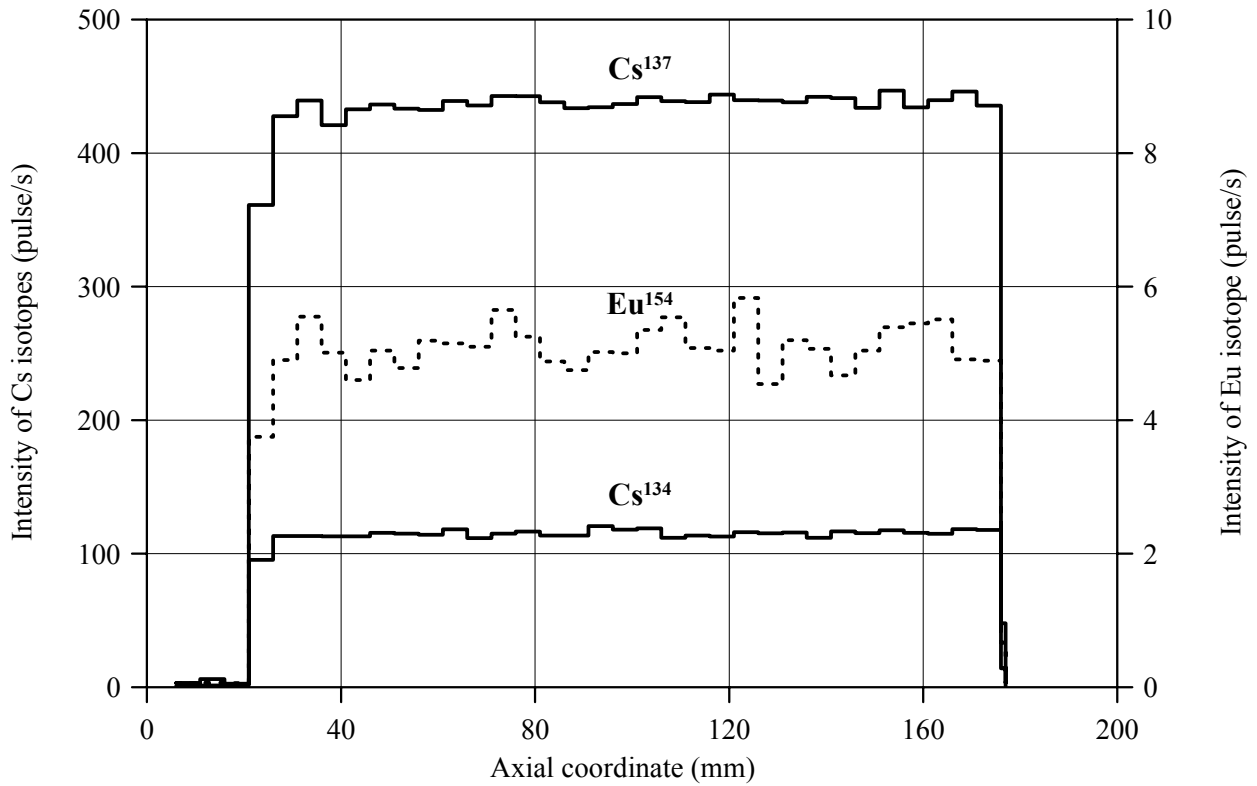
²⁾ Top end coordinate of fuel stack is 177 mm

³⁾ Gas flow area beyond the fuel stack (mm²):

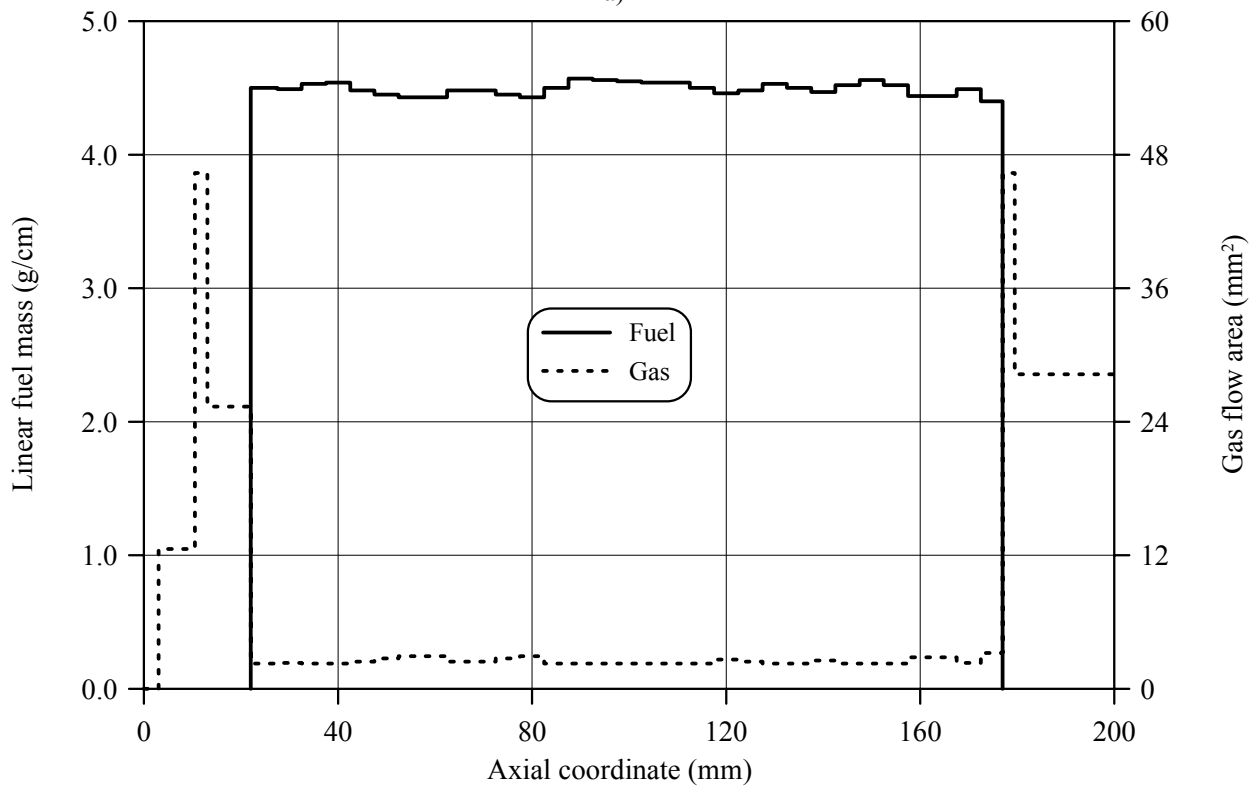
Bottom: 0.0-3.0mm – 0.00; 3.0-10.5mm – 12.56; 10.5-13.1mm – 46.35; 13.1-22.0mm – 25.36

Top: 177-179.5mm – 46.35; 179.5-205.5mm – 28.26; 205.5-282mm – 46.35; 282-291mm – 28.26; 291-300mm – 0.00

RT4

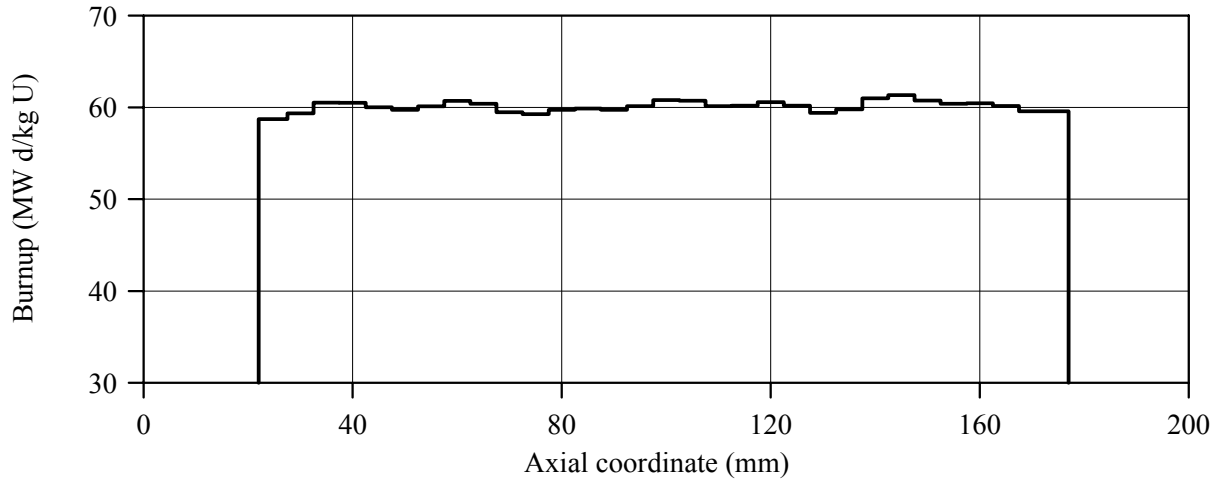


a)

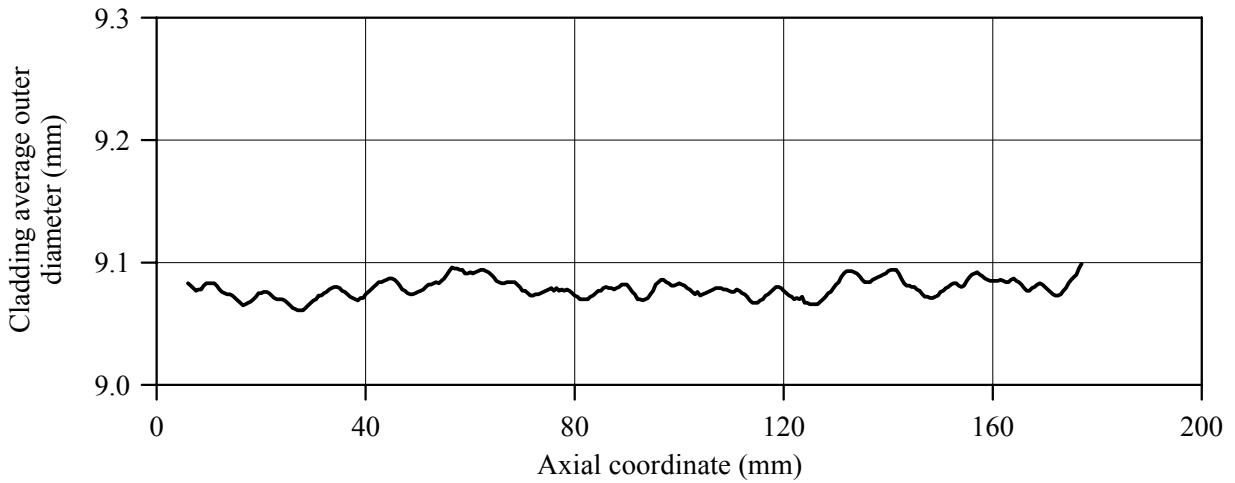


b)

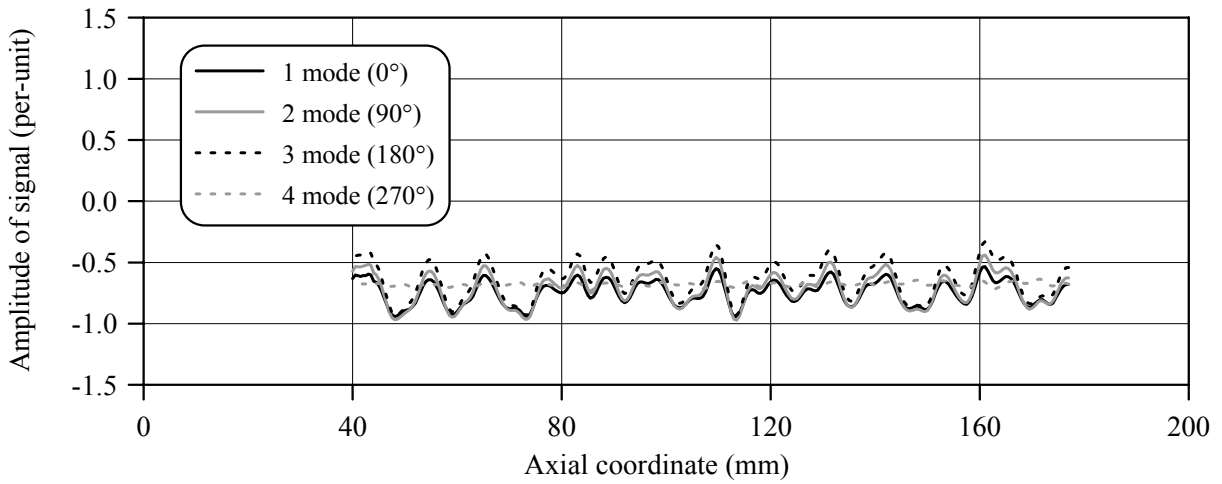
Fig.C-4.1. (a) Results of γ -scanning, (b) Axial fuel mass distribution and axial gas flow area distribution for fuel rod # RT4



a)



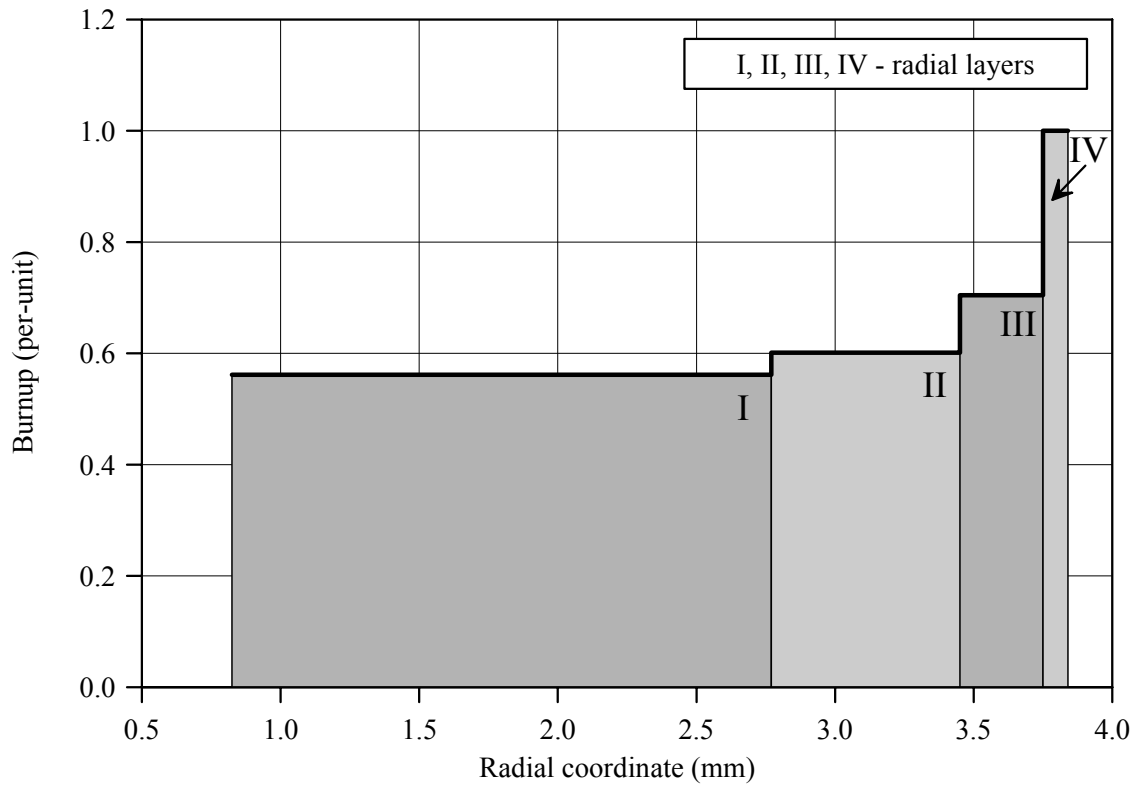
b)



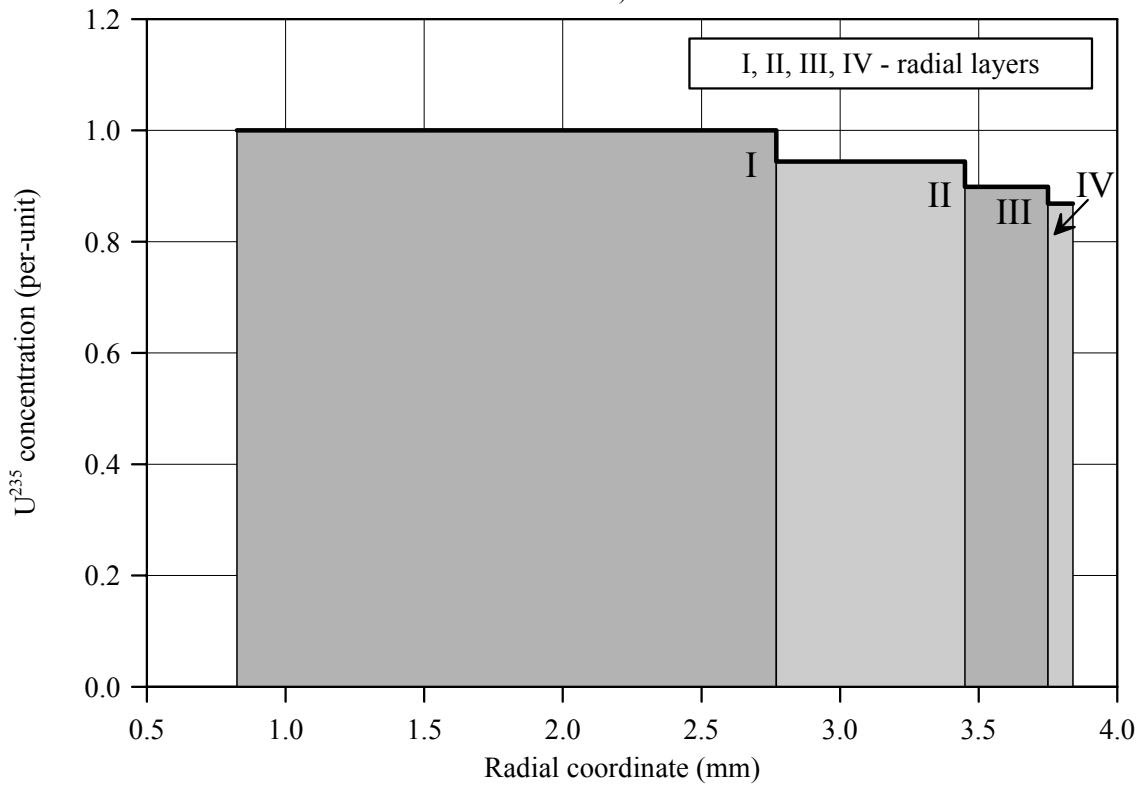
c)

Fig.C-4.2. (a) Axial burnup distribution and (b) results of profilometry and (c) eddy-current examination of fuel rod # RT4

RT4



a)



b)

Fig.C-4.3. (a) Burnup radial distribution and (b) U²³⁵ radial distribution for fuel rod # RT4 (calculated values)

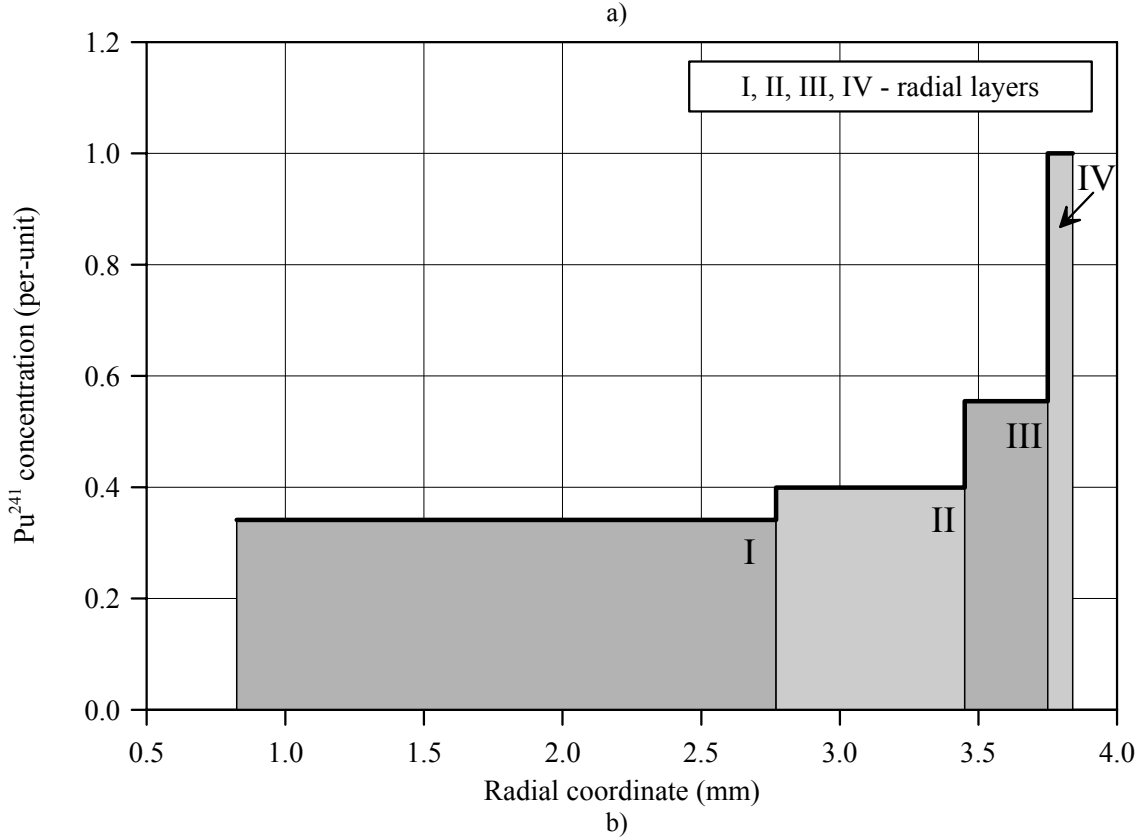
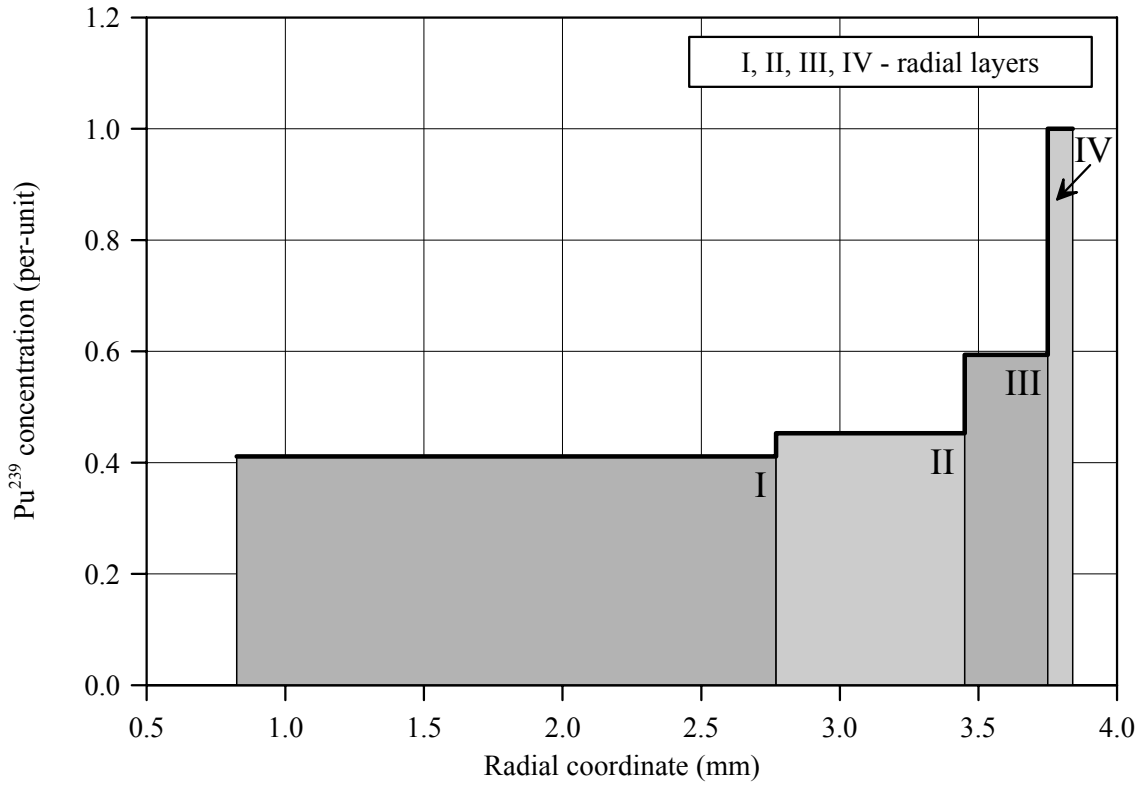


Fig.C-4.4. Radial distribution of (a) Pu^{239} and (b) Pu^{241} for fuel rod # RT4 (calculated values)

Appendix C-5
Individual Characteristics
of Fuel Rod # RT5 before the BGR Test

RT5**Table C-5.1. Radial distribution of isotope nuclear concentrations for fuel rod #RT5
(values averaged of over the fuel stack length)***

| Isotope | Isotopic concentrations (kg/t U) in four fuel radial layers | | | |
|------------------------|---|--------------|--------------|---------------|
| | 1.25-2.84 mm | 2.84-3.47 mm | 3.47-3.74 mm | 3.74-3.808 mm |
| U ²³⁴ | 0.293 | 0.289 | 0.284 | 0.280 |
| U ²³⁵ | 8.104 | 7.783 | 7.488 | 7.286 |
| U ²³⁶ | 6.275 | 6.281 | 6.288 | 6.298 |
| U ²³⁸ | 925.6 | 921.8 | 909.3 | 876.0 |
| Pu ²³⁸ | 0.406 | 0.428 | 0.463 | 0.526 |
| Pu ²³⁹ | 5.032 | 5.598 | 7.550 | 12.74 |
| Pu ²⁴⁰ | 2.661 | 2.807 | 3.592 | 5.795 |
| Pu ²⁴¹ | 0.999 | 1.170 | 1.664 | 2.980 |
| Pu ²⁴² | 0.804 | 0.969 | 1.421 | 2.630 |
| Np ²³⁷ | 0.659 | 0.679 | 0.698 | 0.712 |
| Am ²⁴¹ | 0.514 | 0.595 | 0.839 | 1.503 |
| Oxygen | 134.5 | 134.5 | 134.5 | 134.5 |
| Other fission products | 49.77 | 52.91 | 61.98 | 85.83 |

* Measured averaged concentrations and calculated relative radial distributions of isotopes (TRIFOB code) were used to develop these data

Table C-5.2. Initial individual characteristics of fuel rod # RT5*

| Axial coordinate (from lower cap) (mm) | Cladding average outer diameter (mm) | Fuel mass ** (g) | Linear fuel mass** (g/cm) | Gas flow area ^{3)**} (mm ²) | Burnup** (MW d/kg U) |
|--|---|---------------------|---------------------------------|--|-------------------------|
| 25 ¹⁾ | 9.059 | 1.42 | 4.05 | 5.898 | 47.81 |
| 30 | 9.059 | 2.04 | 4.09 | 5.503 | 49.16 |
| 35 | 9.060 | 2.09 | 4.18 | 4.910 | 48.76 |
| 40 | 9.056 | 2.11 | 4.23 | 4.910 | 48.28 |
| 45 | 9.056 | 2.09 | 4.18 | 4.910 | 48.85 |
| 50 | 9.055 | 2.05 | 4.10 | 5.404 | 49.27 |
| 55 | 9.055 | 2.03 | 4.06 | 5.799 | 48.80 |
| 60 | 9.054 | 2.02 | 4.05 | 5.898 | 48.48 |
| 65 | 9.056 | 2.04 | 4.08 | 5.602 | 48.88 |
| 70 | 9.056 | 2.05 | 4.09 | 5.503 | 48.98 |
| 75 | 9.056 | 2.05 | 4.10 | 5.404 | 48.27 |
| 80 | 9.061 | 2.06 | 4.12 | 5.206 | 47.80 |
| 85 | 9.059 | 2.05 | 4.10 | 5.404 | 48.26 |
| 90 | 9.060 | 2.07 | 4.13 | 5.107 | 49.02 |
| 95 | 9.059 | 2.08 | 4.17 | 4.910 | 49.47 |
| 100 | 9.061 | 2.09 | 4.19 | 4.910 | 49.48 |
| 105 | 9.062 | 2.08 | 4.16 | 4.910 | 49.14 |
| 110 | 9.062 | 2.07 | 4.13 | 5.107 | 48.98 |
| 115 | 9.063 | 2.04 | 4.08 | 5.602 | 49.25 |
| 120 | 9.063 | 2.01 | 4.02 | 6.195 | 49.53 |
| 125 | 9.064 | 2.03 | 4.07 | 5.701 | 49.45 |
| 130 | 9.057 | 2.03 | 4.06 | 5.799 | 49.05 |
| 135 | 9.057 | 2.05 | 4.10 | 5.404 | 48.44 |
| 140 | 9.051 | 2.07 | 4.14 | 5.008 | 47.83 |
| 145 | 9.056 | 2.06 | 4.12 | 5.206 | 47.39 |
| 150 | 9.055 | 2.06 | 4.12 | 5.206 | 47.26 |
| 155 | 9.053 | 2.07 | 4.14 | 5.008 | 47.46 |
| 160 | 9.054 | 2.09 | 4.18 | 4.910 | 47.88 |
| 165 | 9.053 | 2.06 | 4.12 | 5.206 | 48.38 |
| 170 | 9.058 | 2.04 | 4.08 | 5.602 | 48.88 |
| 175 ²⁾ | 9.037 | 1.85 | 4.10 | 5.404 | 49.33 |

* All parameters were determined using results of pre-test examinations

** Average values at the length interval equal to the axial coordinate ± 2.5 mm

¹⁾ Bottom end coordinate of fuel stack is 24 mm;

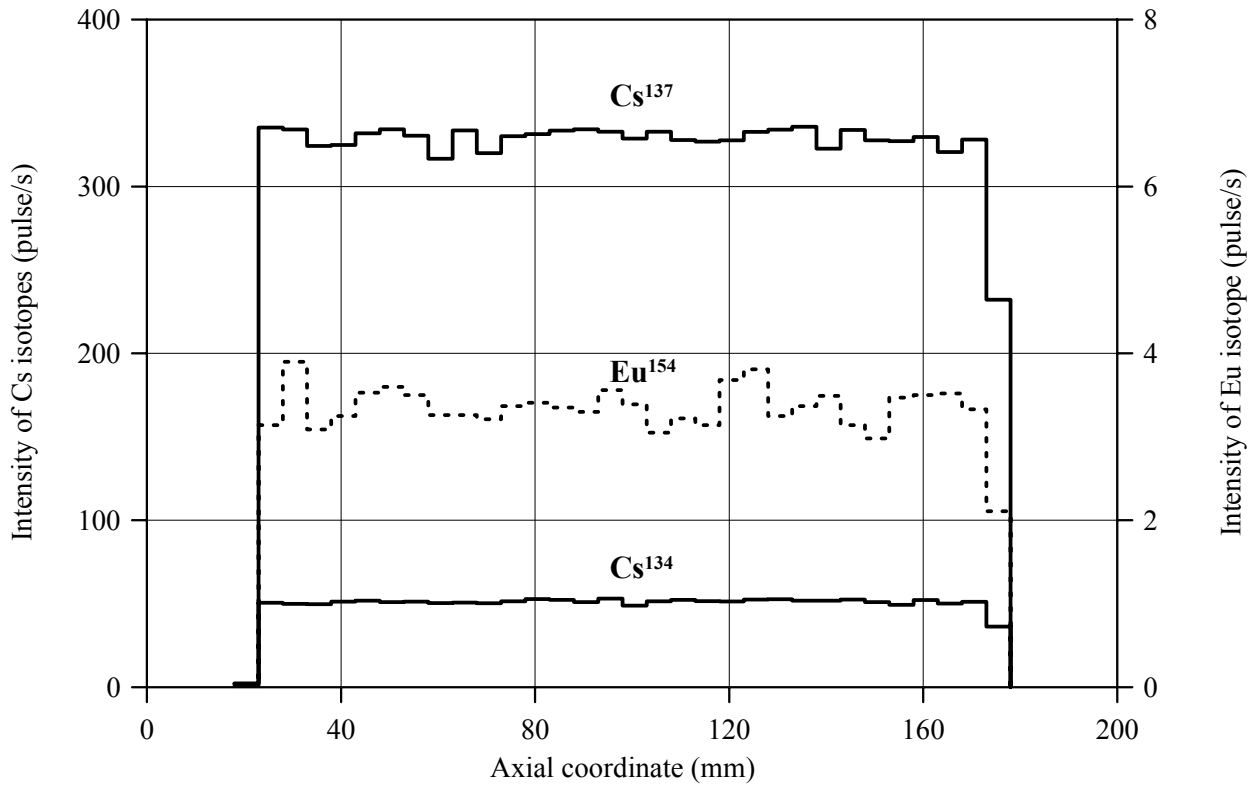
²⁾ Top end coordinate of fuel stack is 177 mm

³⁾ Gas flow area beyond the fuel stack (mm²):

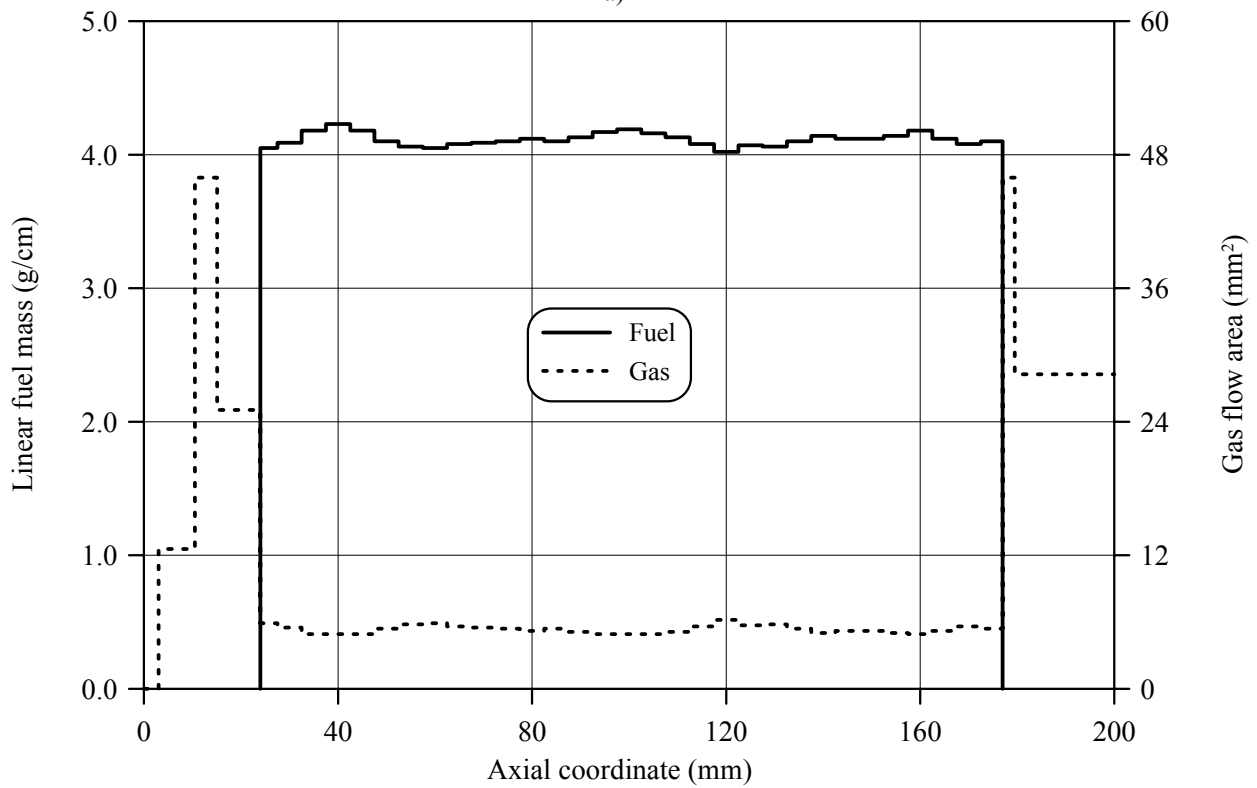
Bottom: 0.0-3.0mm – 0.00; 3.0-10.5mm – 12.56; 10.5-15.1mm – 45.94; 15.1-24.0mm – 25.06

Top: 177.0-179.5mm – 45.94; 179.5-205.5mm – 28.26; 205.5-282.0mm – 45.94; 282-291mm – 28.26; 291-300mm – 0.00

RT5

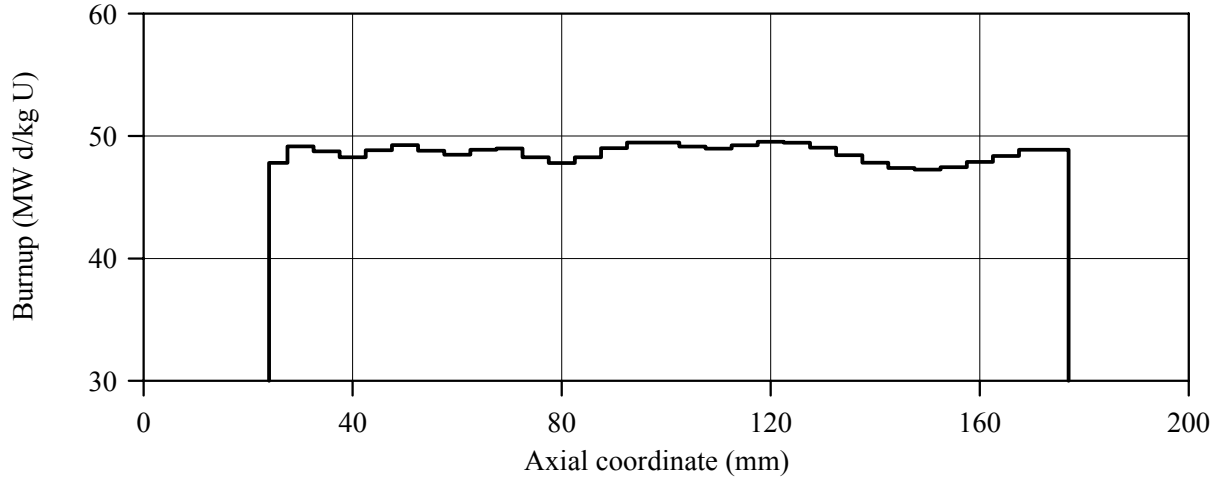


a)

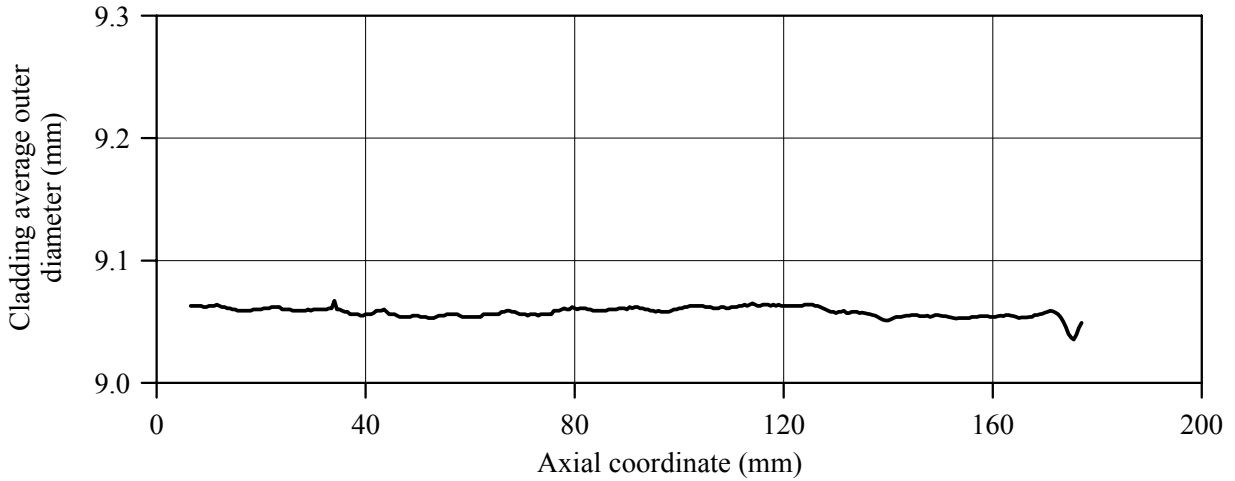


b)

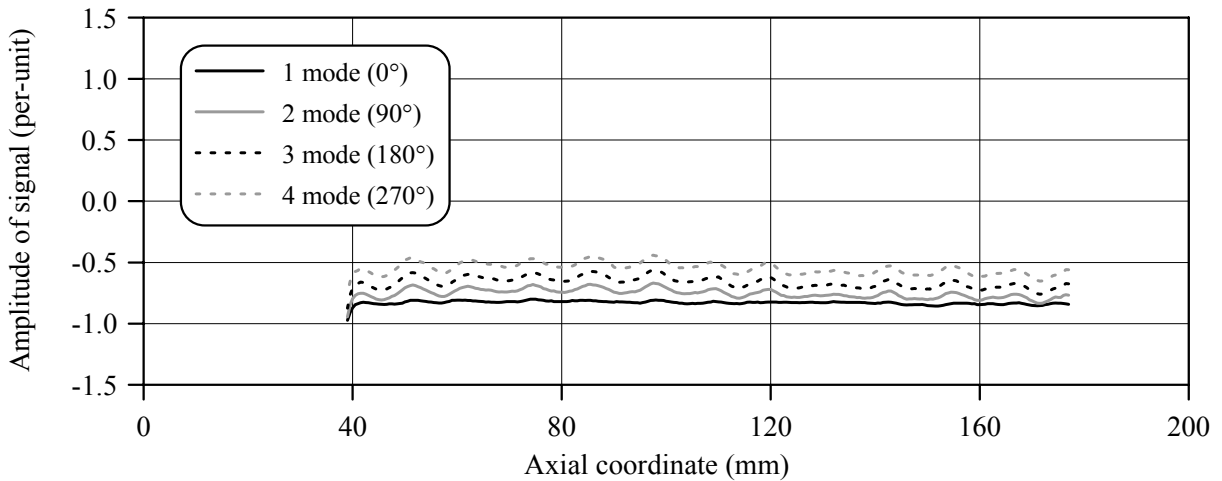
Fig.C-5.1. (a) Results of γ -scanning, (b) Axial fuel mass distribution and axial gas flow area distribution for fuel rod # RT5



a)



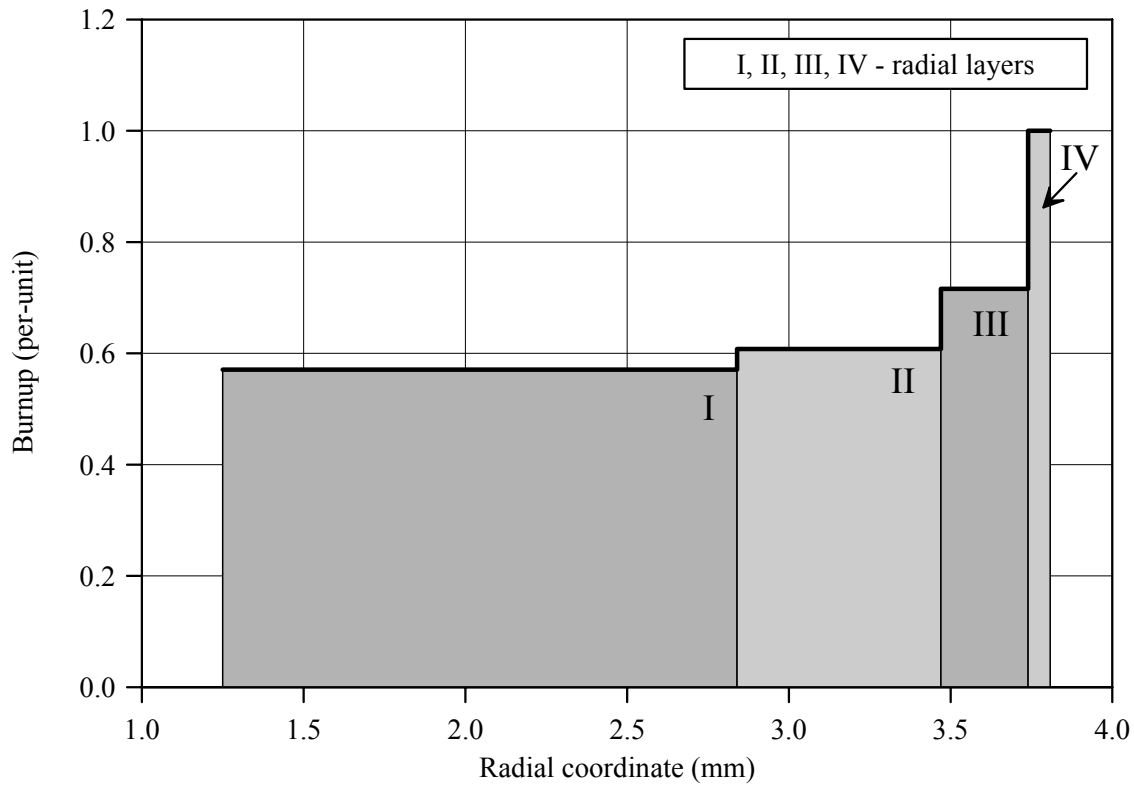
b)



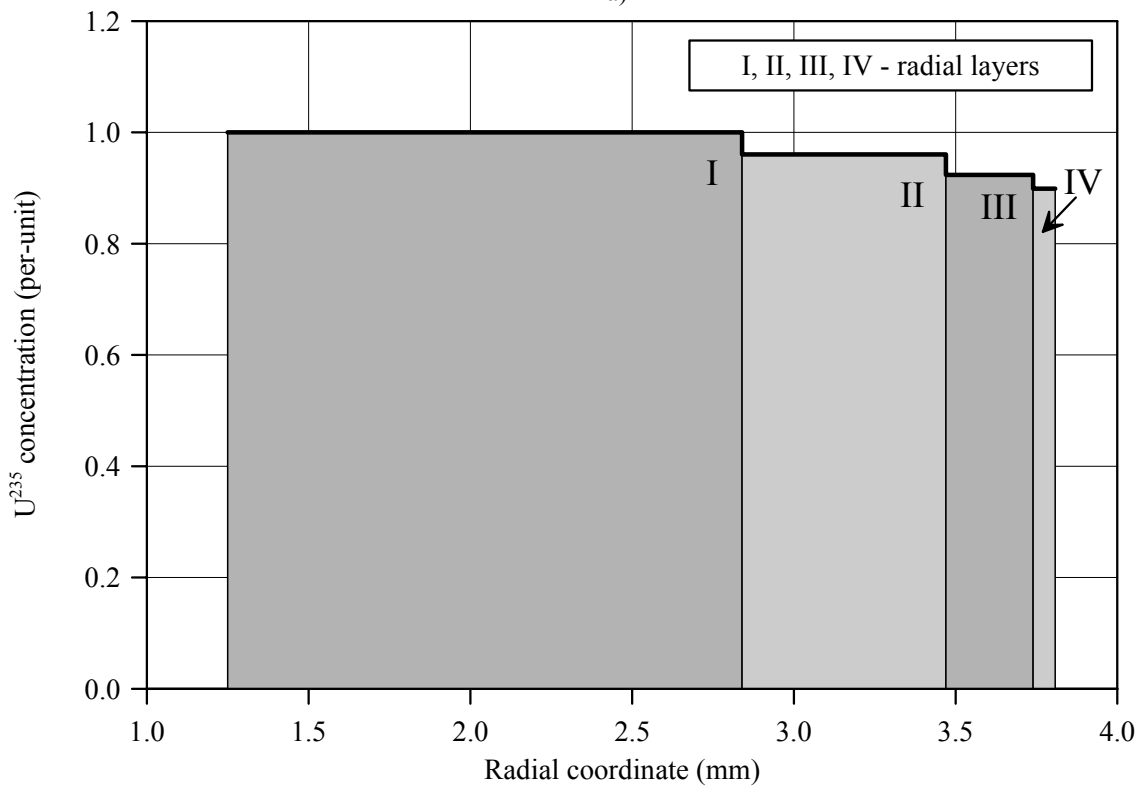
c)

Fig.C-5.2. (a) Axial burnup distribution and (b) results of profilometry and (c) eddy-current examination of fuel rod # RT5

RT5



a)



b)

Fig.C-5.3. (a) Burnup radial distribution and (b) U²³⁵ radial distribution for fuel rod # RT5 (calculated values)

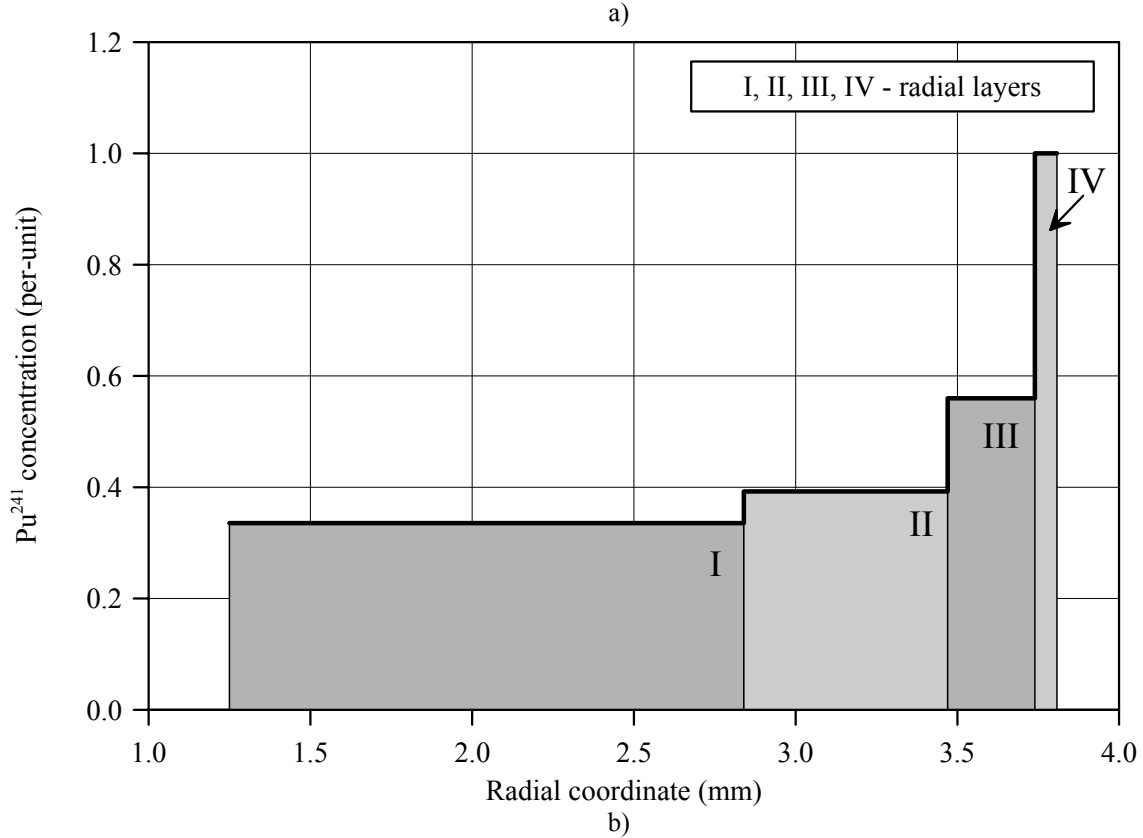
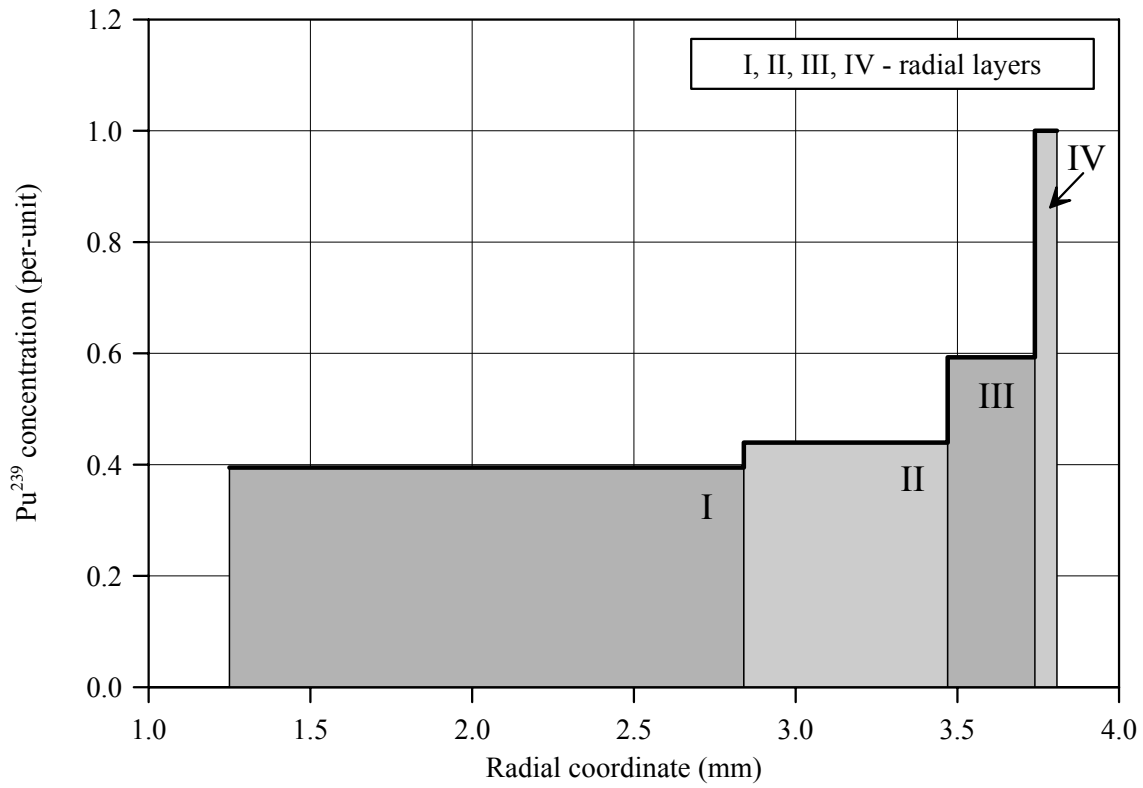


Fig.C-5.4. Radial distribution of (a) Pu²³⁹ and (b) Pu²⁴¹ for fuel rod # RT5 (calculated values)

Appendix C-6
Individual Characteristics
of Fuel Rod # RT6 before the BGR Test

RT6**Table C-6.1. Radial distribution of isotope nuclear concentrations for fuel rod #RT6
(values averaged of over the fuel stack length)***

| Isotope | Isotopic concentrations (kg/t U) in four fuel radial layers | | | |
|------------------------|---|--------------|--------------|---------------|
| | 1.25-2.82 mm | 2.82-3.44 mm | 3.44-3.71 mm | 3.71-3.795 mm |
| U ²³⁴ | 0.273 | 0.269 | 0.265 | 0.261 |
| U ²³⁵ | 8.512 | 8.188 | 7.891 | 7.687 |
| U ²³⁶ | 6.251 | 6.263 | 6.275 | 6.290 |
| U ²³⁸ | 928.4 | 924.6 | 912.9 | 881.2 |
| Pu ²³⁸ | 0.370 | 0.390 | 0.421 | 0.479 |
| Pu ²³⁹ | 4.856 | 5.410 | 7.320 | 12.43 |
| Pu ²⁴⁰ | 2.485 | 2.636 | 3.400 | 5.540 |
| Pu ²⁴¹ | 0.908 | 1.067 | 1.523 | 2.746 |
| Pu ²⁴² | 0.681 | 0.821 | 1.207 | 2.245 |
| Np ²³⁷ | 0.618 | 0.637 | 0.656 | 0.669 |
| Am ²⁴¹ | 0.480 | 0.556 | 0.787 | 1.419 |
| Oxygen | 134.5 | 134.5 | 134.5 | 134.5 |
| Other fission products | 47.25 | 50.28 | 58.81 | 81.35 |

* Measured averaged concentrations and calculated relative radial distributions of isotopes (TRIFOB code) were used to develop these data

Table C-6.2. Initial individual characteristics of fuel rod # RT6*

| Axial coordinate (from lower cap) (mm) | Cladding average outer diameter (mm) | Fuel mass ** (g) | Linear fuel mass** (g/cm) | Gas flow area ^{3)**} (mm ²) | Burnup** (MW d/kg U) |
|--|---|---------------------|---------------------------------|--|-------------------------|
| 25 ¹⁾ | 9.072 | 1.82 | 4.04 | 6.139 | 48.06 |
| 30 | 9.068 | 2.05 | 4.10 | 5.548 | 47.99 |
| 35 | 9.062 | 2.05 | 4.11 | 5.449 | 48.09 |
| 40 | 9.061 | 2.05 | 4.09 | 5.646 | 48.33 |
| 45 | 9.060 | 2.04 | 4.09 | 5.646 | 48.37 |
| 50 | 9.060 | 2.01 | 4.02 | 6.336 | 48.19 |
| 55 | 9.061 | 2.04 | 4.07 | 5.843 | 48.15 |
| 60 | 9.065 | 2.06 | 4.13 | 5.252 | 48.33 |
| 65 | 9.070 | 2.05 | 4.09 | 5.646 | 48.31 |
| 70 | 9.072 | 2.08 | 4.15 | 5.055 | 48.06 |
| 75 | 9.073 | 2.05 | 4.09 | 5.646 | 48.05 |
| 80 | 9.075 | 2.04 | 4.09 | 5.646 | 48.38 |
| 85 | 9.075 | 2.05 | 4.09 | 5.646 | 48.56 |
| 90 | 9.071 | 2.11 | 4.21 | 4.910 | 48.43 |
| 95 | 9.069 | 2.05 | 4.11 | 5.449 | 48.24 |
| 100 | 9.069 | 2.03 | 4.07 | 5.843 | 48.14 |
| 105 | 9.068 | 2.03 | 4.07 | 5.843 | 48.08 |
| 110 | 9.068 | 2.02 | 4.03 | 6.237 | 48.02 |
| 115 | 9.066 | 2.05 | 4.09 | 5.646 | 47.89 |
| 120 | 9.069 | 2.05 | 4.11 | 5.449 | 47.77 |
| 125 | 9.071 | 2.05 | 4.09 | 5.646 | 47.85 |
| 130 | 9.073 | 2.04 | 4.08 | 5.745 | 48.08 |
| 135 | 9.073 | 2.07 | 4.15 | 5.055 | 48.06 |
| 140 | 9.075 | 2.10 | 4.19 | 4.910 | 47.77 |
| 145 | 9.077 | 2.08 | 4.17 | 4.910 | 47.70 |
| 150 | 9.080 | 2.07 | 4.14 | 5.154 | 47.85 |
| 155 | 9.075 | 2.08 | 4.16 | 4.957 | 47.57 |
| 160 | 9.075 | 2.09 | 4.17 | 4.910 | 46.78 |
| 165 | 9.076 | 2.03 | 4.06 | 5.942 | 46.16 |
| 170 | 9.078 | 1.96 | 3.92 | 7.321 | 45.95 |
| 175 ²⁾ | - | 0.58 | 3.88 | 7.715 | 45.71 |

* All parameters were determined using results of pre-test examinations

** Average values at the length interval equal to the axial coordinate ± 2.5 mm

¹⁾ Bottom end coordinate of fuel stack is 23 mm;

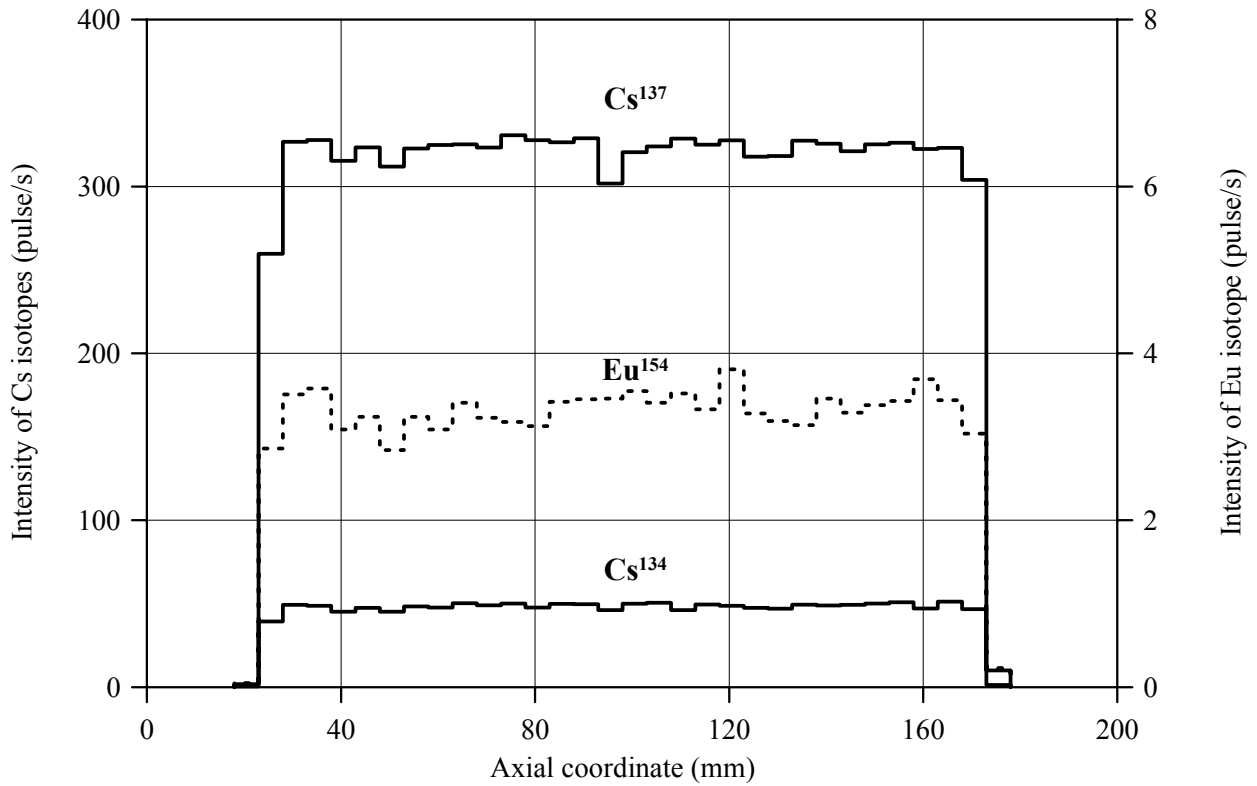
²⁾ Top end coordinate of fuel stack is 174 mm

³⁾ Gas flow area beyond the fuel stack (mm²):

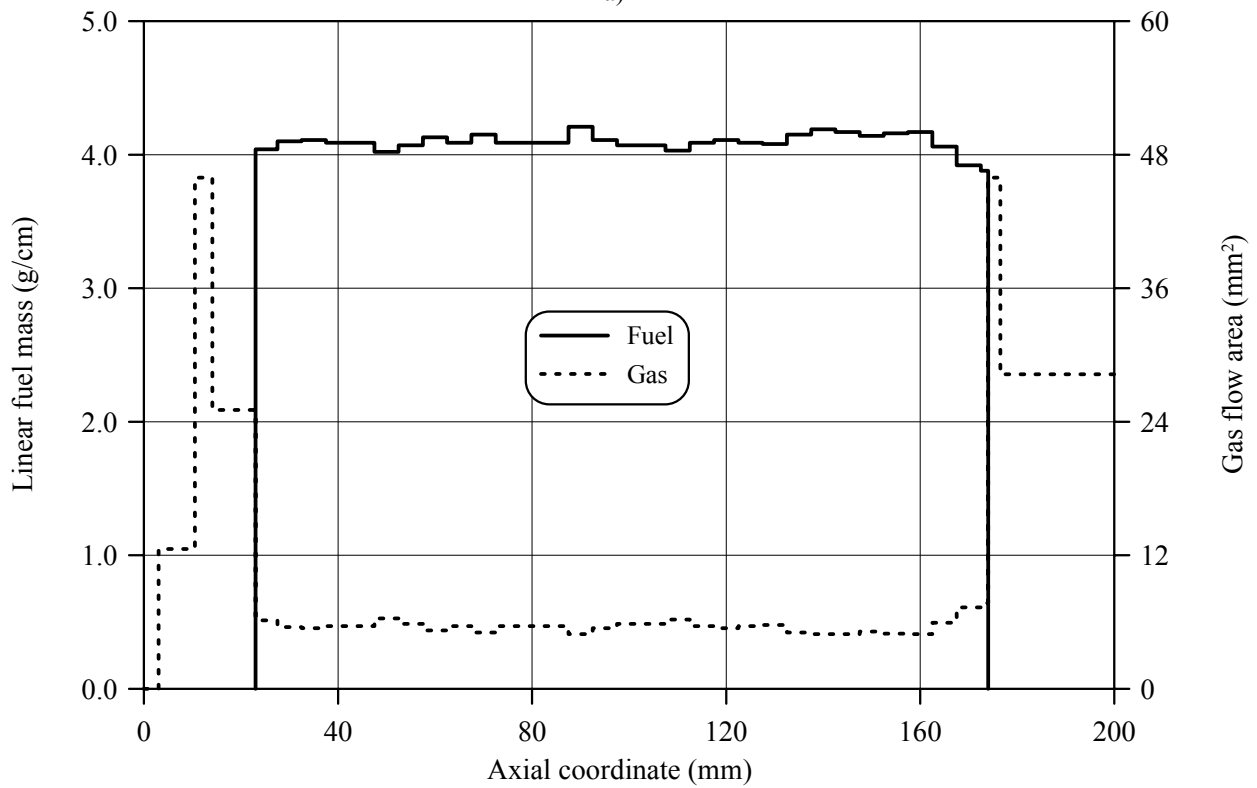
Bottom: 0.0-3.0mm – 0.00; 3.0-10.5mm – 12.56; 10.5-14.1mm – 45.94; 14.1-23.0mm – 25.06

Top: 174.0-176.5mm – 45.94; 176.5-202.5mm – 28.26; 202.5-279mm – 45.94; 279-288mm – 28.26; 288-297mm – 0.00

RT6

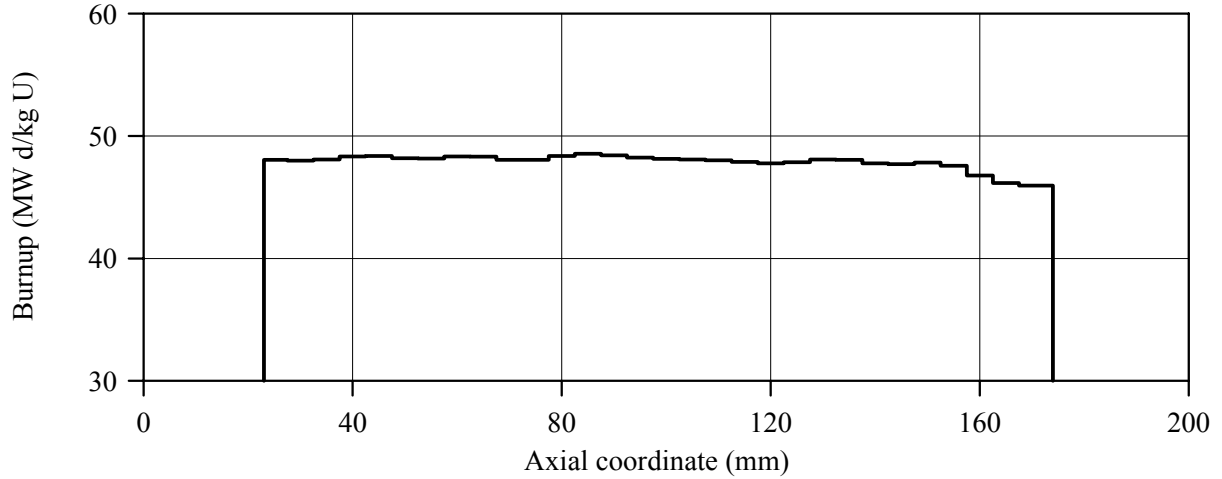


a)

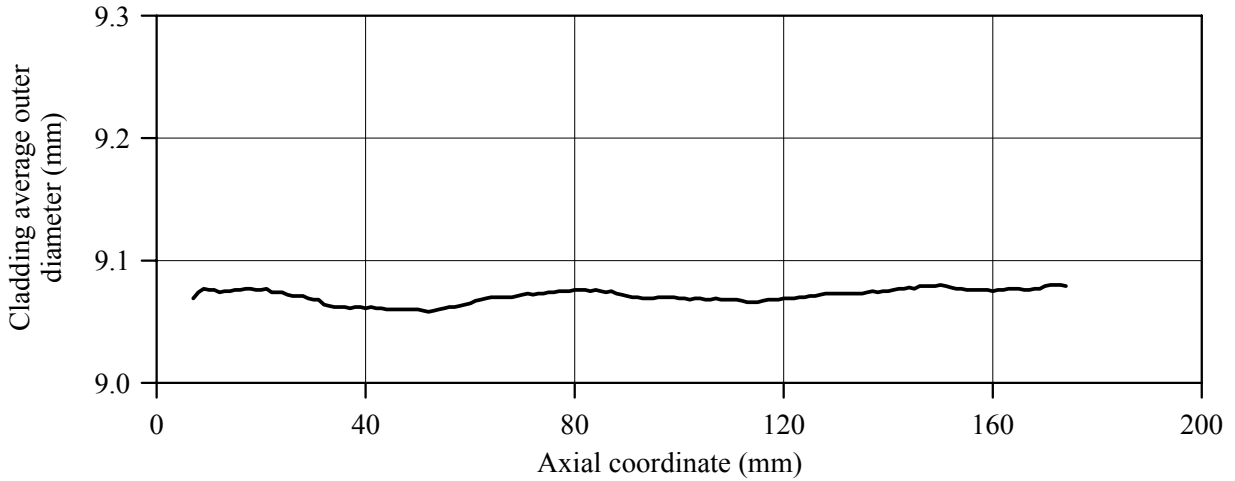


b)

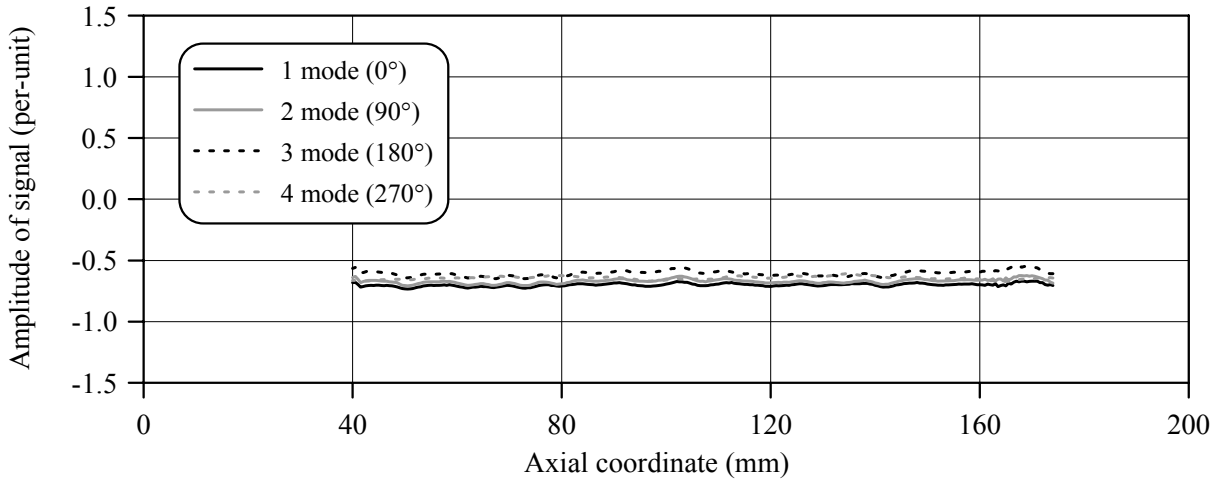
Fig.C-6.1. (a) Results of γ -scanning, (b) Axial fuel mass distribution and axial gas flow area distribution for fuel rod # RT6



a)



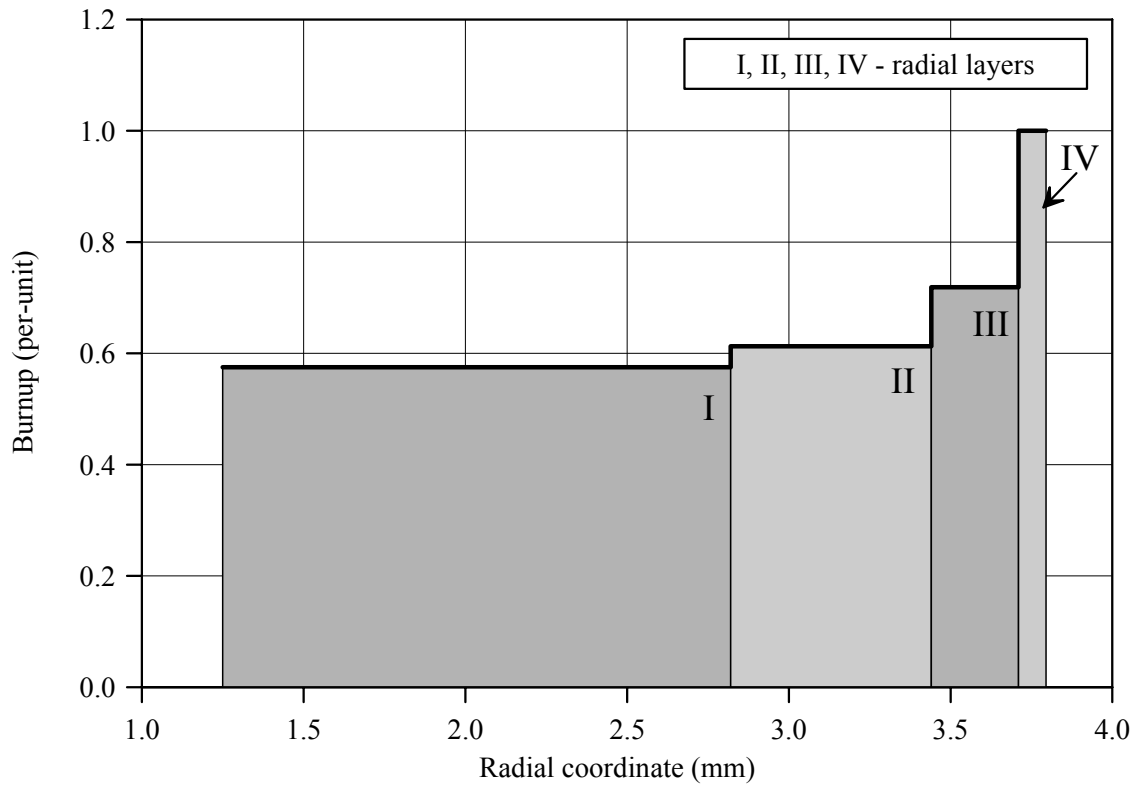
b)



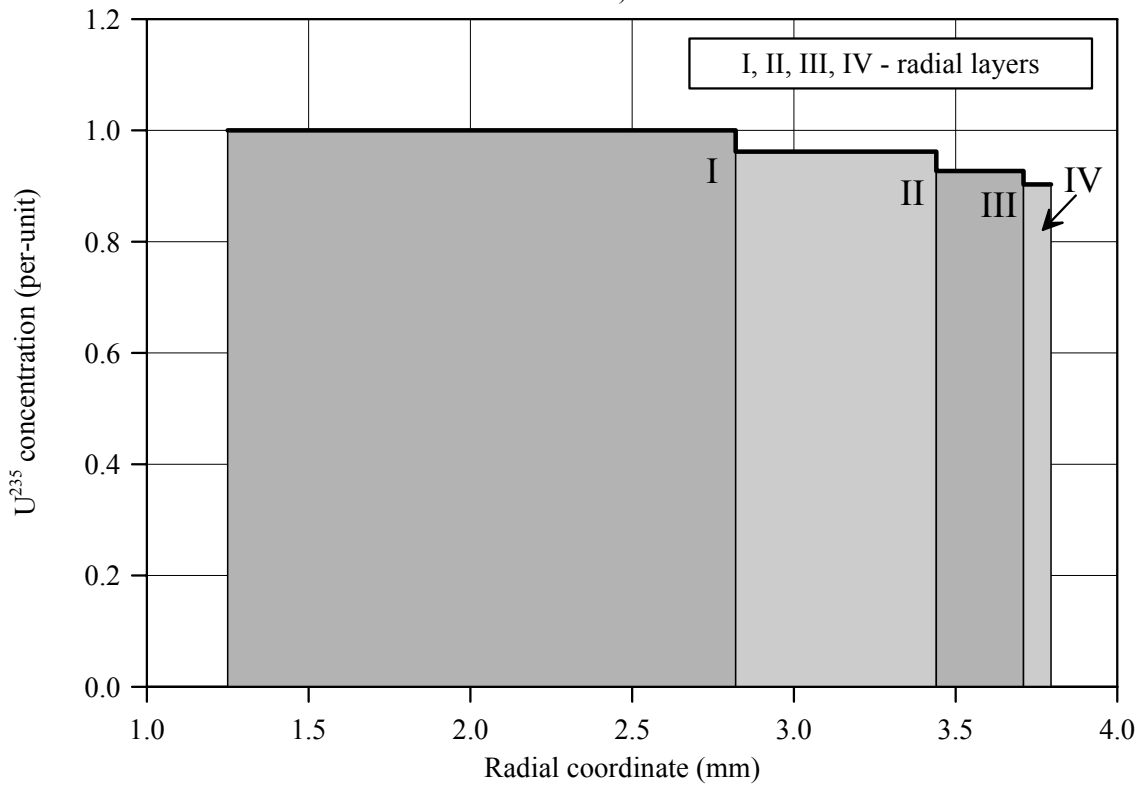
c)

Fig.C-6.2. (a) Axial burnup distribution and (b) results of profilometry and (c) eddy-current examination of fuel rod # RT6

RT6



a)



b)

Fig.C-6.3. (a) Burnup radial distribution and (b) U^{235} radial distribution for fuel rod # RT6 (calculated values)

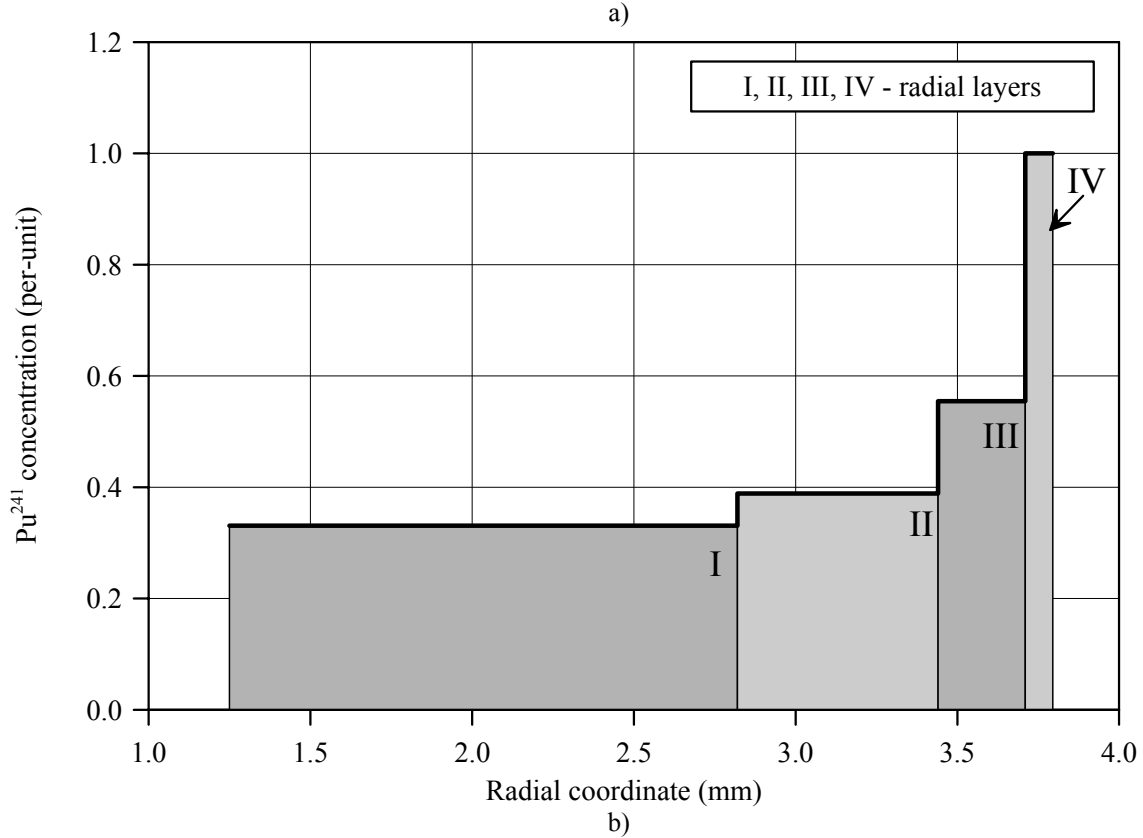
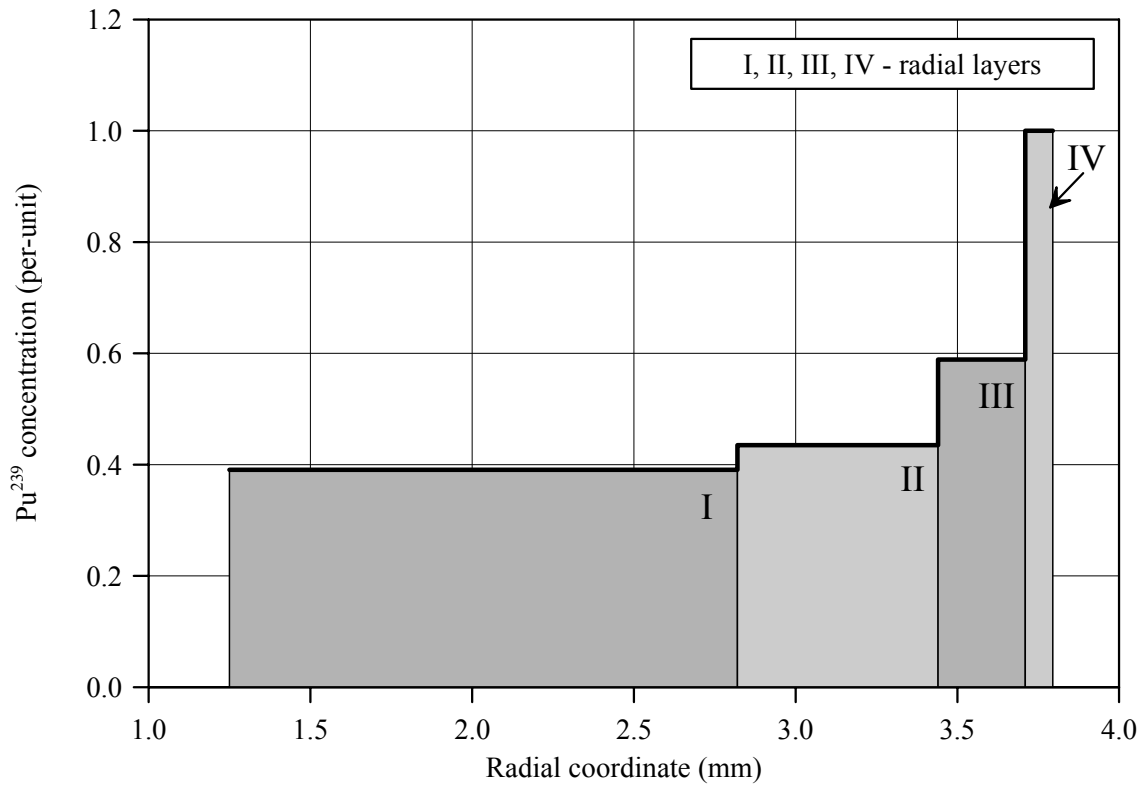


Fig.C-6.4. Radial distribution of (a) Pu^{239} and (b) Pu^{241} for fuel rod # RT6 (calculated values)

Appendix C-7
Individual Characteristics
of Fuel Rod # RT7 before the BGR Test

RT7**Table C-7.1. Radial distribution of isotope nuclear concentrations for fuel rod #RT7
(values averaged of over the fuel stack length)***

| Isotope | Isotopic concentrations (kg/t U) in four fuel radial layers | | | |
|------------------------|---|----------------|----------------|----------------|
| | 0.825-2.777 mm | 2.777-3.454 mm | 3.454-3.747 mm | 3.747-3.840 mm |
| U ²³⁴ | 0.190 | 0.189 | 0.190 | 0.197 |
| U ²³⁵ | 2.435 | 2.297 | 2.185 | 2.111 |
| U ²³⁶ | 5.767 | 5.743 | 5.721 | 5.712 |
| U ²³⁸ | 923.5 | 918.8 | 905.4 | 866.0 |
| Pu ²³⁸ | 0.378 | 0.408 | 0.461 | 0.586 |
| Pu ²³⁹ | 4.744 | 5.223 | 6.840 | 11.50 |
| Pu ²⁴⁰ | 2.978 | 3.063 | 3.755 | 5.978 |
| Pu ²⁴¹ | 1.324 | 1.545 | 2.144 | 3.859 |
| Pu ²⁴² | 1.335 | 1.619 | 2.328 | 4.349 |
| Np ²³⁷ | 0.000 | 0.000 | 0.000 | 0.000 |
| Am ²⁴¹ | 0.162 | 0.188 | 0.261 | 0.470 |
| Oxygen | 134.5 | 134.5 | 134.5 | 134.5 |
| Other fission products | 57.00 | 60.68 | 70.43 | 98.62 |

* Measured averaged concentrations and calculated relative radial distributions of isotopes (TRIFOB code) were used to develop these data

Table C-7.2. Initial individual characteristics of fuel rod # RT7*

| Axial coordinate (from lower cap) (mm) | Cladding average outer diameter (mm) | Fuel mass ** (g) | Linear fuel mass** (g/cm) | Gas flow area ^{3)**} (mm ²) | Burnup** (MW d/kg U) |
|--|---|---------------------|---------------------------------|--|-------------------------|
| 25 ¹⁾ | 9.063 | 2.03 | 4.51 | 2.14 | 58.94 |
| 30 | 9.054 | 2.17 | 4.34 | 3.80 | 59.75 |
| 35 | 9.064 | 2.14 | 4.28 | 4.39 | 61.75 |
| 40 | 9.059 | 2.16 | 4.33 | 3.90 | 60.24 |
| 45 | 9.059 | 2.18 | 4.36 | 3.61 | 60.34 |
| 50 | 9.052 | 2.19 | 4.39 | 3.31 | 59.58 |
| 55 | 9.064 | 2.16 | 4.32 | 4.00 | 59.87 |
| 60 | 9.066 | 2.17 | 4.34 | 3.80 | 61.50 |
| 65 | 9.063 | 2.12 | 4.25 | 4.68 | 60.79 |
| 70 | 9.062 | 2.17 | 4.34 | 3.80 | 59.33 |
| 75 | 9.056 | 2.19 | 4.37 | 3.51 | 60.91 |
| 80 | 9.059 | 2.19 | 4.38 | 3.41 | 59.23 |
| 85 | 9.051 | 2.20 | 4.40 | 3.21 | 59.31 |
| 90 | 9.062 | 2.20 | 4.40 | 3.21 | 60.73 |
| 95 | 9.051 | 2.21 | 4.41 | 3.12 | 59.03 |
| 100 | 9.057 | 2.21 | 4.41 | 3.12 | 60.93 |
| 105 | 9.056 | 2.22 | 4.44 | 2.82 | 59.04 |
| 110 | 9.070 | 2.20 | 4.41 | 3.12 | 60.63 |
| 115 | 9.073 | 2.20 | 4.39 | 3.31 | 60.96 |
| 120 | 9.063 | 2.16 | 4.32 | 4.00 | 59.31 |
| 125 | 9.064 | 2.18 | 4.36 | 3.61 | 61.62 |
| 130 | 9.063 | 2.16 | 4.31 | 4.10 | 61.89 |
| 135 | 9.071 | 2.17 | 4.35 | 3.70 | 60.11 |
| 140 | 9.057 | 2.19 | 4.38 | 3.41 | 61.07 |
| 145 | 9.075 | 2.17 | 4.34 | 3.80 | 60.52 |
| 150 | 9.063 | 2.17 | 4.34 | 3.80 | 59.56 |
| 155 | 9.072 | 2.15 | 4.30 | 4.19 | 61.62 |
| 160 | 9.064 | 2.18 | 4.36 | 3.61 | 60.18 |
| 165 | 9.069 | 2.22 | 4.44 | 2.82 | 61.60 |
| 170 | 9.069 | 2.19 | 4.39 | 3.31 | 60.14 |
| 175 ²⁾ | 9.056 | 1.55 | 4.29 | 4.29 | 59.81 |

* All parameters were determined using results of pre-test examinations

** Average values at the length interval equal to the axial coordinate ± 2.5 mm

¹⁾ Bottom end coordinate of fuel stack is 23 mm;

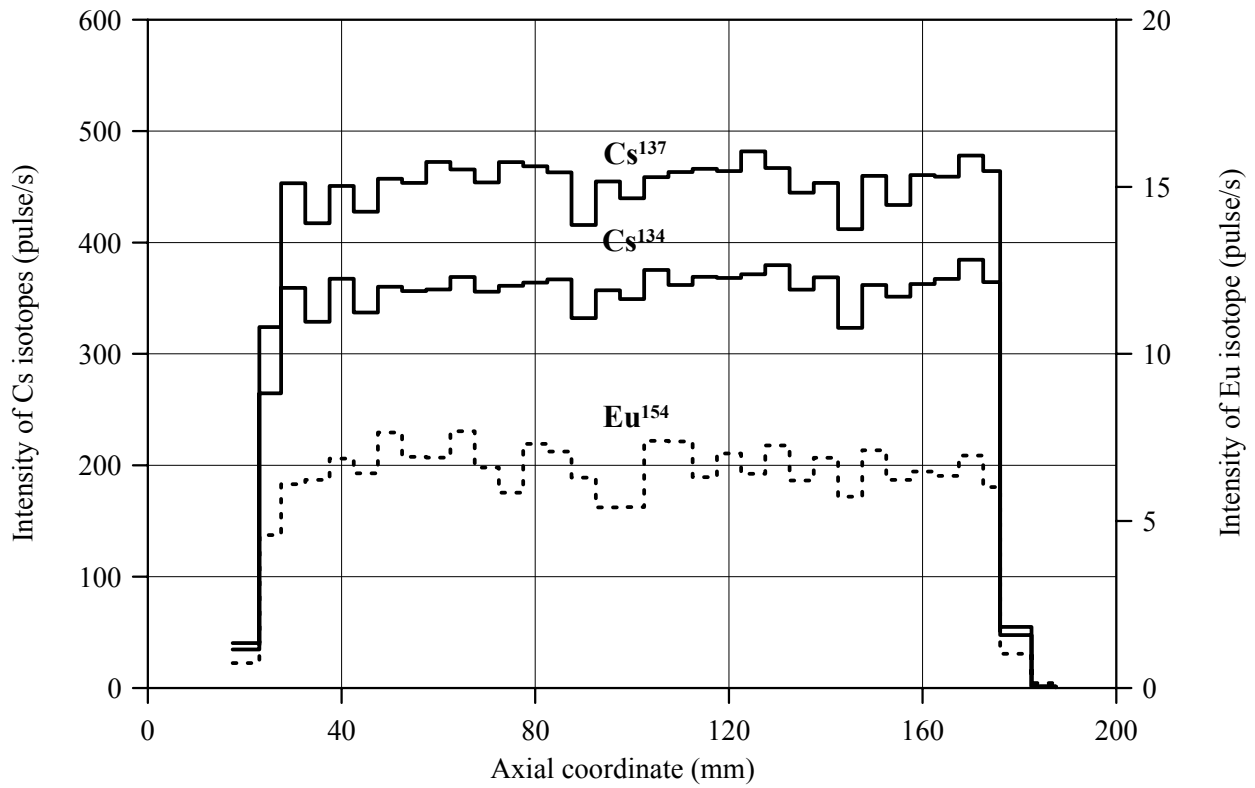
²⁾ Top end coordinate of fuel stack is 176.1 mm

³⁾ Gas flow area beyond the fuel stack (mm²):

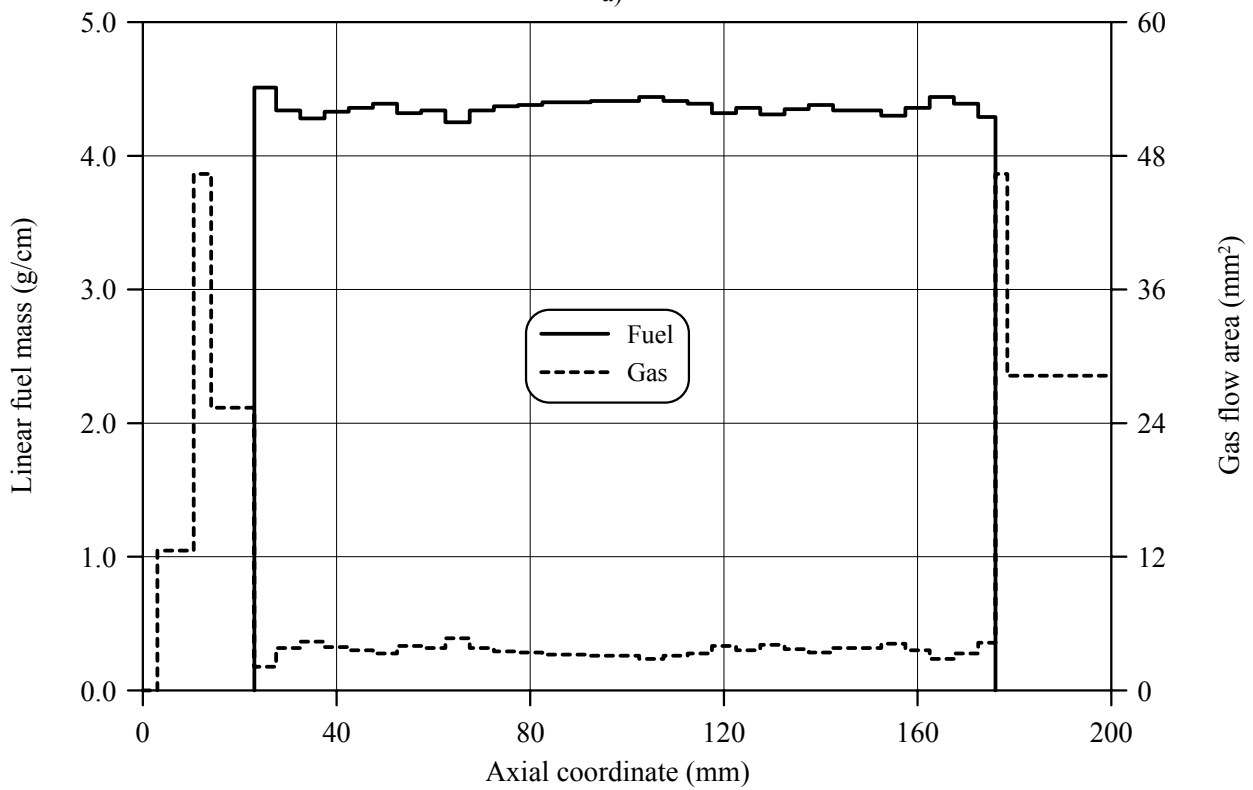
Bottom: 0.0-3.0mm – 0.00; 3.0-10.5mm – 12.56; 10.5-14.1mm – 46.37; 14.1-23.0mm – 25.38

Top: 176.1-178.5mm – 46.37; 178.5-204.5mm – 28.26; 204.5-281mm – 47.27; 281-290mm – 28.26; 290-299mm – 0.00

RT7

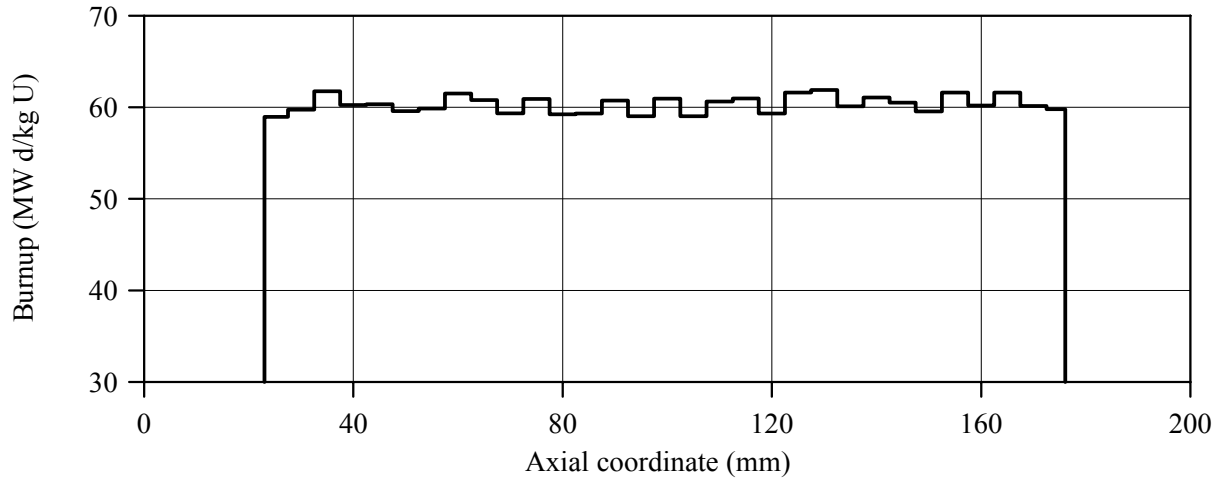


a)

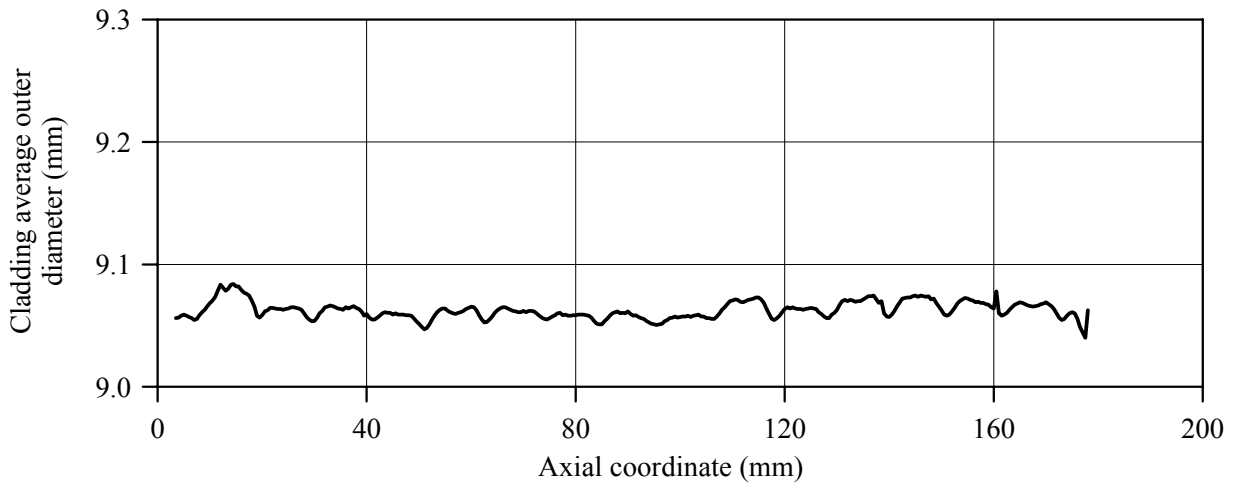


b)

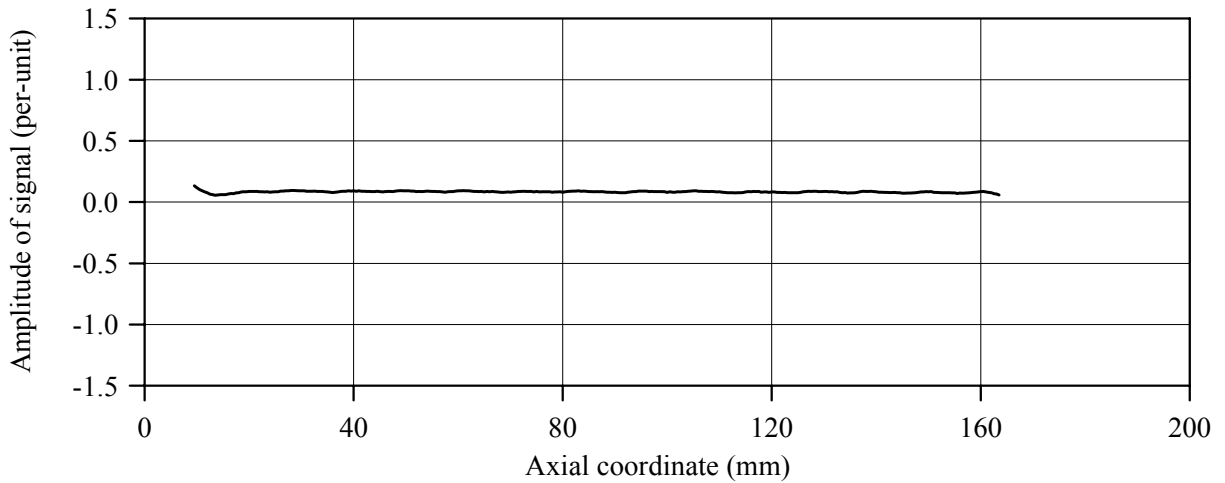
Fig.C-7.1. (a) Results of γ -scanning, (b) Axial fuel mass distribution and axial gas flow area distribution for fuel rod # RT7



a)



b)



c)

Fig.C-7.2. (a) Axial burnup distribution and (b) results of profilometry and (c) eddy-current examination of fuel rod # RT7

RT7

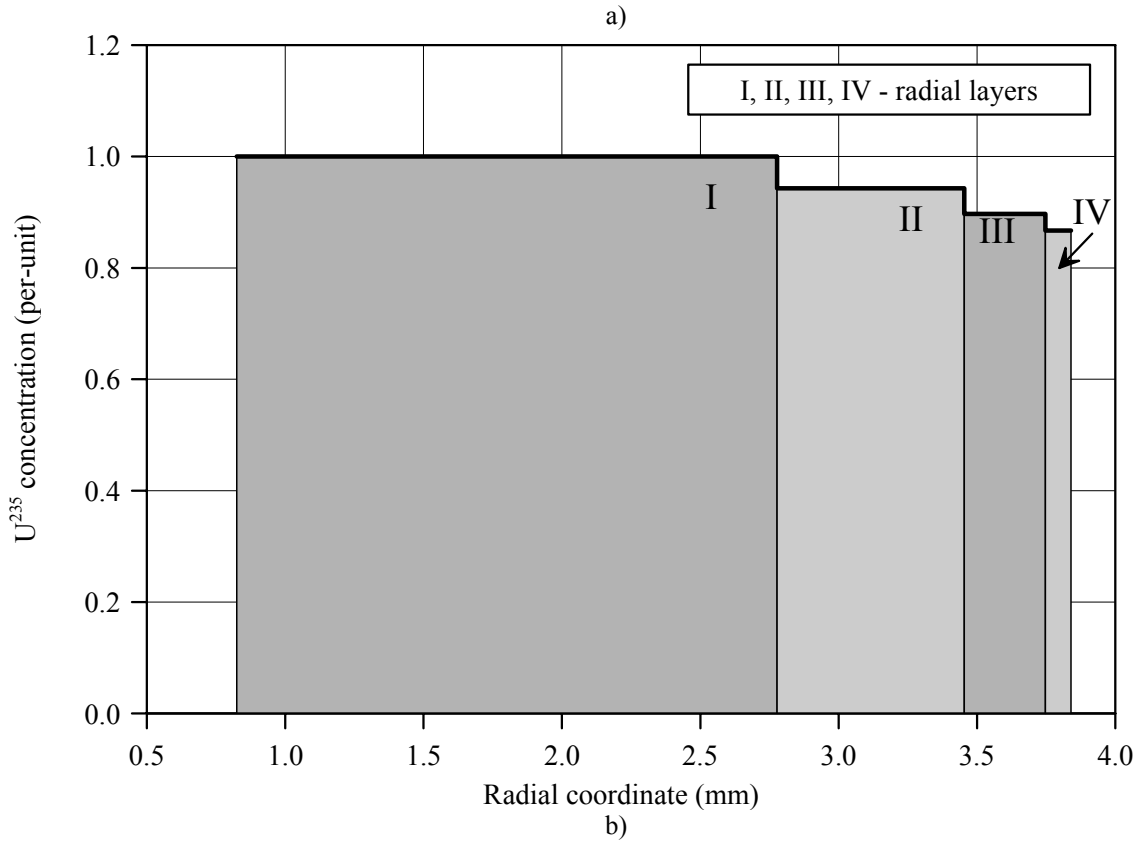
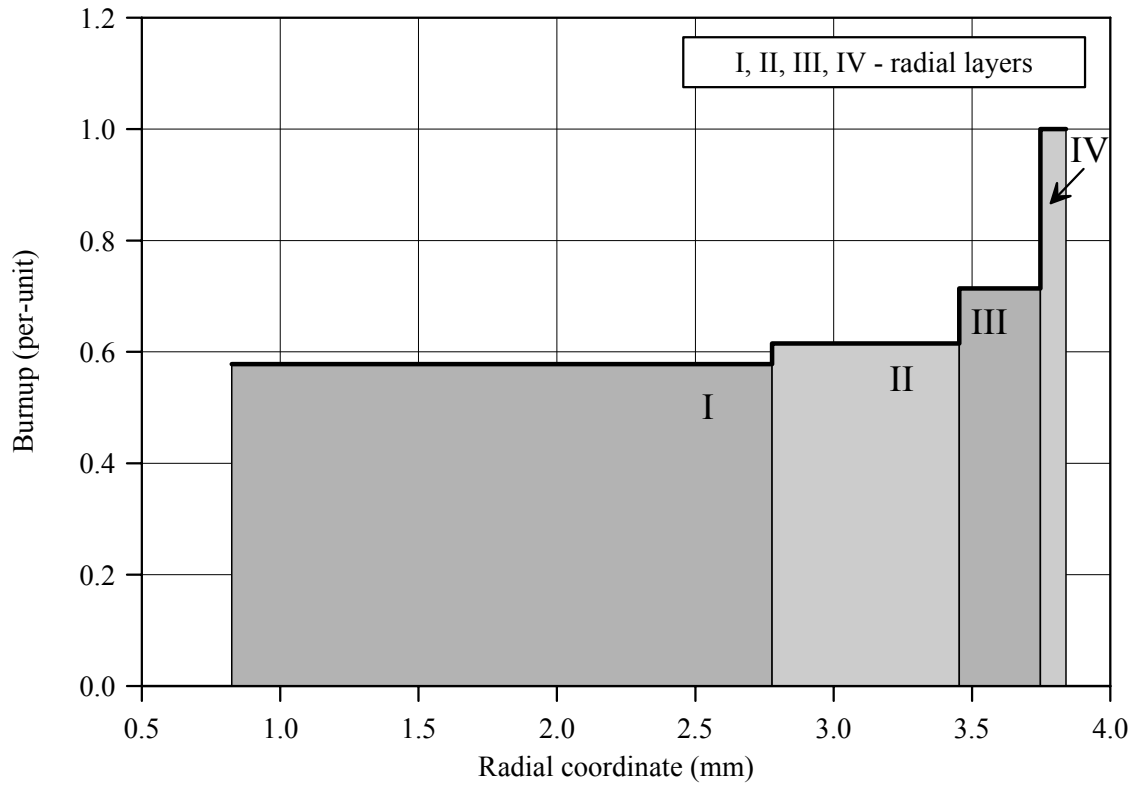
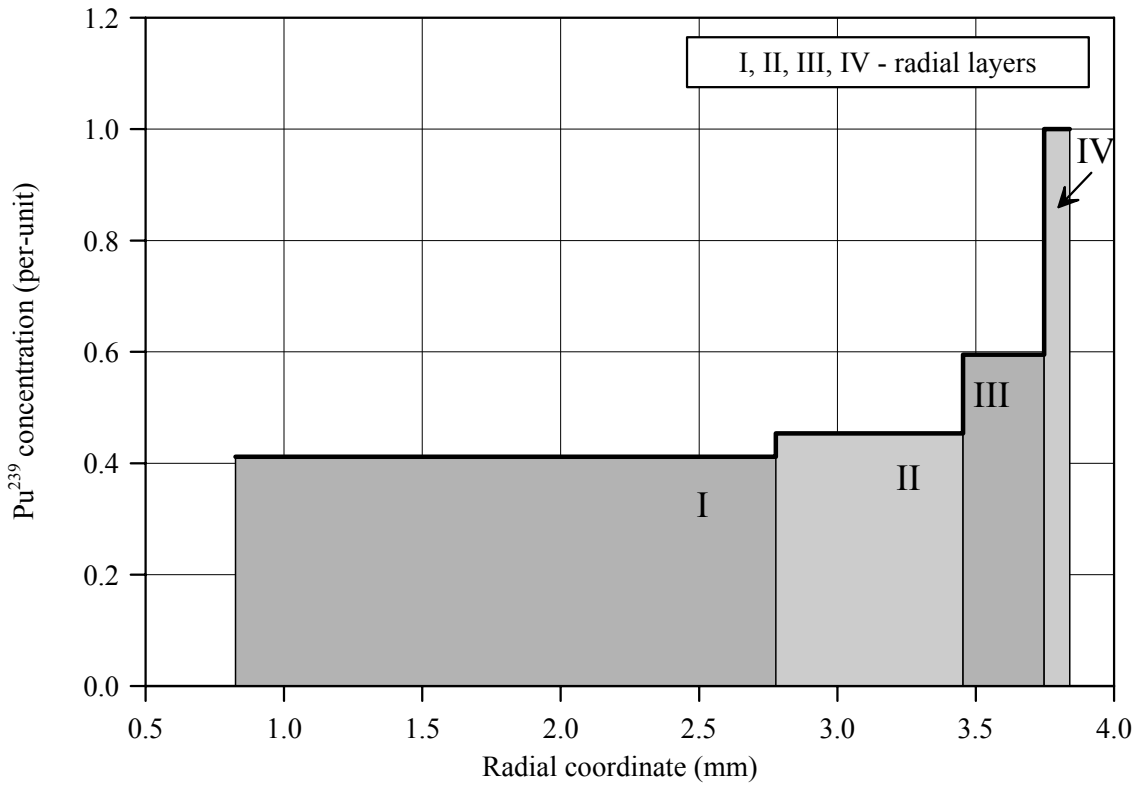
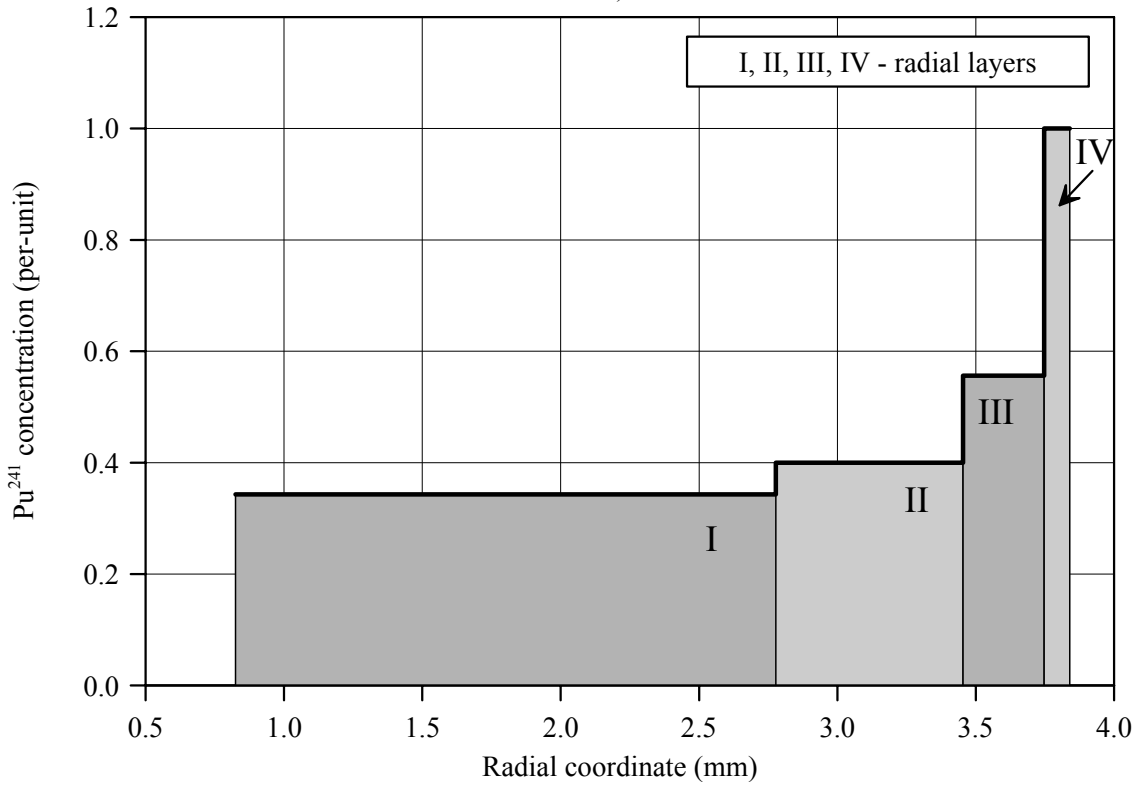


Fig.C-7.3. (a) Burnup radial distribution and (b) U^{235} radial distribution for fuel rod # RT7 (calculated values)



a)



b)

Fig.C-7.4. Radial distribution of (a) Pu^{239} and (b) Pu^{241} for fuel rod # RT7 (calculated values)

Appendix C-8
Individual Characteristics
of Fuel Rod # RT8 before the BGR Test

RT8**Table C-8.1. Radial distribution of isotope nuclear concentrations for fuel rod #RT8
(values averaged of over the fuel stack length)***

| Isotope | Isotopic concentrations (kg/t U) in four fuel radial layers | | | |
|------------------------|---|----------------|----------------|----------------|
| | 0.825-2.777 mm | 2.777-3.454 mm | 3.454-3.747 mm | 3.747-3.840 mm |
| U ²³⁴ | 0.220 | 0.219 | 0.220 | 0.227 |
| U ²³⁵ | 4.898 | 4.625 | 4.403 | 4.255 |
| U ²³⁶ | 6.668 | 6.642 | 6.620 | 6.611 |
| U ²³⁸ | 922.3 | 917.7 | 904.4 | 865.6 |
| Pu ²³⁸ | 0.523 | 0.565 | 0.638 | 0.810 |
| Pu ²³⁹ | 4.920 | 5.419 | 7.104 | 11.97 |
| Pu ²⁴⁰ | 2.755 | 2.838 | 3.487 | 5.565 |
| Pu ²⁴¹ | 0.967 | 1.131 | 1.571 | 2.833 |
| Pu ²⁴² | 0.985 | 1.196 | 1.720 | 3.217 |
| Np ²³⁷ | 1.406 | 1.460 | 1.507 | 1.538 |
| Am ²⁴¹ | 0.052 | 0.060 | 0.084 | 0.151 |
| Oxygen | 134.5 | 134.5 | 134.5 | 134.5 |
| Other fission products | 55.63 | 59.53 | 69.78 | 99.19 |

* Measured averaged concentrations and calculated relative radial distributions of isotopes (TRIFOB code) were used to develop these data

Table C-8.2. Initial individual characteristics of fuel rod # RT8*

| Axial coordinate (from lower cap) (mm) | Cladding average outer diameter (mm) | Fuel mass ** (g) | Linear fuel mass** (g/cm) | Gas flow area ^{3)**} (mm ²) | Burnup** (MW d/kg U) |
|--|---|---------------------|---------------------------------|--|-------------------------|
| 10 ¹⁾ | 9.087 | 0.16 | 3.23 | 15.22 | 60.37 |
| 15 | 9.087 | 1.68 | 3.35 | 14.06 | 60.50 |
| 20 | 9.081 | 2.25 | 4.49 | 3.10 | 59.88 |
| 25 | 9.083 | 2.26 | 4.52 | 2.81 | 59.16 |
| 30 | 9.073 | 2.25 | 4.50 | 3.00 | 59.80 |
| 35 | 9.083 | 2.24 | 4.48 | 3.20 | 60.92 |
| 40 | 9.082 | 2.28 | 4.56 | 2.43 | 60.06 |
| 45 | 9.085 | 2.30 | 4.59 | 2.14 | 58.18 |
| 50 | 9.080 | 2.29 | 4.57 | 2.33 | 58.69 |
| 55 | 9.092 | 2.26 | 4.52 | 2.81 | 60.98 |
| 60 | 9.097 | 2.23 | 4.45 | 3.48 | 61.60 |
| 65 | 9.104 | 2.22 | 4.44 | 3.58 | 60.40 |
| 70 | 9.085 | 2.25 | 4.51 | 2.91 | 59.78 |
| 75 | 9.095 | 2.25 | 4.50 | 3.00 | 60.21 |
| 80 | 9.093 | 2.24 | 4.47 | 3.29 | 60.72 |
| 85 | 9.105 | 2.23 | 4.46 | 3.39 | 60.94 |
| 90 | 9.089 | 2.23 | 4.46 | 3.39 | 60.96 |
| 95 | 9.080 | 2.23 | 4.46 | 3.39 | 60.86 |
| 100 | 9.083 | 2.24 | 4.47 | 3.29 | 60.67 |
| 105 | 9.078 | 2.24 | 4.48 | 3.20 | 60.46 |
| 110 | 9.087 | 2.24 | 4.48 | 3.20 | 60.32 |
| 115 | 9.084 | 2.24 | 4.48 | 3.20 | 60.26 |
| 120 | 9.086 | 2.24 | 4.48 | 3.20 | 60.21 |
| 125 | 9.073 | 2.24 | 4.49 | 3.10 | 60.17 |
| 130 | 9.085 | 2.25 | 4.49 | 3.10 | 60.12 |
| 135 | 9.084 | 2.26 | 4.51 | 2.91 | 59.99 |
| 140 | 9.096 | 2.26 | 4.52 | 2.81 | 59.65 |
| 145 | 9.088 | 2.26 | 4.52 | 2.81 | 59.39 |
| 150 | 9.094 | 2.26 | 4.52 | 2.81 | 59.79 |
| 155 | 9.091 | 2.13 | 4.25 | 5.41 | 60.69 |
| 160 ²⁾ | 9.091 | 1.51 | 3.36 | 13.97 | 61.03 |

* All parameters were determined using results of pre-test examinations

** Average values at the length interval equal to the axial coordinate ± 2.5 mm

¹⁾ Bottom end coordinate of fuel stack is 10.5 mm;

²⁾ Top end coordinate of fuel stack is 160.5 mm

³⁾ Gas flow area beyond the fuel stack (mm²):

Bottom: 0.0-3.0mm – 0.00; 3.0-10.5mm – 12.56

Bepx: 160.5-169.4mm – 25.36; 169.4-178.5mm – 46.35; 178.5-204.5mm – 28.26; 204.5-281mm – 47.27; 281-290mm – 28.26; 290-299mm – 0

RT8

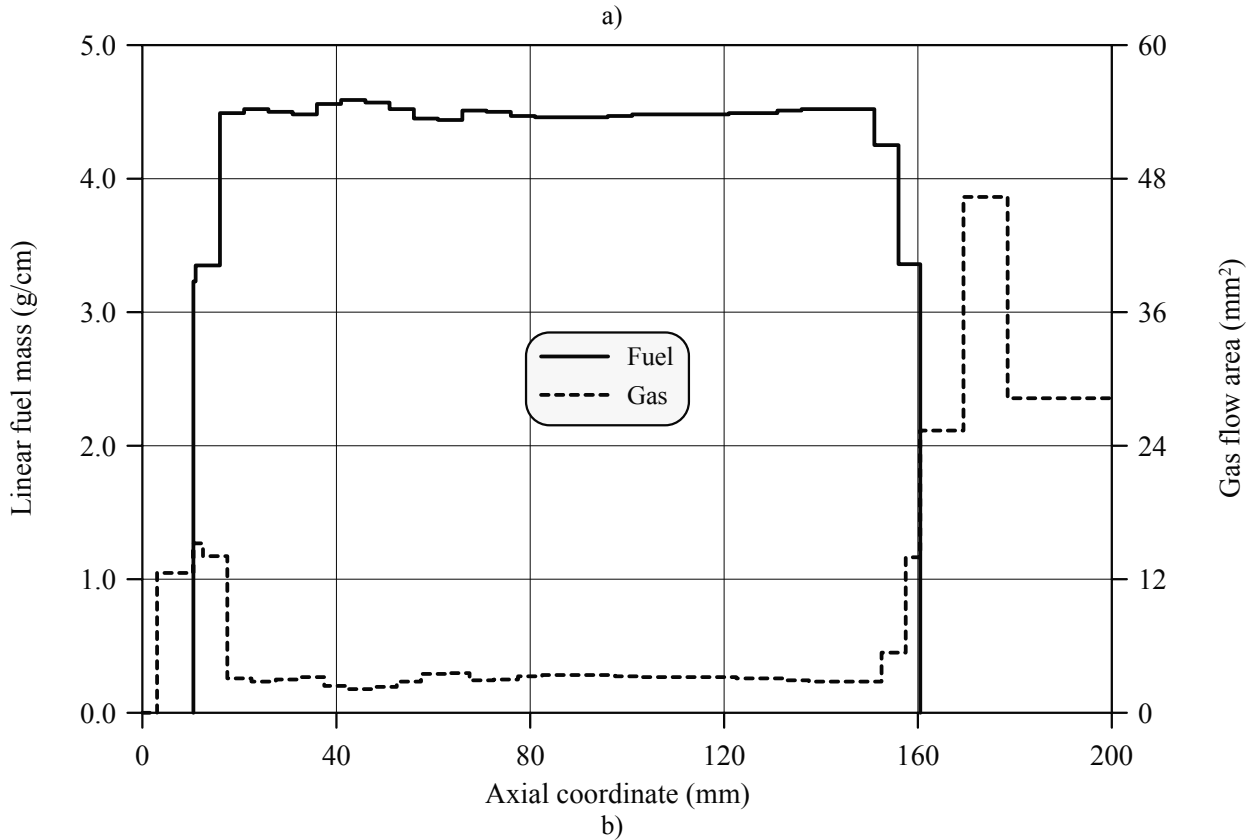
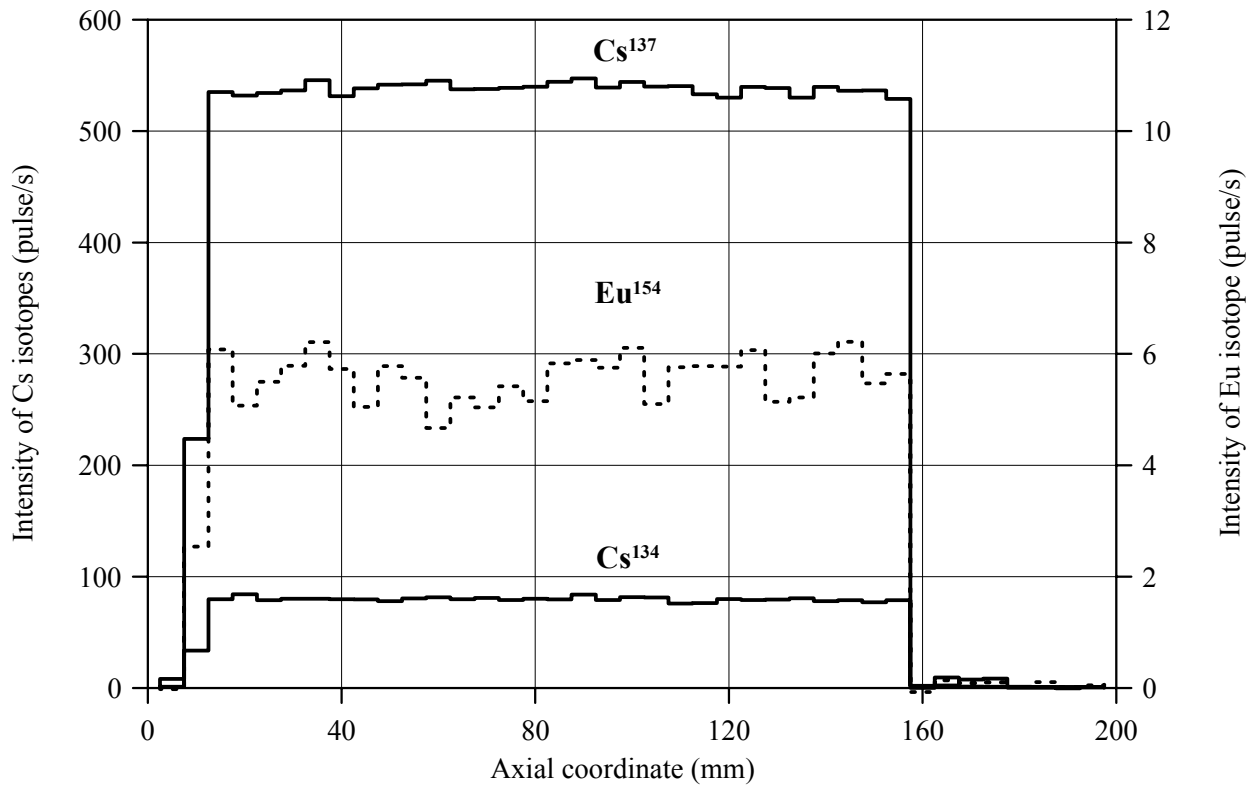
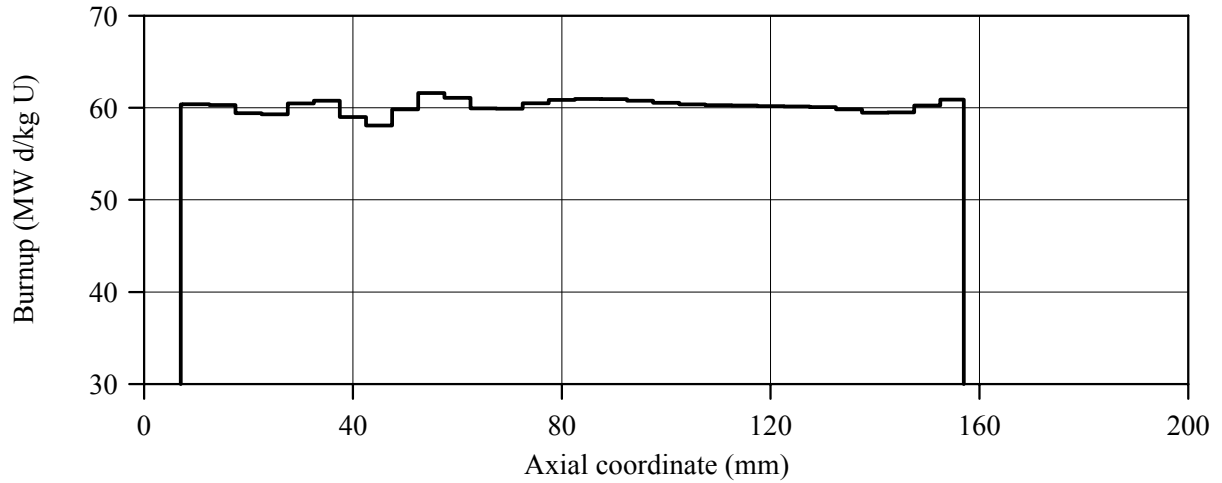
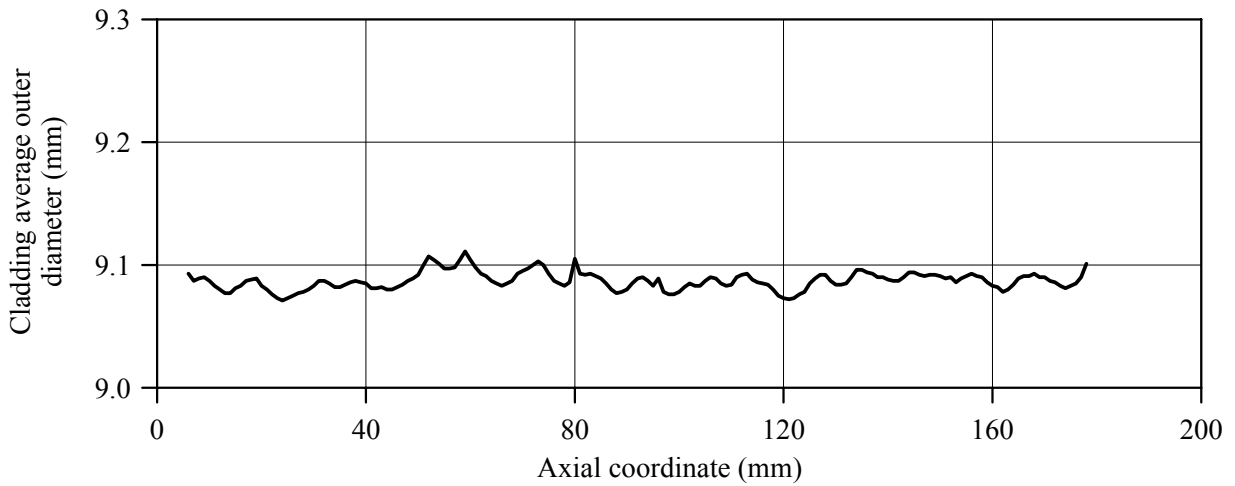


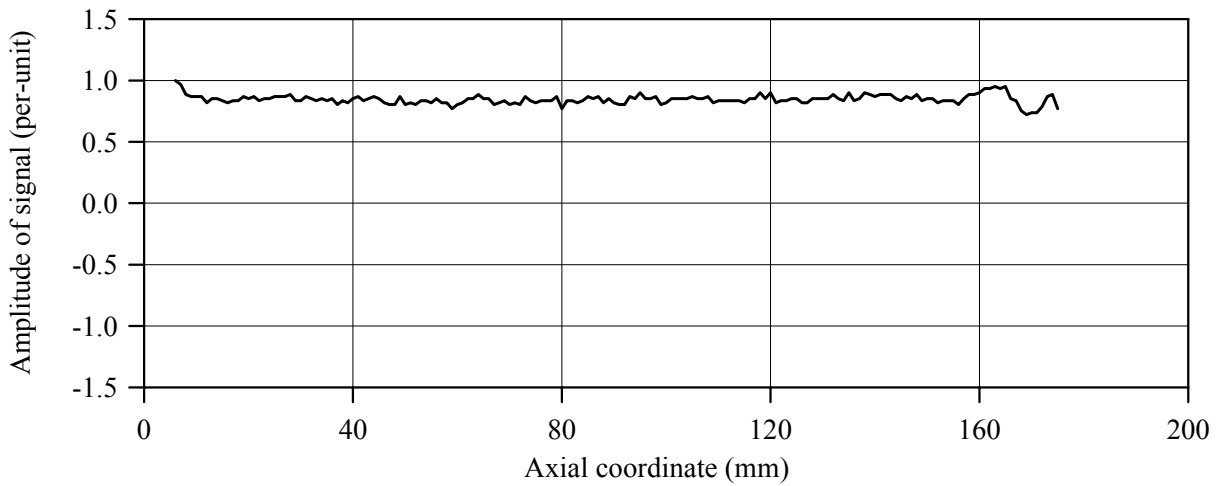
Fig.C-8.1. (a) Results of γ -scanning, (b) Axial fuel mass distribution and axial gas flow area distribution for fuel rod # RT8



a)



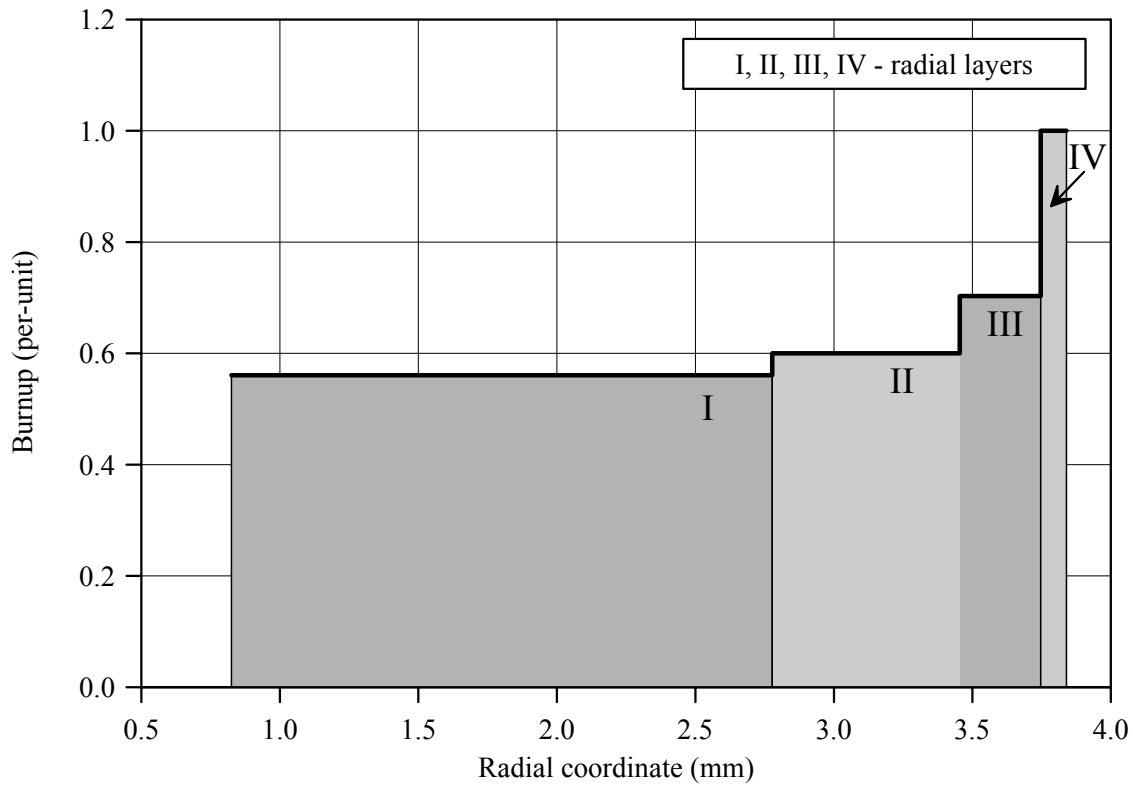
b)



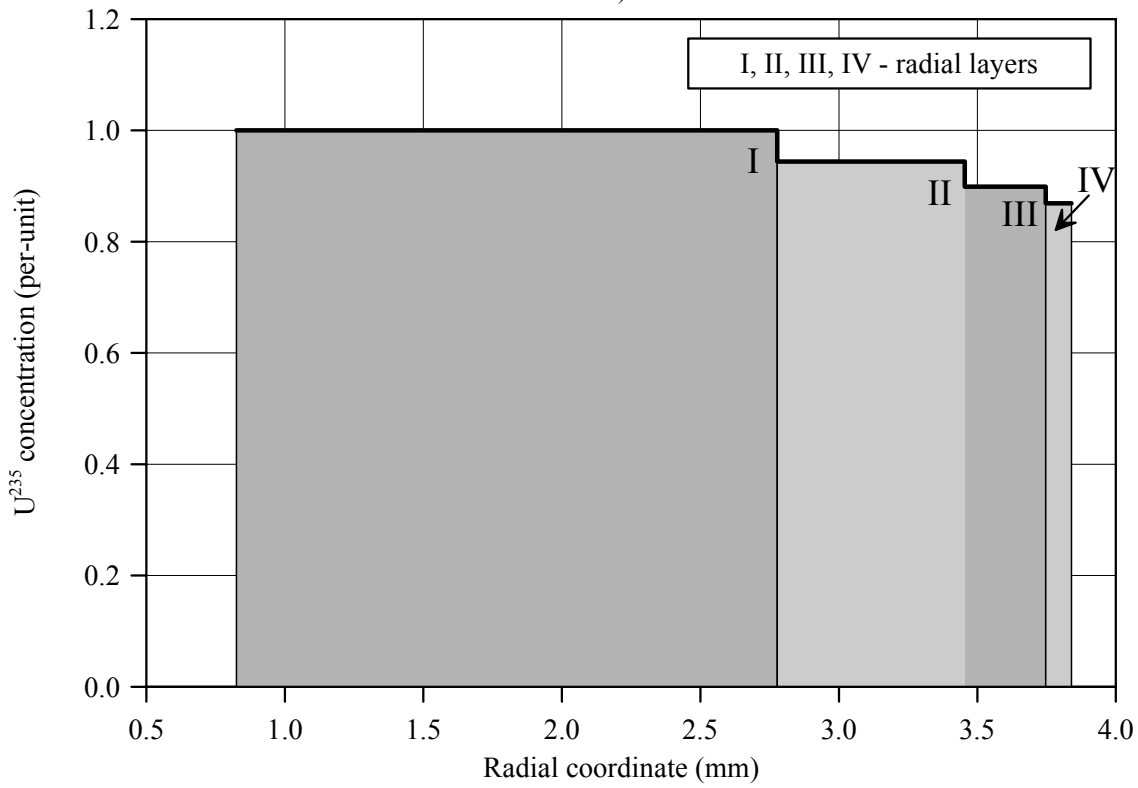
c)

Fig.C-8.2. (a) Axial burnup distribution and (b) results of profilometry and (c) eddy-current examination of fuel rod # RT8

RT8



a)



b)

Fig.C-8.3. (a) Burnup radial distribution and (b) U²³⁵ radial distribution for fuel rod # RT8 (calculated values)

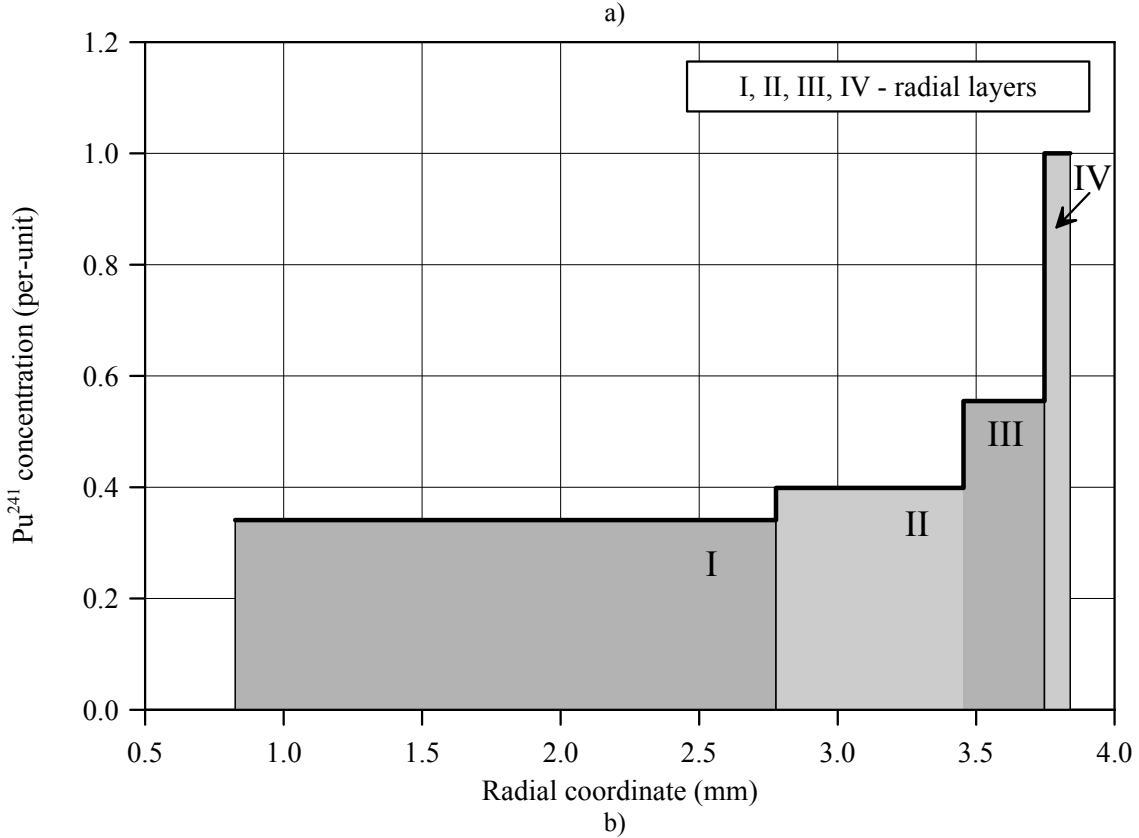
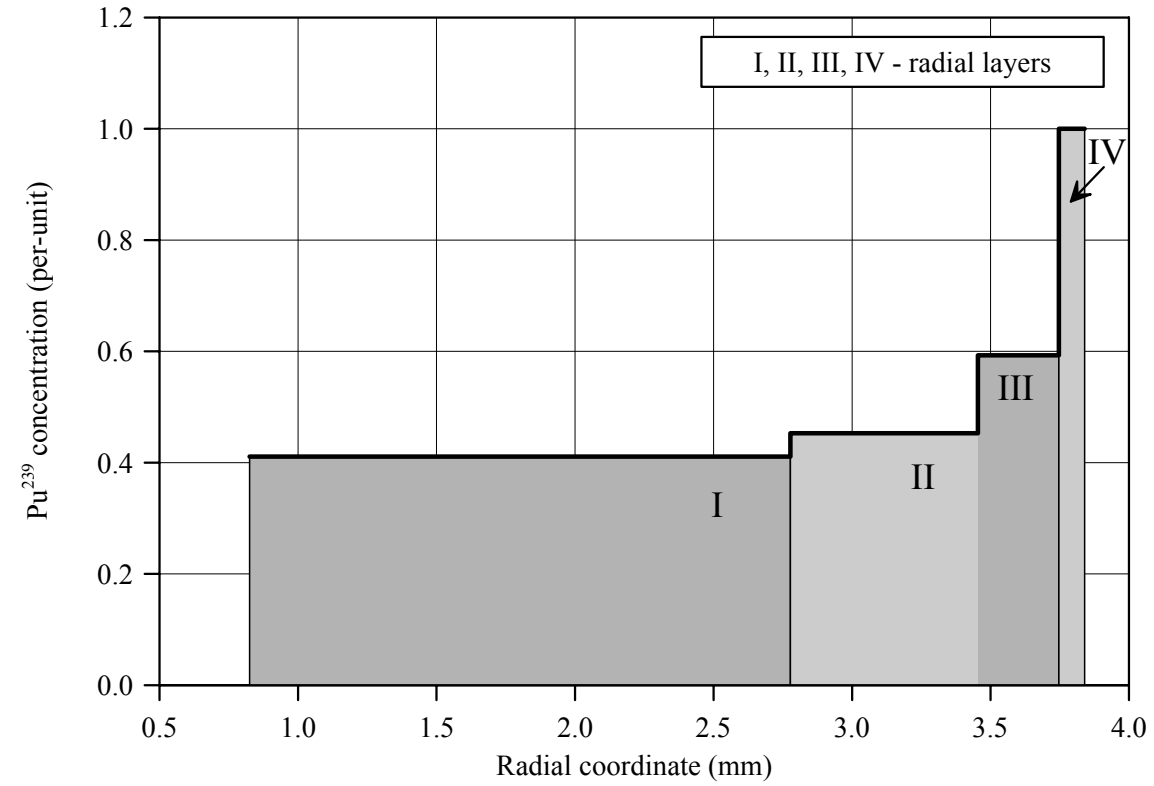


Fig.C-8.4. Radial distribution of (a) Pu^{239} and (b) Pu^{241} for fuel rod # RT8 (calculated values)

Appendix C-9
Individual Characteristics
of Fuel Rod # RT9 before the BGR Test

RT9**Table C-9.1. Radial distribution of isotope nuclear concentrations for fuel rod #RT9
(values averaged of over the fuel stack length)***

| Isotope | Isotopic concentrations (kg/t U) in four fuel radial layers | | | |
|------------------------|---|----------------|----------------|----------------|
| | 0.825-2.777 mm | 2.777-3.454 mm | 3.454-3.747 mm | 3.747-3.840 mm |
| U ²³⁴ | 0.220 | 0.219 | 0.220 | 0.227 |
| U ²³⁵ | 4.898 | 4.625 | 4.403 | 4.255 |
| U ²³⁶ | 6.668 | 6.642 | 6.620 | 6.611 |
| U ²³⁸ | 922.3 | 917.7 | 904.4 | 865.6 |
| Pu ²³⁸ | 0.523 | 0.565 | 0.638 | 0.810 |
| Pu ²³⁹ | 4.920 | 5.419 | 7.104 | 11.97 |
| Pu ²⁴⁰ | 2.755 | 2.838 | 3.487 | 5.565 |
| Pu ²⁴¹ | 0.967 | 1.131 | 1.571 | 2.833 |
| Pu ²⁴² | 0.985 | 1.196 | 1.720 | 3.217 |
| Np ²³⁷ | 1.406 | 1.460 | 1.507 | 1.538 |
| Am ²⁴¹ | 0.052 | 0.060 | 0.084 | 0.151 |
| Oxygen | 134.5 | 134.5 | 134.5 | 134.5 |
| Other fission products | 55.63 | 59.53 | 69.78 | 99.19 |

* Measured averaged concentrations and calculated relative radial distributions of isotopes (TRIFOB code) were used to develop these data

Table C-9.2. Initial individual characteristics of fuel rod # RT9*

| Axial coordinate (from lower cap) (mm) | Cladding average outer diameter (mm) | Fuel mass ** (g) | Linear fuel mass** (g/cm) | Gas flow area ^{3)**} (mm ²) | Burnup** (MW d/kg U) |
|--|---|---------------------|---------------------------------|--|-------------------------|
| 10 ¹⁾ | 9.068 | 1.88 | 4.20 | 5.62 | 58.98 |
| 15 | 9.072 | 2.28 | 4.56 | 2.14 | 59.33 |
| 20 | 9.073 | 2.25 | 4.51 | 2.62 | 59.75 |
| 25 | 9.062 | 2.23 | 4.46 | 3.11 | 59.99 |
| 30 | 9.070 | 2.21 | 4.42 | 3.49 | 60.03 |
| 35 | 9.051 | 2.20 | 4.41 | 3.59 | 60.10 |
| 40 | 9.059 | 2.20 | 4.41 | 3.59 | 60.24 |
| 45 | 9.063 | 2.21 | 4.43 | 3.40 | 60.19 |
| 50 | 9.071 | 2.22 | 4.45 | 3.20 | 59.92 |
| 55 | 9.068 | 2.23 | 4.45 | 3.20 | 59.75 |
| 60 | 9.073 | 2.22 | 4.44 | 3.30 | 59.79 |
| 65 | 9.073 | 2.22 | 4.44 | 3.30 | 59.93 |
| 70 | 9.075 | 2.21 | 4.42 | 3.49 | 60.15 |
| 75 | 9.076 | 2.20 | 4.39 | 3.78 | 60.57 |
| 80 | 9.068 | 2.19 | 4.37 | 3.98 | 61.05 |
| 85 | 9.076 | 2.19 | 4.38 | 3.88 | 61.06 |
| 90 | 9.078 | 2.20 | 4.39 | 3.78 | 60.64 |
| 95 | 9.073 | 2.20 | 4.41 | 3.59 | 60.52 |
| 100 | 9.073 | 2.21 | 4.43 | 3.40 | 60.77 |
| 105 | 9.072 | 2.22 | 4.45 | 3.20 | 60.59 |
| 110 | 9.073 | 2.24 | 4.47 | 3.01 | 59.82 |
| 115 | 9.080 | 2.25 | 4.50 | 2.72 | 59.27 |
| 120 | 9.068 | 2.25 | 4.50 | 2.72 | 59.22 |
| 125 | 9.069 | 2.24 | 4.48 | 2.91 | 59.14 |
| 130 | 9.066 | 2.24 | 4.48 | 2.91 | 58.87 |
| 135 | 9.067 | 2.25 | 4.50 | 2.72 | 58.73 |
| 140 | 9.066 | 2.26 | 4.52 | 2.52 | 58.87 |
| 145 | 9.069 | 2.27 | 4.54 | 2.33 | 59.15 |
| 150 | 9.068 | 2.27 | 4.54 | 2.33 | 59.47 |
| 155 | 9.063 | 1.90 | 4.27 | 4.95 | 59.78 |
| 160 ²⁾ | 9.072 | 1.94 | 4.29 | 4.75 | 60.05 |

* All parameters were determined using results of pre-test examinations

** Average values at the length interval equal to the axial coordinate ± 2.5 mm

¹⁾ Bottom end coordinate of fuel stack is 10.5 mm;

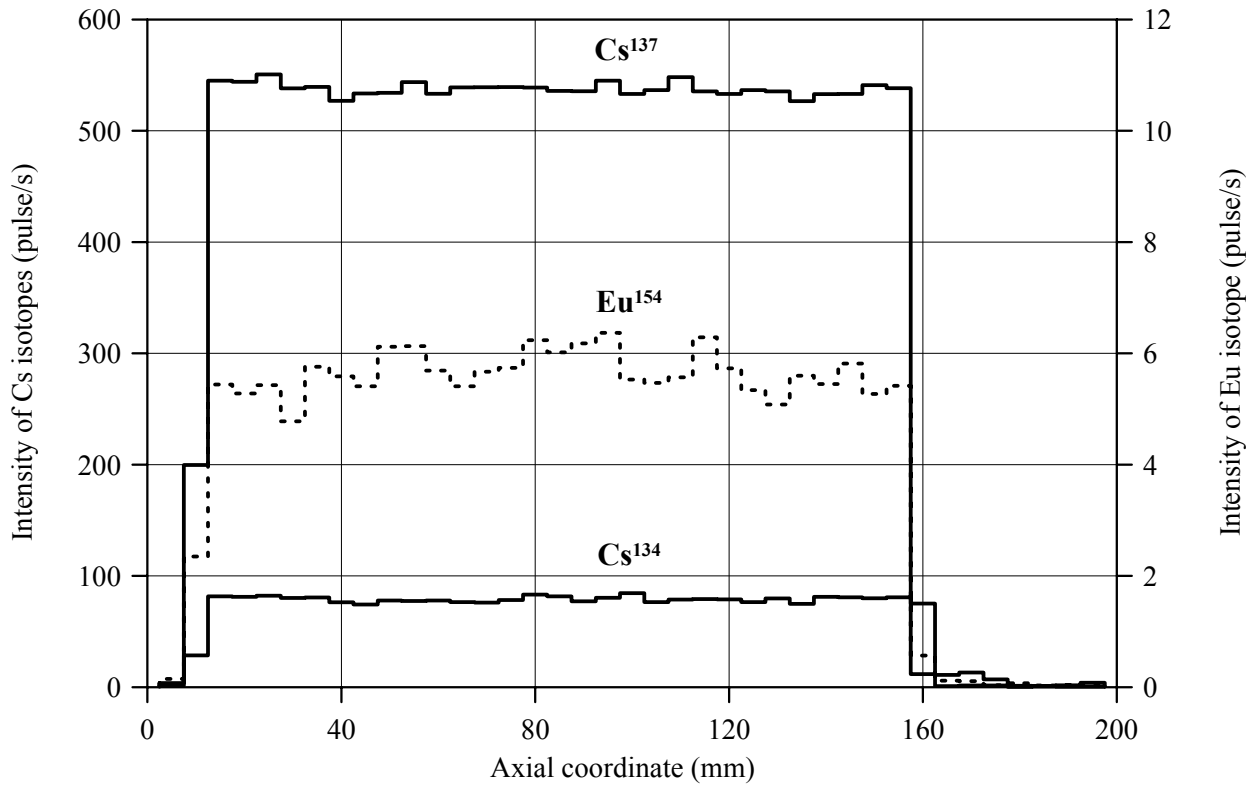
²⁾ Top end coordinate of fuel stack is 159.5 mm

³⁾ Gas flow area beyond the fuel stack (mm²):

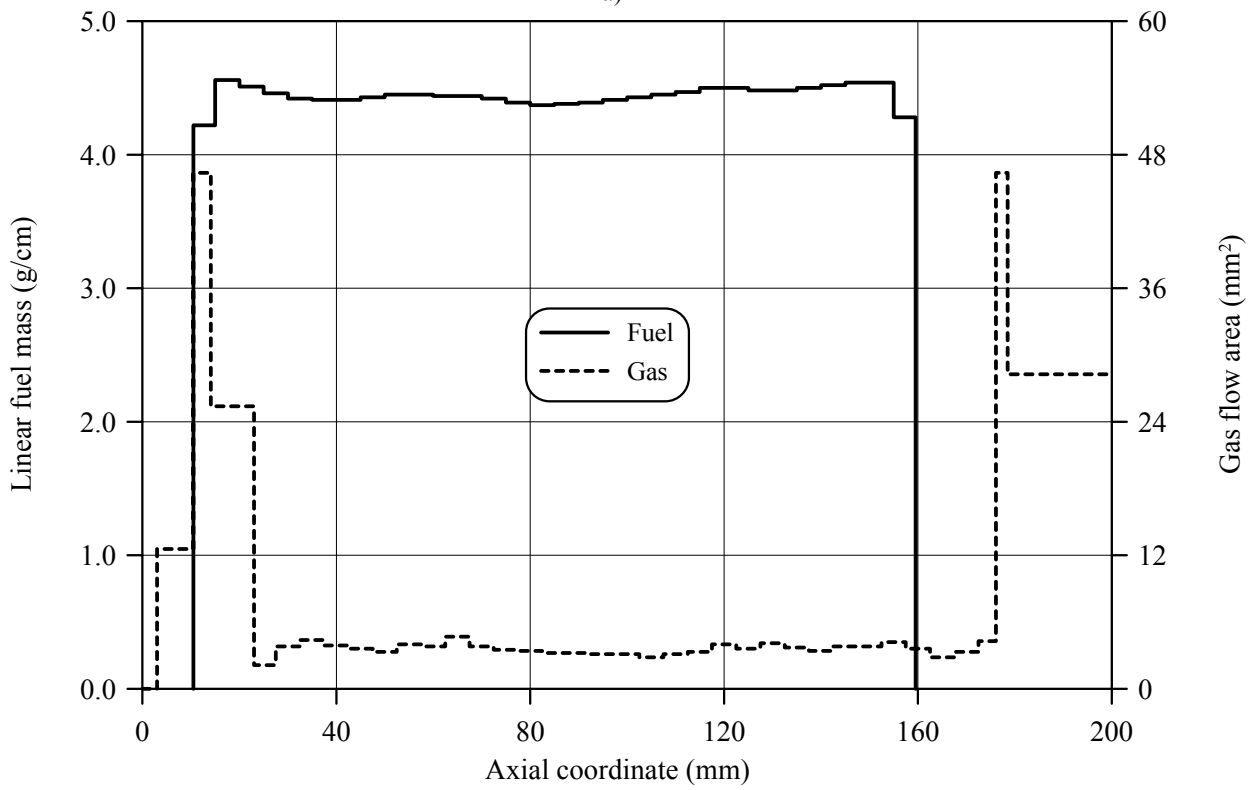
Bottom: 0.0-3.0mm – 0.00; 3.0-10.5mm – 12.56

Top: 159.5-159.4mm–25.34; 159.4-178.5mm–46.35; 178.5-204.5mm–28.26; 204.5-281mm–47.27; 281-290mm–28.26; 290-299mm–0

RT9

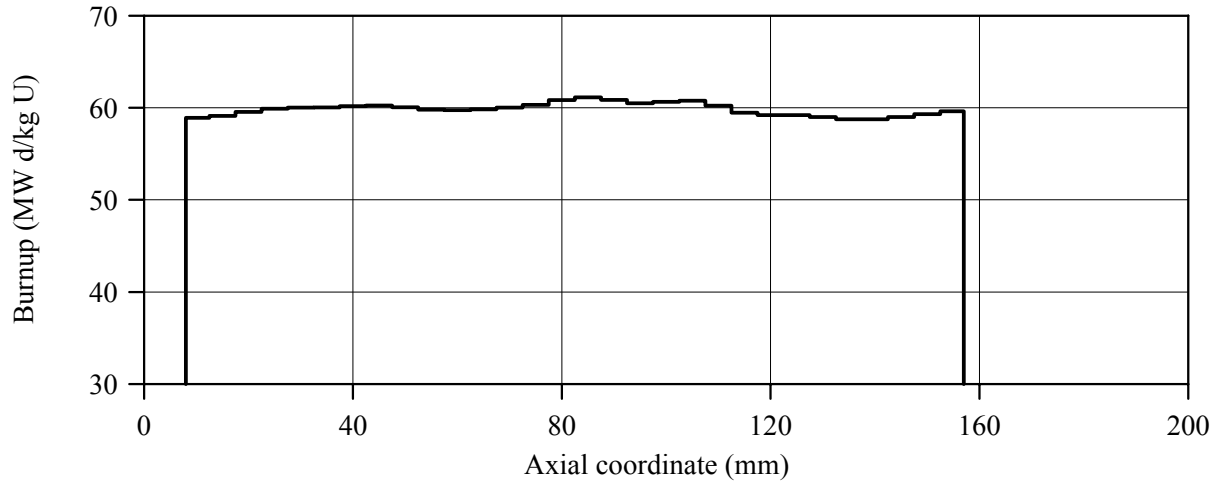


a)

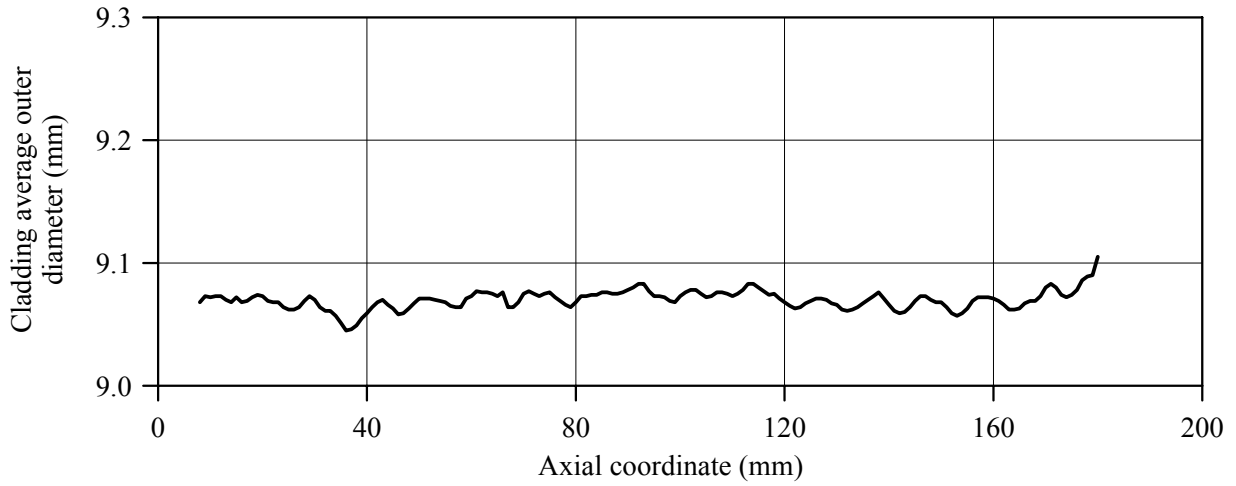


b)

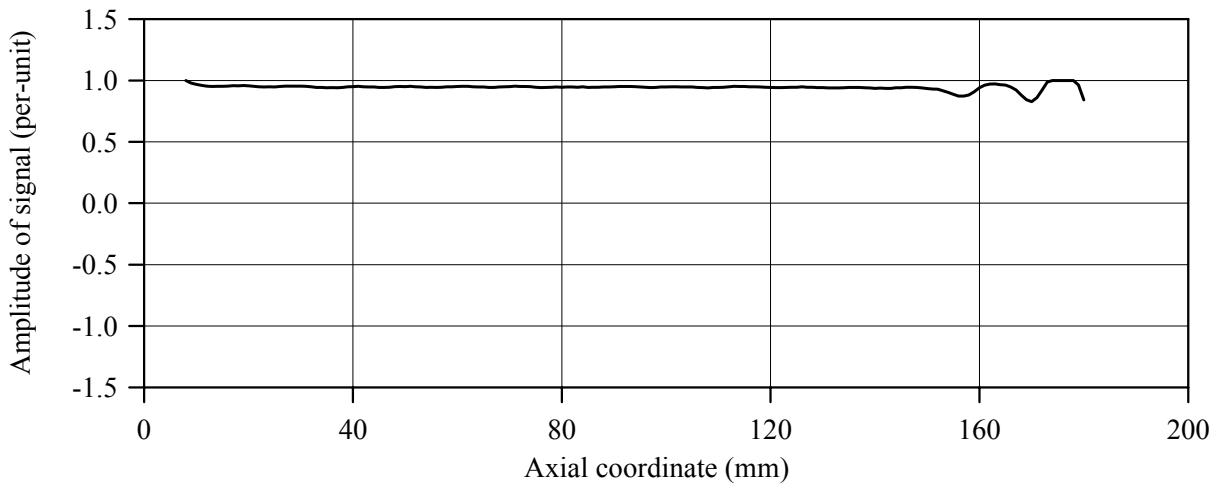
Fig.C-9.1. (a) Results of γ -scanning, (b) Axial fuel mass distribution and axial gas flow area distribution for fuel rod # RT9



a)



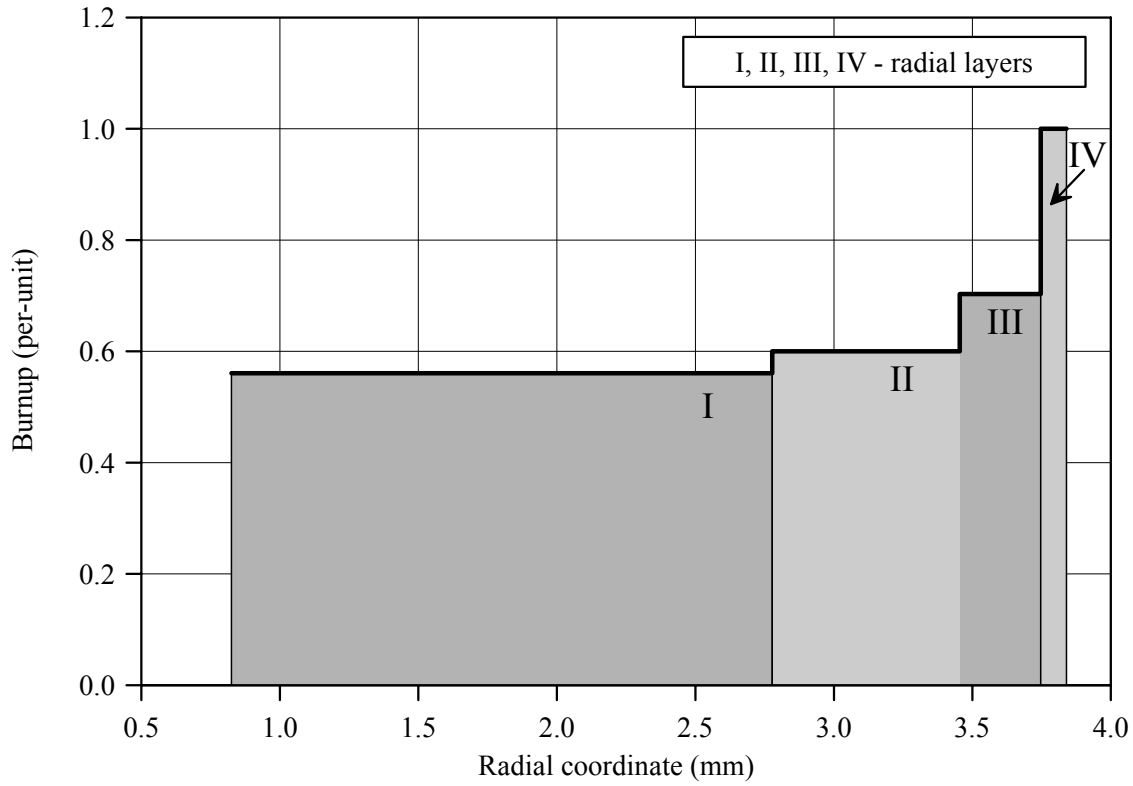
b)



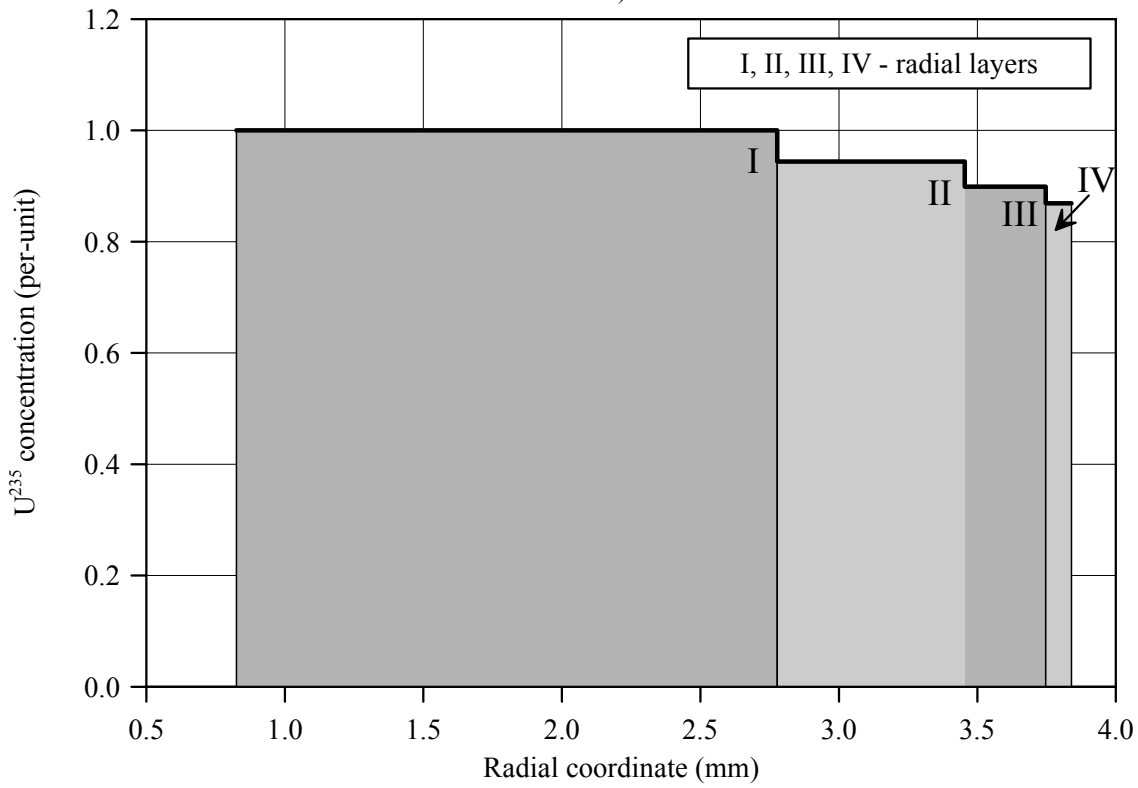
c)

Fig.C-9.2. (a) Axial burnup distribution and (b) results of profilometry and (c) eddy-current examination of fuel rod # RT9

RT9



a)



b)

Fig.C-9.3. (a) Burnup radial distribution and (b) U²³⁵ radial distribution for fuel rod # RT9 (calculated values)

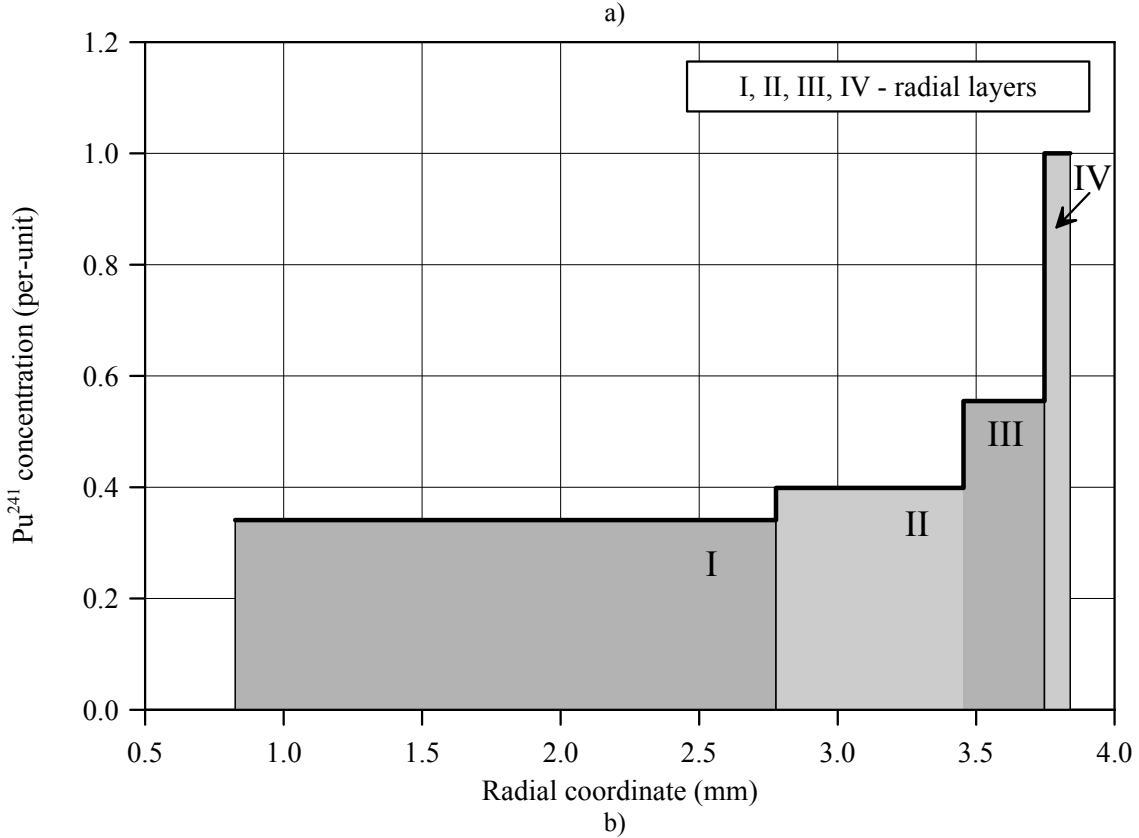
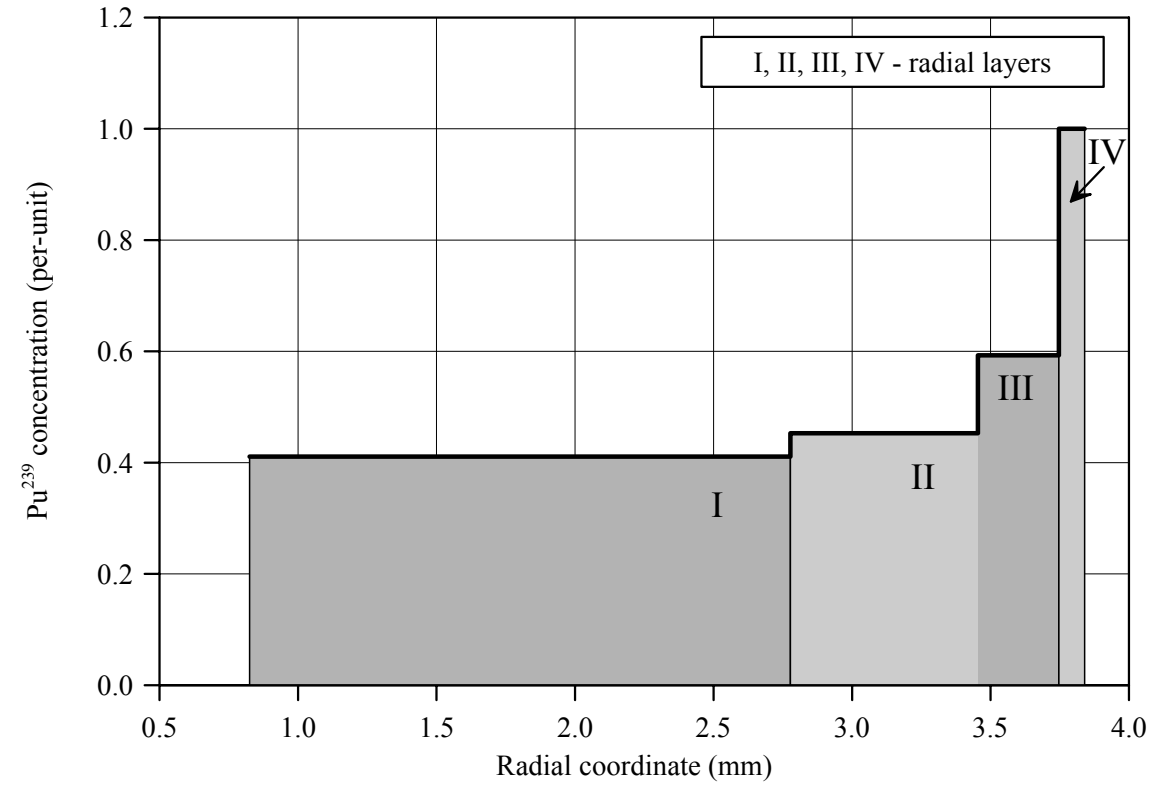


Fig.C-9.4. Radial distribution of (a) Pu^{239} and (b) Pu^{241} for fuel rod # RT9 (calculated values)

Appendix C-10
Individual Characteristics
of Fuel Rod # RT10 before the BGR Test

RT10**Table C-10.1. Radial distribution of isotope nuclear concentrations for fuel rod #RT10
(values averaged of over the fuel stack length)***

| Isotope | Isotopic concentrations (kg/t U) in four fuel radial layers | | | |
|------------------------|---|----------------|----------------|----------------|
| | 1.250-2.834 mm | 2.834-3.452 mm | 3.452-3.722 mm | 3.722-3.808 mm |
| U ²³⁴ | 0.212 | 0.209 | 0.206 | 0.203 |
| U ²³⁵ | 8.058 | 7.767 | 7.500 | 7.316 |
| U ²³⁶ | 6.746 | 6.765 | 6.783 | 6.802 |
| U ²³⁸ | 928.2 | 924.7 | 913.3 | 882.7 |
| Pu ²³⁸ | 0.266 | 0.281 | 0.303 | 0.343 |
| Pu ²³⁹ | 4.835 | 5.389 | 7.299 | 12.42 |
| Pu ²⁴⁰ | 2.546 | 2.711 | 3.509 | 5.742 |
| Pu ²⁴¹ | 0.867 | 1.020 | 1.459 | 2.635 |
| Pu ²⁴² | 0.719 | 0.868 | 1.277 | 2.375 |
| Np ²³⁷ | 1.290 | 1.331 | 1.371 | 1.399 |
| Am ²⁴¹ | 0.990 | 1.149 | 1.625 | 2.932 |
| Oxygen | 134.5 | 134.5 | 134.5 | 134.5 |
| Other fission products | 46.19 | 48.79 | 56.35 | 76.27 |

* Measured averaged concentrations and calculated relative radial distributions of isotopes (TRIFOB code) were used to develop these data

Table C-10.2. Initial individual characteristics of fuel rod # RT10*

| Axial coordinate (from lower cap) (mm) | Cladding average outer diameter (mm) | Fuel mass ** (g) | Linear fuel mass** (g/cm) | Gas flow area ^{3)**} (mm ²) | Burnup** (MW d/kg U) |
|--|---|---------------------|---------------------------------|--|-------------------------|
| 20 ¹⁾ | 9.076 | 0.45 | 4.11 | 5.68 | 46.87 |
| 25 | 9.075 | 2.07 | 4.13 | 5.49 | 46.93 |
| 30 | 9.073 | 2.09 | 4.18 | 5.00 | 46.60 |
| 35 | 9.073 | 2.10 | 4.19 | 4.91 | 46.31 |
| 40 | 9.074 | 2.09 | 4.18 | 5.00 | 46.65 |
| 45 | 9.074 | 2.07 | 4.15 | 5.29 | 47.25 |
| 50 | 9.075 | 2.06 | 4.12 | 5.58 | 47.36 |
| 55 | 9.073 | 2.05 | 4.10 | 5.78 | 47.10 |
| 60 | 9.073 | 2.06 | 4.11 | 5.68 | 47.02 |
| 65 | 9.076 | 2.07 | 4.15 | 5.29 | 47.06 |
| 70 | 9.075 | 2.07 | 4.15 | 5.29 | 46.85 |
| 75 | 9.075 | 2.07 | 4.14 | 5.39 | 46.60 |
| 80 | 9.073 | 2.07 | 4.13 | 5.49 | 46.77 |
| 85 | 9.071 | 2.06 | 4.12 | 5.58 | 47.08 |
| 90 | 9.080 | 2.08 | 4.15 | 5.29 | 46.91 |
| 95 | 9.072 | 2.08 | 4.16 | 5.20 | 46.61 |
| 100 | 9.072 | 2.07 | 4.13 | 5.49 | 46.97 |
| 105 | 9.068 | 2.06 | 4.11 | 5.68 | 47.56 |
| 110 | 9.066 | 2.04 | 4.08 | 5.97 | 47.44 |
| 115 | 9.071 | 2.04 | 4.08 | 5.97 | 46.91 |
| 120 | 9.071 | 2.05 | 4.10 | 5.78 | 46.84 |
| 125 | 9.070 | 2.06 | 4.11 | 5.68 | 47.08 |
| 130 | 9.069 | 2.06 | 4.13 | 5.49 | 47.02 |
| 135 | 9.071 | 2.07 | 4.13 | 5.49 | 46.84 |
| 140 | 9.069 | 2.06 | 4.11 | 5.68 | 47.13 |
| 145 | 9.069 | 2.05 | 4.11 | 5.68 | 47.54 |
| 150 | 9.069 | 2.05 | 4.10 | 5.78 | 47.36 |
| 155 | 9.068 | 2.05 | 4.11 | 5.68 | 46.82 |
| 160 | 9.071 | 2.03 | 4.06 | 6.17 | 46.65 |
| 165 | 9.068 | 1.99 | 3.99 | 6.85 | 46.83 |
| 170 | 9.070 | 2.01 | 4.02 | 6.55 | 46.91 |
| 175 ²⁾ | 9.069 | 0.37 | 4.11 | 5.68 | 46.89 |

* All parameters were determined using results of pre-test examinations

** Average values at the length interval equal to the axial coordinate ± 2.5 mm

¹⁾ Bottom end coordinate of fuel stack is 21.4 mm;

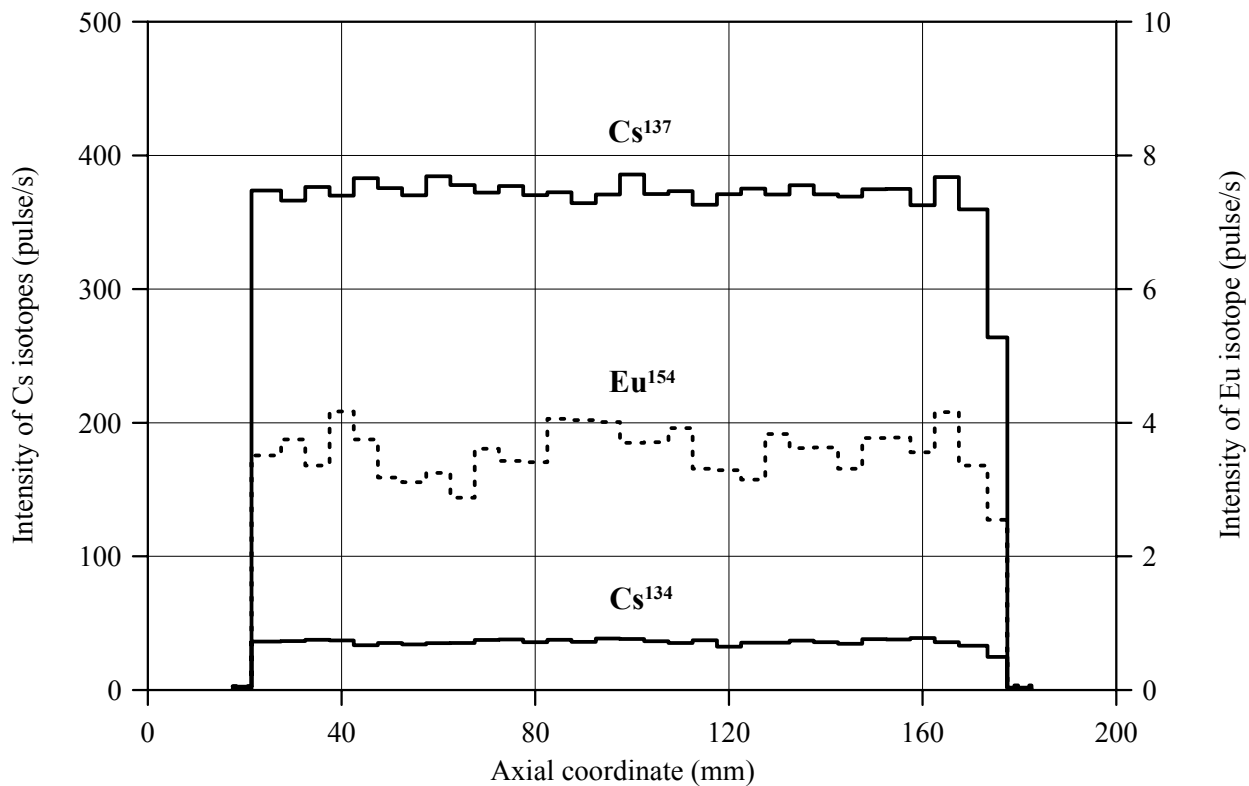
²⁾ Top end coordinate of fuel stack is 173.4 mm

³⁾ Gas flow area beyond the fuel stack (mm²):

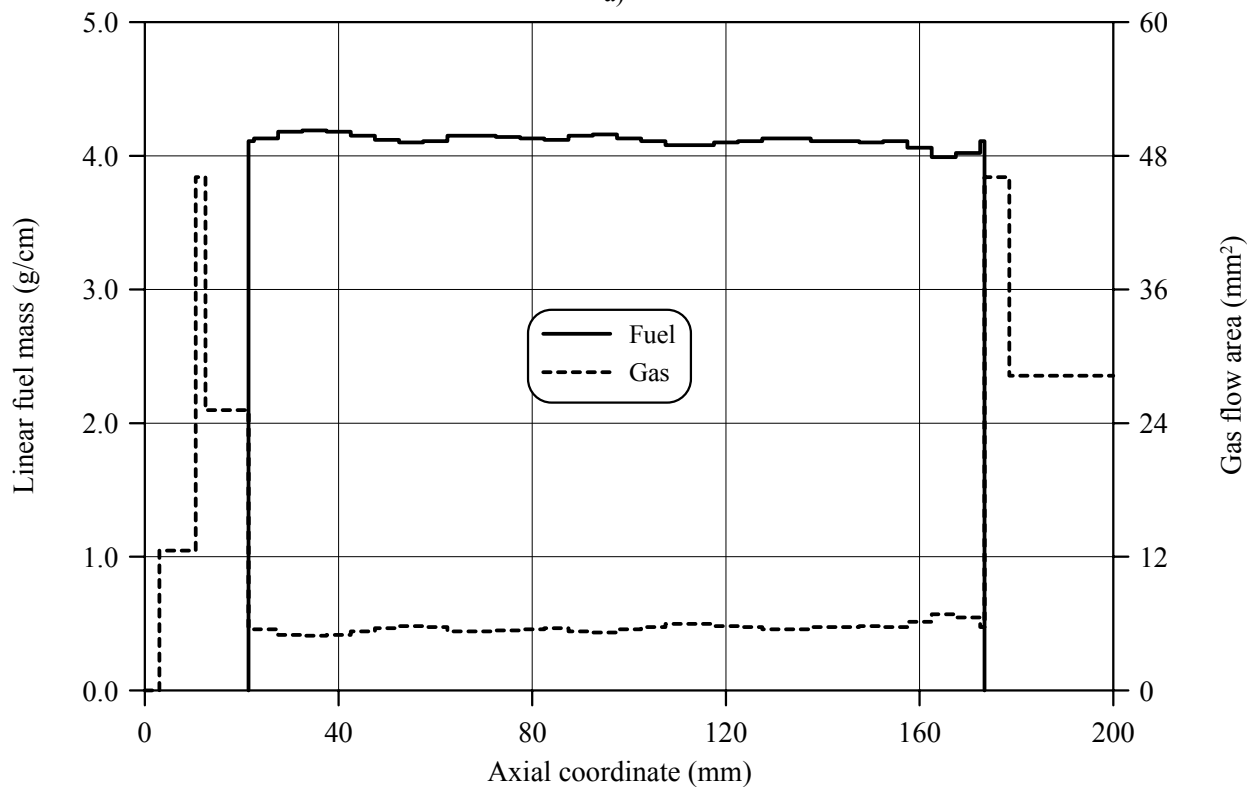
Bottom: 0.0-3.0mm – 0.00; 3.0-10.5mm – 12.56; 10.5-12.5mm – 46.08; 12.5-23.0mm – 25.17

Top: 173.4-178.5mm – 46.08; 178.5-204.5mm – 28.26; 204.5-281mm – 47.27; 281-290mm – 28.26; 290-299mm – 0.00

RT10

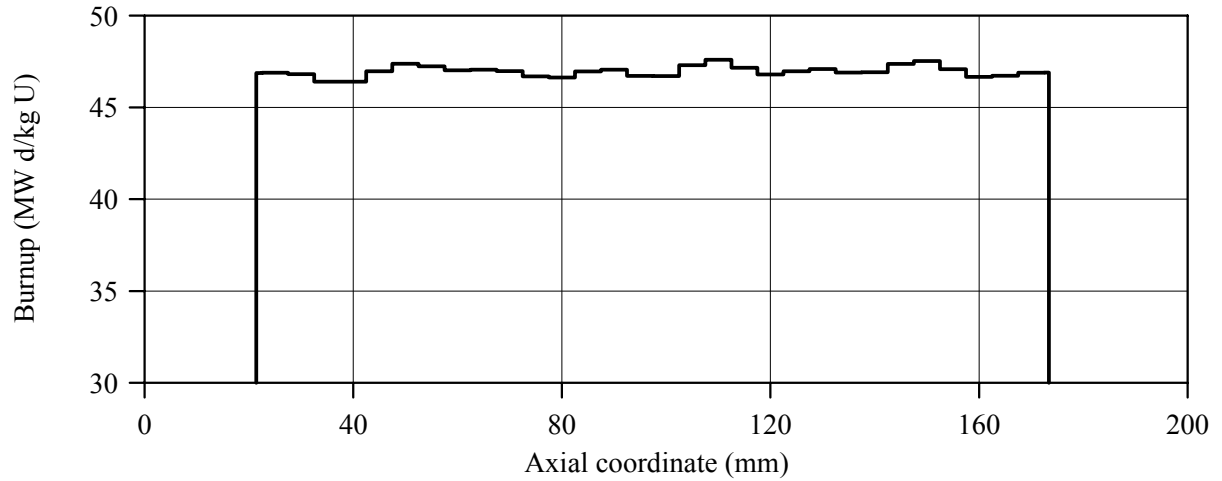


a)

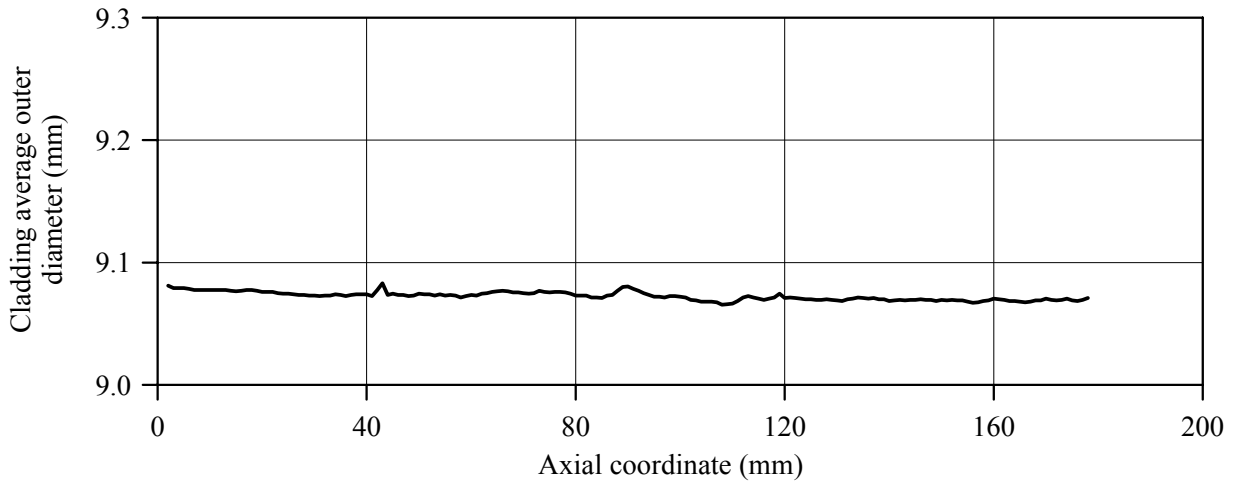


b)

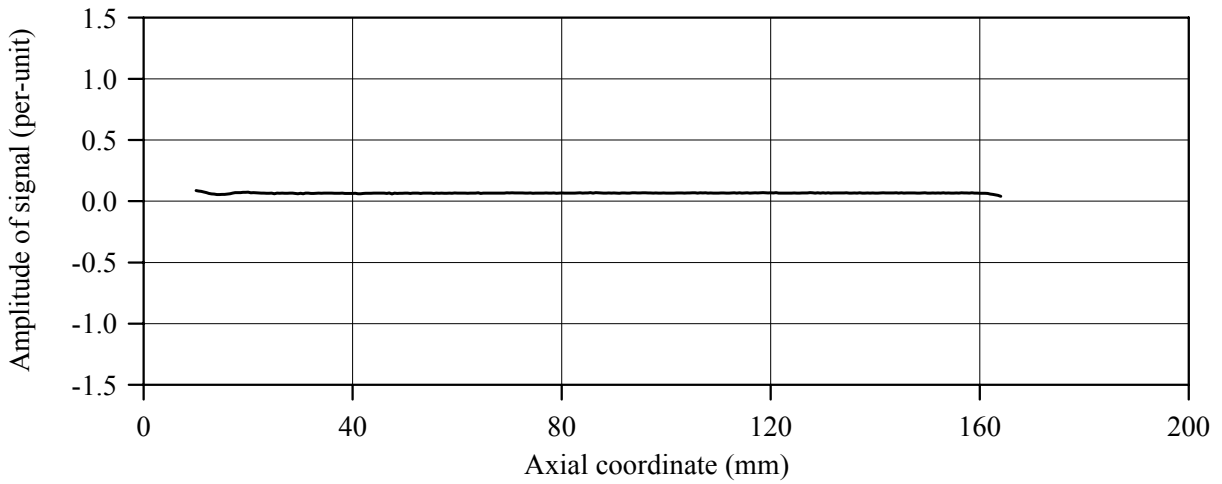
Fig.C-10.1. (a) Results of γ -scanning, (b) Axial fuel mass distribution and axial gas flow area distribution for fuel rod # RT10



a)



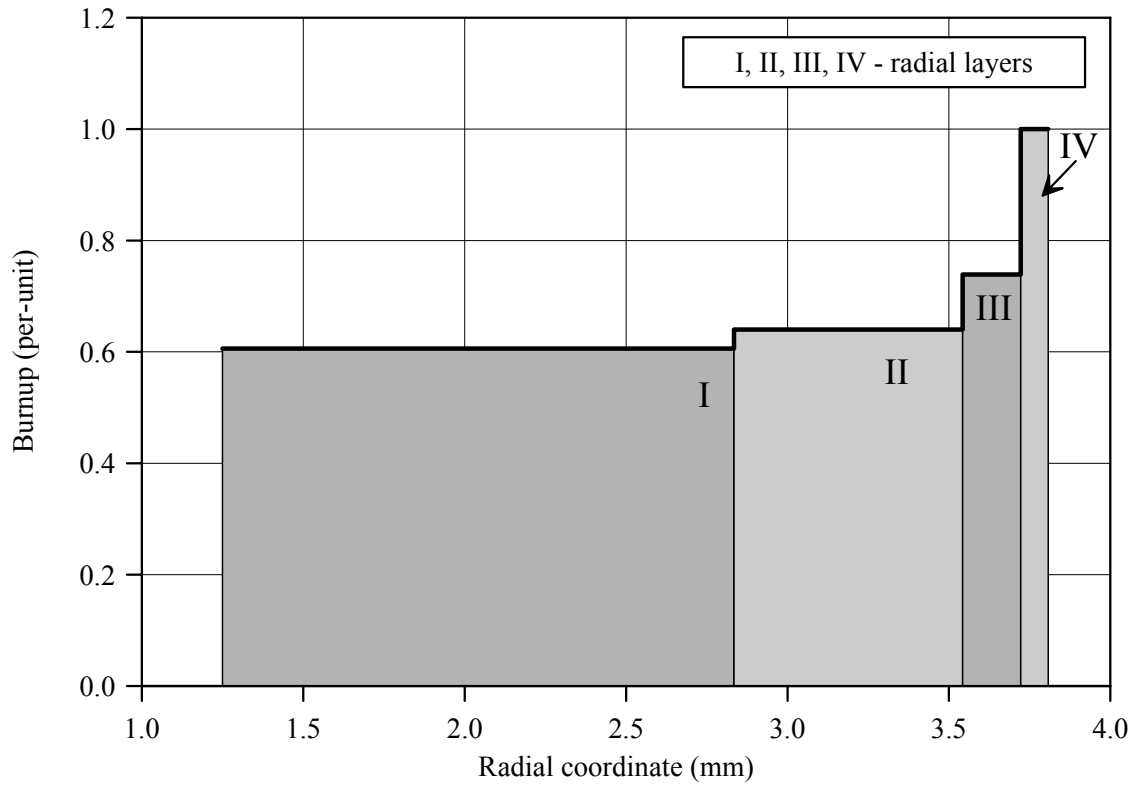
b)



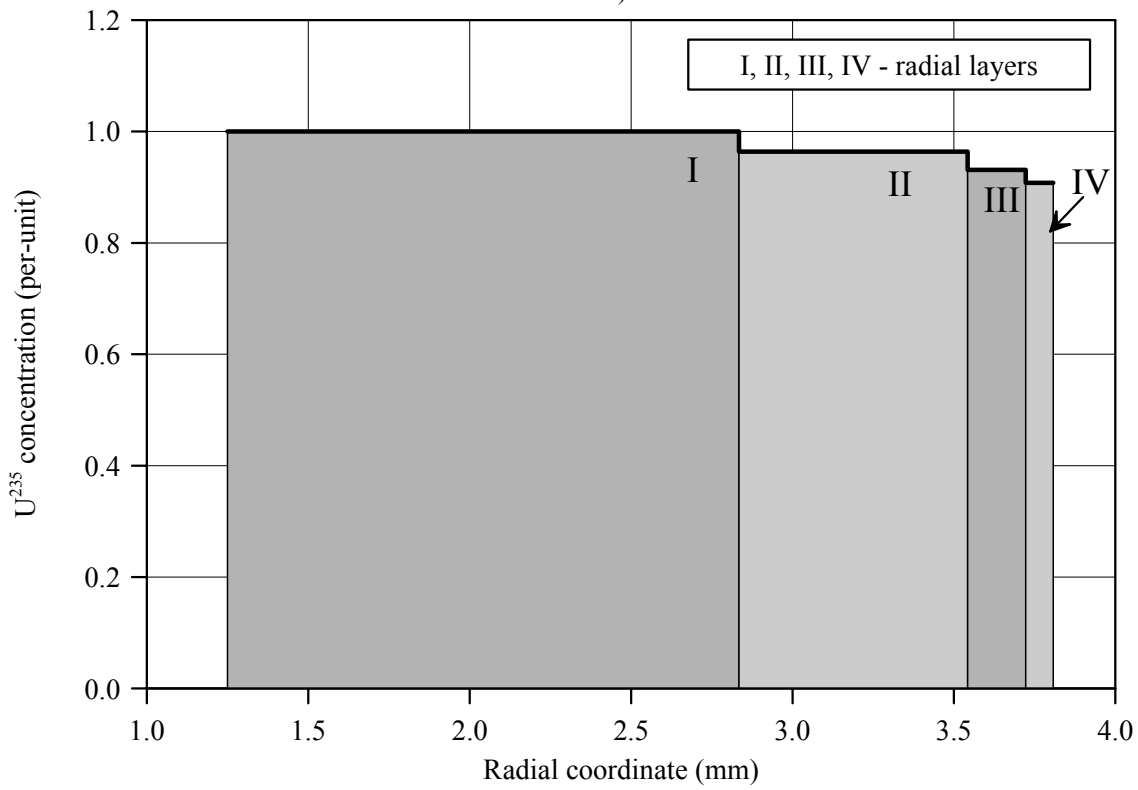
c)

Fig.C-10.2. (a) Axial burnup distribution and (b) results of profilometry and (c) eddy-current examination of fuel rod # RT10

RT10

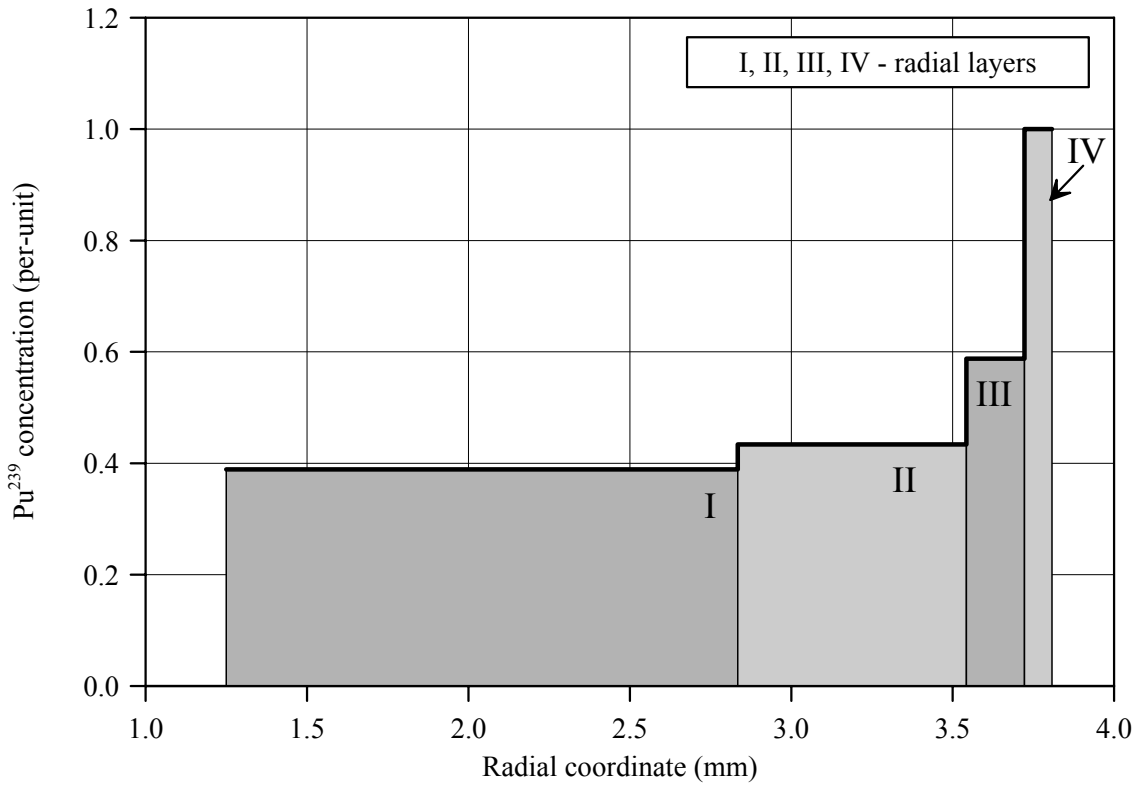


a)

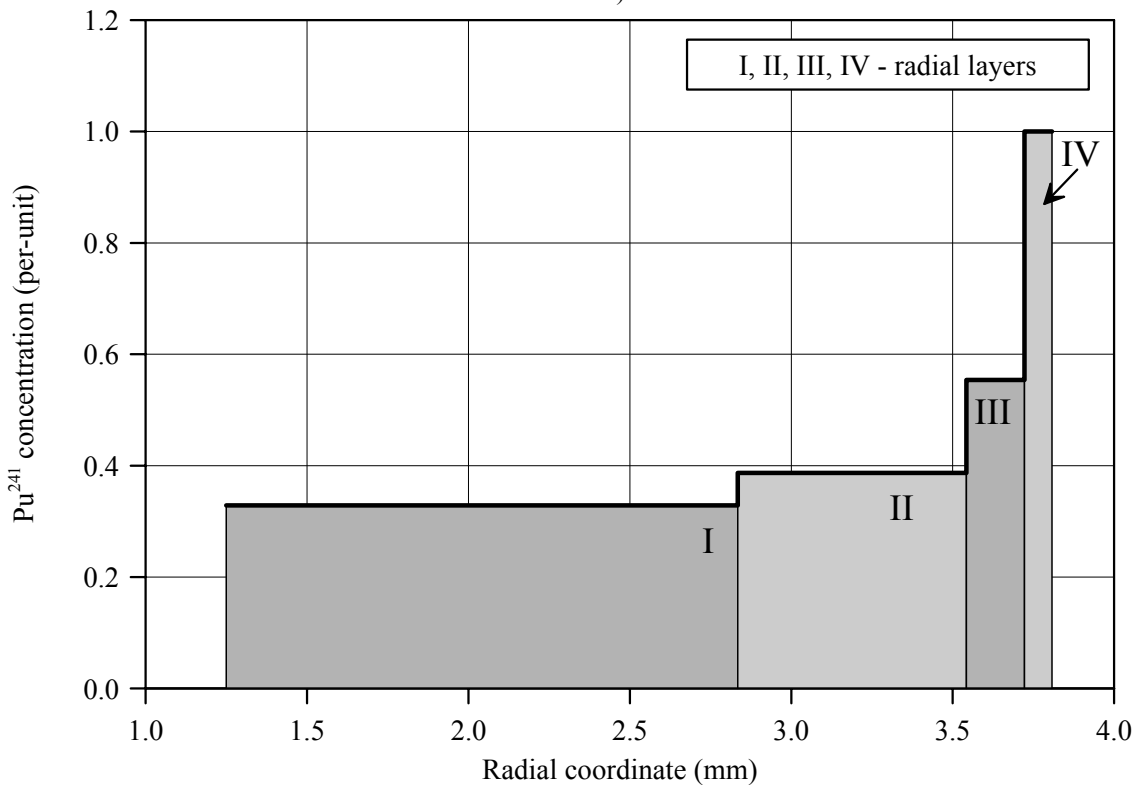


b)

Fig.C-10.3. (a) Burnup radial distribution and (b) U²³⁵ radial distribution for fuel rod # RT10 (calculated values)



a)



b)

Fig.C-10.4. Radial distribution of (a) Pu²³⁹ and (b) Pu²⁴¹ for fuel rod # RT10 (calculated values)

Appendix C-11
Individual Characteristics
of Fuel Rod # RT11 before the BGR Test

RT11**Table C-11.1. Radial distribution of isotope nuclear concentrations for fuel rod #RT11
(values averaged of over the fuel stack length)***

| Isotope | Isotopic concentrations (kg/t U) in four fuel radial layers | | | |
|------------------------|---|----------------|----------------|----------------|
| | 1.250-2.834 mm | 2.834-3.452 mm | 3.452-3.722 mm | 3.722-3.808 mm |
| U ²³⁴ | 0.212 | 0.209 | 0.206 | 0.203 |
| U ²³⁵ | 8.058 | 7.767 | 7.500 | 7.316 |
| U ²³⁶ | 6.746 | 6.765 | 6.783 | 6.802 |
| U ²³⁸ | 928.2 | 924.7 | 913.3 | 882.7 |
| Pu ²³⁸ | 0.266 | 0.281 | 0.303 | 0.343 |
| Pu ²³⁹ | 4.835 | 5.389 | 7.299 | 12.42 |
| Pu ²⁴⁰ | 2.546 | 2.711 | 3.509 | 5.742 |
| Pu ²⁴¹ | 0.851 | 1.001 | 1.432 | 2.587 |
| Pu ²⁴² | 0.719 | 0.868 | 1.277 | 2.375 |
| Np ²³⁷ | 1.290 | 1.331 | 1.371 | 1.399 |
| Am ²⁴¹ | 0.990 | 1.149 | 1.625 | 2.932 |
| Oxygen | 134.5 | 134.5 | 134.5 | 134.5 |
| Other fission products | 46.11 | 48.69 | 56.22 | 76.05 |

* Measured averaged concentrations and calculated relative radial distributions of isotopes (TRIFOB code) were used to develop these data

Table C-11.2. Initial individual characteristics of fuel rod # RT11*

| Axial coordinate (from lower cap) (mm) | Cladding average outer diameter (mm) | Fuel mass ** (g) | Linear fuel mass** (g/cm) | Gas flow area ^{3)**} (mm ²) | Burnup** (MW d/kg U) |
|--|---|---------------------|---------------------------------|--|-------------------------|
| 25 ¹⁾ | 9.095 | 1.76 | 3.91 | 8.59 | 46.49 |
| 30 | 9.088 | 2.02 | 4.03 | 7.46 | 46.30 |
| 35 | 9.087 | 2.10 | 4.19 | 5.95 | 46.26 |
| 40 | 9.089 | 2.15 | 4.30 | 4.91 | 46.41 |
| 45 | 9.087 | 2.15 | 4.30 | 4.91 | 46.39 |
| 50 | 9.089 | 2.15 | 4.29 | 5.00 | 46.22 |
| 55 | 9.088 | 2.14 | 4.27 | 5.19 | 46.44 |
| 60 | 9.083 | 2.13 | 4.26 | 5.28 | 47.02 |
| 65 | 9.083 | 2.13 | 4.26 | 5.28 | 47.16 |
| 70 | 9.083 | 2.11 | 4.22 | 5.66 | 46.77 |
| 75 | 9.082 | 2.11 | 4.21 | 5.76 | 46.81 |
| 80 | 9.081 | 2.11 | 4.21 | 5.76 | 47.48 |
| 85 | 9.083 | 2.09 | 4.18 | 6.04 | 47.93 |
| 90 | 9.083 | 2.08 | 4.16 | 6.23 | 47.81 |
| 95 | 9.082 | 2.07 | 4.15 | 6.32 | 47.56 |
| 100 | 9.085 | 2.08 | 4.15 | 6.32 | 47.40 |
| 105 | 9.082 | 2.09 | 4.18 | 6.04 | 47.28 |
| 110 | 9.085 | 2.11 | 4.21 | 5.76 | 47.23 |
| 115 | 9.082 | 2.10 | 4.20 | 5.85 | 47.42 |
| 120 | 9.081 | 2.08 | 4.17 | 6.13 | 47.76 |
| 125 | 9.085 | 2.06 | 4.13 | 6.51 | 47.76 |
| 130 | 9.081 | 2.07 | 4.14 | 6.42 | 47.42 |
| 135 | 9.085 | 2.07 | 4.13 | 6.51 | 47.32 |
| 140 | 9.080 | 2.07 | 4.14 | 6.42 | 47.62 |
| 145 | 9.082 | 2.07 | 4.14 | 6.42 | 47.81 |
| 150 | 9.080 | 2.06 | 4.12 | 6.61 | 47.72 |
| 155 | 9.080 | 2.07 | 4.13 | 6.51 | 47.68 |
| 160 | 9.082 | 2.07 | 4.14 | 6.42 | 47.76 |
| 165 | 9.080 | 2.10 | 4.21 | 5.76 | 47.64 |
| 170 | 9.083 | 1.82 | 3.64 | 11.14 | 47.27 |
| 175 ²⁾ | 9.082 | 0.71 | 2.84 | 18.70 | 46.92 |

* All parameters were determined using results of pre-test examinations

** Average values at the length interval equal to the axial coordinate ± 2.5 mm

¹⁾ Bottom end coordinate of fuel stack is 23 mm;

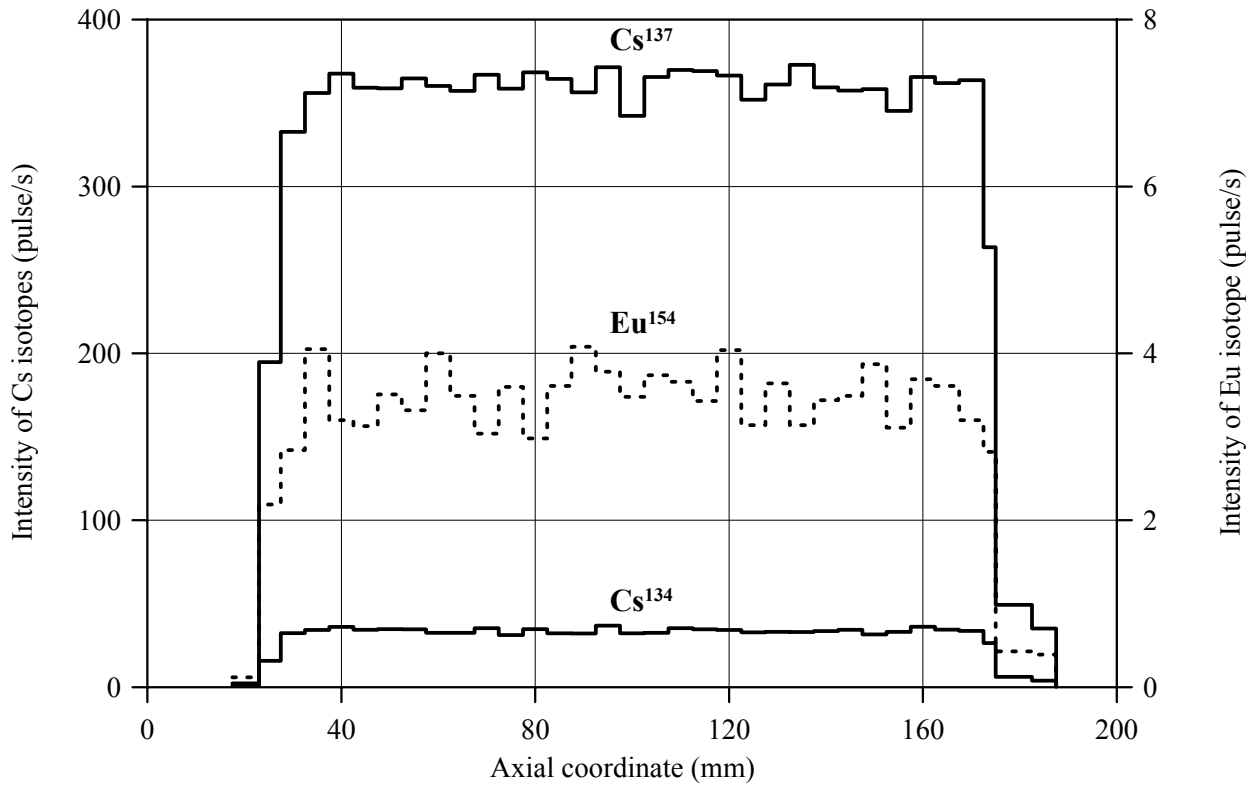
²⁾ Top end coordinate of fuel stack is 175 mm

³⁾ Gas flow area beyond the fuel stack (mm²):

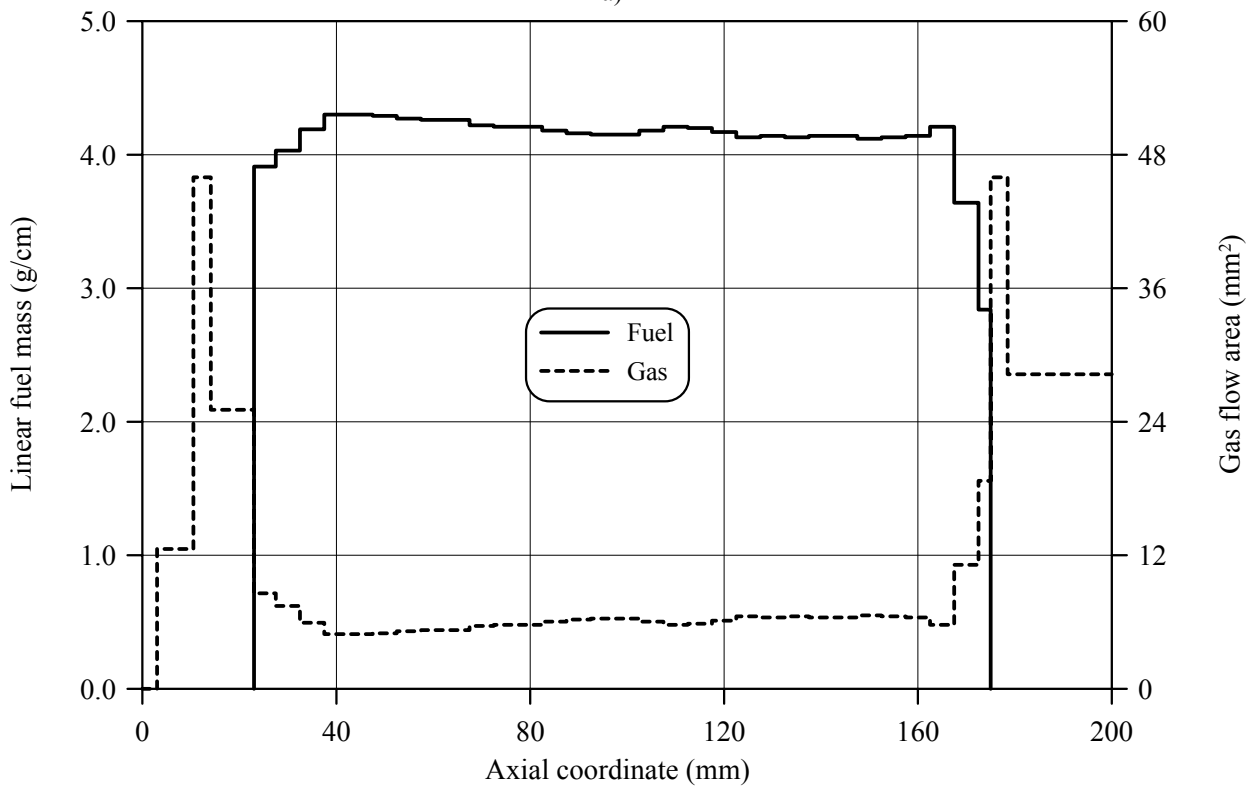
Bottom: 0.0-3.0mm – 0.00; 3.0-10.5mm – 12.56; 10.5-14.1mm – 45.96; 14.1-23.0mm – 25.08

Top: 176.1-178.5mm – 45.96; 178.5-204.5mm – 28.26; 204.5-281mm – 47.27; 281-290mm – 28.26; 290-299mm – 0.00

RT11



a)



b)

Fig.C-11.1. (a) Results of γ -scanning, (b) Axial fuel mass distribution and axial gas flow area distribution for fuel rod # RT11

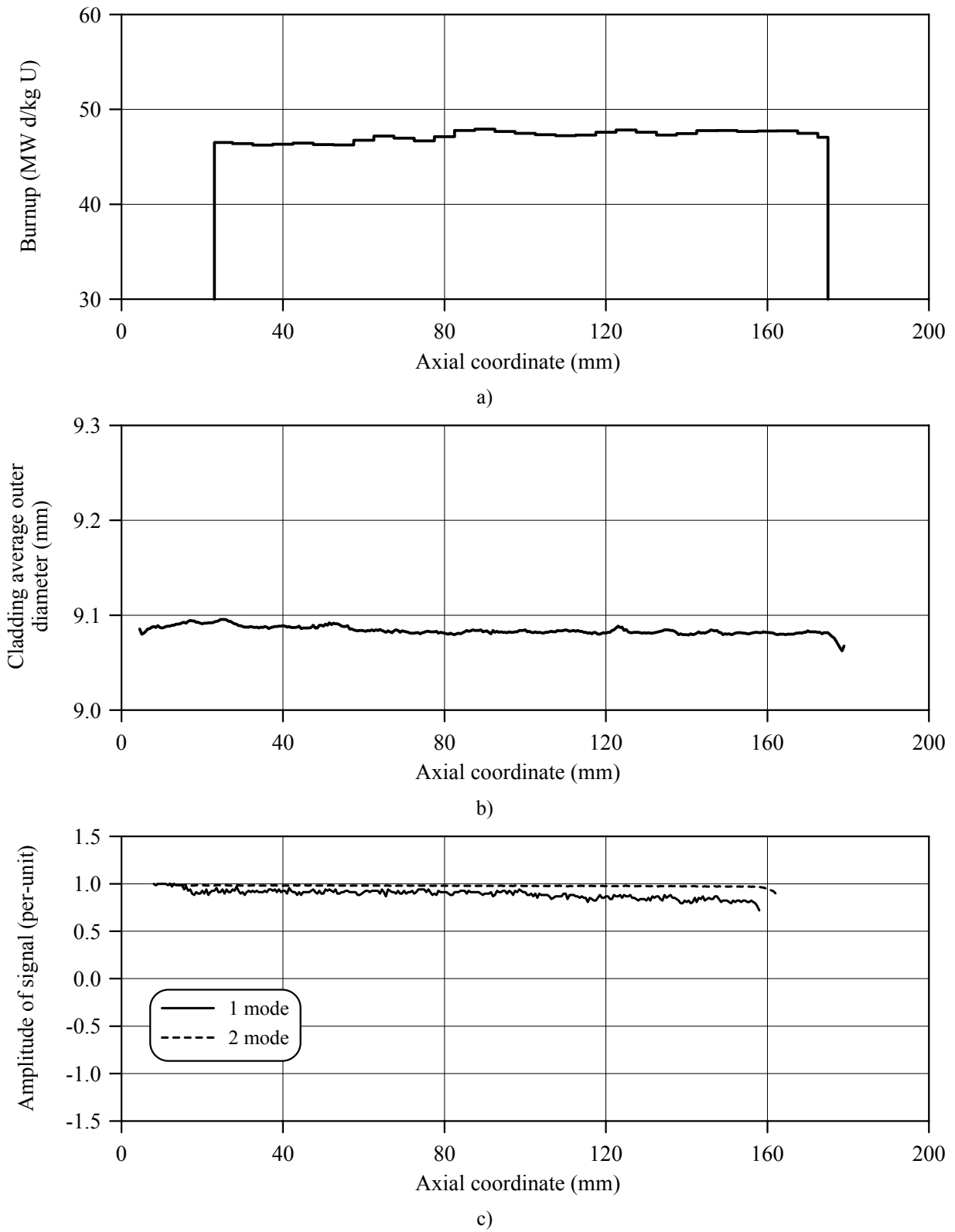
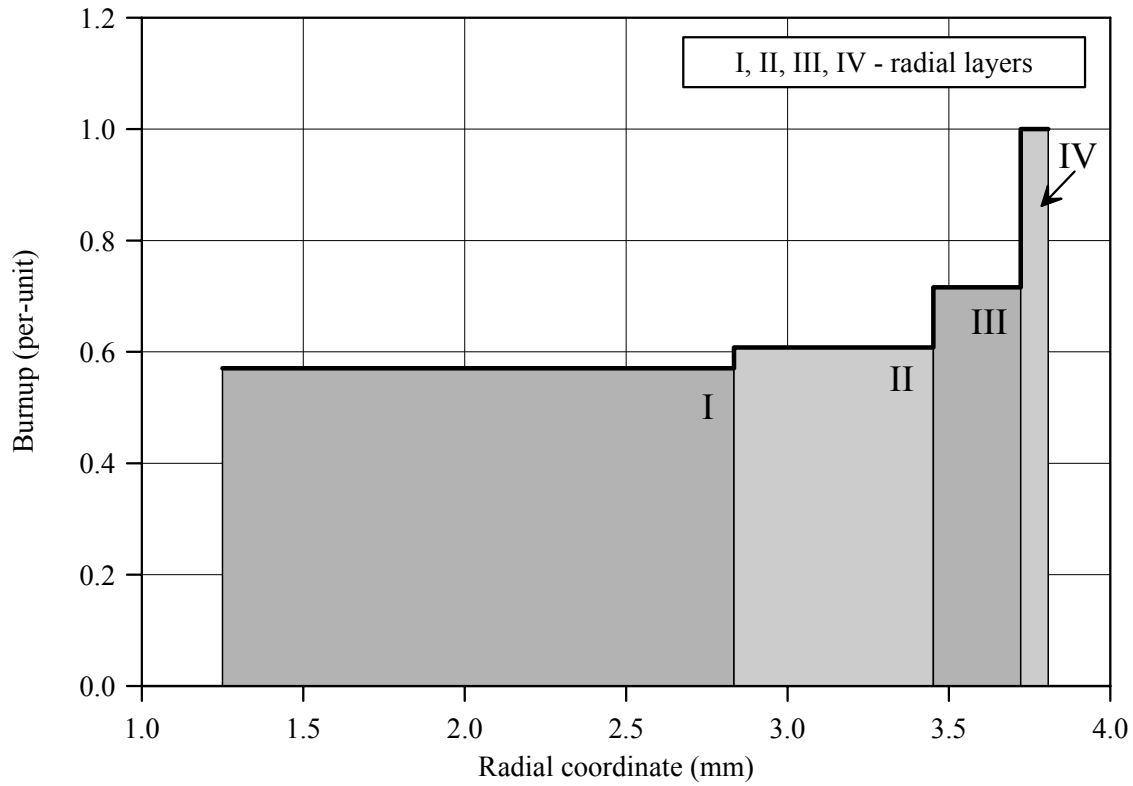
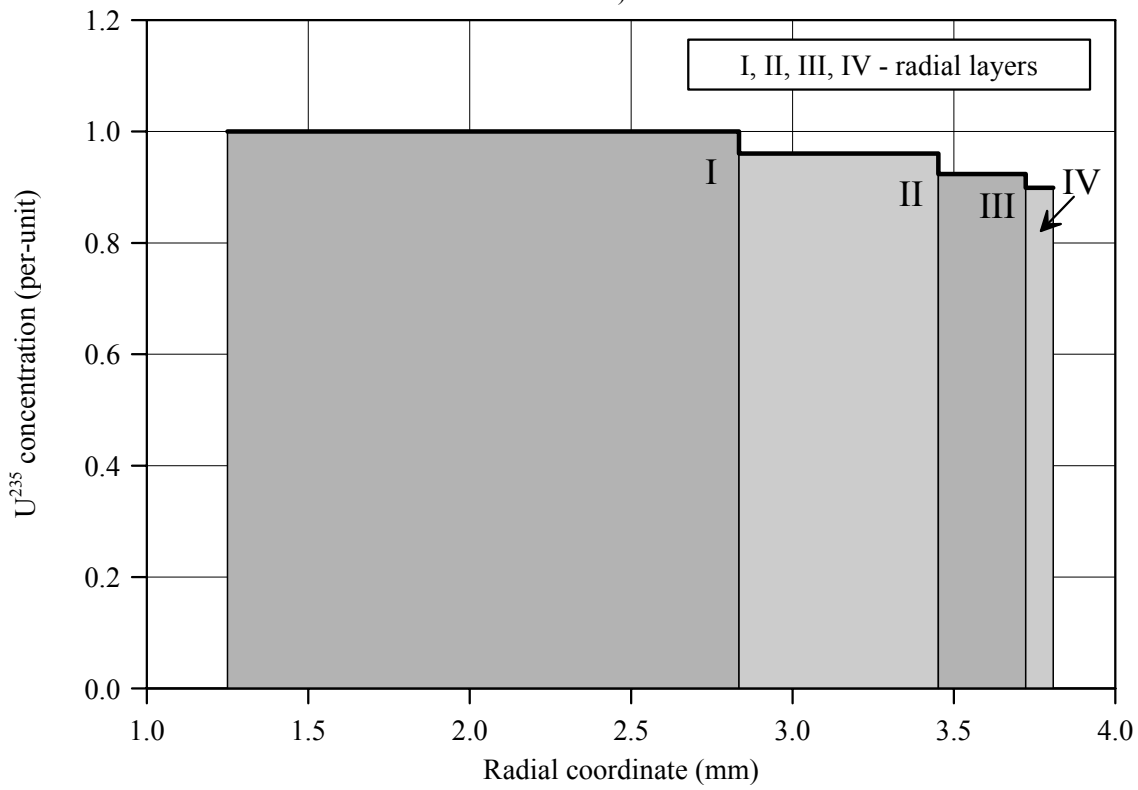


Fig.C-11.2. (a) Axial burnup distribution and (b) results of profilometry and (c) eddy-current examination of fuel rod # RT11

RT11

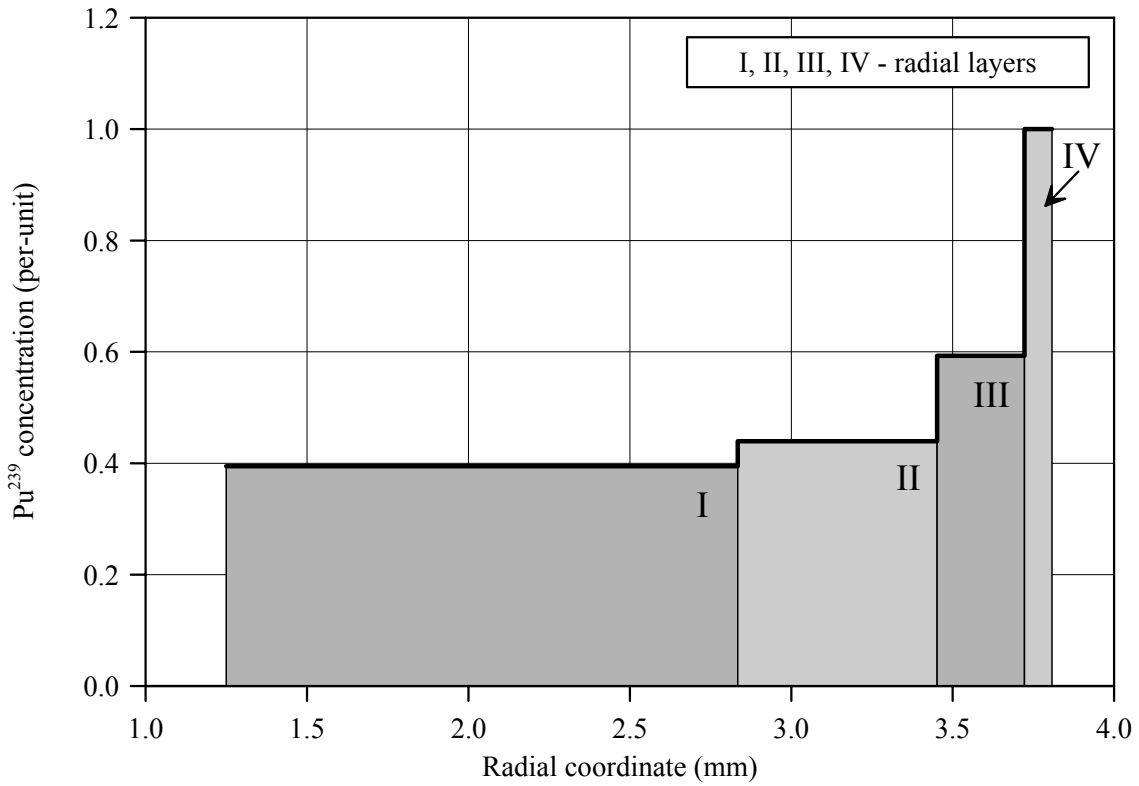


a)

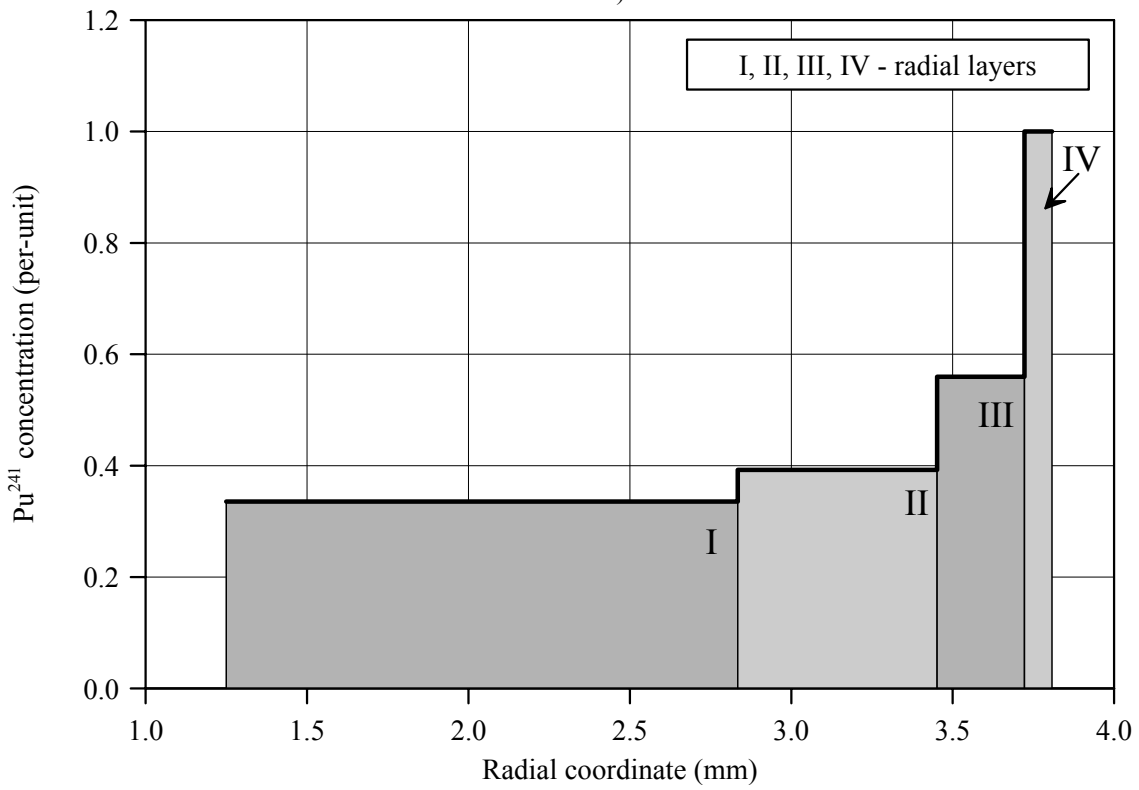


b)

Fig.C-11.3. (a) Burnup radial distribution and (b) U²³⁵ radial distribution for fuel rod # RT11 (calculated values)



a)



b)

Fig.C-11.4. Radial distribution of (a) Pu^{239} and (b) Pu^{241} for fuel rod # RT11 (calculated values)

Appendix C-12
Individual Characteristics
of Fuel Rod # RT12 before the BGR Test

RT12**Table C-12.1. Radial distribution of isotope nuclear concentrations for fuel rod #RT12
(values averaged of over the fuel stack length)***

| Isotope | Isotopic concentrations (kg/t U) in four fuel radial layers | | | |
|------------------------|---|----------------|----------------|----------------|
| | 1.250-2.834 mm | 2.834-3.452 mm | 3.452-3.722 mm | 3.722-3.808 mm |
| U ²³⁴ | 0.212 | 0.209 | 0.206 | 0.203 |
| U ²³⁵ | 8.058 | 7.767 | 7.500 | 7.316 |
| U ²³⁶ | 6.746 | 6.765 | 6.783 | 6.802 |
| U ²³⁸ | 928.2 | 924.7 | 913.3 | 882.7 |
| Pu ²³⁸ | 0.266 | 0.281 | 0.303 | 0.343 |
| Pu ²³⁹ | 4.835 | 5.389 | 7.299 | 12.42 |
| Pu ²⁴⁰ | 2.546 | 2.711 | 3.509 | 5.742 |
| Pu ²⁴¹ | 0.867 | 1.020 | 1.459 | 2.635 |
| Pu ²⁴² | 0.719 | 0.868 | 1.277 | 2.375 |
| Np ²³⁷ | 1.290 | 1.331 | 1.371 | 1.399 |
| Am ²⁴¹ | 0.990 | 1.149 | 1.625 | 2.932 |
| Oxygen | 134.5 | 134.5 | 134.5 | 134.5 |
| Other fission products | 46.19 | 48.79 | 56.35 | 76.27 |

* Measured averaged concentrations and calculated relative radial distributions of isotopes (TRIFOB code) were used to develop these data

Table C-12.2. Initial individual characteristics of fuel rod # RT12*

| Axial coordinate (from lower cap) (mm) | Cladding average outer diameter (mm) | Fuel mass ** (g) | Linear fuel mass** (g/cm) | Gas flow area ^{3)**} (mm ²) | Burnup** (MW d/kg U) |
|--|---|---------------------|---------------------------------|--|-------------------------|
| 20 ¹⁾ | 9.073 | 0.50 | 4.14 | 5.39 | 47.30 |
| 25 | 9.070 | 2.07 | 4.14 | 5.39 | 47.23 |
| 30 | 9.072 | 2.07 | 4.14 | 5.39 | 47.32 |
| 35 | 9.073 | 2.07 | 4.15 | 5.29 | 47.39 |
| 40 | 9.069 | 2.07 | 4.13 | 5.49 | 47.49 |
| 45 | 9.072 | 2.06 | 4.13 | 5.49 | 47.63 |
| 50 | 9.070 | 2.06 | 4.12 | 5.58 | 47.78 |
| 55 | 9.073 | 2.06 | 4.13 | 5.49 | 47.87 |
| 60 | 9.071 | 2.07 | 4.15 | 5.29 | 47.74 |
| 65 | 9.070 | 2.08 | 4.17 | 5.10 | 47.40 |
| 70 | 9.067 | 2.09 | 4.18 | 5.00 | 47.16 |
| 75 | 9.066 | 2.09 | 4.17 | 5.10 | 47.18 |
| 80 | 9.063 | 2.08 | 4.17 | 5.10 | 47.20 |
| 85 | 9.062 | 2.08 | 4.16 | 5.20 | 47.09 |
| 90 | 9.065 | 2.07 | 4.15 | 5.29 | 47.07 |
| 95 | 9.063 | 2.07 | 4.14 | 5.39 | 47.23 |
| 100 | 9.066 | 2.07 | 4.13 | 5.49 | 47.37 |
| 105 | 9.064 | 2.06 | 4.12 | 5.58 | 47.35 |
| 110 | 9.069 | 2.06 | 4.12 | 5.58 | 47.24 |
| 115 | 9.064 | 2.06 | 4.12 | 5.58 | 47.16 |
| 120 | 9.065 | 2.06 | 4.12 | 5.58 | 47.26 |
| 125 | 9.064 | 2.06 | 4.11 | 5.68 | 47.53 |
| 130 | 9.066 | 2.05 | 4.10 | 5.78 | 47.64 |
| 135 | 9.067 | 2.06 | 4.11 | 5.68 | 47.42 |
| 140 | 9.062 | 2.06 | 4.12 | 5.58 | 47.13 |
| 145 | 9.062 | 2.06 | 4.12 | 5.58 | 47.02 |
| 150 | 9.058 | 2.05 | 4.11 | 5.68 | 47.20 |
| 155 | 9.059 | 2.04 | 4.08 | 5.97 | 47.62 |
| 160 | 9.063 | 2.03 | 4.06 | 6.17 | 47.87 |
| 165 | 9.059 | 2.03 | 4.06 | 6.17 | 47.74 |
| 170 | 9.063 | 2.06 | 4.11 | 5.68 | 47.51 |
| 175 ²⁾ | 9.066 | 0.59 | 4.19 | 4.91 | 47.39 |

* All parameters were determined using results of pre-test examinations

** Average values at the length interval equal to the axial coordinate ± 2.5 mm

¹⁾ Bottom end coordinate of fuel stack is 21.3 mm;

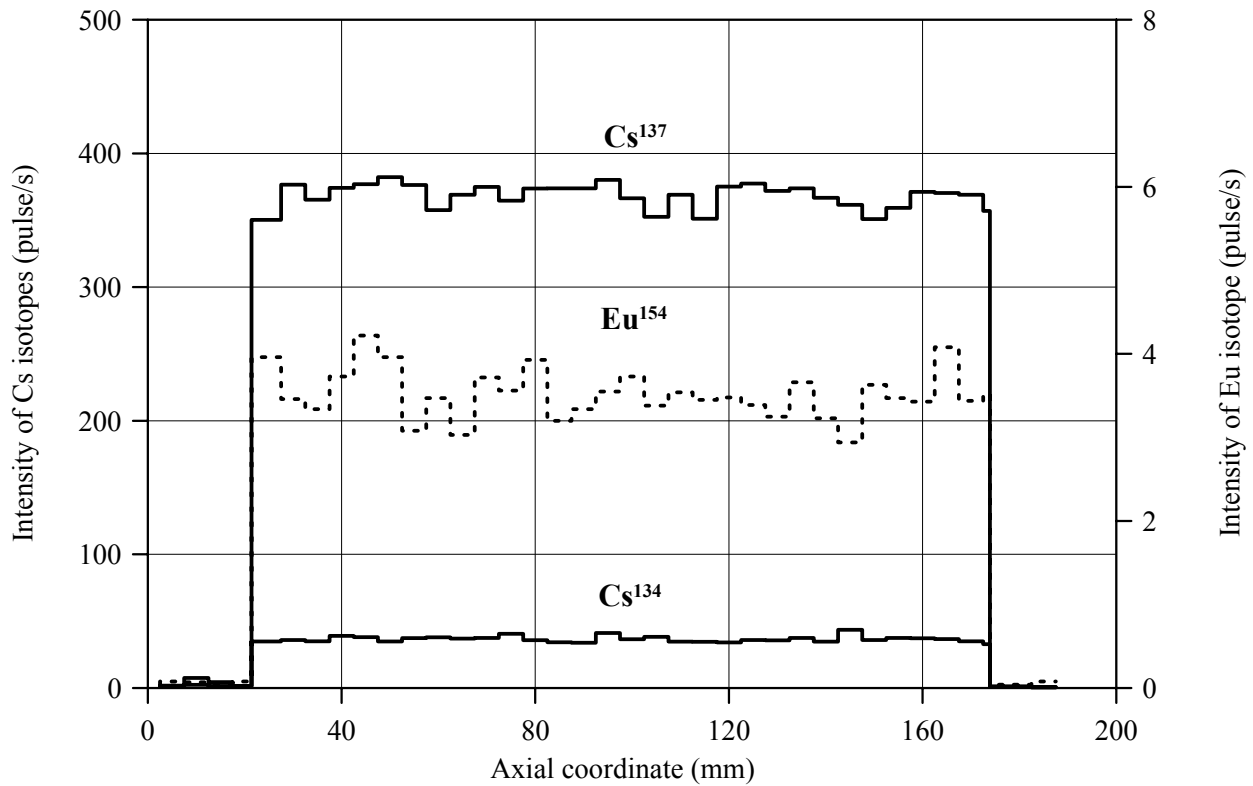
²⁾ Top end coordinate of fuel stack is 173.9 mm

³⁾ Gas flow area beyond the fuel stack (mm²):

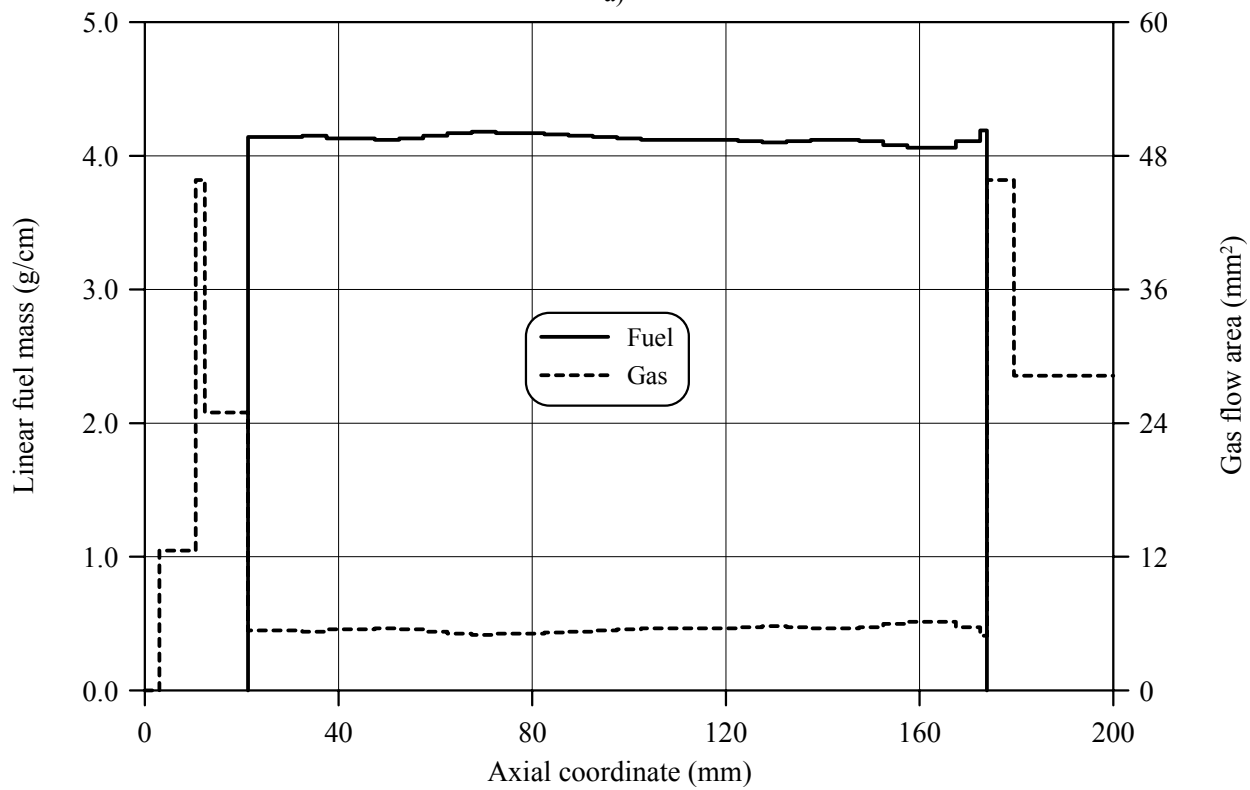
Bottom: 0.0-3.0mm – 0.00; 3.0-10.5mm – 12.56; 10.5-12.4mm – 45.82; 12.4-21.3mm – 24.97

Top: 173.9-180.0mm – 45.82; 180.0-206.0mm – 28.26; 206.0-282mm – 47.27; 282-291mm – 28.26; 291-300mm – 0.00

RT12



a)



b)

Fig.C-12.1. (a) Results of γ -scanning, (b) Axial fuel mass distribution and axial gas flow area distribution for fuel rod # RT12

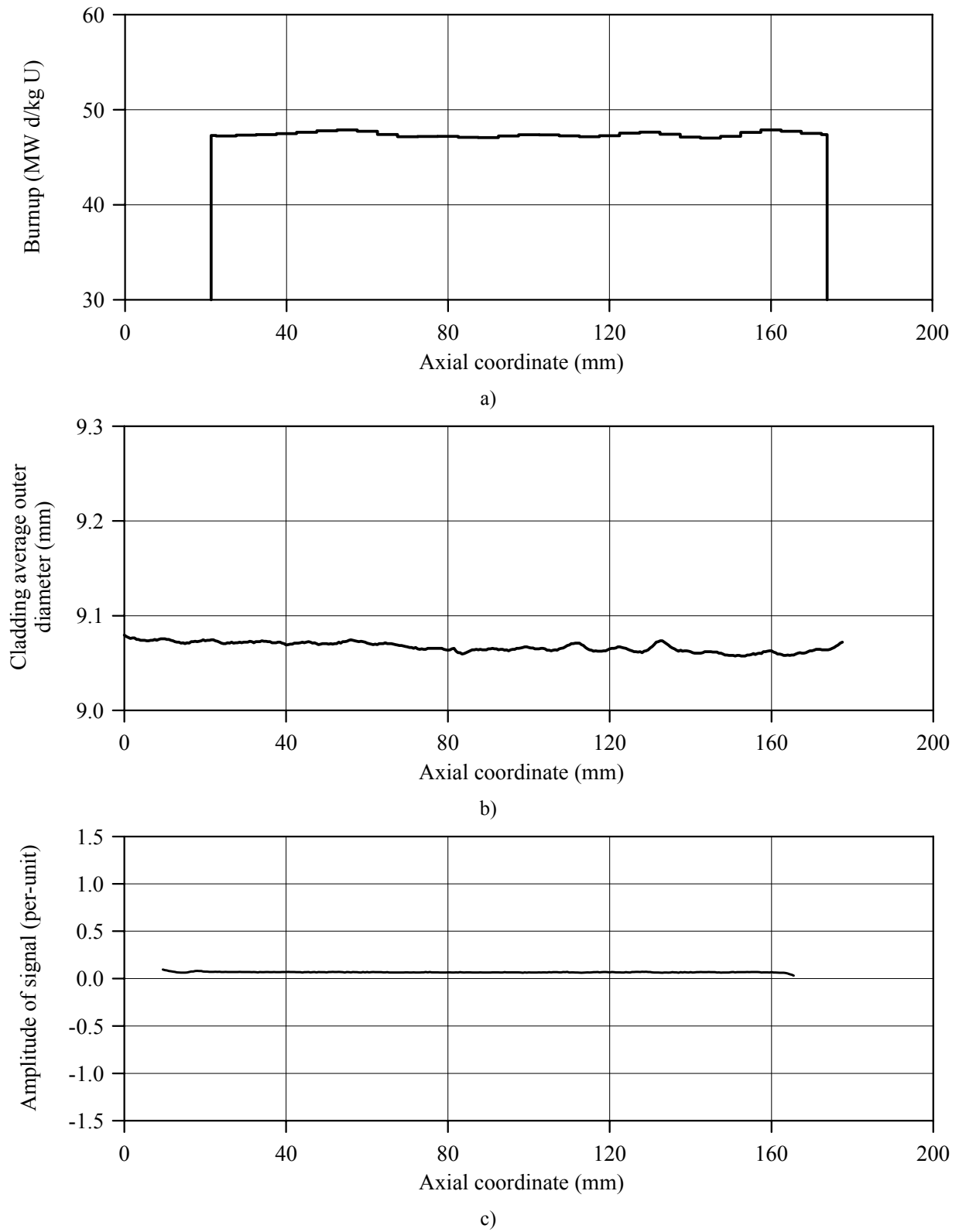


Fig.C-12.2. (a) Axial burnup distribution and (b) results of profilometry and (c) eddy-current examination of fuel rod # RT12

RT12

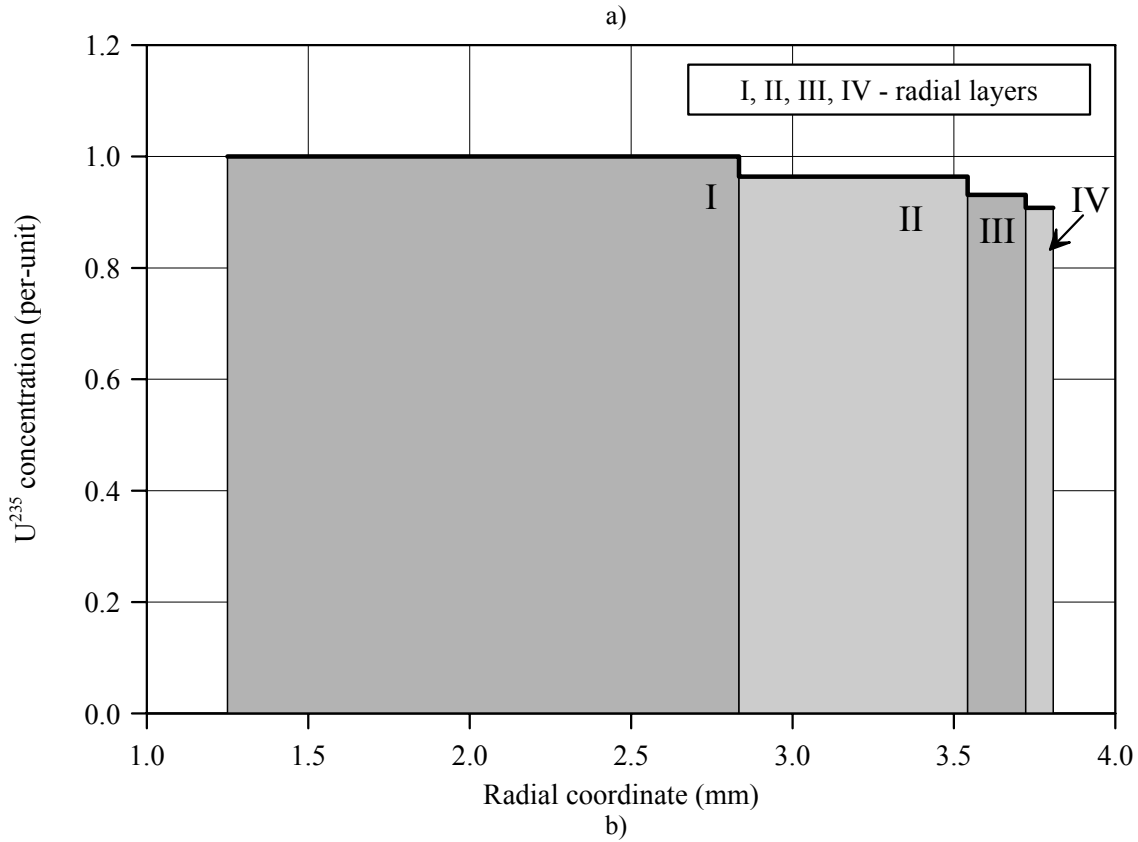
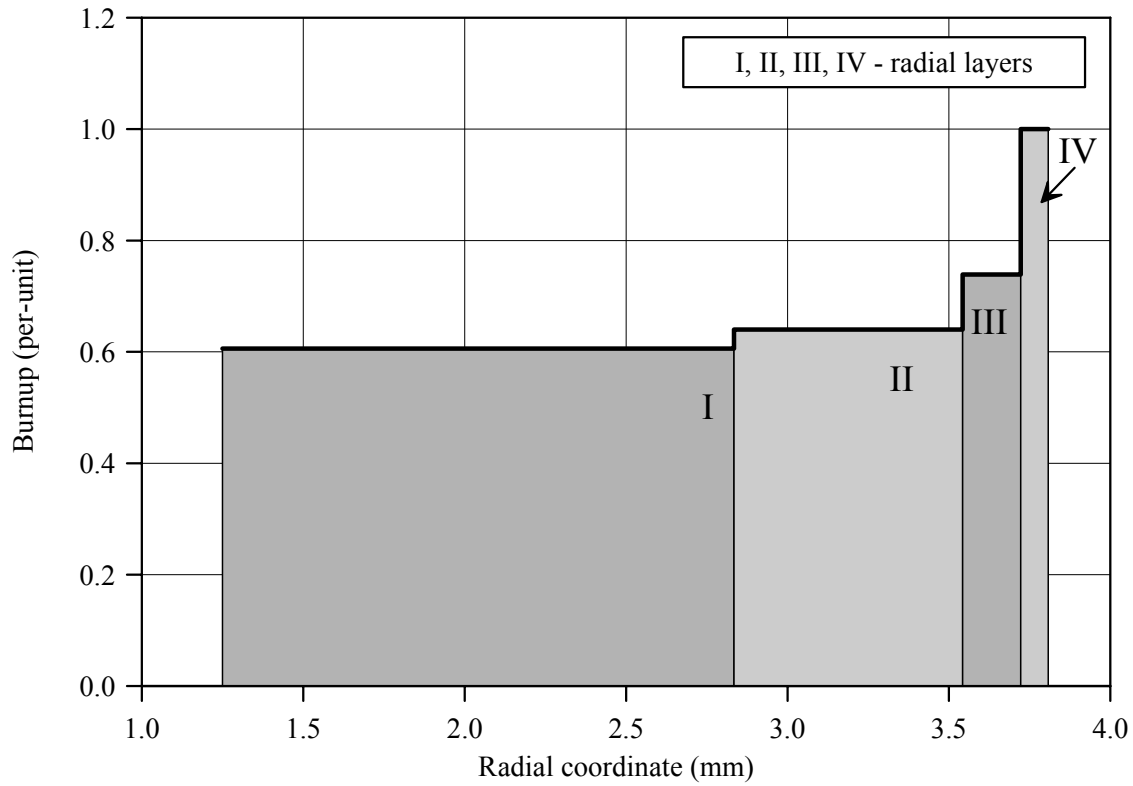
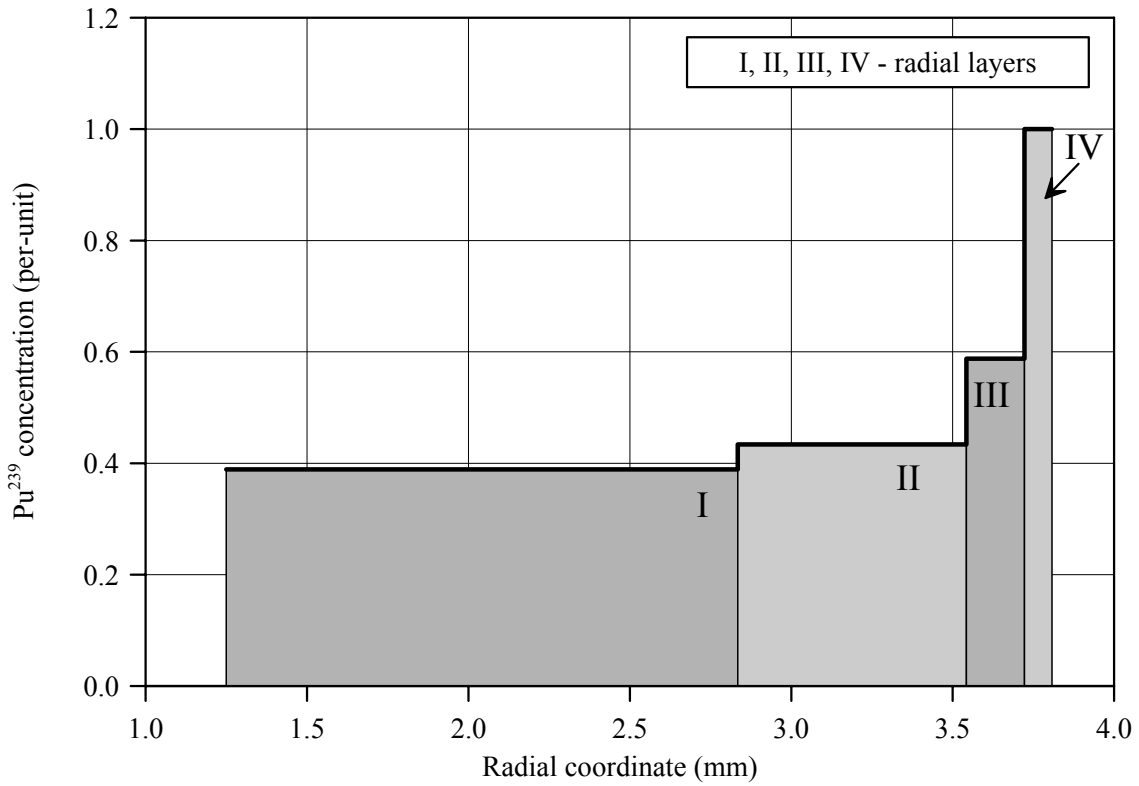
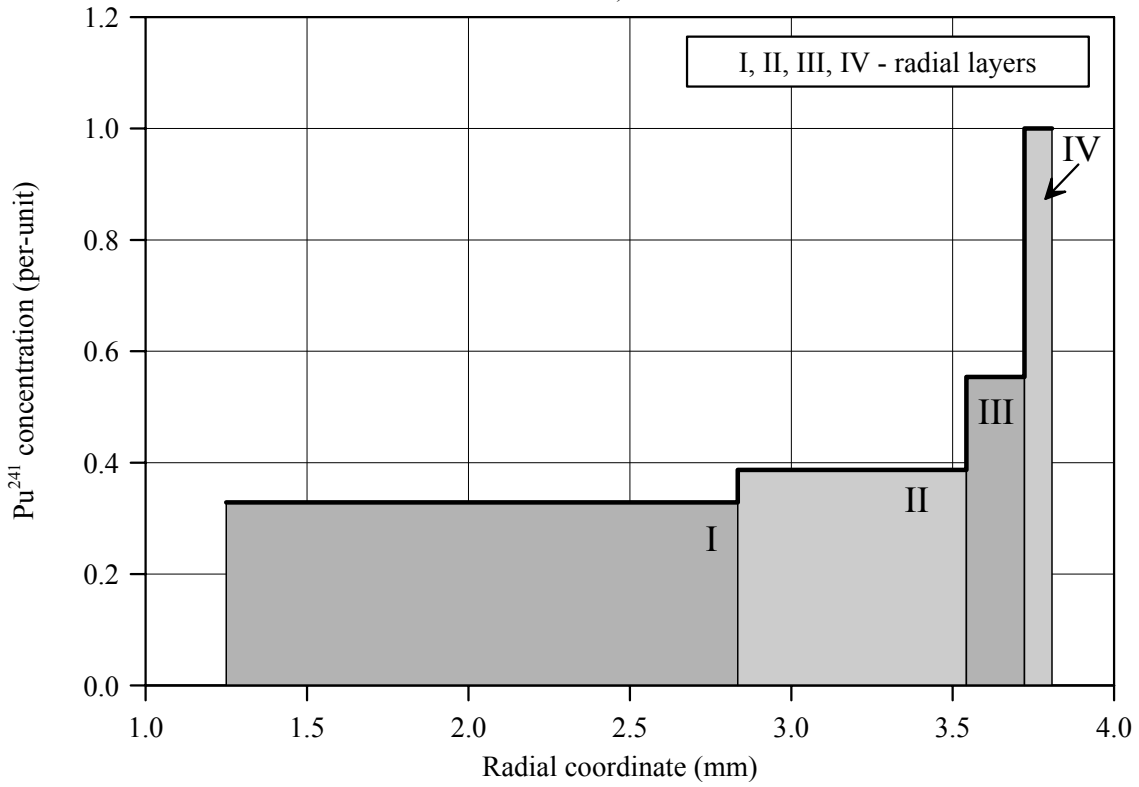


Fig.C-12.3. (a) Burnup radial distribution and (b) U^{235} radial distribution for fuel rod # RT12 (calculated values)



a)



b)

Fig.C-12.4. Radial distribution of (a) Pu²³⁹ and (b) Pu²⁴¹ for fuel rod # RT12 (calculated values)

APPENDIX D

CHARACTERISTICS OF THE BIGR POWER PULSES

Table D.1. Reference data characterizing BGR tests of refabricated fuel rods ## RT 1–12

| Number of fuel rods | Number of BGR test | Date of BGR test | Pulse half width (ms) |
|----------------------------|---------------------------|-------------------------|------------------------------|
| RT1 | 833 | 06.11.97 | 2.6 |
| RT2 | 834 | 10.11.97 | 3.1 |
| RT3 | 832 | 04.11.97 | 2.5 |
| RT4 | 846 | 13.11.97 | 2.5 |
| RT5 | 847 | 16.11.97 | 2.5 |
| RT6 | 845 | 11.11.97 | 2.6 |
| RT7 | 881 | 30.06.2000 | 2.6 |
| RT8 | 889 | 17.11.2000 | 2.6 |
| RT9 | 887 | 11.11.2000 | 2.7 |
| RT10 | 880 | 27.06.2000 | 2.6 |
| RT11 | 888 | 14.11.2000 | 2.6 |
| RT12 | 882 | 05.07.2000 | 2.8 |

**Table D.2. BGR power for fuel rods ## RT1–12 in accordance
with the Neutron detector recording**

| Time (s) | Reactor power (V) | | | | | | | | | | | |
|-------------|--------------------|-------|-------|-------|-------|-------|-------|-------|-------|-------|-------|-------|
| | Number of fuel rod | | | | | | | | | | | |
| | RT1 | RT2 | RT3 | RT4 | RT5 | RT6 | RT7 | RT8 | RT9 | RT10 | RT11 | RT12 |
| 0.000 | 0.000 | 0.000 | 0.000 | 0.000 | 0.000 | 0.000 | 0.001 | 0.000 | 0.000 | 0.000 | 0.000 | 0.000 |
| 0.001 | 0.810 | 1.598 | 0.946 | 0.917 | 0.931 | 0.788 | 0.004 | 0.003 | 0.003 | 0.009 | 0.003 | 0.003 |
| 0.002 | 2.636 | 3.254 | 2.966 | 2.894 | 2.891 | 2.840 | 0.017 | 0.012 | 0.013 | 0.041 | 0.012 | 0.012 |
| 0.003 | 4.545 | 3.384 | 4.800 | 4.800 | 4.900 | 4.500 | 0.076 | 0.055 | 0.057 | 0.185 | 0.053 | 0.049 |
| 0.004 | 3.367 | 2.232 | 3.269 | 3.110 | 3.200 | 3.051 | 0.314 | 0.238 | 0.240 | 0.620 | 0.229 | 0.195 |
| 0.005 | 1.467 | 1.109 | 1.406 | 1.277 | 1.318 | 1.269 | 0.837 | 0.706 | 0.688 | 1.003 | 0.689 | 0.603 |
| 0.006 | 0.759 | 0.562 | 0.710 | 0.682 | 0.715 | 0.684 | 0.939 | 0.990 | 0.998 | 0.684 | 0.993 | 0.997 |
| 0.007 | 0.409 | 0.356 | 0.387 | 0.364 | 0.379 | 0.374 | 0.520 | 0.619 | 0.670 | 0.318 | 0.632 | 0.764 |
| 0.008 | 0.270 | 0.267 | 0.268 | 0.253 | 0.264 | 0.261 | 0.234 | 0.282 | 0.319 | 0.150 | 0.289 | 0.389 |
| 0.009 | 0.241 | 0.238 | 0.236 | 0.216 | 0.221 | 0.218 | 0.119 | 0.136 | 0.155 | 0.086 | 0.138 | 0.192 |
| 0.010 | 0.230 | 0.230 | 0.229 | 0.213 | 0.220 | 0.213 | 0.075 | 0.081 | 0.092 | 0.062 | 0.082 | 0.109 |
| 0.012 | 0.273 | 0.237 | 0.256 | 0.255 | 0.260 | 0.247 | 0.054 | 0.054 | 0.059 | 0.052 | 0.054 | 0.063 |
| 0.014 | 0.337 | 0.250 | 0.316 | 0.321 | 0.321 | 0.300 | 0.056 | 0.054 | 0.061 | 0.057 | 0.054 | 0.059 |
| 0.016 | 0.370 | 0.242 | 0.345 | 0.360 | 0.363 | 0.338 | 0.066 | 0.064 | 0.072 | 0.065 | 0.064 | 0.064 |
| 0.018 | 0.366 | 0.219 | 0.332 | 0.352 | 0.357 | 0.329 | 0.075 | 0.074 | 0.083 | 0.070 | 0.074 | 0.070 |
| 0.020 | 0.315 | 0.188 | 0.275 | 0.310 | 0.300 | 0.275 | 0.076 | 0.078 | 0.086 | 0.067 | 0.079 | 0.070 |
| 0.022 | 0.247 | 0.156 | 0.219 | 0.284 | 0.241 | 0.220 | 0.069 | 0.074 | 0.081 | 0.059 | 0.074 | 0.064 |
| 0.024 | 0.194 | 0.131 | 0.173 | 0.250 | 0.191 | 0.174 | 0.059 | 0.062 | 0.070 | 0.050 | 0.062 | 0.056 |
| 0.026 | 0.151 | 0.115 | 0.139 | 0.201 | 0.146 | 0.140 | 0.049 | 0.050 | 0.058 | 0.042 | 0.050 | 0.047 |
| 0.028 | 0.127 | 0.107 | 0.117 | 0.154 | 0.118 | 0.118 | 0.040 | 0.040 | 0.047 | 0.035 | 0.040 | 0.040 |
| 0.030 | 0.117 | 0.104 | 0.110 | 0.123 | 0.109 | 0.106 | 0.034 | 0.034 | 0.039 | 0.031 | 0.034 | 0.035 |
| 0.050 | 0.107 | 0.104 | 0.112 | 0.091 | 0.091 | 0.091 | 0.028 | 0.027 | 0.030 | 0.026 | 0.028 | 0.031 |
| 0.070 | 0.085 | 0.084 | 0.090 | 0.082 | 0.079 | 0.079 | 0.025 | 0.024 | 0.027 | 0.022 | 0.025 | 0.025 |
| 0.090 | 0.066 | 0.069 | 0.071 | 0.061 | 0.056 | 0.056 | 0.018 | 0.021 | 0.023 | 0.015 | 0.022 | 0.018 |
| 0.110 | 0.042 | 0.038 | 0.038 | 0.039 | 0.034 | 0.035 | 0.005 | 0.012 | 0.013 | 0.003 | 0.013 | 0.008 |
| 0.120 | 0.000 | 0.000 | 0.000 | 0.000 | 0.000 | 0.000 | 0.000 | 0.000 | 0.000 | 0.000 | 0.000 | 0.000 |

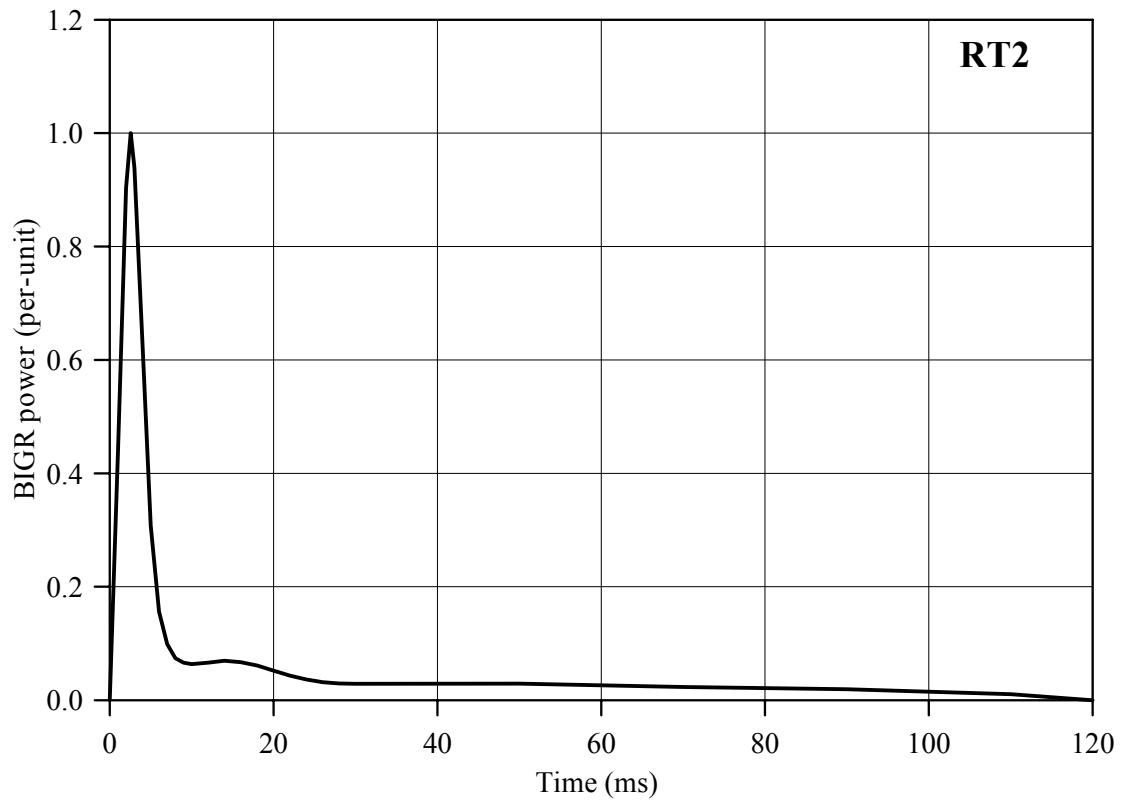
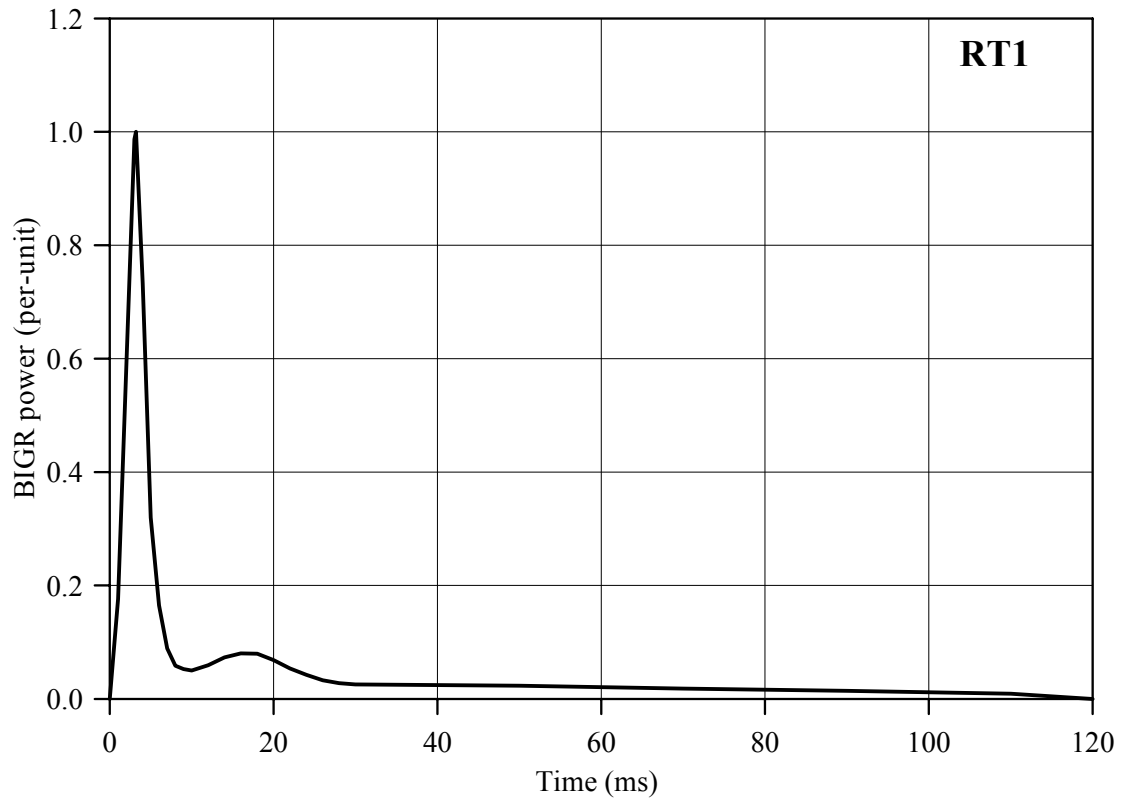


Fig. D.1. BGR power for fuel rods # RT1 and # RT2

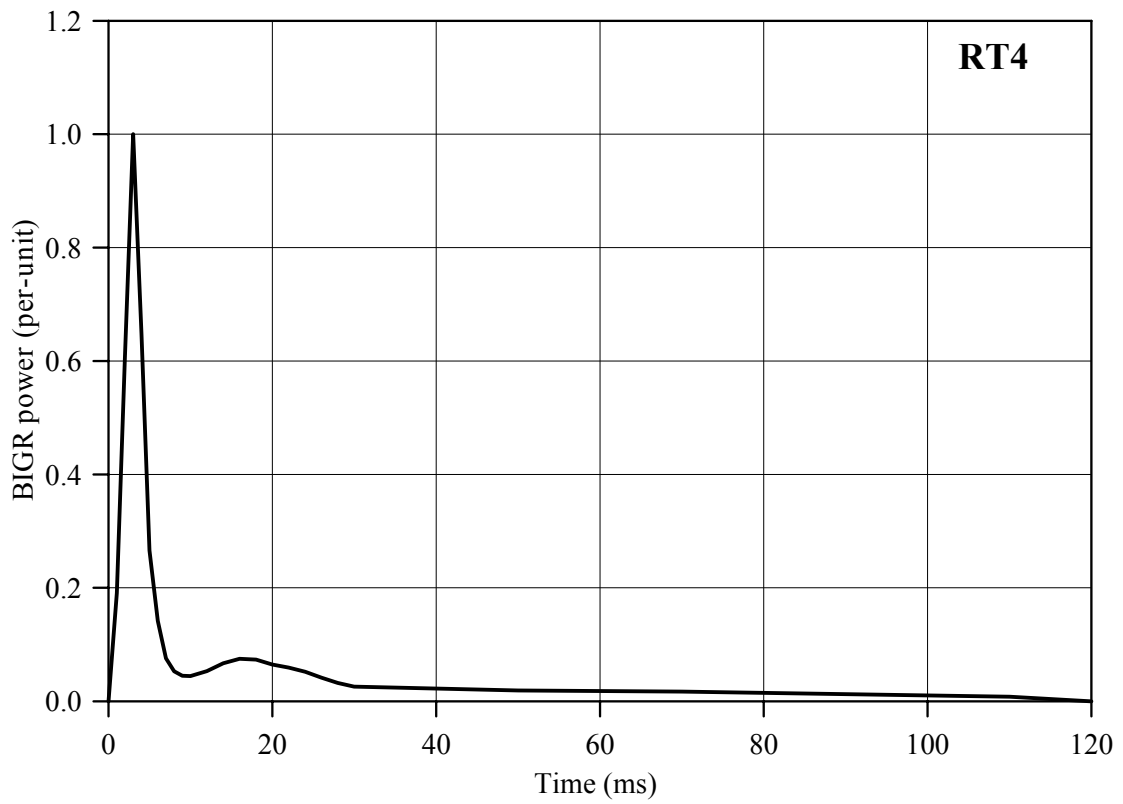
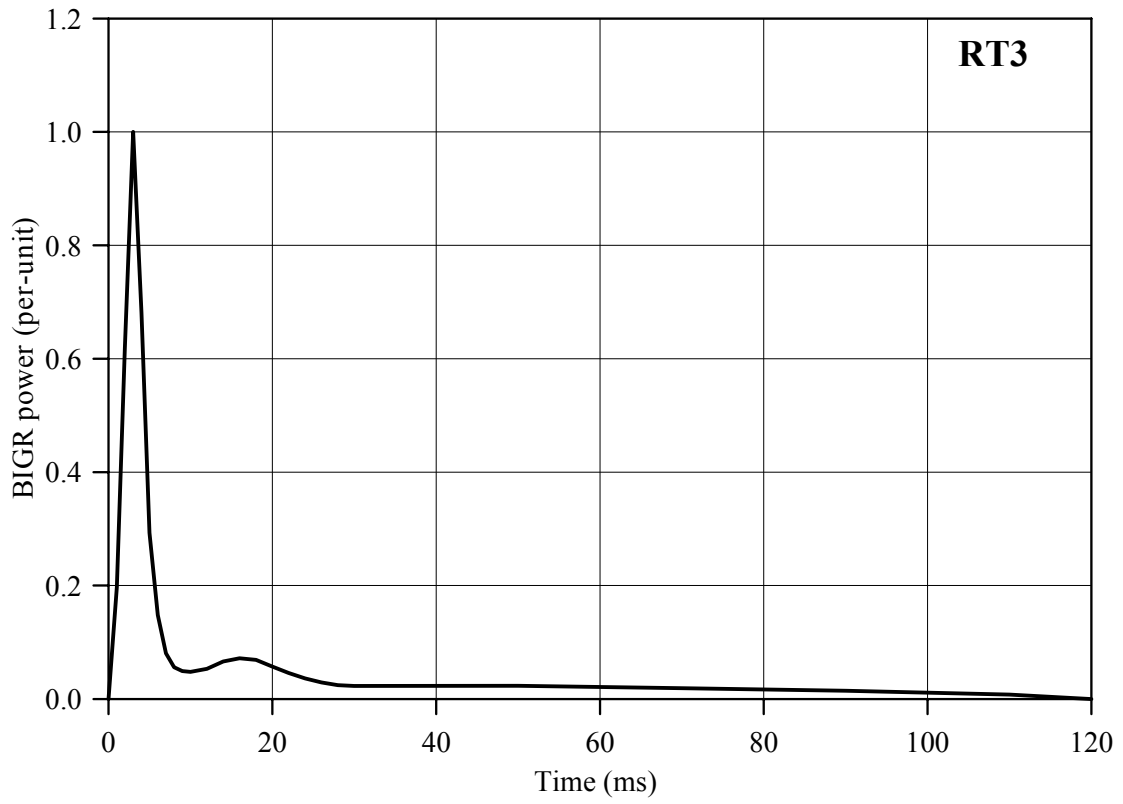


Fig. D.2. BGR power for fuel rods # RT3 and # RT4

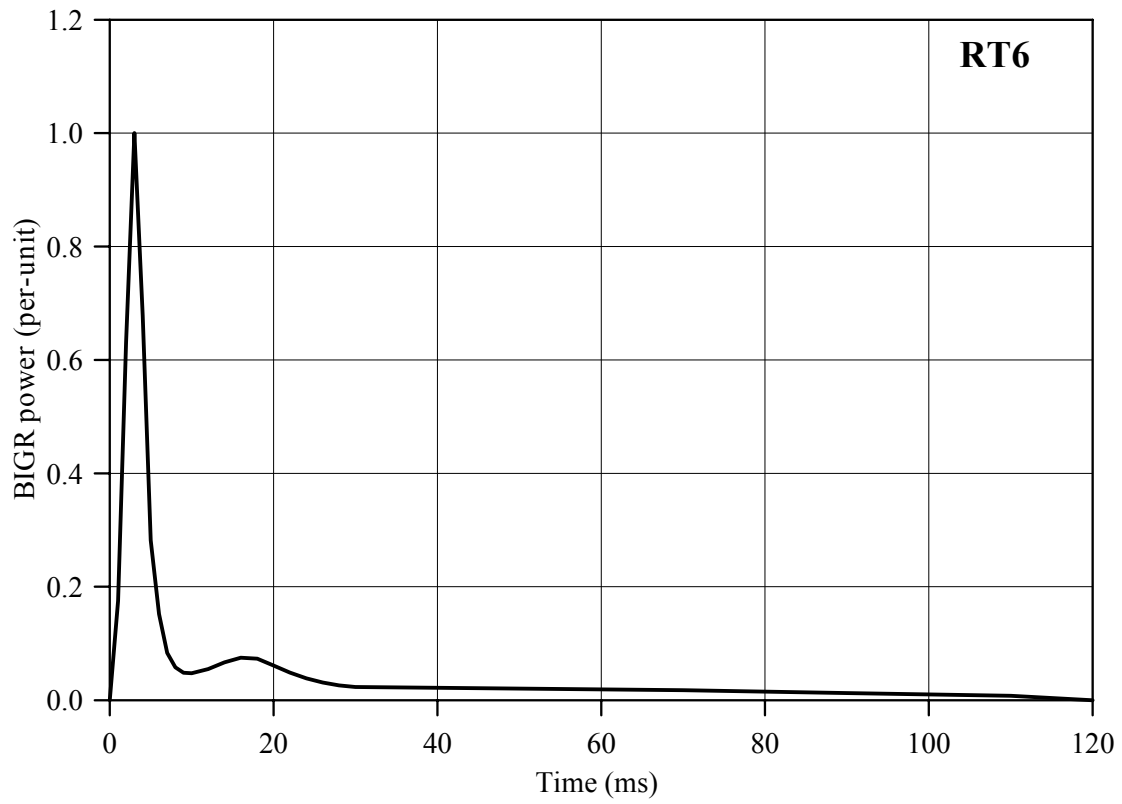
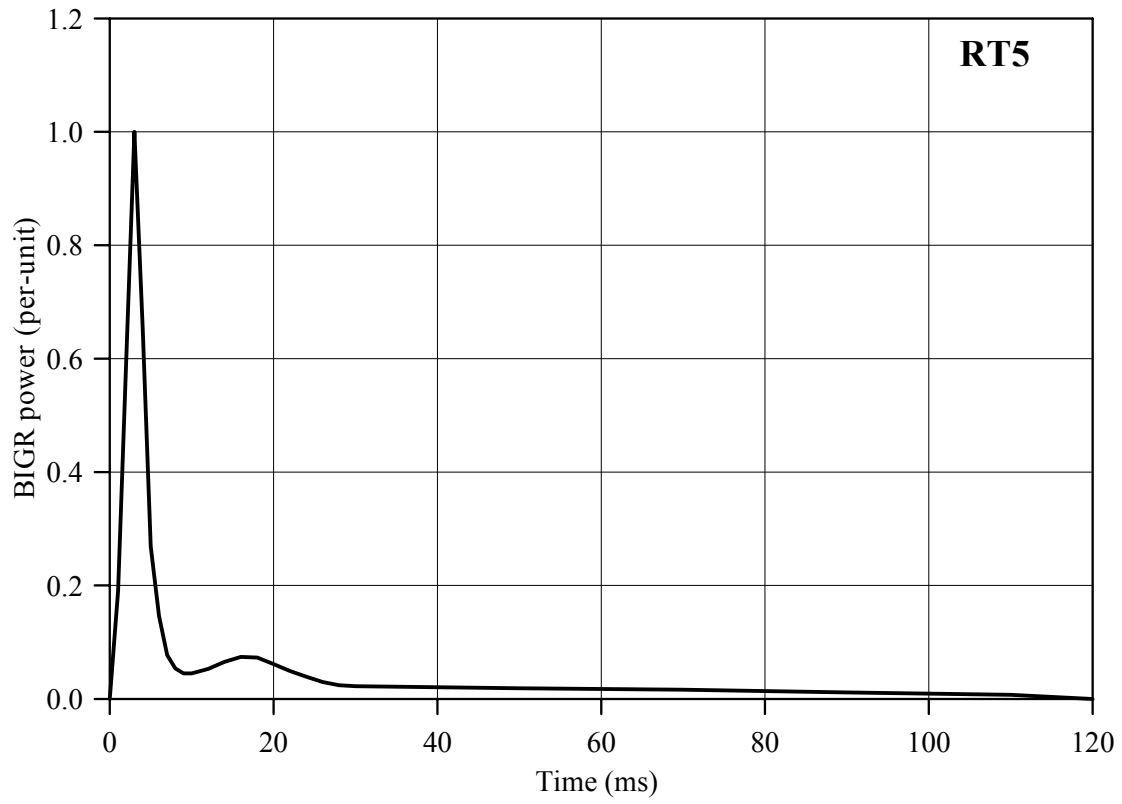


Fig. D.3. BGR power for fuel rods # RT5 and # RT6

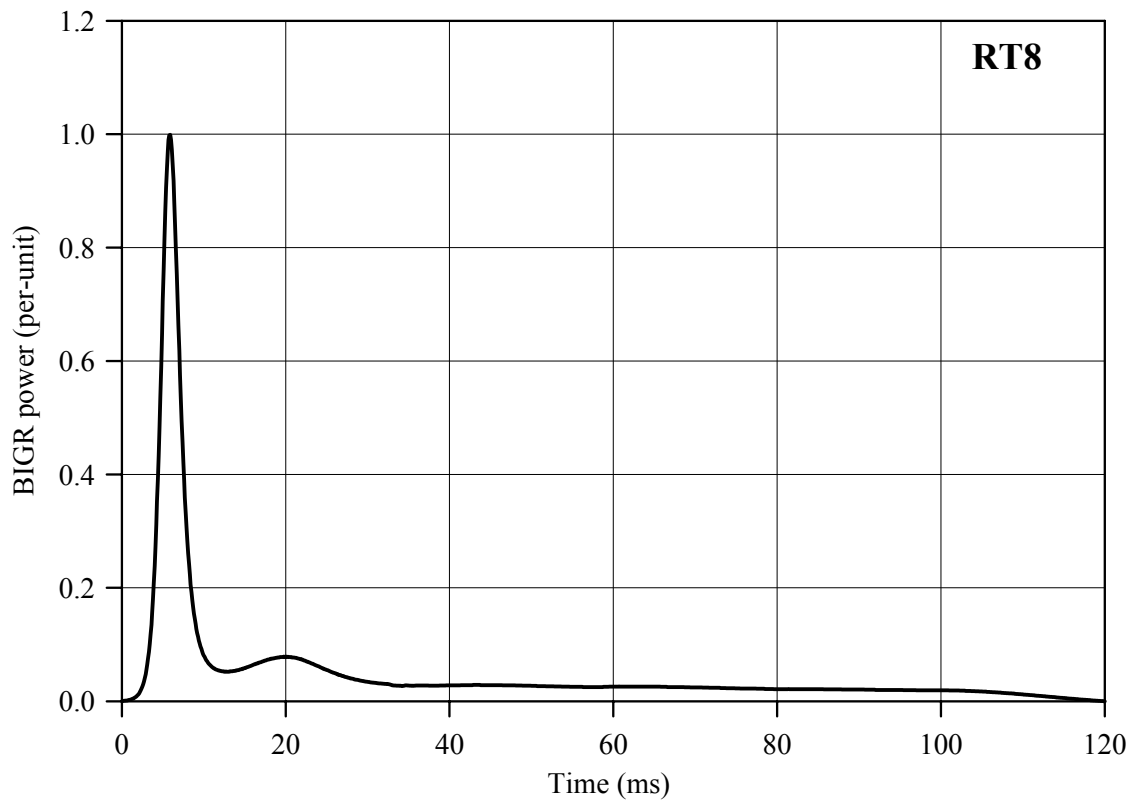
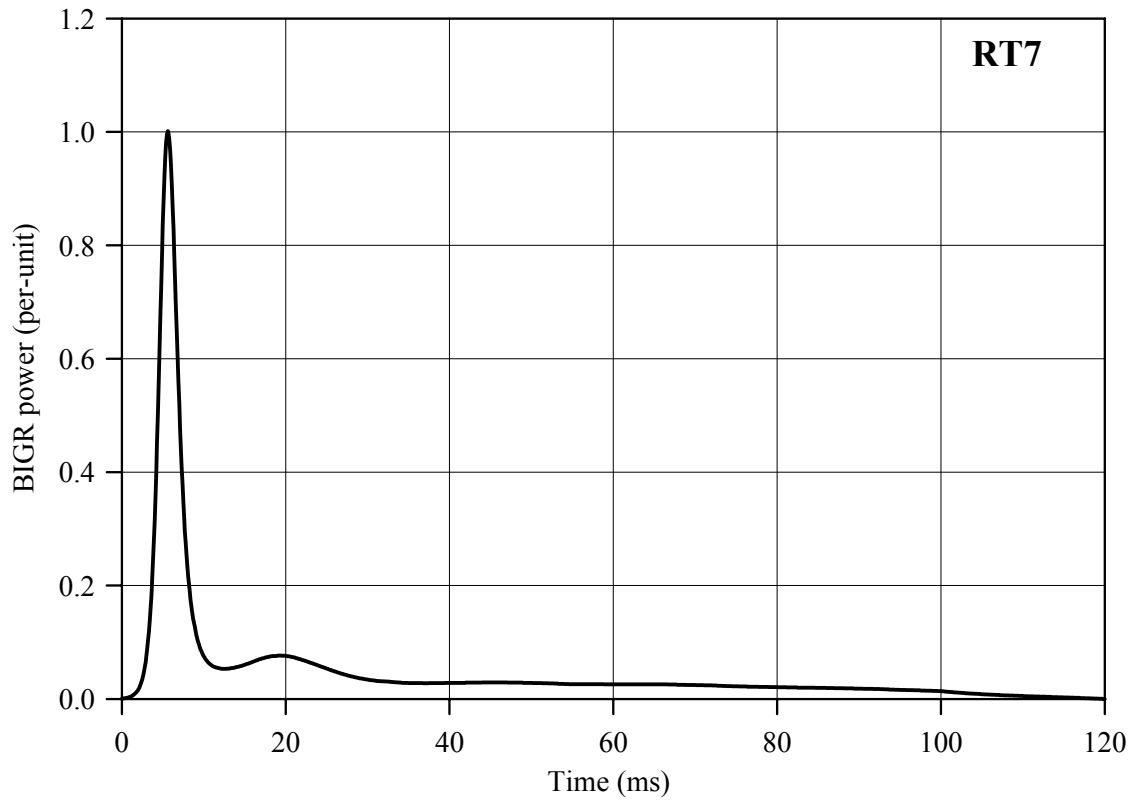


Fig. D.4. BGR power for fuel rods # RT7 and # RT8

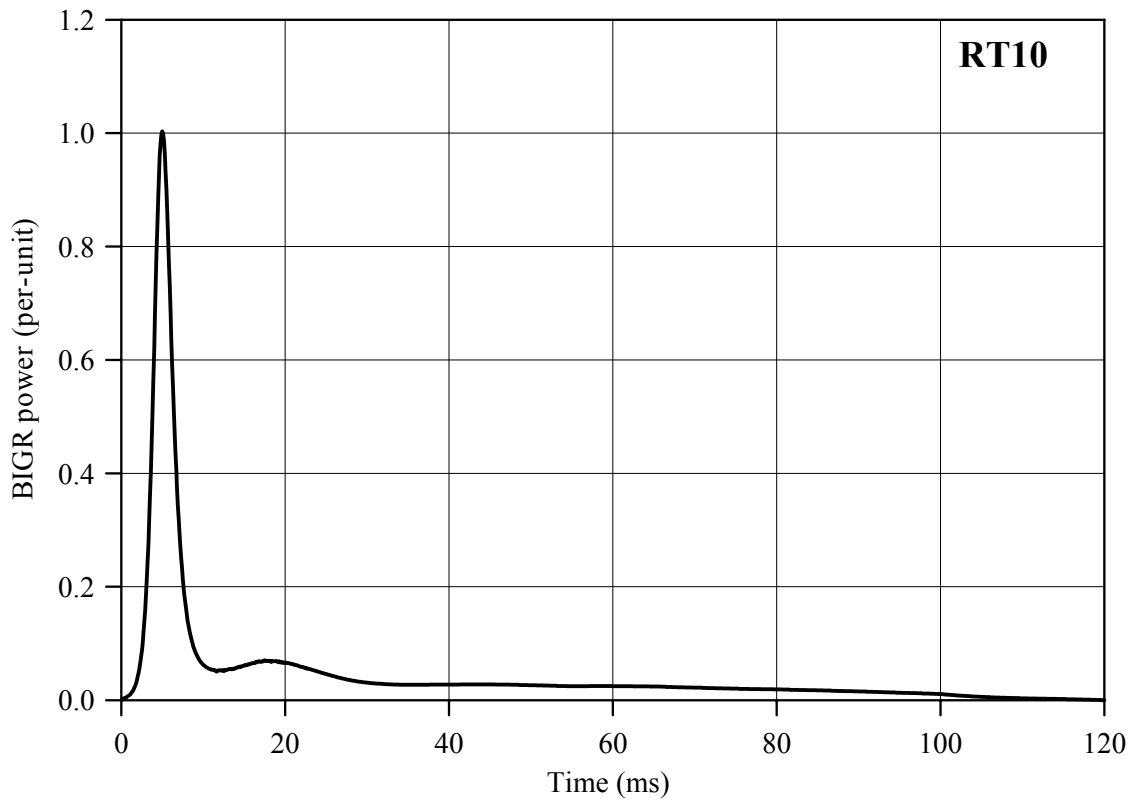
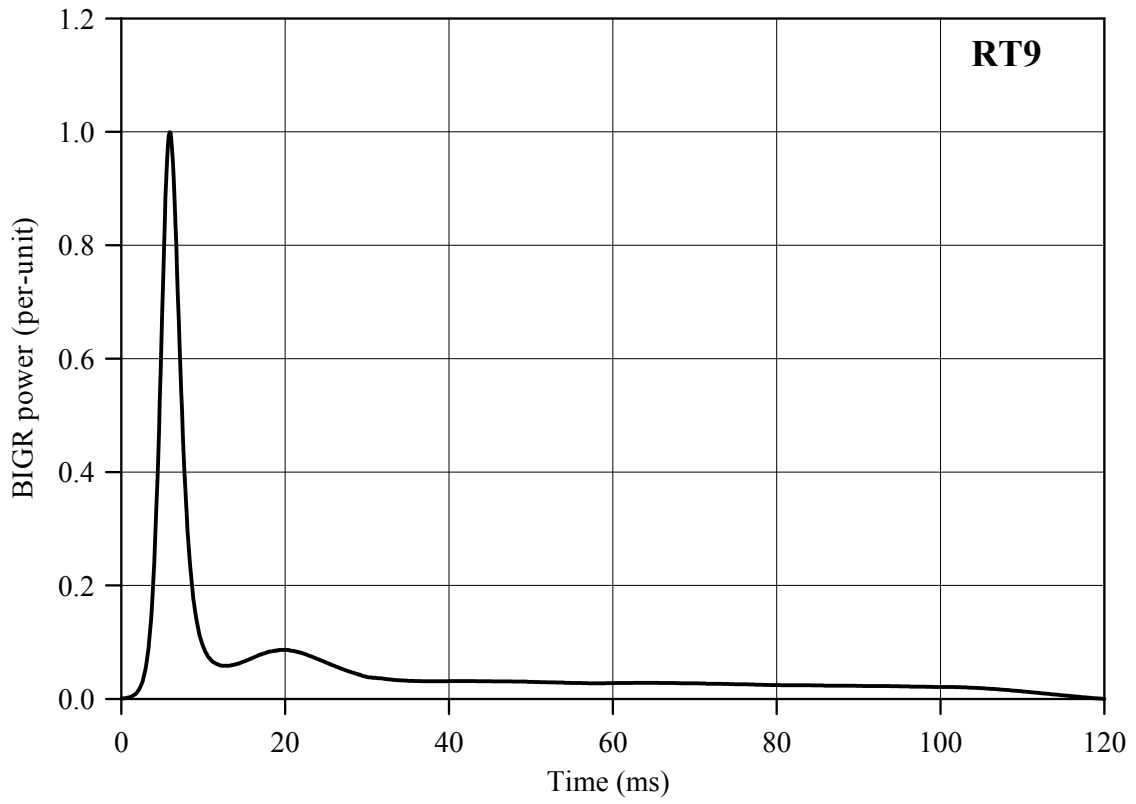


Fig. D.5. BGR power for fuel rods # RT9 and # RT10

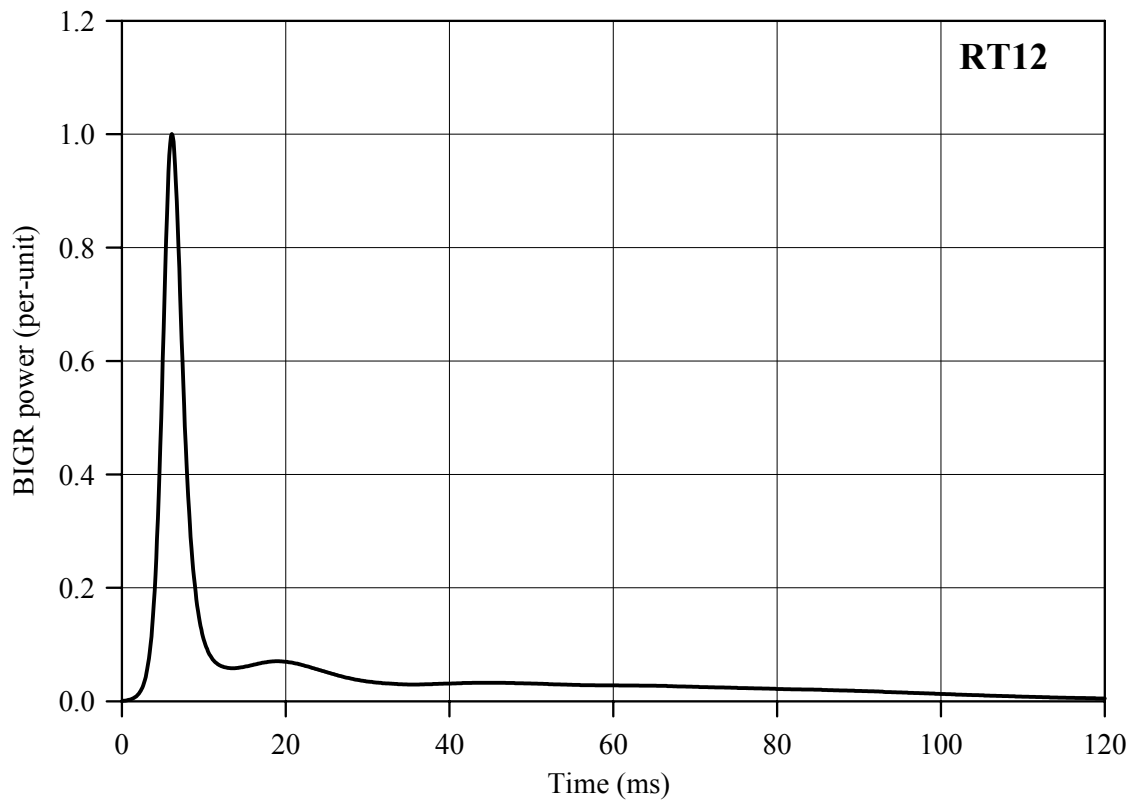
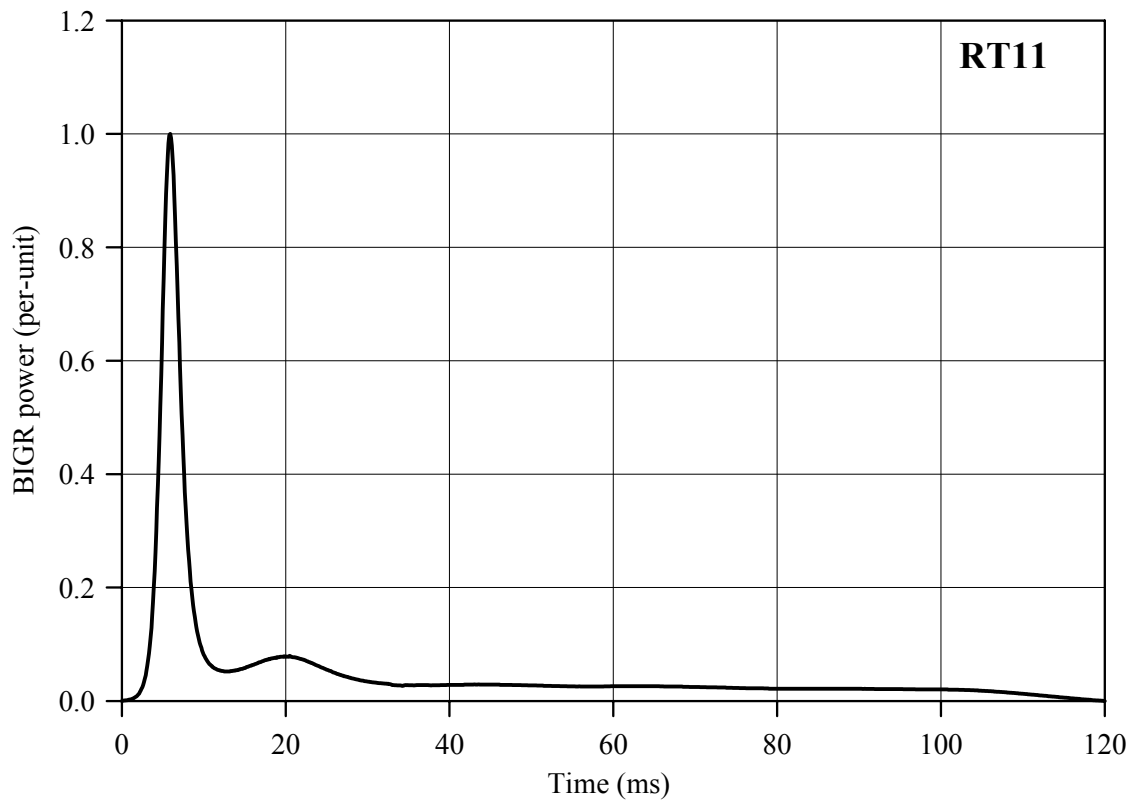


Fig. D.6. BGR power for fuel rods # RT11 and # RT12

APPENDIX E
CHARACTERISTICS OF REFABRICATED FUEL RODS
AFTER THE BGR TESTS

Appendix E-1
Individual Characteristics of Fuel Rod # RT1
after the BGR Test

RT1

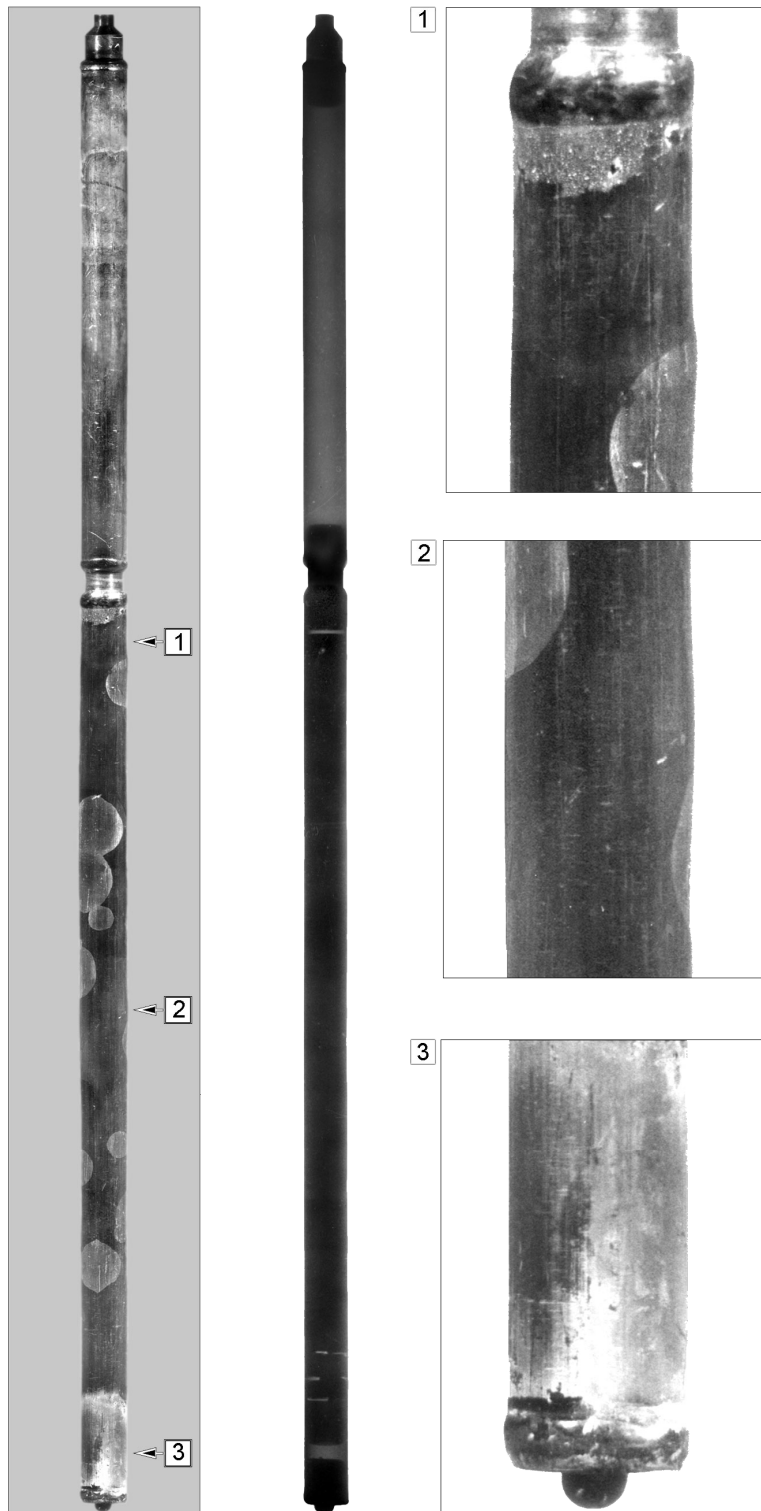


Fig.E-1.1. Appearance of unfailed fuel rod # RT1 after the BGR test (photographs and X-ray photograph)

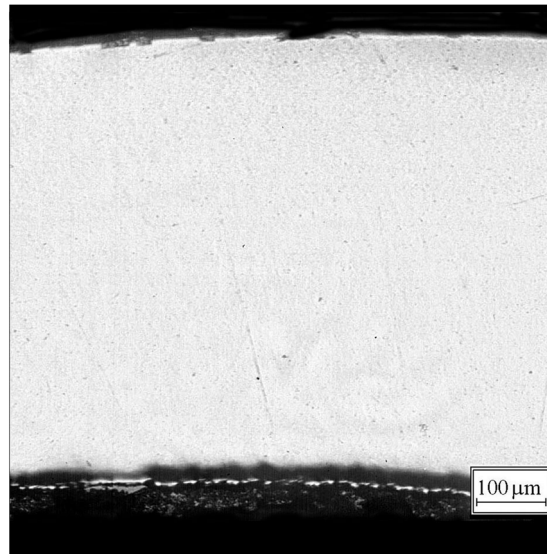
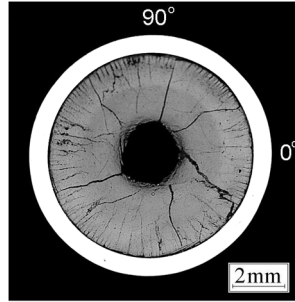


Fig.E-1.2. Cross-section and cladding microstructure of fuel rod # RT1 at 113 mm elevation (from low cap)

RT1

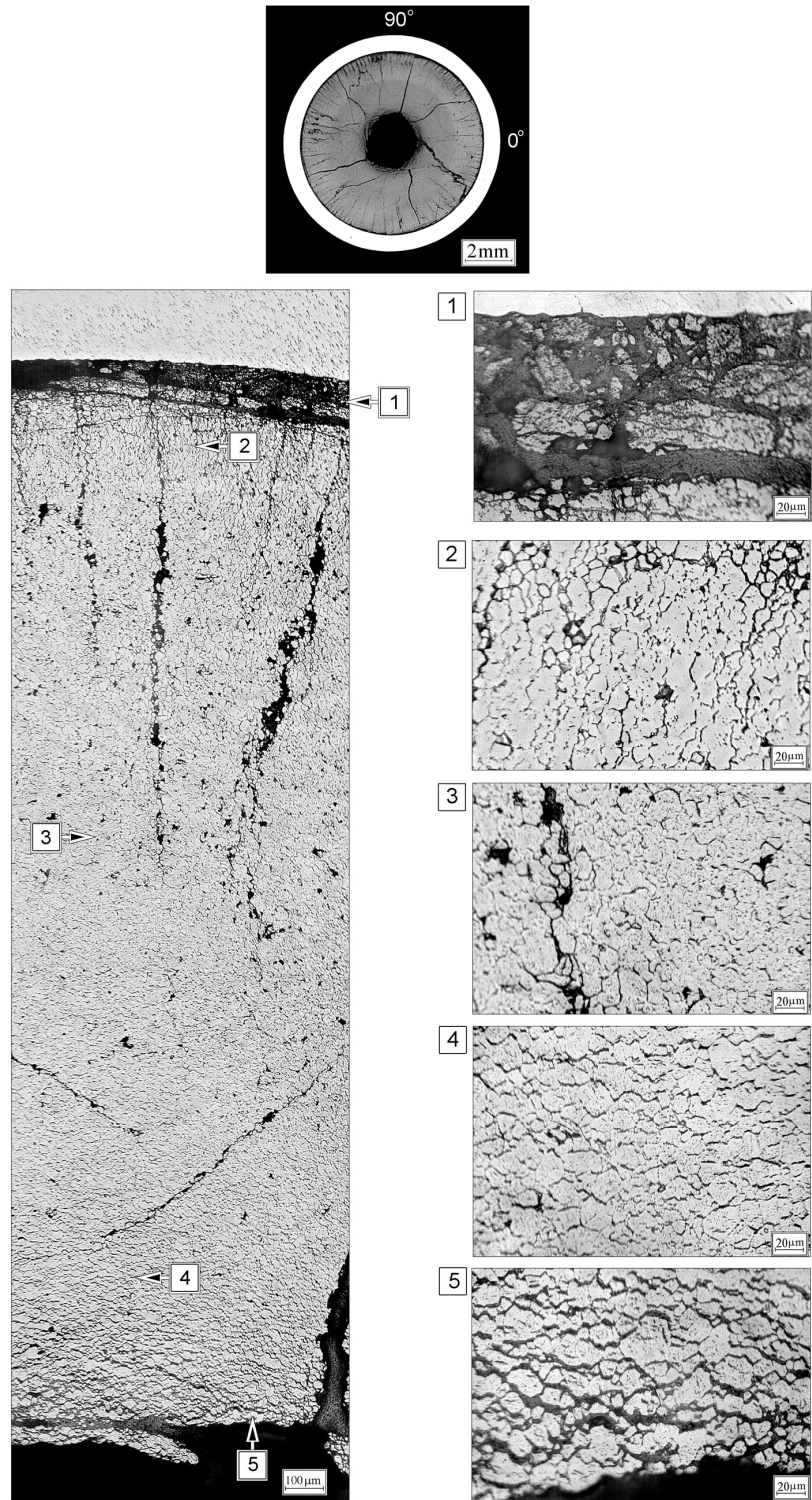


Fig.E-1.3. Cross-section and fuel microstructure of fuel rod # RT1 at 113 mm elevation (from low cap)

Table E-1.1. Time dependent energy characteristics of fuel rod # RT1

| Time (s) | Relative reactor power (current/maximum value) (per-unit) | Cumulative number of fissions in fuel rod (fiss) x10 ⁻¹⁴ | Power of fuel rod ¹⁾²⁾ (kW) | Energy deposition | | Fuel enthalpy ³⁾ | |
|----------|---|---|--|-------------------|------------|-----------------------------|---------|
| | | | | (cal/g fuel) | (J/g fuel) | FRAP-T6 | RAPTA-5 |
| 0.000 | 0.00E+00 | 0.000 | 0.000 | 0.000 | 0.000 | 0.000 | 0.000 |
| 0.001 | 1.76E-01 | 0.240 | 1260 | 2.507 | 10.49 | 3.010 | 2.386 |
| 0.002 | 5.73E-01 | 1.166 | 4095 | 12.13 | 50.79 | 13.201 | 12.045 |
| 0.003 | 9.88E-01 | 3.301 | 7069 | 34.44 | 144.2 | 35.610 | 34.383 |
| 0.004 | 7.32E-01 | 5.690 | 5233 | 59.33 | 248.4 | 60.455 | 59.119 |
| 0.005 | 3.19E-01 | 7.017 | 2281 | 73.16 | 306.3 | 74.106 | 72.559 |
| 0.006 | 1.65E-01 | 7.630 | 1181 | 79.57 | 333.1 | 80.313 | 78.541 |
| 0.007 | 8.90E-02 | 7.949 | 636.8 | 82.88 | 347.0 | 83.360 | 81.459 |
| 0.008 | 5.88E-02 | 8.138 | 420.7 | 84.84 | 355.2 | 85.045 | 83.077 |
| 0.009 | 5.24E-02 | 8.284 | 374.5 | 86.33 | 361.4 | 86.262 | 84.264 |
| 0.010 | 5.00E-02 | 8.416 | 357.7 | 87.72 | 367.3 | 87.385 | 85.379 |
| 0.012 | 5.93E-02 | 8.691 | 424.0 | 90.65 | 379.5 | 89.796 | 87.862 |
| 0.014 | 7.33E-02 | 9.037 | 524.4 | 94.22 | 394.5 | 92.851 | 90.944 |
| 0.016 | 8.05E-02 | 9.446 | 575.8 | 98.50 | 412.4 | 96.592 | 94.697 |
| 0.018 | 7.95E-02 | 9.869 | 568.9 | 102.9 | 430.8 | 100.483 | 98.676 |
| 0.020 | 6.85E-02 | 10.26 | 490.0 | 107.0 | 447.9 | 104.037 | 102.320 |
| 0.022 | 5.38E-02 | 10.58 | 384.7 | 110.3 | 461.9 | 106.885 | 105.220 |
| 0.024 | 4.21E-02 | 10.83 | 301.4 | 112.9 | 472.9 | 109.026 | 107.410 |
| 0.026 | 3.29E-02 | 11.03 | 235.3 | 115.0 | 481.4 | 110.633 | 109.200 |
| 0.028 | 2.76E-02 | 11.18 | 197.8 | 116.6 | 488.1 | 111.865 | 110.410 |
| 0.030 | 2.55E-02 | 11.32 | 182.3 | 118.0 | 494.2 | 112.927 | 111.370 |
| 0.050 | 2.33E-02 | 12.59 | 166.4 | 131.3 | 549.7 | 122.572 | 121.330 |
| 0.070 | 1.84E-02 | 13.68 | 131.8 | 142.7 | 597.5 | 130.730 | 129.710 |
| 0.090 | 1.43E-02 | 14.54 | 102.6 | 151.6 | 634.7 | 136.829 | 135.920 |
| 0.110 | 9.12E-03 | 15.17 | 65.43 | 158.2 | 662.5 | 141.113 | 140.300 |
| 0.130 | 3.38E-03 | 15.48 | 24.39 | 161.4 | 675.7 | 142.614 | 141.550 |
| 0.150 | 1.29E-03 | 15.59 | 9.439 | 162.6 | 680.7 | 142.832 | 141.070 |
| 0.200 | 3.45E-04 | 15.68 | 2.730 | 163.6 | 684.8 | 141.257 | 138.770 |
| 1.000 | 3.11E-05 | 15.81 | 0.341 | 165.4 | 692.3 | 121.068 | 117.990 |
| 10.00 | 3.60E-06 | 16.04 | 0.050 | 169.5 | 709.7 | 29.703 | 27.267 |
| 100.0 | 7.01E-08 | 16.15 | 0.008 | 172.5 | 722.4 | 5.033 | 4.508 |
| 1000 | 2.74E-13 | 16.16 | 1.73E-04 | 174.0 | 728.5 | 0.000 | 0.000 |

¹⁾ Average values determined in accordance with results of RRC KI and VNIIEF calculations

²⁾ Maximum power value is 7152.5 kW (t=0.0032 s)

³⁾ Average radial value

RT1

Table E-1.2. Radial energy characteristics of fuel rod # RT1*

| Parameters | Coordinates of fuel radial layers (mm) | | | |
|---|--|------------------------|------------------------|-------------------------|
| | 1 layer (1.23-2.82) | 2 layer (2.82-3.44) | 3 layer (3.44-3.71) | 4 layer (3.71-3.795) |
| Number of fissions $\times 10^{-14}$ (fiss) | 7.266 | 4.700 | 2.829 | 1.364 |
| Fission density $\times 10^{-13}$ (fiss/g fuel) | 2.292 | 2.431 | 2.997 | 4.417 |
| Power ** (kW) | 3173 | 2086 | 1264 | 629.7 |
| Energy deposition (cal/g fuel) | 156.6 | 166.5 | 205.1 | 303.3 |
| Energy deposition (J/g fuel) | 655.8 | 697.3 | 858.9 | 1270 |
| Energy deposition *** (per-unit) | 0.517 | 0.550 | 0.677 | 1.000 |

* Average values were determined in accordance with results of RRC KI and VNIIEF calculations

** The power for the entire length of each layer at time 0.0032 s

*** Energy deposition in current layer/energy deposition in 4th layer

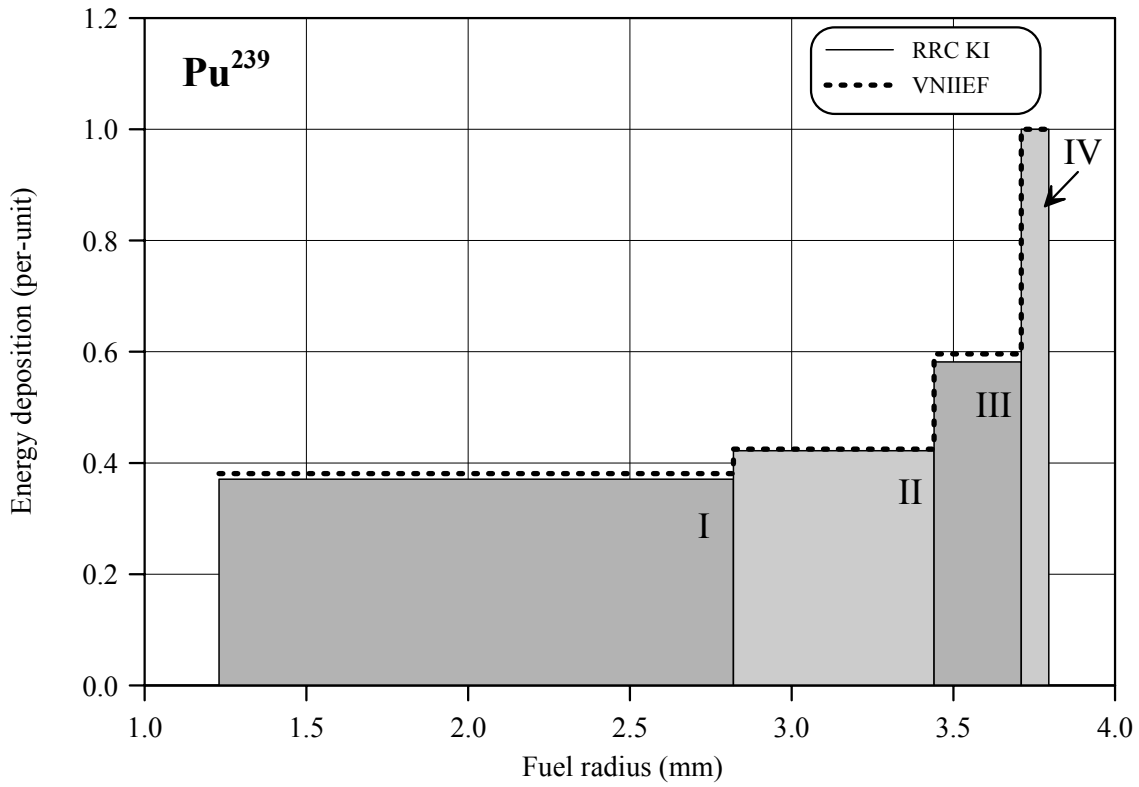
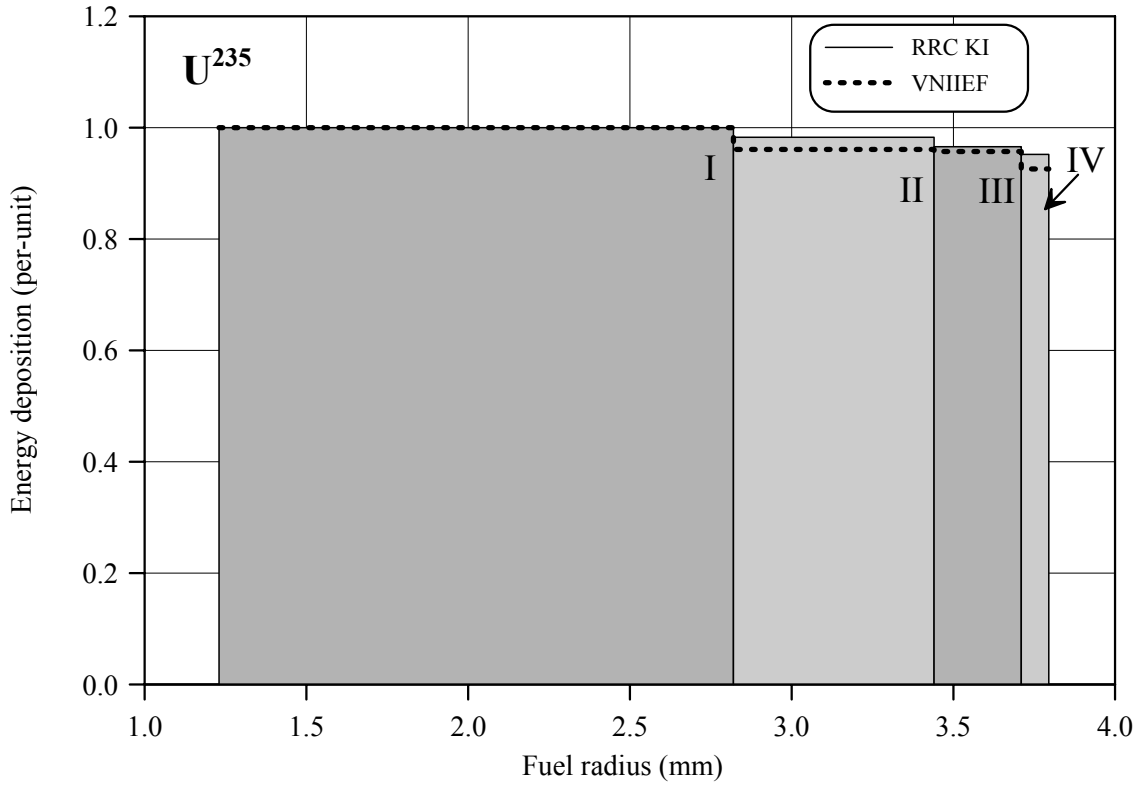


Fig.E-1.4. U^{235} and Pu^{239} radial distribution of energy deposition for fuel rod # RT1

RT1

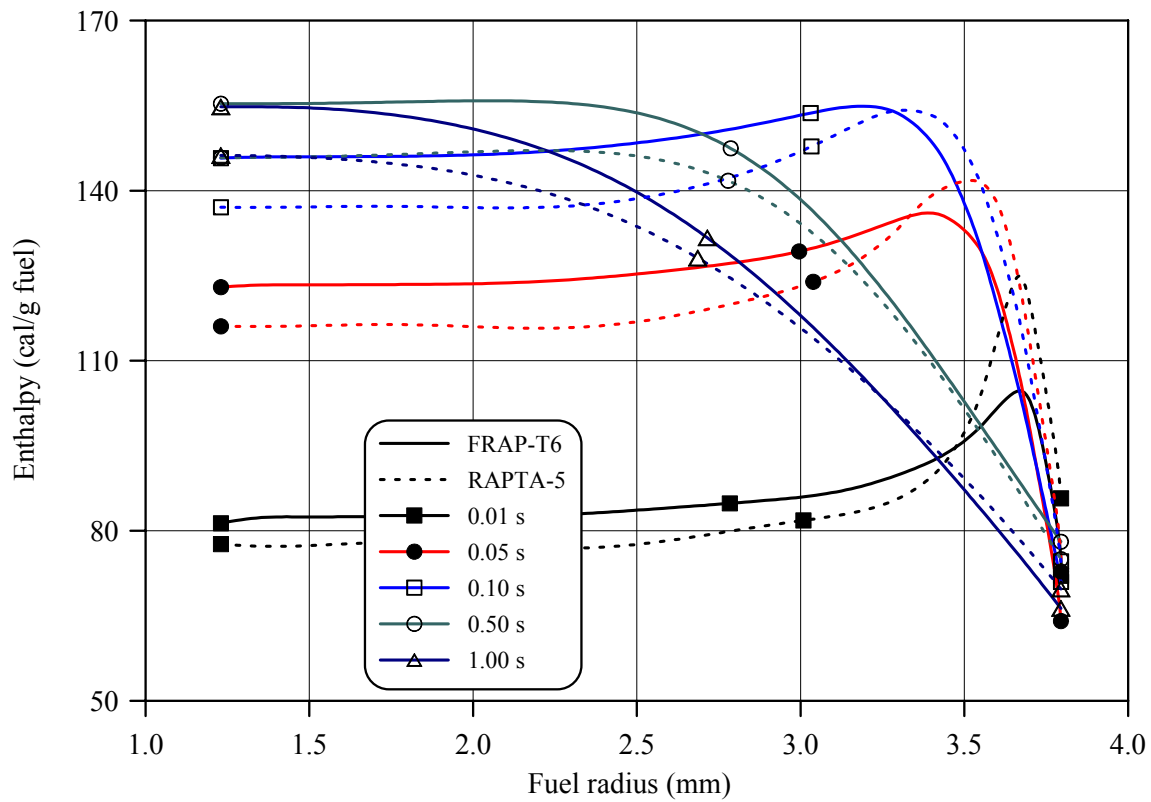
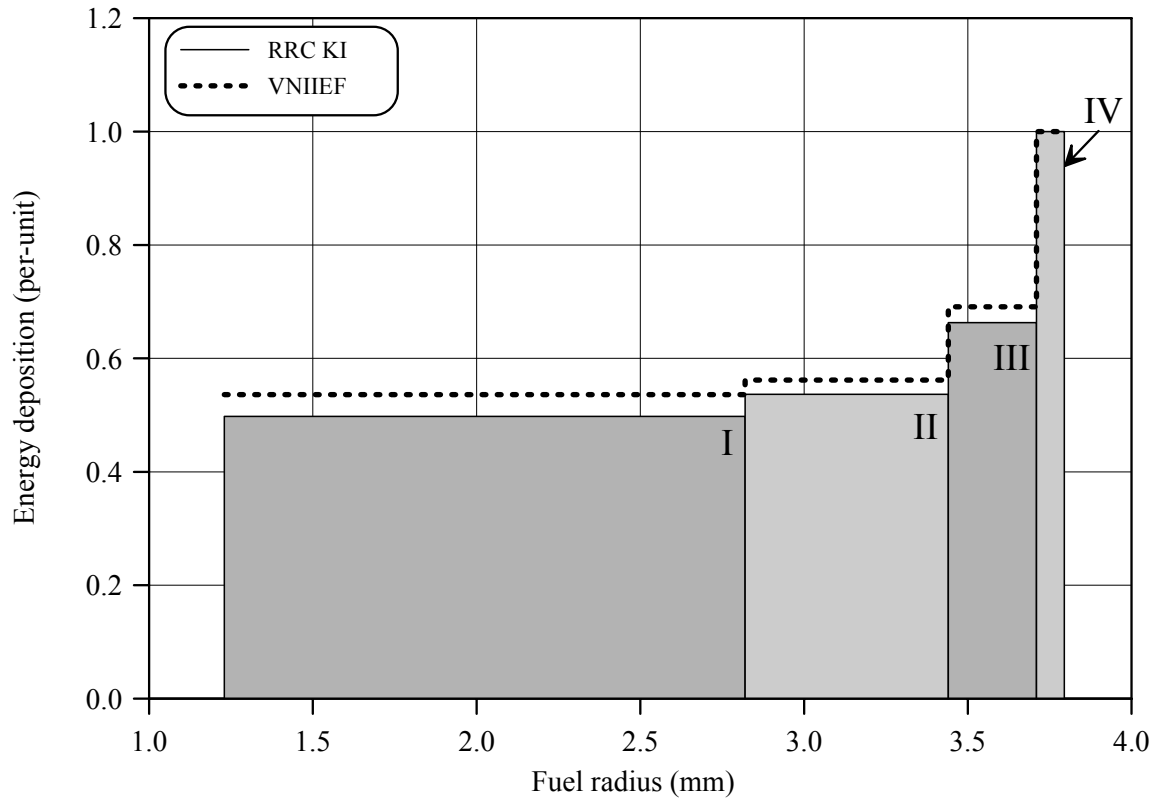


Fig.E-1.5. Radial distribution of energy deposition and fuel enthalpy for fuel rod # RT1

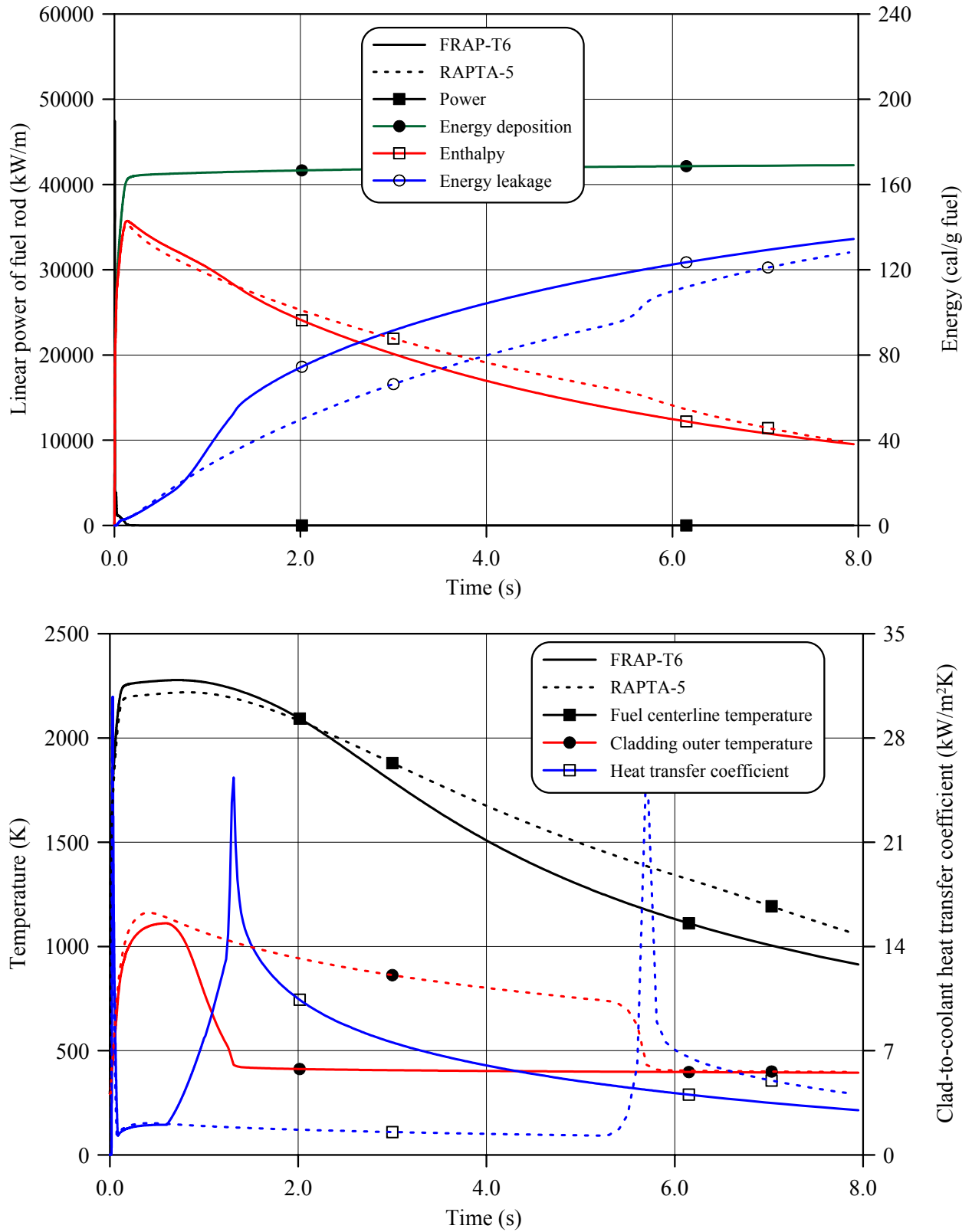


Fig.E-1.6. Thermal history of fuel rod # RT1 during the BGR test in accordance with FRAP-T6/VVER and RAPTA-5 calculations

RT1

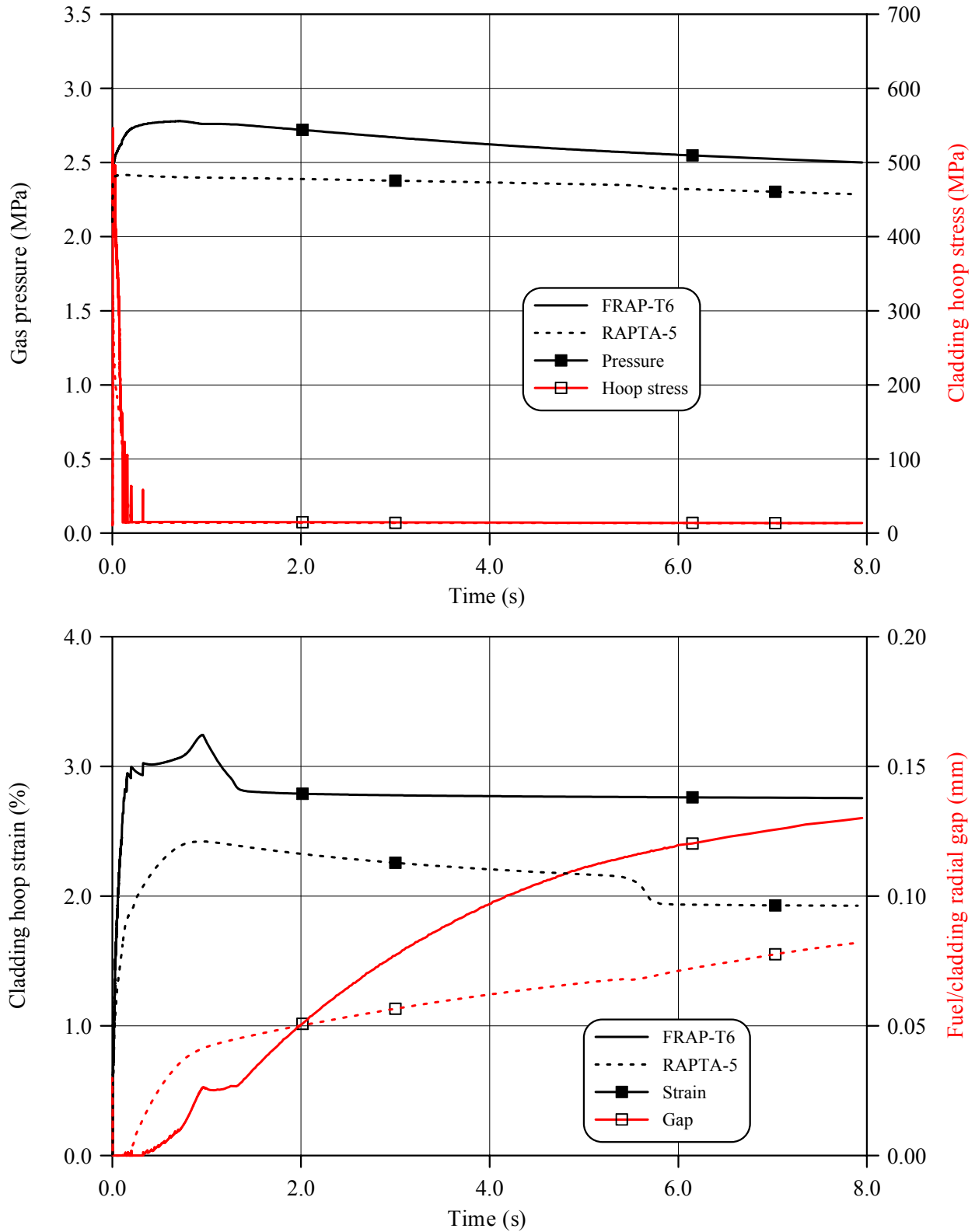


Fig.E-1.7. Mechanical behavior of fuel rod # RT1 during the BGR test in accordance with FRAP-T6/VVER and RAPTA-5 calculations

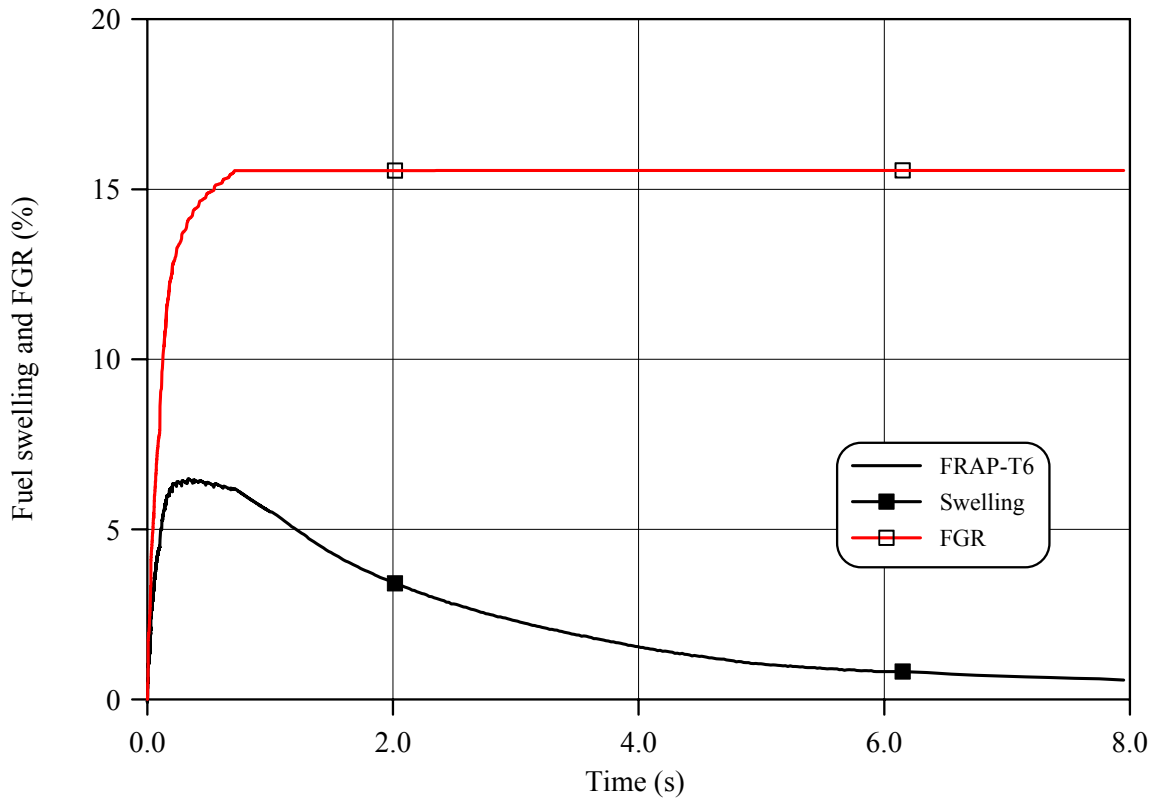
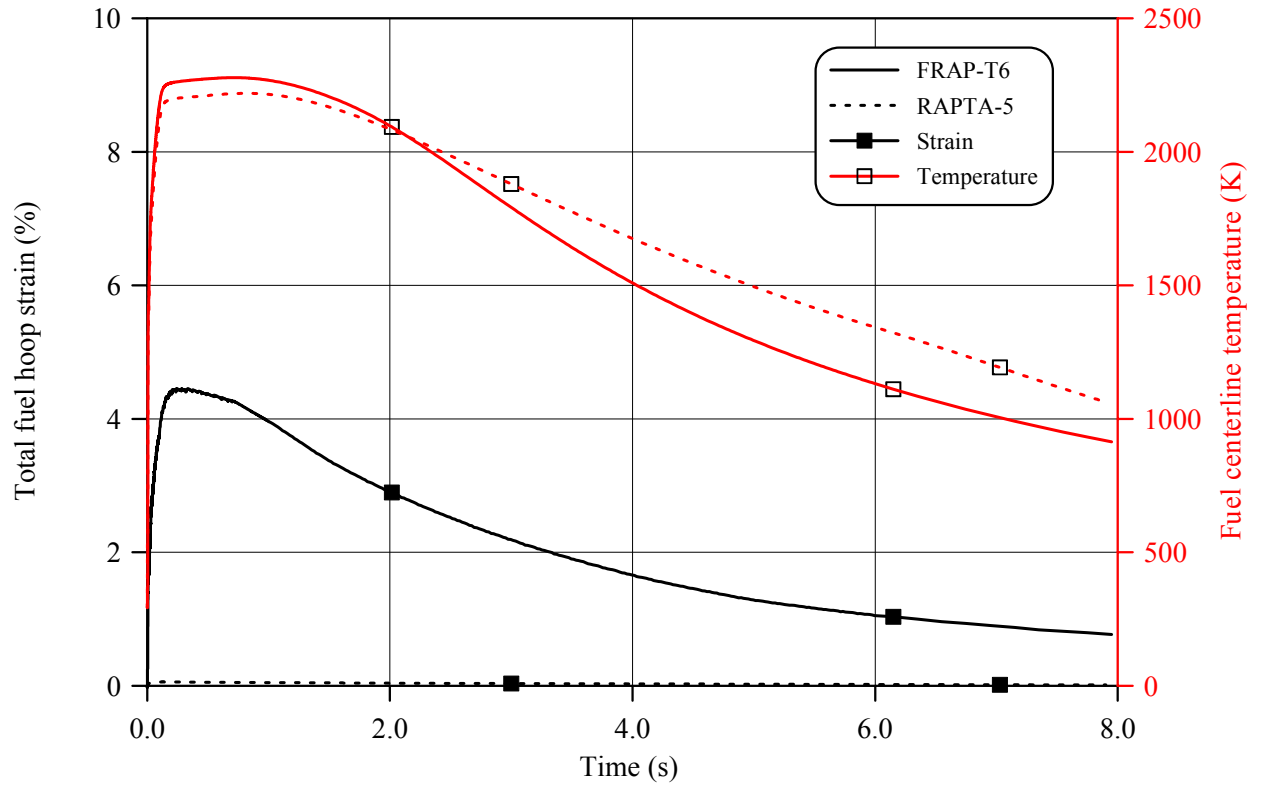


Fig.E-1.8. Fuel behavior during the BGR test of fuel rod # RT1 in accordance with FRAP-T6/VVER and RAPTA-5 calculations

RT1

Table E-1.3. Axial distribution of cladding average outer diameter in fuel rod # RT1*

| Axial coordinate (mm) | Cladding diameter (mm) | Axial coordinate (mm) | Cladding diameter (mm) | Axial coordinate (mm) | Cladding diameter (mm) | Axial coordinate (mm) | Cladding diameter (mm) |
|-----------------------|------------------------|-----------------------|------------------------|-----------------------|------------------------|-----------------------|------------------------|
| 30 | 9.200 | 68 | 9.238 | 106 | 9.248 | 144 | 9.336 |
| 32 | 9.197 | 70 | 9.250 | 108 | 9.265 | 146 | 9.293 |
| 34 | 9.213 | 72 | 9.252 | 110 | 9.248 | 148 | 9.228 |
| 36 | 9.226 | 74 | 9.263 | 112 | 9.220 | 150 | 9.237 |
| 38 | 9.239 | 76 | 9.264 | 114 | 9.198 | 152 | 9.294 |
| 40 | 9.235 | 78 | 9.249 | 116 | 9.245 | 154 | 9.354 |
| 42 | 9.214 | 80 | 9.257 | 118 | 9.304 | 156 | 9.360 |
| 44 | 9.203 | 82 | 9.266 | 120 | 9.344 | 158 | 9.303 |
| 46 | 9.220 | 84 | 9.283 | 122 | 9.308 | 160 | 9.246 |
| 48 | 9.227 | 86 | 9.310 | 124 | 9.244 | 162 | 9.277 |
| 50 | 9.235 | 88 | 9.321 | 126 | 9.221 | 164 | 9.349 |
| 52 | 9.226 | 90 | 9.309 | 128 | 9.268 | 166 | 9.426 |
| 54 | 9.184 | 92 | 9.315 | 130 | 9.310 | 168 | 9.338 |
| 56 | 9.160 | 94 | 9.321 | 132 | 9.325 | 170 | 9.181 |
| 58 | 9.168 | 96 | 9.352 | 134 | 9.312 | 172 | 9.097 |
| 60 | 9.185 | 98 | 9.358 | 136 | 9.289 | 174 | 9.065 |
| 62 | 9.211 | 100 | 9.299 | 138 | 9.306 | 176 | 9.075 |
| 64 | 9.236 | 102 | 9.219 | 140 | 9.340 | 178 | 9.073 |
| 66 | 9.235 | 104 | 9.217 | 142 | 9.346 | 180 | 9.315 |

* Measured value determined on the basis of profilometry data (16 azimuthal directions)

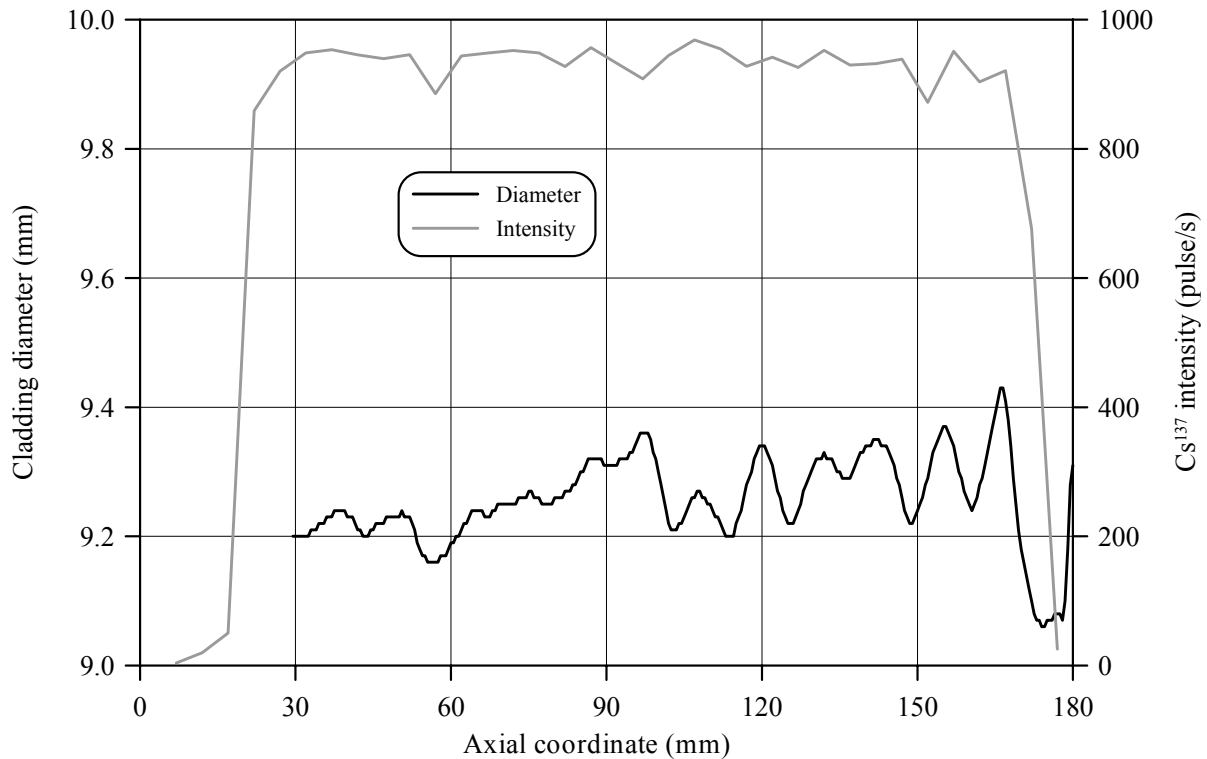


Fig.E-1.9. Cladding measured average diameter and γ -scanning results for fuel rod # RT1

Table E-1.4. The PIE results for fuel rod # RT1

| Parameter | | Value |
|-----------|--|-------|
| 1. | Cladding outer diameter (mm): | |
| 1.1. | Maximum diameter of the bidimensional data sample in "fuel rod length - azimuthal angle" coordinates (mm) | 9.50 |
| 1.2. | Averaged azimuthal diameter and maximum diameter along the length selected from the sample of averaged azimuthal diameter (mm) | 9.43 |
| 1.3. | Averaged diameter of the bidimensional data sample in "fuel rod length - azimuthal angle" coordinates (mm) | 9.26 |
| 2. | Cladding maximum residual hoop strain (%) | 4.06 |
| 3. | Fuel pellet conditional diameter (mm) in cross-section*: at 113 mm elevation | 7.64 |
| 4. | ZrO ₂ outer thickness (μm) in cross-section: at 113 mm elevation | 3–5 |
| 5. | ZrO ₂ inner thickness (μm) in cross-section: at 113 mm elevation | 0 |
| 6. | Parameters characterizing FGR: | |
| 6.1. | Gas composition (% by volume): | |
| | He | 86.08 |
| | N ₂ | 0.70 |
| | O ₂ | 0.13 |
| | Ar | 0.014 |
| | CO ₂ | 0.011 |
| | Kr | 1.19 |
| | Xe | 11.88 |
| 6.2. | Free gas volume (cm ³) | 6.5 |
| 6.3. | Gas volume under normal conditions (cm ³) | 142.3 |
| 6.4. | Gas pressure under normal conditions (MPa) | 2.19 |
| 6.5. | FGR (%) | 22.8 |

* Reference value determined by the processing of fuel cross-section photographs

RT1**Table E-1.5. Organized BGR test results for fuel rod # RT1**

| | Parameter | Unit | Value | | |
|-----|---|------------------|----------|------------|----------|
| | | | Measured | Calculated | |
| | | | | FRAP-T6 | RAPTA-5 |
| 1. | Fuel burnup | MW d/kg U | 48.3 | 48.3 | 48.3 |
| 2. | Initial gas pressure | MPa | 2.1 | 2.1 | 2.1 |
| 3. | Energy deposition | cal/g fuel | 174.0 | 174.0 | 174.0 |
| 4. | Peak fuel enthalpy* | cal/g fuel | - | 142.9 | 141.6 |
| 5. | Fuel maximum temperature | K | - | 2313 | 2327 |
| 6. | Maximum temperature of cladding outer surface | K | - | 1111 | 1162 |
| 7. | Cladding burst | Failed, Unfailed | Unfailed | Unfailed | Unfailed |
| 8. | Cladding residual hoop strain** | % | 2.20 | 2.66 | 1.86 |
| 9. | Kr volume content in gas composition after the BGR test | % | 1.19 | 1.67 | - |
| 10. | Xe volume content in gas composition after the BGR test | % | 11.88 | 10.00 | - |

* Average value of peak fuel enthalpy is 142.2 cal/g fuel

** Average value along the fuel stack length

Appendix E-2

*Individual Characteristics of Fuel Rod # RT2
after the BGR Test*

RT2

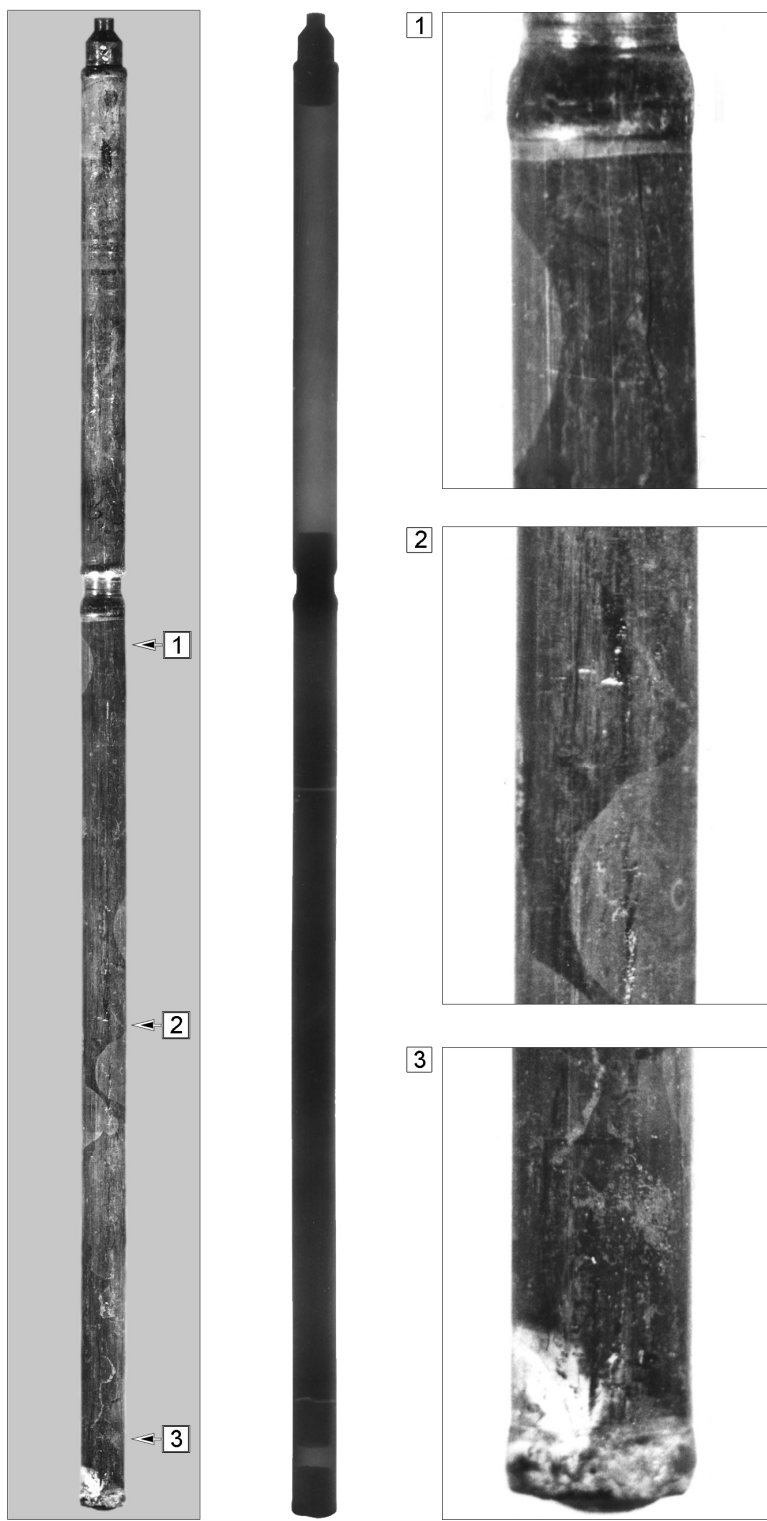


Fig.E-2.1. Appearance of unfailed fuel rod # RT2 after the BGR test (photographs and X-ray photograph)

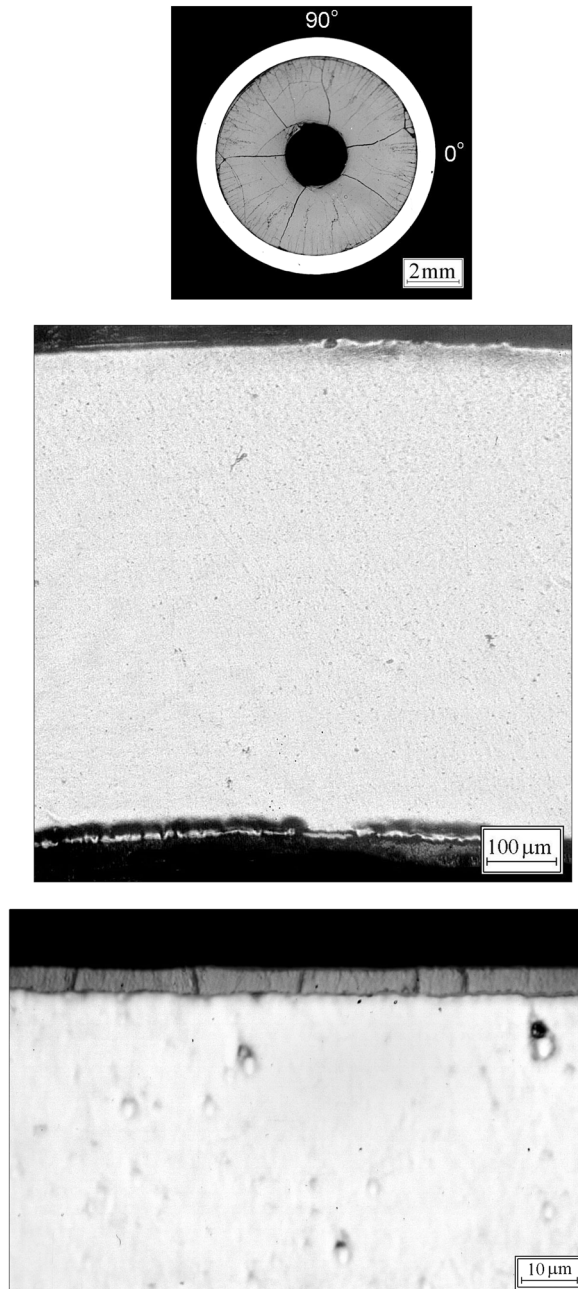


Fig.E-2.2. Cross-section and cladding microstructure of fuel rod # RT2 at 99 mm elevation (from low cap)

RT2

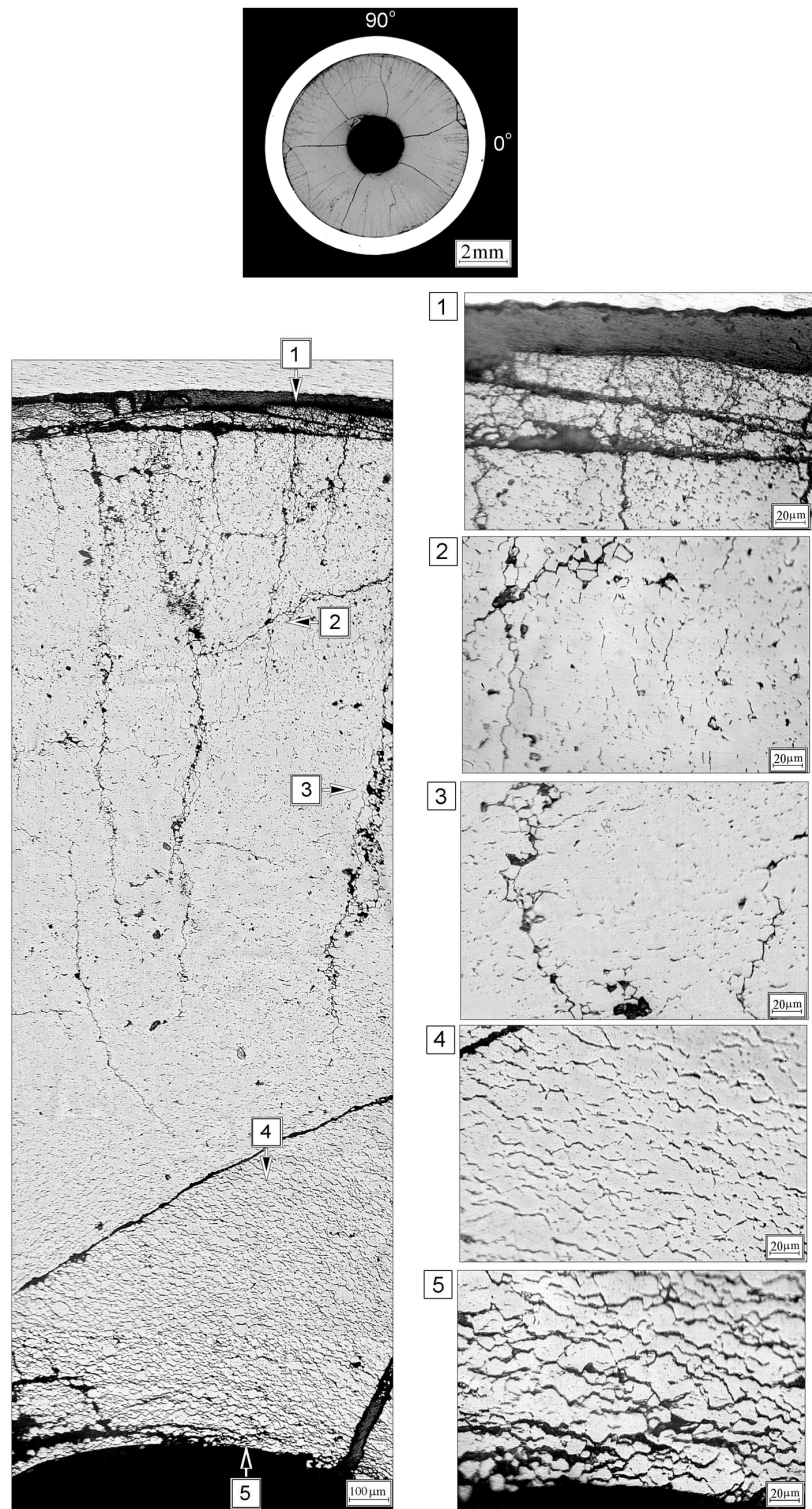


Fig.E-2.3. Cross-section and fuel microstructure of fuel rod # RT2 at 99 mm elevation (from low cap)

Table E-2.1. Time dependent energy characteristics of fuel rod # RT2

| Time (s) | Relative reactor power (current/maximum value) (per-unit) | Cumulative number of fissions in fuel rod (fiss) x10 ⁻¹⁴ | Power of fuel rod ¹⁾²⁾ (kW) | Energy deposition | | Fuel enthalpy ³⁾ | |
|----------|---|---|--|-------------------|------------|-----------------------------|---------|
| | | | | (cal/g fuel) | (J/g fuel) | FRAP-T6 | RAPTA-5 |
| 0.000 | 7.10E-02 | 0.000 | 0.000 | 0.000 | 0.000 | 0.000 | 0.000 |
| 0.001 | 4.44E-01 | 0.516 | 2415 | 5.397 | 22.59 | 5.829 | 5.110 |
| 0.002 | 9.04E-01 | 1.777 | 4917 | 18.76 | 78.52 | 19.119 | 18.520 |
| 0.003 | 9.40E-01 | 3.576 | 5115 | 37.83 | 158.4 | 37.673 | 37.576 |
| 0.004 | 6.20E-01 | 5.042 | 3374 | 53.34 | 223.3 | 52.772 | 52.916 |
| 0.005 | 3.08E-01 | 5.890 | 1673 | 62.41 | 261.3 | 61.506 | 61.691 |
| 0.006 | 1.56E-01 | 6.302 | 846.7 | 66.68 | 279.2 | 65.486 | 65.655 |
| 0.007 | 9.88E-02 | 6.530 | 537.4 | 69.11 | 289.3 | 67.641 | 67.796 |
| 0.008 | 7.42E-02 | 6.685 | 403.6 | 70.79 | 296.4 | 69.046 | 69.202 |
| 0.009 | 6.61E-02 | 6.812 | 359.4 | 72.14 | 302.0 | 70.151 | 70.318 |
| 0.010 | 6.38E-02 | 6.938 | 347.0 | 73.41 | 307.3 | 71.177 | 71.364 |
| 0.012 | 6.59E-02 | 7.176 | 358.7 | 75.94 | 317.9 | 73.233 | 73.405 |
| 0.014 | 6.95E-02 | 7.431 | 378.0 | 78.64 | 329.3 | 75.489 | 75.808 |
| 0.016 | 6.71E-02 | 7.688 | 365.4 | 81.37 | 340.6 | 77.764 | 78.147 |
| 0.018 | 6.08E-02 | 7.926 | 330.8 | 83.91 | 351.3 | 79.884 | 80.304 |
| 0.020 | 5.21E-02 | 8.138 | 283.6 | 86.14 | 360.6 | 81.698 | 82.379 |
| 0.022 | 4.33E-02 | 8.309 | 235.8 | 88.02 | 368.5 | 83.194 | 83.861 |
| 0.024 | 3.65E-02 | 8.460 | 198.7 | 89.58 | 375.0 | 84.396 | 85.038 |
| 0.026 | 3.20E-02 | 8.590 | 174.5 | 90.92 | 380.7 | 85.397 | 86.178 |
| 0.028 | 2.96E-02 | 8.699 | 161.1 | 92.13 | 385.7 | 86.280 | 87.089 |
| 0.030 | 2.88E-02 | 8.809 | 156.8 | 93.27 | 390.5 | 87.109 | 87.794 |
| 0.050 | 2.90E-02 | 9.936 | 157.8 | 105.2 | 440.4 | 95.999 | 97.218 |
| 0.070 | 2.33E-02 | 10.90 | 126.9 | 115.4 | 483.3 | 103.409 | 104.960 |
| 0.090 | 1.92E-02 | 11.70 | 104.8 | 123.8 | 518.4 | 109.210 | 111.040 |
| 0.110 | 1.06E-02 | 12.27 | 57.66 | 129.9 | 544.0 | 113.001 | 115.210 |
| 0.130 | 3.90E-03 | 12.51 | 21.44 | 132.6 | 555.1 | 114.296 | 116.180 |
| 0.150 | 1.49E-03 | 12.61 | 8.302 | 133.6 | 559.2 | 114.072 | 115.740 |
| 0.200 | 4.00E-04 | 12.68 | 2.414 | 134.4 | 562.6 | 112.792 | 113.770 |
| 1.000 | 3.59E-05 | 12.79 | 0.300 | 135.9 | 568.8 | 96.970 | 96.035 |
| 10.00 | 4.15E-06 | 12.98 | 0.044 | 139.3 | 583.1 | 20.562 | 17.632 |
| 100.0 | 8.08E-08 | 13.07 | 0.007 | 141.8 | 593.8 | 4.773 | 4.276 |
| 1000 | 3.16E-13 | 13.08 | 1.59E-04 | 143.0 | 598.8 | 0.000 | 0.000 |

¹⁾ Average values determined in accordance with results of RRC KI and VNIIEF calculations

²⁾ Maximum power value is 5440.5 kW (t=0.0026 s)

³⁾ Average radial value

RT2

Table E-2.2. Radial energy characteristics of fuel rod # RT2*

| Parameters | Coordinates of fuel radial layers (mm) | | | |
|---|--|------------------------|------------------------|-------------------------|
| | 1 layer (1.23-2.82) | 2 layer (2.82-3.44) | 3 layer (3.44-3.71) | 4 layer (3.71-3.795) |
| Number of fissions $\times 10^{-14}$ (fiss) | 5.879 | 3.819 | 2.269 | 1.103 |
| Fission density $\times 10^{-13}$ (fiss/g fuel) | 1.878 | 2.008 | 2.444 | 3.629 |
| Power ** (kW) | 2426 | 1585 | 955.5 | 474.6 |
| Energy deposition (cal/g fuel) | 128.6 | 137.3 | 167.4 | 252.3 |
| Energy deposition (J/g fuel) | 538.6 | 574.9 | 700.8 | 1056 |
| Energy deposition *** (per-unit) | 0.510 | 0.544 | 0.663 | 1.000 |

* Average values were determined in accordance with results of RRC KI and VNIIEF calculations

** The power for the entire length of each layer at time 0.0026 s

*** Energy deposition in current layer/energy deposition in 4th layer

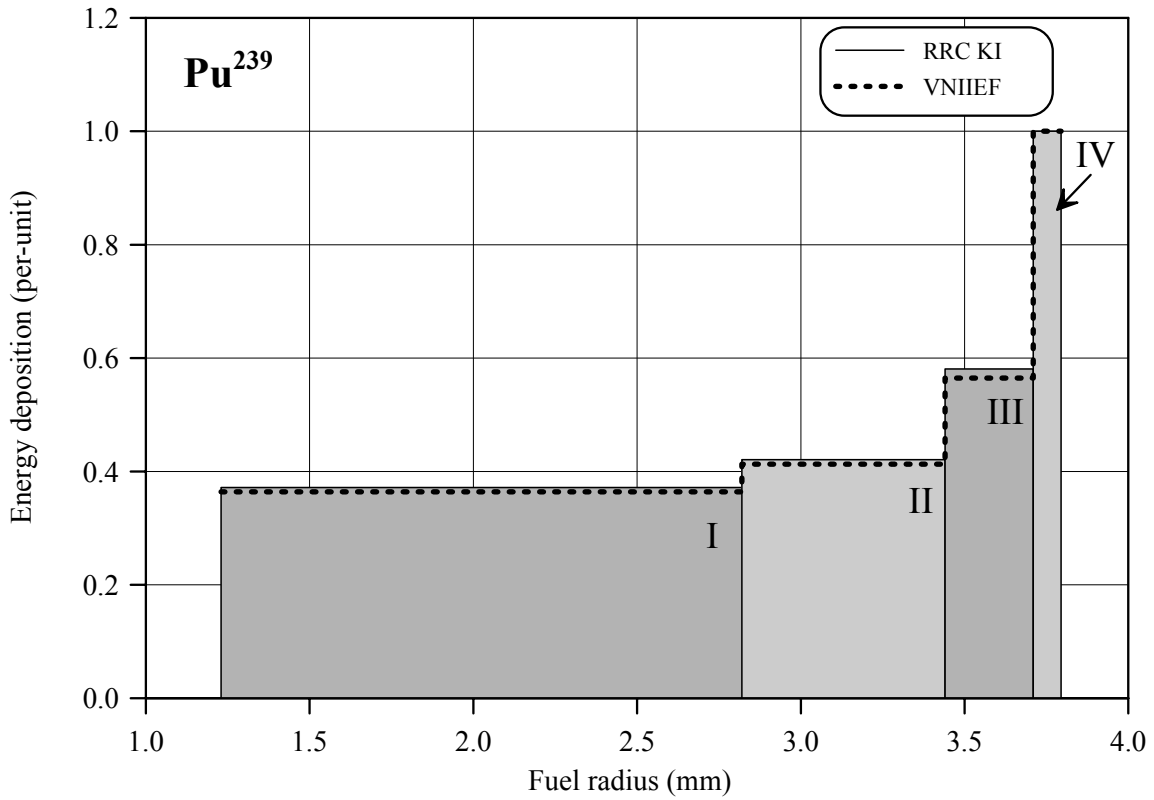
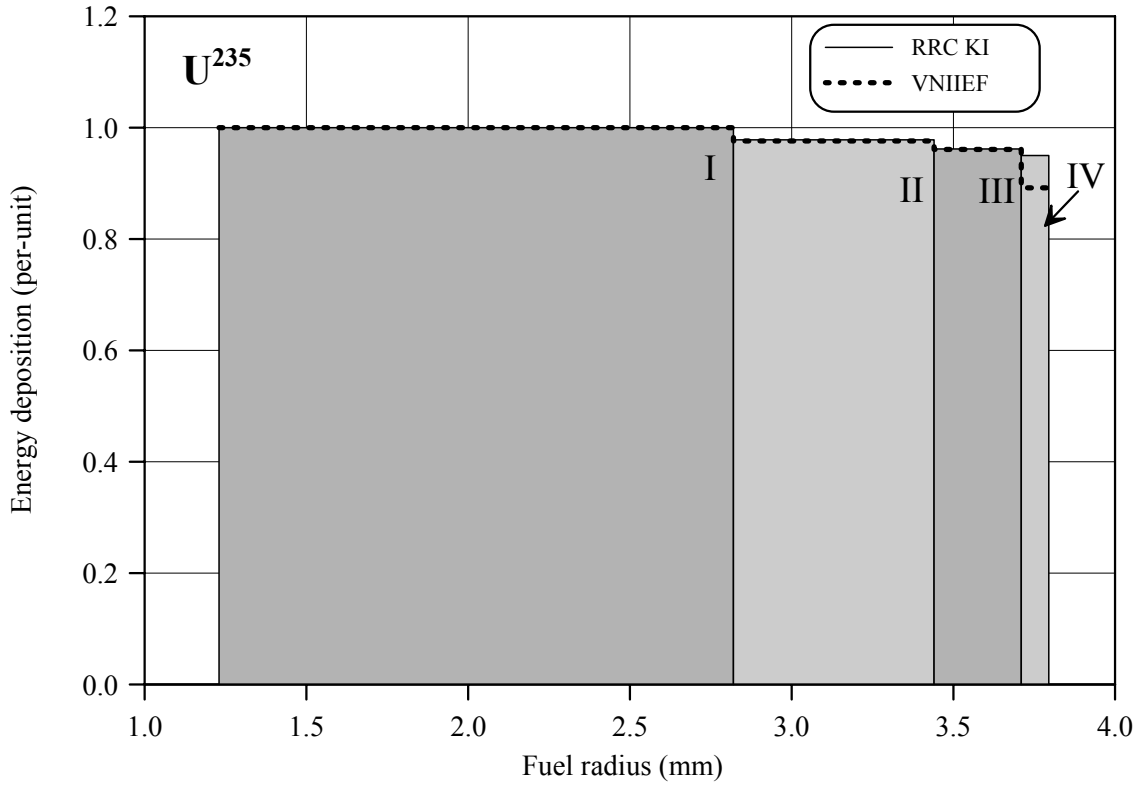


Fig.E-2.4. U²³⁵ and Pu²³⁹ radial distribution of energy deposition for fuel rod # RT2

RT2

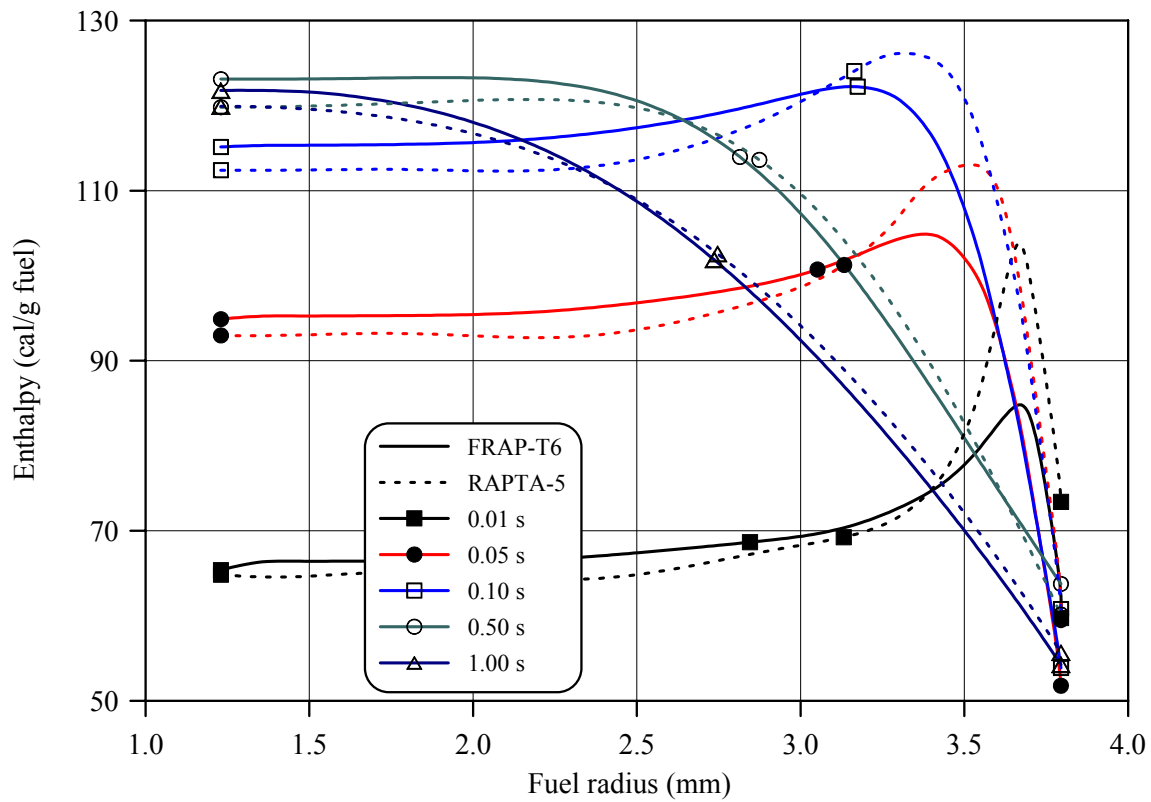
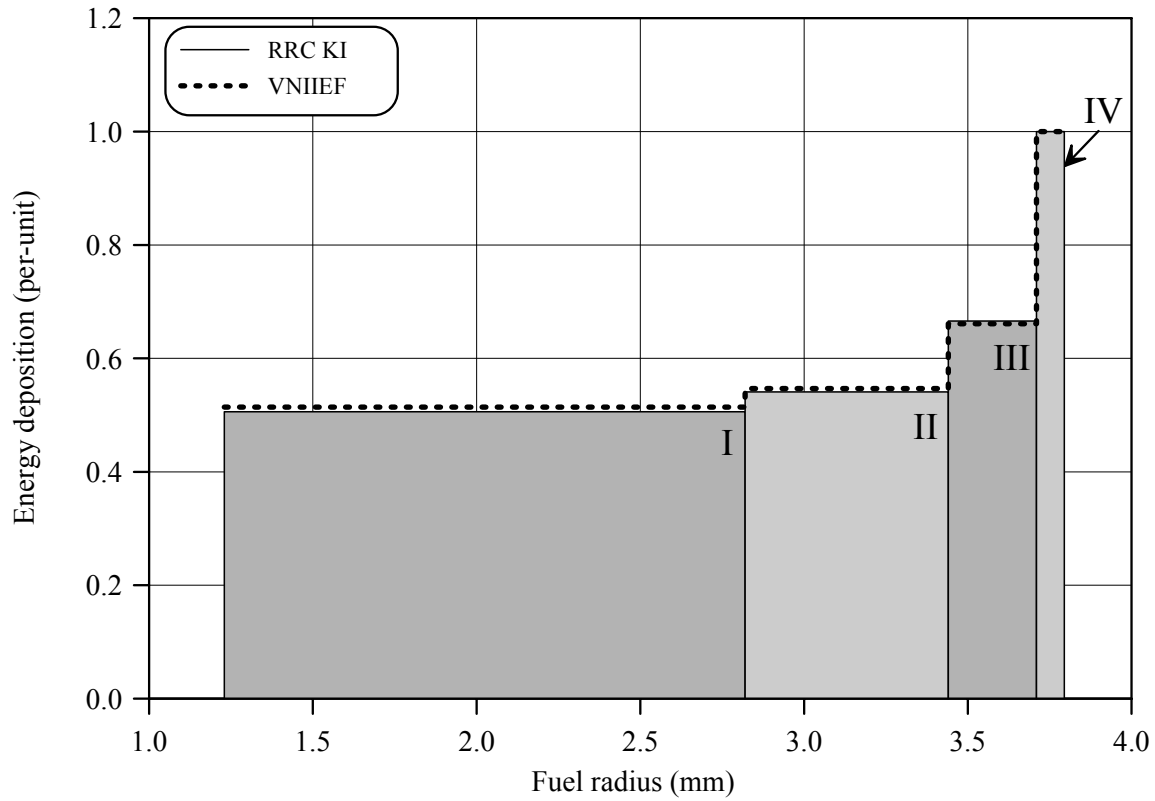


Fig.E-2.5. Radial distribution of energy deposition and fuel enthalpy for fuel rod # RT2

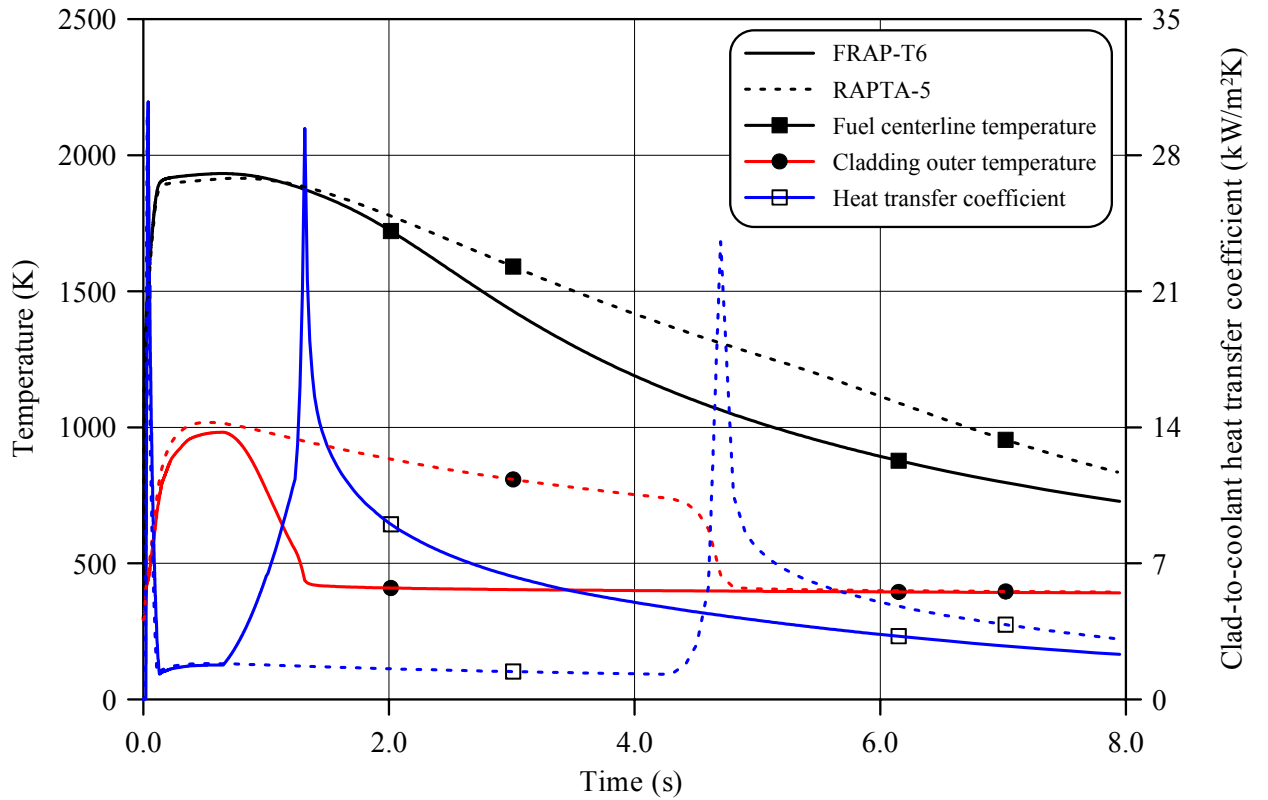
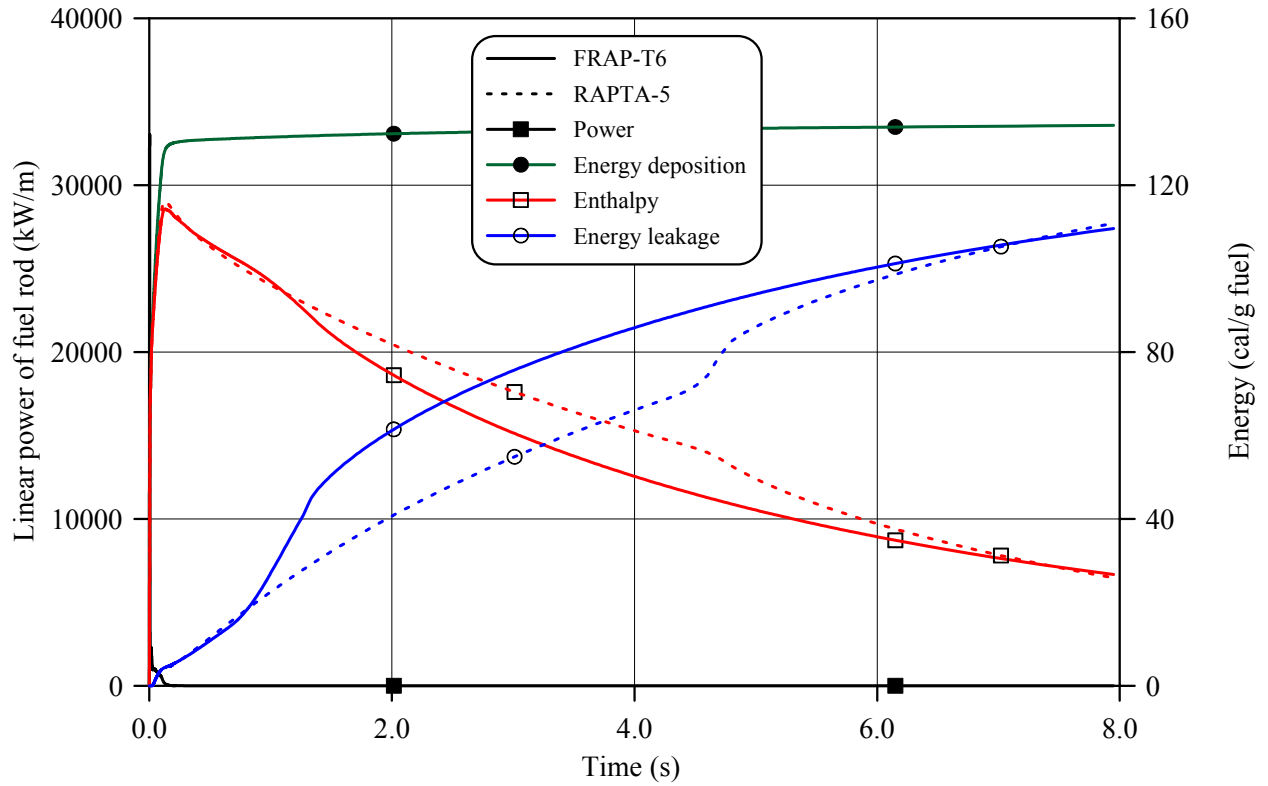


Fig.E-2.6. Thermal history of fuel rod # RT2 during the BGR test in accordance with FRAP-T6/VVER and RAPTA-5 calculations

RT2

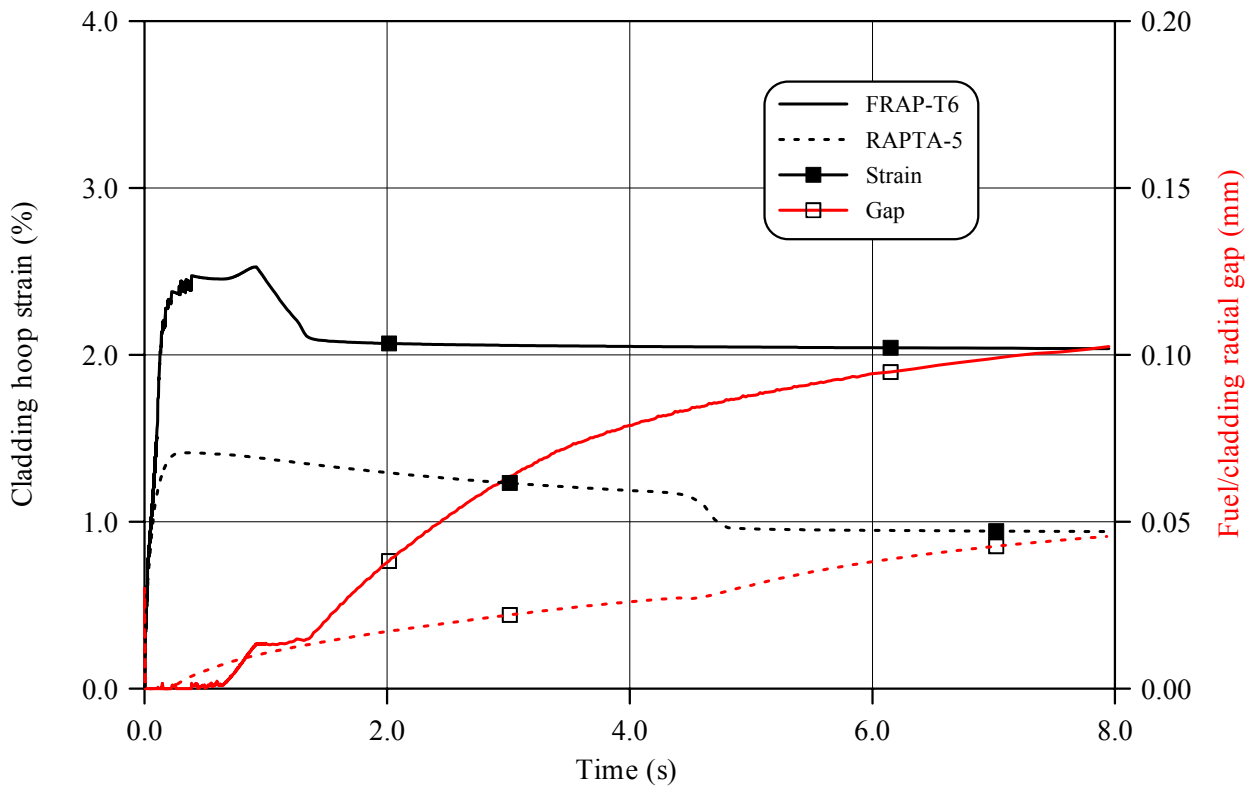
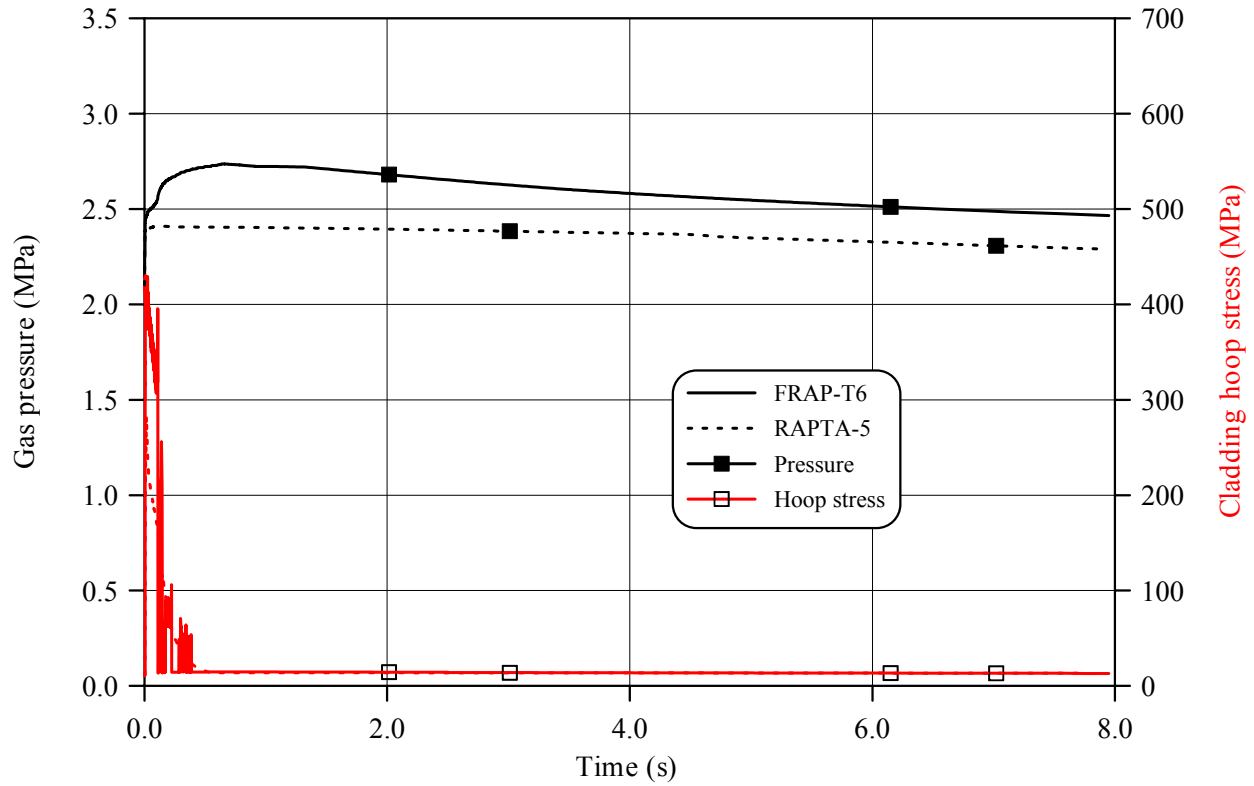


Fig.E-2.7. Mechanical behavior of fuel rod # RT2 during the BGR test in accordance with FRAP-T6/VVER and RAPTA-5 calculations

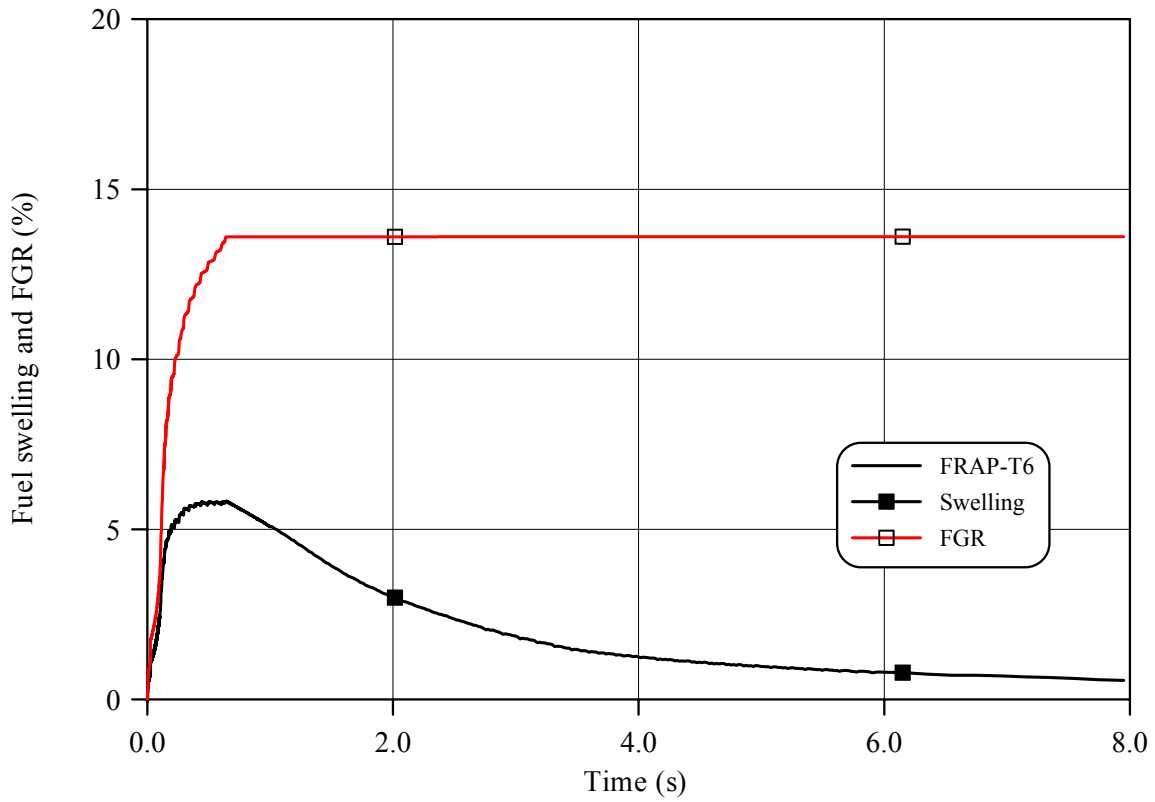
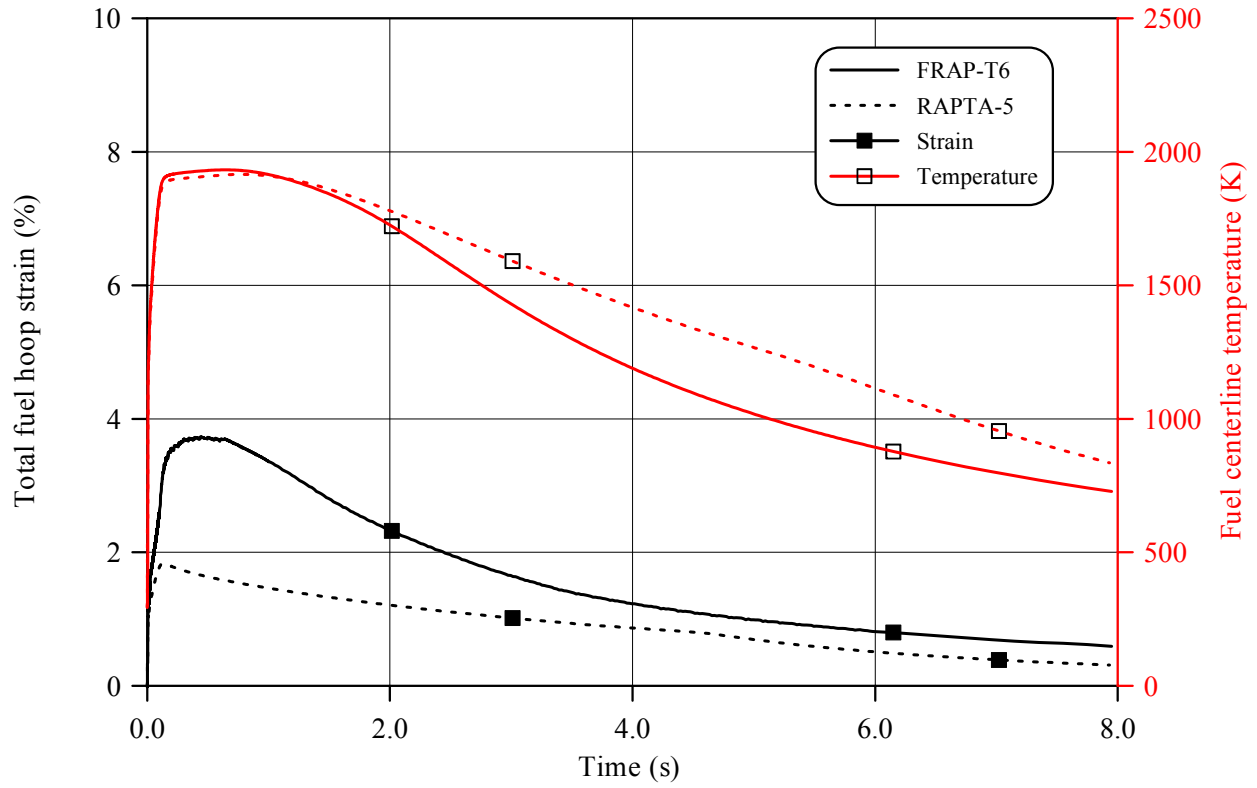


Fig.E-2.8. Fuel behavior during the BGR test of fuel rod # RT2 in accordance with FRAP-T6/VVER and RAPTA-5 calculations

RT2

Table E-2.3. Axial distribution of cladding average outer diameter in fuel rod # RT2*

| Axial coordinate (mm) | Cladding diameter (mm) | Axial coordinate (mm) | Cladding diameter (mm) | Axial coordinate (mm) | Cladding diameter (mm) | Axial coordinate (mm) | Cladding diameter (mm) |
|-----------------------|------------------------|-----------------------|------------------------|-----------------------|------------------------|-----------------------|------------------------|
| 30 | 9.102 | 68 | 9.112 | 106 | 9.116 | 144 | 9.124 |
| 32 | 9.103 | 70 | 9.114 | 108 | 9.123 | 146 | 9.129 |
| 34 | 9.105 | 72 | 9.112 | 110 | 9.125 | 148 | 9.130 |
| 36 | 9.108 | 74 | 9.114 | 112 | 9.128 | 150 | 9.128 |
| 38 | 9.098 | 76 | 9.111 | 114 | 9.129 | 152 | 9.133 |
| 40 | 9.112 | 78 | 9.112 | 116 | 9.129 | 154 | 9.134 |
| 42 | 9.111 | 80 | 9.116 | 118 | 9.118 | 156 | 9.134 |
| 44 | 9.110 | 82 | 9.119 | 120 | 9.132 | 158 | 9.135 |
| 46 | 9.113 | 84 | 9.111 | 122 | 9.137 | 160 | 9.128 |
| 48 | 9.108 | 86 | 9.126 | 124 | 9.140 | 162 | 9.119 |
| 50 | 9.108 | 88 | 9.125 | 126 | 9.137 | 164 | 9.112 |
| 52 | 9.109 | 90 | 9.124 | 128 | 9.136 | 166 | 9.098 |
| 54 | 9.108 | 92 | 9.127 | 130 | 9.129 | 168 | 9.072 |
| 56 | 9.112 | 94 | 9.126 | 132 | 9.135 | 170 | 9.067 |
| 58 | 9.120 | 96 | 9.121 | 134 | 9.139 | 172 | 9.065 |
| 60 | 9.118 | 98 | 9.124 | 136 | 9.138 | 174 | 9.042 |
| 62 | 9.111 | 100 | 9.127 | 138 | 9.132 | 176 | 9.141 |
| 64 | 9.119 | 102 | 9.129 | 140 | 9.131 | 178 | 9.433 |
| 66 | 9.120 | 104 | 9.127 | 142 | 9.124 | 180 | 8.937 |

* Measured value determined on the basis of profilometry data (16 azimuthal directions)

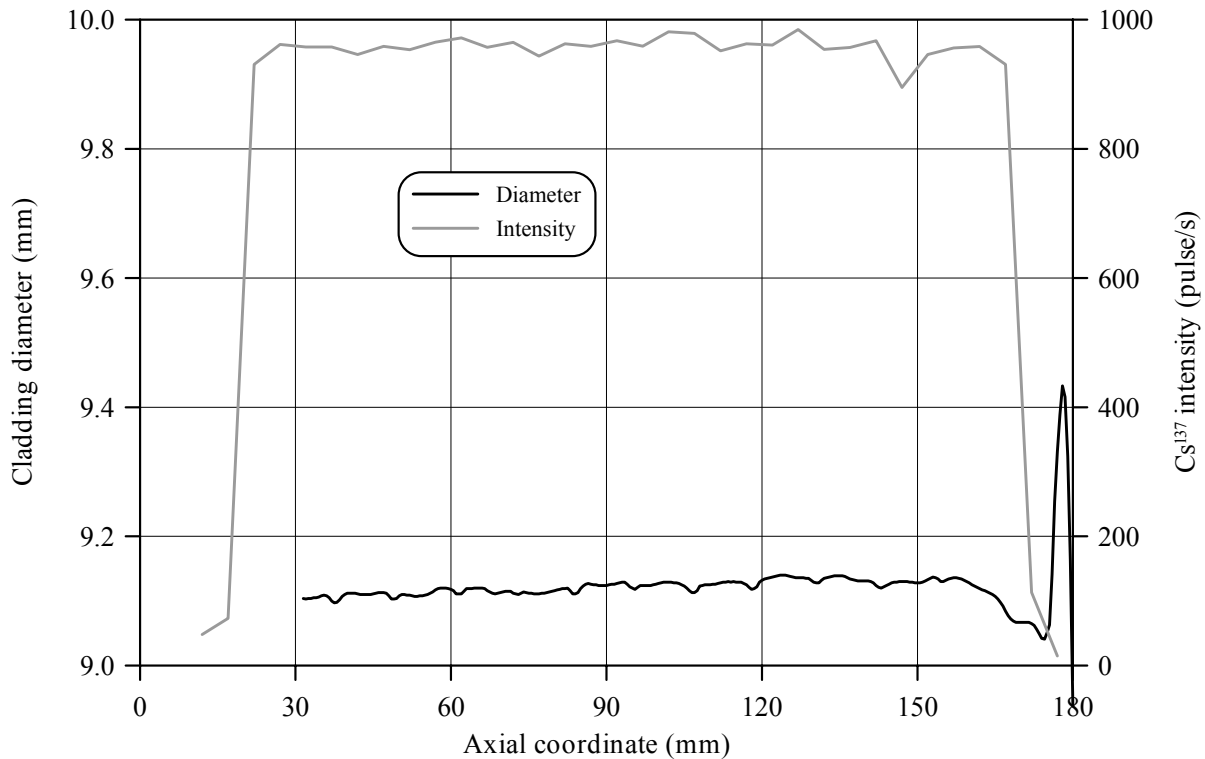


Fig.E-2.9. Cladding measured average diameter and γ -scanning results for fuel rod # RT2

Table E-2.4. The PIE results for fuel rod # RT2

| Parameter | | Value |
|-----------|--|-------|
| 1. | Cladding outer diameter (mm): | |
| 1.1. | Maximum diameter of the bidimensional data sample in "fuel rod length - azimuthal angle" coordinates (mm) | 9.15 |
| 1.2. | Averaged azimuthal diameter and maximum diameter along the length selected from the sample of averaged azimuthal diameter (mm) | 9.14 |
| 1.3. | Averaged diameter of the bidimensional data sample in "fuel rod length - azimuthal angle" coordinates (mm) | 9.12 |
| 2. | Cladding maximum residual hoop strain (%) | 0.85 |
| 3. | Fuel pellet conditional diameter (mm) in cross-section*: at 99 mm elevation | 7.64 |
| 4. | ZrO ₂ outer thickness (μm) in cross-section: at 99 mm elevation | 3-5 |
| 5. | ZrO ₂ inner thickness (μm) in cross-section: at 99 mm elevation | 0 |
| 6. | Parameters characterizing FGR: | |
| 6.1. | Gas composition (% by volume): | |
| | He | 86.08 |
| | N ₂ | 4.05 |
| | O ₂ | 0.12 |
| | Ar | 0.018 |
| | CO ₂ | 0.010 |
| | Kr | 0.90 |
| | Xe | 8.97 |
| 6.2. | Free gas volume (cm ³) | 6.2 |
| 6.3. | Gas volume under normal conditions (cm ³) | 137.5 |
| 6.4. | Gas pressure under normal conditions (MPa) | 2.22 |
| 6.5. | FGR (%) | 16.1 |

* Reference value determined by the processing of fuel cross-section photographs

RT2**Table E-2.5. Organized BGR test results for fuel rod # RT2**

| Parameter | Unit | Value | | |
|---|---------------------|----------|------------|----------|
| | | Measured | Calculated | |
| | | | FRAP-T6 | RAPTA-5 |
| 1. Fuel burnup | MW d/kg U | 48.0 | 48.0 | 48.0 |
| 2. Initial gas pressure | MPa | 2.1 | 2.1 | 2.1 |
| 3. Energy deposition | cal/g fuel | 143.0 | 143.0 | 143.0 |
| 4. Peak fuel enthalpy* | cal/g fuel | - | 114.3 | 116.2 |
| 5. Fuel maximum temperature | K | - | 1963 | 2011 |
| 6. Maximum temperature of cladding outer surface | K | - | 982 | 1019 |
| 7. Cladding burst | Failed, Unfailed | Unfailed | Unfailed | Unfailed |
| 8. Cladding residual hoop strain** | % | 0.63 | 1.94 | 0.88 |
| 9. Kr volume content in gas composition after the BGR test | % | 0.90 | 1.50 | - |
| 10. Xe volume content in gas composition after the BGR test | % | 8.97 | 9.01 | - |

* Average value of peak fuel enthalpy is 115.2 cal/g fuel

** Average value along the fuel stack length

Appendix E-3

*Individual Characteristics of Fuel Rod # RT3
after the BGR Test*

RT3

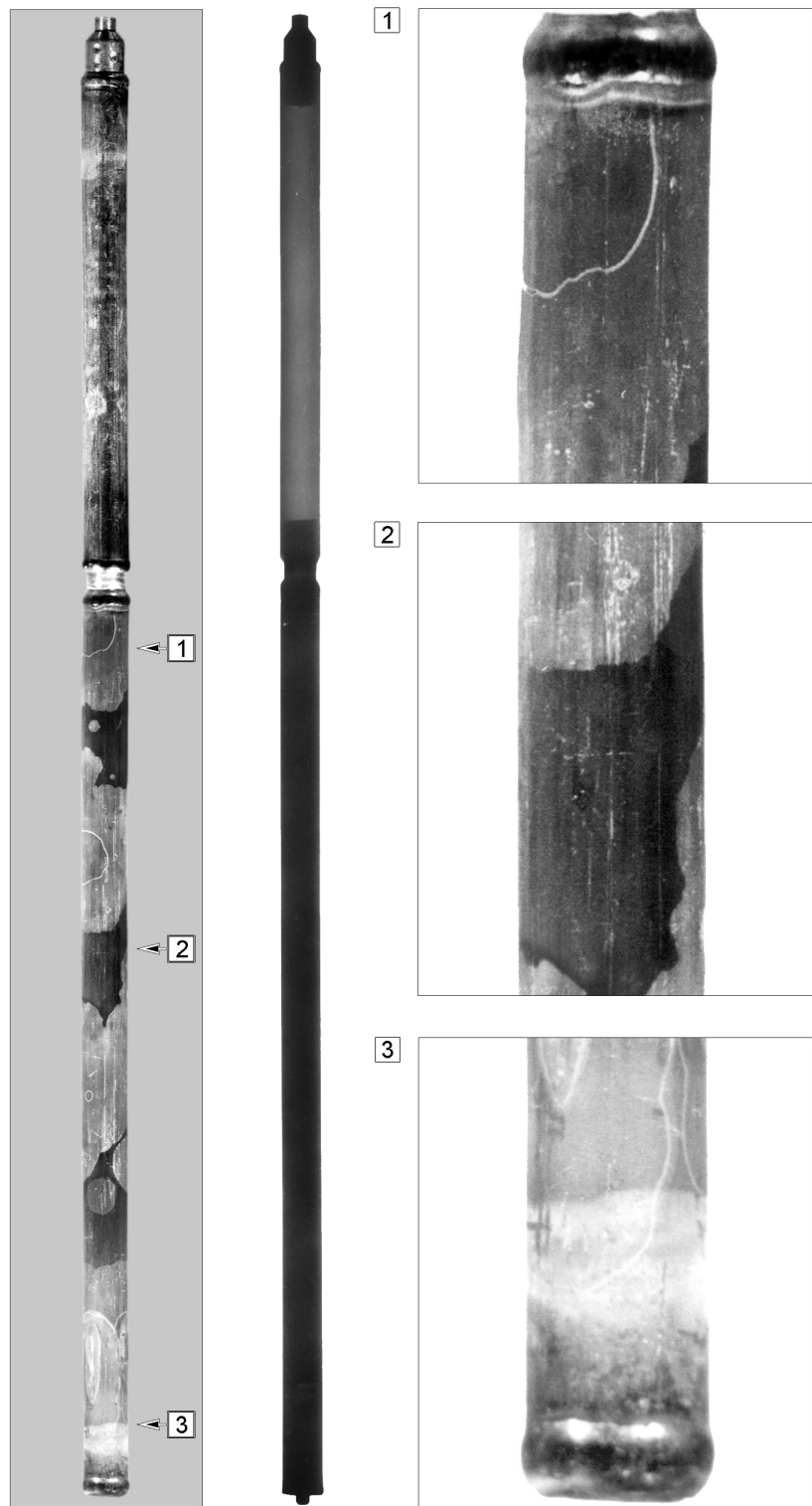


Fig.E-3.1. Appearance of unfailed fuel rod # RT3 after the BGR test (photographs and X-ray photograph)

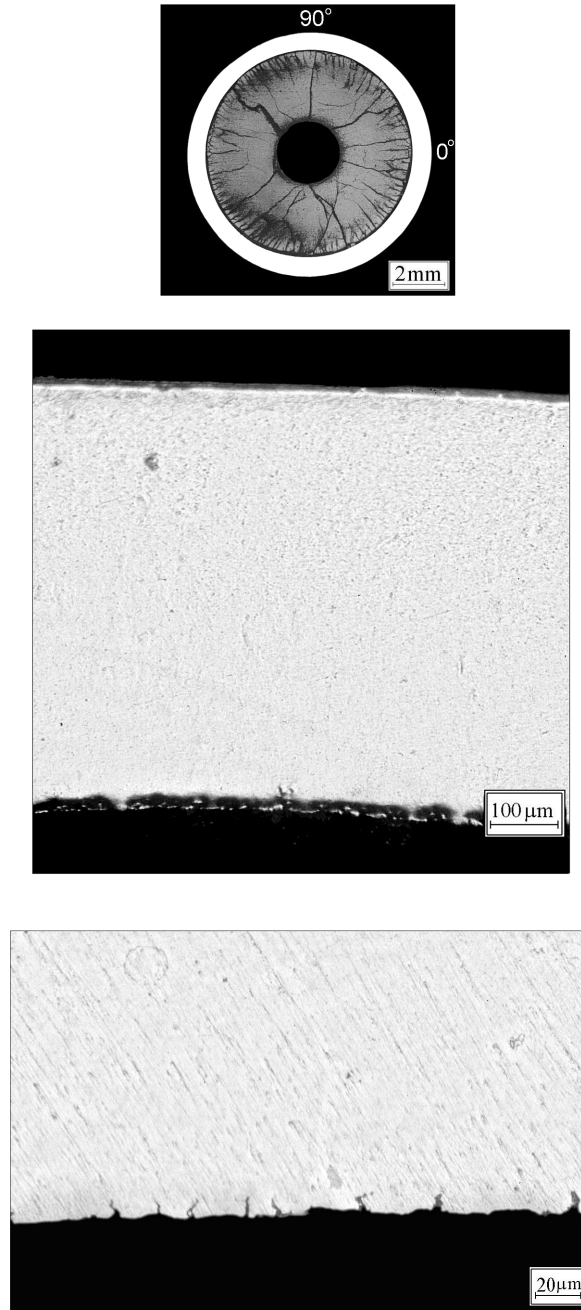


Fig.E-3.2. Cross-section and cladding microstructure of fuel rod # RT3 at 113 mm elevation (from low cap)

RT3

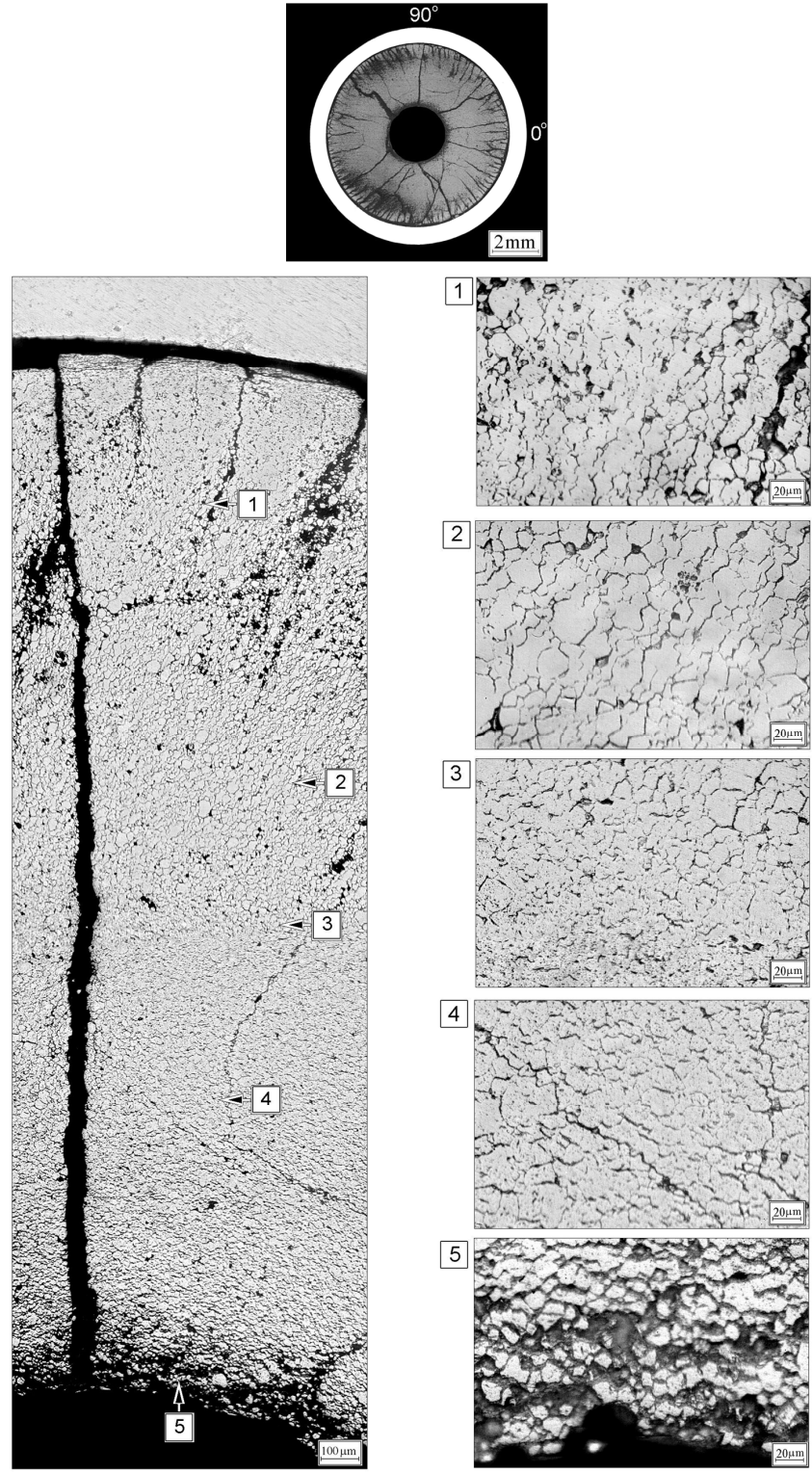


Fig.E-3.3. Cross-section and fuel microstructure of fuel rod # RT3 at 113 mm elevation (from low cap)

Table E-3.1. Time dependent energy characteristics of fuel rod # RT3

| Time (s) | Relative reactor power (current/maximum value) (per-unit) | Cumulative number of fissions in fuel rod (fiss) x10 ⁻¹⁴ | Power of fuel rod ¹⁾²⁾ (kW) | Energy deposition | | Fuel enthalpy ³⁾ | |
|----------|---|---|--|-------------------|------------|-----------------------------|---------|
| | | | | (cal/g fuel) | (J/g fuel) | FRAP-T6 | RAPTA-5 |
| 0.000 | 2.09E-02 | 0.000 | 0.000 | 0.000 | 0.000 | 0.000 | 0.000 |
| 0.001 | 1.97E-01 | 0.080 | 408.2 | 2.791 | 11.68 | 3.323 | 2.662 |
| 0.002 | 6.18E-01 | 0.376 | 1283 | 13.35 | 55.89 | 14.463 | 13.272 |
| 0.003 | 1.00E+00 | 1.028 | 2076 | 36.58 | 153.1 | 37.846 | 36.544 |
| 0.004 | 6.81E-01 | 1.702 | 1413 | 60.68 | 254.1 | 61.942 | 60.481 |
| 0.005 | 2.93E-01 | 2.065 | 608.2 | 73.47 | 307.6 | 74.603 | 72.889 |
| 0.006 | 1.48E-01 | 2.228 | 307.8 | 79.25 | 331.8 | 80.187 | 78.245 |
| 0.007 | 8.06E-02 | 2.310 | 167.3 | 82.23 | 344.3 | 82.916 | 80.850 |
| 0.008 | 5.58E-02 | 2.361 | 115.7 | 84.04 | 351.8 | 84.446 | 82.319 |
| 0.009 | 4.91E-02 | 2.401 | 102.0 | 85.45 | 357.7 | 85.585 | 83.429 |
| 0.010 | 4.78E-02 | 2.440 | 99.15 | 86.76 | 363.2 | 86.639 | 84.475 |
| 0.012 | 5.33E-02 | 2.514 | 110.7 | 89.50 | 374.7 | 88.872 | 86.778 |
| 0.014 | 6.59E-02 | 2.606 | 136.7 | 92.76 | 388.4 | 91.647 | 89.527 |
| 0.016 | 7.19E-02 | 2.715 | 149.2 | 96.53 | 404.1 | 94.924 | 92.891 |
| 0.018 | 6.92E-02 | 2.820 | 143.6 | 100.4 | 420.4 | 98.329 | 96.463 |
| 0.020 | 5.73E-02 | 2.915 | 119.0 | 103.9 | 434.9 | 101.320 | 99.371 |
| 0.022 | 4.57E-02 | 2.995 | 94.94 | 106.7 | 446.7 | 103.683 | 101.860 |
| 0.024 | 3.61E-02 | 3.062 | 74.92 | 108.9 | 456.1 | 105.485 | 103.670 |
| 0.026 | 2.90E-02 | 3.112 | 60.31 | 110.7 | 463.5 | 106.859 | 105.120 |
| 0.028 | 2.43E-02 | 3.148 | 50.46 | 112.1 | 469.4 | 107.931 | 106.030 |
| 0.030 | 2.29E-02 | 3.186 | 47.61 | 113.4 | 474.7 | 108.843 | 106.940 |
| 0.050 | 2.33E-02 | 3.558 | 48.44 | 126.5 | 529.7 | 118.563 | 116.950 |
| 0.070 | 1.88E-02 | 3.877 | 39.07 | 138.0 | 577.8 | 126.855 | 125.630 |
| 0.090 | 1.47E-02 | 4.139 | 30.65 | 147.2 | 616.4 | 133.304 | 132.350 |
| 0.110 | 7.95E-03 | 4.313 | 16.57 | 153.5 | 642.7 | 137.205 | 136.340 |
| 0.130 | 2.98E-03 | 4.394 | 6.240 | 156.3 | 654.5 | 138.624 | 137.210 |
| 0.150 | 1.13E-03 | 4.418 | 2.415 | 157.3 | 658.8 | 138.338 | 136.620 |
| 0.200 | 3.05E-04 | 4.440 | 0.701 | 158.2 | 662.4 | 136.674 | 134.300 |
| 1.000 | 2.77E-05 | 4.477 | 0.089 | 159.8 | 669.2 | 116.316 | 113.690 |
| 10.00 | 3.16E-06 | 4.537 | 0.013 | 163.6 | 685.1 | 23.629 | 24.851 |
| 100.0 | 6.15E-08 | 4.567 | 0.002 | 166.5 | 696.9 | 4.865 | 4.419 |
| 1000 | 2.40E-13 | 4.568 | 4.46E-05 | 167.9 | 702.8 | 0.000 | 0.000 |

¹⁾ Average values determined in accordance with results of RRC KI and VNIIEF calculations

²⁾ Maximum power value is 2075.5 kW (t=0.003 c)

³⁾ Average radial value

RT3

Table E-3.2. Radial energy characteristics of fuel rod # RT3*

| Parameters** | Coordinates of fuel radial layers (mm) | | | |
|---|--|------------------------|------------------------|-------------------------|
| | 1 layer (1.23-2.82) | 2 layer (2.82-3.44) | 3 layer (3.44-3.71) | 4 layer (3.71-3.795) |
| Number of fissions $\times 10^{-14}$ (fiss) | 4.417 | 2.893 | 1.730 | 0.848 |
| Fission density $\times 10^{-13}$ (fiss/g fuel) | 2.192 | 2.357 | 2.896 | 4.358 |
| Power*** (kW) | 920.8 | 605.2 | 366.6 | 182.5 |
| Energy deposition (cal/g fuel) | 149.8 | 161.5 | 198.7 | 299.2 |
| Energy deposition (J/g fuel) | 627.4 | 676.0 | 832.0 | 1253 |
| Energy deposition**** (per-unit) | 0.501 | 0.540 | 0.664 | 1.000 |

* Average values were determined in accordance with results of RRC KI and VNIIEF calculations

** All parameters were determined for the undamaged section of a fuel stack (see Table C.2)

*** The power for the entire length of each layer at time 0.003 s

**** Energy deposition in current layer/energy deposition in 4th layer

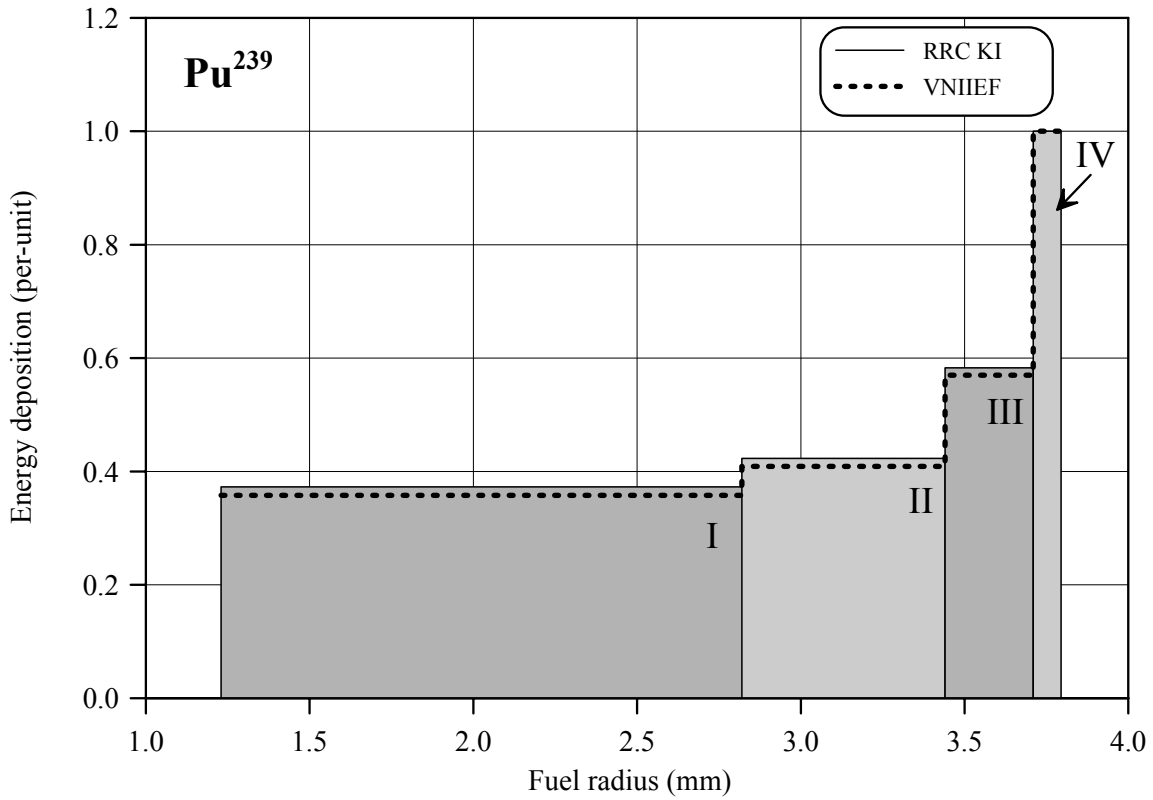
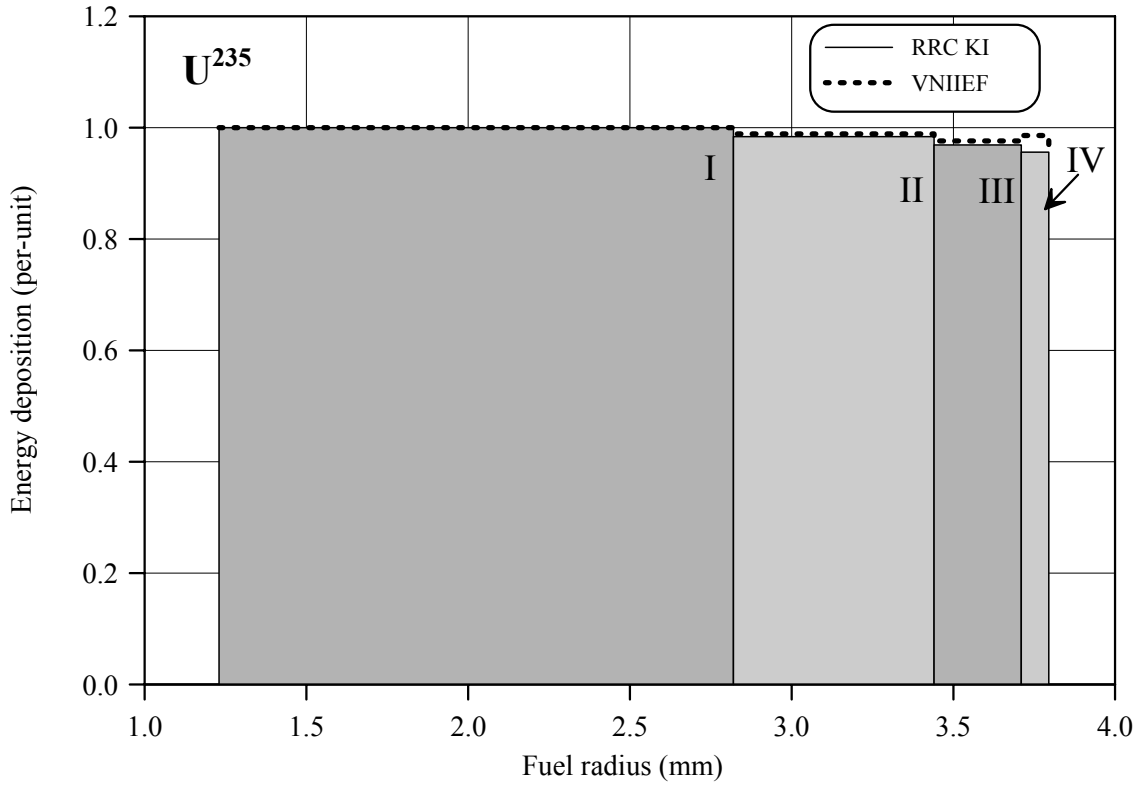


Fig.E-3.4. U²³⁵ and Pu²³⁹ radial distribution of energy deposition for fuel rod # RT3

RT3

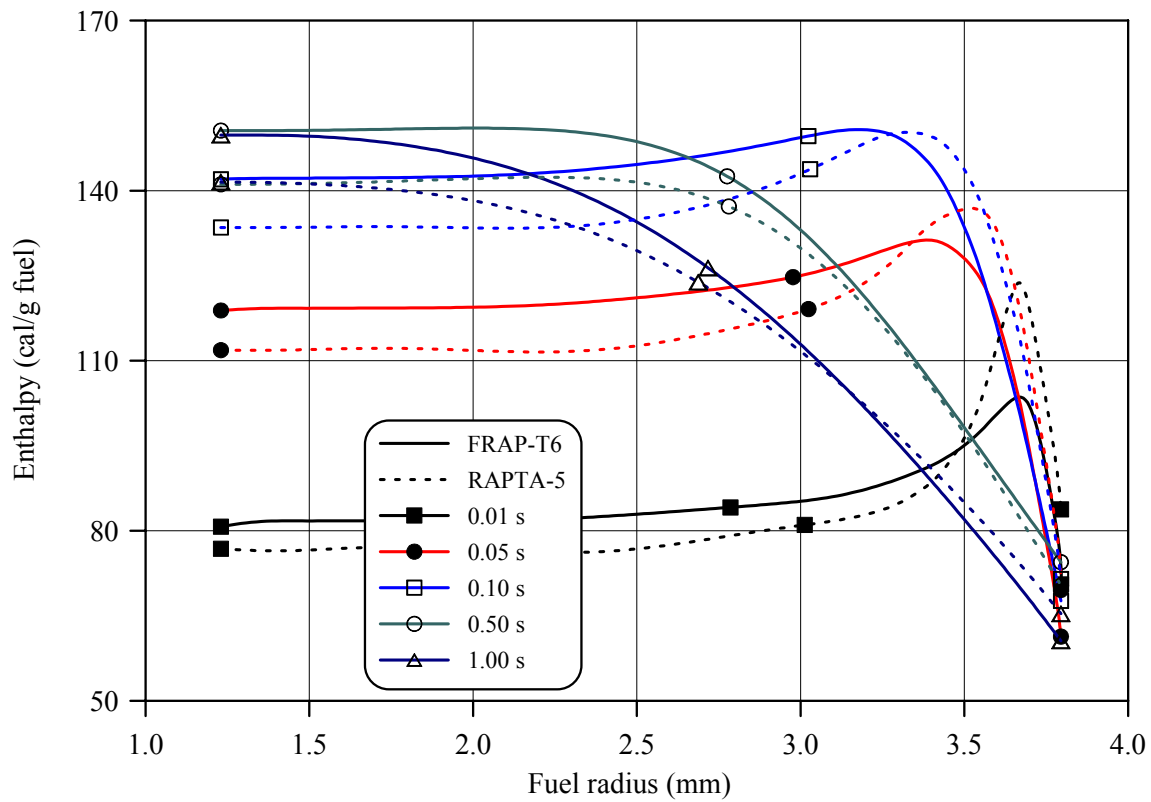
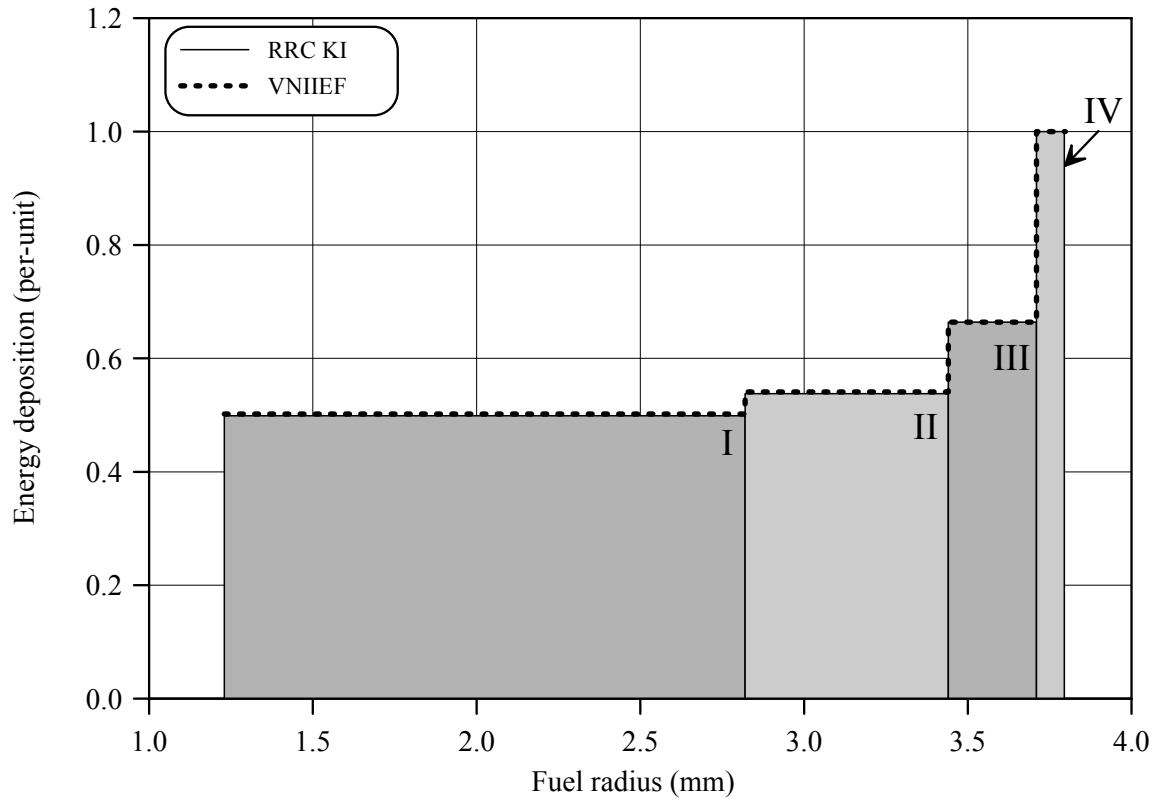


Fig.E-3.5. Radial distribution of energy deposition and fuel enthalpy for fuel rod # RT3

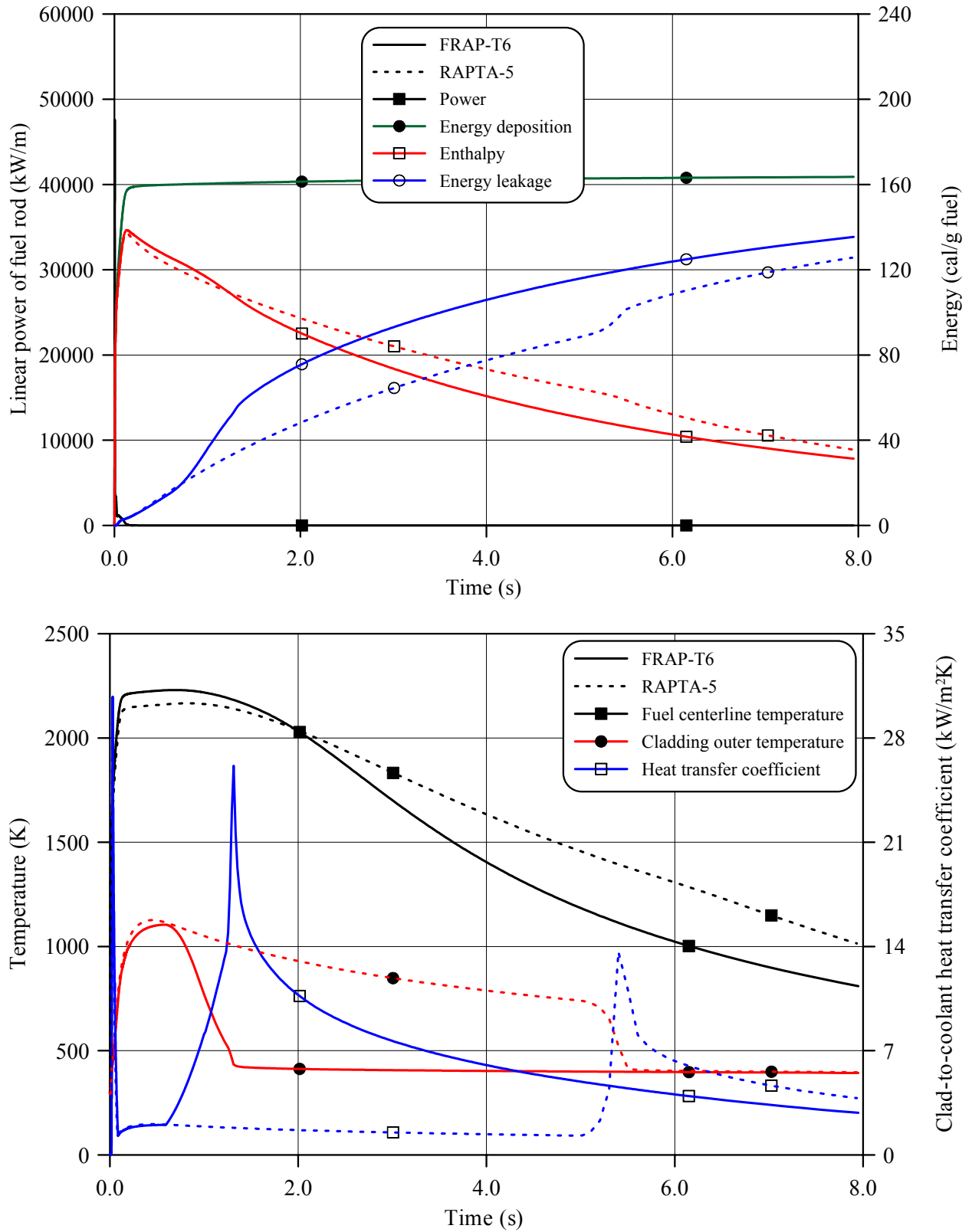


Fig.E-3.6. Thermal history of fuel rod # RT3 during the BGR test in accordance with FRAP-T6/VVER and RAPTA-5 calculations

RT3

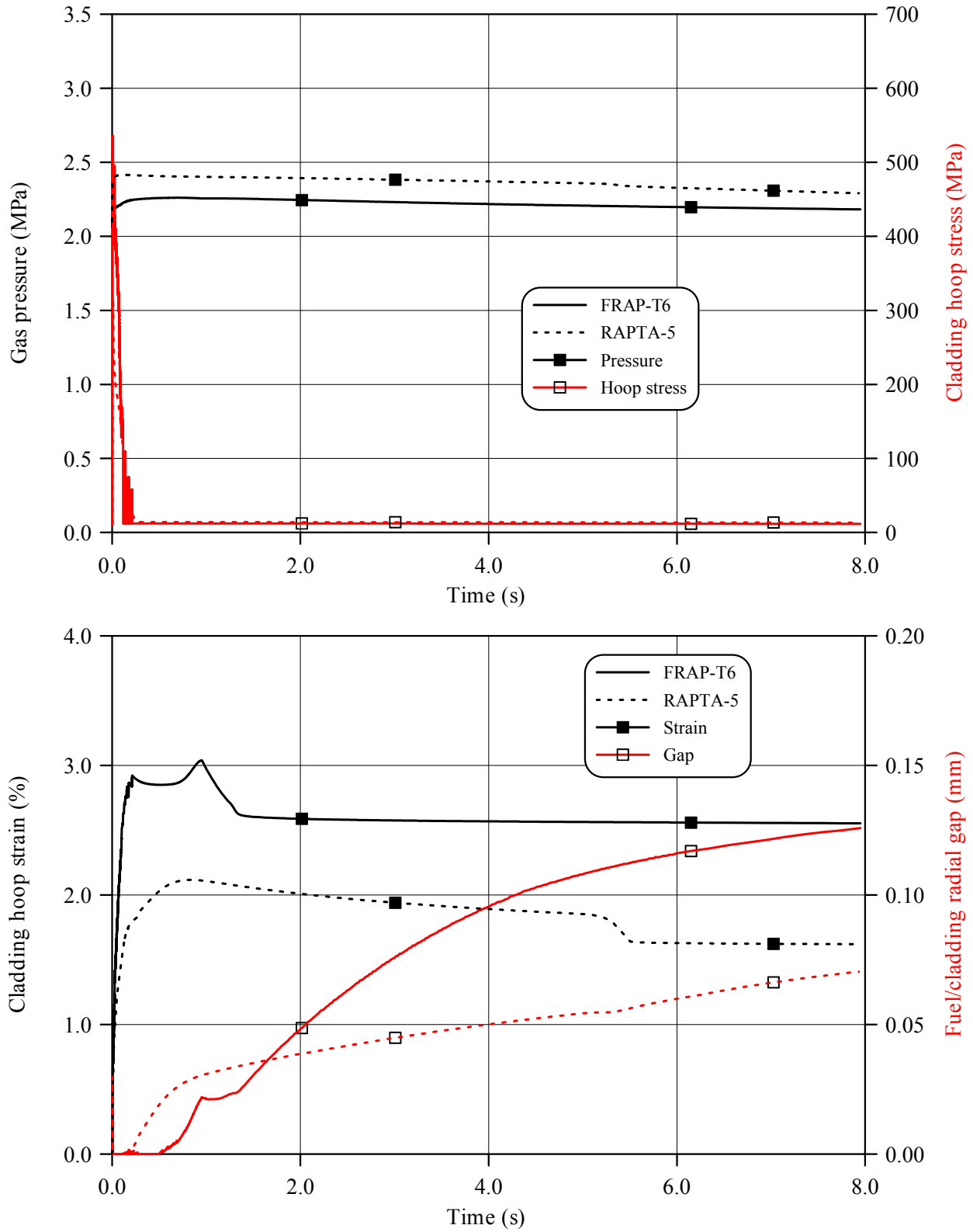


Fig.E-3.7. Mechanical behavior of fuel rod # RT3 during the BGR test in accordance with FRAP-T6/VVER and RAPTA-5 calculations

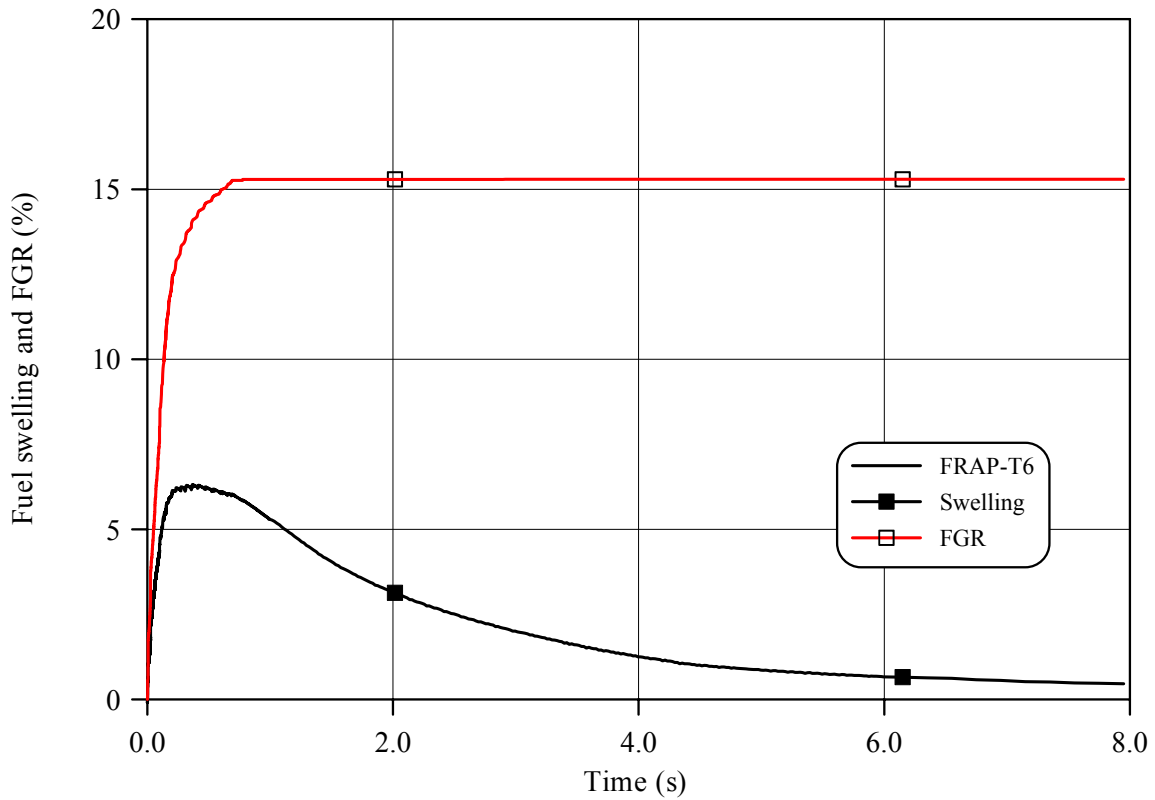
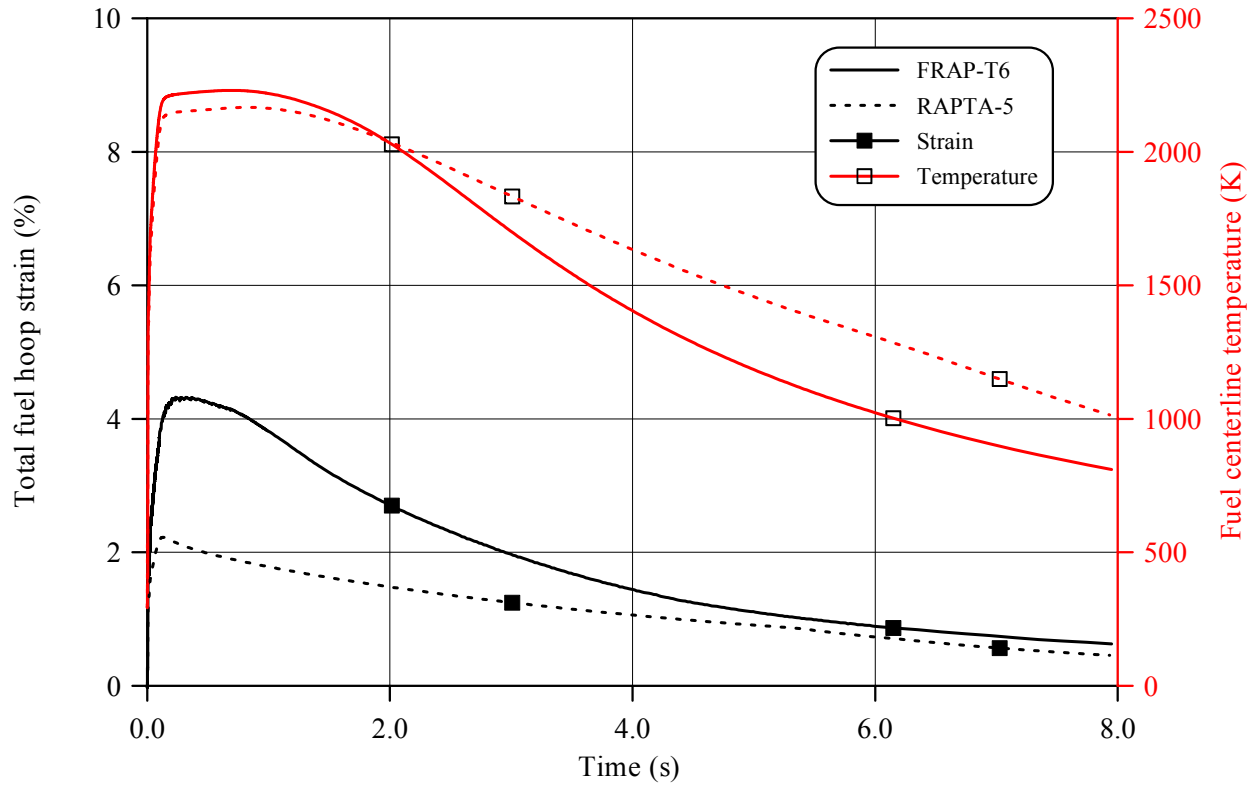


Fig.E-3.8. Fuel behavior during the BGR test of fuel rod # RT3 in accordance with FRAP-T6/VVER and RAPTA-5 calculations

RT3

Table E-3.3. Axial distribution of cladding average outer diameter in fuel rod # RT3*

| Axial coordinate (mm) | Cladding diameter (mm) | Axial coordinate (mm) | Cladding diameter (mm) | Axial coordinate (mm) | Cladding diameter (mm) | Axial coordinate (mm) | Cladding diameter (mm) |
|-----------------------|------------------------|-----------------------|------------------------|-----------------------|------------------------|-----------------------|------------------------|
| 36 | 9.208 | 74 | 9.251 | 112 | 9.293 | 150 | 9.314 |
| 38 | 9.231 | 76 | 9.265 | 114 | 9.286 | 152 | 9.307 |
| 40 | 9.245 | 78 | 9.286 | 116 | 9.267 | 154 | 9.300 |
| 42 | 9.242 | 80 | 9.302 | 118 | 9.235 | 156 | 9.308 |
| 44 | 9.242 | 82 | 9.296 | 120 | 9.245 | 158 | 9.340 |
| 46 | 9.205 | 84 | 9.271 | 122 | 9.260 | 160 | 9.365 |
| 48 | 9.150 | 86 | 9.261 | 124 | 9.259 | 162 | 9.372 |
| 50 | 9.131 | 88 | 9.271 | 126 | 9.252 | 164 | 9.323 |
| 52 | 9.092 | 90 | 9.298 | 128 | 9.227 | 166 | 9.225 |
| 54 | 9.064 | 92 | 9.300 | 130 | 9.226 | 168 | 9.129 |
| 56 | 9.059 | 94 | 9.270 | 132 | 9.269 | 170 | 9.070 |
| 58 | 9.058 | 96 | 9.237 | 134 | 9.316 | 172 | 9.052 |
| 60 | 9.059 | 98 | 9.255 | 136 | 9.328 | 174 | 9.051 |
| 62 | 9.073 | 100 | 9.278 | 138 | 9.292 | 176 | 9.045 |
| 64 | 9.137 | 102 | 9.308 | 140 | 9.252 | 178 | 9.409 |
| 66 | 9.198 | 104 | 9.303 | 142 | 9.241 | 180 | 8.521 |
| 68 | 9.251 | 106 | 9.278 | 144 | 9.272 | | |
| 70 | 9.260 | 108 | 9.270 | 146 | 9.298 | | |
| 72 | 9.253 | 110 | 9.281 | 148 | 9.314 | | |

* Measured value determined on the basis of profilometry data (16 azimuthal directions)

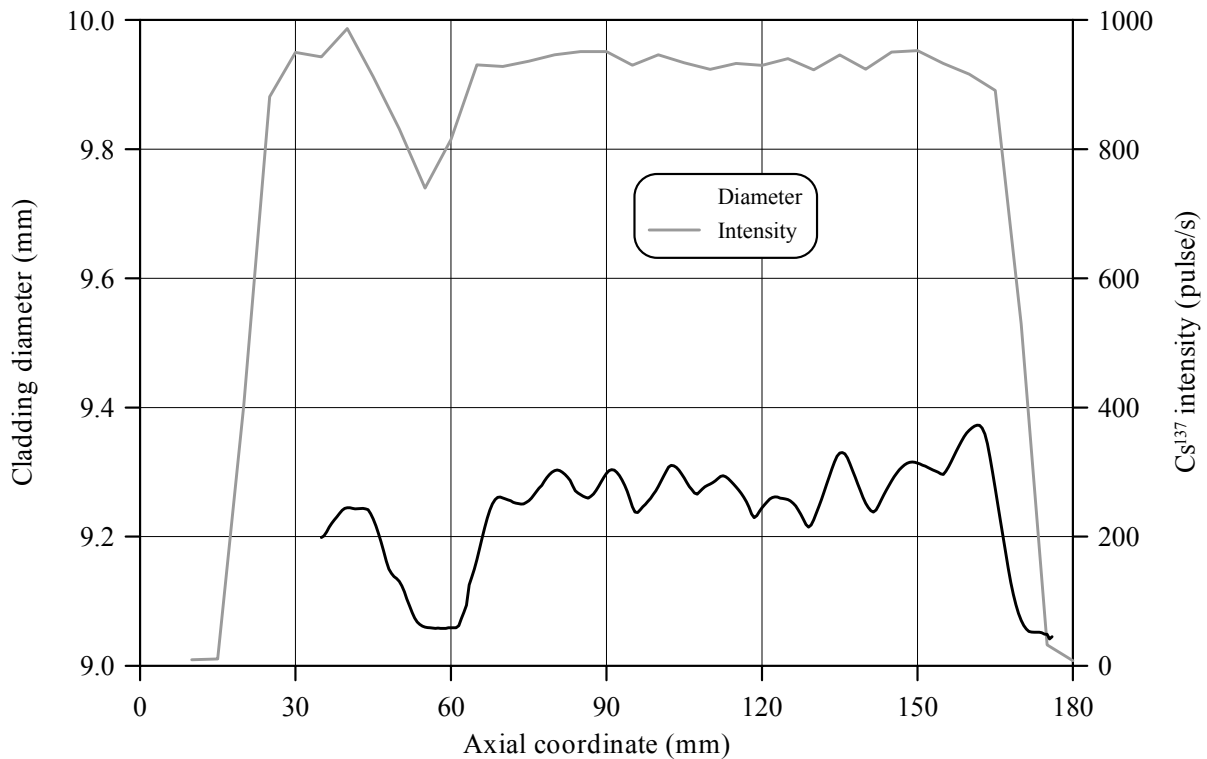


Fig.E-3.9. Cladding measured average diameter and γ -scanning results for fuel rod # RT3

Table E-3.4. The PIE results for fuel rod # RT3

| Parameter | | Value |
|-----------|--|-------|
| 1. | Cladding outer diameter (mm): | |
| 1.1. | Maximum diameter of the bidimensional data sample in "fuel rod length - azimuthal angle" coordinates (mm) | 9.47 |
| 1.2. | Averaged azimuthal diameter and maximum diameter along the length selected from the sample of averaged azimuthal diameter (mm) | 9.37 |
| 1.3. | Averaged diameter of the bidimensional data sample in "fuel rod length - azimuthal angle" coordinates (mm) | 9.24 |
| 2. | Cladding maximum residual hoop strain (%) | 3.40 |
| 3. | Fuel pellet conditional diameter (mm) in cross-section*: at 113 mm elevation | 7.71 |
| 4. | ZrO ₂ outer thickness (μm) in cross-section: at 113 mm elevation | 3–5 |
| 5. | ZrO ₂ inner thickness (μm) in cross-section: at 113 mm elevation | 0 |
| 6. | Parameters characterizing FGR: | |
| 6.1. | Gas composition (% by volume): | |
| | He | 84.76 |
| | N ₂ | 0.91 |
| | O ₂ | 0.17 |
| | Ar | 0.015 |
| | CO ₂ | 0.010 |
| | Kr | 1.28 |
| | Xe | 12.85 |
| 6.2. | Free gas volume (cm ³) | 6.1 |
| 6.3. | Gas volume under normal conditions (cm ³) | 143.5 |
| 6.4. | Gas pressure under normal conditions (MPa) | 2.35 |
| 6.5. | FGR (%) | 21.30 |

* Reference value determined by the processing of fuel cross-section photographs

RT3**Table E-3.5. Organized BGR test results for fuel rod # RT3**

| Parameter | | Unit | Value | | |
|-----------|---|---------------------|----------|------------|----------|
| | | | Measured | Calculated | |
| | | | | FRAP-T6 | RAPTA-5 |
| 1. | Fuel burnup | MW d/kg U | 47.5 | 47.5 | 47.5 |
| 2. | Initial gas pressure | MPa | 2.1 | 2.1 | 2.1 |
| 3. | Energy deposition | cal/g fuel | 167.9 | 167.9 | 167.9 |
| 4. | Peak fuel enthalpy* | cal/g fuel | - | 138.6 | 137.2 |
| 5. | Fuel maximum temperature | K | - | 2266 | 2279 |
| 6. | Maximum temperature of cladding outer surface | K | - | 1104 | 1127 |
| 7. | Cladding burst | Failed, Unfailed | Unfailed | Unfailed | Unfailed |
| 8. | Cladding residual hoop strain** | % | 2.00 | 2.46 | 1.55 |
| 9. | Kr volume content in gas composition after the BGR test | % | 1.28 | 0.56 | - |
| 10. | Xe volume content in gas composition after the BGR test | % | 12.85 | 3.37 | - |

* Average value of peak fuel enthalpy is 137.9 cal/g fuel

** Average value along the fuel stack length

Appendix E-4

*Individual Characteristics of Fuel Rod # RT4
after the BGR Test*

RT4

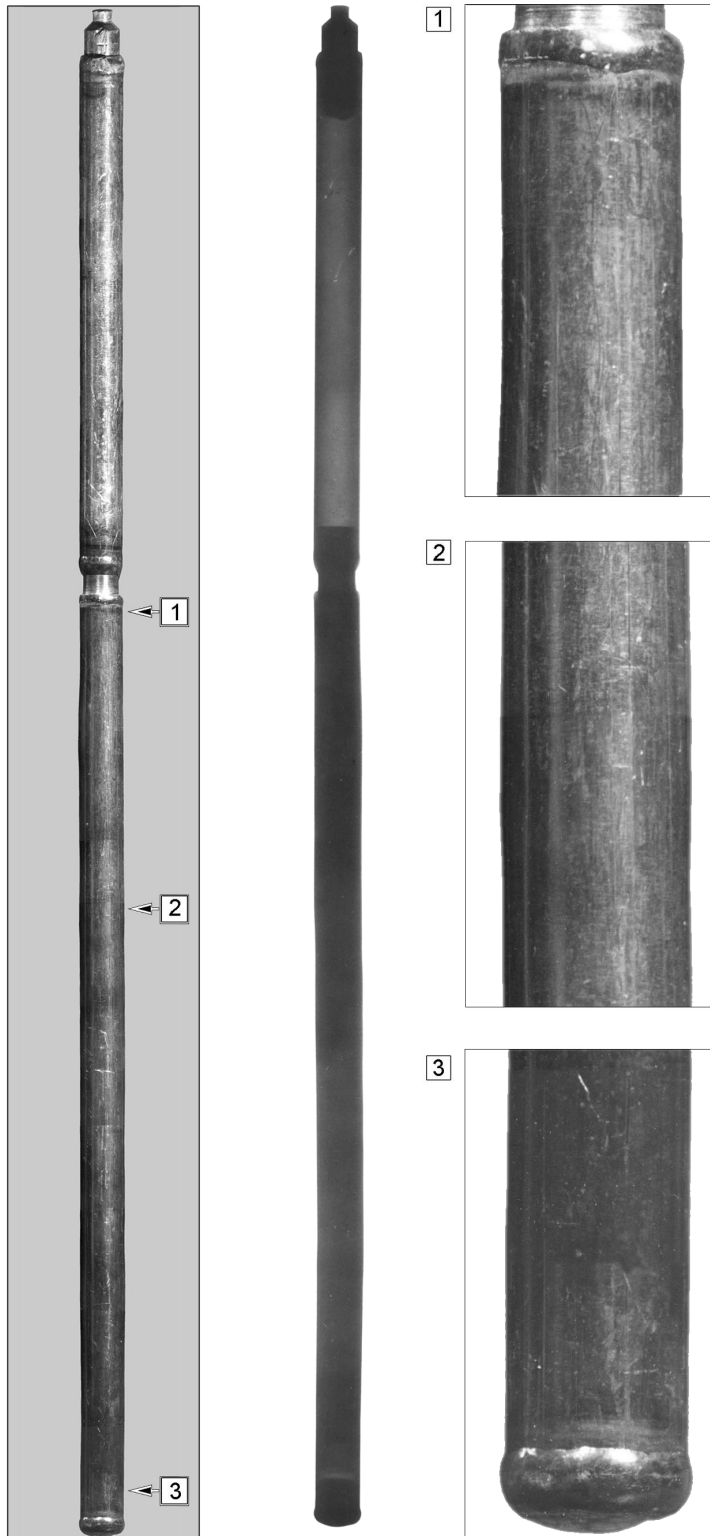


Fig.E-4.1. Appearance of unfailed fuel rod # RT4 after the BGR test (photographs and X-ray photograph)

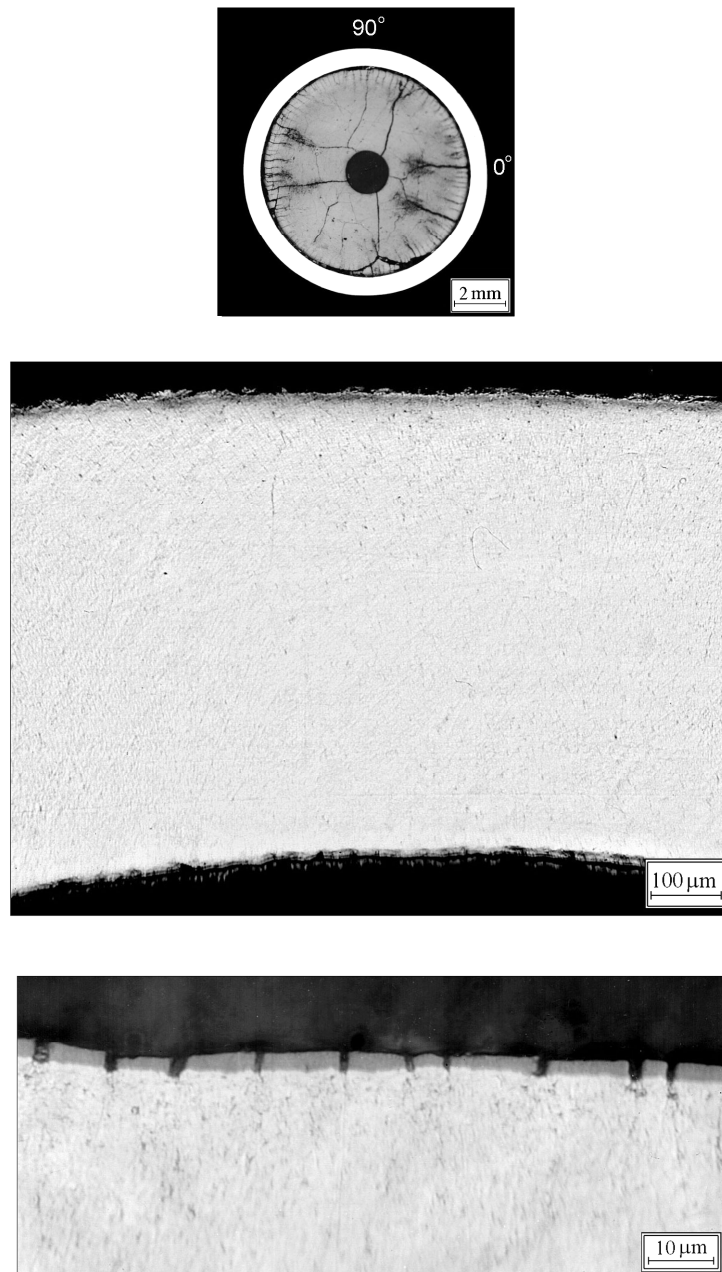


Fig.E-4.2. Cross-section and cladding microstructure of fuel rod # RT4 at 108 mm elevation (from low cap)

RT4

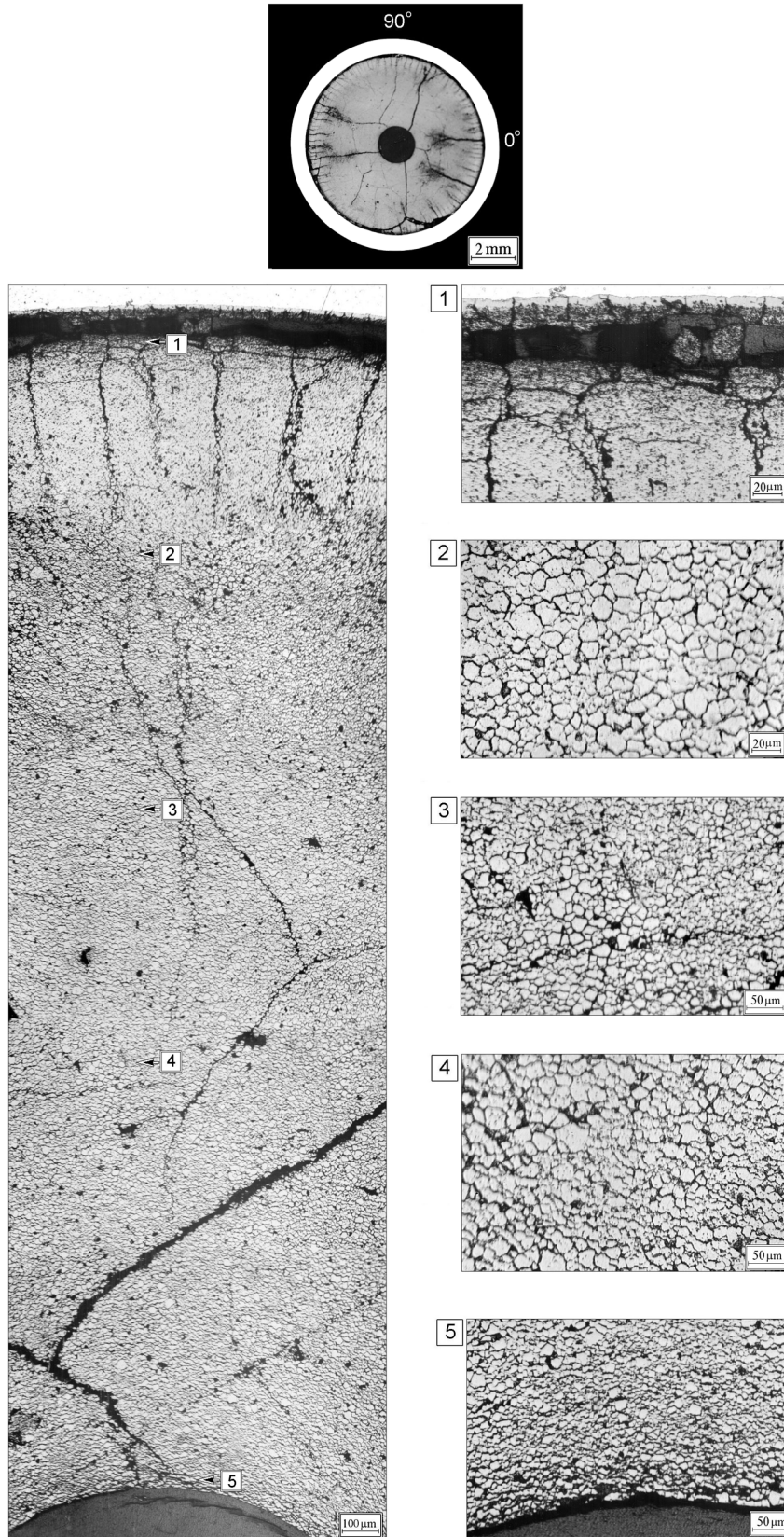


Fig.E-4.3. Cross-section and fuel microstructure of fuel rod # RT4 at 108 mm elevation (from low cap)

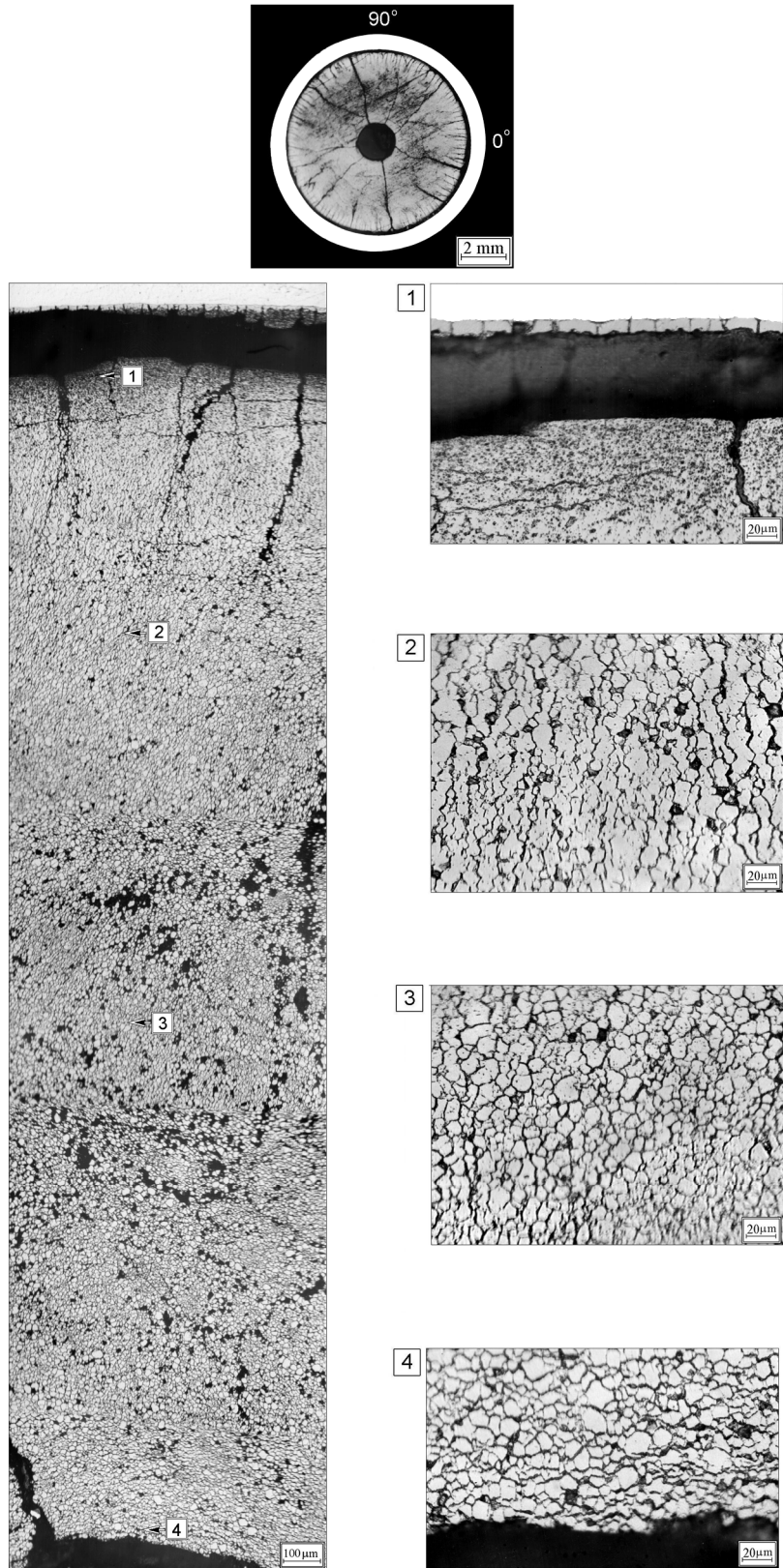


Fig.E-4.4. Cross-section and fuel microstructure of fuel rod # RT4 after the BGR test at 117 mm elevation (from low cap)

RT4

Table E-4.1. Time dependent energy characteristics of fuel rod # RT4

| Time (s) | Relative reactor power (current/maximum value) (per-unit) | Cumulative number of fissions in fuel rod (fiss) x10 ⁻¹⁴ | Power of fuel rod ¹⁾²⁾ (kW) | Energy deposition | | Fuel enthalpy ³⁾ | |
|----------|---|---|--|-------------------|------------|-----------------------------|---------|
| | | | | (cal/g fuel) | (J/g fuel) | FRAP-T6 | RAPTA-5 |
| 0.000 | 1.88E-02 | 0.000 | 0.000 | 0.000 | 0.000 | 0.000 | 0.000 |
| 0.001 | 1.91E-01 | 0.257 | 1297 | 2.477 | 10.37 | 3.138 | 2.366 |
| 0.002 | 6.03E-01 | 1.247 | 4085 | 12.07 | 50.51 | 13.615 | 11.950 |
| 0.003 | 1.00E+00 | 3.438 | 6778 | 33.38 | 139.8 | 35.372 | 33.202 |
| 0.004 | 6.48E-01 | 5.663 | 4393 | 54.98 | 230.2 | 56.687 | 54.522 |
| 0.005 | 2.66E-01 | 6.805 | 1804 | 66.06 | 276.6 | 67.189 | 65.110 |
| 0.006 | 1.42E-01 | 7.321 | 961.5 | 71.06 | 297.5 | 71.731 | 69.656 |
| 0.007 | 7.58E-02 | 7.575 | 513.9 | 73.49 | 307.7 | 73.952 | 71.890 |
| 0.008 | 5.27E-02 | 7.756 | 357.1 | 75.28 | 315.2 | 75.188 | 73.149 |
| 0.009 | 4.50E-02 | 7.878 | 304.8 | 76.50 | 320.3 | 76.058 | 74.091 |
| 0.010 | 4.44E-02 | 8.001 | 300.7 | 77.61 | 324.9 | 76.919 | 74.963 |
| 0.012 | 5.31E-02 | 8.252 | 359.8 | 80.07 | 335.2 | 78.844 | 76.956 |
| 0.014 | 6.69E-02 | 8.567 | 453.3 | 83.11 | 348.0 | 81.379 | 79.559 |
| 0.016 | 7.50E-02 | 8.938 | 508.6 | 86.75 | 363.2 | 84.510 | 82.711 |
| 0.018 | 7.34E-02 | 9.332 | 497.6 | 90.55 | 379.1 | 87.719 | 86.298 |
| 0.020 | 6.46E-02 | 9.694 | 438.0 | 94.09 | 393.9 | 90.803 | 89.384 |
| 0.022 | 5.92E-02 | 10.02 | 401.4 | 97.21 | 407.0 | 93.371 | 92.225 |
| 0.024 | 5.21E-02 | 10.31 | 353.2 | 100.0 | 418.9 | 95.776 | 94.529 |
| 0.026 | 4.18E-02 | 10.56 | 283.4 | 102.4 | 428.8 | 97.670 | 96.723 |
| 0.028 | 3.21E-02 | 10.75 | 217.4 | 104.3 | 436.6 | 99.134 | 98.213 |
| 0.030 | 2.57E-02 | 10.90 | 174.0 | 105.7 | 442.7 | 100.164 | 99.336 |
| 0.050 | 1.89E-02 | 12.02 | 128.4 | 116.6 | 488.0 | 108.491 | 107.080 |
| 0.070 | 1.71E-02 | 12.98 | 116.4 | 126.0 | 527.3 | 114.982 | 114.030 |
| 0.090 | 1.27E-02 | 13.76 | 86.32 | 133.5 | 558.9 | 120.271 | 119.230 |
| 0.110 | 8.10E-03 | 14.32 | 55.07 | 138.9 | 581.7 | 124.073 | 122.830 |
| 0.130 | 3.02E-03 | 14.59 | 20.66 | 141.6 | 592.8 | 125.177 | 123.870 |
| 0.150 | 1.15E-03 | 14.69 | 7.992 | 142.6 | 596.9 | 125.119 | 123.500 |
| 0.200 | 3.10E-04 | 14.77 | 2.316 | 143.4 | 600.3 | 123.882 | 121.670 |
| 1.000 | 2.83E-05 | 14.88 | 0.295 | 144.9 | 606.6 | 104.923 | 104.430 |
| 10.00 | 3.21E-06 | 15.09 | 0.042 | 148.4 | 621.2 | 32.490 | 25.516 |
| 100.0 | 6.25E-08 | 15.20 | 0.006 | 151.0 | 632.2 | 5.621 | 4.506 |
| 1000 | 2.45E-13 | 15.20 | 1.49E-04 | 152.3 | 637.5 | 0.000 | 0.000 |

¹⁾ Average values determined in accordance with results of RRC KI and VNIIEF calculations

²⁾ Maximum power value is 6778 κВт (t=0.003 c)

³⁾ Average radial value

Table E-4.2. Radial energy characteristics of fuel rod # RT4*

| Parameters | Coordinates of fuel radial layers (mm) | | | |
|---|--|------------------------|------------------------|------------------------|
| | 1 layer (0.825-2.77) | 2 layer (2.77-3.45) | 3 layer (3.45-3.75) | 4 layer (3.75-3.84) |
| Number of fissions $\times 10^{-14}$ (fiss) | 6.702 | 4.402 | 2.759 | 1.333 |
| Fission density $\times 10^{-13}$ (fiss/g fuel) | 1.960 | 2.134 | 2.629 | 4.165 |
| Power** (kW) | 2990 | 1948 | 1238 | 600.5 |
| Energy deposition (cal/g fuel) | 146.0 | 155.1 | 191.7 | 288.5 |
| Energy deposition (J/g fuel) | 611.4 | 649.3 | 802.5 | 1208 |
| Energy deposition*** (per-unit) | 0.506 | 0.538 | 0.664 | 1.000 |

* Average values were determined in accordance with results of RRC KI and VNIIEF calculations

** The power for the entire length of each layer at time 0.003 s

*** Energy deposition in current layer/energy deposition in 4th layer

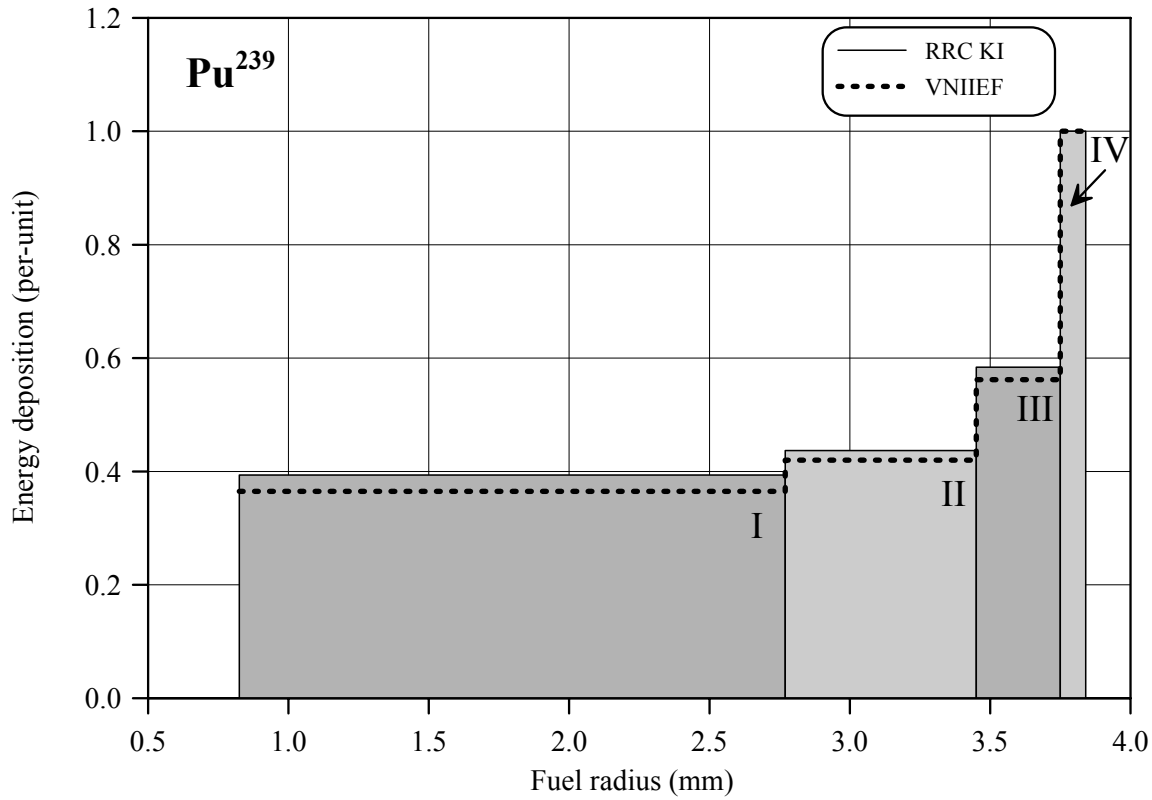
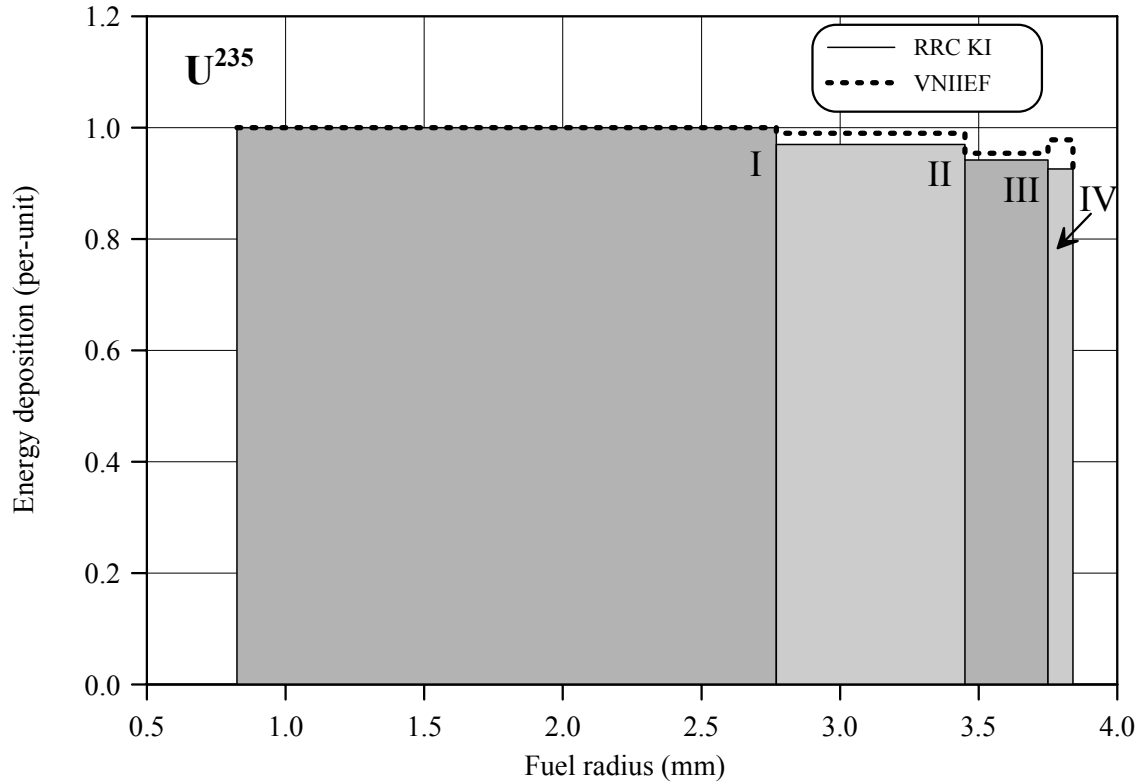


Fig.E-4.5. U²³⁵ and Pu²³⁹ radial distribution of energy deposition for fuel rod # RT4

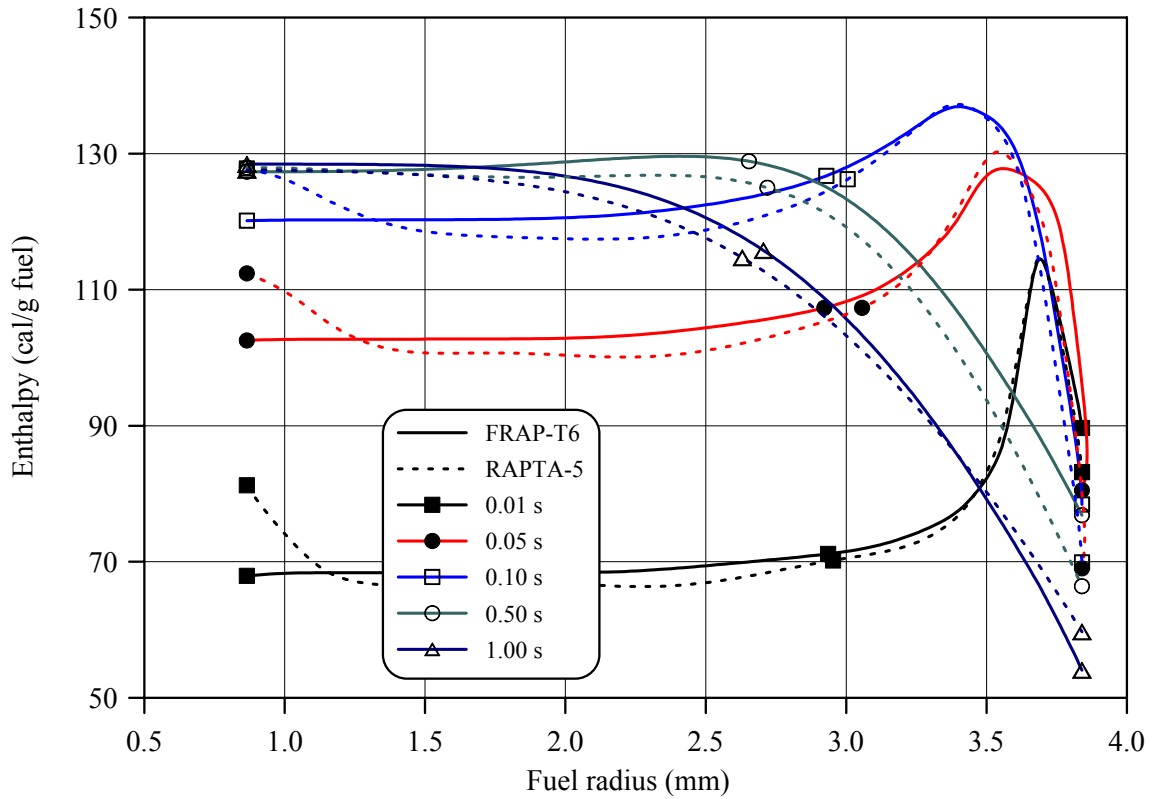
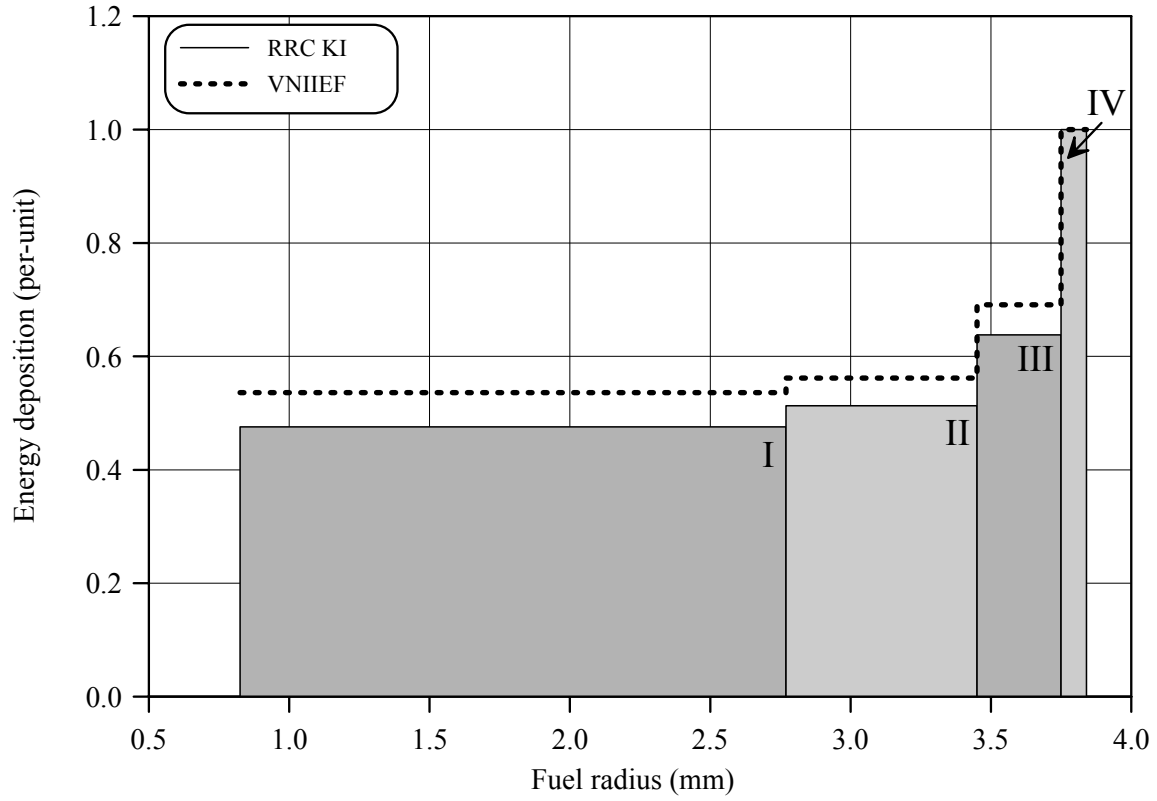


Fig.E-4.6. Radial distribution of energy deposition and fuel enthalpy for fuel rod # RT4

RT4

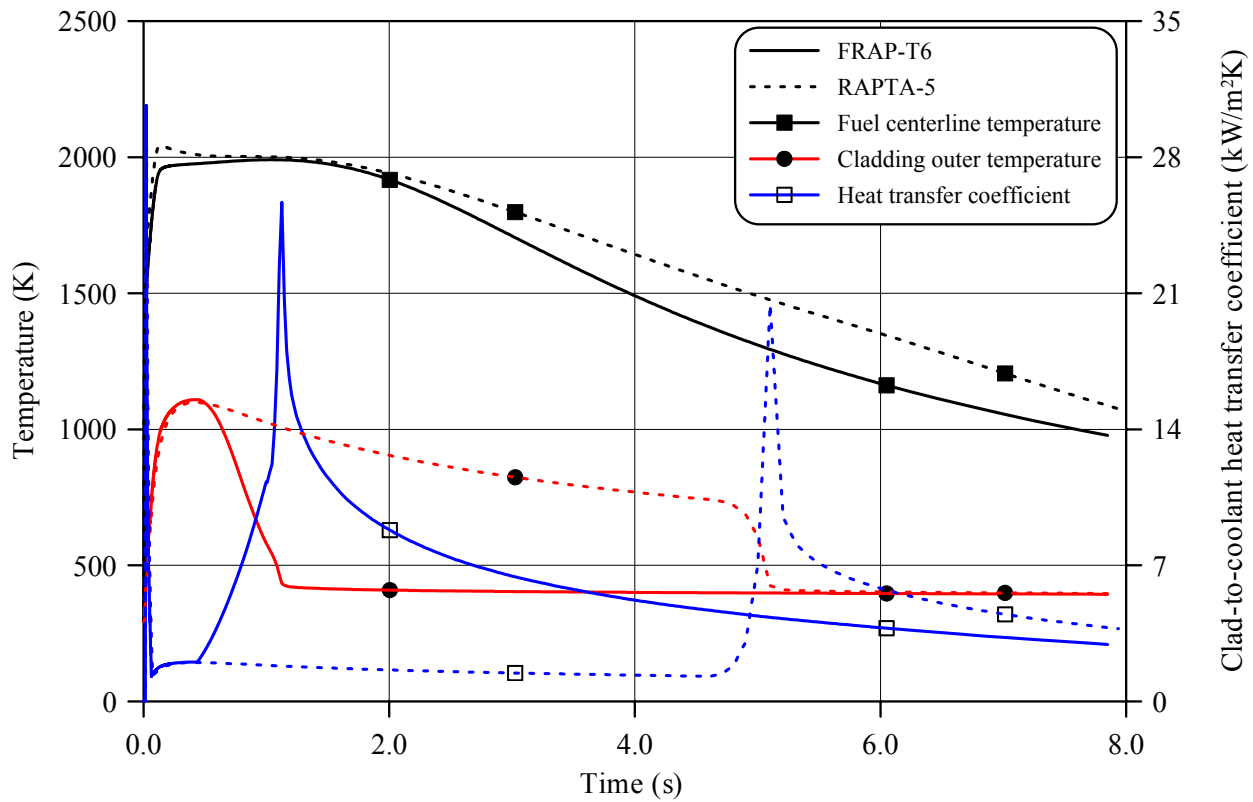
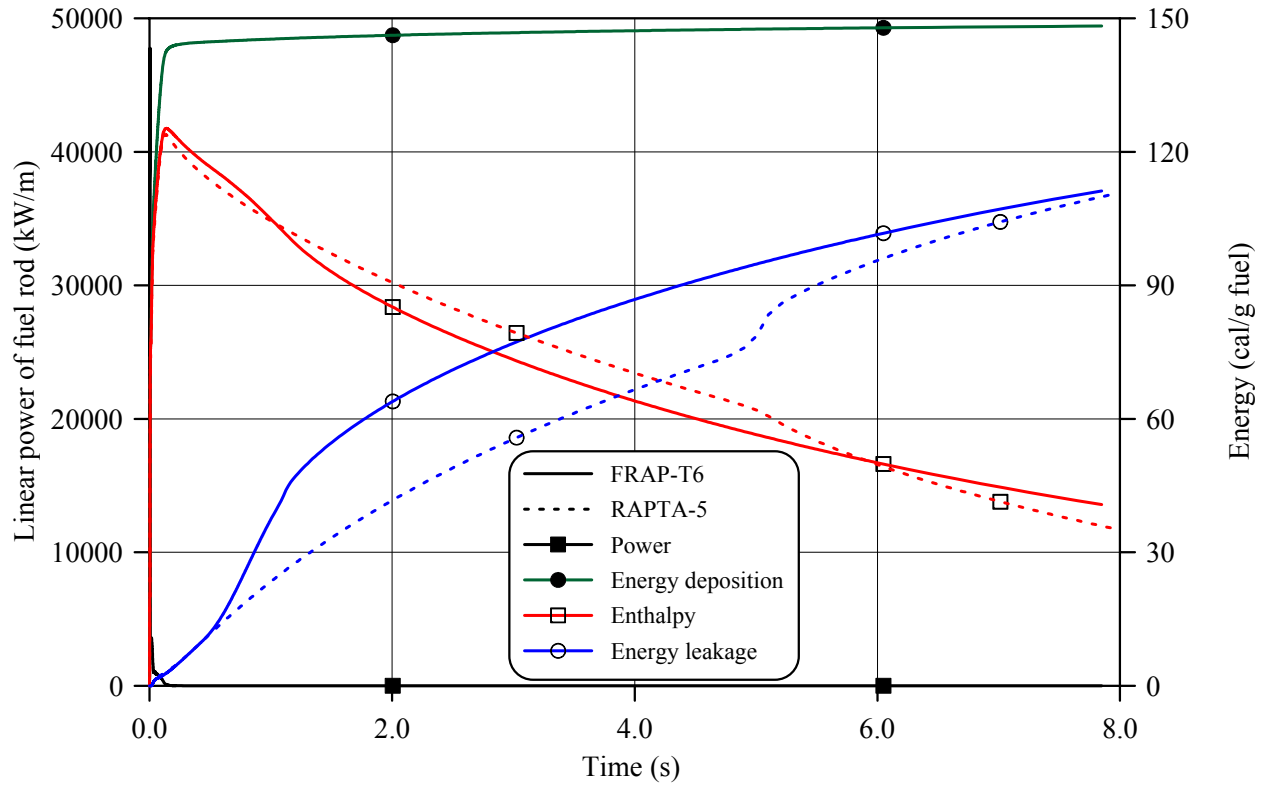


Fig.E-4.7. Thermal history of fuel rod # RT4 during the BGR test in accordance with FRAP-T6/VVER and RAPTA-5 calculations

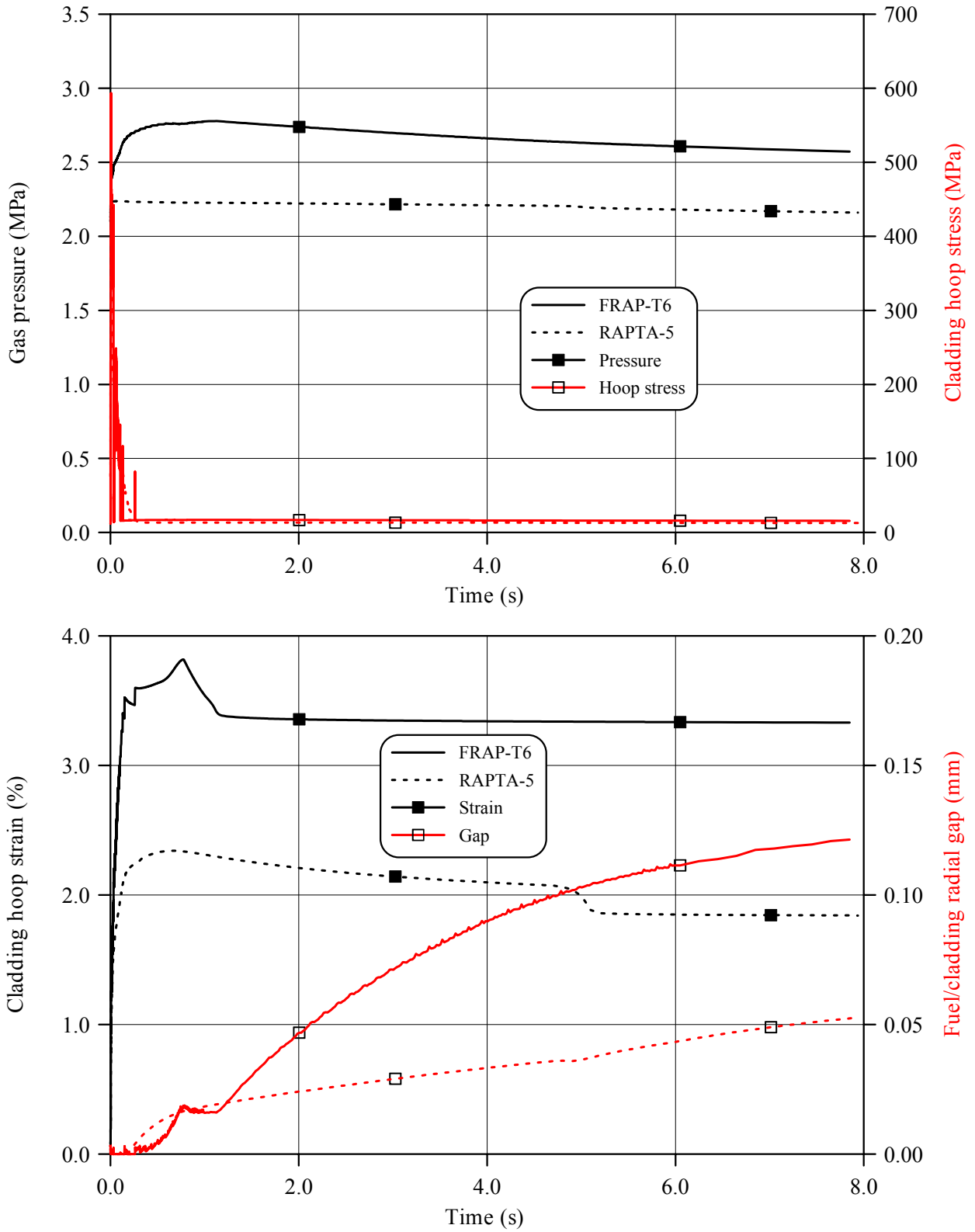


Fig.E-4.8. Mechanical behavior of fuel rod # RT4 during the BGR test in accordance with FRAP-T6/VVER and RAPTA-5 calculations

RT4

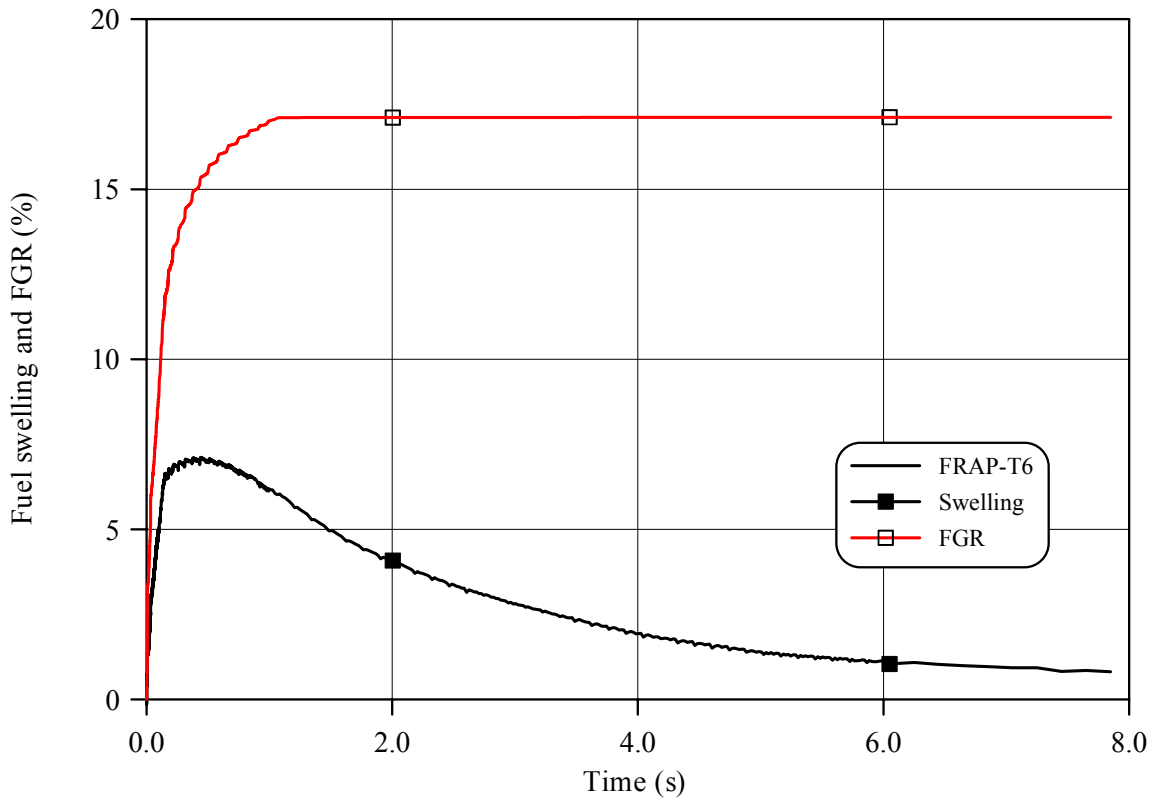
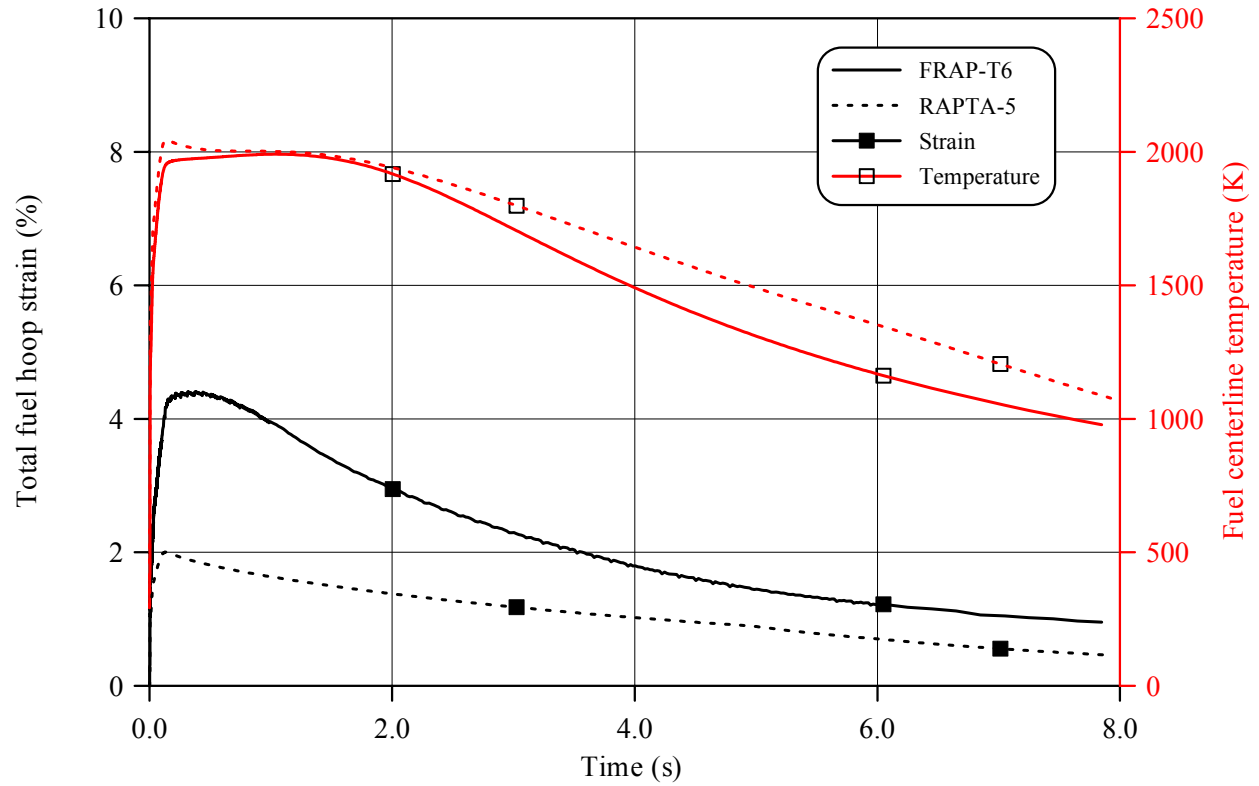
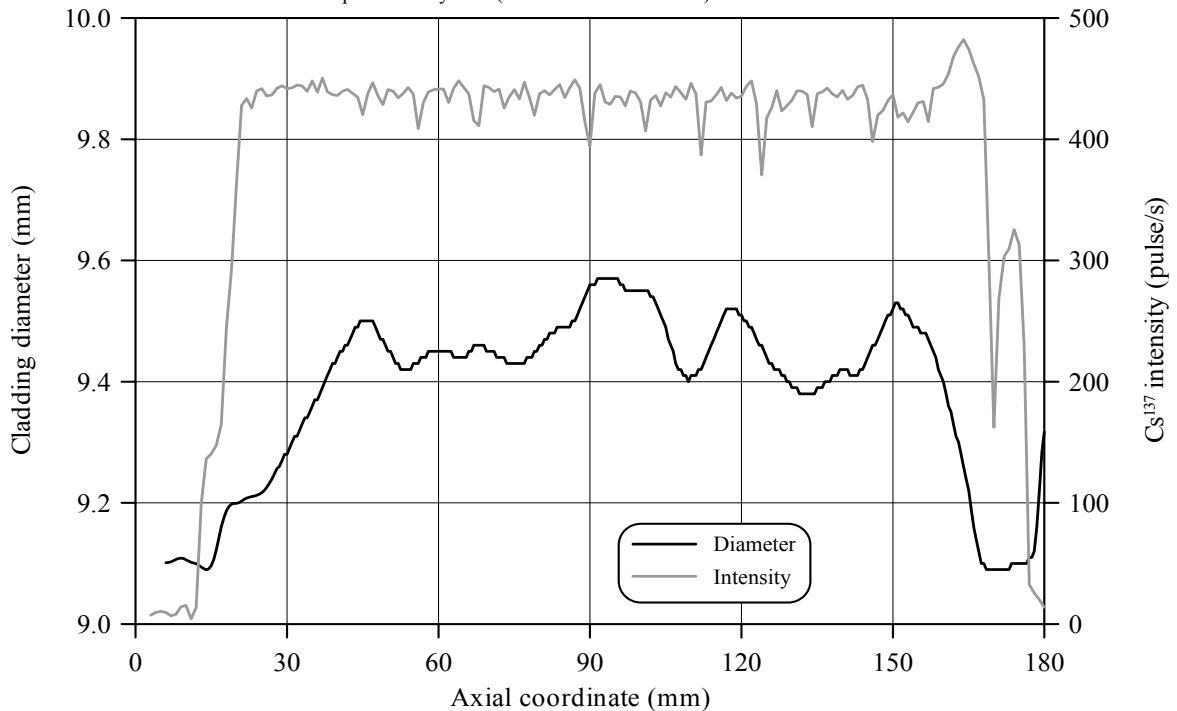


Fig.E-4.9. Fuel behavior during the B1GR test of fuel rod # RT4 in accordance with FRAP-T6/VVER and RAPTA-5 calculations

Table E-4.3. Axial distribution of cladding average outer diameter in fuel rod # RT4*

| Axial coordinate (mm) | Cladding diameter (mm) | Axial coordinate (mm) | Cladding diameter (mm) | Axial coordinate (mm) | Cladding diameter (mm) | Axial coordinate (mm) | Cladding diameter (mm) |
|-----------------------|------------------------|-----------------------|------------------------|-----------------------|------------------------|-----------------------|------------------------|
| 6 | 9.101 | 50 | 9.452 | 94 | 9.573 | 138 | 9.408 |
| 8 | 9.107 | 52 | 9.428 | 96 | 9.562 | 140 | 9.417 |
| 10 | 9.106 | 54 | 9.423 | 98 | 9.546 | 142 | 9.412 |
| 12 | 9.100 | 56 | 9.435 | 100 | 9.550 | 144 | 9.422 |
| 14 | 9.090 | 58 | 9.446 | 102 | 9.542 | 146 | 9.455 |
| 16 | 9.123 | 60 | 9.448 | 104 | 9.510 | 148 | 9.488 |
| 18 | 9.187 | 62 | 9.447 | 106 | 9.459 | 150 | 9.521 |
| 20 | 9.199 | 64 | 9.438 | 108 | 9.416 | 152 | 9.521 |
| 22 | 9.208 | 66 | 9.446 | 110 | 9.406 | 154 | 9.493 |
| 24 | 9.212 | 68 | 9.459 | 112 | 9.424 | 156 | 9.481 |
| 26 | 9.226 | 70 | 9.452 | 114 | 9.460 | 158 | 9.450 |
| 28 | 9.257 | 72 | 9.441 | 116 | 9.502 | 160 | 9.395 |
| 30 | 9.284 | 74 | 9.432 | 118 | 9.523 | 162 | 9.332 |
| 32 | 9.314 | 76 | 9.427 | 120 | 9.510 | 164 | 9.259 |
| 34 | 9.344 | 78 | 9.440 | 122 | 9.486 | 166 | 9.163 |
| 36 | 9.374 | 80 | 9.456 | 124 | 9.456 | 168 | 9.098 |
| 38 | 9.409 | 82 | 9.477 | 126 | 9.429 | 170 | 9.091 |
| 40 | 9.440 | 84 | 9.489 | 128 | 9.412 | 172 | 9.088 |
| 42 | 9.465 | 86 | 9.494 | 130 | 9.394 | 174 | 9.098 |
| 44 | 9.494 | 88 | 9.521 | 132 | 9.382 | 176 | 9.100 |
| 46 | 9.503 | 90 | 9.556 | 134 | 9.381 | 178 | 9.121 |
| 48 | 9.482 | 92 | 9.568 | 136 | 9.392 | 180 | 9.317 |

* Measured value determined on the basis of profilometry data (16 azimuthal directions)

Fig.E-4.10. Cladding measured average diameter and γ -scanning results for fuel rod # RT4

RT4

Table E-4.4. The PIE results for fuel rod # RT4

| Parameter | | Value |
|-----------|--|-------|
| 1. | Cladding outer diameter (mm): | |
| 1.1. | Maximum diameter of the bidimensional data sample in "fuel rod length - azimuthal angle" coordinates (mm) | 9.65 |
| 1.2. | Averaged azimuthal diameter and maximum diameter along the length selected from the sample of averaged azimuthal diameter (mm) | 9.58 |
| 1.3. | Averaged diameter of the bidimensional data sample in "fuel rod length - azimuthal angle" coordinates (mm) | 9.41 |
| 2. | Cladding maximum residual hoop strain (%) | 5.50 |
| 3. | Fuel pellet conditional diameter (mm) in cross-section*: | |
| | at 108 mm elevation | 7.98 |
| | at 117 mm elevation | 7.88 |
| 4. | ZrO ₂ outer thickness (μm) in cross-section: | |
| | at 108 mm elevation | 3-5 |
| | at 117 mm elevation | 3-5 |
| 5. | ZrO ₂ inner thickness (μm) in cross-section: | |
| | at 108 mm elevation | 6 |
| | at 117 mm elevation | 8 |
| 6. | Parameters characterizing FGR: | |
| 6.1. | Gas composition (% by volume): | |
| | He | - |
| | N ₂ | - |
| | O ₂ | - |
| | Ar | - |
| | CO ₂ | - |
| | Kr | - |
| | Xe | - |
| 6.2. | Free gas volume (cm ³) | - |
| 6.3. | Gas volume under normal conditions (cm ³) | - |
| 6.4. | Gas pressure under normal conditions (MPa) | - |

* Reference value determined by the processing of fuel cross-section photographs

Table E-4.5. Organized BGR test results for fuel rod # RT4

| Parameter | Unit | Value | | |
|---|---------------------|----------|------------|----------|
| | | Measured | Calculated | |
| | | | FRAP-T6 | RAPTA-5 |
| 1. Fuel burnup | MW d/kg U | 60.1 | 60.1 | 60.1 |
| 2. Initial gas pressure | MPa | 2.1 | 2.1 | 2.1 |
| 3. Energy deposition | cal/g fuel | 152.3 | 152.3 | 152.3 |
| 4. Peak fuel enthalpy* | cal/g fuel | - | 125.3 | 123.9 |
| 5. Fuel maximum temperature | K | - | 2099 | 2126 |
| 6. Maximum temperature of cladding outer surface | K | - | 1110 | 1099 |
| 7. Cladding burst | Failed, Unfailed | Unfailed | Unfailed | Unfailed |
| 8. Cladding residual hoop strain** | % | 3.70 | 3.23 | 1.77 |
| 9. Kr volume content in gas composition after the BGR test | % | - | 2.81 | - |
| 10. Xe volume content in gas composition after the BGR test | % | - | 16.82 | - |

* Average value of peak fuel enthalpy is 124.6 cal/g fuel

** Average value along the fuel stack length

Appendix E-5

***Individual Characteristics of Fuel Rod # RT5
after the BGR Test***

RT5

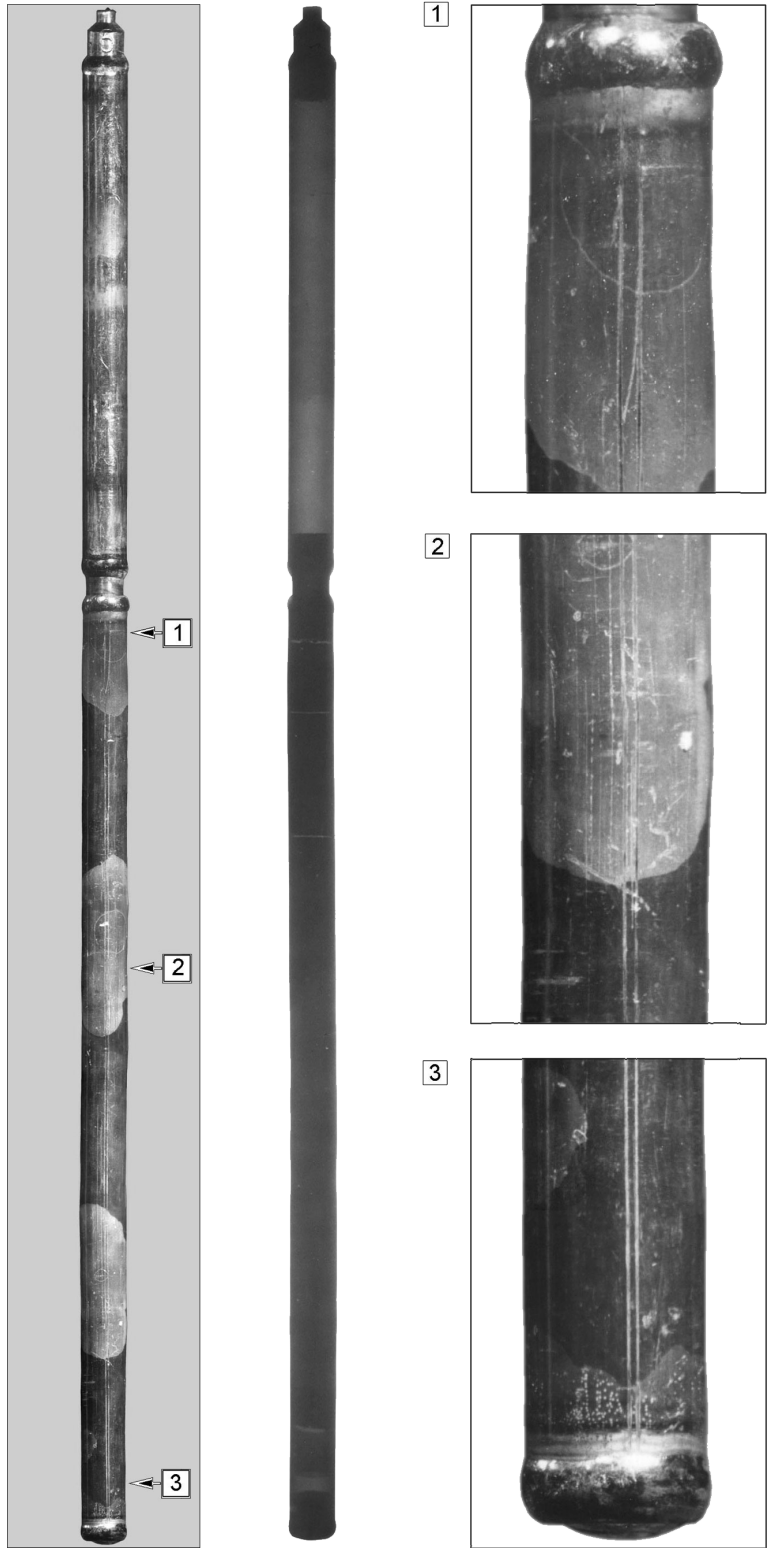


Fig.E-5.1. Appearance of unfailed fuel rod # RT5 after the BGR test (photographs and X-ray photograph)

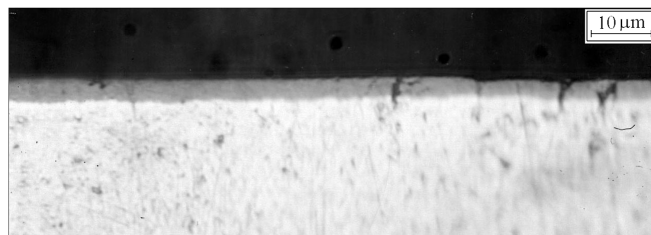
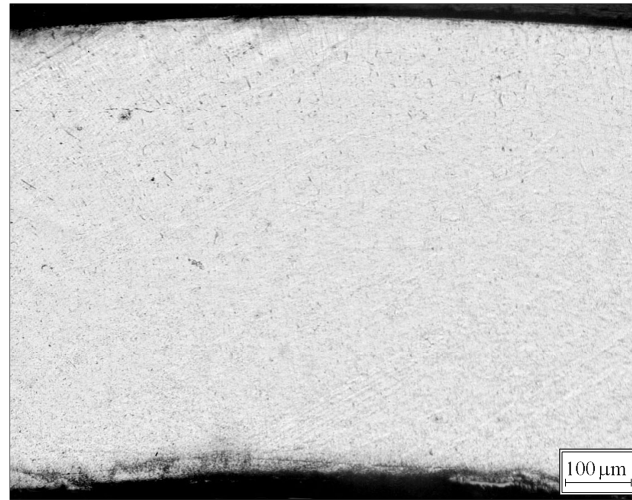
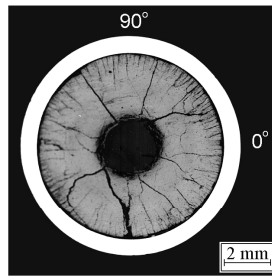


Fig.E-5.2. Cross-section and cladding microstructure of fuel rod # RT5 at 105 mm elevation (from low cap)

RT5

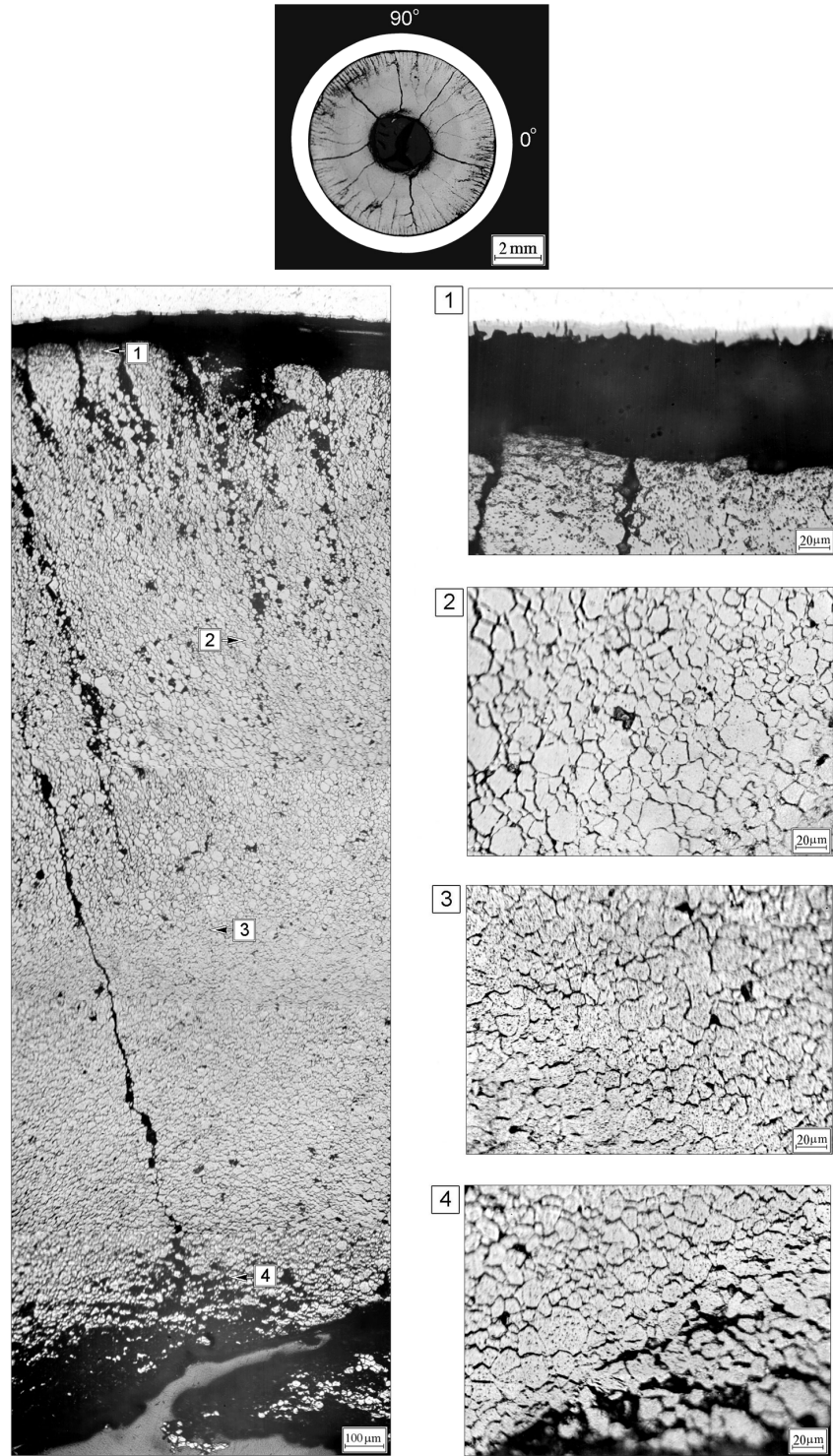


Fig.E-5.3. Cross-section and fuel microstructure of fuel rod # RT5 at 105 mm elevation (from low cap)

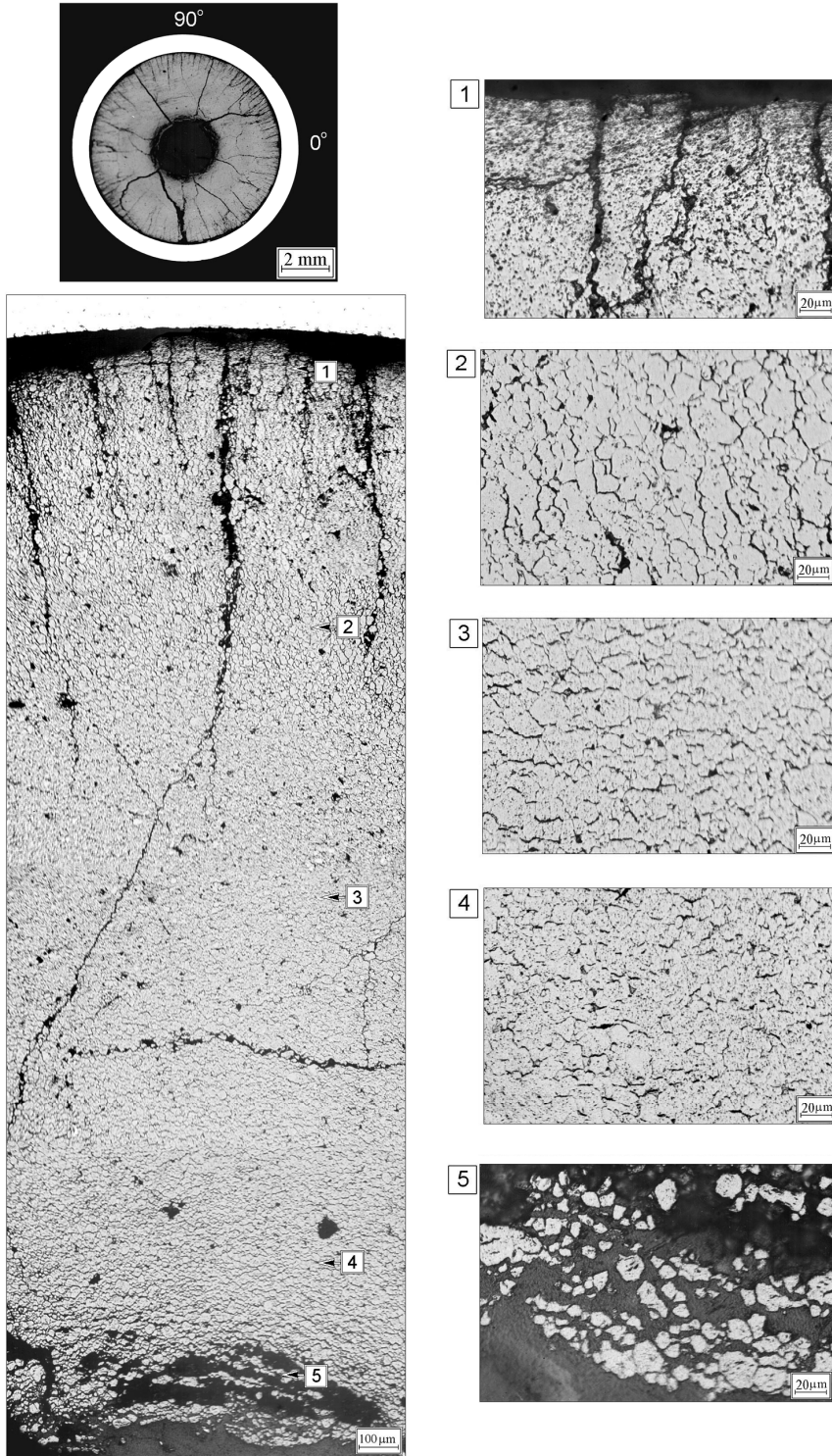


Fig.E-5.4. Cross-section and fuel microstructure of fuel rod # RT5 after the BGR test at 122 mm elevation (from low cap)

RT5

Table E-5.1. Time dependent energy characteristics of fuel rod # RT5

| Time (s) | Relative reactor power (current/maximum value) (per-unit) | Cumulative number of fissions in fuel rod (fiss) x 10 ⁻¹⁴ | Power of fuel rod ¹⁾²⁾ (kW) | Energy deposition | | Fuel enthalpy ³⁾ | |
|----------|---|--|--|-------------------|------------|-----------------------------|---------|
| | | | | (cal/g fuel) | (J/g fuel) | FRAP-T6 | RAPTA-5 |
| 0.000 | 1.74E-02 | 0.000 | 0.000 | 0.000 | 0.000 | 0.000 | 0.000 |
| 0.001 | 1.90E-01 | 0.287 | 1455 | 3.009 | 12.60 | 3.560 | 2.884 |
| 0.002 | 5.90E-01 | 1.377 | 4520 | 14.46 | 60.52 | 15.511 | 14.376 |
| 0.003 | 1.00E+00 | 3.803 | 7661 | 39.97 | 167.3 | 41.007 | 39.902 |
| 0.004 | 6.53E-01 | 6.297 | 5005 | 66.17 | 277.0 | 66.919 | 65.870 |
| 0.005 | 2.69E-01 | 7.583 | 2061 | 79.70 | 333.7 | 80.280 | 78.956 |
| 0.006 | 1.46E-01 | 8.172 | 1121 | 85.91 | 359.7 | 86.224 | 84.688 |
| 0.007 | 7.73E-02 | 8.482 | 591.8 | 89.17 | 373.3 | 89.159 | 87.538 |
| 0.008 | 5.38E-02 | 8.673 | 411.8 | 91.14 | 381.6 | 90.806 | 89.143 |
| 0.009 | 4.52E-02 | 8.816 | 346.1 | 92.64 | 387.9 | 92.001 | 90.323 |
| 0.010 | 4.49E-02 | 8.948 | 344.0 | 94.03 | 393.7 | 93.086 | 91.409 |
| 0.012 | 5.30E-02 | 9.231 | 406.1 | 97.02 | 406.2 | 95.520 | 93.875 |
| 0.014 | 6.55E-02 | 9.583 | 501.5 | 100.7 | 421.5 | 98.613 | 96.972 |
| 0.016 | 7.41E-02 | 9.995 | 567.8 | 105.0 | 439.6 | 102.367 | 100.780 |
| 0.018 | 7.28E-02 | 10.42 | 557.8 | 109.5 | 458.6 | 106.351 | 104.820 |
| 0.020 | 6.12E-02 | 10.82 | 468.9 | 113.8 | 476.3 | 109.976 | 108.800 |
| 0.022 | 4.91E-02 | 11.15 | 376.0 | 117.2 | 490.5 | 112.797 | 111.730 |
| 0.024 | 3.90E-02 | 11.40 | 298.9 | 119.9 | 501.8 | 115.005 | 113.980 |
| 0.026 | 2.98E-02 | 11.60 | 228.6 | 122.0 | 510.7 | 116.645 | 115.540 |
| 0.028 | 2.41E-02 | 11.76 | 185.0 | 123.6 | 517.5 | 117.847 | 116.750 |
| 0.030 | 2.22E-02 | 11.90 | 170.4 | 125.0 | 523.4 | 118.850 | 117.940 |
| 0.050 | 1.85E-02 | 13.14 | 142.0 | 138.1 | 578.3 | 128.238 | 127.630 |
| 0.070 | 1.62E-02 | 14.18 | 124.2 | 149.1 | 624.2 | 135.808 | 135.660 |
| 0.090 | 1.15E-02 | 14.99 | 88.35 | 157.6 | 660.0 | 141.600 | 141.310 |
| 0.110 | 6.98E-03 | 15.54 | 53.63 | 163.5 | 684.4 | 145.075 | 144.810 |
| 0.130 | 2.60E-03 | 15.81 | 20.14 | 166.2 | 695.9 | 146.269 | 145.590 |
| 0.150 | 9.92E-04 | 15.91 | 7.801 | 167.2 | 700.2 | 146.280 | 144.940 |
| 0.200 | 2.67E-04 | 15.98 | 2.270 | 168.1 | 703.9 | 144.671 | 142.520 |
| 1.000 | 2.44E-05 | 16.09 | 0.294 | 169.7 | 710.5 | 123.856 | 121.150 |
| 10.00 | 2.76E-06 | 16.29 | 0.043 | 173.6 | 726.8 | 31.755 | 28.725 |
| 100.0 | 5.38E-08 | 16.39 | 0.007 | 176.5 | 739.0 | 5.054 | 4.463 |
| 1000 | 2.11E-13 | 16.39 | 1.52E-04 | 178.0 | 745.3 | 0.000 | 0.000 |

¹⁾ Average values determined in accordance with results of RRC KI and VNIIEF calculations

²⁾ Maximum power value is 7660.5 kW (t=0.003 s)

³⁾ Average radial value

Table E-5.2. Radial energy characteristics of fuel rod # RT5*

| Parameters | Coordinates of fuel radial layers (mm) | | | |
|---|--|------------------------|------------------------|-------------------------|
| | 1 layer (1.25-2.84) | 2 layer (2.84-3.47) | 3 layer (3.47-3.74) | 4 layer (3.74-3.808) |
| Number of fissions $\times 10^{-14}$ (fiss) | 7.363 | 4.783 | 2.872 | 1.381 |
| Fission density $\times 10^{-13}$ (fiss/g fuel) | 2.341 | 2.493 | 3.068 | 4.513 |
| Power** (kW) | 3414 | 2238 | 1346 | 662.4 |
| Energy deposition (cal/g fuel) | 156.4 | 166.0 | 203.8 | 299.2 |
| Energy deposition (J/g fuel) | 654.8 | 695.0 | 853.2 | 1253 |
| Energy deposition*** (per-unit) | 0.523 | 0.555 | 0.681 | 1.000 |

* Average values were determined in accordance with results of RRC KI and VNIIEF calculations

** The power for the entire length of each layer at time 0.003 s

*** Energy deposition in current layer/energy deposition in 4th layer

RT5

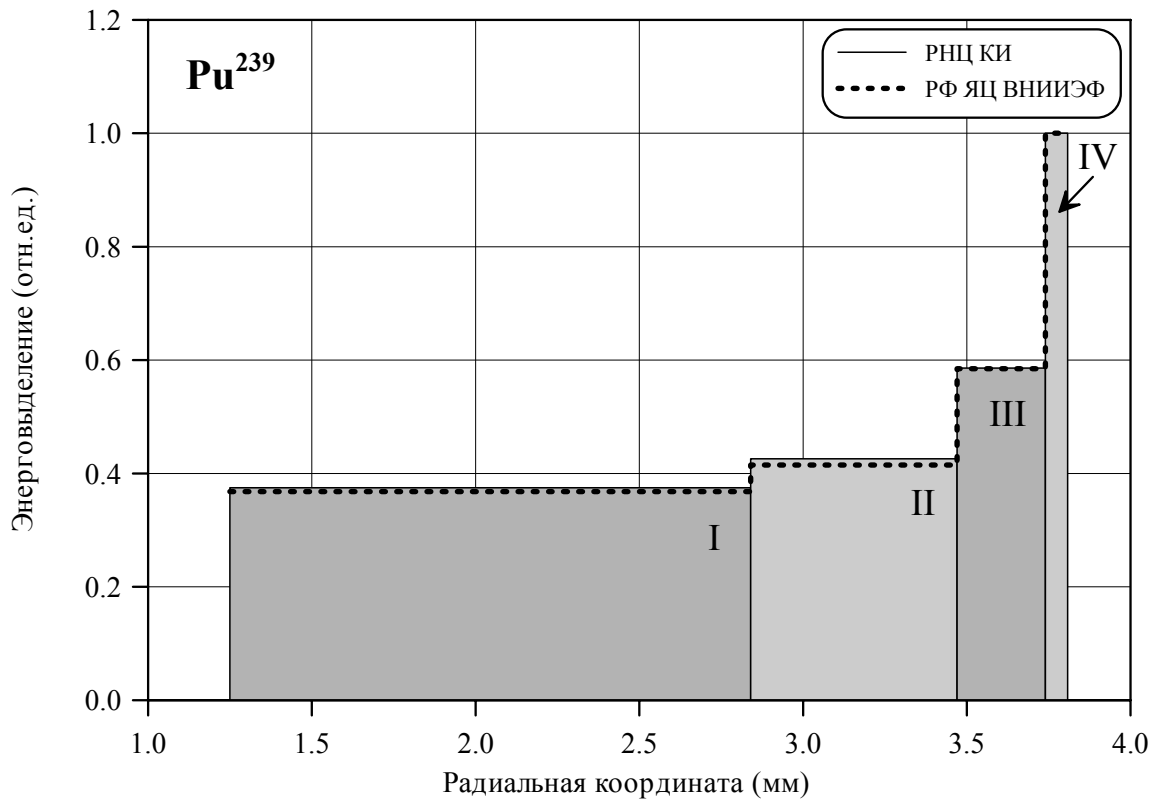
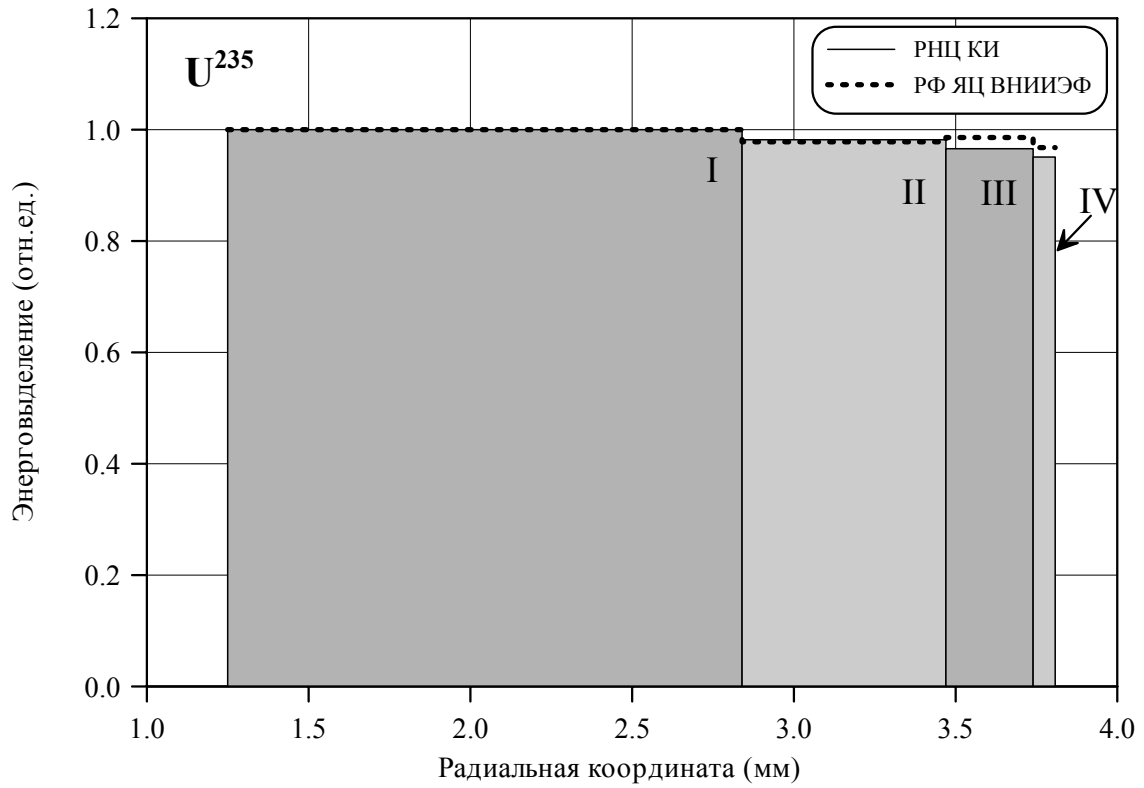


Fig.E-5.5. U²³⁵ and Pu²³⁹ radial distribution of energy deposition for fuel rod # RT5

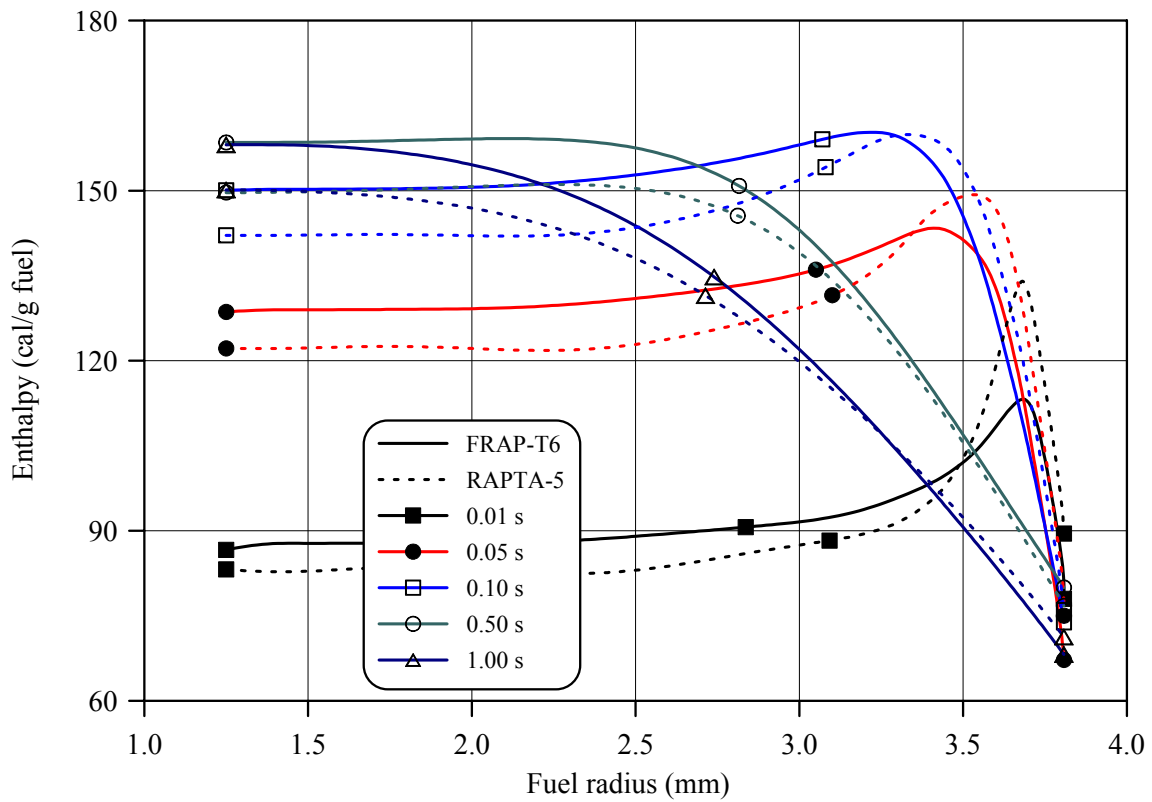
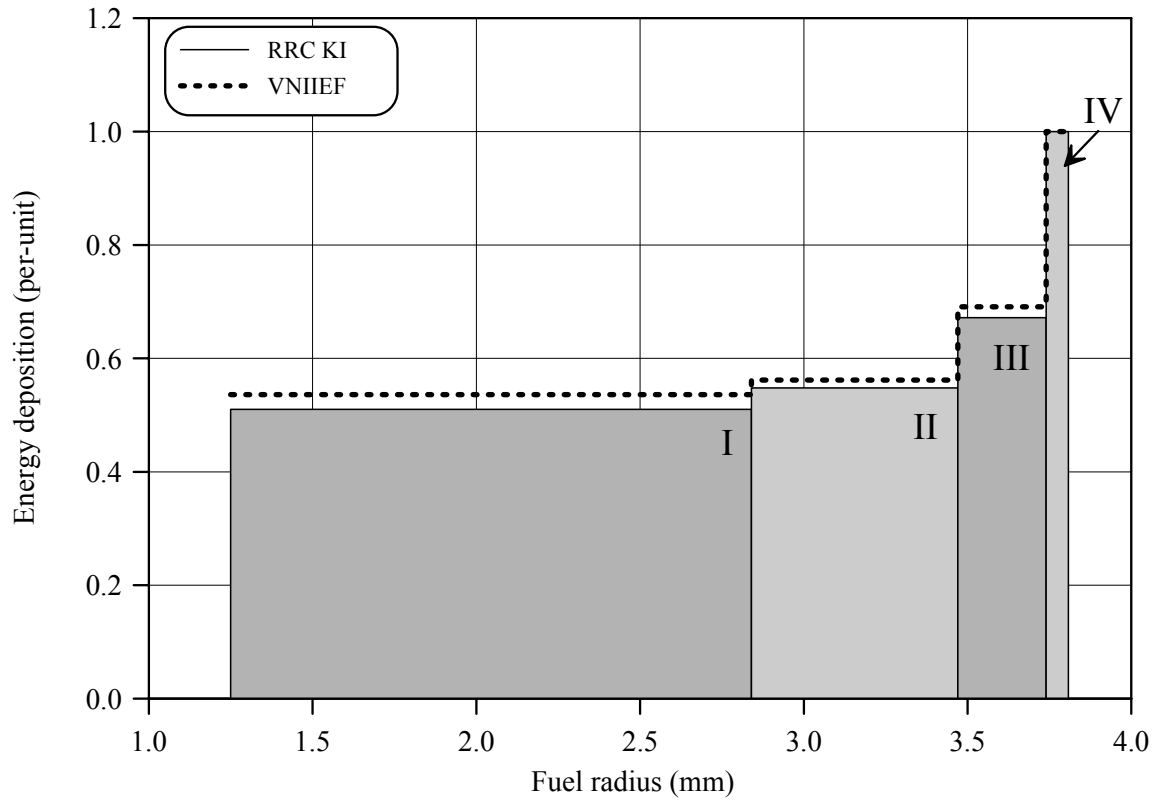


Fig.E-5.6. Radial distribution of energy deposition and fuel enthalpy for fuel rod # RT5

RT5

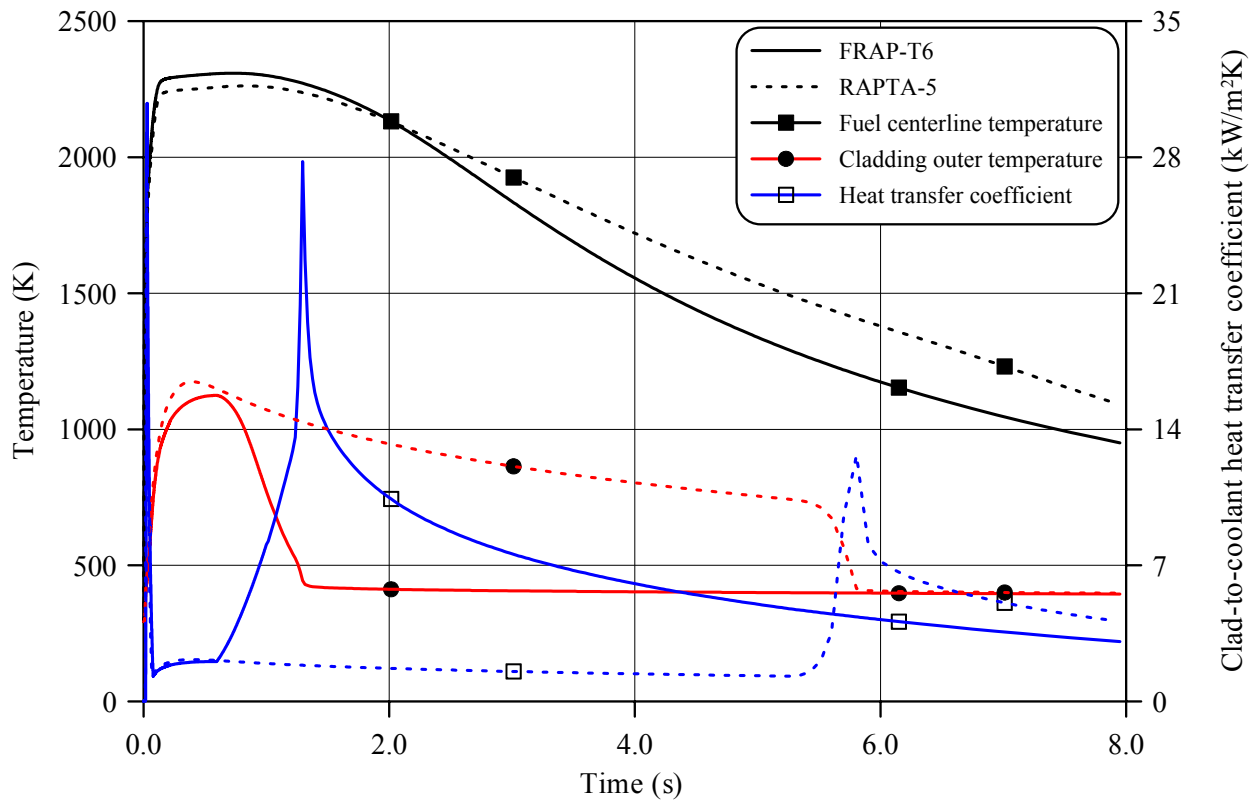
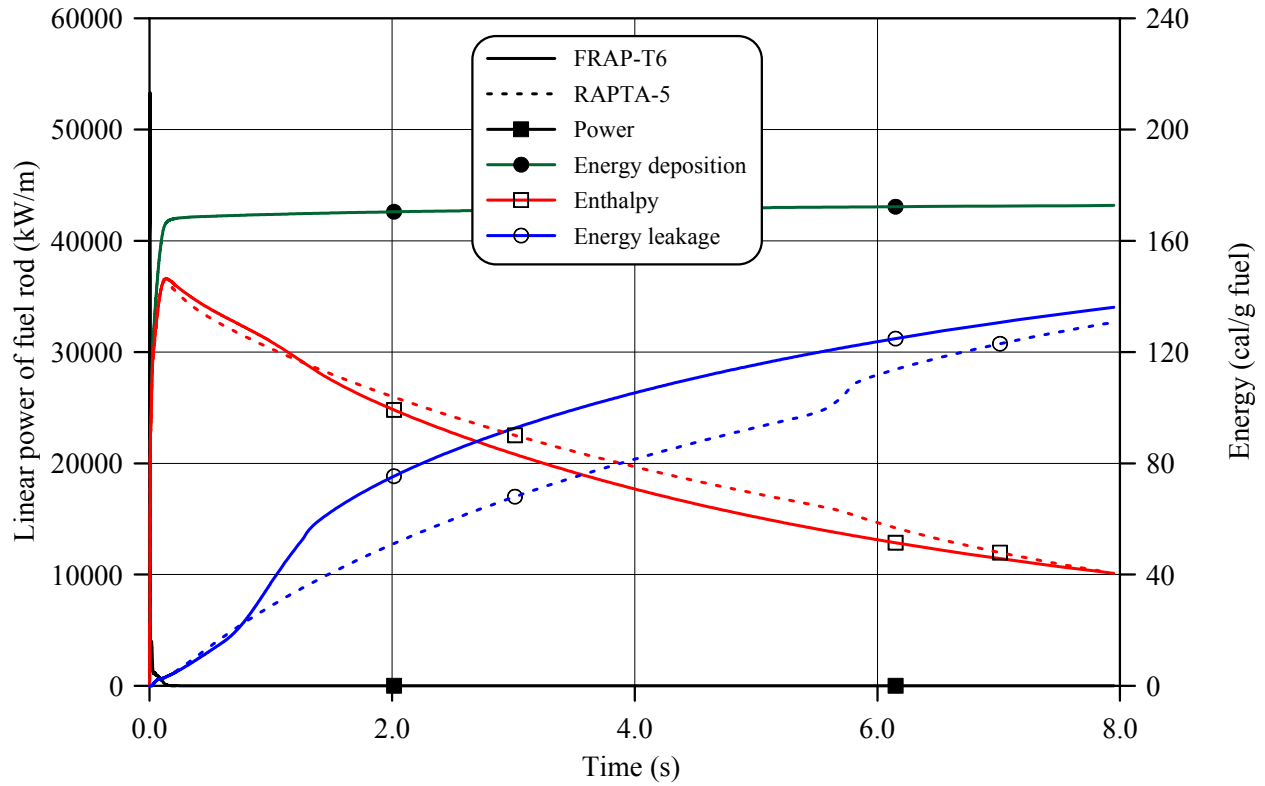


Fig.E-5.7. Thermal history of fuel rod # RT5 during the BGR test in accordance with FRAP-T6/VVER and RAPTA-5 calculations

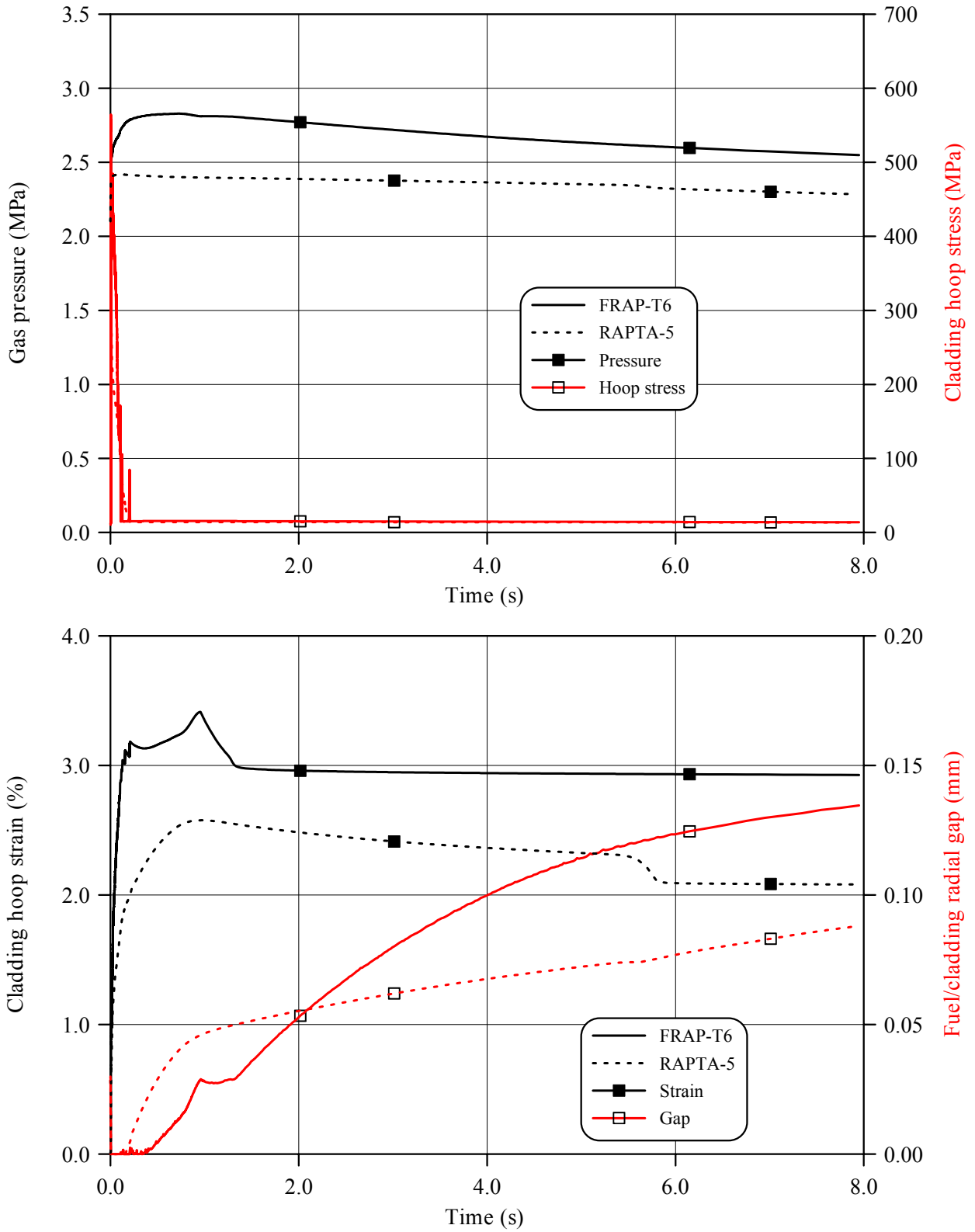


Fig.E-5.8. Mechanical behavior of fuel rod # RT5 during the B1GR test in accordance with FRAP-T6/VVER and RAPTA-5 calculations

RT5

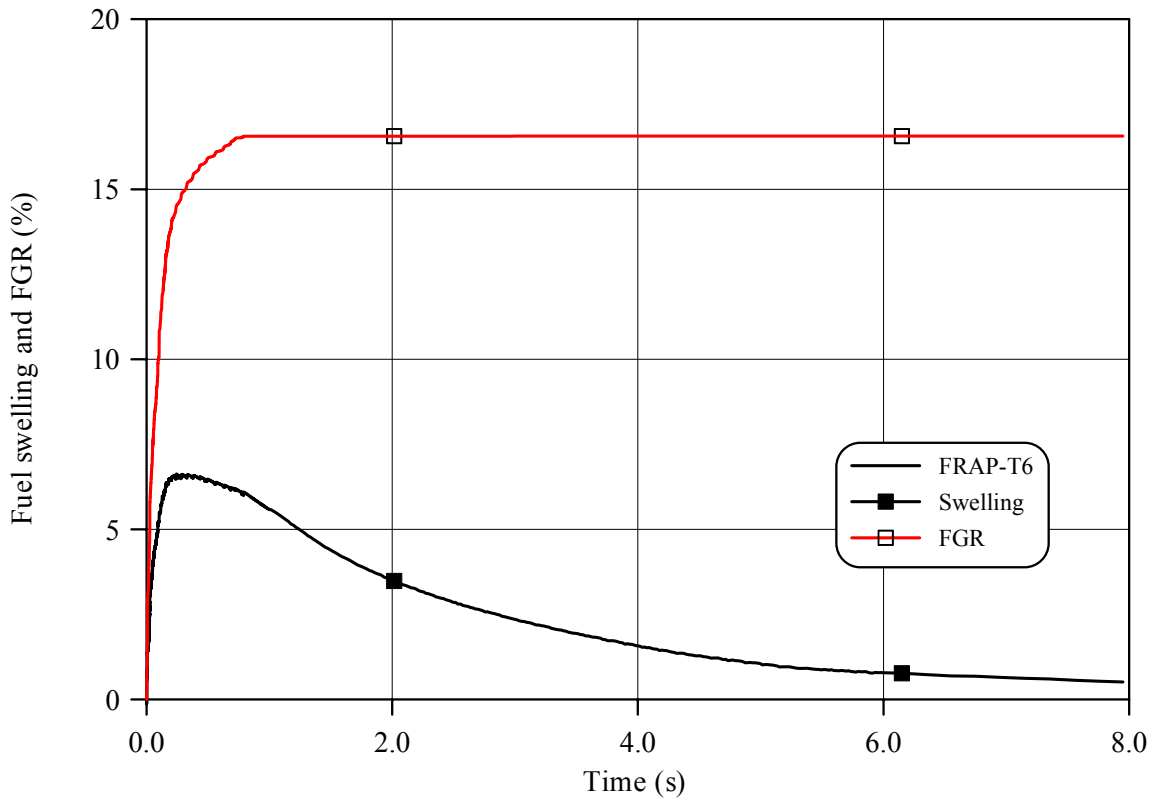
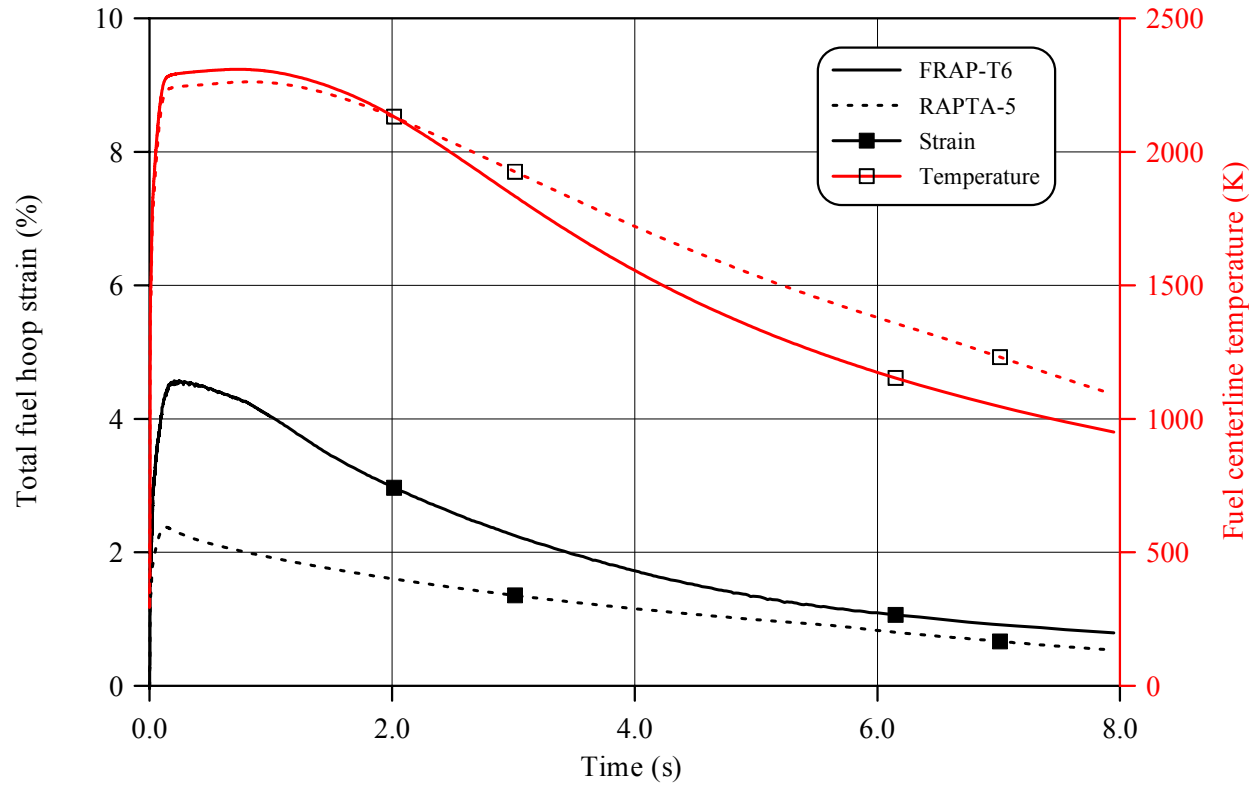
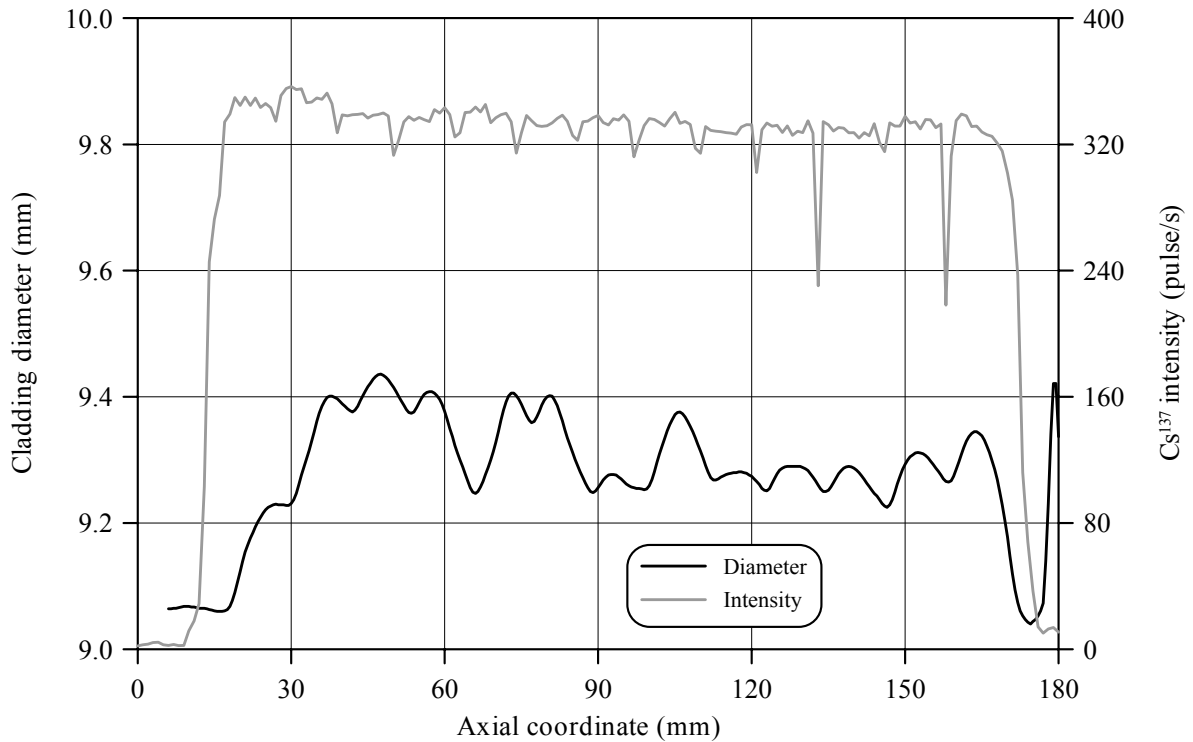


Fig.E-5.9. Fuel behavior during the B1GR test of fuel rod # RT5 in accordance with FRAP-T6/VVER and RAPTA-5 calculations

Table E-5.3. Axial distribution of cladding average outer diameter in fuel rod # RT5*

| Axial coordinate (mm) | Cladding diameter (mm) | Axial coordinate (mm) | Cladding diameter (mm) | Axial coordinate (mm) | Cladding diameter (mm) | Axial coordinate (mm) | Cladding diameter (mm) |
|-----------------------|------------------------|-----------------------|------------------------|-----------------------|------------------------|-----------------------|------------------------|
| 6 | 9.064 | 50 | 9.415 | 94 | 9.273 | 138 | 9.287 |
| 8 | 9.066 | 52 | 9.387 | 96 | 9.259 | 140 | 9.287 |
| 10 | 9.068 | 54 | 9.376 | 98 | 9.255 | 142 | 9.269 |
| 12 | 9.065 | 56 | 9.404 | 100 | 9.259 | 144 | 9.247 |
| 14 | 9.063 | 58 | 9.406 | 102 | 9.310 | 146 | 9.227 |
| 16 | 9.060 | 60 | 9.377 | 104 | 9.356 | 148 | 9.249 |
| 18 | 9.068 | 62 | 9.323 | 106 | 9.376 | 150 | 9.293 |
| 20 | 9.123 | 64 | 9.278 | 108 | 9.353 | 152 | 9.311 |
| 22 | 9.176 | 66 | 9.247 | 110 | 9.314 | 154 | 9.307 |
| 24 | 9.209 | 68 | 9.277 | 112 | 9.272 | 156 | 9.287 |
| 26 | 9.227 | 70 | 9.328 | 114 | 9.273 | 158 | 9.266 |
| 28 | 9.229 | 72 | 9.392 | 116 | 9.279 | 160 | 9.285 |
| 30 | 9.231 | 74 | 9.402 | 118 | 9.281 | 162 | 9.330 |
| 32 | 9.276 | 76 | 9.370 | 120 | 9.274 | 164 | 9.345 |
| 34 | 9.330 | 78 | 9.368 | 122 | 9.255 | 166 | 9.322 |
| 36 | 9.385 | 80 | 9.400 | 124 | 9.263 | 168 | 9.269 |
| 38 | 9.401 | 82 | 9.386 | 126 | 9.287 | 170 | 9.178 |
| 40 | 9.389 | 84 | 9.335 | 128 | 9.290 | 172 | 9.074 |
| 42 | 9.376 | 86 | 9.291 | 130 | 9.288 | 174 | 9.043 |
| 44 | 9.402 | 88 | 9.256 | 132 | 9.273 | 176 | 9.053 |
| 46 | 9.428 | 90 | 9.256 | 134 | 9.250 | 178 | 9.231 |
| 48 | 9.434 | 92 | 9.276 | 136 | 9.264 | 180 | 9.337 |

* Measured value determined on the basis of profilometry data (16 azimuthal directions)

Fig.E-5.10. Cladding measured average diameter and γ -scanning results for fuel rod # RT5

RT5

Table E-5.4. The PIE results for fuel rod # RT5

| Parameter | | Value |
|-----------|--|-------|
| 1. | Cladding outer diameter (mm): | |
| 1.1. | Maximum diameter of the bidimensional data sample in "fuel rod length - azimuthal angle" coordinates (mm) | 9.49 |
| 1.2. | Averaged azimuthal diameter and maximum diameter along the length selected from the sample of averaged azimuthal diameter (mm) | 9.44 |
| 1.3. | Averaged diameter of the bidimensional data sample in "fuel rod length - azimuthal angle" coordinates (mm) | 9.30 |
| 2. | Cladding maximum residual hoop strain (%) | 4.20 |
| 3. | Fuel pellet conditional diameter (mm) in cross-section*: | |
| | at 105 mm elevation | 7.72 |
| | at 122 mm elevation | 7.76 |
| 4. | ZrO ₂ outer thickness (μm) in cross-section: | |
| | at 105 mm elevation | 3-5 |
| | at 122 mm elevation | 3-5 |
| 5. | ZrO ₂ inner thickness (μm) in cross-section: | |
| | at 105 mm elevation | 7 |
| 6. | Parameters characterizing FGR: | |
| 6.1. | Gas composition (% by volume): | |
| | He | 81.16 |
| | N ₂ | 0.52 |
| | O ₂ | 0.033 |
| | Ar | 0.017 |
| | CO ₂ | 0.01 |
| | Kr | 1.52 |
| | Xe | 16.75 |
| 6.2. | Free gas volume (cm ³) | 6.2 |
| 6.3. | Gas volume under normal conditions (cm ³) | 138.7 |
| 6.4. | Gas pressure under normal conditions (MPa) | 2.24 |
| 6.5. | FGR (%) | 26.00 |

* Reference value determined by the processing of fuel cross-section photographs

Table E-5.5. Organized BGR test results for fuel rod # RT5

| Parameter | Unit | Value | | |
|---|---------------------|----------|------------|----------|
| | | Measured | Calculated | |
| | | | FRAP-T6 | RAPTA-5 |
| 1. Fuel burnup | MW d/kg U | 48.6 | 48.6 | 48.6 |
| 2. Initial gas pressure | MPa | 2.1 | 2.1 | 2.1 |
| 3. Energy deposition | cal/g fuel | 178.0 | 178.0 | 178.0 |
| 4. Peak fuel enthalpy* | cal/g fuel | - | 146.4 | 145.6 |
| 5. Fuel maximum temperature | K | - | 2353 | 2379 |
| 6. Maximum temperature of cladding outer surface | K | - | 1125 | 1175 |
| 7. Cladding burst | Failed, Unfailed | Unfailed | Unfailed | Unfailed |
| 8. Cladding residual hoop strain** | % | 2.70 | 2.83 | 2.01 |
| 9. Kr volume content in gas composition after the BGR test | % | 1.52 | 1.87 | - |
| 10. Xe volume content in gas composition after the BGR test | % | 16.75 | 11.18 | - |

* Average value of peak fuel enthalpy is 146.0 cal/g fuel

** Average value along the fuel stack length

Appendix E-6

*Individual Characteristics of Fuel Rod # RT6
after the BGR Test*

RT6

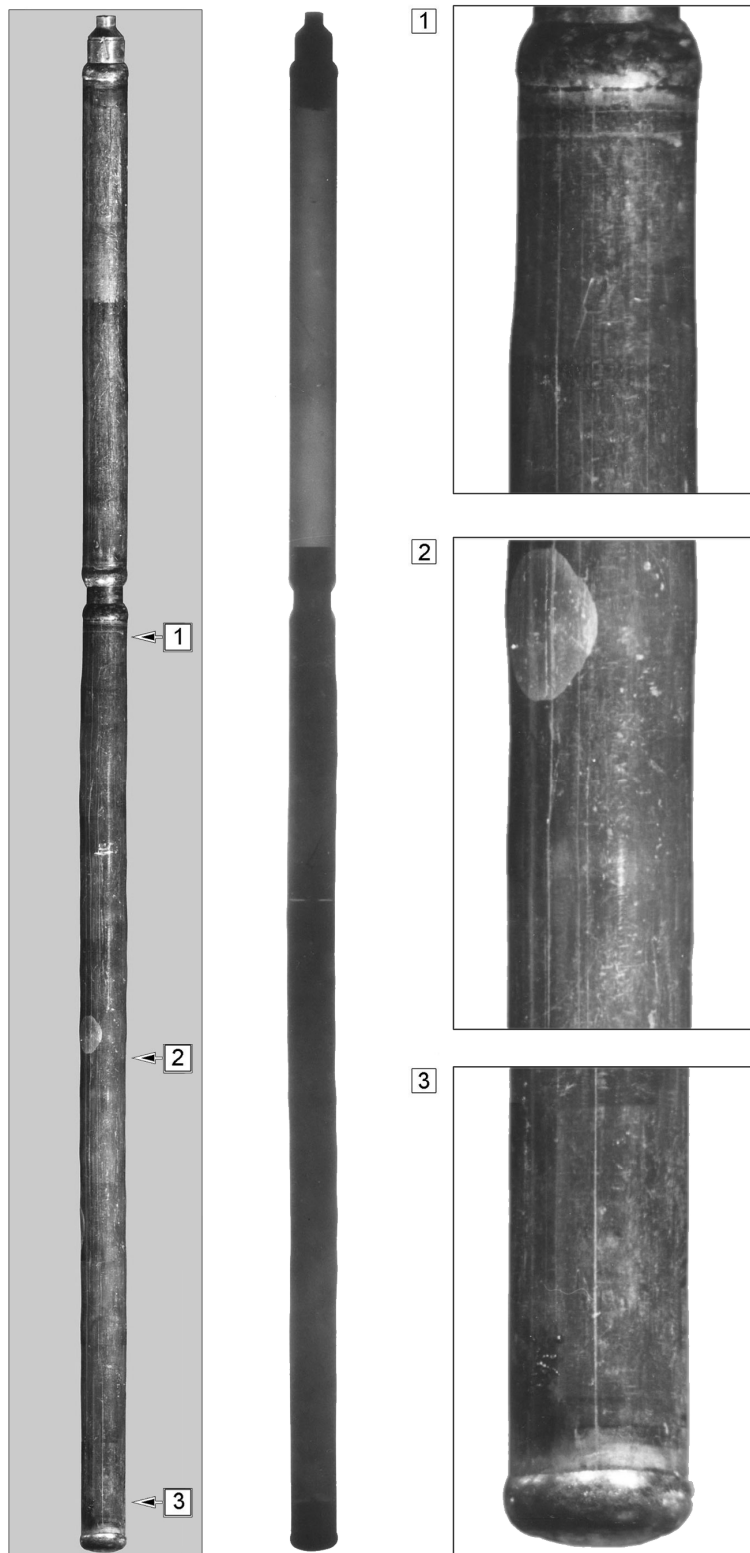


Fig.E-6.1. Appearance of unfailed fuel rod # RT6 after the BGR test (photographs and X-ray photograph)

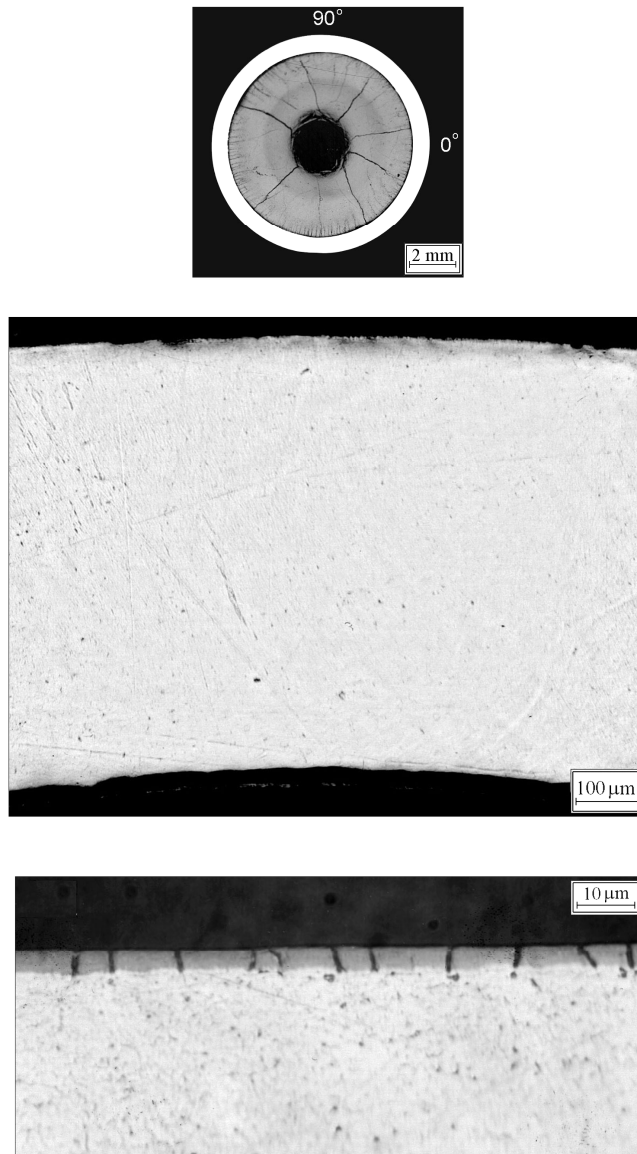


Fig.E-6.2. Cross-section and cladding microstructure of fuel rod # RT6 at 114 mm elevation (from low cap)

RT6

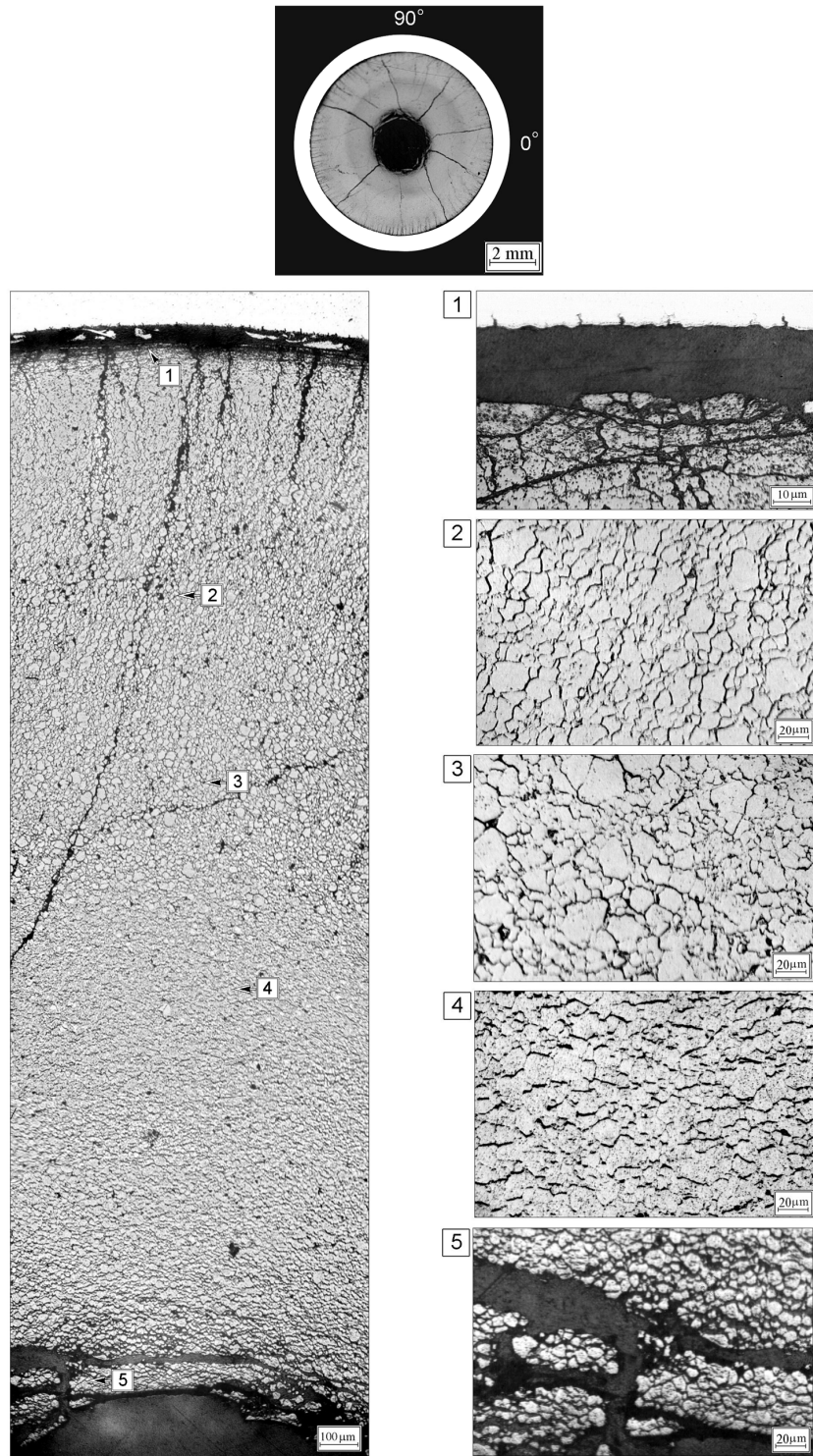


Fig.E-6.3. Cross-section and fuel microstructure of fuel rod # RT6 at 114 mm elevation (from low cap)

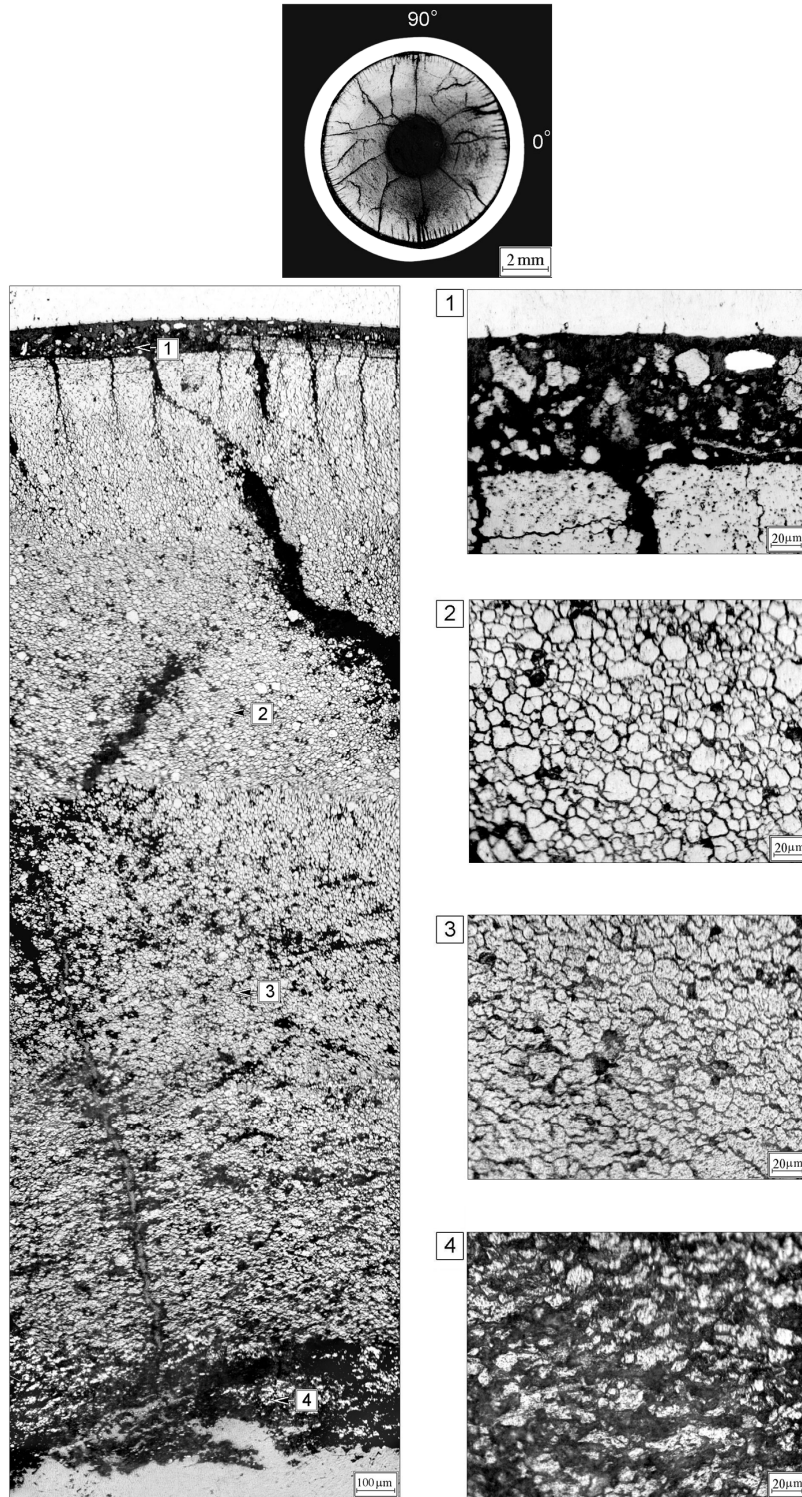


Fig.E-6.4. Cross-section and fuel microstructure of fuel rod # RT6 after the BGR test at 132 mm elevation (from low cap)

RT6

Table E-6.1. Time dependent energy characteristics of fuel rod # RT6

| Time (s) | Relative reactor power (current/maximum value) (per-unit) | Cumulative number of fissions in fuel rod (fiss) x 10 ⁻¹⁴ | Power of fuel rod ¹⁾²⁾ (kW) | Energy deposition | | Fuel enthalpy ³⁾ | |
|----------|---|--|--|-------------------|------------|-----------------------------|---------|
| | | | | (cal/g fuel) | (J/g fuel) | FRAP-T6 | RAPTA-5 |
| 0.000 | 5.55E-03 | 0.000 | 0.000 | 0.000 | 0.000 | 0.000 | 0.000 |
| 0.001 | 1.75E-01 | 0.192 | 1286 | 2.184 | 9.142 | 3.244 | 2.139 |
| 0.002 | 6.31E-01 | 1.266 | 4633 | 14.20 | 59.45 | 13.059 | 14.203 |
| 0.003 | 1.00E+00 | 3.620 | 7340 | 40.77 | 170.7 | 44.285 | 40.783 |
| 0.004 | 6.78E-01 | 6.040 | 4979 | 68.03 | 284.8 | 66.083 | 67.795 |
| 0.005 | 2.82E-01 | 7.294 | 2069 | 82.17 | 344.0 | 83.034 | 81.459 |
| 0.006 | 1.52E-01 | 7.878 | 1118 | 88.69 | 371.3 | 88.089 | 87.484 |
| 0.007 | 8.32E-02 | 8.183 | 610.4 | 92.17 | 385.9 | 91.939 | 90.526 |
| 0.008 | 5.79E-02 | 8.372 | 425.3 | 94.30 | 394.8 | 93.381 | 92.280 |
| 0.009 | 4.84E-02 | 8.519 | 355.1 | 95.92 | 401.6 | 94.956 | 93.567 |
| 0.010 | 4.74E-02 | 8.644 | 347.7 | 97.37 | 407.7 | 95.869 | 94.721 |
| 0.012 | 5.49E-02 | 8.923 | 403.3 | 100.5 | 420.8 | 98.352 | 97.226 |
| 0.014 | 6.67E-02 | 9.262 | 489.5 | 104.3 | 436.6 | 101.475 | 100.620 |
| 0.016 | 7.50E-02 | 9.661 | 550.3 | 108.8 | 455.6 | 105.267 | 104.490 |
| 0.018 | 7.30E-02 | 10.08 | 535.8 | 113.4 | 474.9 | 109.262 | 108.870 |
| 0.020 | 6.10E-02 | 10.44 | 447.7 | 117.7 | 492.7 | 112.878 | 112.560 |
| 0.022 | 4.89E-02 | 10.75 | 358.8 | 121.1 | 506.9 | 115.719 | 115.520 |
| 0.024 | 3.86E-02 | 10.99 | 283.7 | 123.8 | 518.2 | 117.902 | 117.770 |
| 0.026 | 3.11E-02 | 11.18 | 228.0 | 125.9 | 527.2 | 119.573 | 119.360 |
| 0.028 | 2.62E-02 | 11.33 | 192.7 | 127.7 | 534.5 | 120.880 | 120.620 |
| 0.030 | 2.35E-02 | 11.47 | 172.5 | 129.2 | 540.8 | 121.980 | 121.860 |
| 0.050 | 2.02E-02 | 12.73 | 148.7 | 143.4 | 600.5 | 132.238 | 132.490 |
| 0.070 | 1.76E-02 | 13.80 | 129.4 | 155.5 | 650.9 | 140.860 | 141.510 |
| 0.090 | 1.24E-02 | 14.62 | 91.47 | 164.7 | 689.6 | 147.338 | 147.820 |
| 0.110 | 7.71E-03 | 15.19 | 56.77 | 171.1 | 716.5 | 151.832 | 151.750 |
| 0.130 | 2.88E-03 | 15.46 | 21.30 | 174.2 | 729.2 | 152.508 | 152.670 |
| 0.150 | 1.10E-03 | 15.56 | 8.248 | 175.3 | 734.0 | 152.417 | 152.040 |
| 0.200 | 2.93E-04 | 15.64 | 2.397 | 176.3 | 738.1 | 151.207 | 149.570 |
| 1.000 | 2.63E-05 | 15.75 | 0.302 | 178.0 | 745.3 | 131.264 | 127.660 |
| 10.00 | 3.06E-06 | 15.96 | 0.044 | 182.3 | 763.0 | 38.467 | 32.063 |
| 100.0 | 5.95E-08 | 16.06 | 0.007 | 185.4 | 776.1 | 5.210 | 4.530 |
| 1000 | 2.32E-13 | 16.07 | 1.57E-04 | 186.9 | 782.7 | 0.000 | 0.000 |

¹⁾ Average values determined in accordance with results of RRC KI and VNIIEF calculations

²⁾ Maximum power value is 7340 kW (t=0.003 s)

³⁾ Average radial value

Table E-6.2. Radial energy characteristics of fuel rod # RT6*

| Parameters** | Coordinates of fuel radial layers (mm) | | | |
|---|--|------------------------|------------------------|-------------------------|
| | 1 layer (1.25-2.82) | 2 layer (2.82-3.44) | 3 layer (3.44-3.71) | 4 layer (3.71-3.795) |
| Number of fissions $\times 10^{-14}$ (fiss) | 7.469 | 4.829 | 2.876 | 1.404 |
| Fission density $\times 10^{-13}$ (fiss/g fuel) | 2.469 | 2.618 | 3.195 | 4.766 |
| Power*** (kW) | 3281 | 2145 | 1285 | 629.6 |
| Energy deposition (cal/g fuel) | 163.6 | 173.5 | 212.5 | 311.5 |
| Energy deposition (J/g fuel) | 684.9 | 726.4 | 889.6 | 1304 |
| Energy deposition**** (per-unit) | 0.526 | 0.557 | 0.683 | 1.000 |

* Average values were determined in accordance with results of RRC KI and VNIIEF calculations

** All parameters were determined for the undamaged section of a fuel stack (see Table C.2)

*** The power for the entire length of each layer at time 0.003 s

**** Energy deposition in current layer/energy deposition in 4th layer

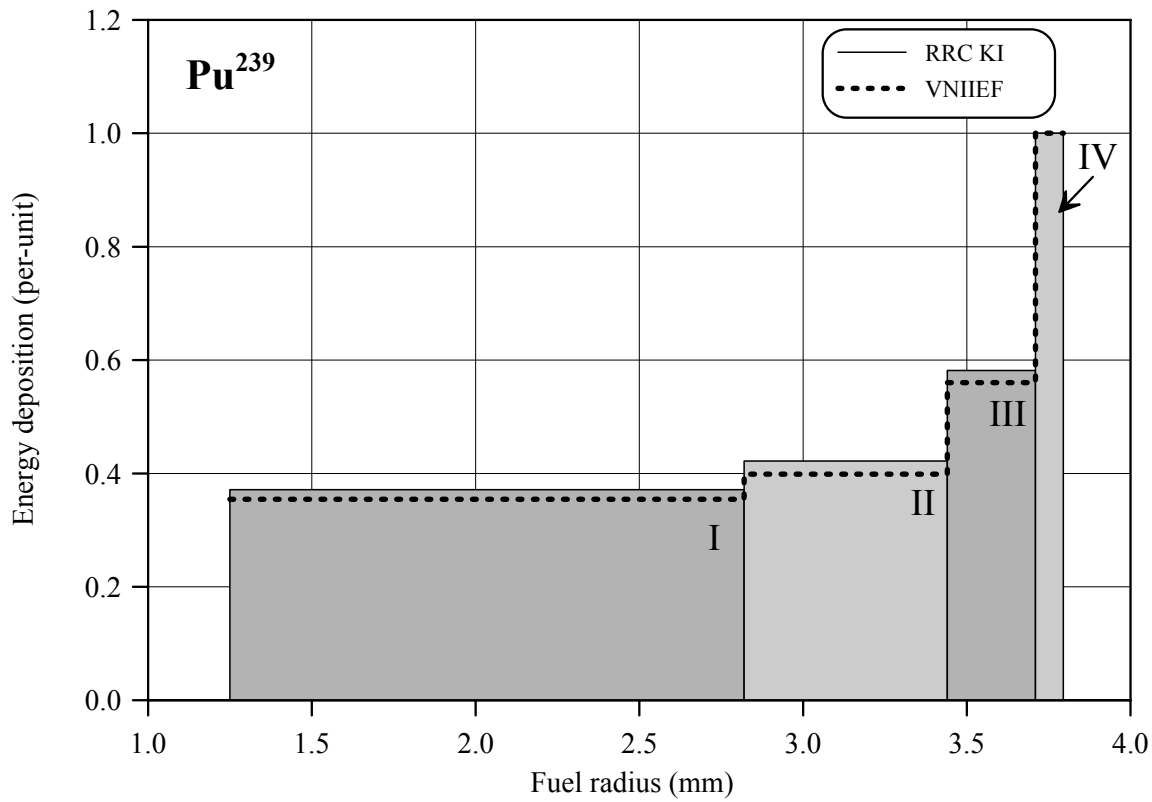
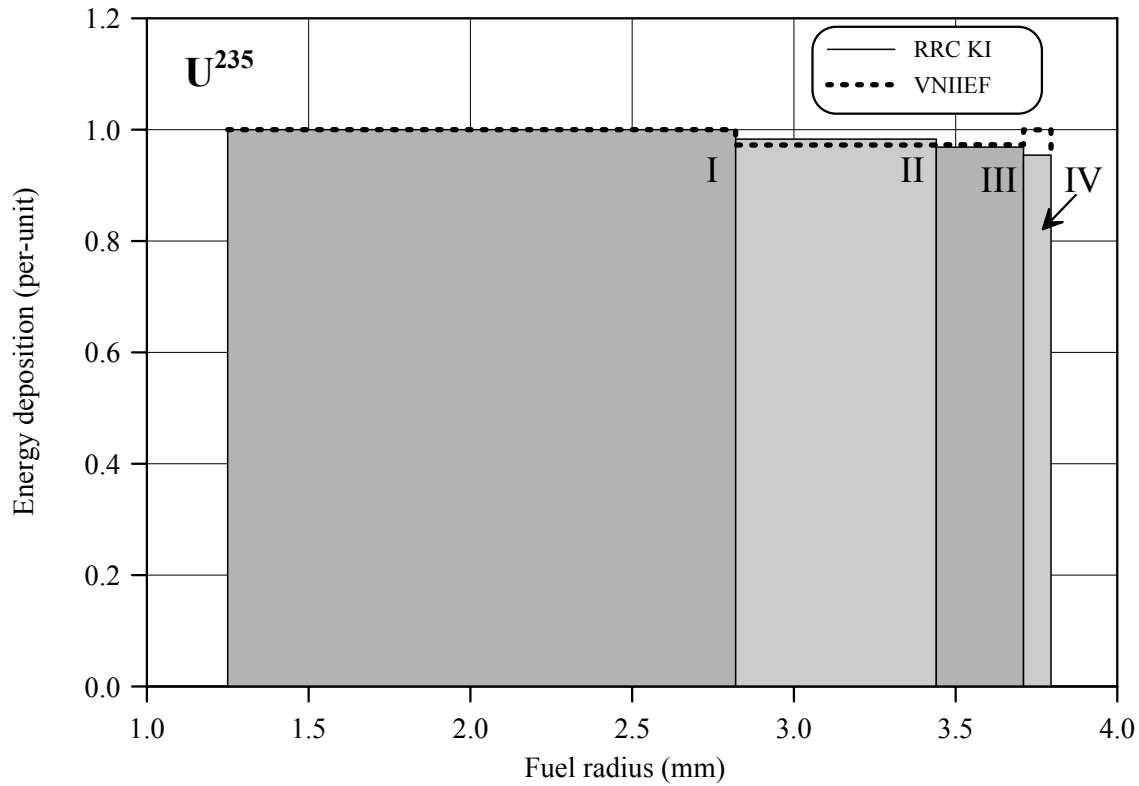


Fig.E-6.5. U²³⁵ and Pu²³⁹ radial distribution of energy deposition for fuel rod # RT6

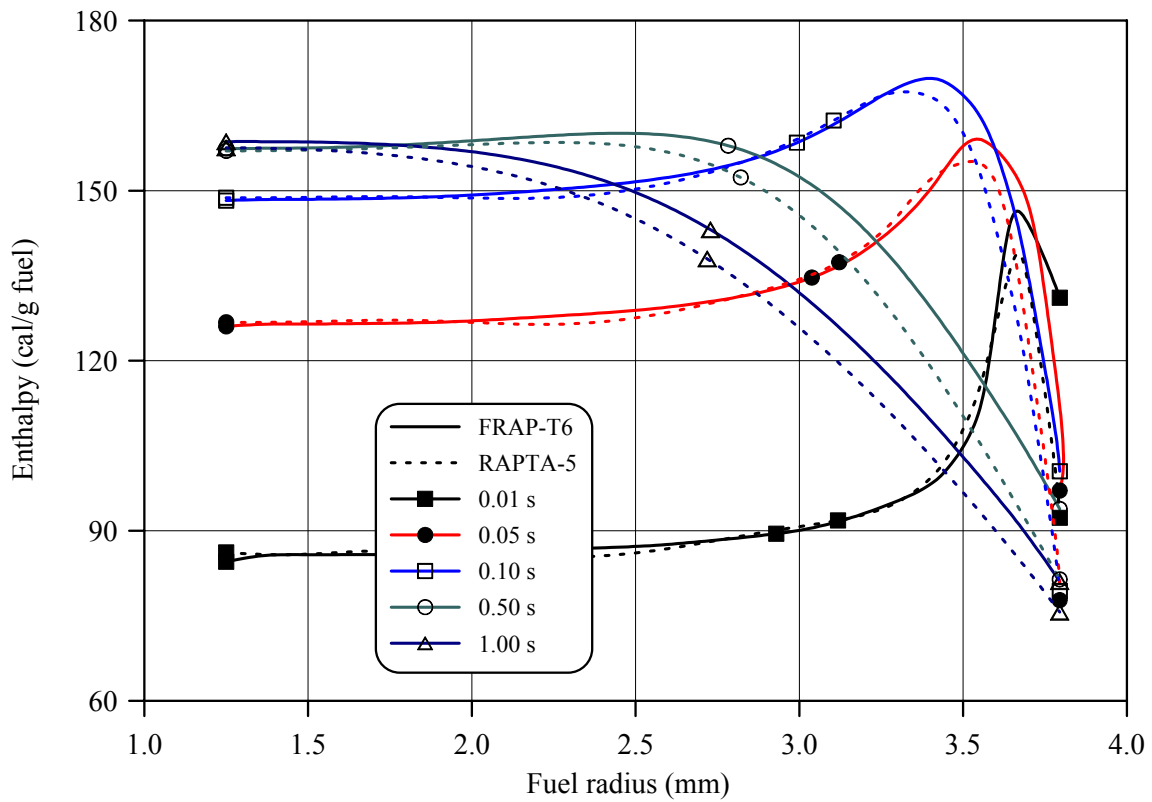
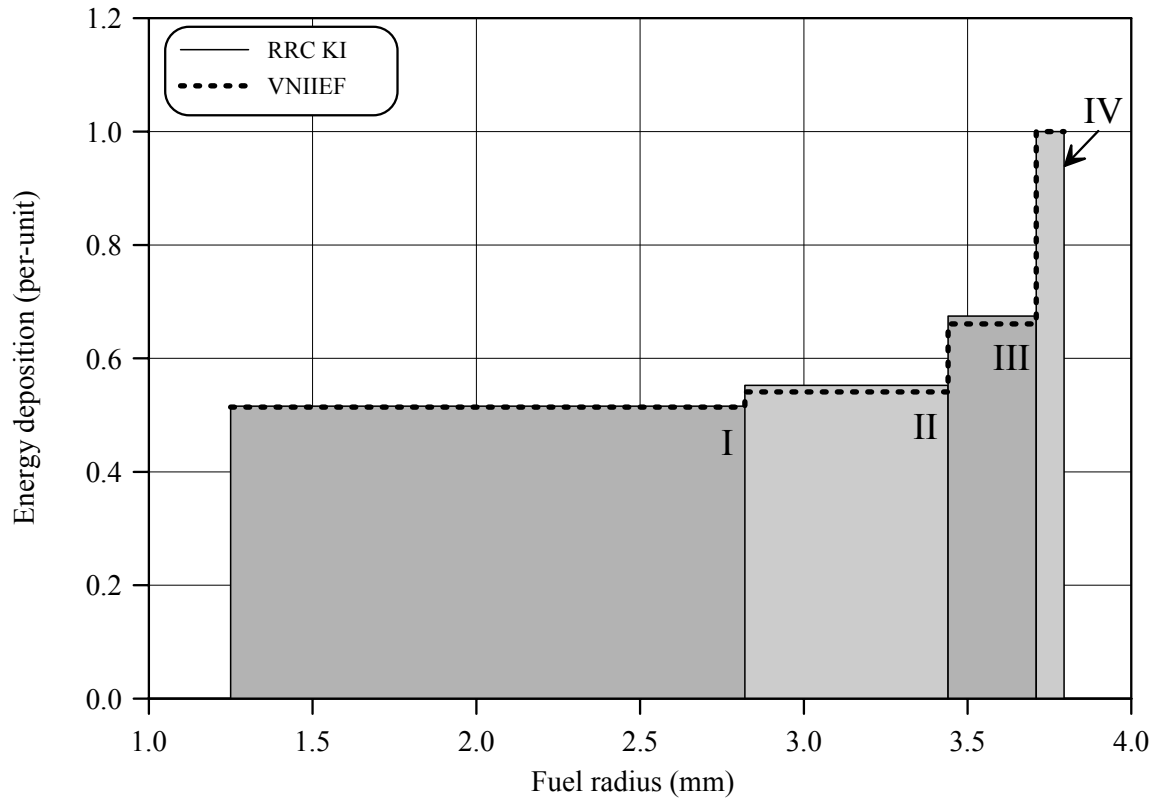


Fig.E-6.6. Radial distribution of energy deposition and fuel enthalpy for fuel rod # RT6

RT6

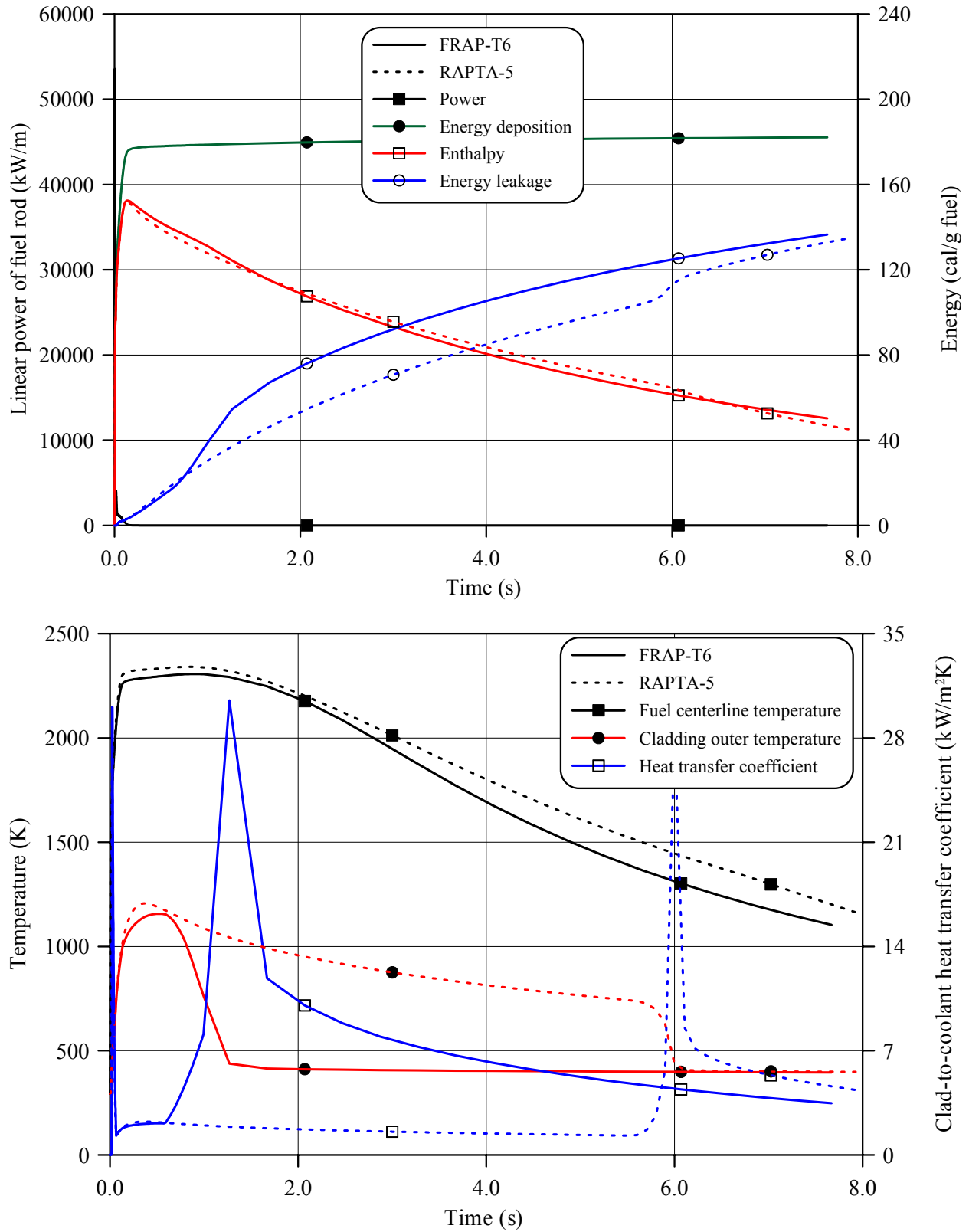


Fig.E-6.7. Thermal history of fuel rod # RT6 during the BGR test in accordance with FRAP-T6/VVER and RAPTA-5 calculations

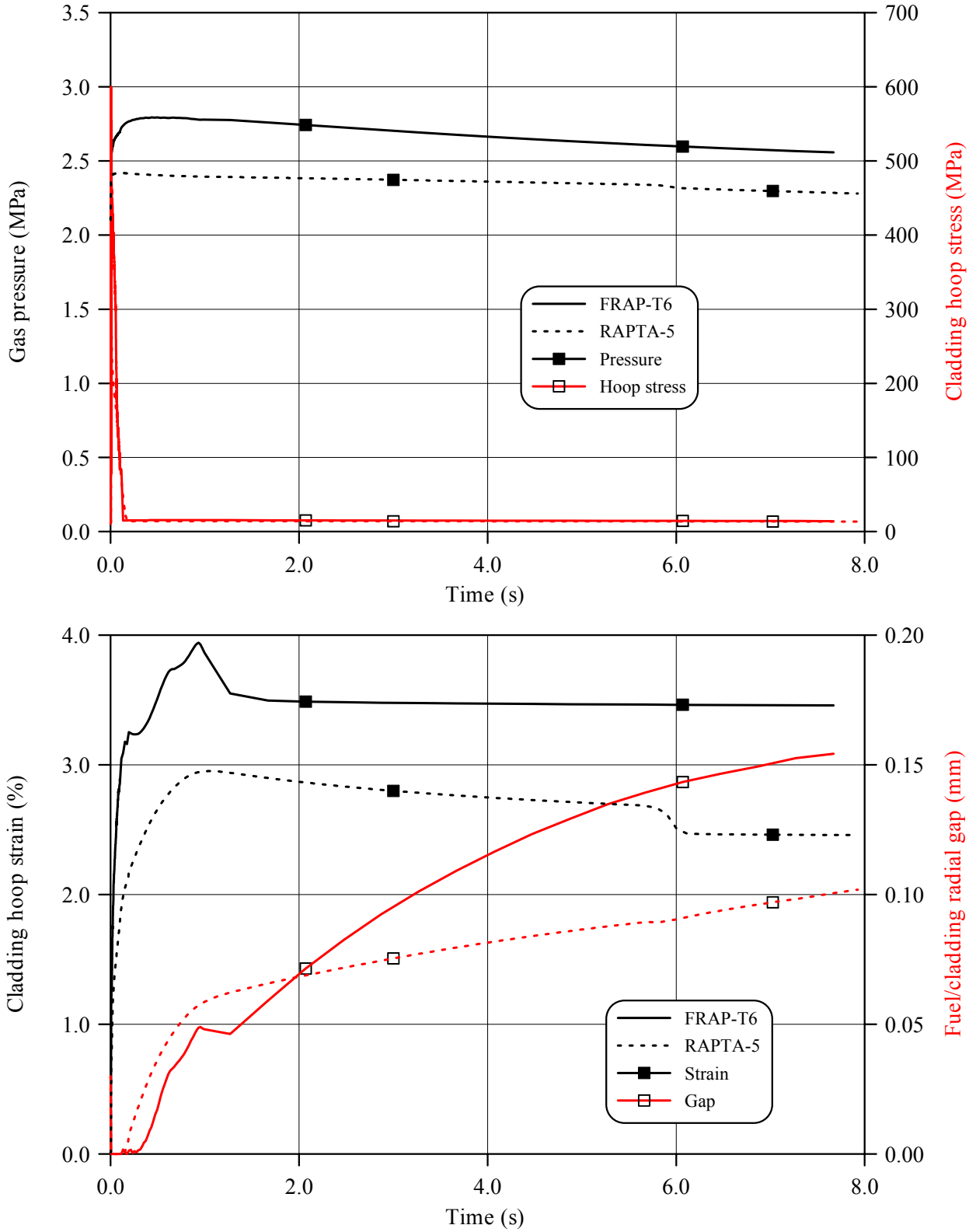


Fig.E-6.8. Mechanical behavior of fuel rod # RT6 during the B1GR test in accordance with FRAP-T6/VVER and RAPTA-5 calculations

RT6

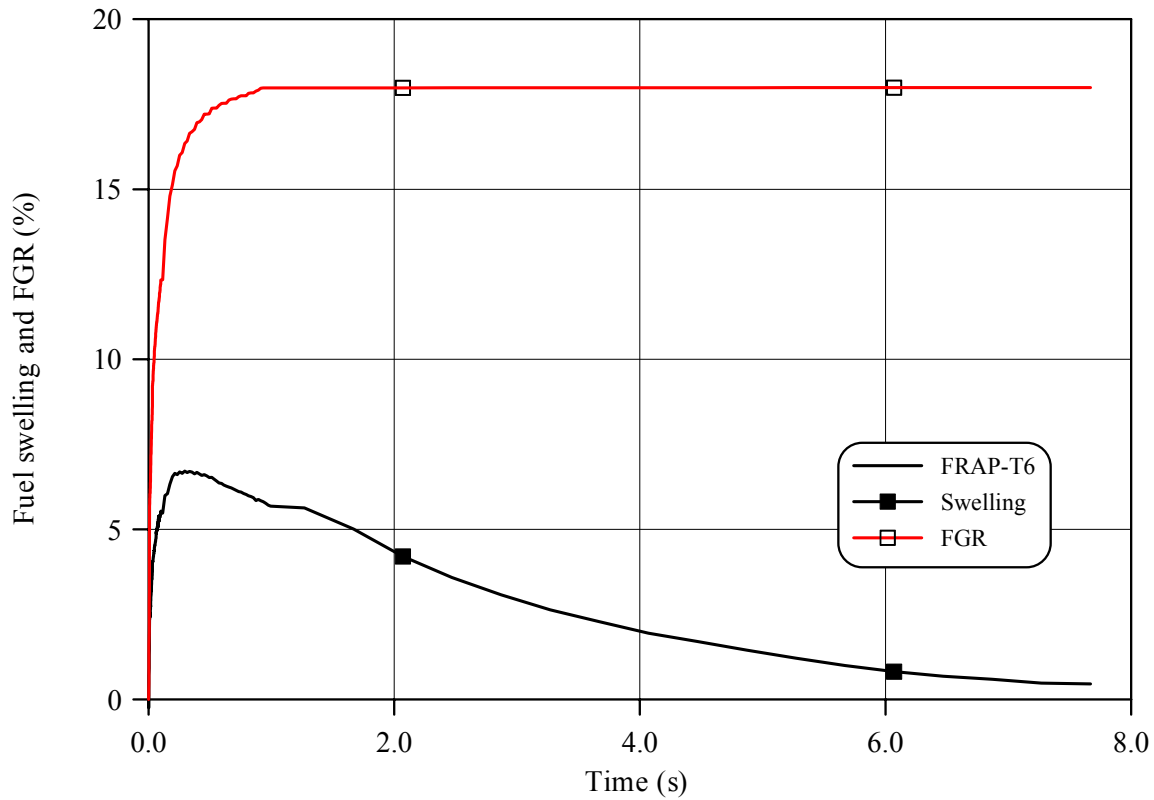
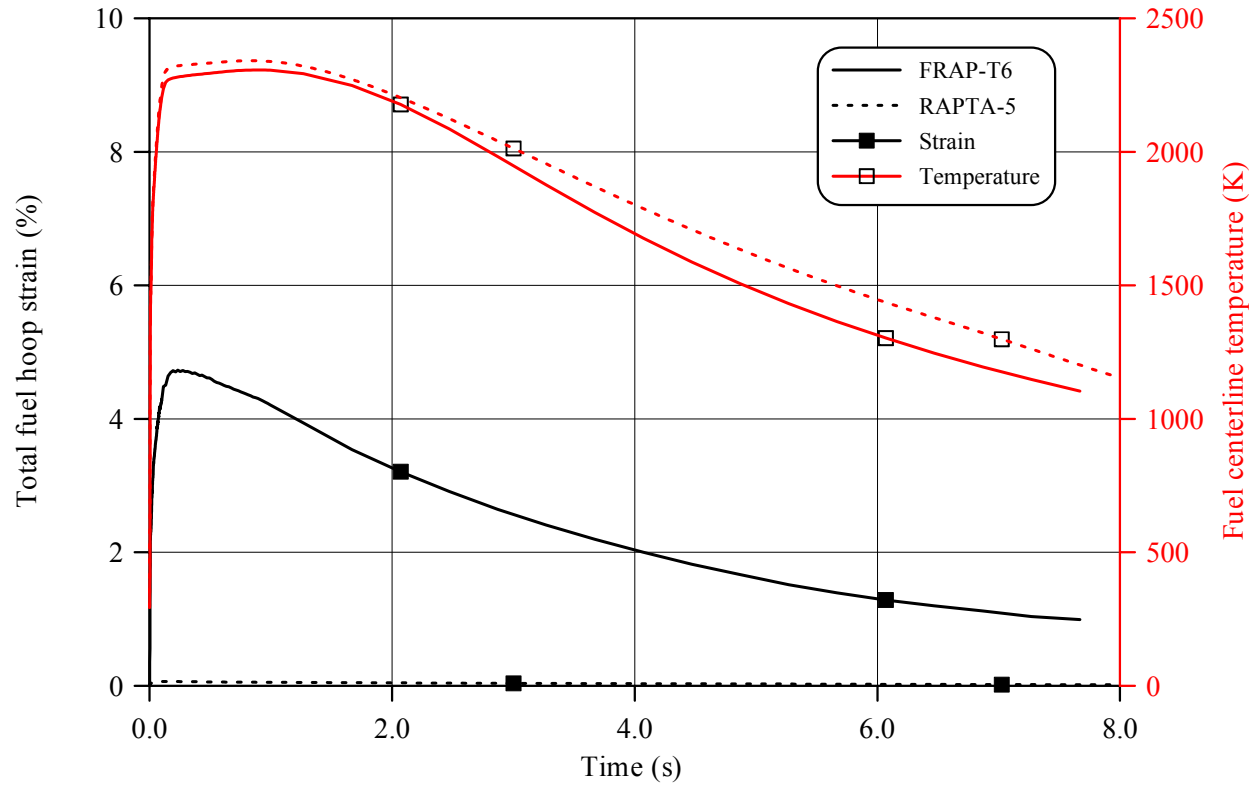


Fig.E-6.9. Fuel behavior during the B1GR test of fuel rod # RT6 in accordance with FRAP-T6/VVER and RAPTA-5 calculations

Table E-6.3. Axial distribution of cladding average outer diameter in fuel rod # RT6*

| Axial coordinate (mm) | Cladding diameter (mm) | Axial coordinate (mm) | Cladding diameter (mm) | Axial coordinate (mm) | Cladding diameter (mm) | Axial coordinate (mm) | Cladding diameter (mm) |
|-----------------------|------------------------|-----------------------|------------------------|-----------------------|------------------------|-----------------------|------------------------|
| 6 | 9.073 | 50 | 9.327 | 94 | 9.316 | 138 | 9.428 |
| 8 | 9.074 | 52 | 9.377 | 96 | 9.417 | 140 | 9.460 |
| 10 | 9.072 | 54 | 9.322 | 98 | 9.488 | 142 | 9.473 |
| 12 | 9.071 | 56 | 9.234 | 100 | 9.420 | 144 | 9.459 |
| 14 | 9.072 | 58 | 9.214 | 102 | 9.344 | 146 | 9.405 |
| 16 | 9.071 | 60 | 9.277 | 104 | 9.337 | 148 | 9.355 |
| 18 | 9.073 | 62 | 9.385 | 106 | 9.388 | 150 | 9.392 |
| 20 | 9.108 | 64 | 9.428 | 108 | 9.456 | 152 | 9.500 |
| 22 | 9.156 | 66 | 9.357 | 110 | 9.461 | 154 | 9.555 |
| 24 | 9.195 | 68 | 9.284 | 112 | 9.362 | 156 | 9.511 |
| 26 | 9.233 | 70 | 9.291 | 114 | 9.286 | 158 | 9.437 |
| 28 | 9.267 | 72 | 9.360 | 116 | 9.314 | 160 | 9.387 |
| 30 | 9.301 | 74 | 9.461 | 118 | 9.384 | 162 | 9.397 |
| 32 | 9.307 | 76 | 9.447 | 120 | 9.429 | 164 | 9.418 |
| 34 | 9.300 | 78 | 9.324 | 122 | 9.429 | 166 | 9.372 |
| 36 | 9.323 | 80 | 9.279 | 124 | 9.363 | 168 | 9.216 |
| 38 | 9.357 | 82 | 9.317 | 126 | 9.343 | 170 | 9.109 |
| 40 | 9.393 | 84 | 9.391 | 128 | 9.411 | 172 | 9.070 |
| 42 | 9.358 | 86 | 9.486 | 130 | 9.522 | 174 | 9.066 |
| 44 | 9.266 | 88 | 9.427 | 132 | 9.597 | 176 | 9.063 |
| 46 | 9.229 | 90 | 9.306 | 134 | 9.554 | 178 | 9.122 |
| 48 | 9.265 | 92 | 9.272 | 136 | 9.454 | 180 | 9.222 |

* Measured value determined on the basis of profilometry data (16 azimuthal directions)

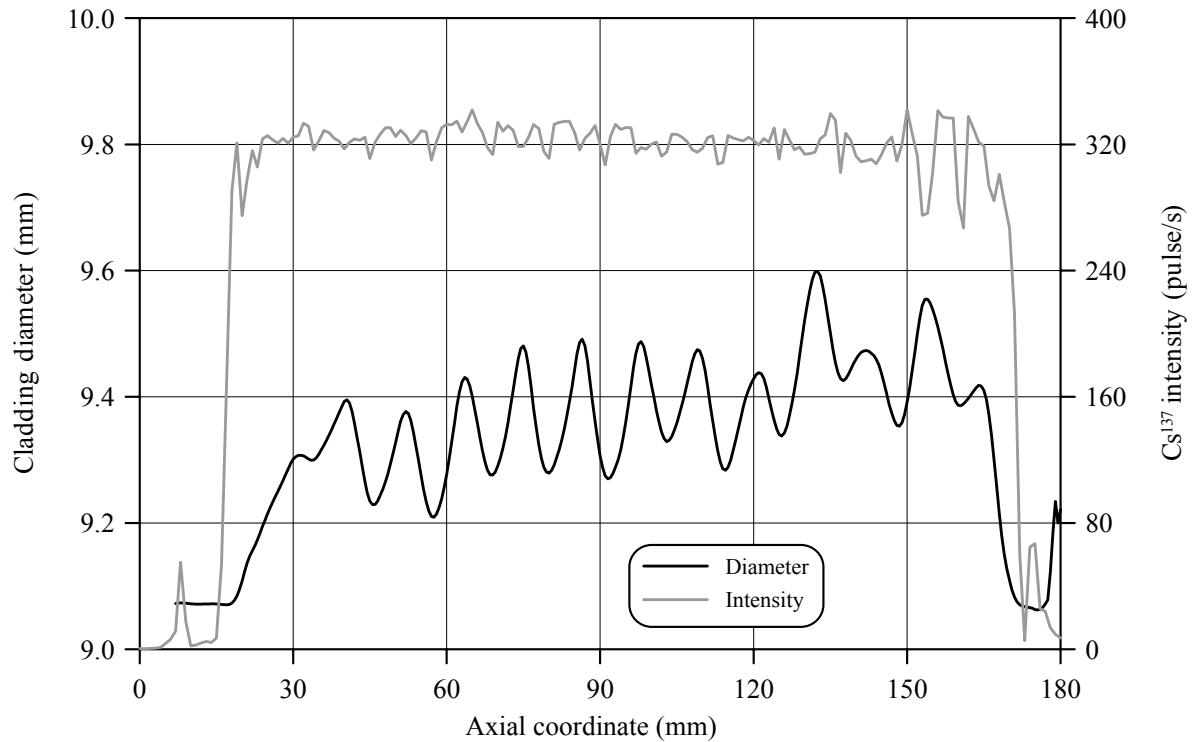
Fig.E-6.10. Cladding measured average diameter and γ -scanning results for fuel rod # RT6

Table E-6.4. The PIE results for fuel rod # RT6

| Parameter | | Value |
|-----------|--|-------|
| 1. | Cladding outer diameter (mm): | |
| 1.1. | Maximum diameter of the bidimensional data sample in "fuel rod length - azimuthal angle" coordinates (mm) | 9.76 |
| 1.2. | Averaged azimuthal diameter and maximum diameter along the length selected from the sample of averaged azimuthal diameter (mm) | 9.61 |
| 1.3. | Averaged diameter of the bidimensional data sample in "fuel rod length - azimuthal angle" coordinates (mm) | 9.36 |
| 2. | Cladding maximum residual hoop strain (%) | 6.00 |
| 3. | Fuel pellet conditional diameter (mm) in cross-section*: | |
| | at 114 mm elevation | 7.84 |
| | at 132 mm elevation | 7.92 |
| 4. | ZrO ₂ outer thickness (μm) in cross-section: | |
| | at 114 mm elevation | 3-5 |
| | at 132 mm elevation | 3-5 |
| 5. | ZrO ₂ inner thickness (μm) in cross-section: | |
| | at 114 mm elevation | 0 |
| | at 132 mm elevation | 0 |
| 6. | Parameters characterizing FGR: | |
| 6.1. | Gas composition (% by volume): | |
| | He | 81.53 |
| | N ₂ | 1.11 |
| | O ₂ | 0.09 |
| | Ar | 0.021 |
| | CO ₂ | 0.015 |
| | Kr | 1.53 |
| | Xe | 15.69 |
| 6.2. | Free gas volume (cm ³) | 6.2 |
| 6.3. | Gas volume under normal conditions (cm ³) | 141.8 |
| 6.4. | Gas pressure under normal conditions (MPa) | 2.29 |
| 6.5. | FGR (%) | 26.50 |

* Reference value determined by the processing of fuel cross-section photographs

Table E-6.5. Organized BGR test results for fuel rod # RT6

| Parameter | Unit | Value | | |
|---|---------------------|----------|------------|----------|
| | | Measured | Calculated | |
| | | | FRAP-T6 | RAPTA-5 |
| 1. Fuel burnup | MW d/kg U | 47.84 | 47.84 | 47.84 |
| 2. Initial gas pressure | MPa | 2.1 | 2.1 | 2.1 |
| 3. Energy deposition | cal/g fuel | 186.9 | 186.9 | 186.9 |
| 4. Peak fuel enthalpy* | cal/g fuel | - | 152.5 | 152.7 |
| 5. Fuel maximum temperature | K | - | 2421 | 2459 |
| 6. Maximum temperature of cladding outer surface | K | - | 1157 | 1207 |
| 7. Cladding burst | Failed, Unfailed | Unfailed | Unfailed | Unfailed |
| 8. Cladding residual hoop strain** | % | 3.20 | 3.36 | 2.39 |
| 9. Kr volume content in gas composition after the BGR test | % | 1.53 | 1.89 | - |
| 10. Xe volume content in gas composition after the BGR test | % | 15.69 | 11.30 | - |

* Average value of peak fuel enthalpy is 152.6 cal/g fuel

** Average value along the fuel stack length

Appendix E-7

*Individual Characteristics of Fuel Rod # RT7
after the BGR Test*

RT7

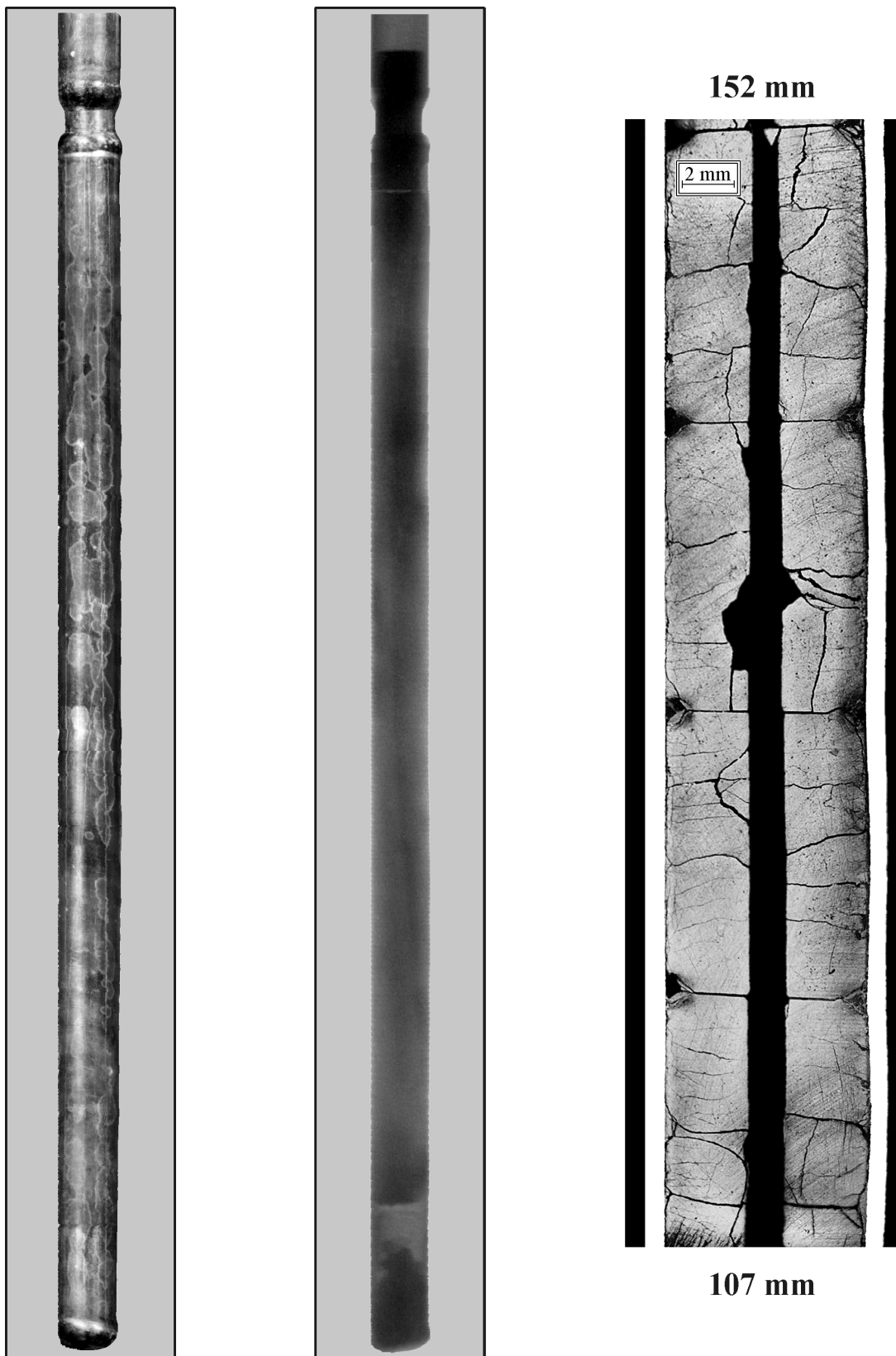


Fig.E-7.1. Appearance of unfailed fuel rod # RT7 after the BGR test (photographs and X-ray photograph) and longitudinal metallographic specimen image

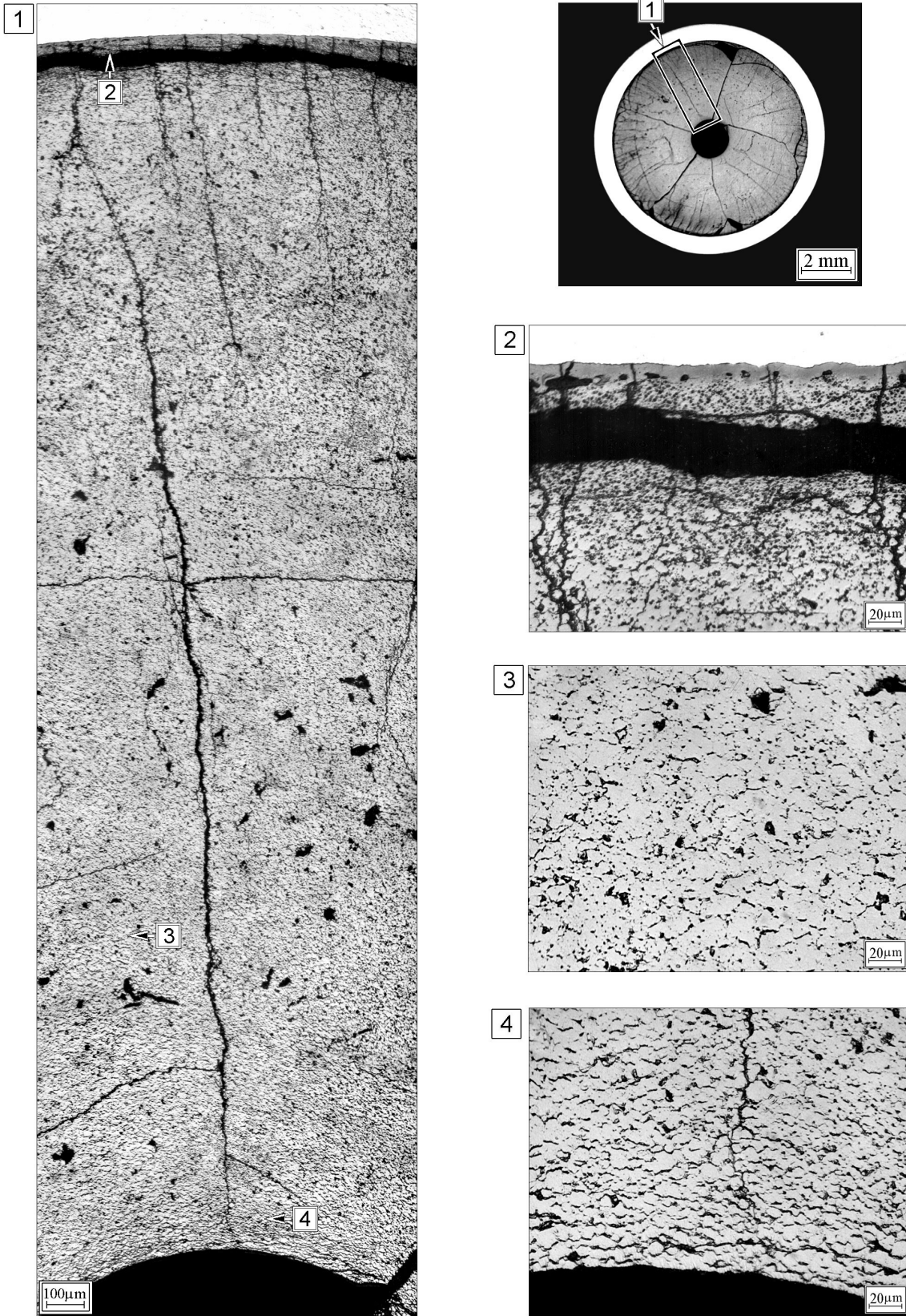


Fig.E-7.2. Cross-section and cladding microstructure of fuel rod # RT7 at 107 mm elevation (from low cap)

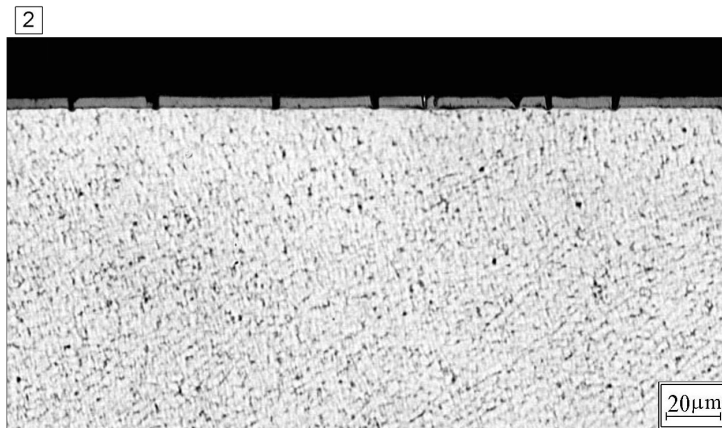
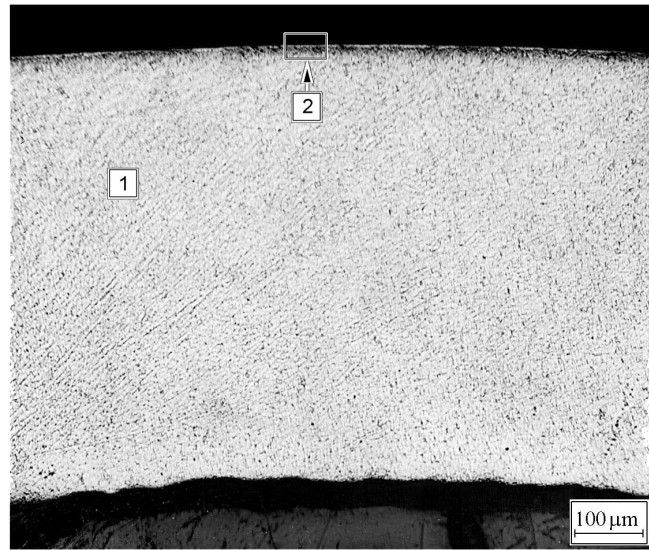


Fig.E-7.3. Cladding microstructure of fuel rod # RT7 at 107 mm elevation (from low cap)

Table E-7.1. Time dependent energy characteristics of fuel rod # RT7

| Time (s) | Relative reactor power (current/maximum value) (per-unit) | Cumulative number of fissions in fuel rod (fiss) x10 ⁻¹⁴ | Power of fuel rod ¹⁾²⁾ (kW) | Energy deposition | | Fuel enthalpy ³⁾ | |
|----------|---|---|--|-------------------|------------|-----------------------------|---------|
| | | | | (cal/g fuel) | (J/g fuel) | FRAP-T6 | RAPTA-5 |
| 0.000 | 0.00E+00 | 0.000 | 0.000 | 0.000 | 0.000 | 0.000 | 0.000 |
| 0.001 | 3.77E-03 | 0.045 | 25.09 | 0.046 | 0.194 | 0.671 | 0.004 |
| 0.002 | 1.65E-02 | 0.248 | 109.7 | 0.255 | 1.067 | 0.671 | 0.013 |
| 0.003 | 7.63E-02 | 1.153 | 508.5 | 1.187 | 4.968 | 0.671 | 0.031 |
| 0.004 | 3.14E-01 | 5.134 | 2090 | 5.268 | 22.06 | 0.671 | 0.130 |
| 0.005 | 8.37E-01 | 18.27 | 5577 | 18.73 | 78.42 | 0.844 | 0.542 |
| 0.006 | 9.39E-01 | 40.46 | 6260 | 41.56 | 174.0 | 2.954 | 2.713 |
| 0.007 | 5.20E-01 | 57.56 | 3462 | 59.10 | 247.4 | 11.084 | 10.941 |
| 0.008 | 2.34E-01 | 65.86 | 1560 | 67.63 | 283.1 | 30.369 | 30.902 |
| 0.009 | 1.19E-01 | 69.64 | 796.4 | 71.61 | 299.8 | 51.815 | 53.058 |
| 0.010 | 7.54E-02 | 71.86 | 502.5 | 73.84 | 309.2 | 64.176 | 65.721 |
| 0.012 | 5.38E-02 | 74.73 | 358.3 | 76.74 | 321.3 | 72.209 | 73.965 |
| 0.014 | 5.62E-02 | 77.15 | 374.7 | 79.31 | 332.1 | 74.823 | 76.698 |
| 0.016 | 6.56E-02 | 79.97 | 437.0 | 82.20 | 344.1 | 76.831 | 78.858 |
| 0.018 | 7.47E-02 | 83.30 | 497.7 | 85.56 | 358.2 | 79.111 | 81.308 |
| 0.020 | 7.60E-02 | 86.80 | 506.6 | 89.18 | 373.4 | 81.899 | 84.282 |
| 0.022 | 6.89E-02 | 90.20 | 459.1 | 92.67 | 388.0 | 85.046 | 87.624 |
| 0.024 | 5.89E-02 | 93.23 | 393.0 | 95.72 | 400.8 | 88.160 | 90.927 |
| 0.026 | 4.85E-02 | 95.64 | 323.6 | 98.28 | 411.5 | 90.906 | 93.838 |
| 0.028 | 3.99E-02 | 97.71 | 266.2 | 100.4 | 420.4 | 93.182 | 96.258 |
| 0.030 | 3.41E-02 | 99.42 | 227.6 | 102.1 | 427.5 | 94.995 | 98.186 |
| 0.050 | 2.83E-02 | 113.0 | 189.0 | 116.0 | 485.8 | 106.142 | 110.175 |
| 0.070 | 2.46E-02 | 125.1 | 163.7 | 128.4 | 537.7 | 116.336 | 120.734 |
| 0.090 | 1.83E-02 | 134.5 | 121.9 | 138.5 | 579.7 | 124.433 | 129.209 |
| 0.110 | 9.39E-03 | 141.3 | 62.72 | 145.1 | 607.3 | 129.425 | 134.525 |
| 0.130 | 3.68E-03 | 143.7 | 24.68 | 147.9 | 619.4 | 131.404 | 136.246 |
| 0.150 | 1.69E-03 | 145.3 | 11.46 | 149.1 | 624.3 | 131.628 | 136.222 |
| 0.200 | 4.93E-04 | 146.3 | 3.441 | 150.3 | 629.1 | 130.640 | 134.603 |
| 1.000 | 7.30E-05 | 148.5 | 0.594 | 152.9 | 640.2 | 115.626 | 116.979 |
| 10.00 | 8.50E-06 | 153.4 | 0.079 | 159.5 | 667.8 | 46.313 | 33.119 |
| 100.0 | 1.72E-07 | 155.7 | 0.003 | 163.7 | 685.4 | 7.031 | 5.041 |
| 1000 | 6.74E-13 | 155.7 | 1.43E-04 | 165.2 | 691.7 | 0.000 | 0.000 |

¹⁾ Average values determined in accordance with results of RRC KI and VNIIEF calculations

²⁾ Maximum power value is 6663 kW (t=0.00555 s)

³⁾ Average radial value

RT7**Table E-7.2. Radial energy characteristics of fuel rod # RT7***

| Parameters | Coordinates of fuel radial layers (mm) | | | |
|---|--|--------------------------|--------------------------|--------------------------|
| | 1 layer (0.825-2.777) | 2 layer (2.777-3.454) | 3 layer (3.454-3.747) | 4 layer (3.747-3.840) |
| Number of fissions $\times 10^{-14}$ (fiss) | 6.673 | 4.455 | 2.879 | 1.590 |
| Fission density $\times 10^{-13}$ (fiss/g fuel) | 1.999 | 2.224 | 2.873 | 4.745 |
| Power ** (kW) | 2847 | 1903 | 1231 | 681.5 |
| Energy deposition (cal/g fuel) | 141.2 | 157.3 | 203.4 | 336.6 |
| Energy deposition (J/g fuel) | 591.2 | 658.5 | 851.8 | 1409 |
| Energy deposition *** (per-unit) | 0.420 | 0.467 | 0.604 | 1.000 |

* Average values were determined in accordance with results of RRC KI and VNIIEF calculations

** The power for the entire length of each layer at time 0.00555 s

*** Energy deposition in current layer/energy deposition in 4th layer

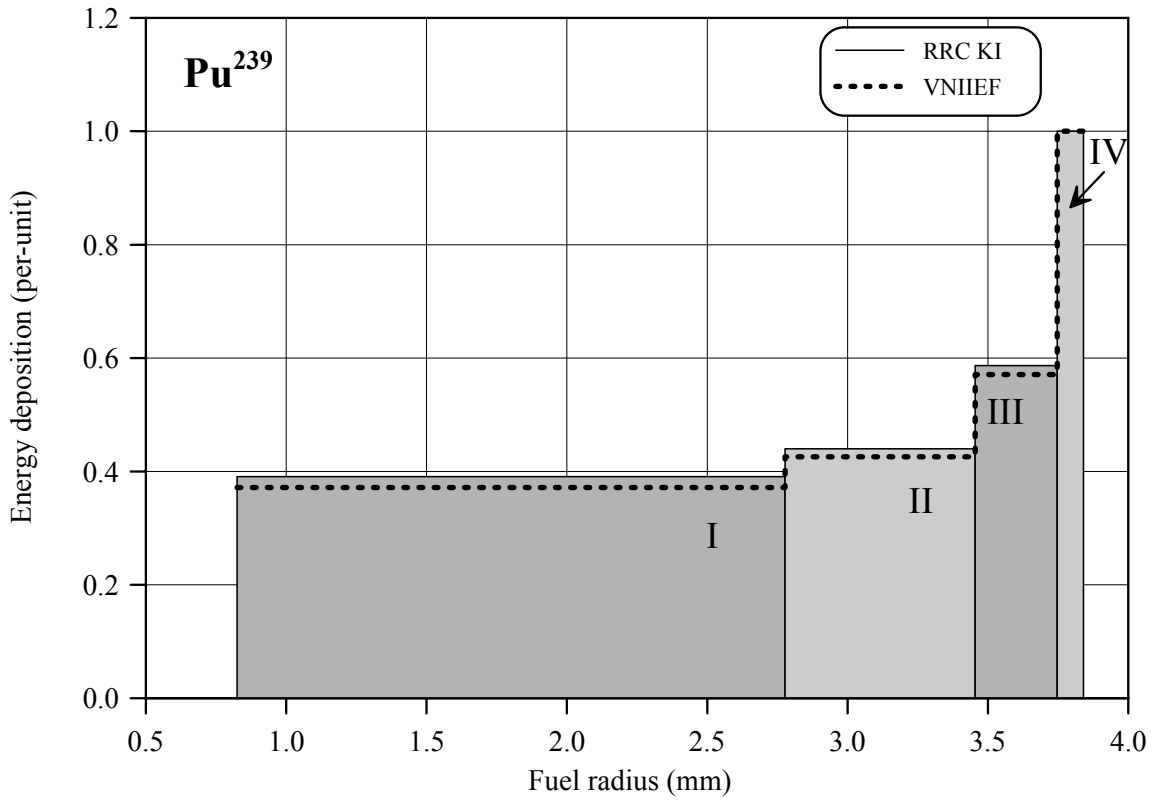
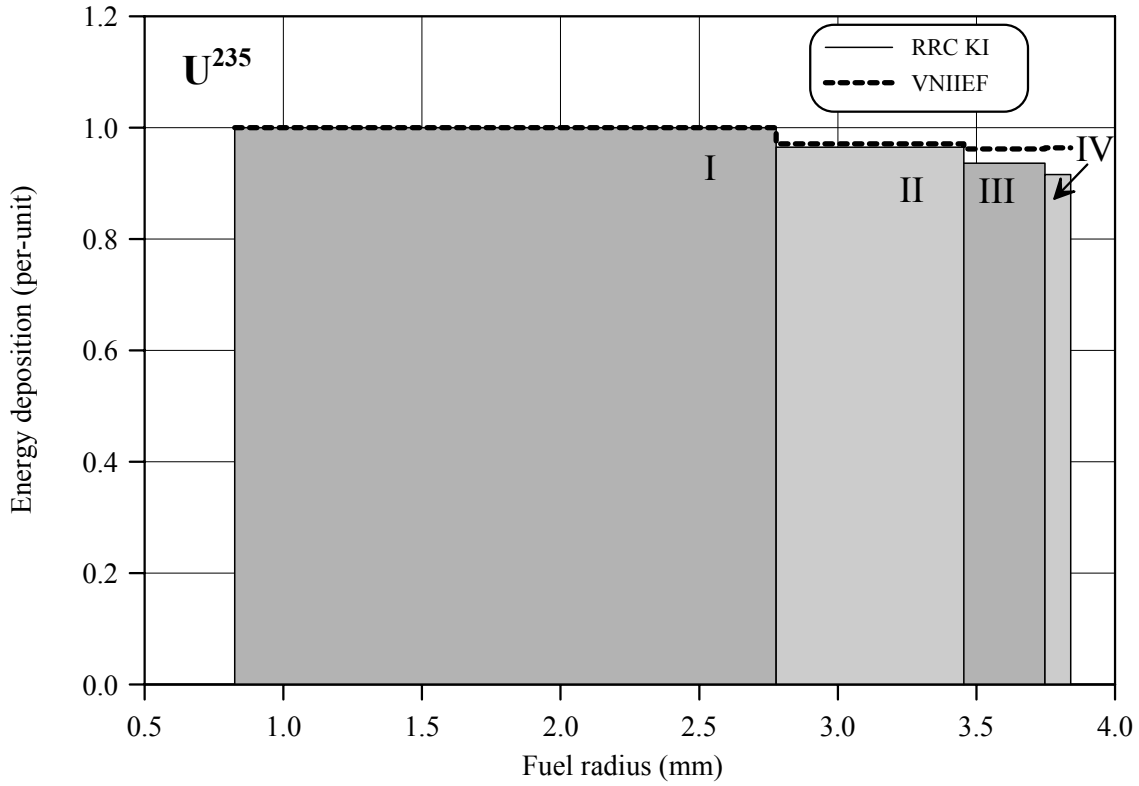


Fig.E-7.4. U²³⁵ and Pu²³⁹ radial distribution of energy deposition for fuel rod # RT7

RT7

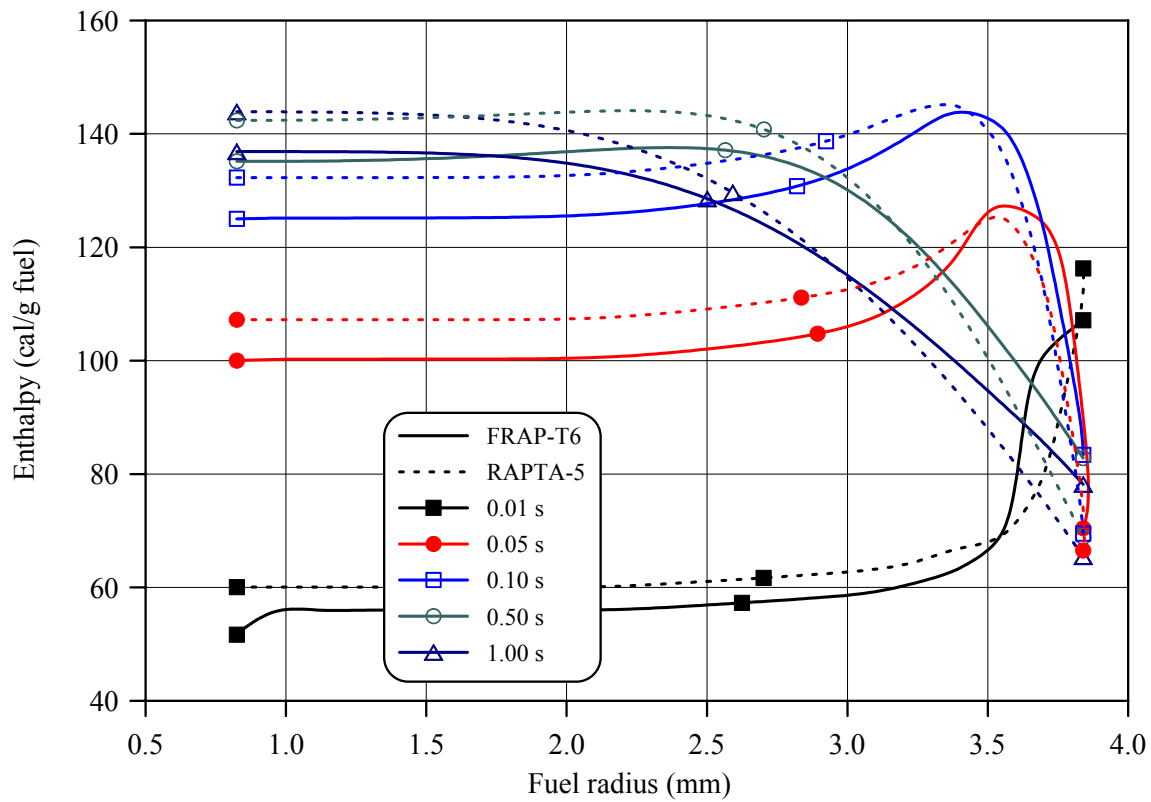
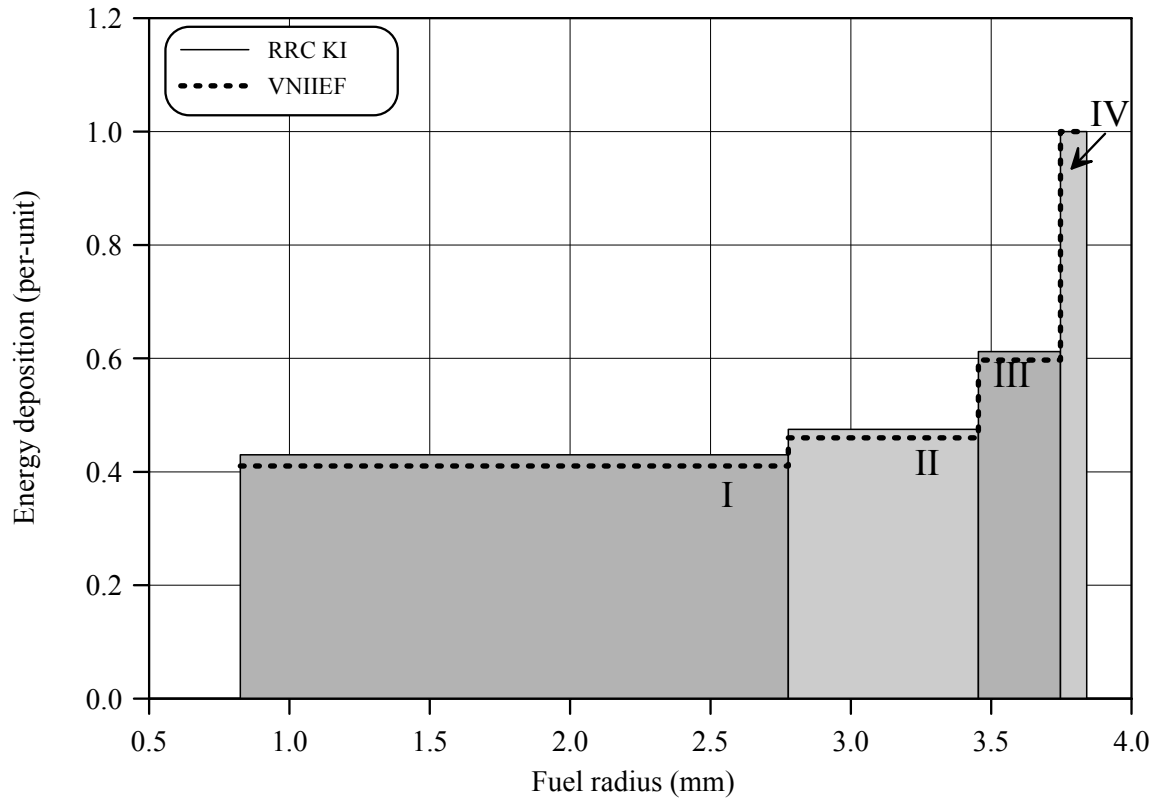


Fig.E-7.5. Radial distribution of energy deposition and fuel enthalpy for fuel rod # RT7

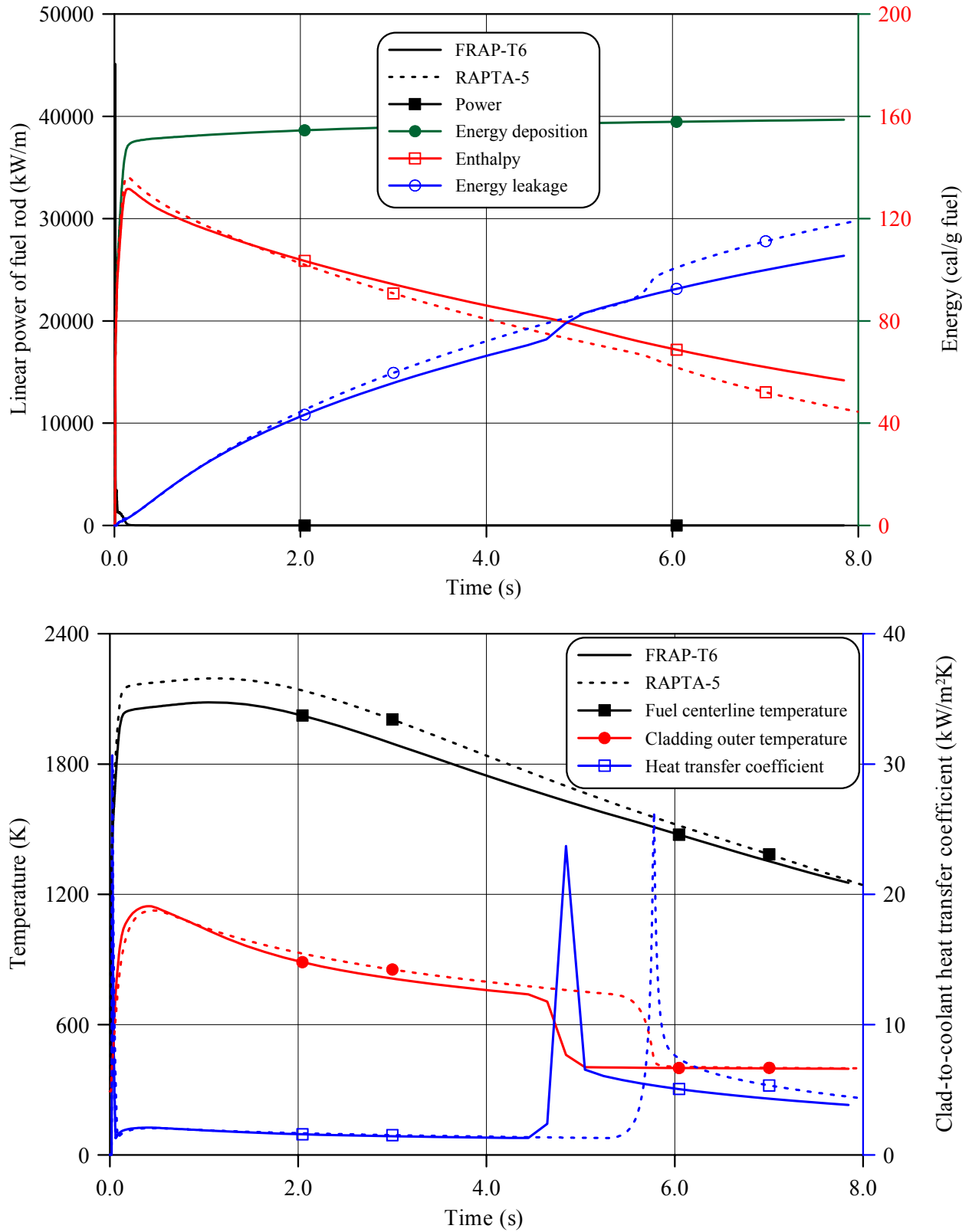


Fig.E-7.6. Thermal history of fuel rod # RT7 during the BGR test in accordance with FRAP-T6/VVER and RAPTA-5 calculations

RT7

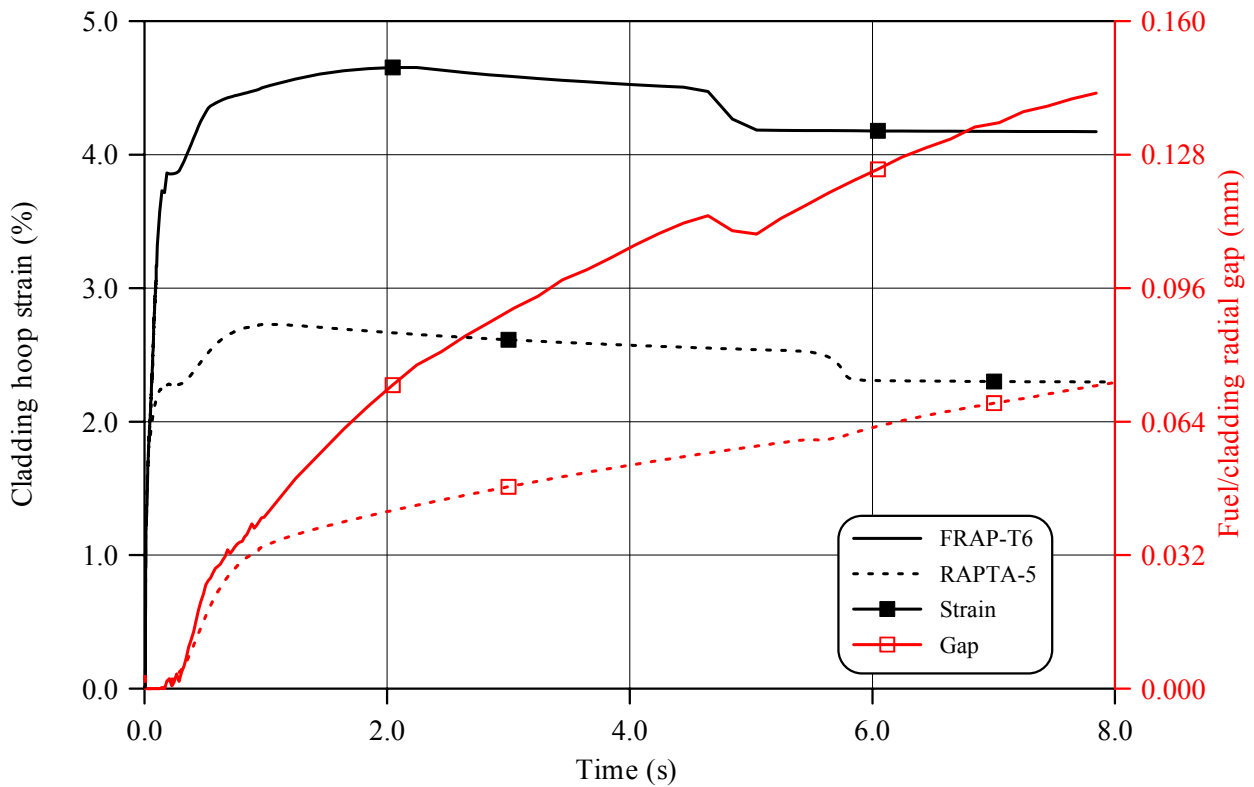
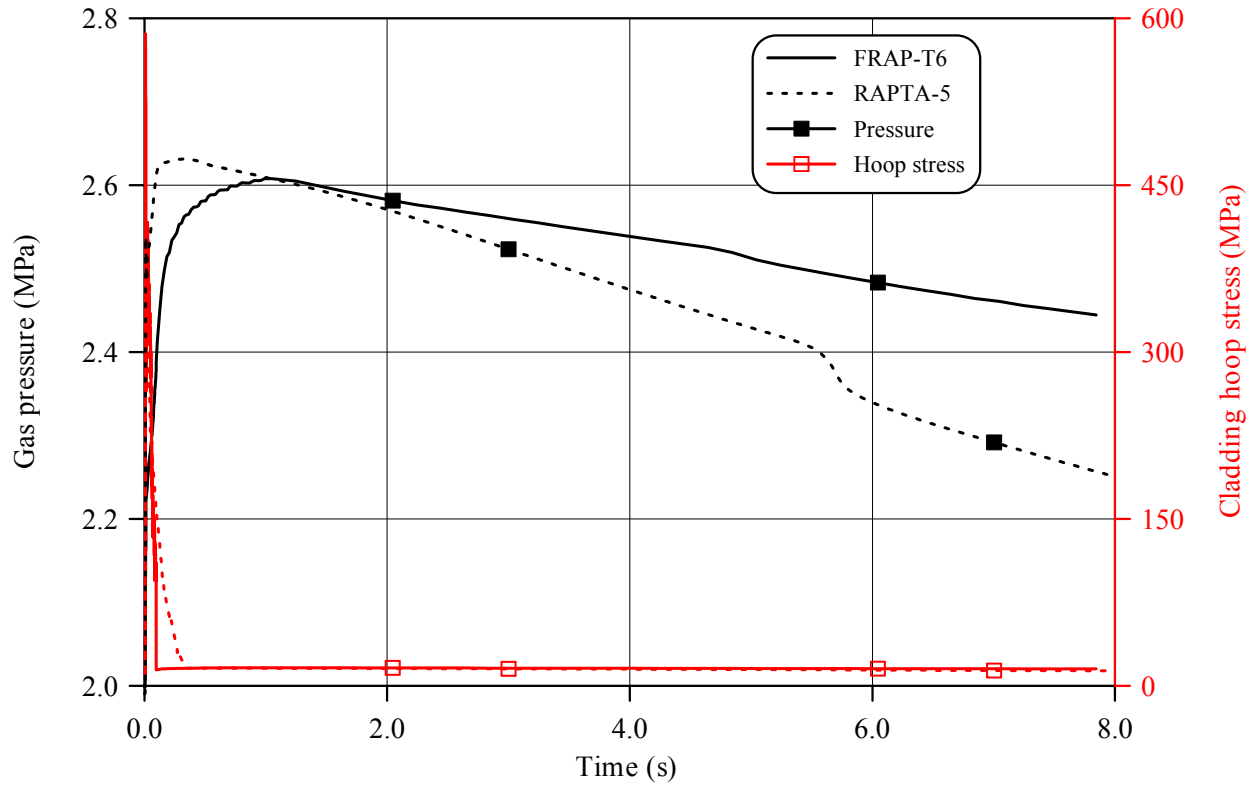


Fig.E-7.7. Mechanical behavior of fuel rod # RT7 during the BGR test in accordance with FRAP-T6/VVER and RAPTA-5 calculations

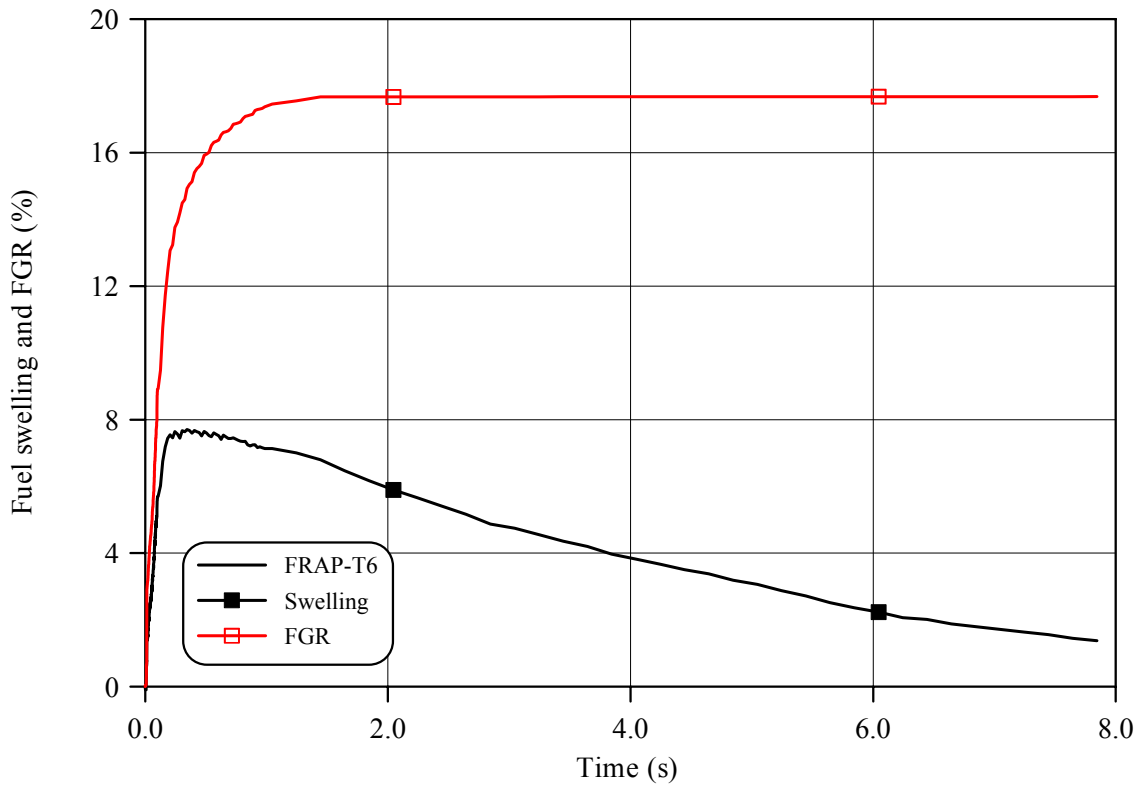
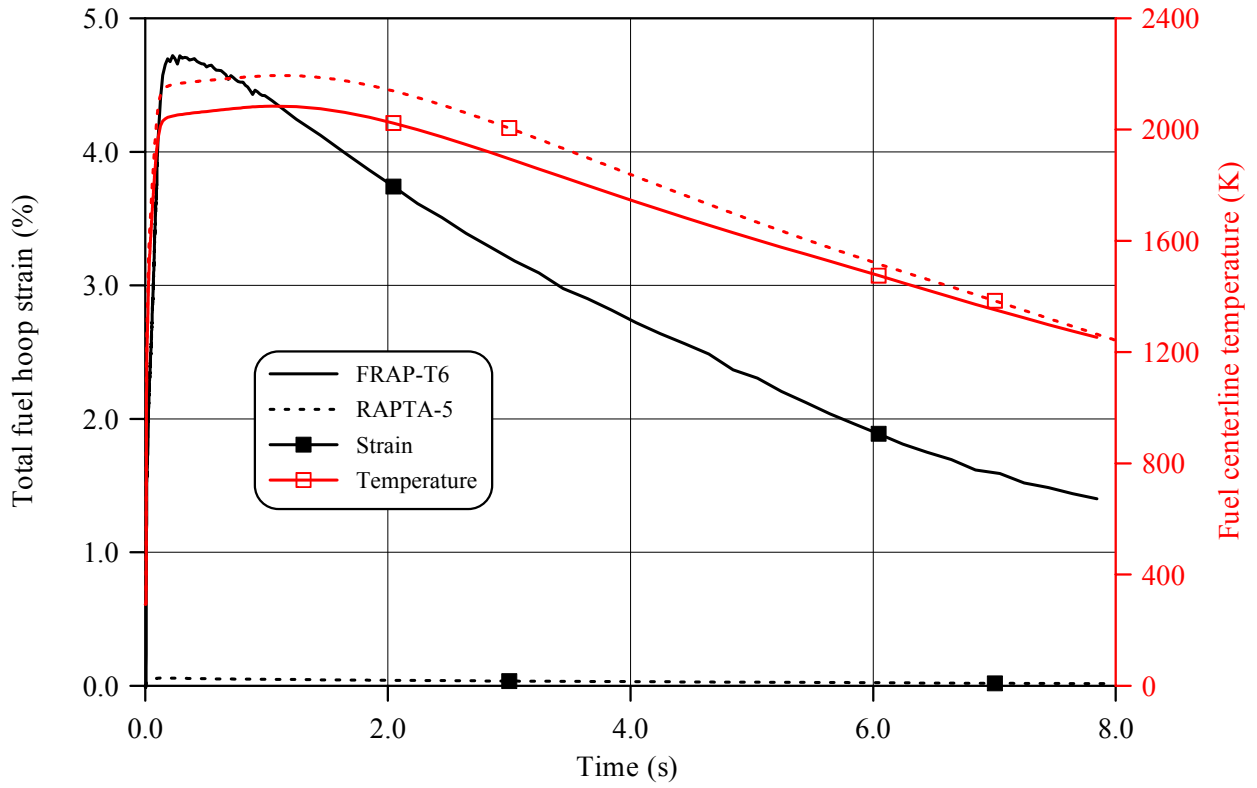


Fig.E-7.8. Fuel behavior during the BGR test of fuel rod # RT7 in accordance with FRAP-T6/VVER and RAPTA-5 calculations

RT7

Table E-7.3. Axial distribution of cladding average outer diameter in fuel rod # RT7*

| Axial coordinate (mm) | Cladding diameter (mm) | Axial coordinate (mm) | Cladding diameter (mm) | Axial coordinate (mm) | Cladding diameter (mm) | Axial coordinate (mm) | Cladding diameter (mm) |
|-----------------------|------------------------|-----------------------|------------------------|-----------------------|------------------------|-----------------------|------------------------|
| 26 | 9.180 | 64 | 9.250 | 102 | 9.330 | 140 | 9.130 |
| 28 | 9.150 | 66 | 9.320 | 104 | 9.270 | 142 | 9.180 |
| 30 | 9.160 | 68 | 9.370 | 106 | 9.230 | 144 | 9.220 |
| 32 | 9.220 | 70 | 9.330 | 108 | 9.270 | 146 | 9.240 |
| 34 | 9.260 | 72 | 9.280 | 110 | 9.310 | 148 | 9.210 |
| 36 | 9.280 | 74 | 9.300 | 112 | 9.310 | 150 | 9.160 |
| 38 | 9.250 | 76 | 9.350 | 114 | 9.310 | 152 | 9.180 |
| 40 | 9.220 | 78 | 9.380 | 116 | 9.230 | 154 | 9.250 |
| 42 | 9.260 | 80 | 9.370 | 118 | 9.230 | 156 | 9.290 |
| 44 | 9.290 | 82 | 9.310 | 120 | 9.240 | 158 | 9.310 |
| 46 | 9.270 | 84 | 9.260 | 122 | 9.270 | 160 | 9.290 |
| 48 | 9.260 | 86 | 9.290 | 124 | 9.270 | 162 | 9.270 |
| 50 | 9.180 | 88 | 9.320 | 126 | 9.200 | 164 | 9.290 |
| 52 | 9.210 | 90 | 9.350 | 128 | 9.140 | 166 | 9.310 |
| 54 | 9.280 | 92 | 9.310 | 130 | 9.160 | 168 | 9.310 |
| 56 | 9.340 | 94 | 9.240 | 132 | 9.190 | 170 | 9.290 |
| 58 | 9.310 | 96 | 9.240 | 134 | 9.230 | 172 | 9.190 |
| 60 | 9.270 | 98 | 9.300 | 136 | 9.220 | 174 | 9.100 |
| 62 | 9.220 | 100 | 9.340 | 138 | 9.170 | 176 | 9.100 |

* Measured value determined on the basis of profilometry data (16 azimuthal directions)

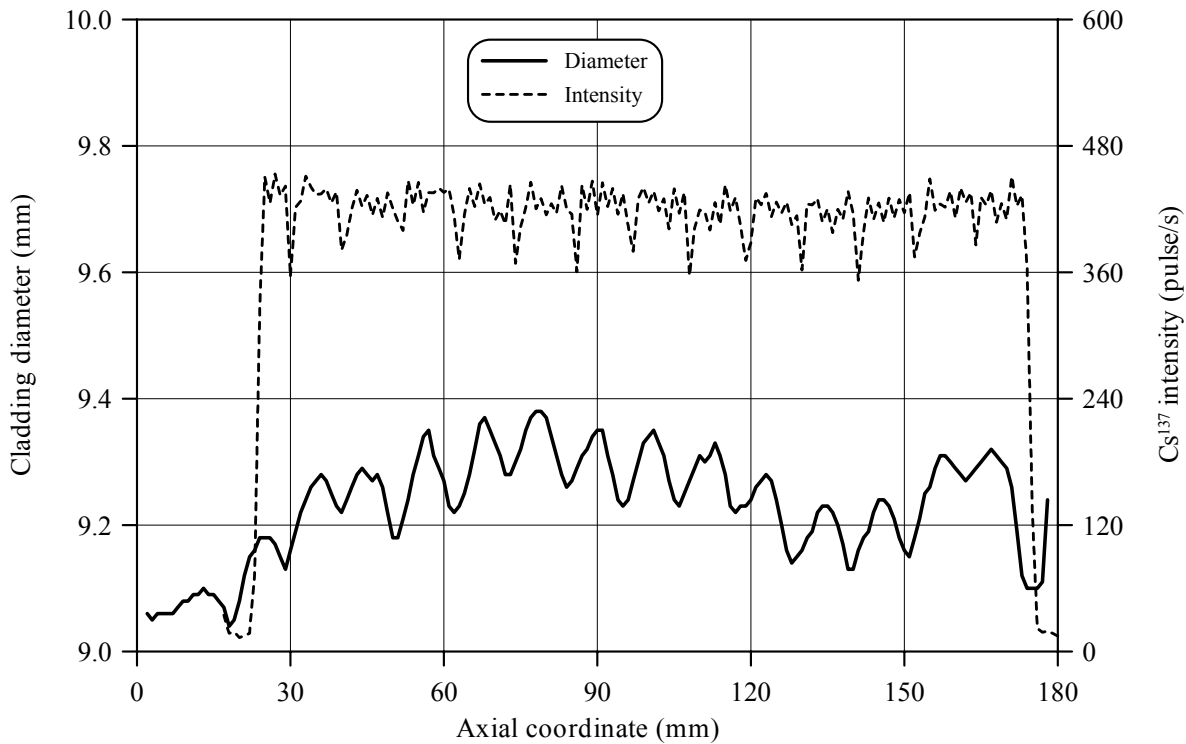


Fig.E-7.9. Cladding measured average diameter and γ -scanning results for fuel rod # RT7

Table E-7.4. The PIE results for fuel rod # RT7

| Parameter | | Value |
|-----------|--|-------|
| 1. | Cladding outer diameter (mm): | |
| 1.1. | Maximum diameter of the bidimensional data sample in "fuel rod length - azimuthal angle" coordinates (mm) | 9.38 |
| 1.2. | Averaged azimuthal diameter and maximum diameter along the length selected from the sample of averaged azimuthal diameter (mm) | 9.38 |
| 1.3. | Averaged diameter of the bidimensional data sample in "fuel rod length - azimuthal angle" coordinates (mm) | 9.25 |
| 2. | Cladding maximum residual hoop strain (%) | 3.50 |
| 3. | Fuel pellet conditional diameter (mm) in cross-section*: at 107 mm elevation | 7.74 |
| 4. | ZrO ₂ outer thickness (μm) in cross-section: at 107 mm elevation | 3-5 |
| 5. | ZrO ₂ inner thickness (μm) in cross-section: at 107 mm elevation | 9 |
| 6. | Parameters characterizing FGR: | |
| 6.1. | Gas composition (% by volume): | |
| | He | 76.83 |
| | N ₂ | 1.92 |
| | O ₂ | 0.05 |
| | Ar | 0.014 |
| | CO ₂ | 0.080 |
| | Kr | 1.82 |
| | Xe | 19.29 |
| 6.2. | Free gas volume (cm ³) | 5.9 |
| 6.3. | Gas volume under normal conditions (cm ³) | 158.9 |
| 6.4. | Gas pressure under normal conditions (MPa) | 2.7 |
| 6.5. | FGR (%) | 26.8 |

* Reference value determined by the processing of fuel cross-section photographs

RT7

Table E-7.5. Organized BGR test results for fuel rod # RT7

| Parameter | Unit | Value | | |
|---|------------------|----------|------------|----------|
| | | Measured | Calculated | |
| | | | FRAP-T6 | RAPTA-5 |
| 1. Fuel burnup | MW d/kg U | 60.3 | 60.3 | 60.3 |
| 2. Initial gas pressure | MPa | 2.0 | 2.0 | 2.0 |
| 3. Energy deposition | cal/g fuel | 165.2 | 165.2 | 165.2 |
| 4. Peak fuel enthalpy* | cal/g fuel | - | 131.7 | 136.4 |
| 5. Fuel maximum temperature | K | - | 2183 | 2251 |
| 6. Maximum temperature of cladding outer surface | K | - | 1146 | 1126 |
| 7. Cladding burst | Failed, Unfailed | Unfailed | Unfailed | Unfailed |
| 8. Cladding residual hoop strain | | | | |
| - average** | % | 2.07 | 3.68 | 2.73 |
| - maximum | % | 3.50 | 3.68 | 2.73 |
| 9. Kr volume content in gas composition after the BGR test | % | 1.82 | 2.99 | - |
| 10. Xe volume content in gas composition after the BGR test | % | 19.29 | 17.93 | - |

* Average value of peak fuel enthalpy 134.0 cal/g fuel

** Average value along the fuel stack length

Appendix E-8

***Individual Characteristics of Fuel Rod # RT8
after the BGR Test***

RT8

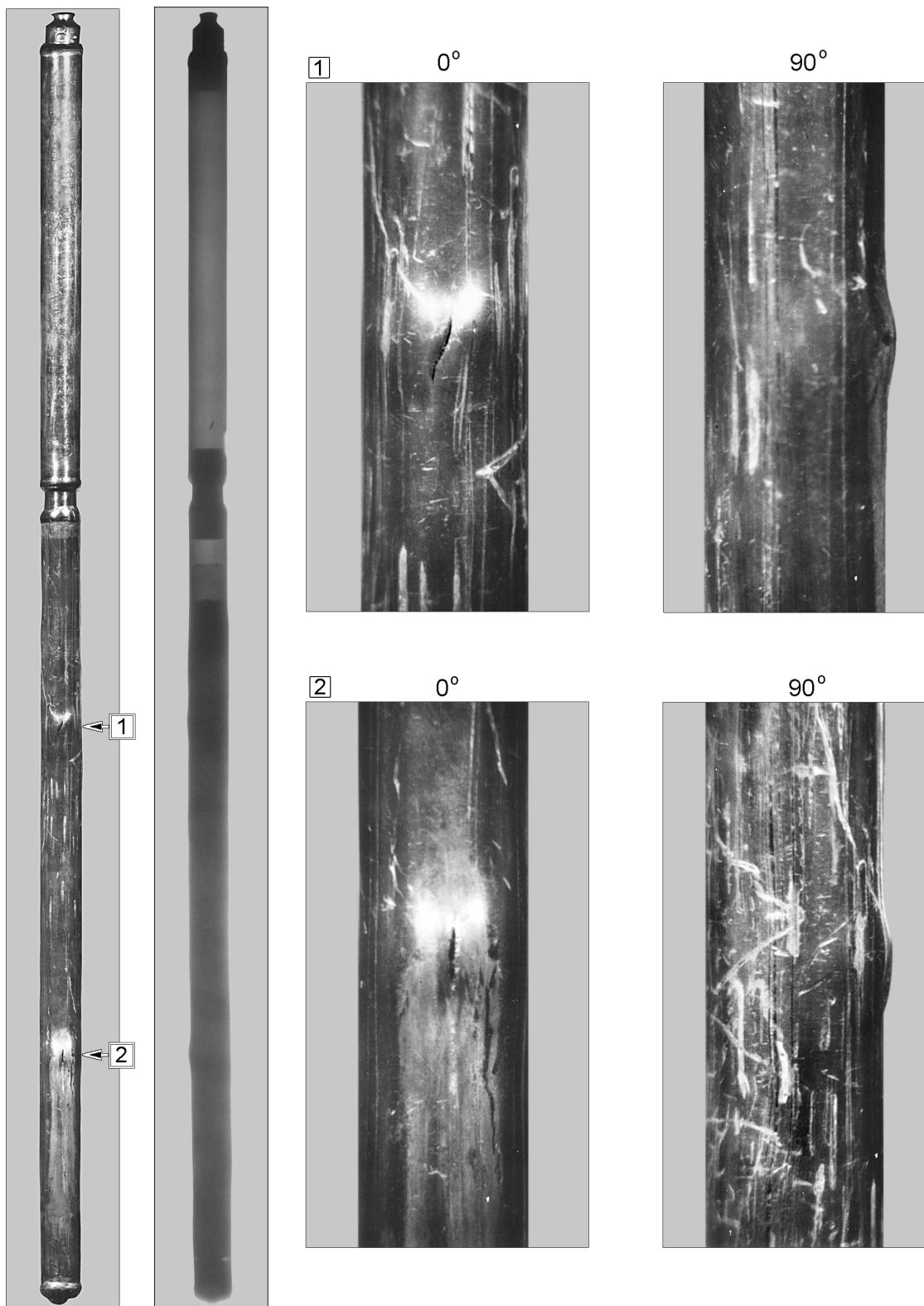


Fig.E-8.1. Appearance of failed fuel rod # RT8 after the BGR test (photographs and X-ray photograph)

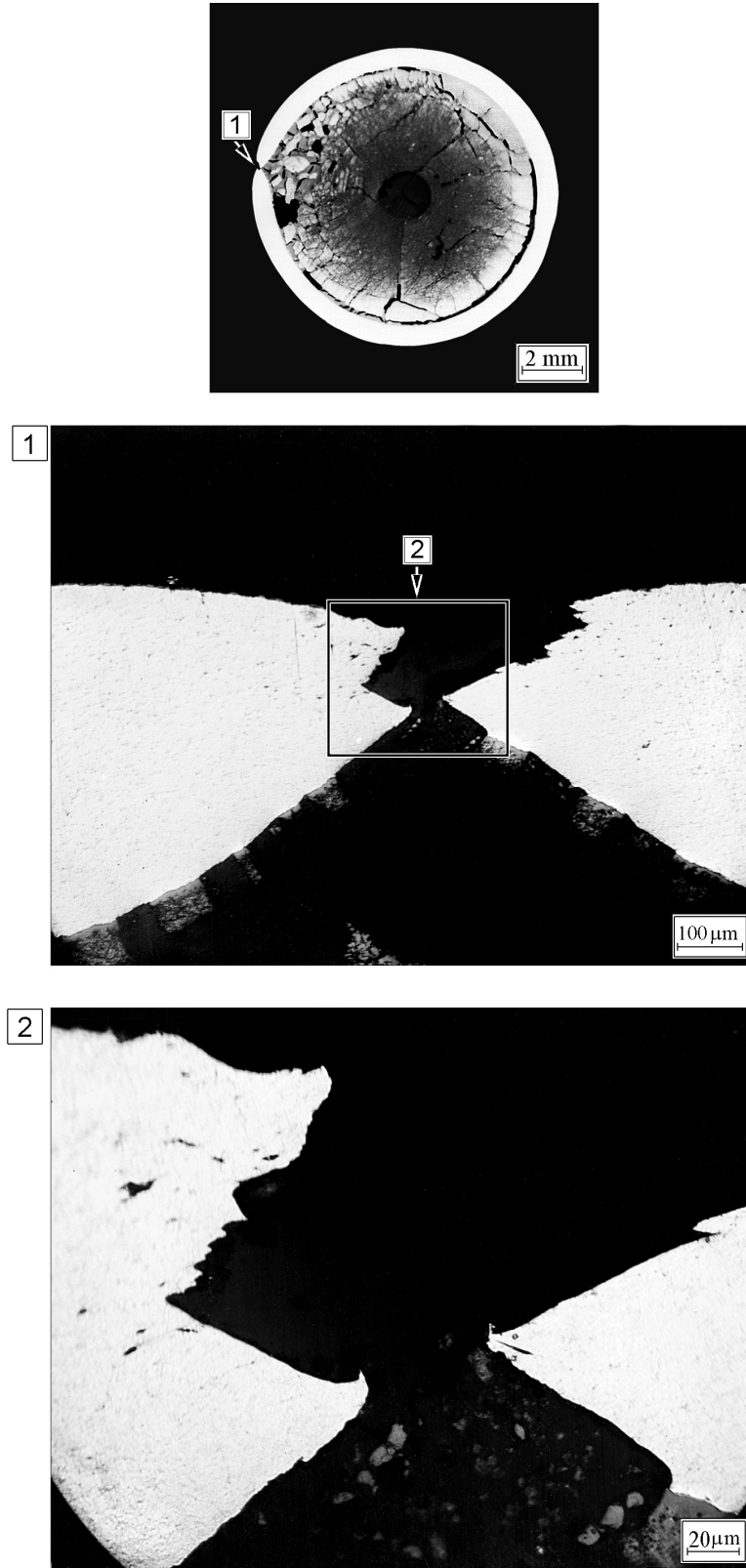


Fig.E-8.2. Cross-section and cladding microstructure in the burst area of fuel rod # RT8 at 53 mm elevation (from low cap)

RT8

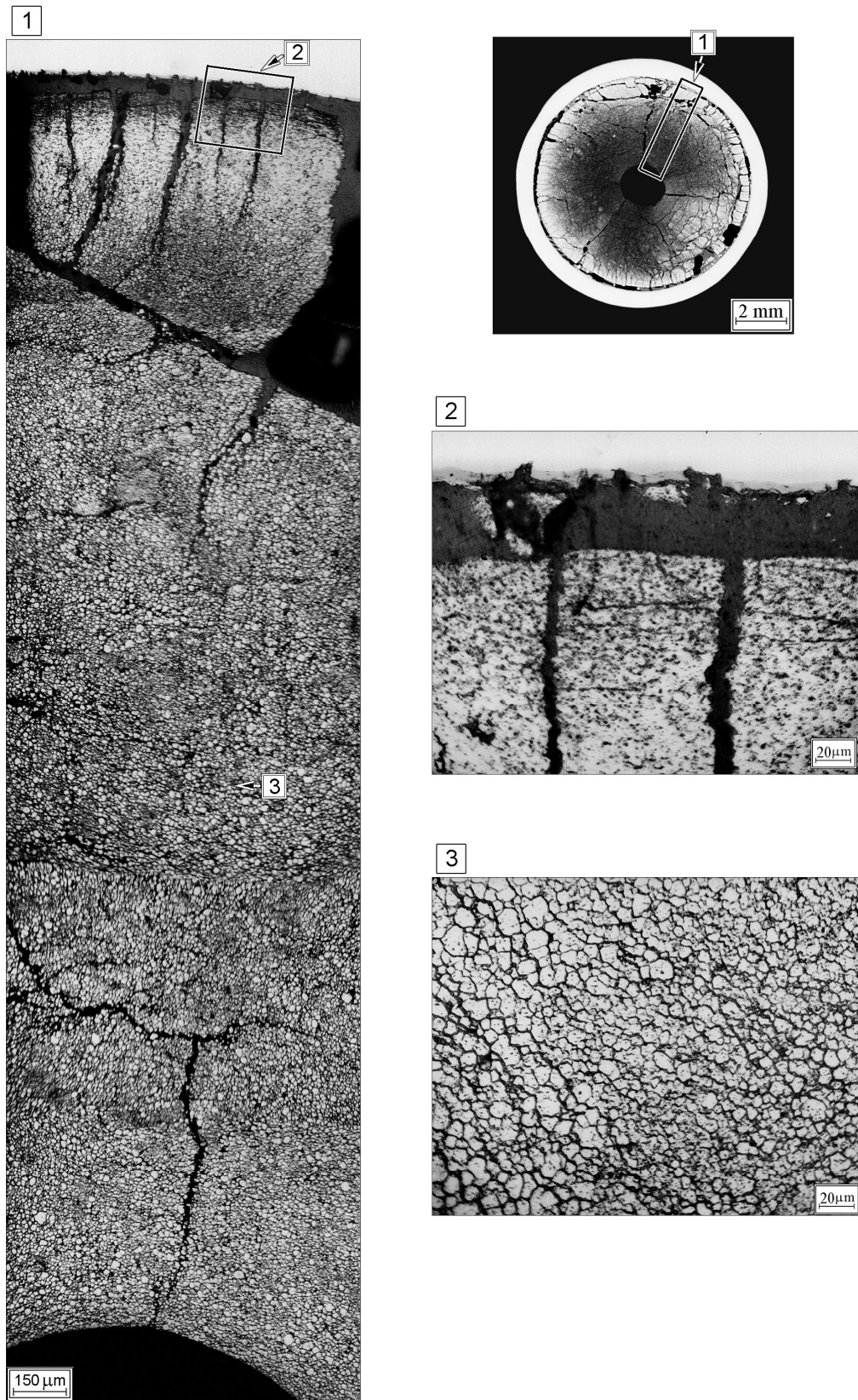


Fig.E-8.3. Cross-section and fuel microstructure of fuel rod # RT8 at 97 mm elevation (from low cap)

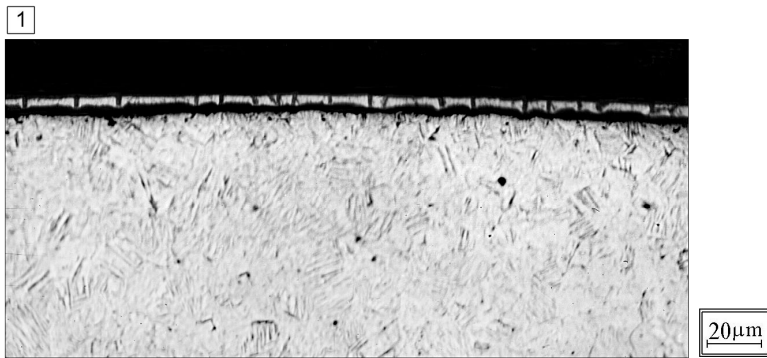


Fig.E-8.4. Cladding microstructure of fuel rod # RT8 at 97 mm elevation (from low cap)

RT8

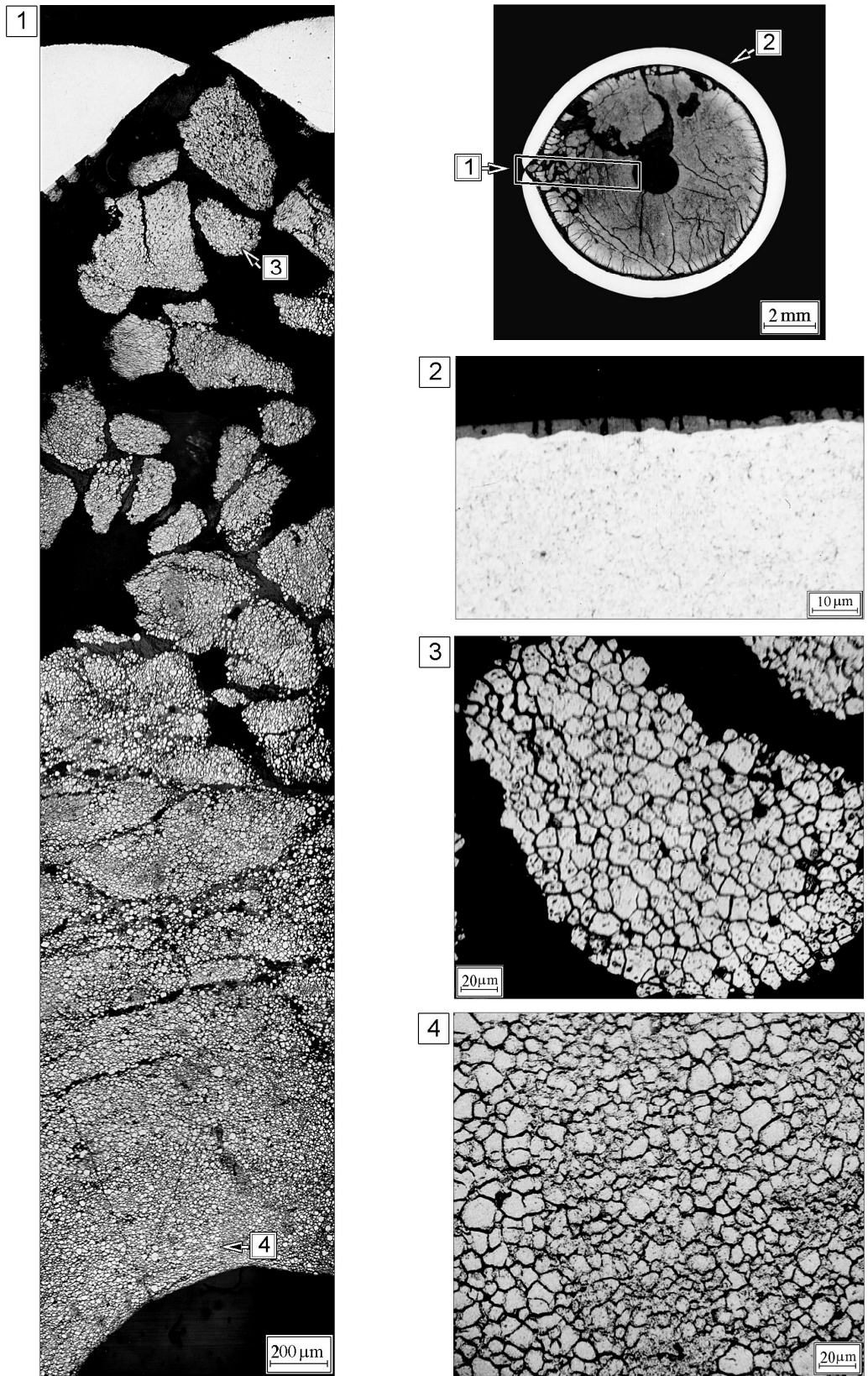


Fig.E-8.5. Cross-section and cladding microstructure of fuel rod # RT8 at 133 mm elevation (from low cap)

Table E-8.1. Time dependent energy characteristics of fuel rod # RT8

| Time (s) | Relative reactor power (current/maximum value) (per-unit) | Cumulative number of fissions in fuel rod (fiss) x10 ⁻¹⁴ | Power of fuel rod ¹⁾²⁾ (kW) | Energy deposition | | Fuel enthalpy ³⁾ | |
|----------|---|---|--|-------------------|------------|-----------------------------|---------|
| | | | | (cal/g fuel) | (J/g fuel) | FRAP-T6 | RAPTA-5 |
| 0.000 | 0.00E+00 | 0.000 | 0.000 | 0.000 | 0.000 | 0.000 | 0.000 |
| 0.001 | 2.74E-03 | 0.037 | 21.08 | 0.038 | 0.161 | 0.671 | 0.039 |
| 0.002 | 1.20E-02 | 0.206 | 92.68 | 0.213 | 0.890 | 0.671 | 0.204 |
| 0.003 | 5.50E-02 | 0.970 | 423.4 | 1.001 | 4.191 | 1.276 | 1.074 |
| 0.004 | 2.39E-01 | 4.391 | 1836 | 4.530 | 18.97 | 4.939 | 4.676 |
| 0.005 | 7.06E-01 | 16.47 | 5432 | 17.01 | 71.21 | 17.598 | 17.715 |
| 0.006 | 9.90E-01 | 40.90 | 7613 | 42.26 | 176.9 | 42.949 | 43.901 |
| 0.007 | 6.19E-01 | 63.22 | 4758 | 65.26 | 273.2 | 65.896 | 67.516 |
| 0.008 | 2.82E-01 | 74.86 | 2171 | 77.26 | 323.5 | 77.575 | 79.466 |
| 0.009 | 1.36E-01 | 80.15 | 1046 | 82.74 | 346.4 | 82.629 | 84.594 |
| 0.010 | 8.10E-02 | 82.97 | 623.4 | 85.62 | 358.5 | 85.108 | 87.175 |
| 0.012 | 5.36E-02 | 86.35 | 412.1 | 89.11 | 373.1 | 87.862 | 90.099 |
| 0.014 | 5.43E-02 | 89.18 | 417.8 | 92.05 | 385.4 | 90.164 | 92.594 |
| 0.016 | 6.39E-02 | 92.32 | 492.1 | 95.30 | 399.0 | 92.864 | 95.506 |
| 0.018 | 7.43E-02 | 96.12 | 572.0 | 99.15 | 415.1 | 96.196 | 99.043 |
| 0.020 | 7.80E-02 | 100.2 | 600.6 | 103.4 | 432.9 | 99.972 | 103.046 |
| 0.022 | 7.36E-02 | 104.3 | 566.3 | 107.7 | 450.8 | 103.748 | 107.029 |
| 0.024 | 6.17E-02 | 108.2 | 474.9 | 111.4 | 466.4 | 107.027 | 110.502 |
| 0.026 | 4.96E-02 | 111.2 | 381.7 | 114.5 | 479.3 | 109.629 | 113.275 |
| 0.028 | 4.02E-02 | 113.3 | 309.2 | 117.0 | 489.6 | 111.646 | 115.445 |
| 0.030 | 3.42E-02 | 115.4 | 263.2 | 119.1 | 498.4 | 113.264 | 117.197 |
| 0.050 | 2.72E-02 | 130.6 | 209.4 | 134.9 | 564.7 | 125.680 | 130.399 |
| 0.070 | 2.44E-02 | 144.6 | 187.7 | 149.1 | 624.3 | 137.020 | 142.329 |
| 0.090 | 2.06E-02 | 156.1 | 158.5 | 161.3 | 675.4 | 147.055 | 152.391 |
| 0.110 | 1.57E-02 | 166.2 | 120.7 | 171.8 | 719.1 | 155.898 | 160.736 |
| 0.130 | 7.95E-03 | 173.0 | 61.39 | 178.4 | 746.9 | 160.853 | 165.400 |
| 0.150 | 3.05E-03 | 175.7 | 23.65 | 181.2 | 758.8 | 162.225 | 166.440 |
| 0.200 | 6.92E-04 | 177.3 | 5.511 | 183.3 | 767.3 | 161.502 | 164.962 |
| 1.000 | 7.64E-05 | 180.3 | 0.717 | 186.7 | 781.8 | 151.533 | 147.195 |
| 10.00 | 8.86E-06 | 186.3 | 0.095 | 194.7 | 815.4 | 76.383 | 55.533 |
| 100.0 | 1.79E-07 | 189.4 | 0.004 | 199.9 | 836.7 | 8.643 | 5.231 |
| 1000 | 7.01E-13 | 189.5 | 1.70E-04 | 201.7 | 844.3 | 0.000 | 0.000 |

¹⁾ Average values determined in accordance with results of RRC KI and VNIIEF calculations

²⁾ Maximum power value is 7693 kW (t=0.00588 s)

³⁾ Average radial value

RT8**Table E-8.2. Radial energy characteristics of fuel rod # RT8***

| Parameters | Coordinates of fuel radial layers (mm) | | | |
|---|--|--------------------------|--------------------------|--------------------------|
| | 1 layer (0.825-2.777) | 2 layer (2.777-3.454) | 3 layer (3.454-3.747) | 4 layer (3.747-3.840) |
| Number of fissions $\times 10^{-14}$ (fiss) | 8.381 | 5.429 | 3.366 | 1.780 |
| Fission density $\times 10^{-13}$ (fiss/g fuel) | 2.533 | 2.734 | 3.389 | 5.360 |
| Power ** (kW) | 3396 | 2202 | 1369 | 726.3 |
| Energy deposition (cal/g fuel) | 178.1 | 192.5 | 239.1 | 379.1 |
| Energy deposition (J/g fuel) | 745.6 | 805.8 | 1000.9 | 1587 |
| Energy deposition *** (per-unit) | 0.470 | 0.508 | 0.631 | 1.000 |

* Average values were determined in accordance with results of RRC KI and VNIIEF calculations

** The power for the entire length of each layer at time 0.00588 s

*** Energy deposition in current layer/energy deposition in 4th layer

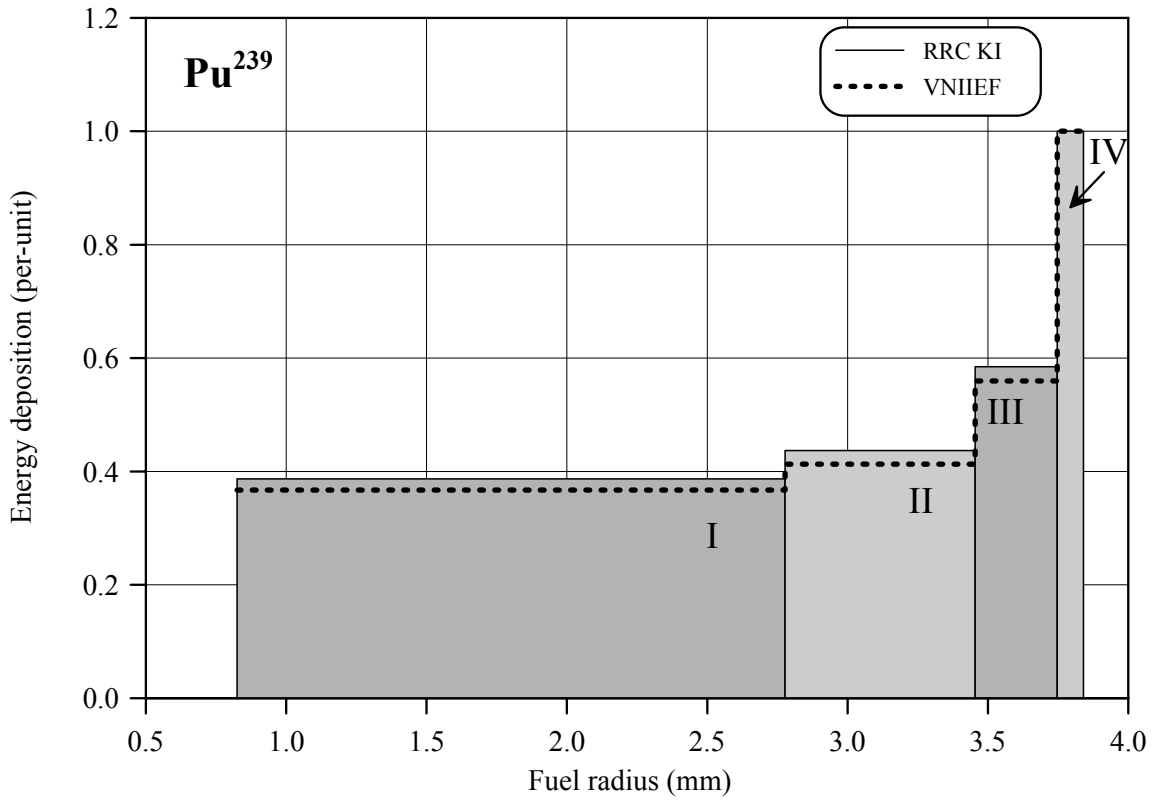
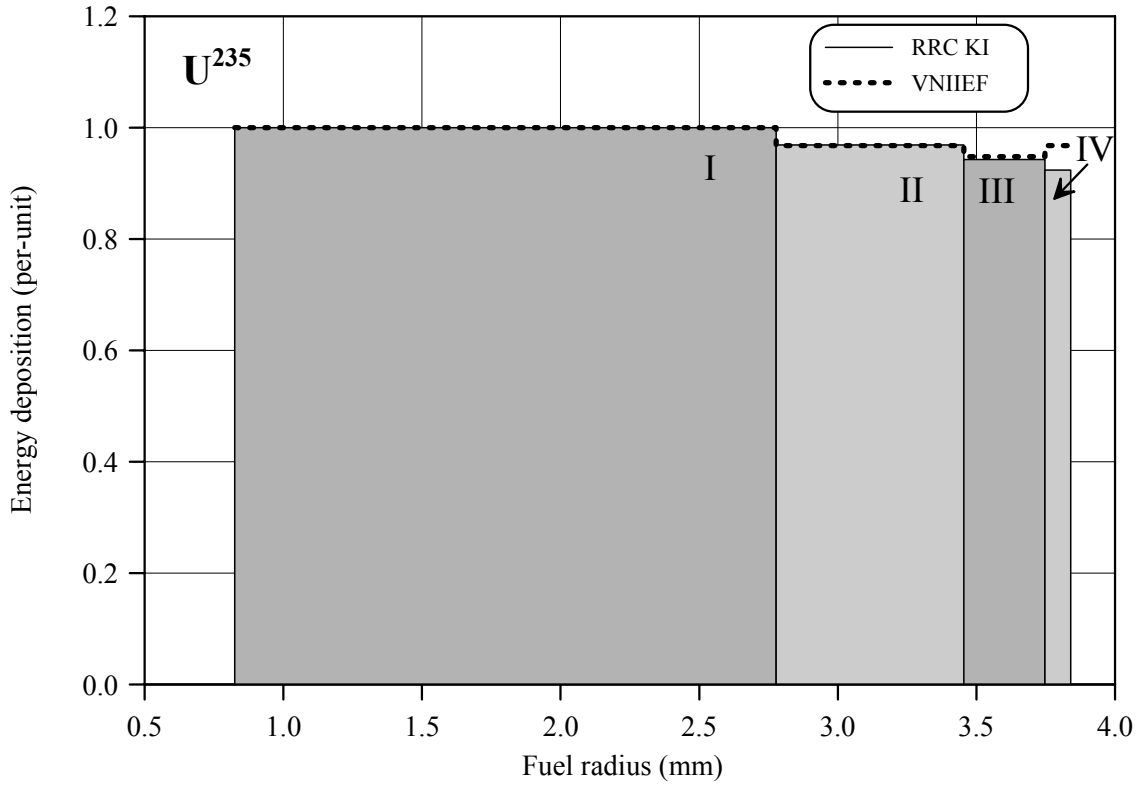


Fig.E-8.6. U²³⁵ and Pu²³⁹ radial distribution of energy deposition for fuel rod # RT8

RT8

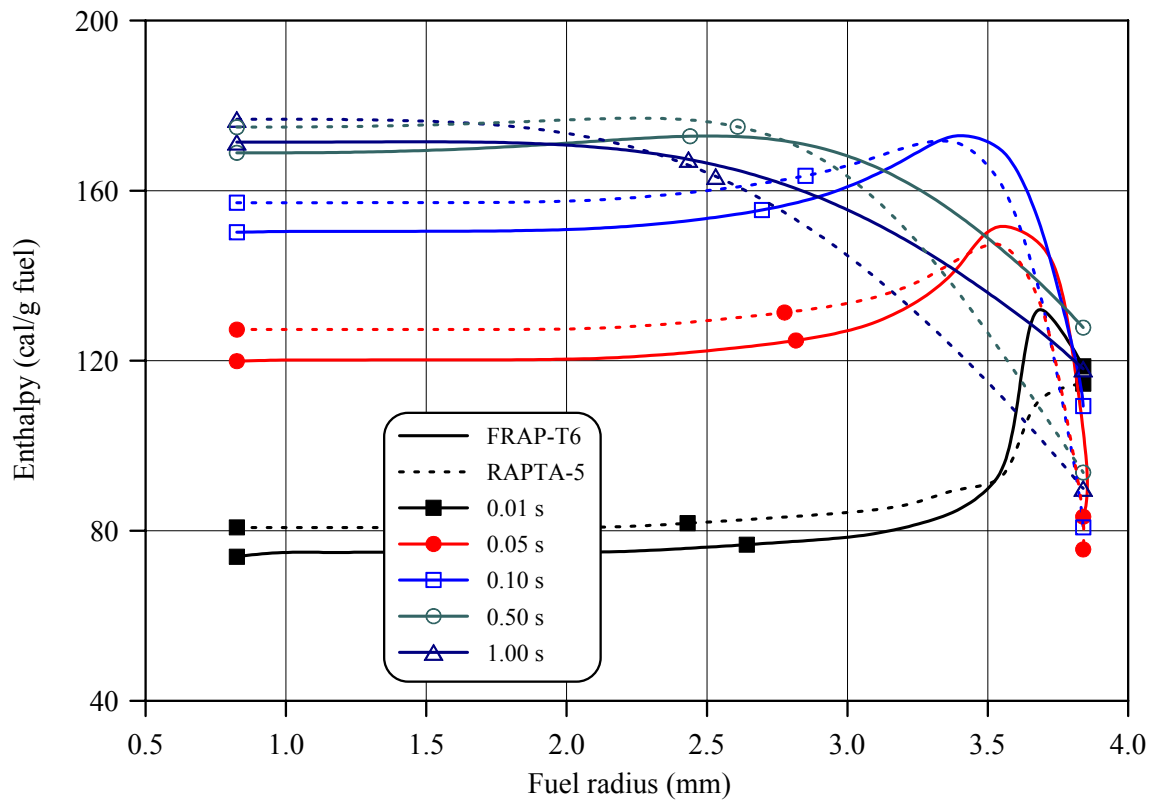
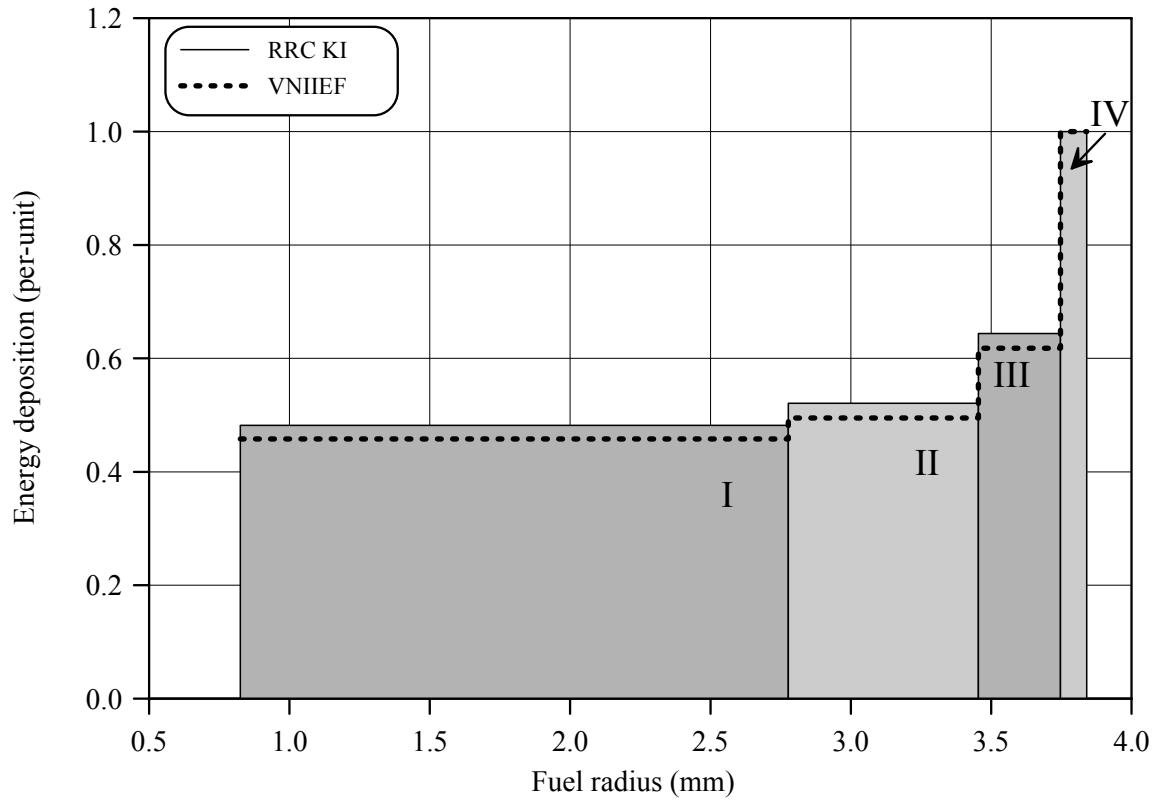


Fig.E-8.7. Radial distribution of energy deposition and fuel enthalpy for fuel rod # RT8

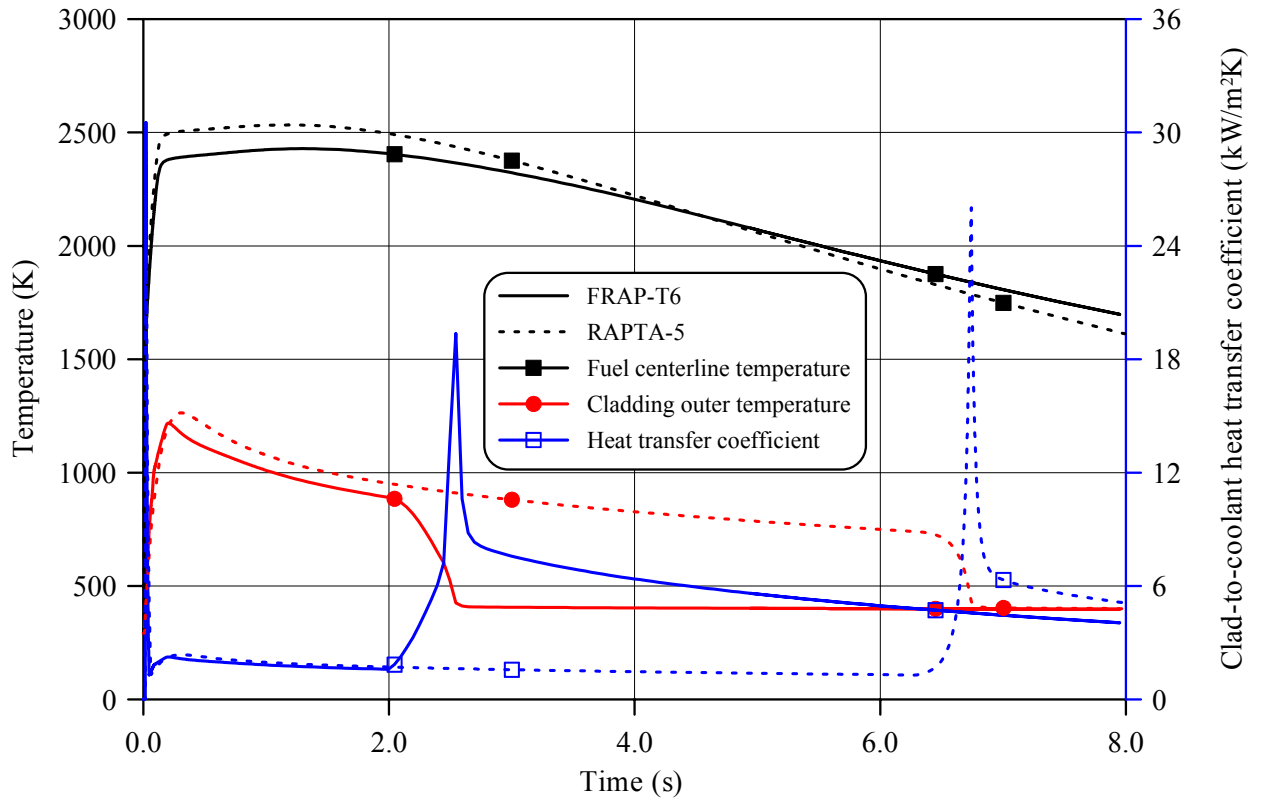
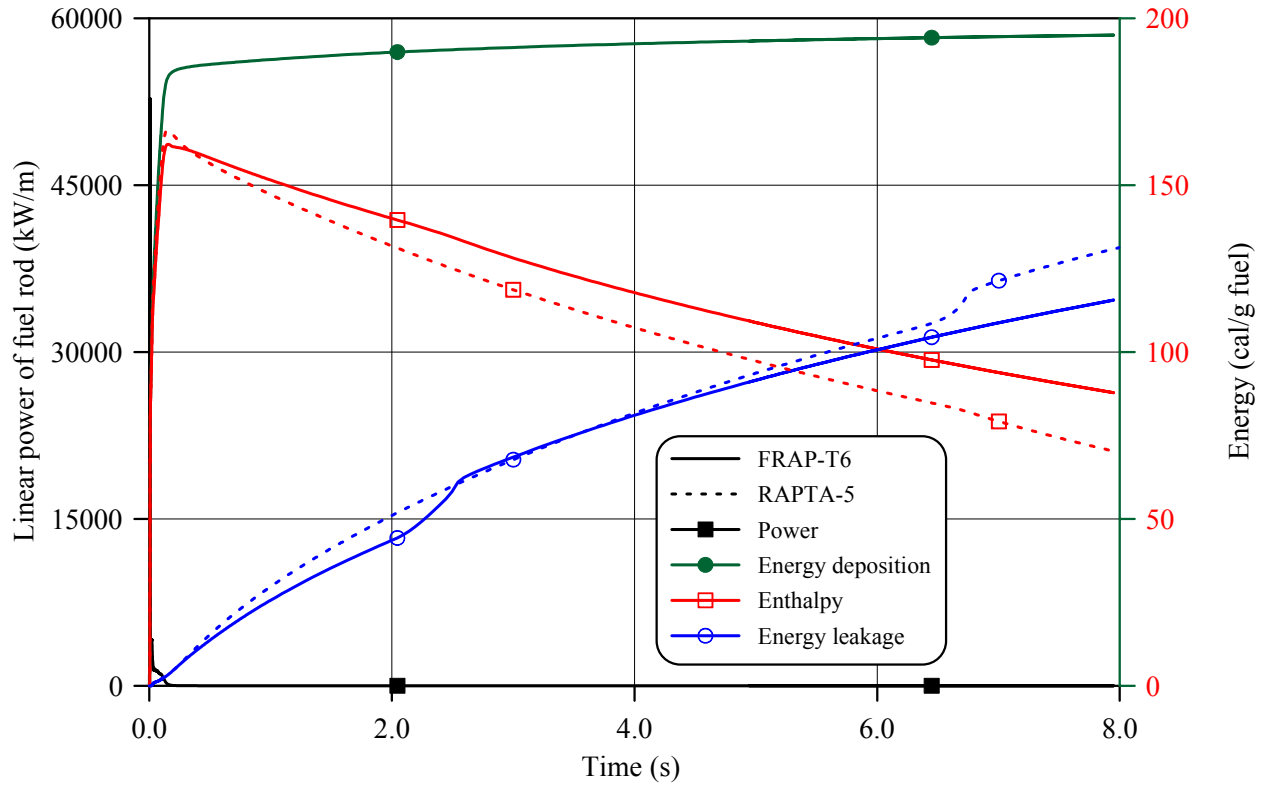


Fig.E-8.8. Thermal history of fuel rod # RT8 during the BGR test in accordance with FRAP-T6/VVER and RAPTA-5 calculations

RT8

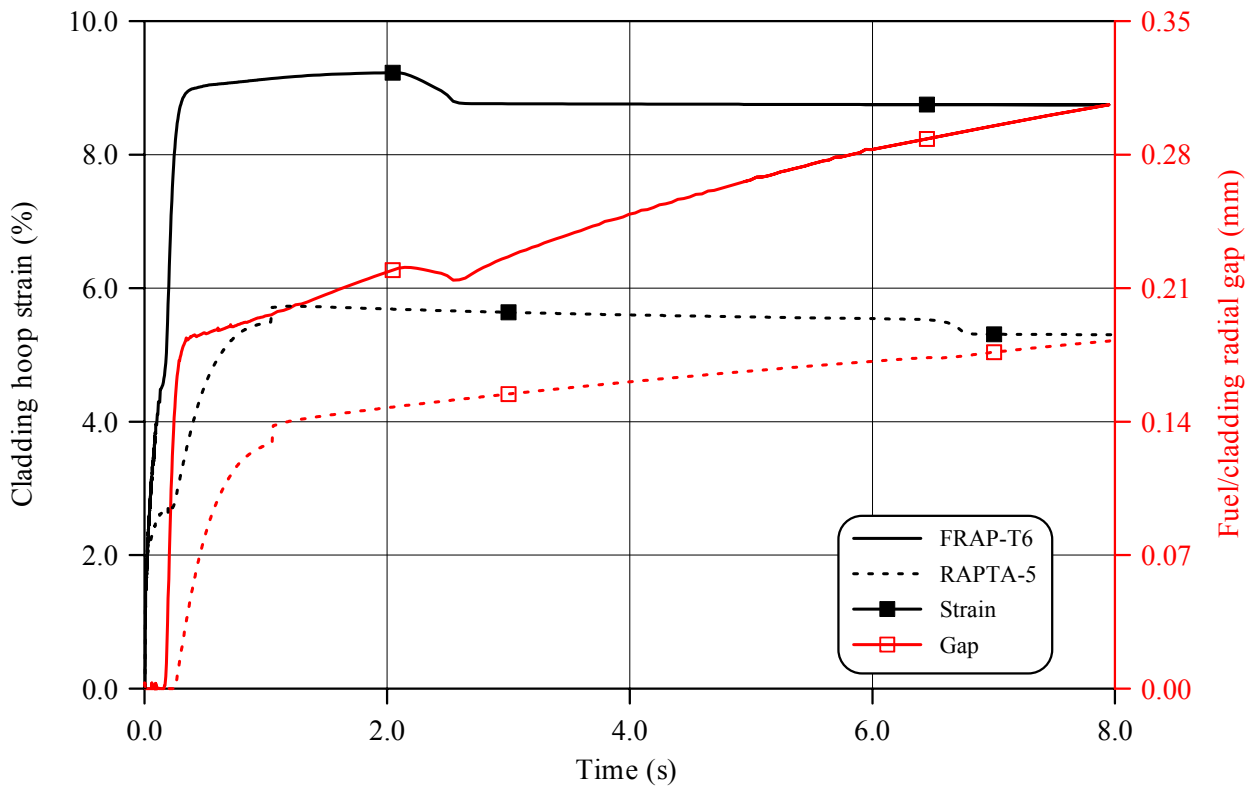
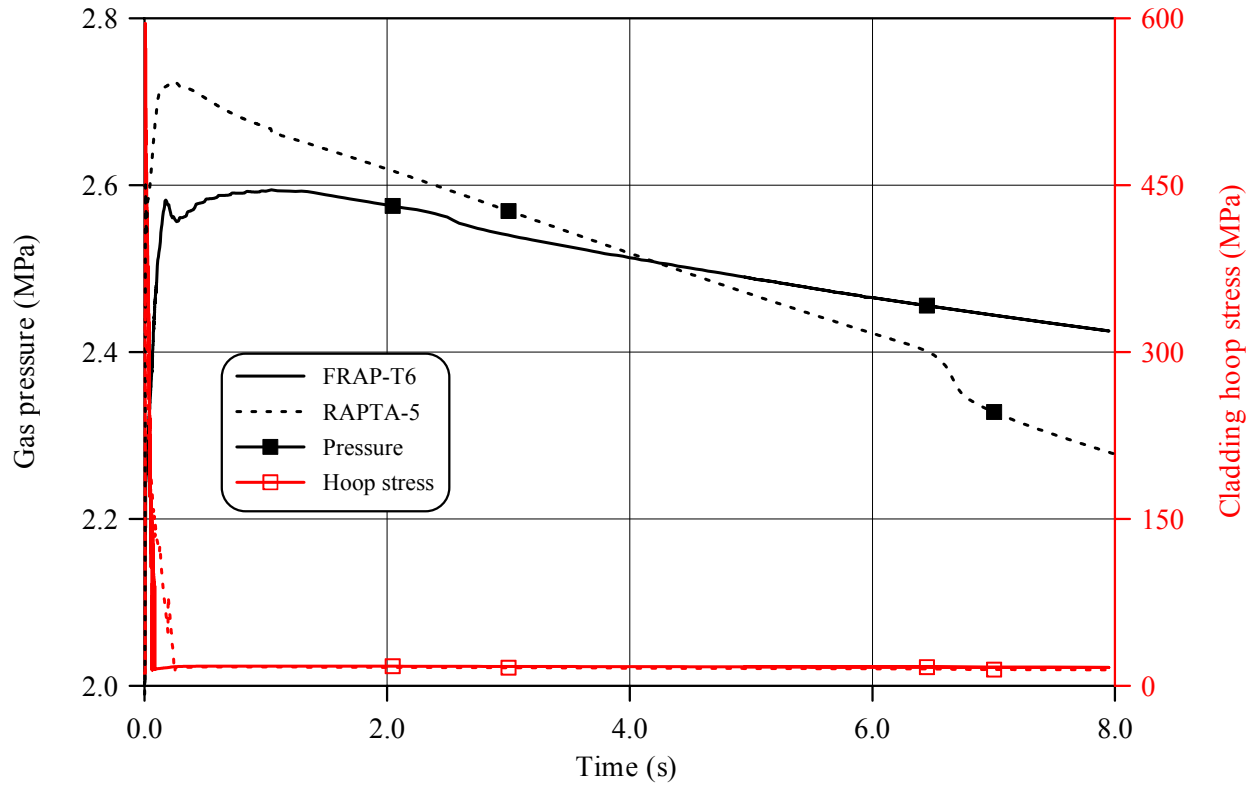


Fig.E-8.9. Mechanical behavior of fuel rod # RT8 during the BGR test in accordance with FRAP-T6/VVER and RAPTA-5 calculations

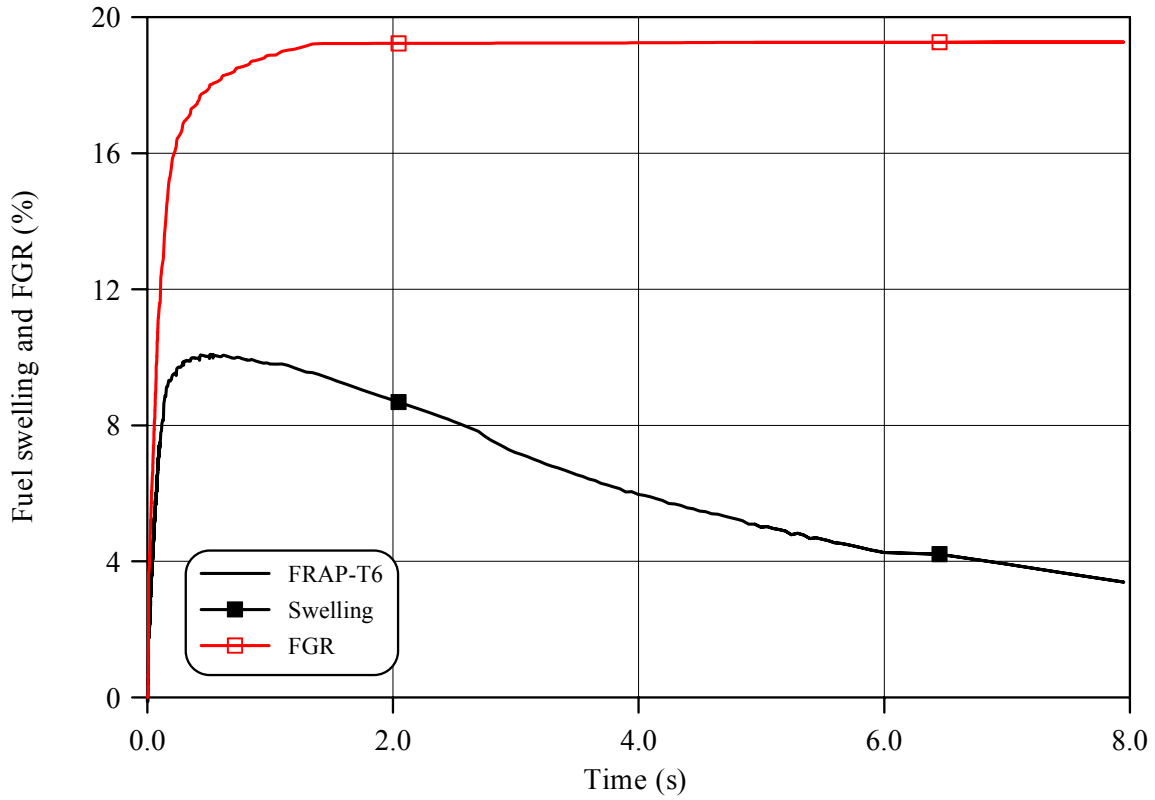
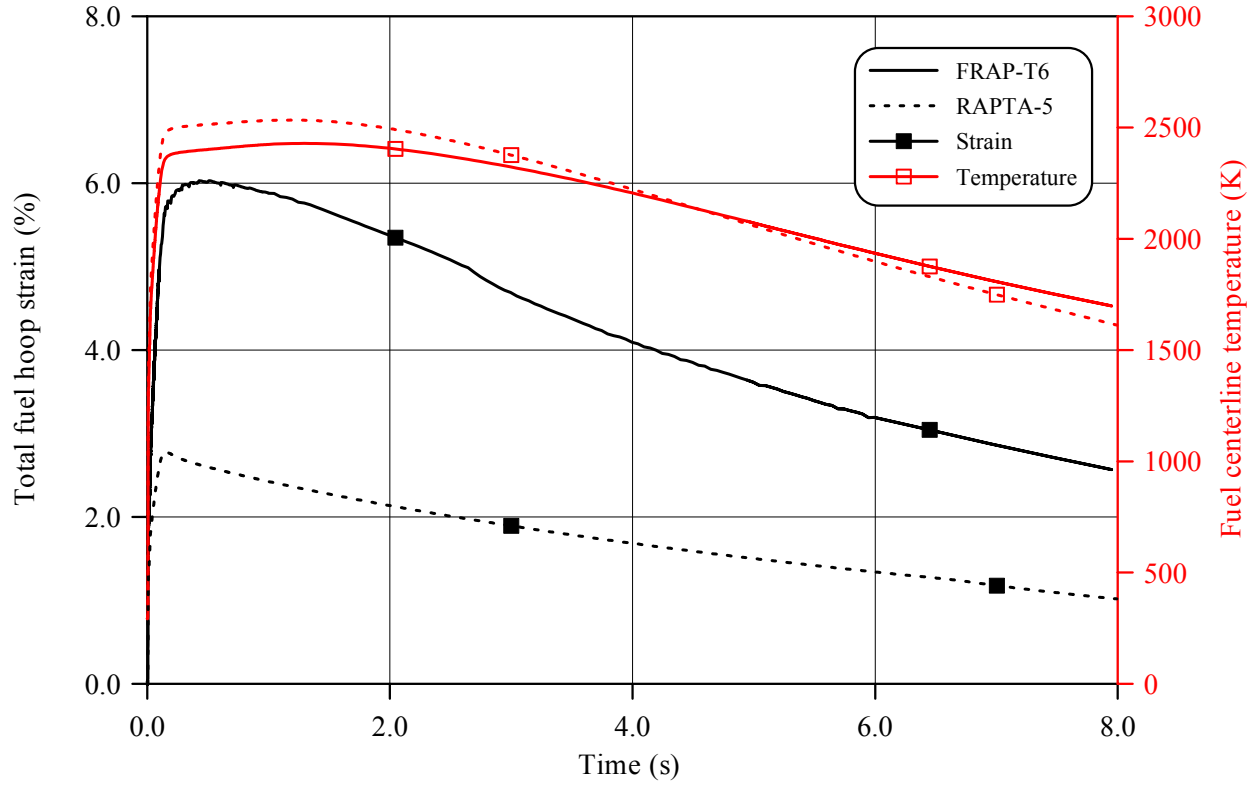


Fig.E-8.10. Fuel behavior during the BGR test of fuel rod # RT8 in accordance with FRAP-T6/VVER and RAPTA-5 calculations

RT8

Table E-8.3. Axial distribution of cladding average outer diameter in fuel rod # RT8*

| Axial coordinate (mm) | Cladding diameter (mm) | Axial coordinate (mm) | Cladding diameter (mm) | Axial coordinate (mm) | Cladding diameter (mm) | Axial coordinate (mm) | Cladding diameter (mm) |
|-----------------------|------------------------|-----------------------|------------------------|-----------------------|------------------------|-----------------------|------------------------|
| 7 | 9.128 | 45 | 9.663 | 83 | 9.695 | 121 | 9.703 |
| 9 | 9.223 | 47 | 9.694 | 85 | 9.713 | 123 | 9.655 |
| 11 | 9.290 | 49 | 9.783 | 87 | 9.714 | 125 | 9.626 |
| 13 | 9.326 | 51 | 9.914 | 89 | 9.723 | 127 | 9.649 |
| 15 | 9.296 | 53 | 10.058 | 91 | 9.702 | 129 | 9.734 |
| 17 | 9.257 | 55 | 10.085 | 93 | 9.701 | 131 | 9.824 |
| 19 | 9.247 | 57 | 9.938 | 95 | 9.733 | 133 | 9.801 |
| 21 | 9.277 | 59 | 9.795 | 97 | 9.731 | 135 | 9.680 |
| 23 | 9.343 | 61 | 9.745 | 99 | 9.688 | 137 | 9.670 |
| 25 | 9.409 | 63 | 9.716 | 101 | 9.620 | 139 | 9.694 |
| 27 | 9.496 | 65 | 9.701 | 103 | 9.642 | 141 | 9.715 |
| 29 | 9.584 | 67 | 9.680 | 105 | 9.733 | 143 | 9.703 |
| 31 | 9.626 | 69 | 9.664 | 107 | 9.783 | 145 | 9.650 |
| 33 | 9.645 | 71 | 9.681 | 109 | 9.751 | 147 | 9.613 |
| 35 | 9.634 | 73 | 9.733 | 111 | 9.663 | 149 | 9.602 |
| 37 | 9.619 | 75 | 9.745 | 113 | 9.608 | 151 | 9.567 |
| 39 | 9.651 | 77 | 9.728 | 115 | 9.615 | 153 | 9.521 |
| 41 | 9.676 | 79 | 9.681 | 117 | 9.670 | 155 | 9.442 |
| 43 | 9.673 | 81 | 9.659 | 119 | 9.705 | 157 | 9.261 |

* Measured value determined on the basis of profilometry data (16 azimuthal directions)

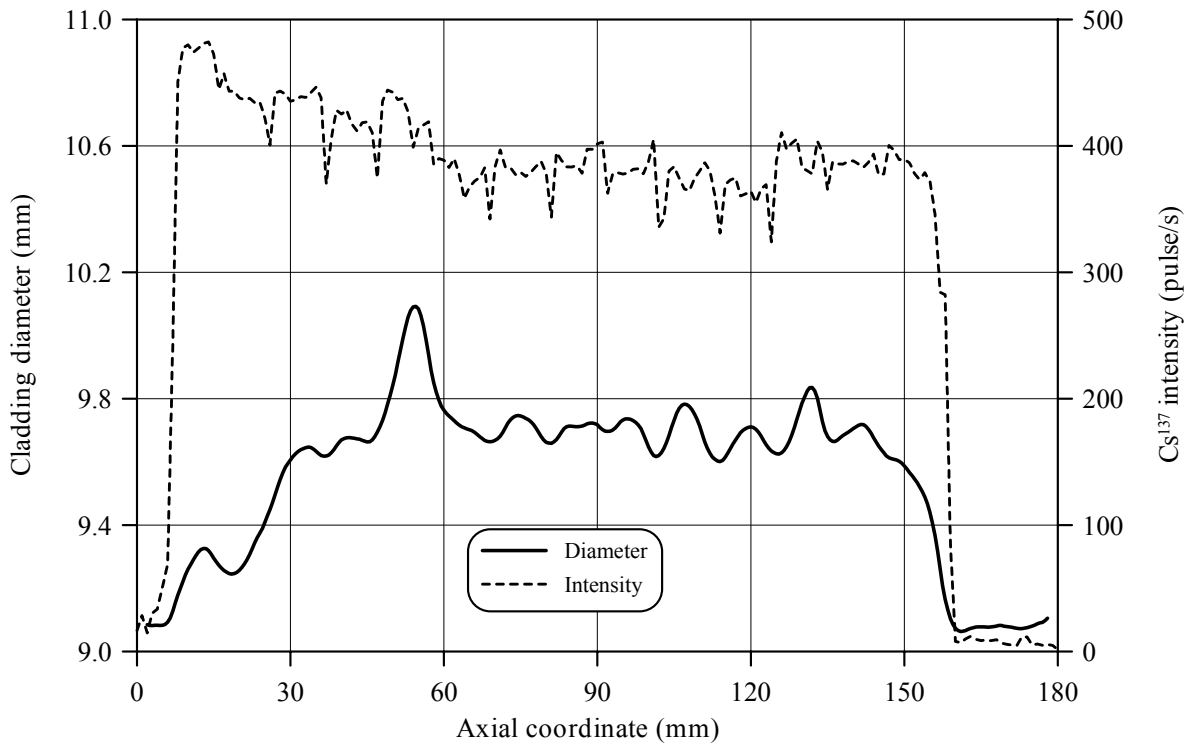


Fig.E-8.11. Cladding measured average diameter and γ -scanning results for fuel rod # RT8

Table E-8.4. The PIE results for fuel rod # RT8

| Parameter | | Value |
|-----------|--|-----------|
| 1. | Cladding outer diameter (mm): | |
| 1.1. | Maximum diameter of the bidimensional data sample in "fuel rod length - azimuthal angle" coordinates (mm) | 10.35 |
| 1.2. | Averaged azimuthal diameter and maximum diameter along the length selected from the sample of averaged azimuthal diameter (mm) | 10.09 |
| 1.3. | Averaged diameter of the bidimensional data sample in "fuel rod length - azimuthal angle" coordinates (mm) | 9.60 |
| 2. | Cladding residual hoop strain (%): | |
| 2.1. | Maximum hoop strain | 11.10 |
| 2.2. | Hoop strain at rupture | 11.1, 8.3 |
| 3. | Fuel pellet conditional diameter (mm) in cross-section*: | |
| | at 53 mm elevation | 8.33 |
| | at 97 mm elevation | 8.28 |
| | at 133 mm elevation | 8.22 |
| 4. | ZrO ₂ outer thickness (μm) in cross-section: | |
| | at 53, 97, 133 mm elevations | 5-7 |
| 5. | ZrO ₂ inner thickness (μm) in cross-section: | |
| | at 97 mm elevation | 4 |
| 6. | Parameters characterizing FGR: | |
| 6.1. | Gas composition (% by volume): | |
| | He | - |
| | N ₂ | - |
| | O ₂ | - |
| | Ar | - |
| | CO ₂ | - |
| | Kr | - |
| | Xe | - |
| 6.2. | Free gas volume (cm ³) | - |
| 6.3. | Gas volume under normal conditions (cm ³) | - |
| 6.4. | Gas pressure under normal conditions (MPa) | - |

* Reference value determined by the processing of fuel cross-section photographs

RT8

Table E-8.5. Organized BGR test results for fuel rod # RT8

| Parameter | | Unit | Value | | |
|-----------|---|---------------------|----------|------------|---------|
| | | | Measured | Calculated | |
| | | | | FRAP-T6 | RAPTA-5 |
| 1. | Fuel burnup | MW d/kg U | 60.2 | 60.2 | 60.2 |
| 2. | Initial gas pressure | MPa | 2.0 | 2.0 | 2.0 |
| 3. | Energy deposition | cal/g fuel | 201.7 | 201.7 | 201.7 |
| 4. | Peak fuel enthalpy* | cal/g fuel | - | 162.3 | 166.4 |
| 5. | Fuel maximum temperature | K | - | 2514 | 2580 |
| 6. | Maximum temperature of cladding outer surface | K | - | 1219 | 1264 |
| 7. | Cladding burst | Failed, Unfailed | Failed | -** | -** |
| 8. | Cladding residual hoop strain | | | | |
| | - average*** | % | 6.08 | 8.64 | 5.73 |
| | - maximum | % | 11.10 | 8.64 | 5.73 |

* Average value of peak fuel enthalpy 164.3 cal/g fuel

** This parameter was not calculated

*** Average value along the fuel stack length

Appendix E-9

*Individual Characteristics of Fuel Rod # RT9
after the BGR Test*

RT9

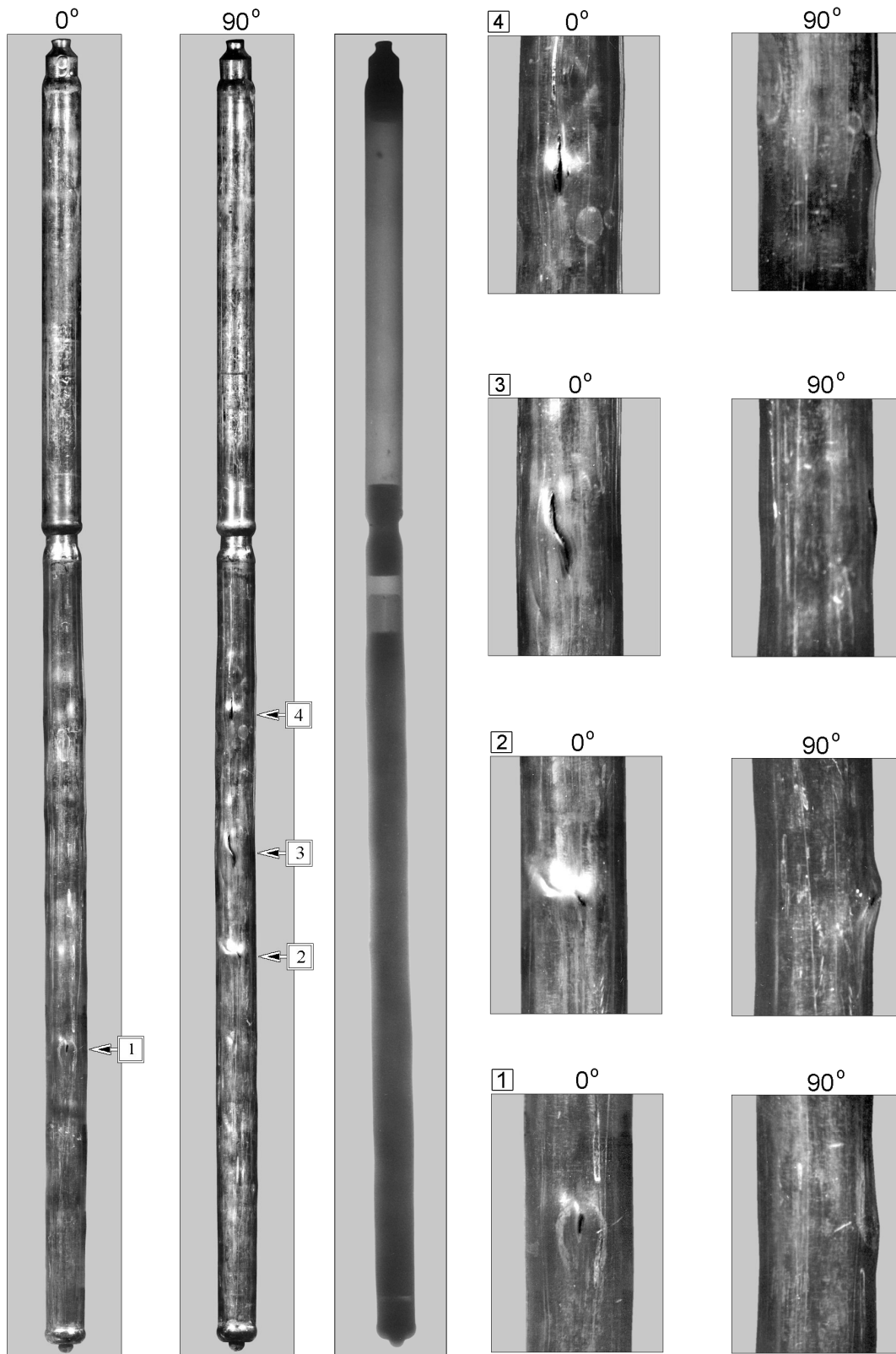


Fig.E-9.1. Appearance of failed fuel rod # RT9 after the BGR test (photographs and X-ray photograph)

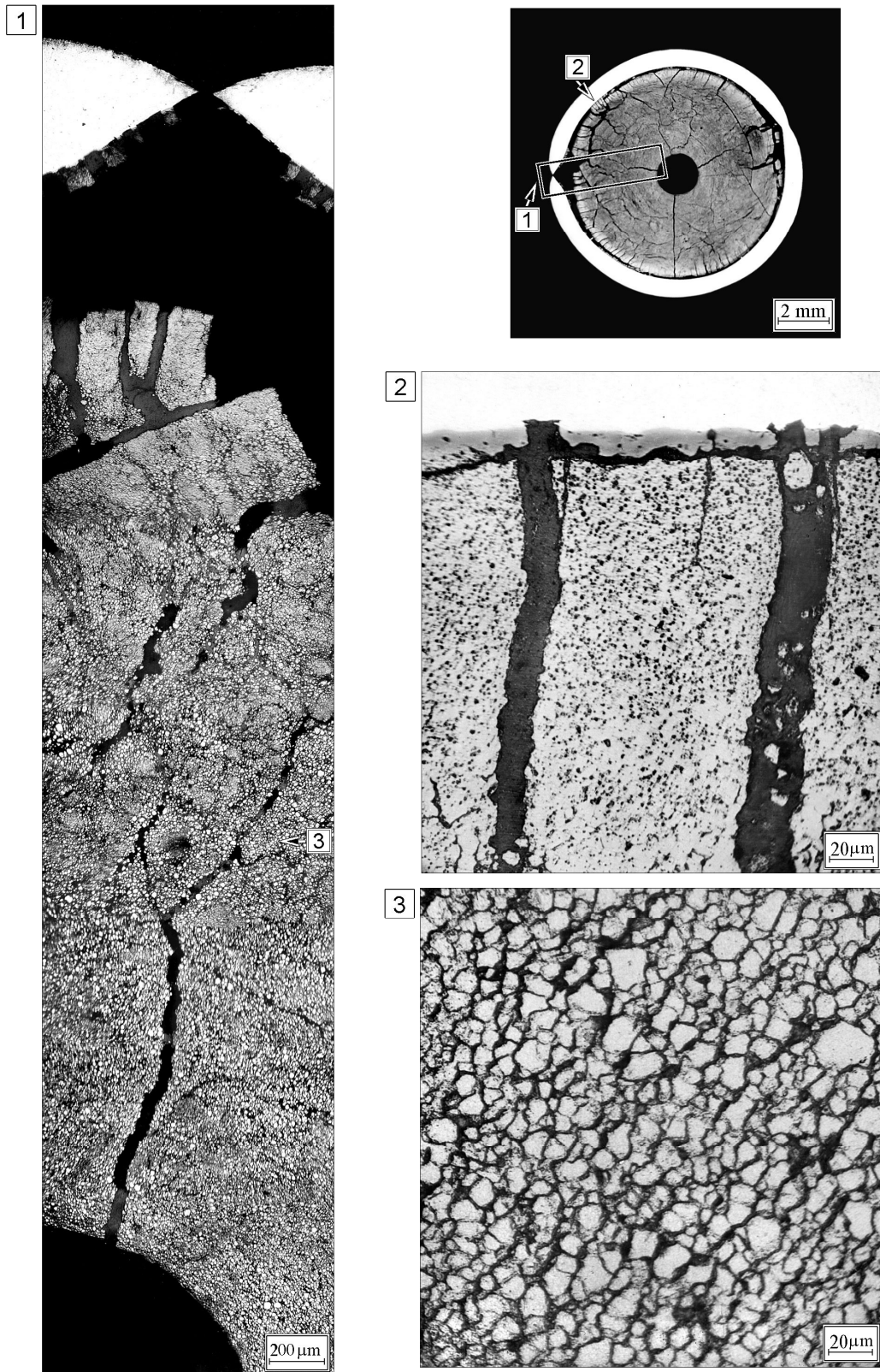


Fig.E-9.2. Cross-section and microstructure of fuel and cladding of fuel rod # RT9 at 69 mm elevation (from low cap)

RT9

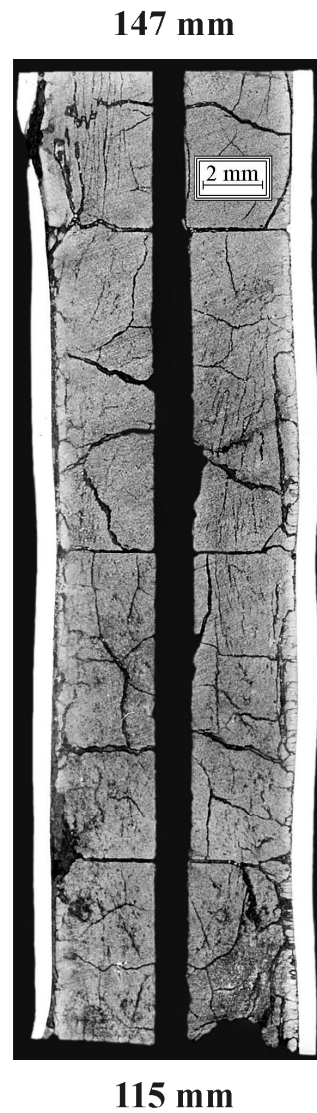
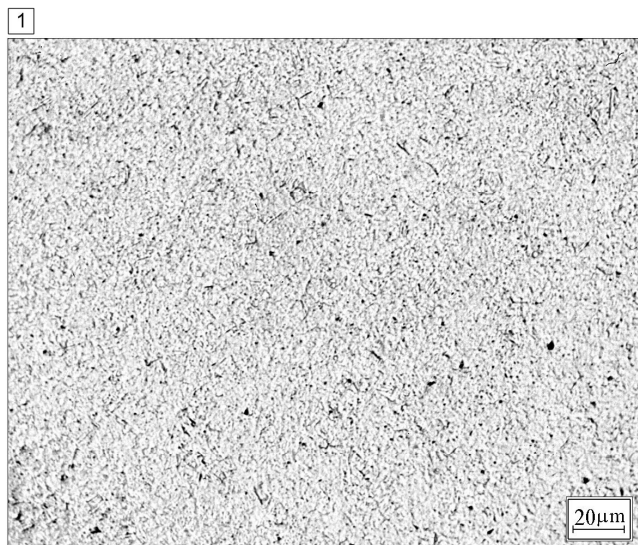
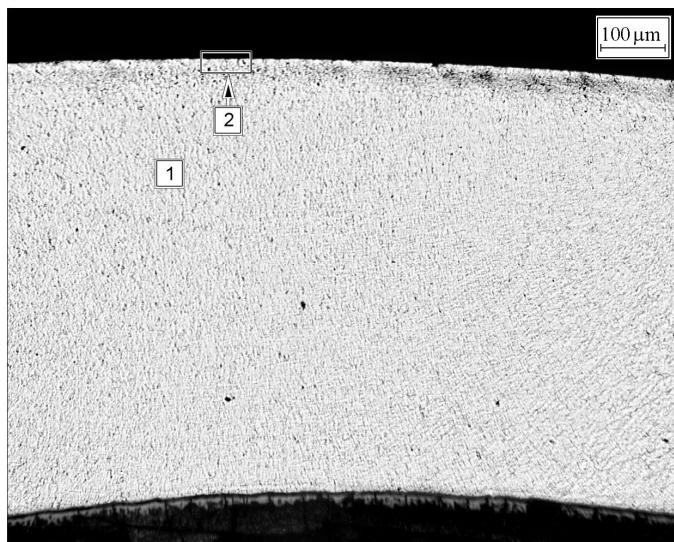


Fig.E-9.3. Cladding microstructure at 69 mm elevation (from low cap) and longitudinal metallographic specimen image of fuel rod # RT9

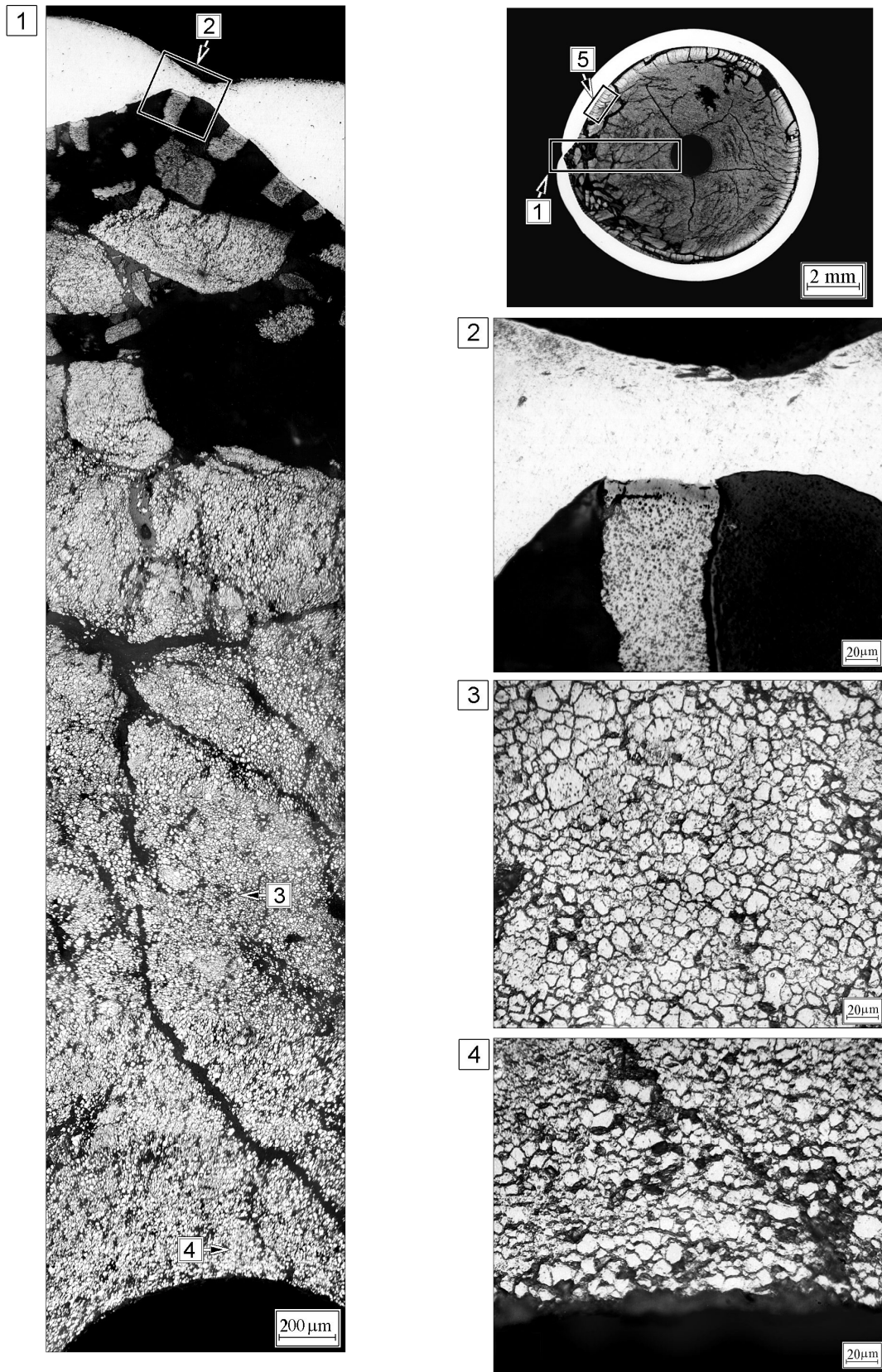


Fig.E-9.4. Cross-section and microstructure of fuel and cladding of fuel rod # RT9 at 88 mm elevation (from low cap)

RT9

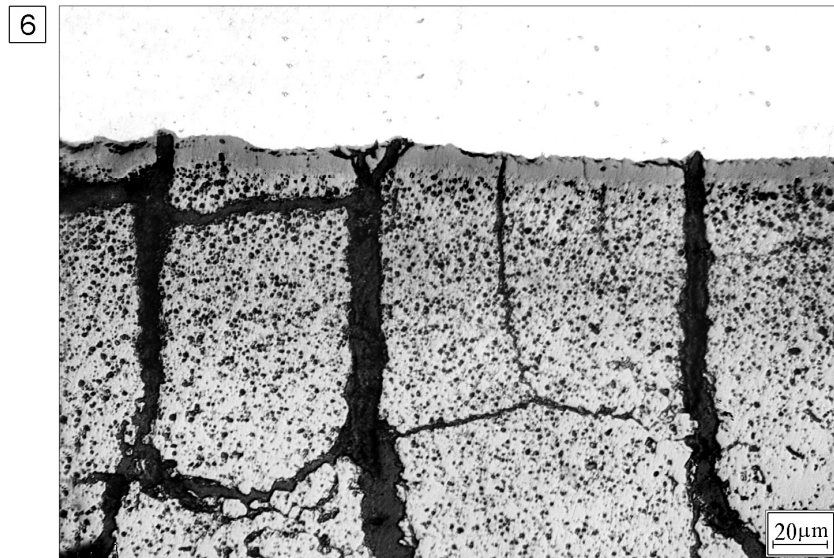
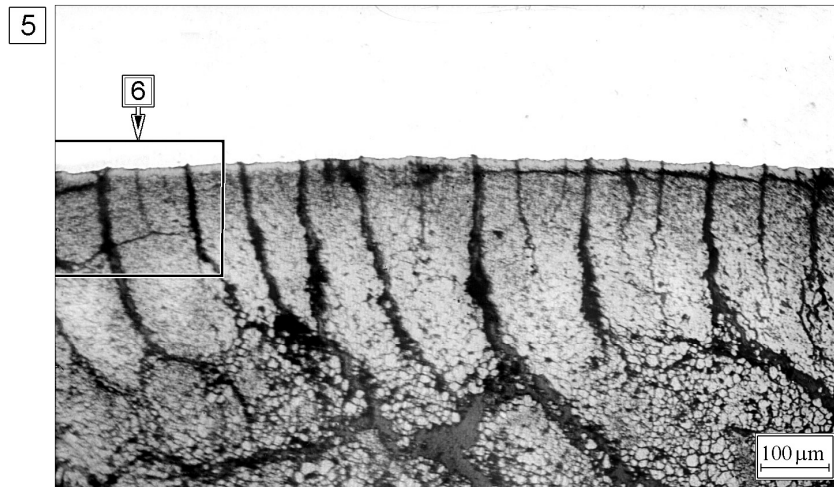
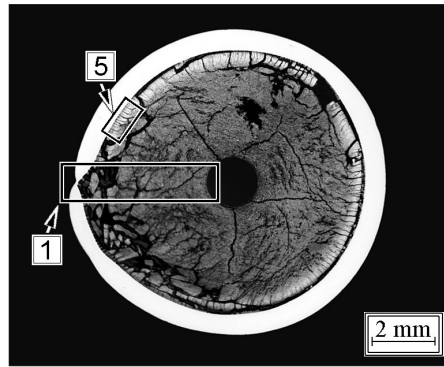


Fig.E-9.5. Microstructure of fuel and cladding in their interaction area for fuel rod # RT9 at 88 mm elevation (from low cap)

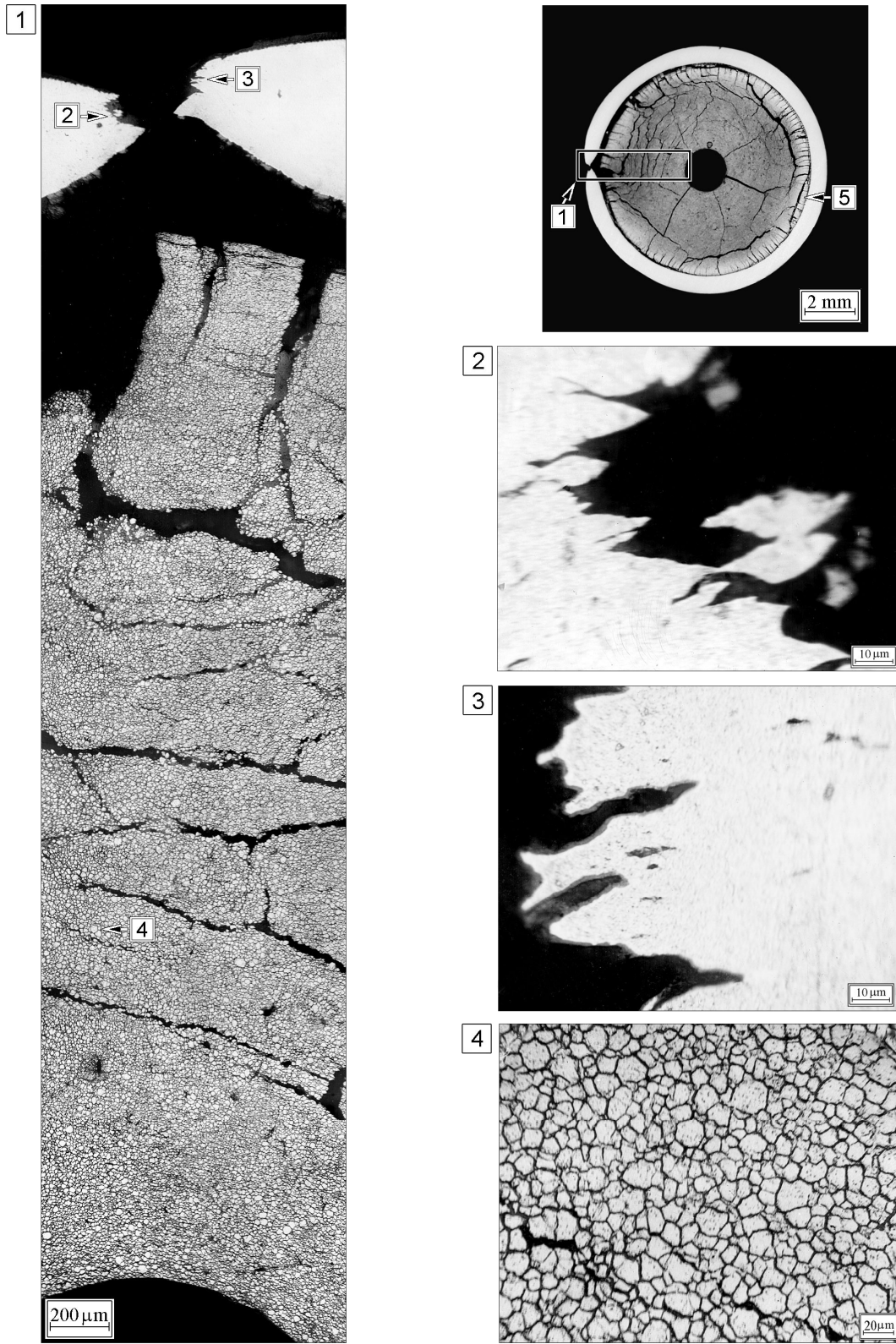


Fig.E-9.6. Cross-section and microstructure of fuel and cladding of fuel rod # RT9 at 110 mm elevation (from low cap)

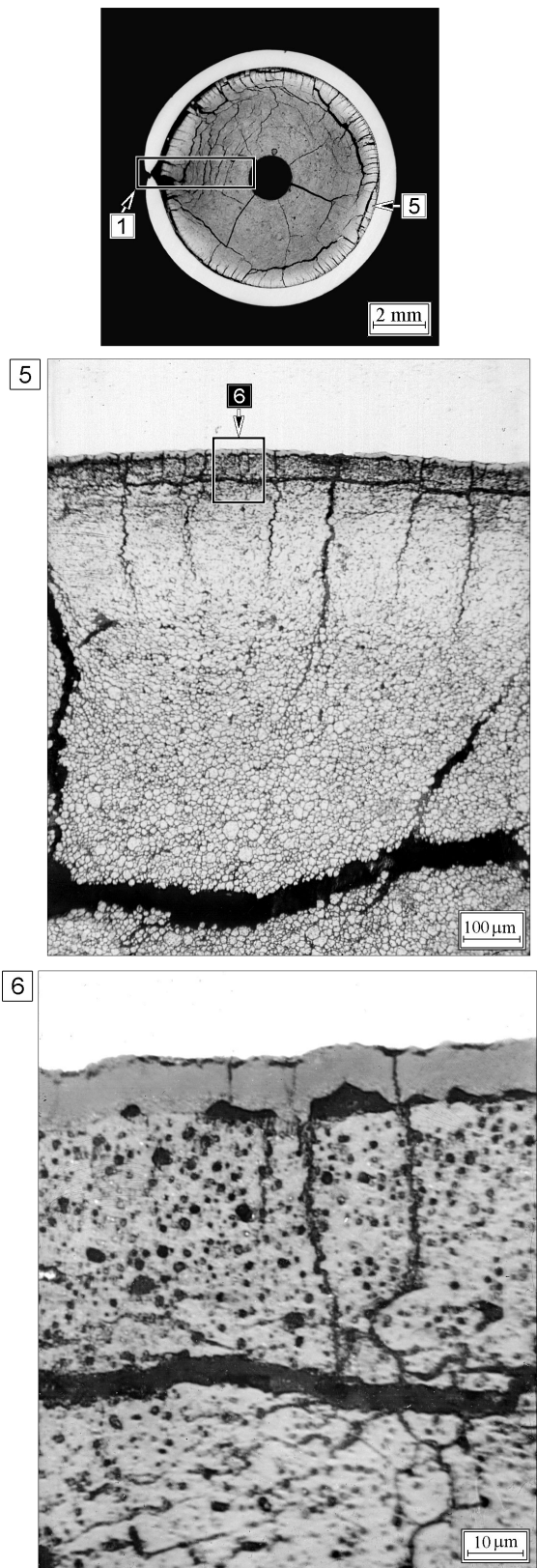


Fig.E-9.7. Microstructure of fuel and cladding in their interaction area for fuel rod # RT9 at 110 mm elevation (from low cap)

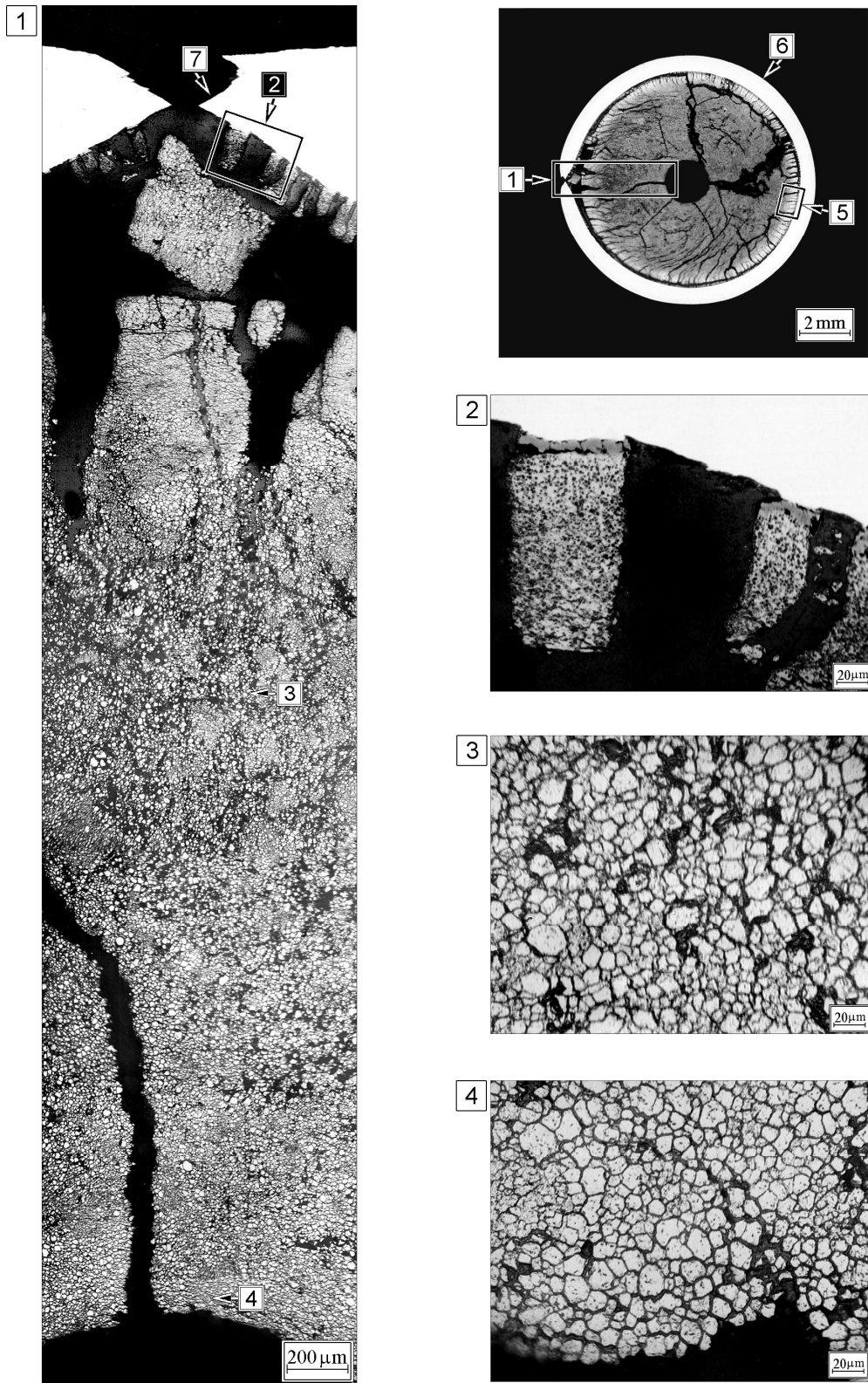


Fig.E-9.8. Cross-section and microstructure of fuel and cladding of fuel rod # RT9 at 144 mm elevation (from low cap)

RT9

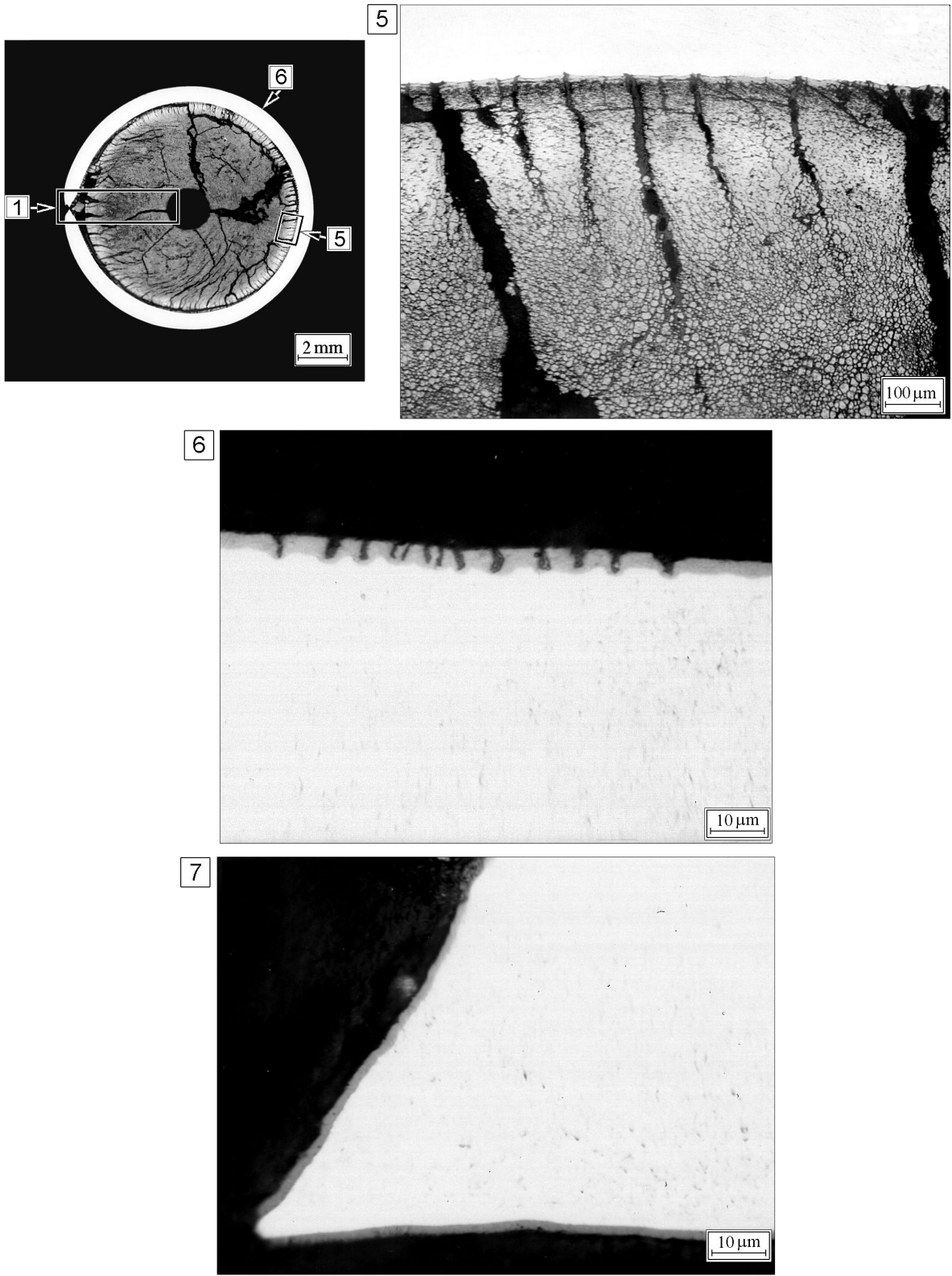


Fig.E-9.9. Fuel and cladding microstructures in their interaction area, cladding microstructure in the burst area at 144 mm elevation (from low cap) for fuel rod # RT9

Table E-9.1. Time dependent energy characteristics of fuel rod # RT9

| Time (s) | Relative reactor power (current/maximum value) (per-unit) | Cumulative number of fissions in fuel rod (fiss) x10 ⁻¹⁴ | Power of fuel rod ¹⁾²⁾ (kW) | Energy deposition | | Fuel enthalpy ³⁾ | |
|----------|---|---|--|-------------------|------------|-----------------------------|---------|
| | | | | (cal/g fuel) | (J/g fuel) | FRAP-T6 | RAPTA-5 |
| 0.000 | 0.00E+00 | 0.000 | 0.000 | 0.000 | 0.000 | 0.000 | 0.000 |
| 0.001 | 3.10E-03 | 0.040 | 22.09 | 0.041 | 0.173 | 0.671 | 0.044 |
| 0.002 | 1.31E-02 | 0.211 | 93.19 | 0.218 | 0.911 | 0.671 | 0.213 |
| 0.003 | 5.73E-02 | 0.961 | 408.0 | 0.990 | 4.143 | 1.257 | 1.037 |
| 0.004 | 2.40E-01 | 4.153 | 1705 | 4.283 | 17.93 | 4.653 | 4.408 |
| 0.005 | 6.88E-01 | 15.16 | 4895 | 15.62 | 65.38 | 16.101 | 16.216 |
| 0.006 | 9.98E-01 | 37.52 | 7104 | 38.64 | 161.8 | 39.125 | 40.065 |
| 0.007 | 6.70E-01 | 59.06 | 4767 | 60.82 | 254.7 | 61.314 | 62.915 |
| 0.008 | 3.19E-01 | 70.98 | 2269 | 73.10 | 306.0 | 73.501 | 75.284 |
| 0.009 | 1.55E-01 | 76.58 | 1103 | 78.87 | 330.2 | 79.094 | 80.938 |
| 0.010 | 9.19E-02 | 79.51 | 654.8 | 81.91 | 342.9 | 81.940 | 83.814 |
| 0.012 | 5.93E-02 | 82.98 | 422.2 | 85.52 | 358.1 | 85.168 | 86.986 |
| 0.014 | 6.09E-02 | 85.98 | 433.6 | 88.56 | 370.8 | 87.826 | 89.659 |
| 0.016 | 7.20E-02 | 89.32 | 513.0 | 91.96 | 385.0 | 90.861 | 92.773 |
| 0.018 | 8.32E-02 | 93.20 | 592.4 | 95.97 | 401.8 | 94.503 | 96.536 |
| 0.020 | 8.64E-02 | 97.43 | 615.1 | 100.4 | 420.1 | 98.522 | 100.700 |
| 0.022 | 8.11E-02 | 101.7 | 577.3 | 104.7 | 438.2 | 102.487 | 104.809 |
| 0.024 | 7.01E-02 | 105.6 | 499.5 | 108.6 | 454.7 | 106.028 | 108.464 |
| 0.026 | 5.82E-02 | 108.7 | 414.5 | 111.9 | 468.4 | 108.974 | 111.515 |
| 0.028 | 4.75E-02 | 111.1 | 338.1 | 114.6 | 479.7 | 111.362 | 113.964 |
| 0.030 | 3.86E-02 | 113.6 | 275.4 | 116.8 | 489.0 | 113.405 | 115.907 |
| 0.050 | 3.01E-02 | 129.2 | 214.8 | 133.3 | 558.2 | 127.090 | 129.994 |
| 0.070 | 2.74E-02 | 143.4 | 195.0 | 147.8 | 618.7 | 135.847 | 142.414 |
| 0.090 | 2.31E-02 | 156.1 | 164.4 | 160.6 | 672.3 | 145.515 | 153.144 |
| 0.110 | 1.78E-02 | 166.3 | 127.1 | 171.3 | 717.2 | 154.950 | 161.897 |
| 0.130 | 8.36E-03 | 173.1 | 59.70 | 178.1 | 745.7 | 160.310 | 166.618 |
| 0.150 | 3.09E-03 | 175.2 | 22.14 | 180.7 | 756.5 | 161.988 | 167.474 |
| 0.200 | 7.25E-04 | 177.3 | 5.351 | 182.8 | 765.1 | 162.116 | 165.632 |
| 1.000 | 8.18E-05 | 180.2 | 0.712 | 186.1 | 779.1 | 145.296 | 142.784 |
| 10.00 | 9.48E-06 | 186.5 | 0.094 | 194.1 | 812.4 | 77.015 | 42.662 |
| 100.0 | 1.91E-07 | 189.1 | 0.004 | 199.1 | 833.6 | 8.681 | 4.998 |
| 1000 | 7.50E-13 | 189.2 | 1.70E-04 | 200.9 | 841.1 | 0.000 | 0.000 |

¹⁾ Average values determined in accordance with results of RRC KI and VNIIEF calculations

²⁾ Maximum power value is 7120.5 kW (t=0.00594 s)

³⁾ Average radial value

RT9**Table E-9.2. Radial energy characteristics of fuel rod # RT9***

| Parameters | Coordinates of fuel radial layers (mm) | | | |
|---|--|--------------------------|--------------------------|--------------------------|
| | 1 layer (0.825-2.777) | 2 layer (2.777-3.454) | 3 layer (3.454-3.747) | 4 layer (3.747-3.840) |
| Number of fissions $\times 10^{-14}$ (fiss) | 8.494 | 5.371 | 3.326 | 1.737 |
| Fission density $\times 10^{-13}$ (fiss/g fuel) | 2.567 | 2.705 | 3.349 | 5.230 |
| Power ** (kW) | 3190 | 2020 | 1254 | 657.0 |
| Energy deposition (cal/g fuel) | 180.1 | 190.0 | 235.8 | 369.2 |
| Energy deposition (J/g fuel) | 754.0 | 795.6 | 987.1 | 1546 |
| Energy deposition *** (per-unit) | 0.488 | 0.515 | 0.639 | 1.000 |

* Average values were determined in accordance with results of RRC KI and VNIIEF calculations

** The power for the entire length of each layer at time 0.00594 s

*** Energy deposition in current layer/energy deposition in 4th layer

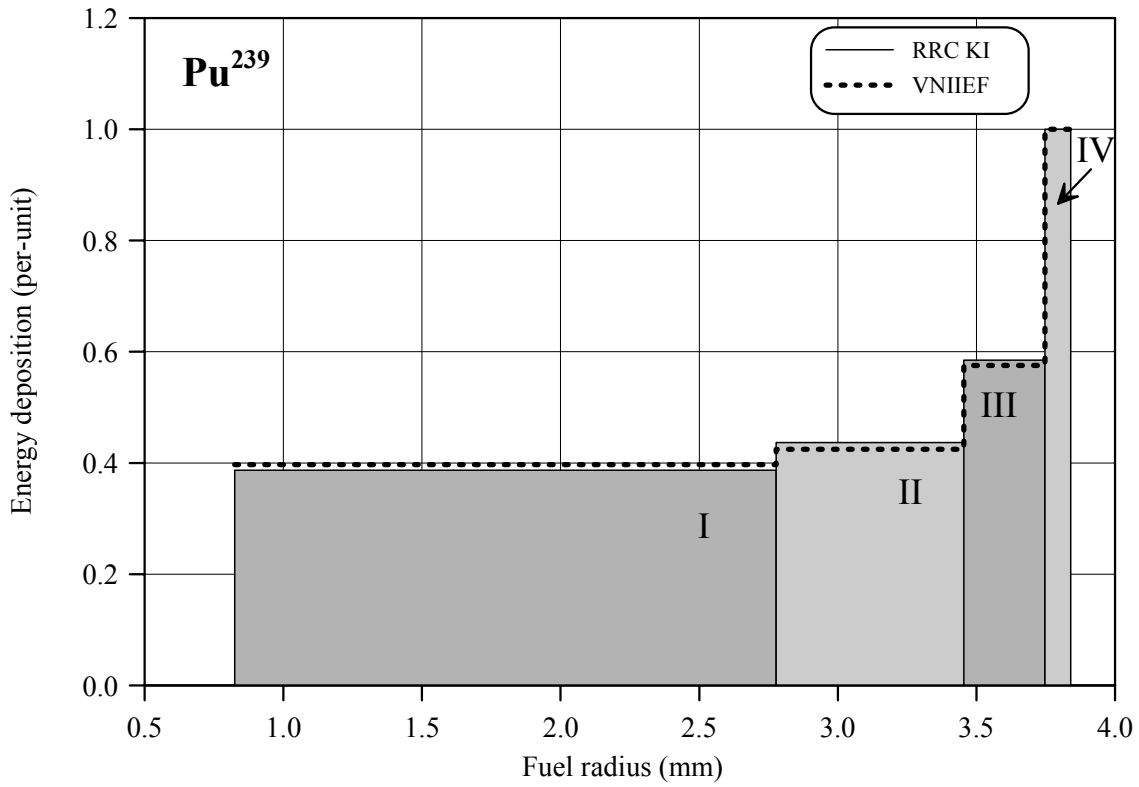
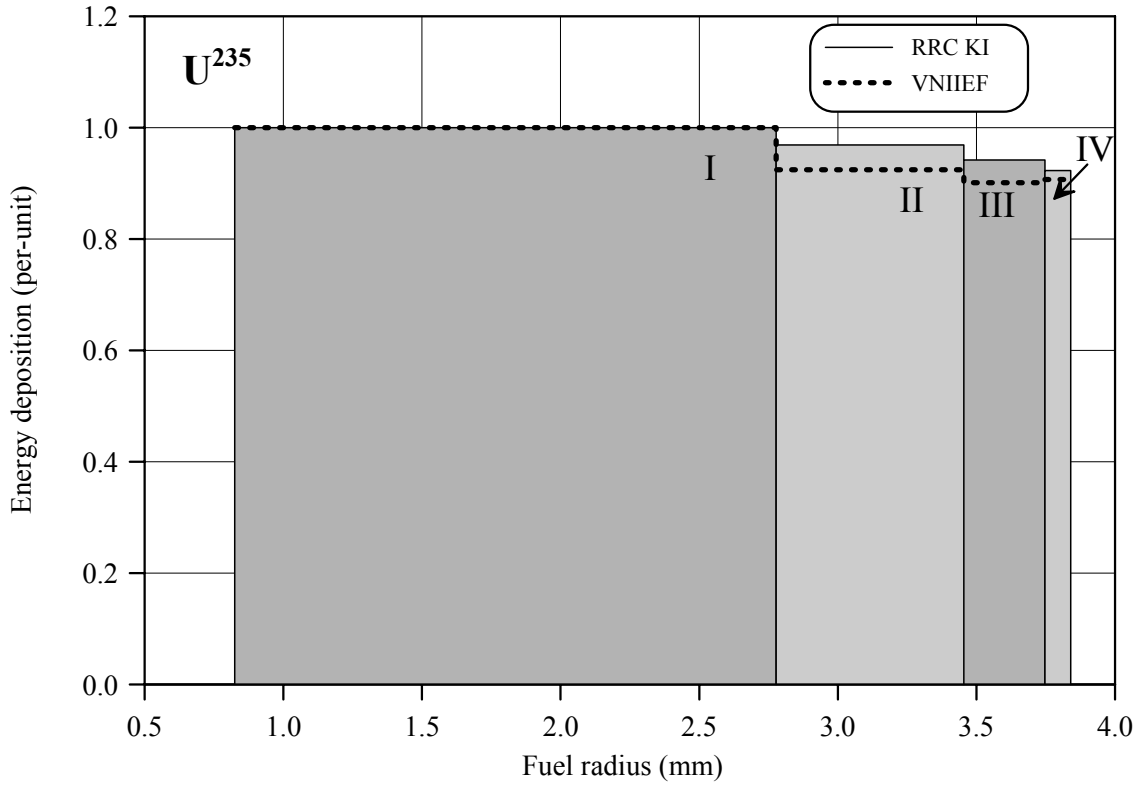


Fig.E-9.10. U²³⁵ and Pu²³⁹ radial distribution of energy deposition for fuel rod # RT9

RT9

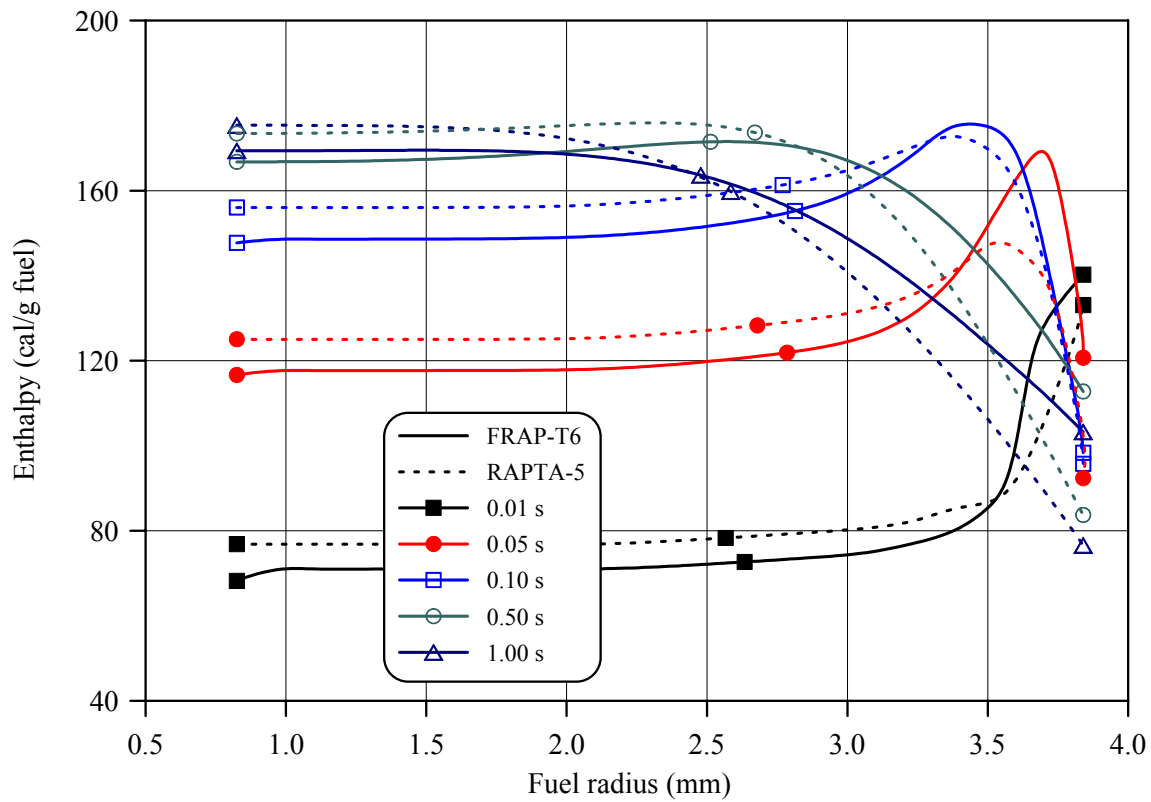
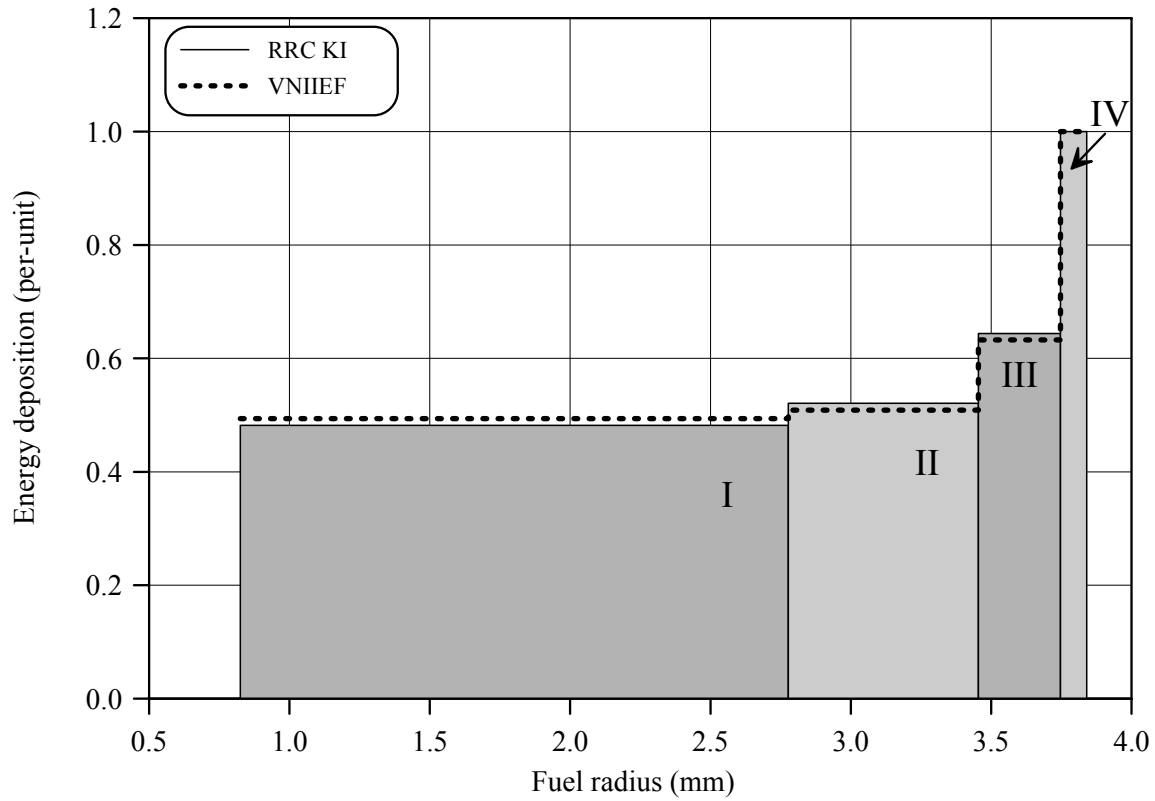


Fig.E-9.11. Radial distribution of energy deposition and fuel enthalpy for fuel rod # RT9

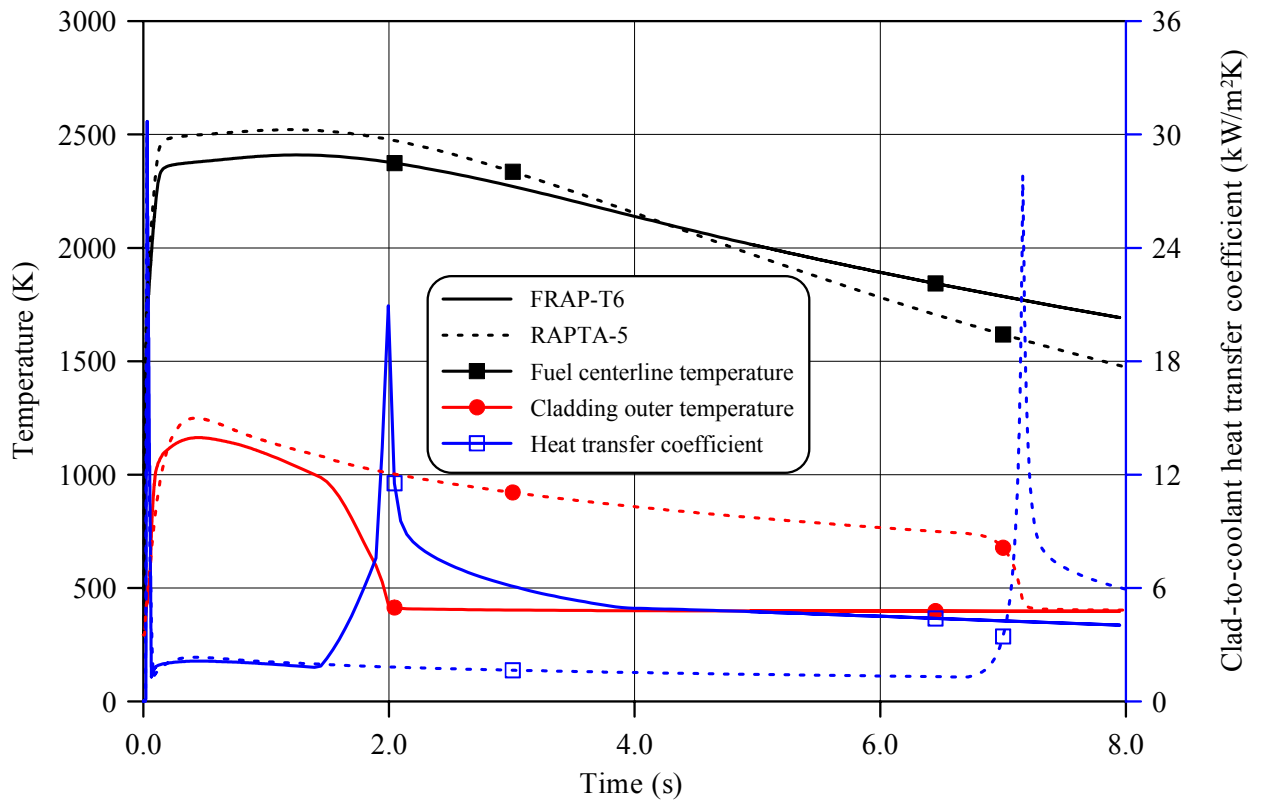
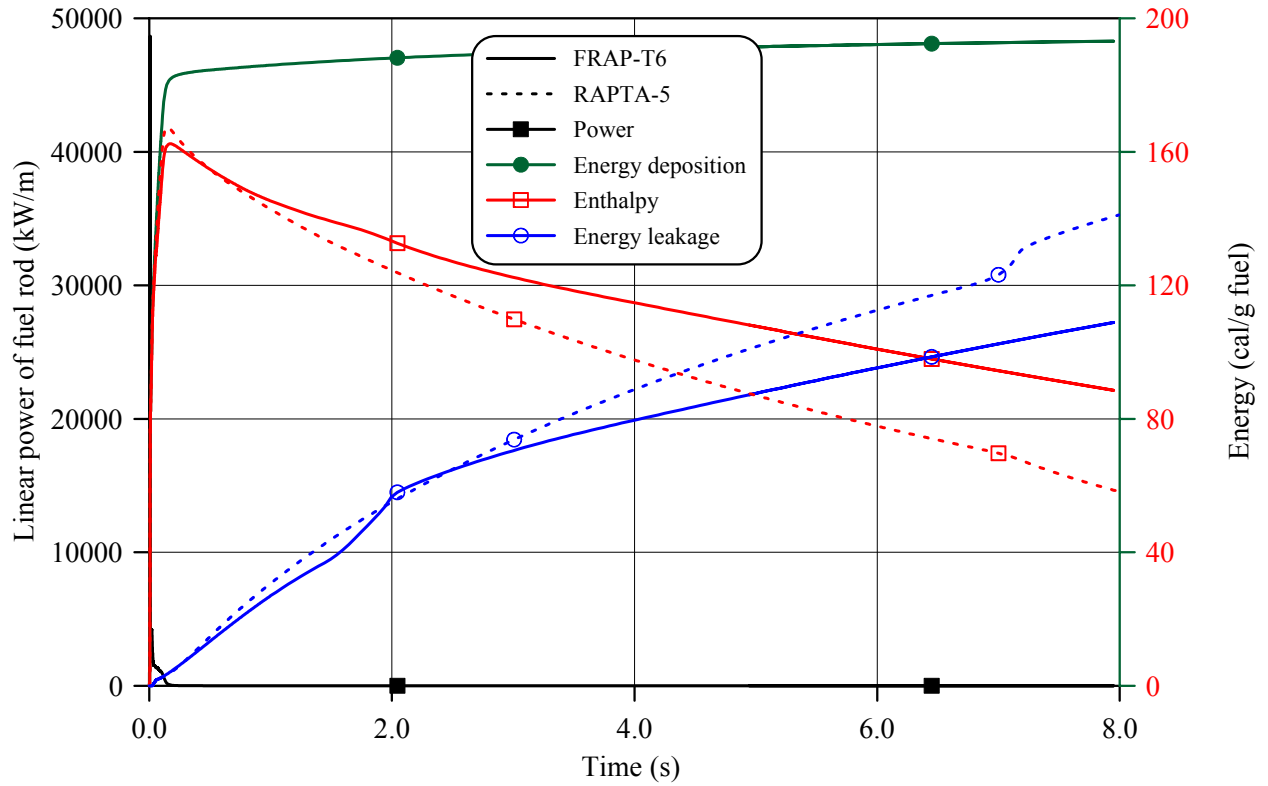


Fig.E-9.12. Thermal history of fuel rod # RT9 during the BGR test in accordance with FRAP-T6/VVER and RAPTA-5 calculations

RT9

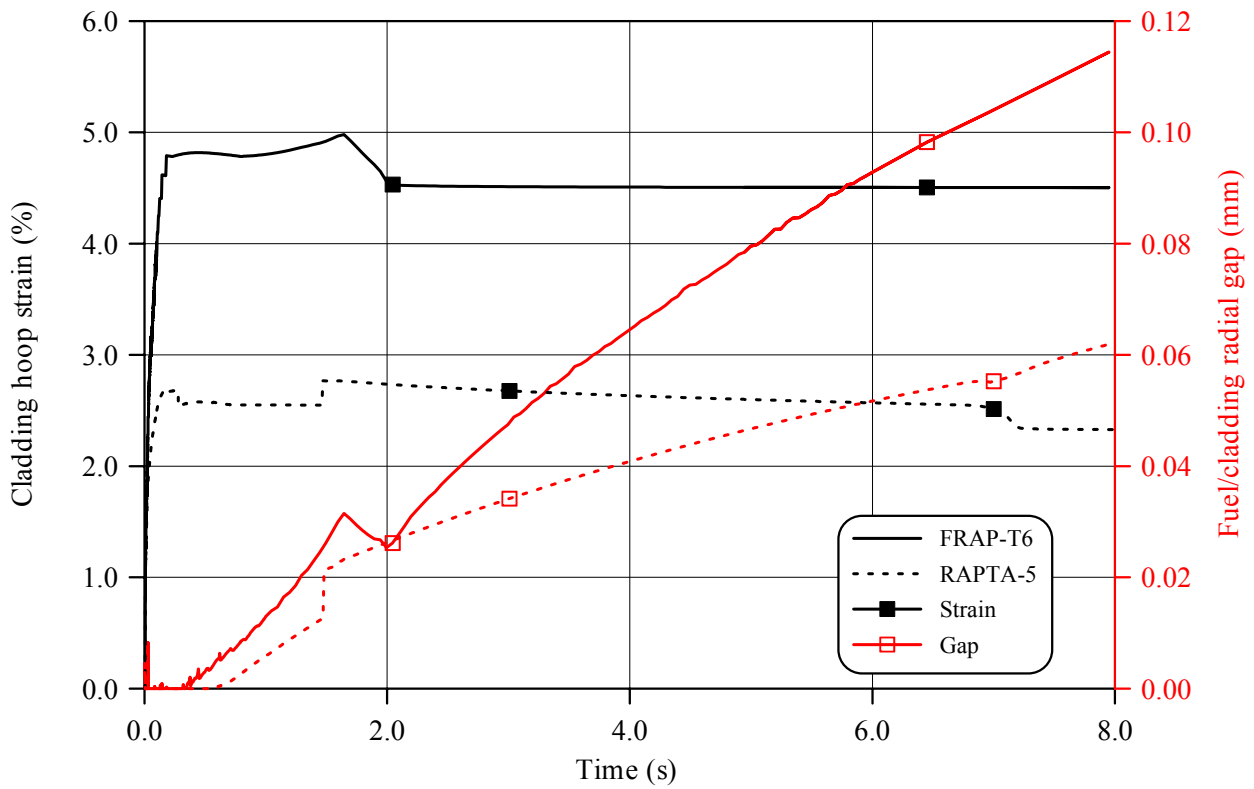
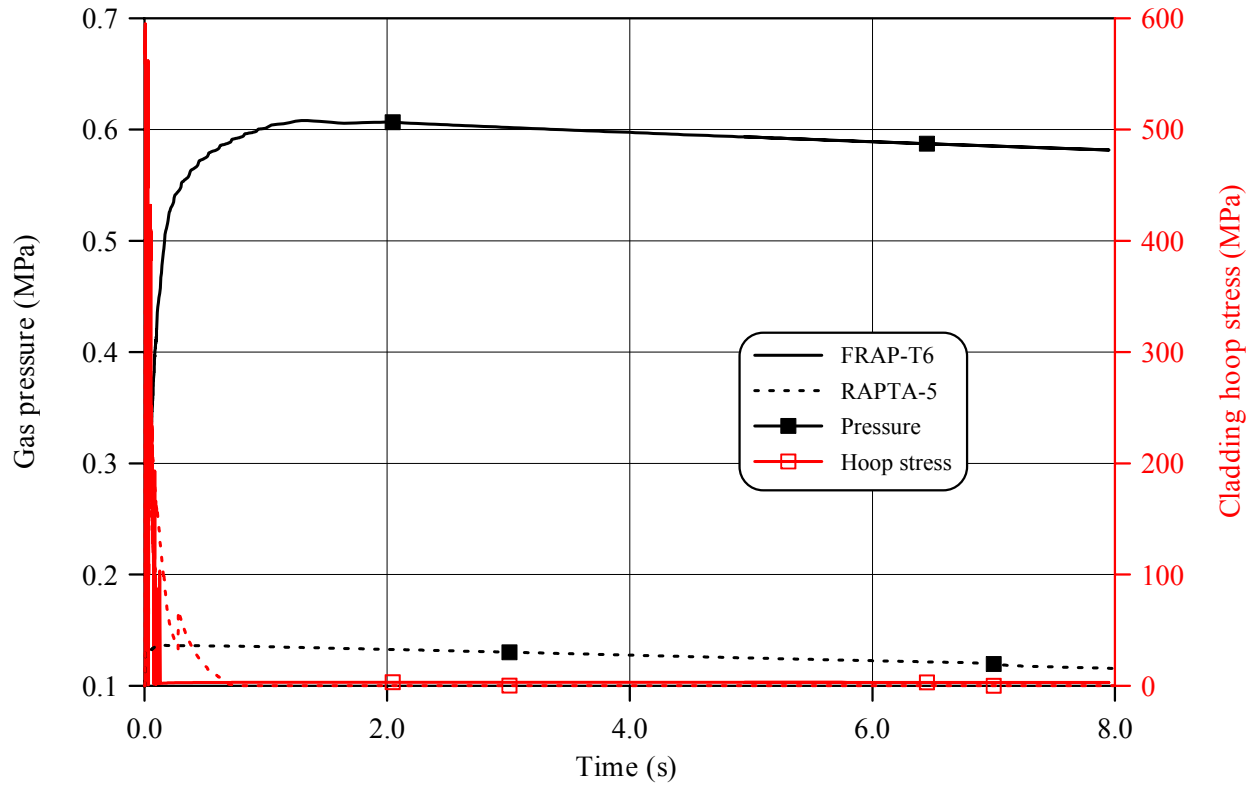


Fig.E-9.13. Mechanical behavior of fuel rod # RT9 during the BGR test in accordance with FRAP-T6/VVER and RAPTA-5 calculations

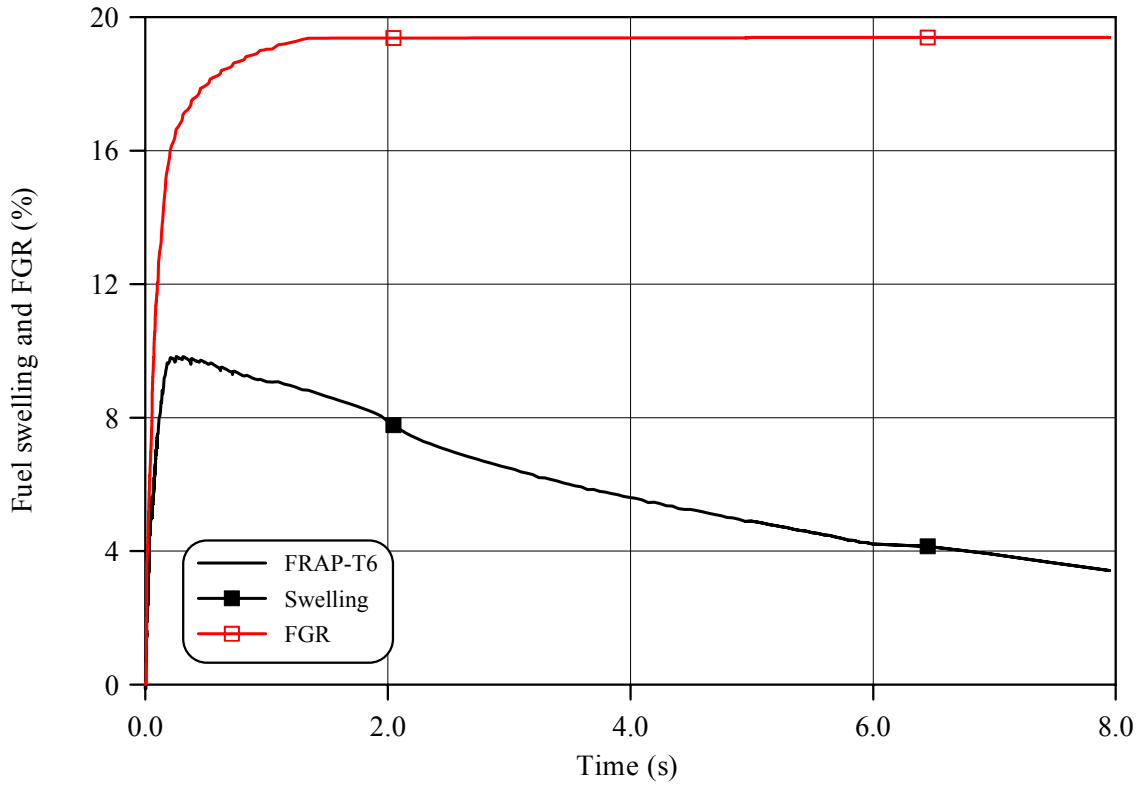
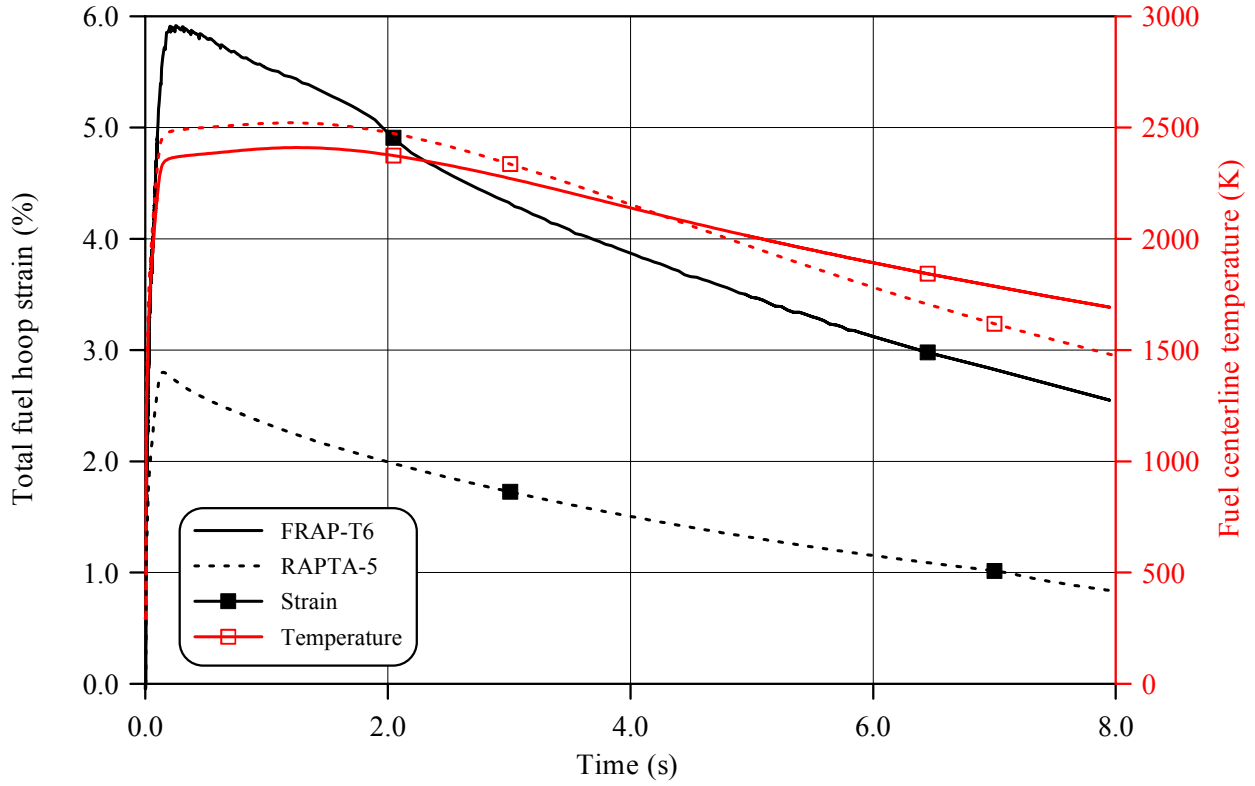


Fig.E-9.14. Fuel behavior during the BGR test of fuel rod # RT9 in accordance with FRAP-T6/VVER and RAPTA-5 calculations

RT9

Table E-9.3. Axial distribution of cladding average outer diameter in fuel rod # RT9*

| Axial coordinate (mm) | Cladding diameter (mm) | Axial coordinate (mm) | Cladding diameter (mm) | Axial coordinate (mm) | Cladding diameter (mm) | Axial coordinate (mm) | Cladding diameter (mm) |
|-----------------------|------------------------|-----------------------|------------------------|-----------------------|------------------------|-----------------------|------------------------|
| 8 | 9.185 | 46 | 9.804 | 84 | 9.695 | 122 | 9.710 |
| 10 | 9.265 | 48 | 9.741 | 86 | 9.859 | 124 | 9.648 |
| 12 | 9.321 | 50 | 9.726 | 88 | 9.944 | 126 | 9.553 |
| 14 | 9.334 | 52 | 9.770 | 90 | 9.734 | 128 | 9.577 |
| 16 | 9.330 | 54 | 9.753 | 92 | 9.569 | 130 | 9.673 |
| 18 | 9.350 | 56 | 9.687 | 94 | 9.580 | 132 | 9.694 |
| 20 | 9.404 | 58 | 9.639 | 96 | 9.633 | 134 | 9.643 |
| 22 | 9.480 | 60 | 9.668 | 98 | 9.623 | 136 | 9.592 |
| 24 | 9.551 | 62 | 9.733 | 100 | 9.559 | 138 | 9.600 |
| 26 | 9.549 | 64 | 9.823 | 102 | 9.517 | 140 | 9.679 |
| 28 | 9.537 | 66 | 9.897 | 104 | 9.556 | 142 | 9.780 |
| 30 | 9.578 | 68 | 9.836 | 106 | 9.651 | 144 | 9.856 |
| 32 | 9.642 | 70 | 9.694 | 108 | 9.729 | 146 | 9.742 |
| 34 | 9.678 | 72 | 9.680 | 110 | 9.790 | 148 | 9.642 |
| 36 | 9.634 | 74 | 9.727 | 112 | 9.802 | 150 | 9.638 |
| 38 | 9.625 | 76 | 9.734 | 114 | 9.680 | 152 | 9.624 |
| 40 | 9.677 | 78 | 9.688 | 116 | 9.569 | 154 | 9.520 |
| 42 | 9.763 | 80 | 9.645 | 118 | 9.555 | 156 | 9.399 |
| 44 | 9.801 | 82 | 9.646 | 120 | 9.636 | 158 | 9.248 |

* Measured value determined on the basis of profilometry data (16 azimuthal directions)

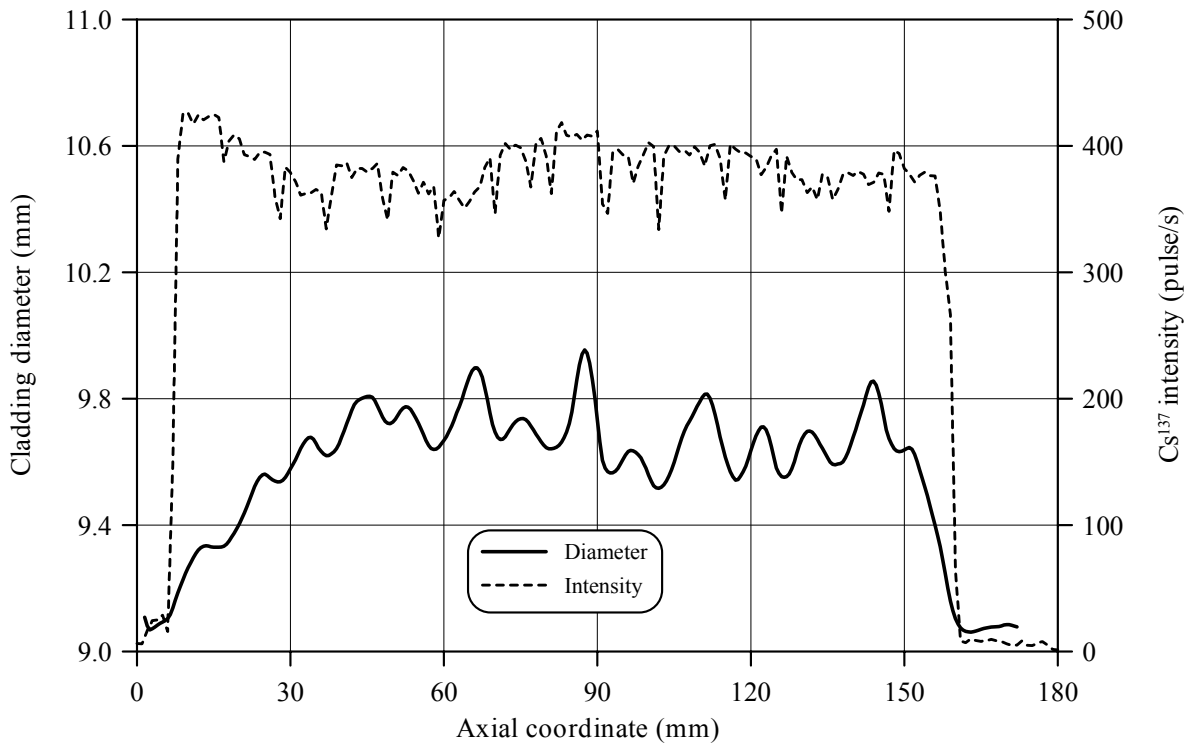


Fig.E-9.15. Cladding measured average diameter and γ -scanning results for fuel rod # RT9

Table E-9.4. The PIE results for fuel rod # RT9

| Parameter | | Value |
|-----------|--|-----------------------|
| 1. | Cladding outer diameter (mm): | |
| 1.1. | Maximum diameter of the bidimensional data sample in "fuel rod length - azimuthal angle" coordinates (mm) | 10.37 |
| 1.2. | Averaged azimuthal diameter and maximum diameter along the length selected from the sample of averaged azimuthal diameter (mm) | 9.95 |
| 1.3. | Averaged diameter of the bidimensional data sample in "fuel rod length - azimuthal angle" coordinates (mm) | 9.62 |
| 2. | Cladding residual hoop strain (%): | |
| 2.1. | Maximum hoop strain | 9.60 |
| 2.2. | Hoop strain at rupture | 9.1; 9.6; 8.2; 8.6 |
| 3. | Fuel pellet conditional diameter (mm) in cross-section*: | |
| | at 69 mm elevation | 8.21 |
| | at 88 mm elevation | 8.19 |
| | at 110 mm elevation | 8.24 |
| | at 144 mm elevation | 8.20 |
| 4. | ZrO ₂ outer thickness (μm) in cross-section: | |
| | at 69, 88, 110, 144 mm elevations | 5 |
| 5. | ZrO ₂ inner thickness (μm) in cross-section: | |
| | at 69 mm elevation | 8 |
| | at 110 mm elevation | 8 |
| 6. | Parameters characterizing FGR: | |
| 6.1. | Gas composition (% by volume): | |
| | He | - |
| | N ₂ | - |
| | O ₂ | - |
| | Ar | - |
| | CO ₂ | - |
| | Kr | - |
| | Xe | - |
| 6.2. | Free gas volume (cm ³) | - |
| 6.3. | Gas volume under normal conditions (cm ³) | - |
| 6.4. | Gas pressure under normal conditions (MPa) | - |

* Reference value determined by the processing of fuel cross-section photographs

RT9

Table E-9.5. Organized BGR test results for fuel rod # RT9

| Parameter | | Unit | Value | | |
|-----------|---|---------------------|----------|------------|---------|
| | | | Measured | Calculated | |
| | | | | FRAP-T6 | RAPTA-5 |
| 1. | Fuel burnup | MW d/kg U | 59.9 | 59.9 | 59.9 |
| 2. | Initial gas pressure | MPa | 0.1 | 0.1 | 0.1 |
| 3. | Energy deposition | cal/g fuel | 200.9 | 200.9 | 200.9 |
| 4. | Peak fuel enthalpy* | cal/g fuel | - | 162.4 | 167.5 |
| 5. | Fuel maximum temperature | K | - | 2524 | 2584 |
| 6. | Maximum temperature of cladding outer surface | K | - | 1164 | 1249 |
| 7. | Cladding burst | Failed, Unfailed | Failed | -** | -** |
| 8. | Cladding residual hoop strain | | | | |
| | - average*** | % | 6.27 | 4.41 | 2.77 |
| | - maximum | % | 9.60 | 4.98 | 2.77 |

* Average value of peak fuel enthalpy 164.9 cal/g fuel

** This parameter was not calculated

*** Average value along the fuel stack length

Appendix E-10
Individual Characteristics of Fuel Rod # RT10
after the BGR Test

RT10

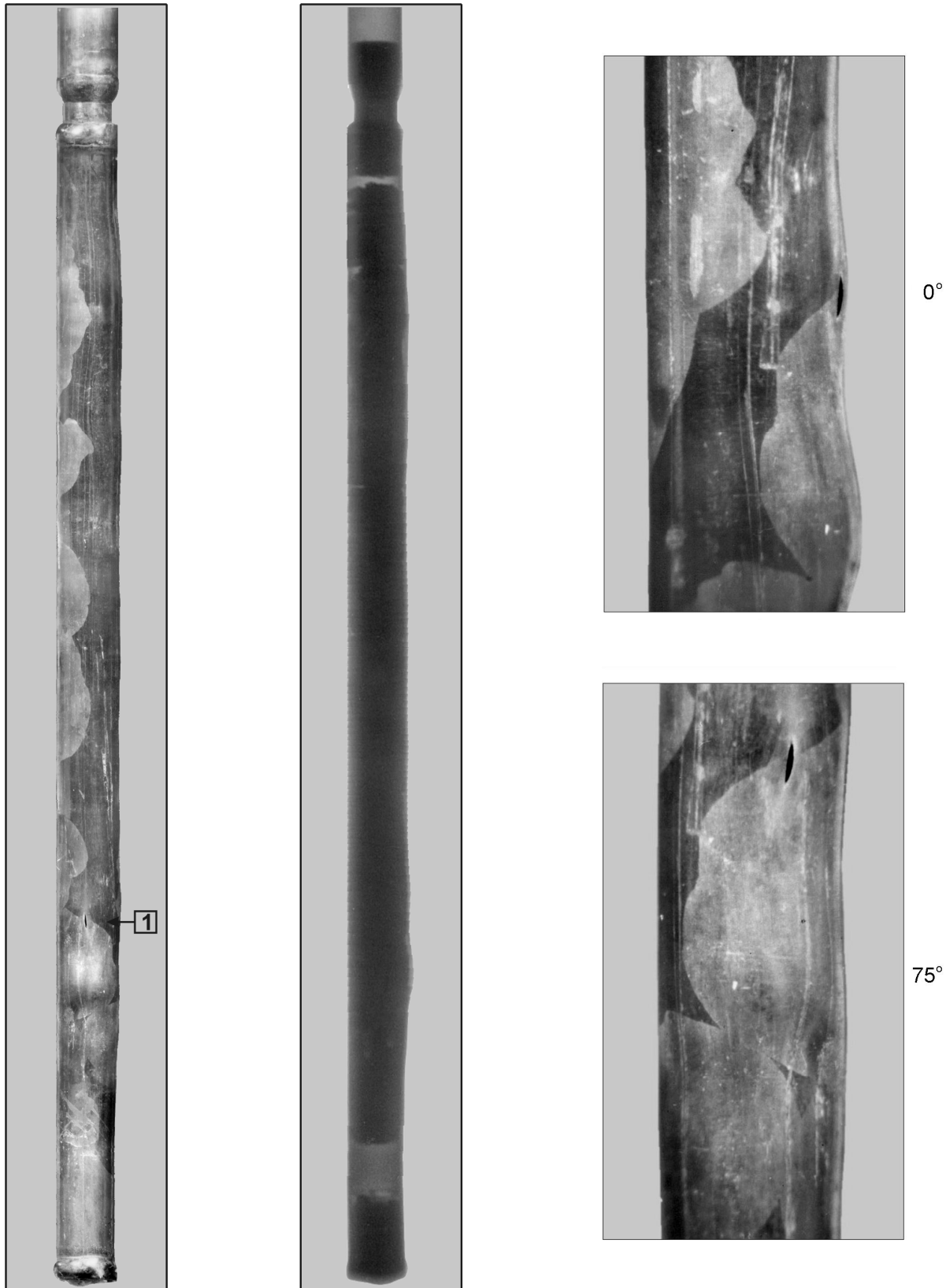


Fig.E-10.1. Appearance of failed fuel rod # RT10 after the BGR test (photographs and X-ray photograph)

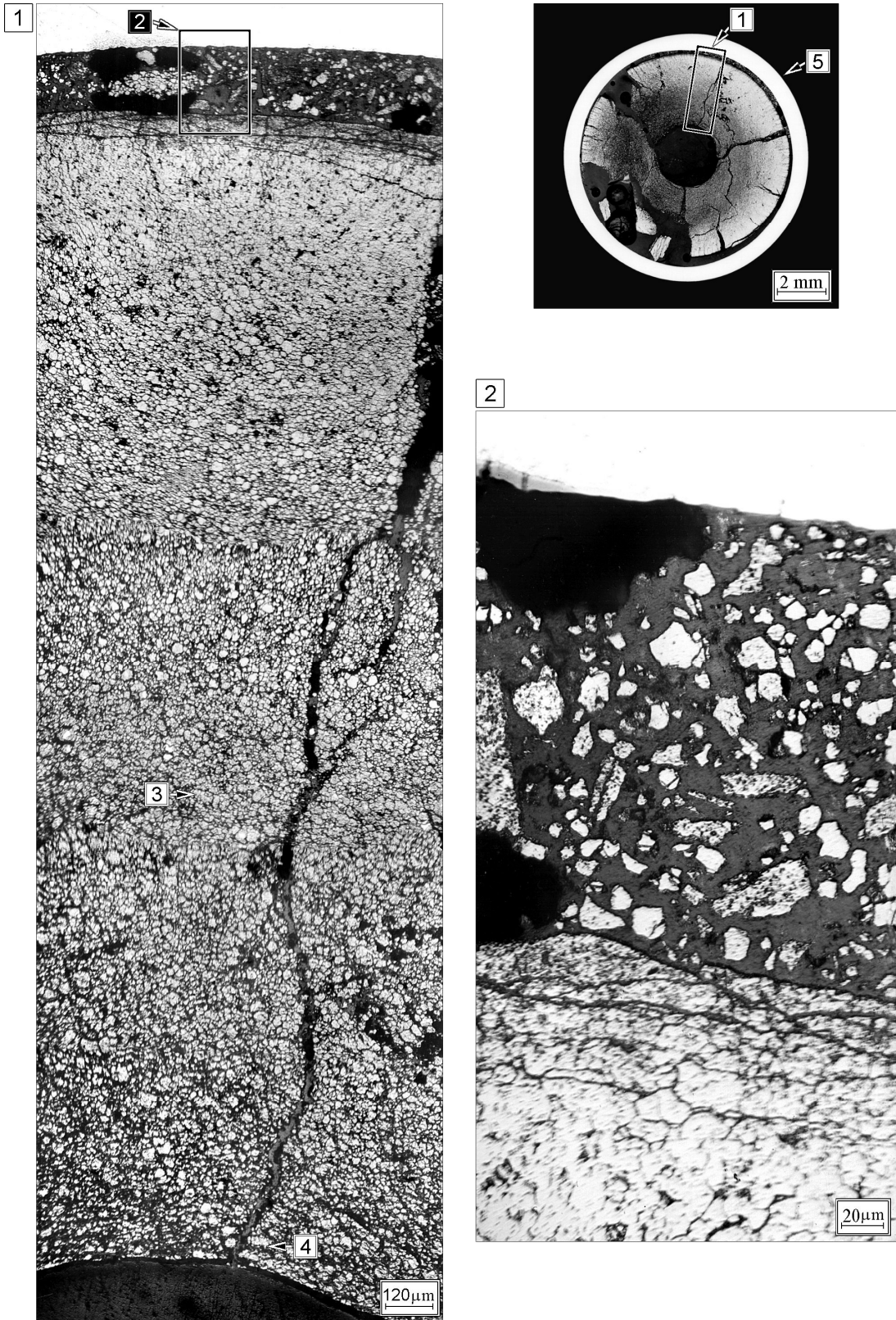


Fig.E-10.2. Cross-section and fuel microstructure of fuel rod # RT10 at 33 mm elevation (from low cap)

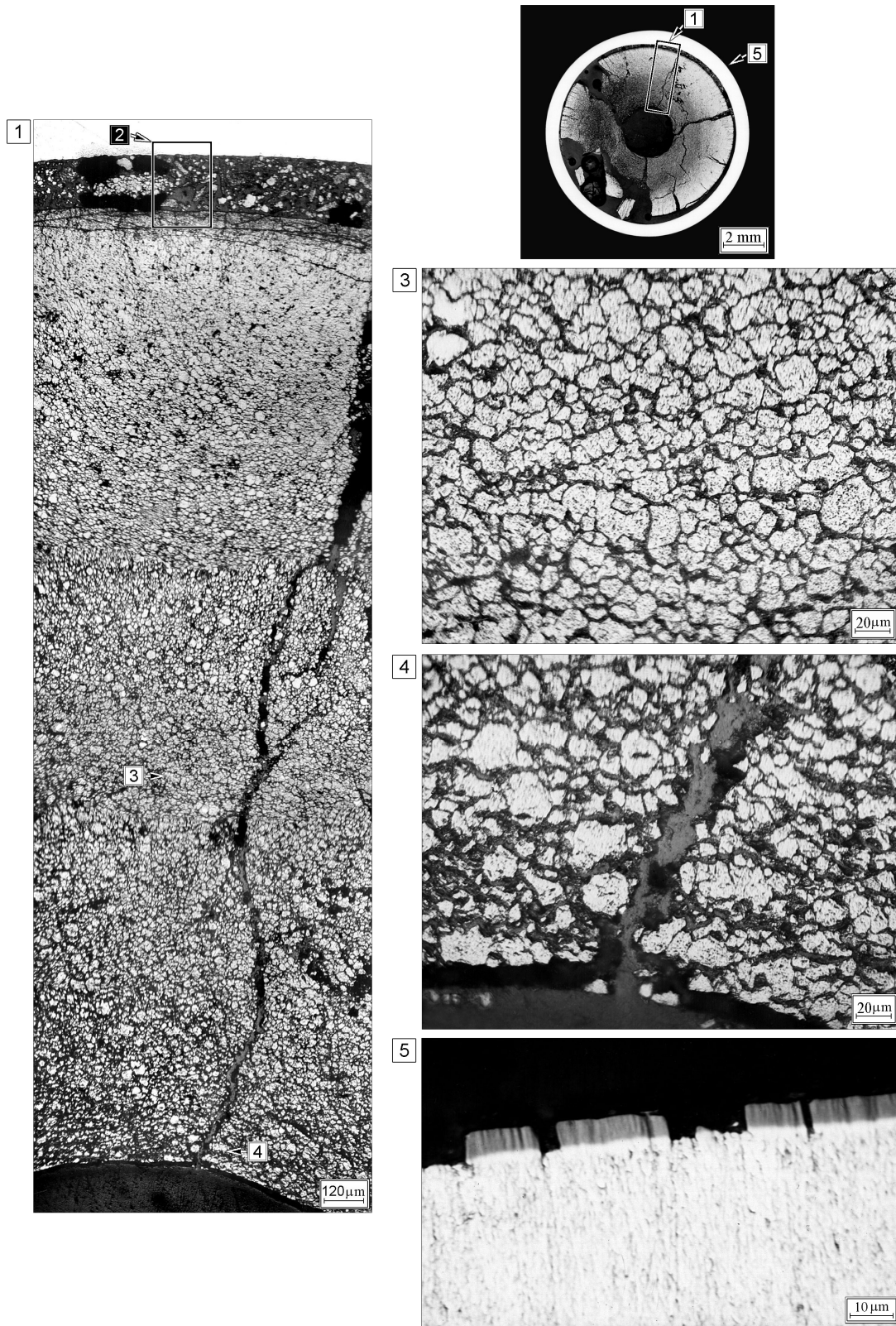


Fig.E-10.3. Cross-section and microstructure of fuel and cladding of fuel rod # RT10 at 33 mm elevation (from low cap)

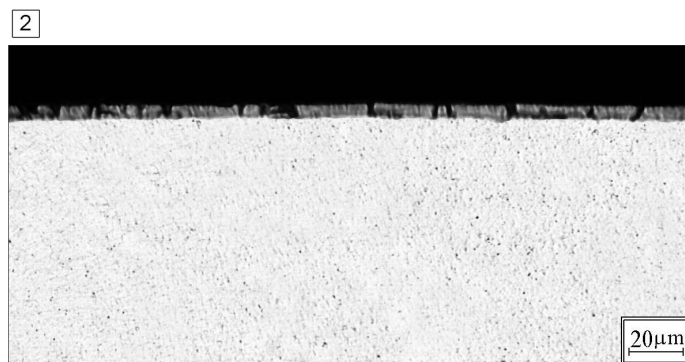
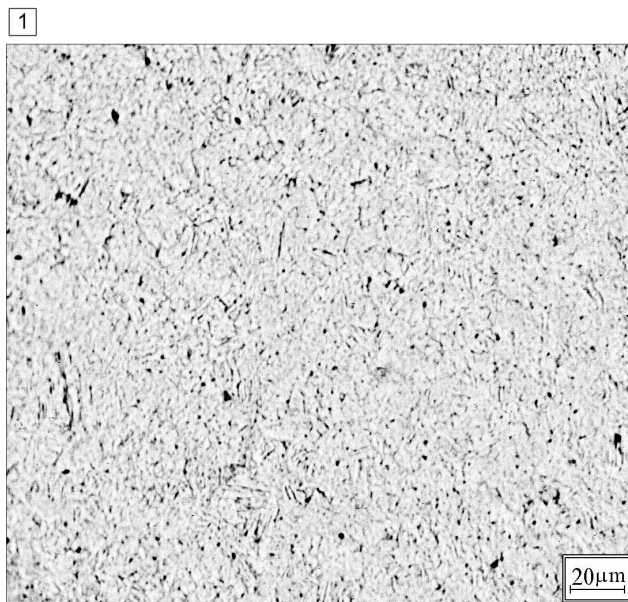
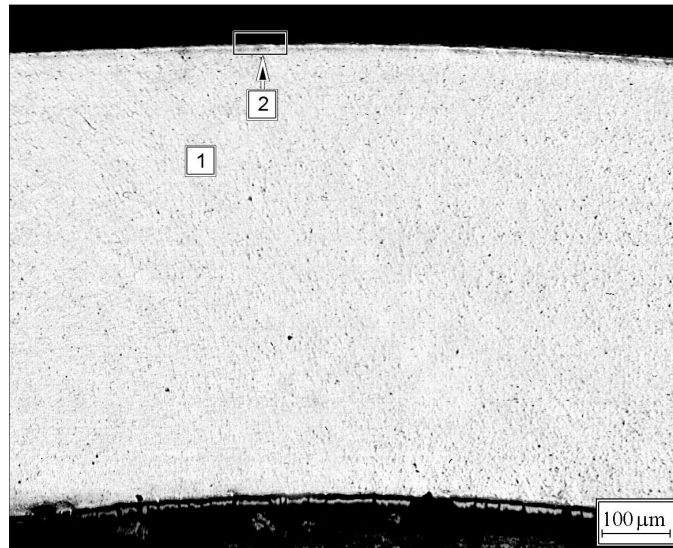


Fig.E-10.4. Cladding microstructure of fuel rod # RT10 at 33 mm elevation (from low cap)

RT10

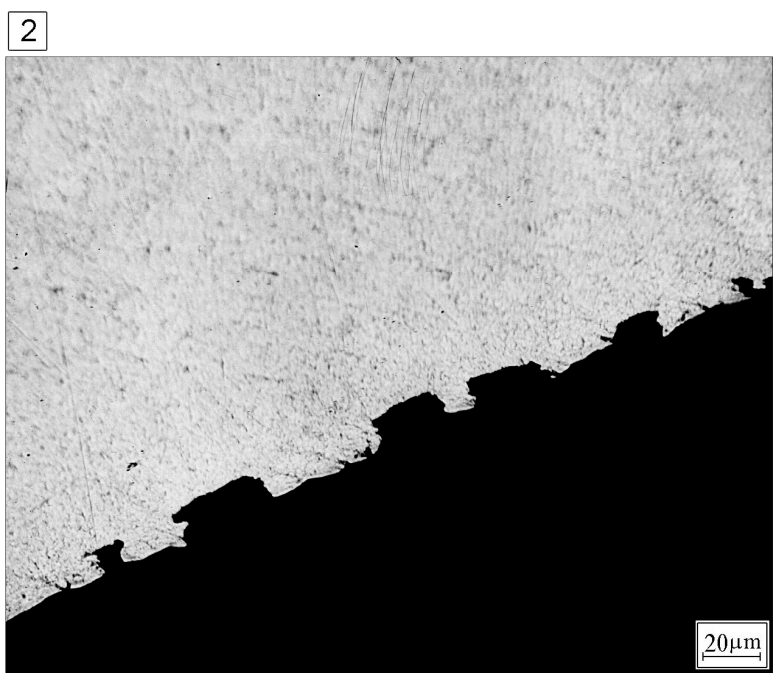
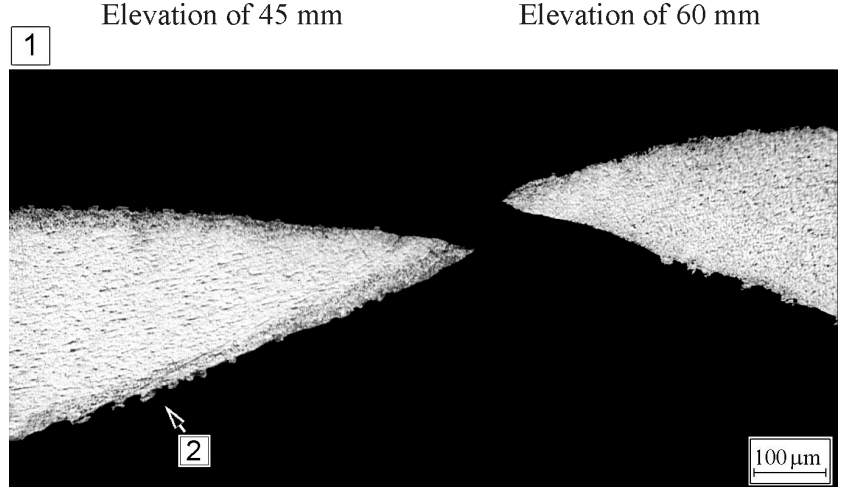
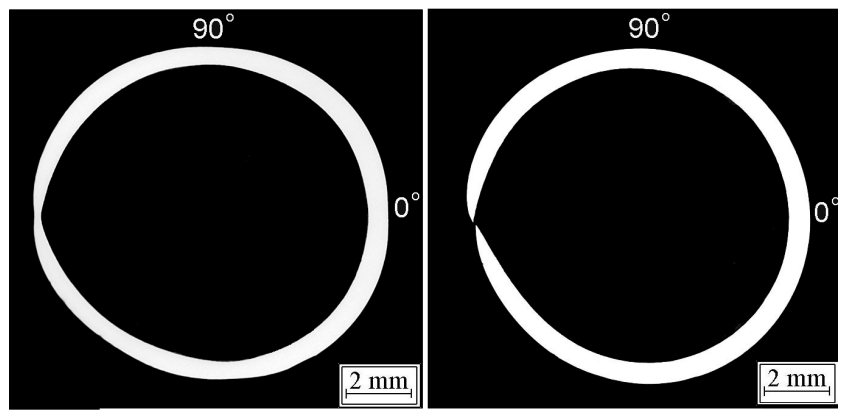


Fig.E-10.5. Cladding cross-sections at elevations 45 and 60 mm and cladding microstructure at 60 mm elevation (from low cap) for fuel rod # RT10

Table E-10.1. Time dependent energy characteristics of fuel rod # RT10

| Time (s) | Relative reactor power (current/maximum value) (per-unit) | Cumulative number of fissions in fuel rod (fiss) x10 ⁻¹⁴ | Power of fuel rod ¹⁾²⁾ (kW) | Energy deposition | | Fuel enthalpy ³⁾ | |
|----------|---|---|--|-------------------|------------|-----------------------------|---------|
| | | | | (cal/g fuel) | (J/g fuel) | FRAP-T6 | RAPTA-5 |
| 0.000 | 0.00E+00 | 0.000 | 0.000 | 0.000 | 0.000 | 0.000 | 0.000 |
| 0.001 | 9.16E-03 | 0.140 | 75.14 | 0.151 | 0.634 | 0.671 | 0.008 |
| 0.002 | 4.13E-02 | 0.748 | 338.9 | 0.811 | 3.397 | 0.671 | 0.048 |
| 0.003 | 1.85E-01 | 3.508 | 1516 | 3.803 | 15.92 | 0.671 | 0.195 |
| 0.004 | 6.20E-01 | 14.31 | 5085 | 15.52 | 64.96 | 1.091 | 0.805 |
| 0.005 | 9.98E-01 | 39.15 | 8186 | 42.50 | 177.9 | 4.076 | 3.976 |
| 0.006 | 6.84E-01 | 64.62 | 5613 | 70.07 | 293.4 | 15.499 | 15.977 |
| 0.007 | 3.18E-01 | 78.53 | 2607 | 85.21 | 356.7 | 41.590 | 42.989 |
| 0.008 | 1.50E-01 | 84.89 | 1229 | 92.13 | 385.7 | 68.273 | 70.367 |
| 0.009 | 8.59E-02 | 88.17 | 705.1 | 95.67 | 400.5 | 82.848 | 85.261 |
| 0.010 | 6.22E-02 | 90.27 | 510.7 | 97.93 | 410.0 | 89.376 | 91.781 |
| 0.012 | 5.26E-02 | 93.44 | 431.1 | 101.4 | 424.4 | 94.495 | 96.818 |
| 0.014 | 5.67E-02 | 96.53 | 465.2 | 104.8 | 438.6 | 97.283 | 99.638 |
| 0.016 | 6.50E-02 | 99.88 | 533.4 | 108.6 | 454.5 | 100.010 | 102.487 |
| 0.018 | 6.93E-02 | 103.8 | 568.7 | 112.8 | 472.3 | 103.191 | 105.803 |
| 0.020 | 6.68E-02 | 107.7 | 547.9 | 117.1 | 490.1 | 106.810 | 109.590 |
| 0.022 | 5.90E-02 | 111.6 | 484.4 | 121.0 | 506.6 | 110.476 | 113.402 |
| 0.024 | 5.04E-02 | 114.6 | 413.3 | 124.5 | 521.1 | 113.842 | 116.911 |
| 0.026 | 4.19E-02 | 117.4 | 343.9 | 127.4 | 533.2 | 116.717 | 119.900 |
| 0.028 | 3.51E-02 | 119.5 | 288.4 | 129.7 | 543.2 | 119.070 | 122.357 |
| 0.030 | 3.09E-02 | 121.4 | 253.4 | 131.8 | 551.8 | 120.976 | 124.333 |
| 0.050 | 2.64E-02 | 137.3 | 217.2 | 149.1 | 624.3 | 134.540 | 138.386 |
| 0.070 | 2.21E-02 | 151.7 | 181.6 | 164.5 | 688.6 | 146.907 | 150.845 |
| 0.090 | 1.54E-02 | 162.6 | 126.8 | 176.3 | 738.0 | 154.873 | 160.149 |
| 0.110 | 6.66E-03 | 168.8 | 54.79 | 183.1 | 766.6 | 160.862 | 165.043 |
| 0.130 | 2.39E-03 | 170.9 | 19.80 | 185.7 | 777.4 | 162.471 | 165.870 |
| 0.150 | 1.23E-03 | 171.9 | 10.33 | 186.8 | 782.2 | 162.444 | 165.233 |
| 0.200 | 4.18E-04 | 172.9 | 3.614 | 188.0 | 787.1 | 160.937 | 162.802 |
| 1.000 | 6.97E-05 | 175.6 | 0.700 | 191.2 | 800.5 | 148.795 | 147.640 |
| 10.00 | 8.13E-06 | 181.6 | 0.093 | 199.5 | 835.3 | 61.291 | 66.612 |
| 100.0 | 1.64E-07 | 184.5 | 0.004 | 204.8 | 857.5 | 6.053 | 10.345 |
| 1000 | 6.45E-13 | 184.6 | 1.65E-04 | 206.7 | 865.2 | 0.000 | 0.000 |

¹⁾ Average values determined in accordance with results of RRC KI and VNIIEF calculations

²⁾ Maximum power value is 8204 kW (t=0.00491 s)

³⁾ Average radial value

RT10**Table E-10.2. Radial energy characteristics of fuel rod # RT10***

| Parameters | Coordinates of fuel radial layers (mm) | | | |
|---|--|--------------------------|--------------------------|--------------------------|
| | 1 layer (1.250-2.834) | 2 layer (2.834-3.452) | 3 layer (3.452-3.722) | 4 layer (3.722-3.808) |
| Number of fissions $\times 10^{-14}$ (fiss) | 8.317 | 5.305 | 3.238 | 1.607 |
| Fission density $\times 10^{-13}$ (fiss/g fuel) | 2.657 | 2.824 | 3.452 | 5.122 |
| Power ** (kW) | 3688 | 2356 | 1442 | 718.6 |
| Energy deposition (cal/g fuel) | 185.8 | 197.7 | 242.4 | 360.8 |
| Energy deposition (J/g fuel) | 778.1 | 827.8 | 1015 | 1511 |
| Energy deposition *** (per-unit) | 0.515 | 0.548 | 0.672 | 1.000 |

* Average values were determined in accordance with results of RRC KI and VNIIEF calculations

** The power for the entire length of each layer at time 0.00491 s

*** Energy deposition in current layer/energy deposition in 4th layer

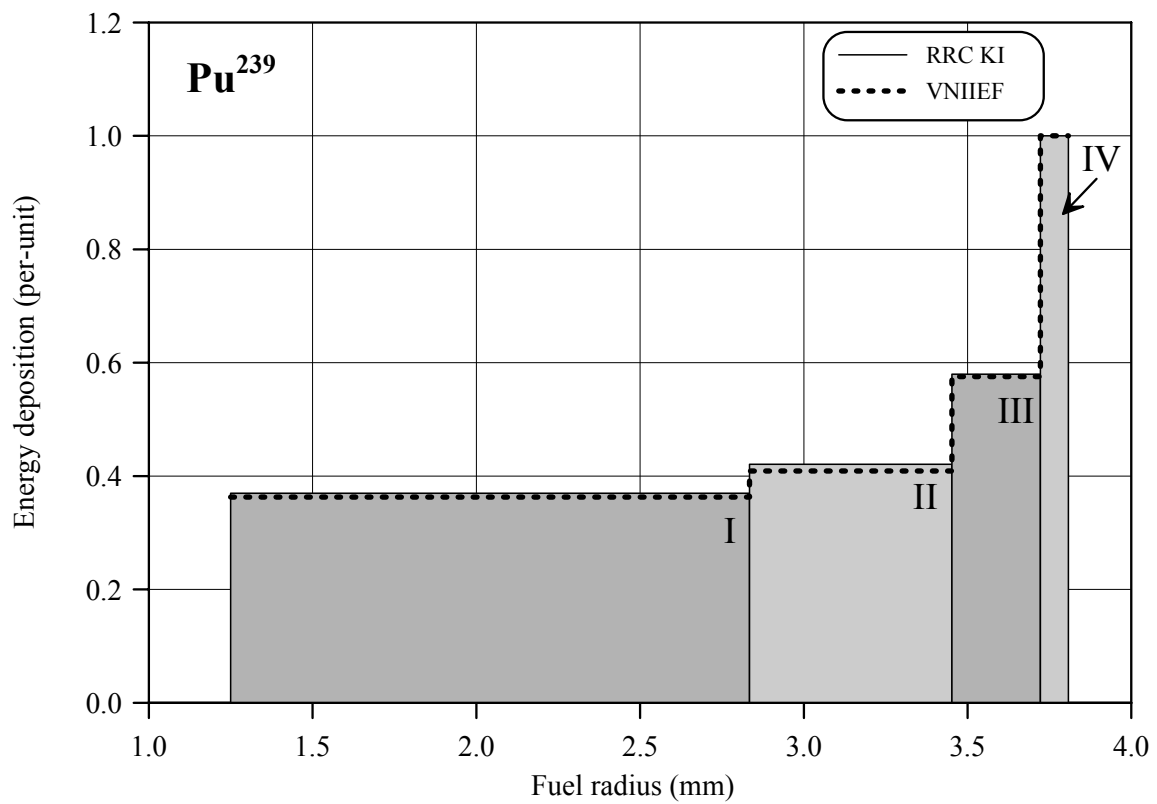
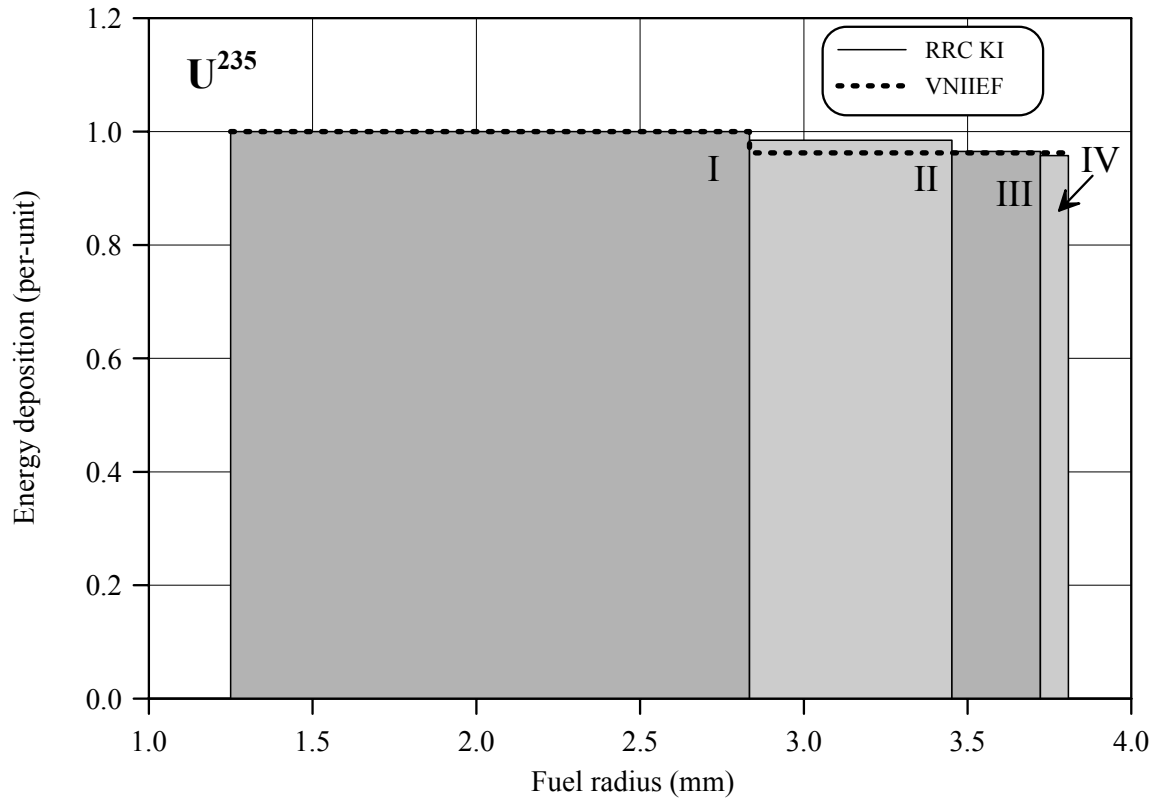


Fig.E-10.6. U²³⁵ and Pu²³⁹ radial distribution of energy deposition for fuel rod # RT10

RT10

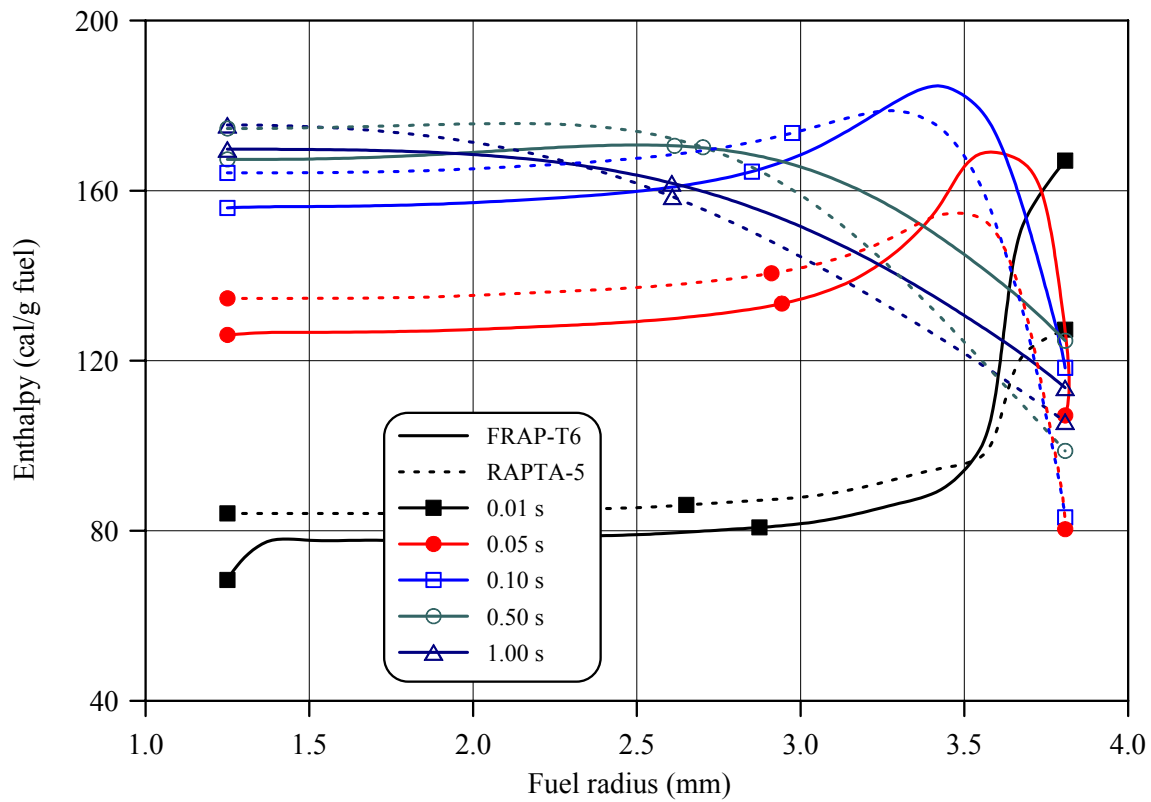
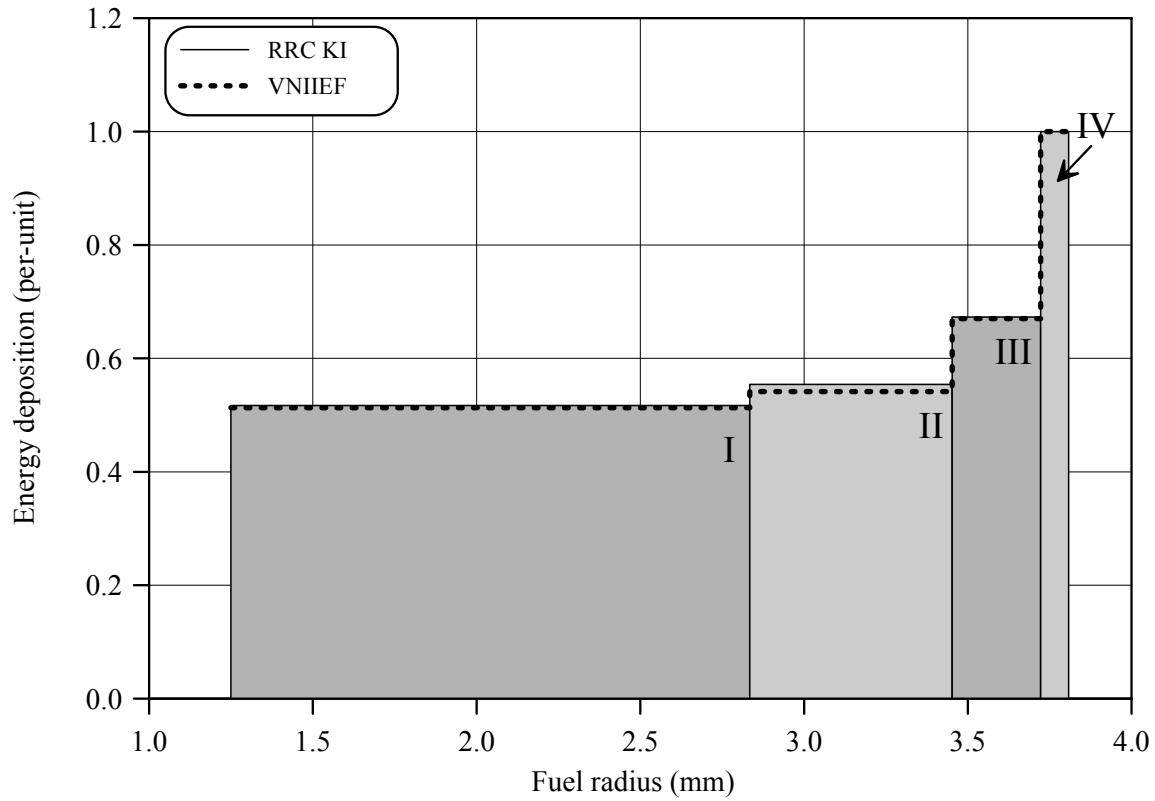


Fig.E-10.7. Radial distribution of energy deposition and fuel enthalpy for fuel rod # RT10

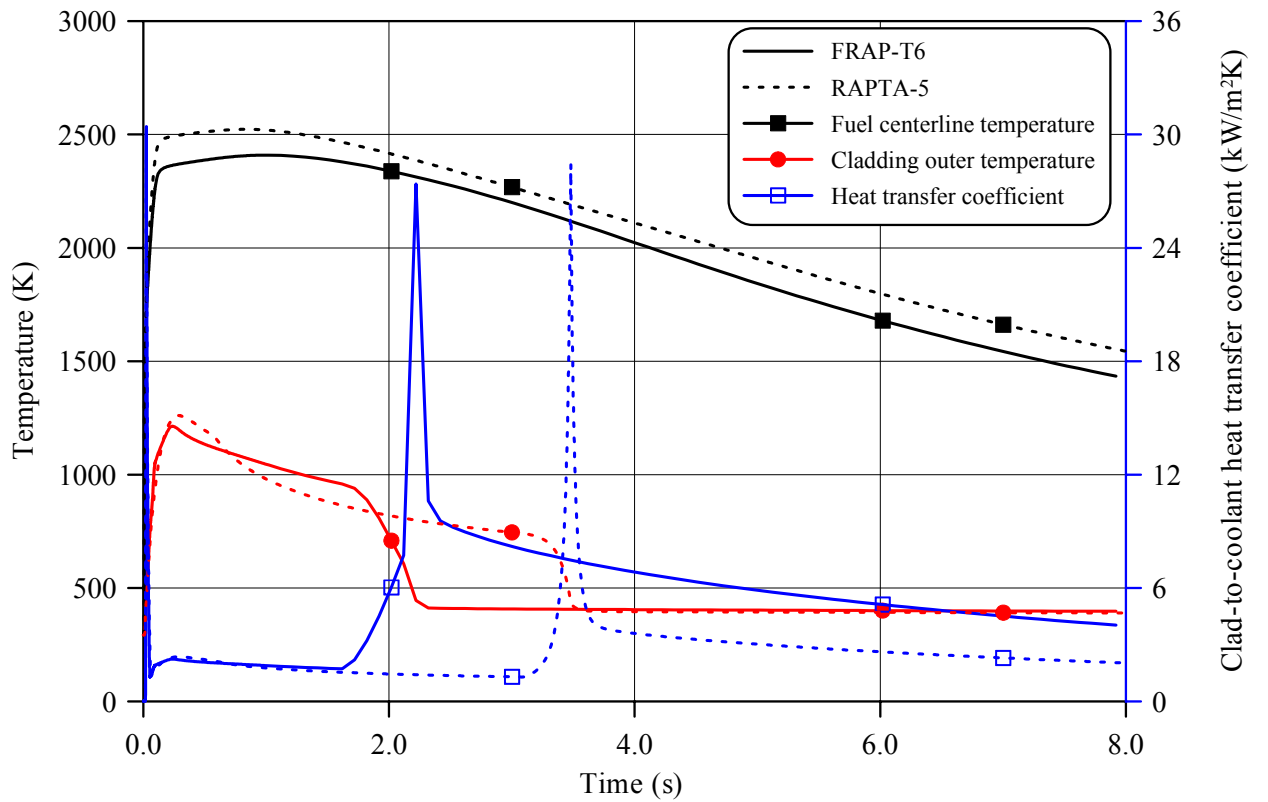
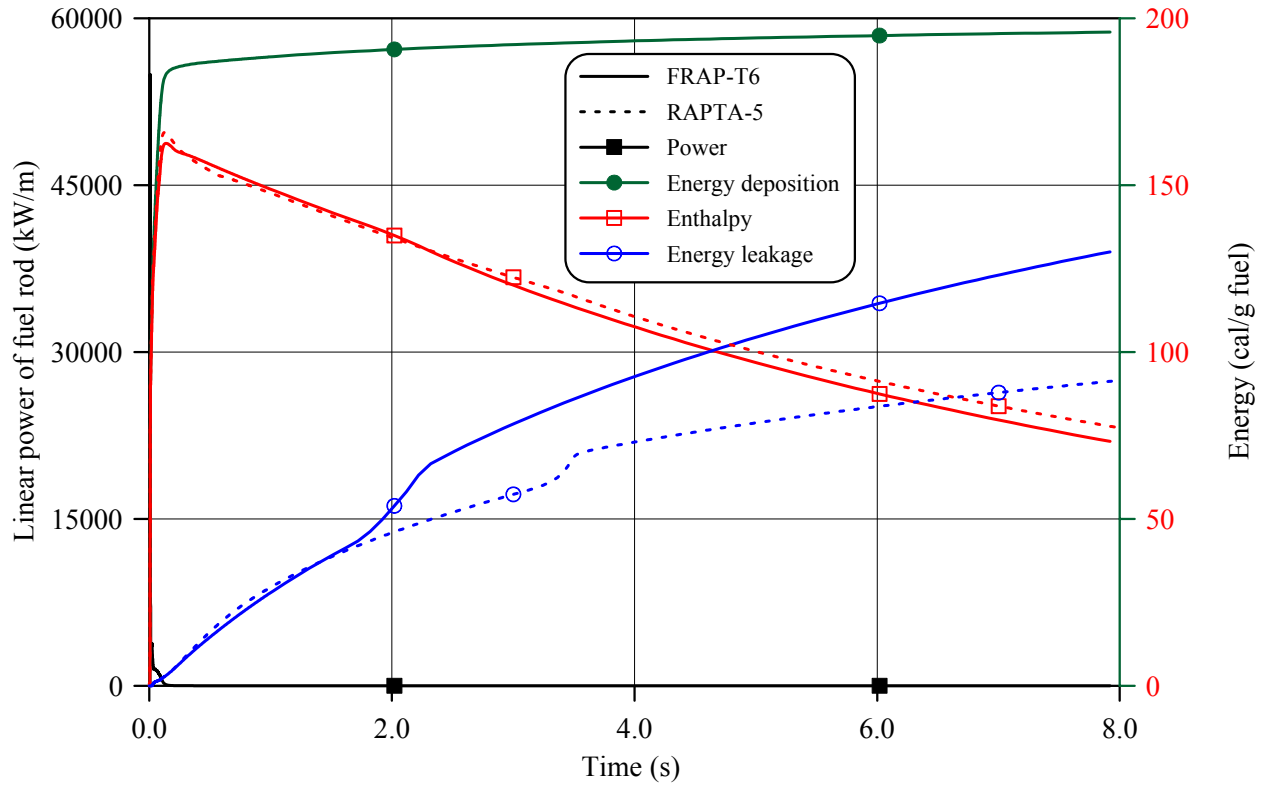


Fig.E-10.8. Thermal history of fuel rod # RT10 during the B1GR test in accordance with FRAP-T6/VVER and RAPTA-5 calculations

RT10

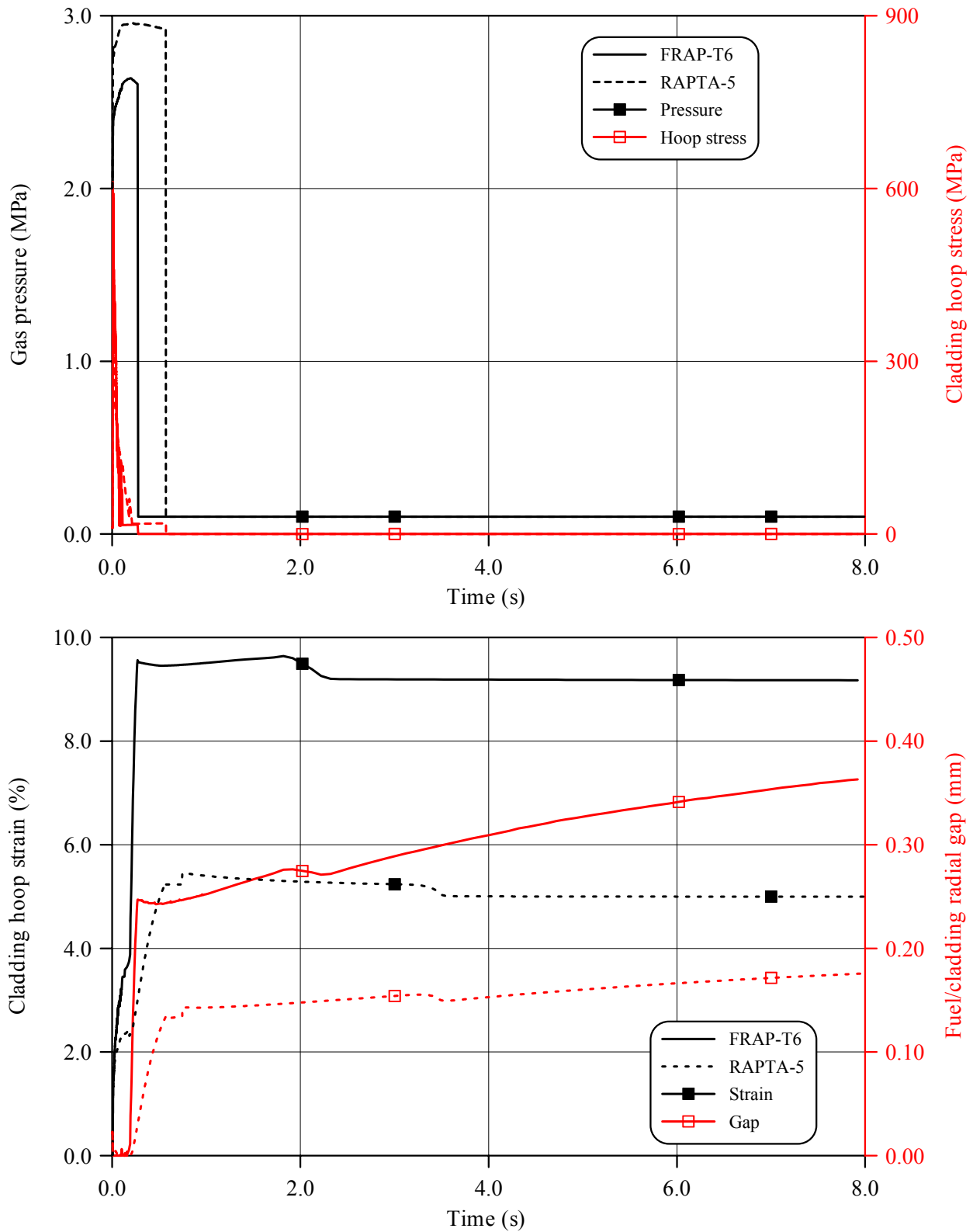


Fig.E-10.9. Mechanical behavior of fuel rod # RT10 during the BGR test in accordance with FRAP-T6/VVER and RAPTA-5 calculations

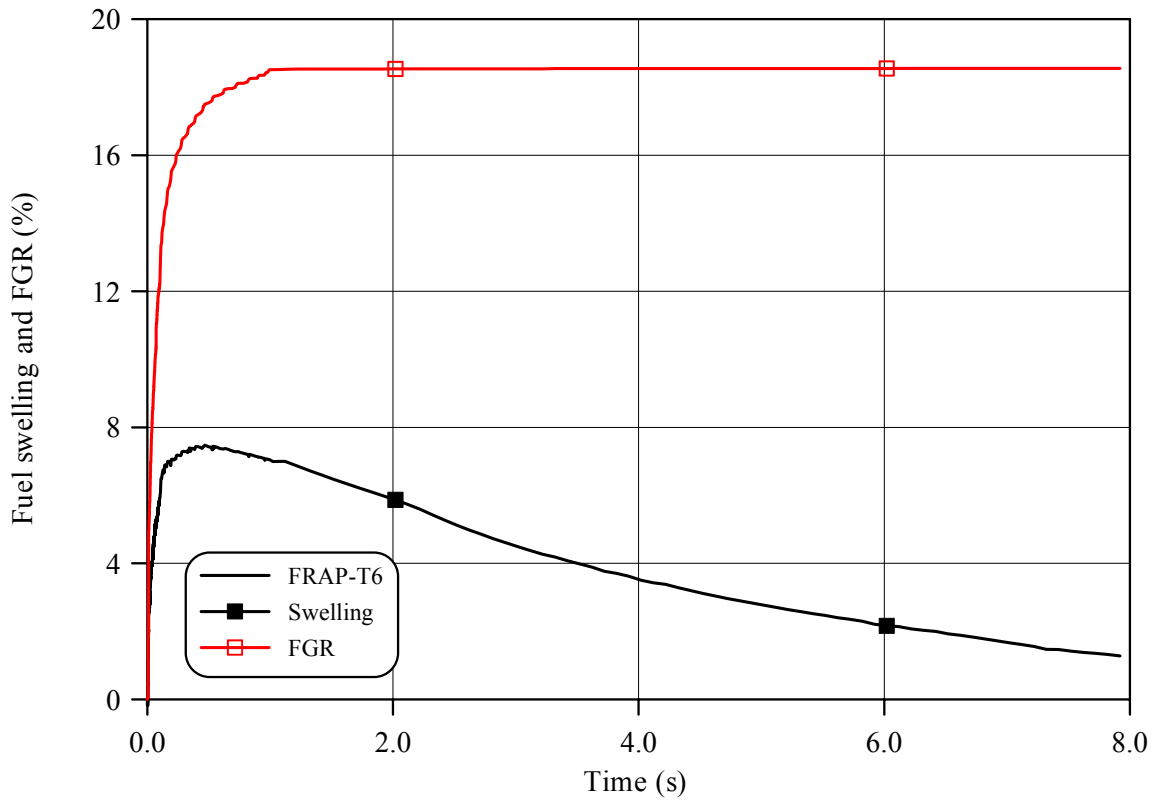
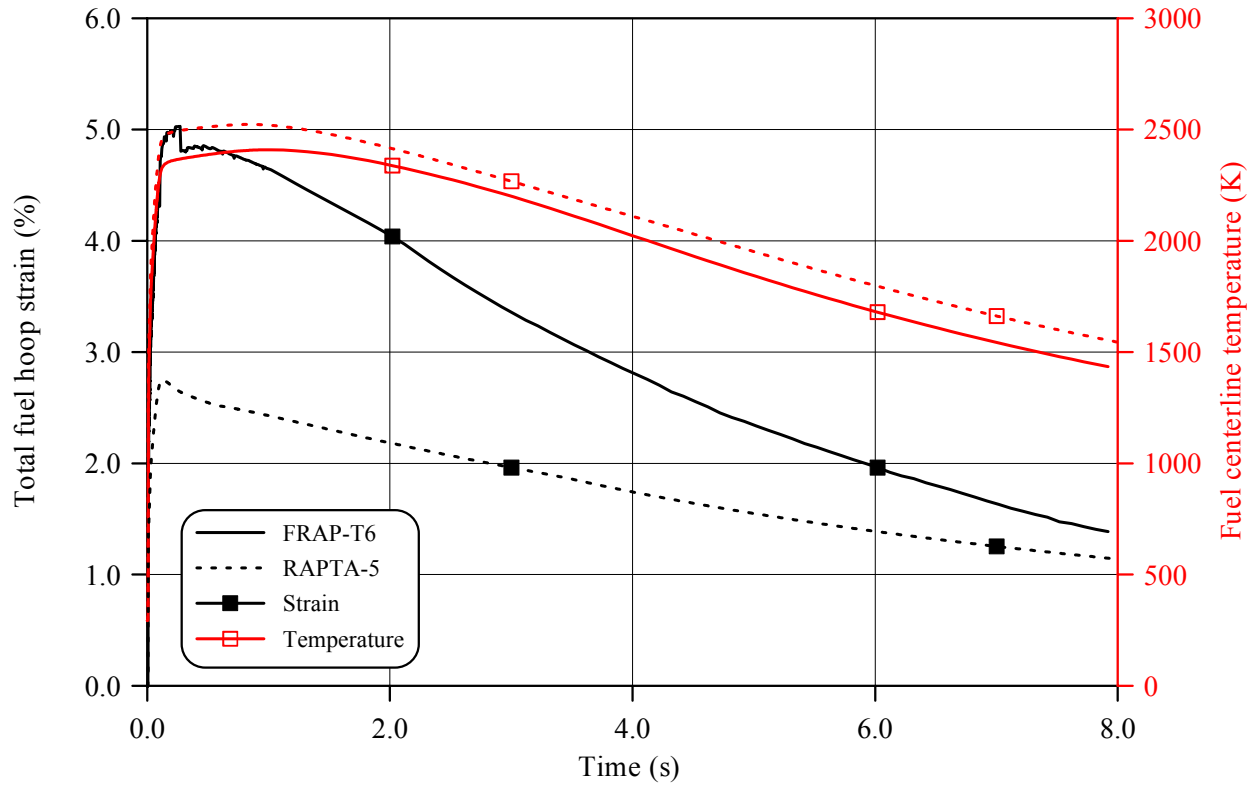


Fig.E-10.10. Fuel behavior during the BGR test of fuel rod # RT10 in accordance with FRAP-T6/VVER and RAPTA-5 calculations

RT10

Table E-10.3. Axial distribution of cladding average outer diameter in fuel rod # RT10*

| Axial coordinate (mm) | Cladding diameter (mm) | Axial coordinate (mm) | Cladding diameter (mm) | Axial coordinate (mm) | Cladding diameter (mm) | Axial coordinate (mm) | Cladding diameter (mm) |
|-----------------------|------------------------|-----------------------|------------------------|-----------------------|------------------------|-----------------------|------------------------|
| 24 | 9.394 | 62 | 10.219 | 100 | 9.962 | 138 | 9.999 |
| 26 | 9.435 | 64 | 10.099 | 102 | 9.987 | 140 | 10.031 |
| 28 | 9.496 | 66 | 10.084 | 104 | 10.000 | 142 | 10.068 |
| 30 | 9.588 | 68 | 10.104 | 106 | 9.976 | 144 | 10.106 |
| 32 | 9.755 | 70 | 10.112 | 108 | 9.930 | 146 | 10.129 |
| 34 | 9.931 | 72 | 10.090 | 110 | 9.871 | 148 | 10.161 |
| 36 | 10.081 | 74 | 10.033 | 112 | 9.821 | 150 | 10.213 |
| 38 | 10.149 | 76 | 10.037 | 114 | 9.814 | 152 | 10.197 |
| 40 | 10.284 | 78 | 10.084 | 116 | 9.819 | 154 | 10.118 |
| 42 | 10.566 | 80 | 10.110 | 118 | 9.819 | 156 | 10.050 |
| 44 | 10.754 | 82 | 10.109 | 120 | 9.802 | 158 | 9.977 |
| 46 | 10.747 | 84 | 10.066 | 122 | 9.781 | 160 | 9.918 |
| 48 | 10.588 | 86 | 10.000 | 124 | 9.784 | 162 | 9.885 |
| 50 | 10.377 | 88 | 9.979 | 126 | 9.852 | 164 | 9.771 |
| 52 | 10.230 | 90 | 10.011 | 128 | 9.936 | 166 | 9.604 |
| 54 | 10.250 | 92 | 10.025 | 130 | 9.996 | 168 | 9.444 |
| 56 | 10.330 | 94 | 10.018 | 132 | 10.028 | 170 | 9.311 |
| 58 | 10.394 | 96 | 10.010 | 134 | 10.020 | 172 | 9.186 |
| 60 | 10.356 | 98 | 9.984 | 136 | 9.983 | 174 | 9.166 |

* Measured value determined on the basis of profilometry data (16 azimuthal directions)

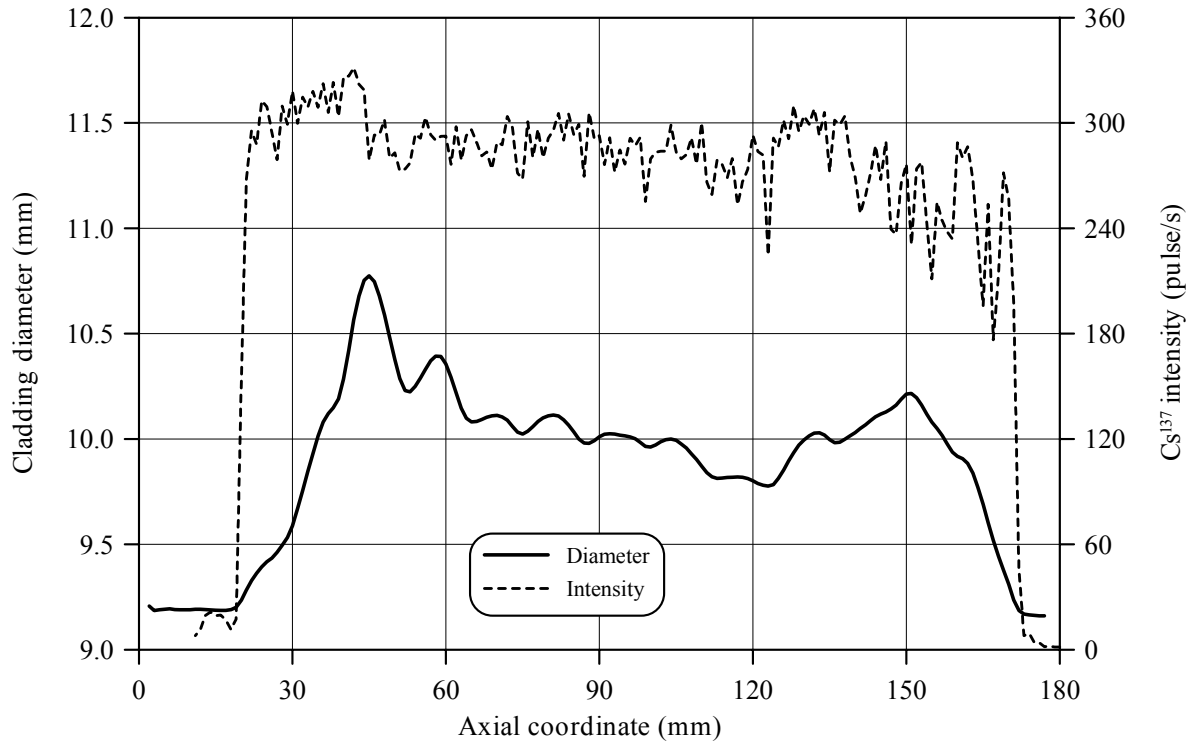


Fig.E-10.11. Cladding measured average diameter and γ -scanning results for fuel rod # RT10

Table E-10.4. The PIE results for fuel rod # RT10

| Parameter | | Value |
|-----------|--|-------|
| 1. | Cladding outer diameter (mm): | |
| 1.1. | Maximum diameter of the bidimensional data sample in "fuel rod length - azimuthal angle" coordinates (mm) | 11.03 |
| 1.2. | Averaged azimuthal diameter and maximum diameter along the length selected from the sample of averaged azimuthal diameter (mm) | 10.75 |
| 1.3. | Averaged diameter of the bidimensional data sample in "fuel rod length - azimuthal angle" coordinates (mm) | 9.88 |
| 2. | Cladding residual hoop strain (%): | |
| 2.1. | Maximum hoop strain | 18.90 |
| 2.2. | Hoop strain at rupture | 14.75 |
| 3. | Fuel pellet conditional diameter (mm) in cross-section*: | |
| | at 33 mm elevation | 8.19 |
| 4. | ZrO ₂ outer thickness (μm) in cross-section: | |
| | at 33, 45, 60 mm elevations | 4-7 |
| 5. | ZrO ₂ inner thickness (μm) in cross-section: | |
| | at 45, 60 mm elevations | 0 |
| 6. | Parameters characterizing FGR: | |
| 6.1. | Gas composition (% by volume): | |
| | He | - |
| | N ₂ | - |
| | O ₂ | - |
| | Ar | - |
| | CO ₂ | - |
| | Kr | - |
| | Xe | - |
| 6.2. | Free gas volume (cm ³) | - |
| 6.3. | Gas volume under normal conditions (cm ³) | - |
| 6.4. | Gas pressure under normal conditions (MPa) | - |

* Reference value determined by the processing of fuel cross-section photographs

RT10**Table E-10.5. Organized BGR test results for fuel rod # RT10**

| Parameter | | Unit | Value | | |
|-----------|---|---------------------|----------|------------|---------|
| | | | Measured | Calculated | |
| | | | | FRAP-T6 | RAPTA-5 |
| 1. | Fuel burnup | MW d/kg U | 47.0 | 47.0 | 47.0 |
| 2. | Initial gas pressure | MPa | 2.0 | 2.0 | 2.0 |
| 3. | Energy deposition | cal/g fuel | 206.7 | 206.7 | 206.7 |
| 4. | Peak fuel enthalpy* | cal/g fuel | - | 162.5 | 165.9 |
| 5. | Fuel maximum temperature | K | - | 2542 | 2578 |
| 6. | Maximum temperature of cladding outer surface | K | - | 1214 | 1261 |
| 7. | Cladding burst | Failed, Unfailed | Failed | Failed | Failed |
| 8. | Cladding residual hoop strain** | | | | |
| | - average | % | 8.94 | 6.12 | 5.45 |
| | - maximum | % | 18.90 | 9.09 | 5.45 |

* Average value of peak fuel enthalpy 164.2 cal/g fuel

** Average value along the fuel stack length

Appendix E-11
Individual Characteristics of Fuel Rod # RT11
after the BGR Test

RT11

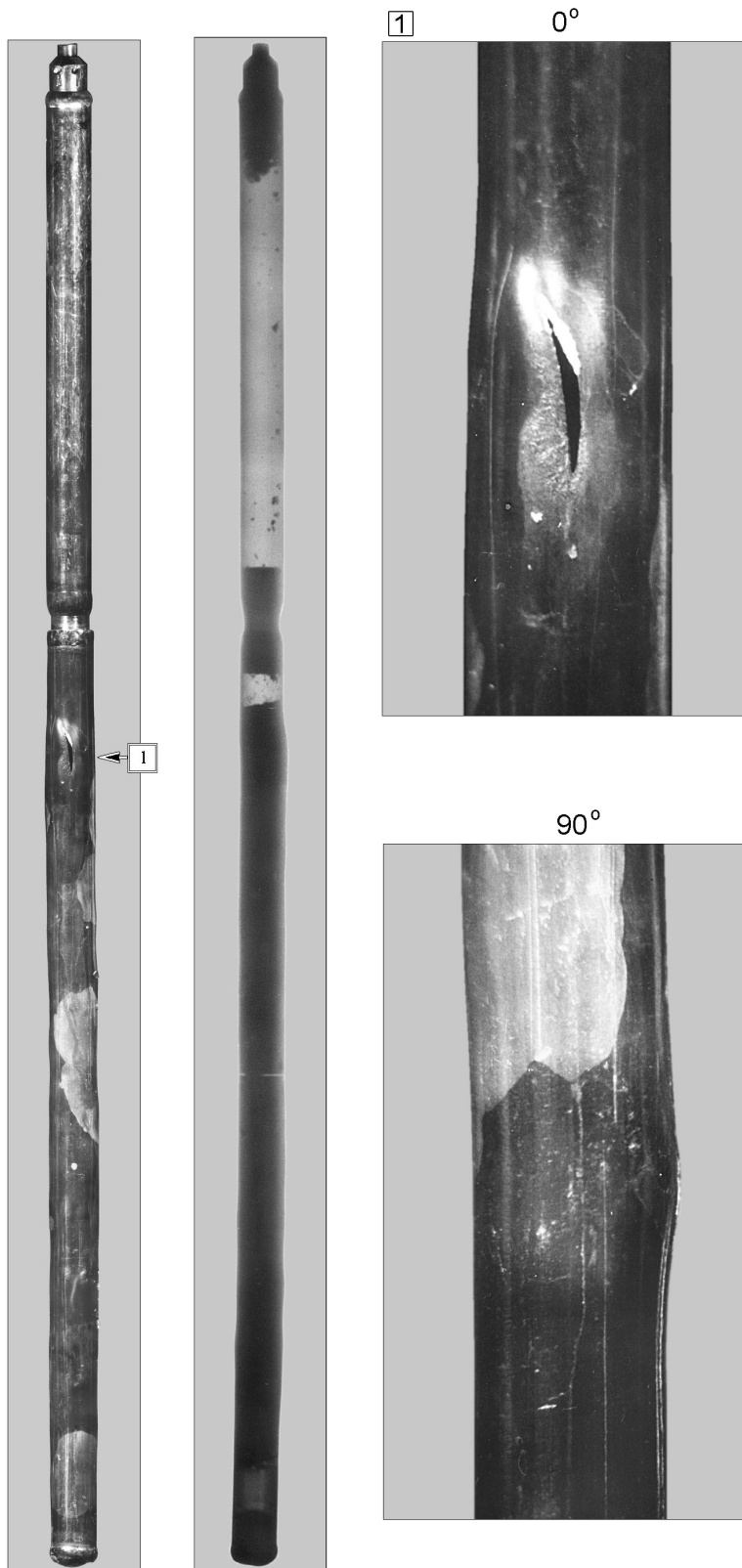


Fig.E-11.1. Appearance of failed fuel rod # RT11 after the BGR test (photographs and X-ray photograph)

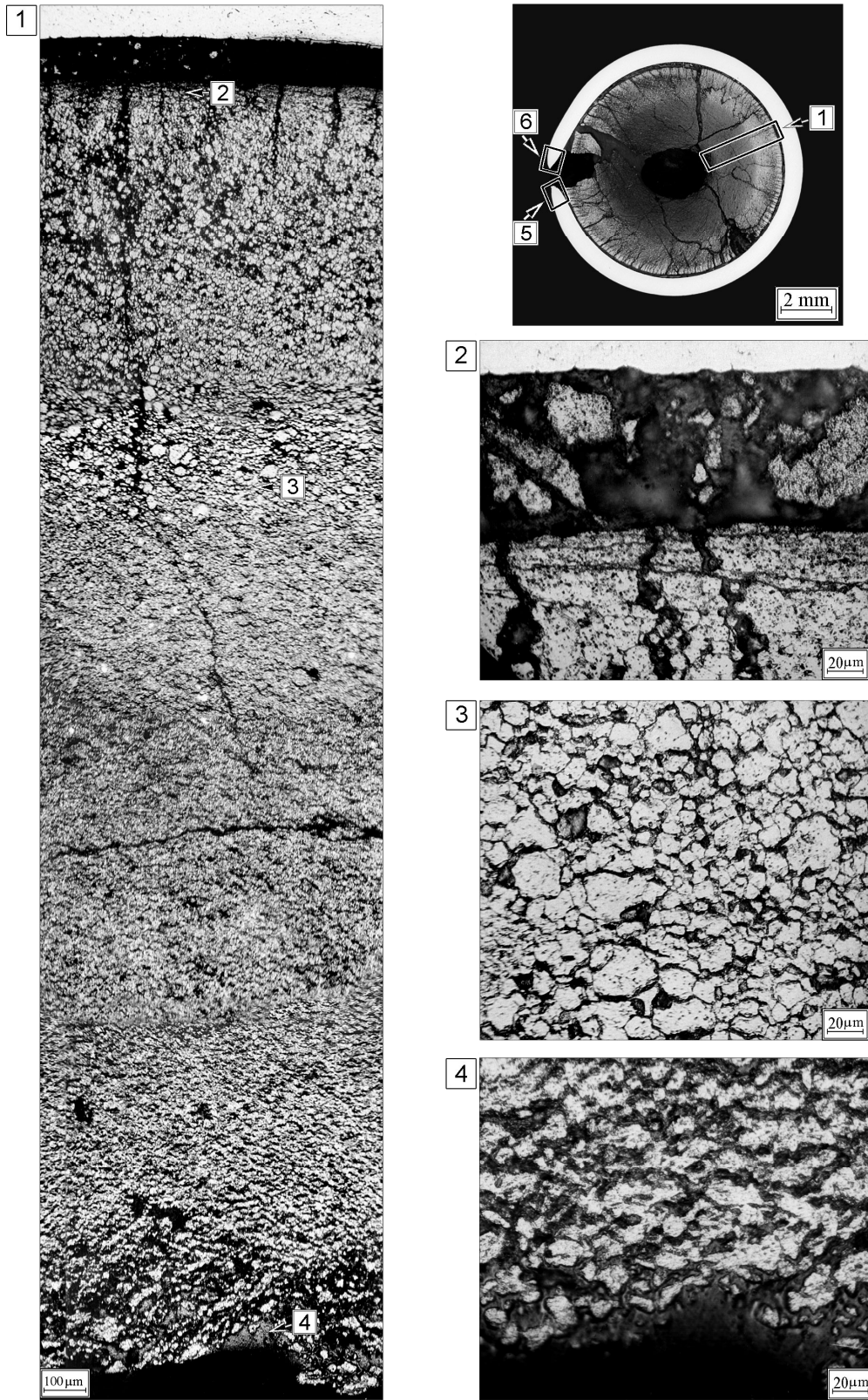


Fig.E-11.2. Cross-section and fuel microstructure of fuel rod # RT11 at 157 mm elevation (from low cap)

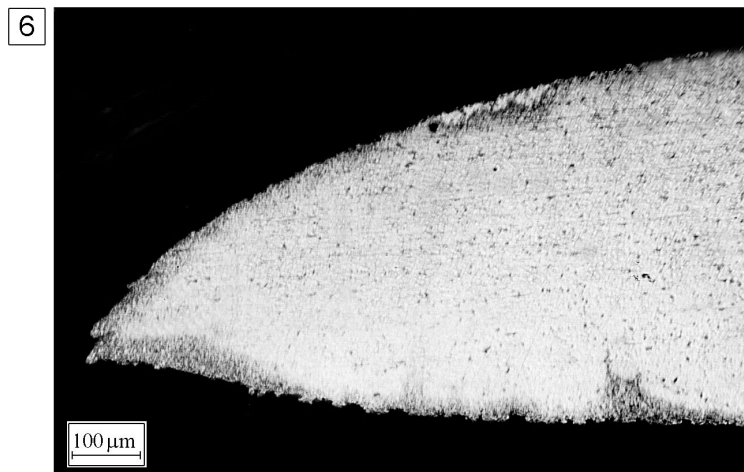
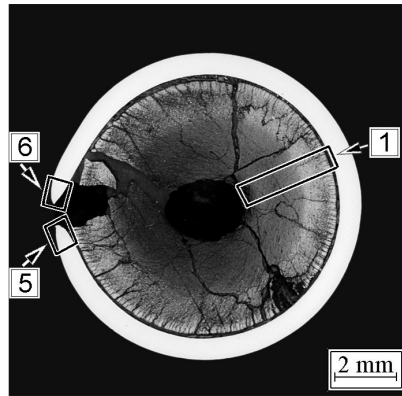
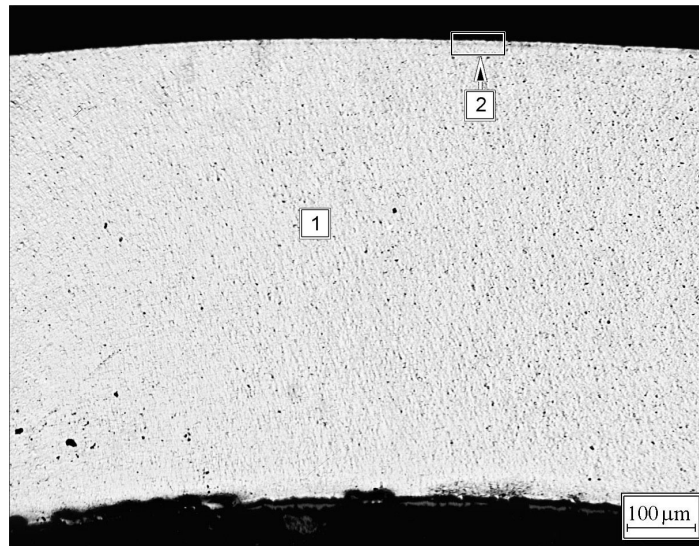
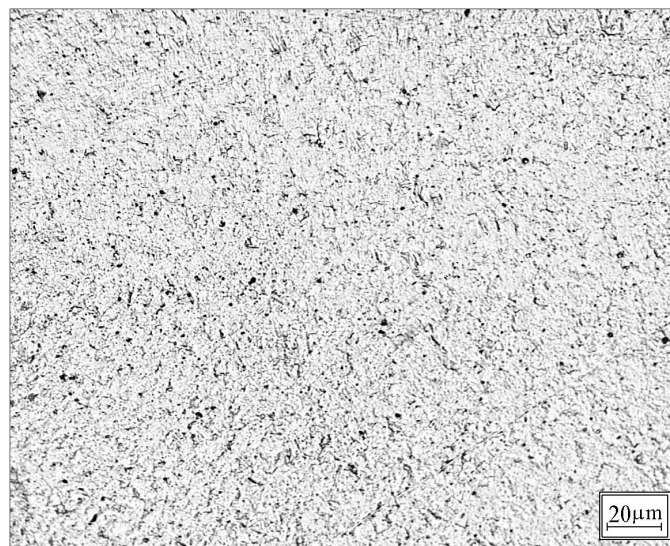


Fig.E-11.3. Cross-section and cladding microstructure of fuel rod # RT11 in the burst area at 157 mm elevation (from low cap)



1



2

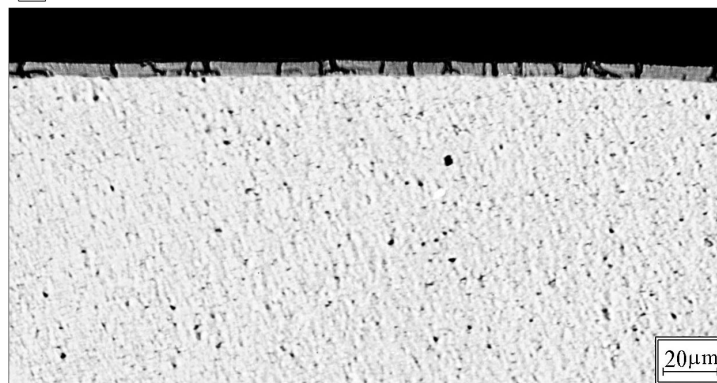


Fig.E-11.4. Cladding microstructure of fuel rod # RT11 at 157 mm elevation (from low cap)

RT11

Table E-11.1. Time dependent energy characteristics of fuel rod # RT11

| Time (s) | Relative reactor power (current/maximum value) (per-unit) | Cumulative number of fissions in fuel rod (fiss) x 10 ⁻¹⁴ | Power of fuel rod ¹⁾²⁾ (kW) | Energy deposition | | Fuel enthalpy ³⁾ | |
|----------|---|--|--|-------------------|------------|-----------------------------|---------|
| | | | | (cal/g fuel) | (J/g fuel) | FRAP-T6 | RAPTA-5 |
| 0.000 | 0.00E+00 | 0.000 | 0.000 | 0.000 | 0.000 | 0.000 | 0.000 |
| 0.001 | 2.61E-03 | 0.039 | 22.11 | 0.042 | 0.177 | 0.671 | 0.041 |
| 0.002 | 1.16E-02 | 0.217 | 98.28 | 0.235 | 0.983 | 0.671 | 0.226 |
| 0.003 | 5.28E-02 | 1.024 | 447.3 | 1.108 | 4.637 | 1.345 | 1.121 |
| 0.004 | 2.29E-01 | 4.652 | 1942 | 5.023 | 21.03 | 5.256 | 5.196 |
| 0.005 | 6.89E-01 | 17.65 | 5836 | 19.04 | 79.72 | 18.922 | 19.396 |
| 0.006 | 9.93E-01 | 44.50 | 8414 | 48.02 | 201.1 | 46.962 | 48.187 |
| 0.007 | 6.32E-01 | 69.48 | 5352 | 75.04 | 314.2 | 73.074 | 74.807 |
| 0.008 | 2.89E-01 | 82.68 | 2451 | 89.26 | 373.7 | 86.708 | 88.540 |
| 0.009 | 1.38E-01 | 88.68 | 1171 | 95.76 | 400.9 | 92.802 | 94.659 |
| 0.010 | 8.17E-02 | 91.83 | 692.7 | 99.15 | 415.1 | 96.005 | 97.592 |
| 0.012 | 5.36E-02 | 95.59 | 453.8 | 103.3 | 432.3 | 99.478 | 100.921 |
| 0.014 | 5.43E-02 | 98.76 | 460.0 | 106.6 | 446.5 | 102.185 | 103.704 |
| 0.016 | 6.37E-02 | 102.2 | 539.7 | 110.4 | 462.2 | 105.277 | 106.937 |
| 0.018 | 7.36E-02 | 106.3 | 623.5 | 114.9 | 480.9 | 109.043 | 110.867 |
| 0.020 | 7.85E-02 | 111.1 | 665.4 | 119.8 | 501.5 | 113.303 | 115.318 |
| 0.022 | 7.36E-02 | 115.3 | 623.5 | 124.7 | 522.1 | 117.572 | 119.748 |
| 0.024 | 6.17E-02 | 119.3 | 522.9 | 129.1 | 540.5 | 121.301 | 123.610 |
| 0.026 | 4.96E-02 | 123.0 | 420.3 | 132.7 | 555.4 | 124.284 | 126.707 |
| 0.028 | 4.02E-02 | 125.6 | 340.6 | 135.5 | 567.5 | 126.612 | 129.092 |
| 0.030 | 3.43E-02 | 127.8 | 290.4 | 137.9 | 577.4 | 128.479 | 131.024 |
| 0.050 | 2.75E-02 | 144.9 | 232.9 | 156.4 | 654.7 | 143.008 | 145.560 |
| 0.070 | 2.46E-02 | 160.1 | 208.8 | 173.1 | 724.6 | 154.413 | 158.770 |
| 0.090 | 2.16E-02 | 173.6 | 183.2 | 187.5 | 784.9 | 167.473 | 169.947 |
| 0.110 | 1.72E-02 | 185.5 | 146.1 | 200.2 | 838.2 | 178.630 | 179.596 |
| 0.130 | 8.76E-03 | 193.3 | 74.46 | 208.7 | 873.6 | 185.748 | 185.120 |
| 0.150 | 3.37E-03 | 196.7 | 28.83 | 212.2 | 888.5 | 188.096 | 186.670 |
| 0.200 | 7.24E-04 | 198.9 | 6.354 | 214.9 | 899.6 | 187.774 | 185.441 |
| 1.000 | 7.72E-05 | 202.2 | 0.801 | 218.9 | 916.6 | 164.951 | 170.085 |
| 10.00 | 8.95E-06 | 208.6 | 0.106 | 228.3 | 956.0 | 51.589 | 73.945 |
| 100.0 | 1.80E-07 | 212.3 | 0.004 | 234.4 | 981.2 | 5.968 | 11.422 |
| 1000 | 7.08E-13 | 212.4 | 1.89E-04 | 236.5 | 990.0 | 0.000 | 0.000 |

¹⁾ Average values determined in accordance with results of RRC KI and VNIIEF calculations

²⁾ Maximum power value is 8470 kW (t=0.00588 s)

³⁾ Average radial value

Table E-11.2. Radial energy characteristics of fuel rod # RT11*

| Parameters | Coordinates of fuel radial layers (mm) | | | |
|---|--|--------------------------|--------------------------|--------------------------|
| | 1 layer (1.250-2.834) | 2 layer (2.834-3.452) | 3 layer (3.452-3.722) | 4 layer (3.722-3.808) |
| Number of fissions $\times 10^{-14}$ (fiss) | 9.593 | 6.117 | 3.707 | 1.824 |
| Fission density $\times 10^{-13}$ (fiss/g fuel) | 3.050 | 3.239 | 3.937 | 5.793 |
| Power** (kW) | 3818 | 2438 | 1482 | 732.3 |
| Energy deposition (cal/g fuel) | 213.2 | 226.7 | 276.2 | 408.0 |
| Energy deposition (J/g fuel) | 892.7 | 949.0 | 1157 | 1708 |
| Energy deposition*** (per-unit) | 0.523 | 0.556 | 0.677 | 1.000 |

* Average values were determined in accordance with results of RRC KI and VNIIEF calculations

** The power for the entire length of each layer at time 0.00588 s

*** Energy deposition in current layer/energy deposition in 4th layer

RT11

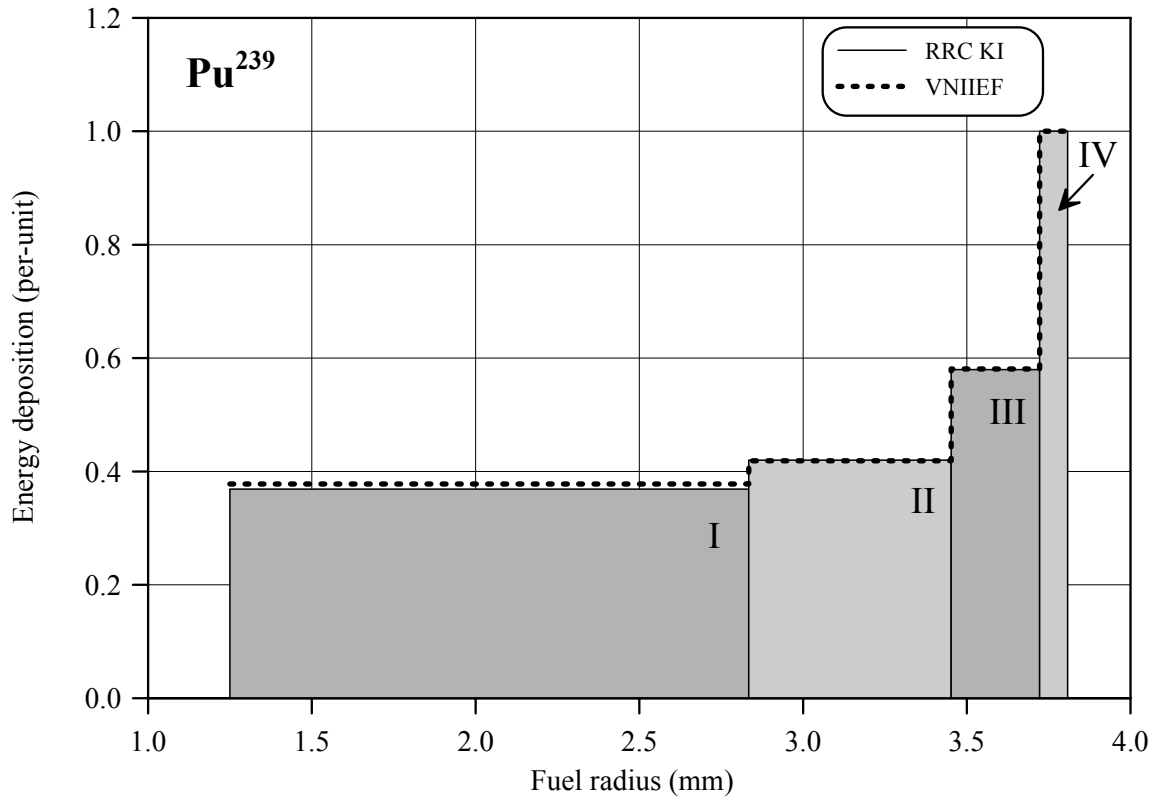
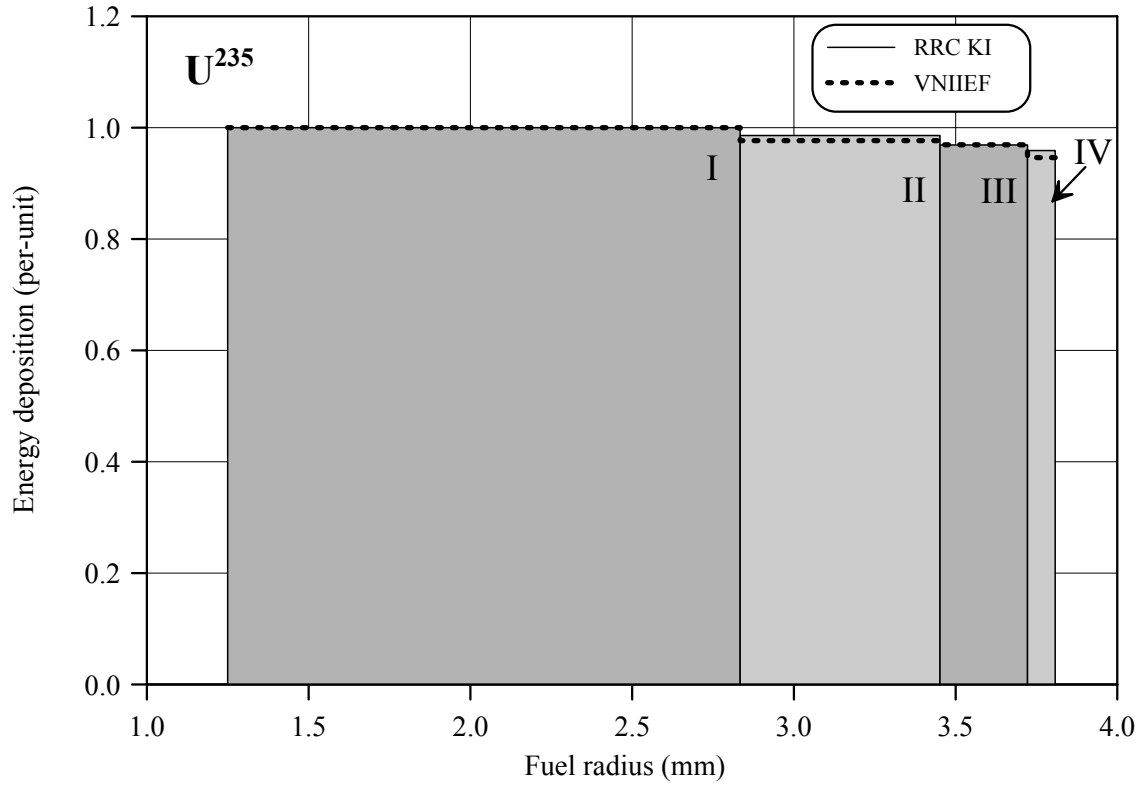


Fig.E-11.5. U²³⁵ and Pu²³⁹ radial distribution of energy deposition for fuel rod # RT11

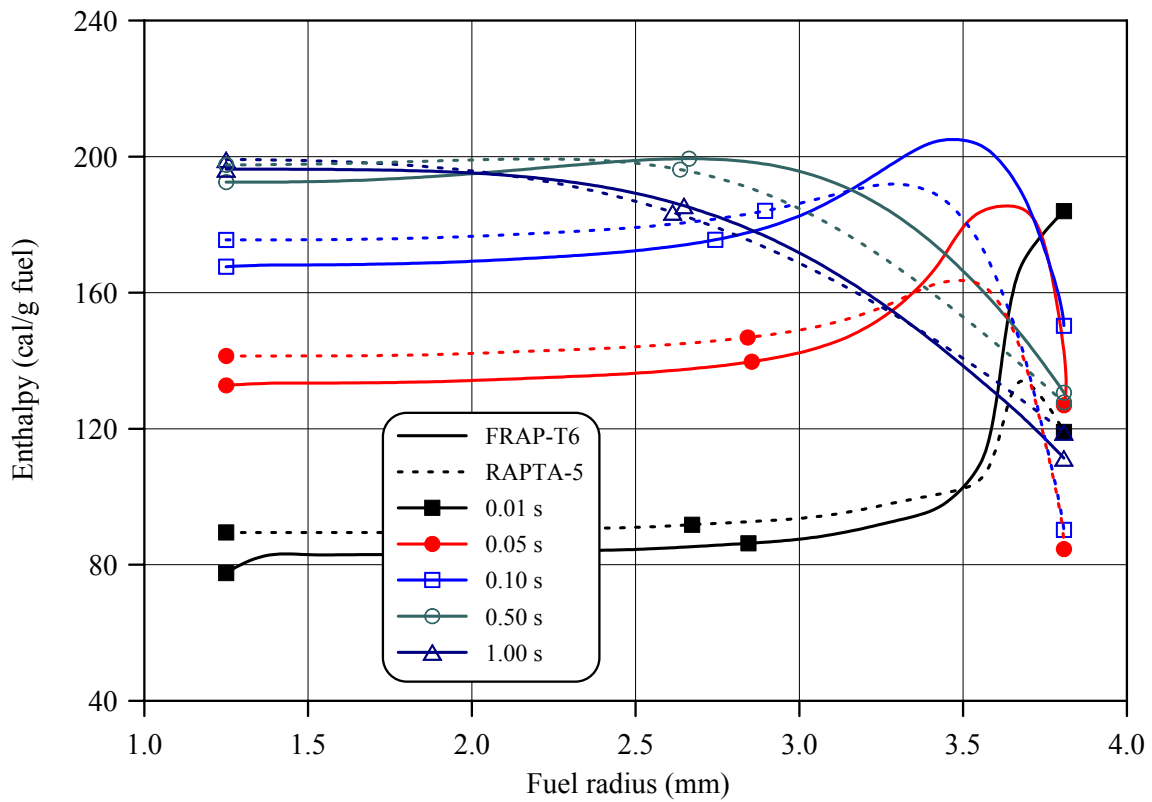
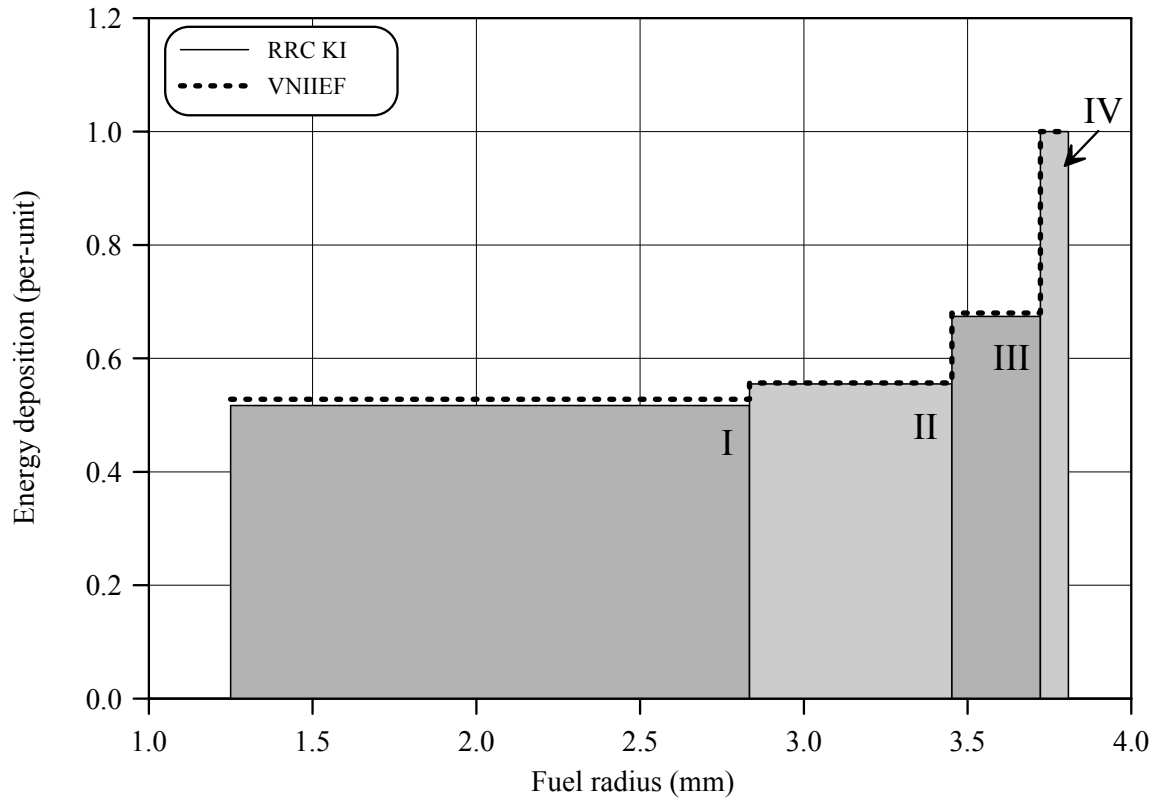


Fig.E-11.6. Radial distribution of energy deposition and fuel enthalpy for fuel rod # RT11

RT11

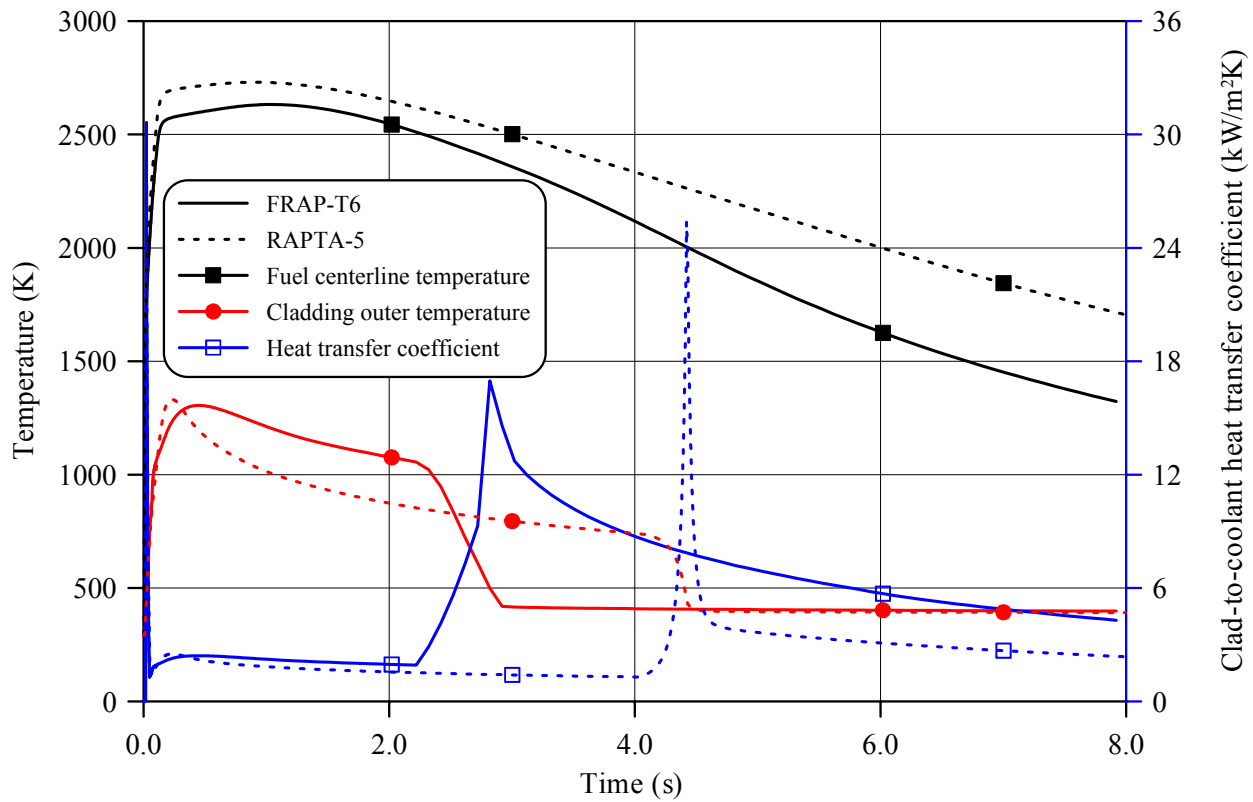
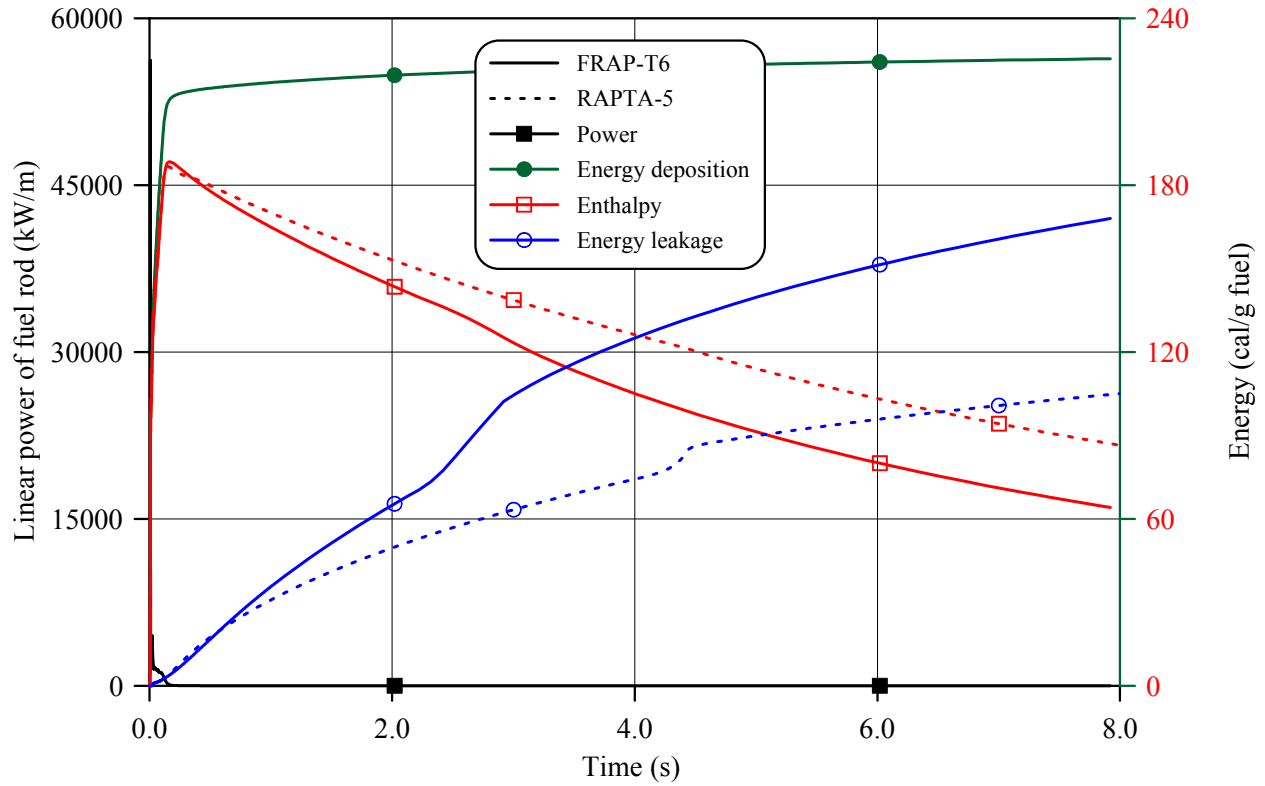


Fig.E-11.7. Thermal history of fuel rod # RT11 during the B1GR test in accordance with FRAP-T6/VVER and RAPTA-5 calculations

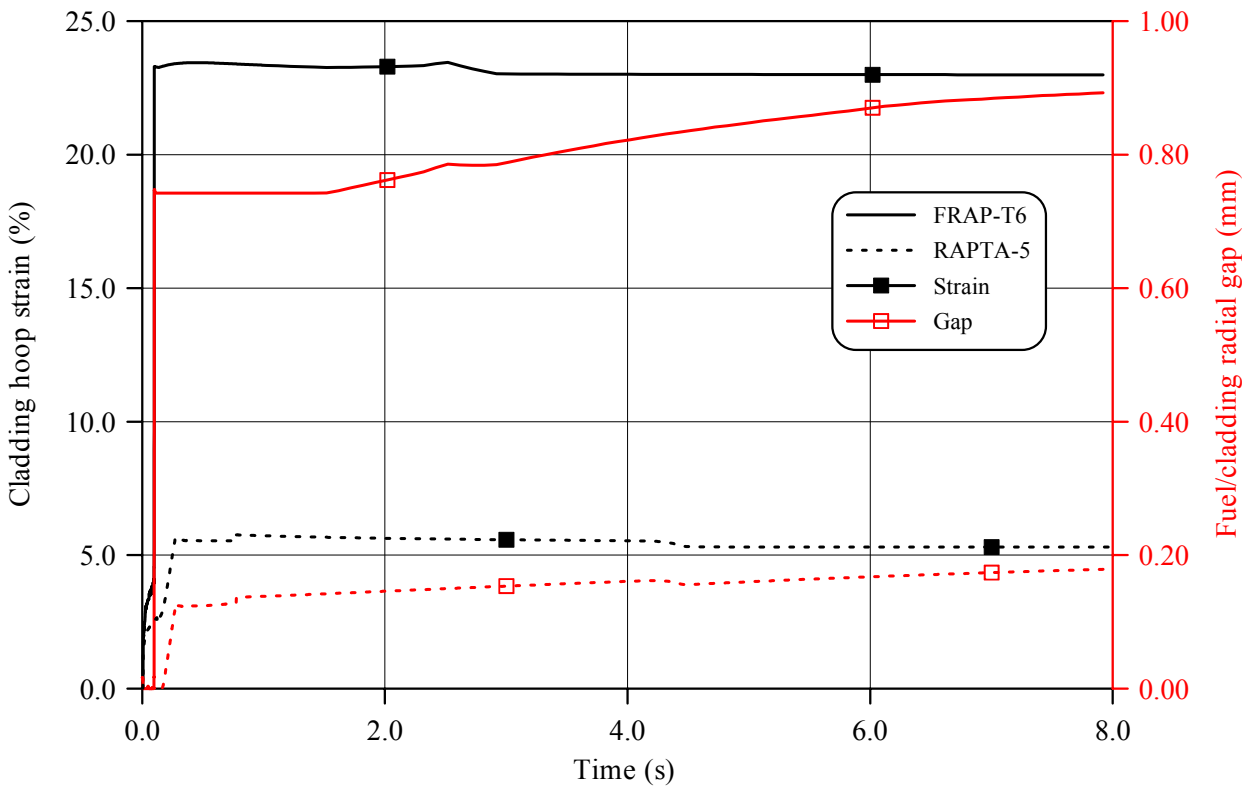
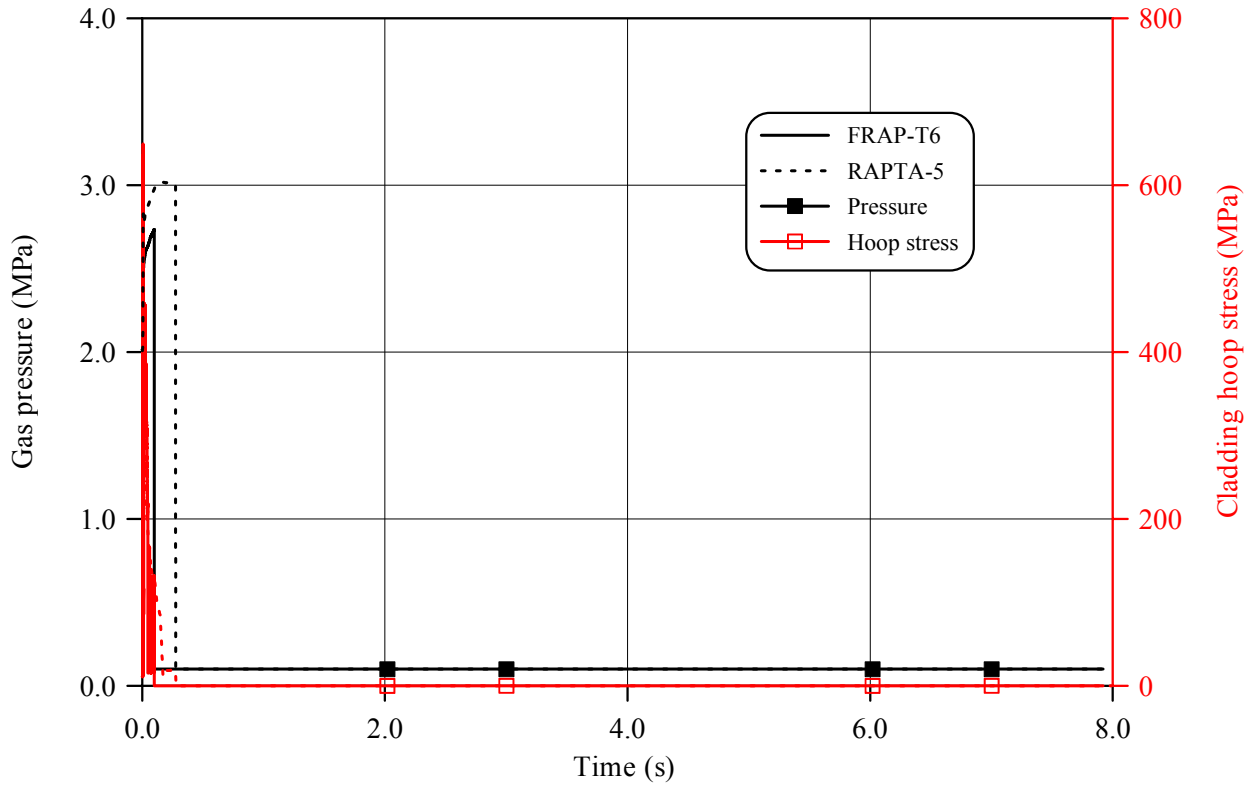


Fig.E-11.8. Mechanical behavior of fuel rod # RT11 during the BGR test in accordance with FRAP-T6/VVER and RAPTA-5 calculations

RT11

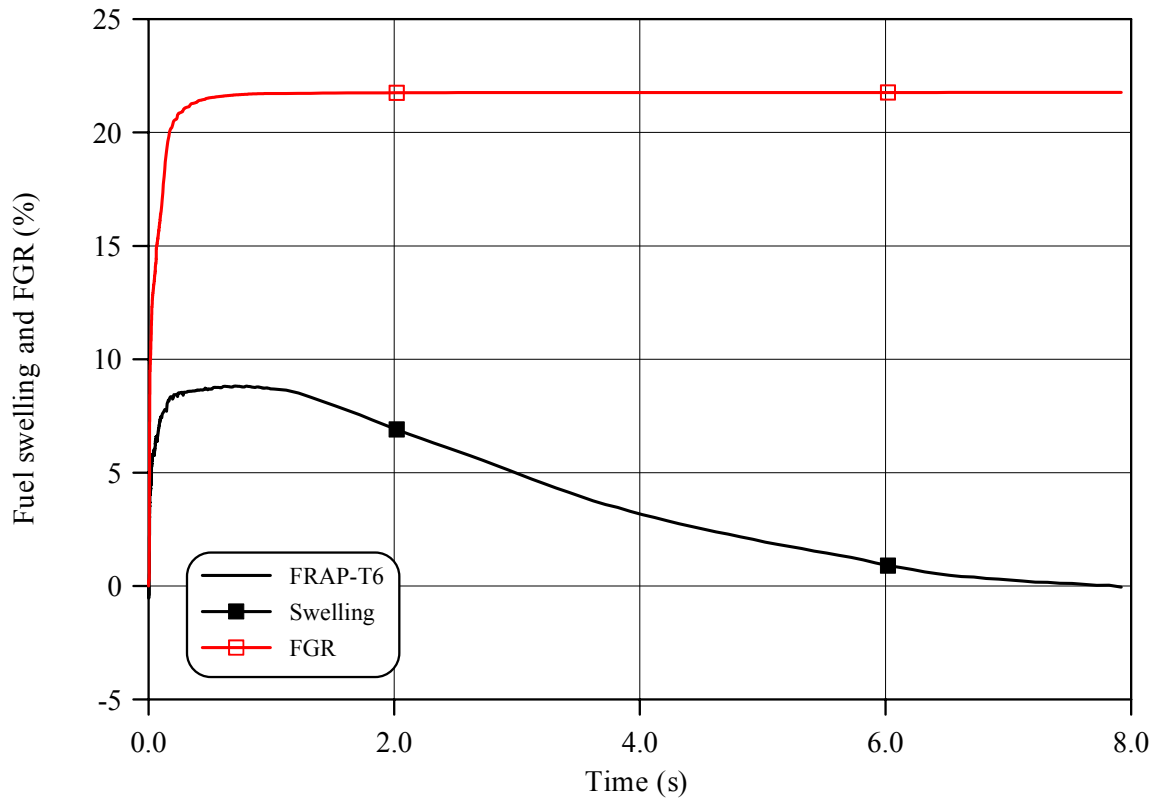
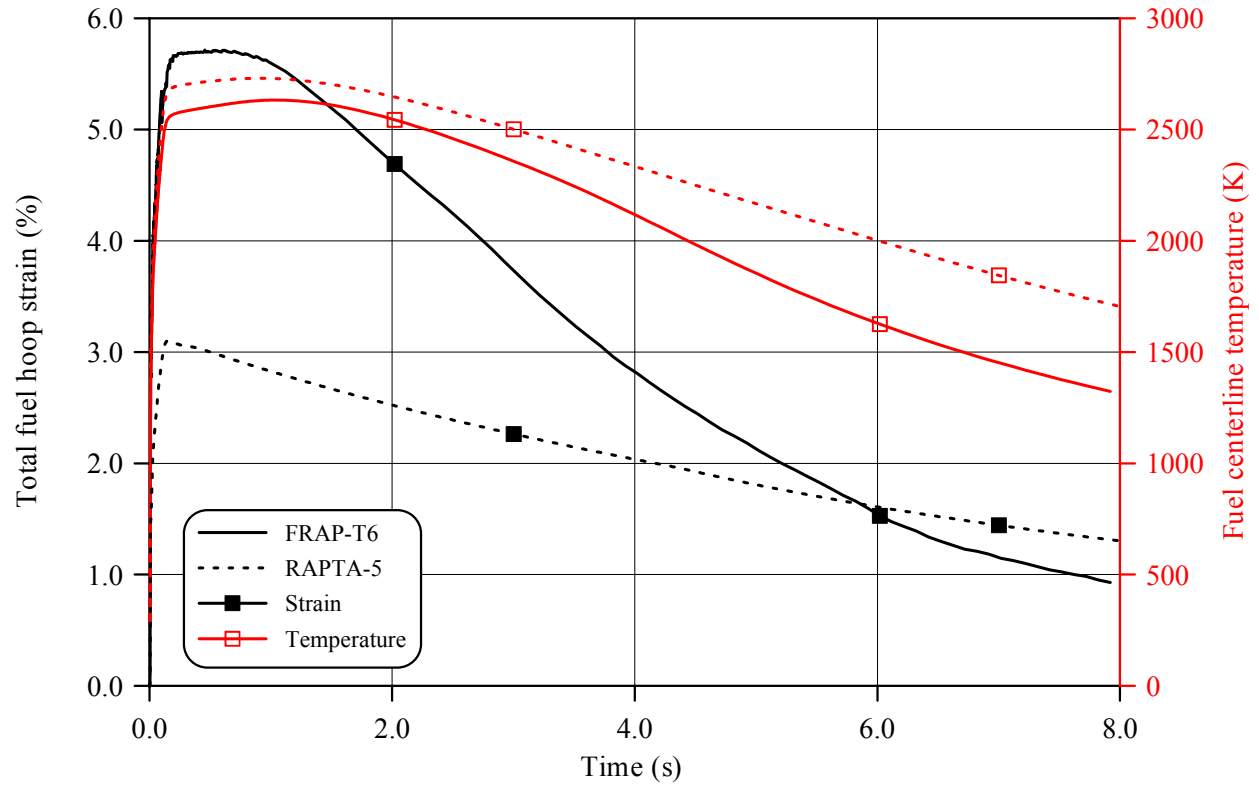


Fig.E-11.9. Fuel behavior during the B1GR test of fuel rod # RT11 in accordance with FRAP-T6/VVER and RAPTA-5 calculations

Table E-11.3. Axial distribution of cladding average outer diameter in fuel rod # RT11*

| Axial coordinate (mm) | Cladding diameter (mm) | Axial coordinate (mm) | Cladding diameter (mm) | Axial coordinate (mm) | Cladding diameter (mm) | Axial coordinate (mm) | Cladding diameter (mm) |
|-----------------------|------------------------|-----------------------|------------------------|-----------------------|------------------------|-----------------------|------------------------|
| 25 | 9.229 | 63 | 9.702 | 101 | 9.611 | 139 | 9.623 |
| 27 | 9.296 | 65 | 9.804 | 103 | 9.597 | 141 | 9.609 |
| 29 | 9.404 | 67 | 9.808 | 105 | 9.522 | 143 | 9.571 |
| 31 | 9.550 | 69 | 9.727 | 107 | 9.492 | 145 | 9.607 |
| 33 | 9.579 | 71 | 9.646 | 109 | 9.541 | 147 | 9.691 |
| 35 | 9.579 | 73 | 9.676 | 111 | 9.594 | 149 | 9.743 |
| 37 | 9.681 | 75 | 9.747 | 113 | 9.606 | 151 | 9.766 |
| 39 | 9.804 | 77 | 9.791 | 115 | 9.573 | 153 | 9.762 |
| 41 | 9.847 | 79 | 9.797 | 117 | 9.546 | 155 | 9.753 |
| 43 | 9.713 | 81 | 9.749 | 119 | 9.555 | 157 | 9.781 |
| 45 | 9.518 | 83 | 9.681 | 121 | 9.587 | 159 | 9.830 |
| 47 | 9.481 | 85 | 9.727 | 123 | 9.625 | 161 | 9.769 |
| 49 | 9.591 | 87 | 9.762 | 125 | 9.596 | 163 | 9.568 |
| 51 | 9.747 | 89 | 9.672 | 127 | 9.543 | 165 | 9.304 |
| 53 | 9.783 | 91 | 9.558 | 129 | 9.479 | 167 | 9.141 |
| 55 | 9.661 | 93 | 9.466 | 131 | 9.430 | 169 | 9.064 |
| 57 | 9.539 | 95 | 9.435 | 133 | 9.422 | 171 | 9.060 |
| 59 | 9.493 | 97 | 9.505 | 135 | 9.488 | 173 | 9.063 |
| 61 | 9.573 | 99 | 9.568 | 137 | 9.569 | 175 | 9.062 |

* Measured value determined on the basis of profilometry data (16 azimuthal directions)

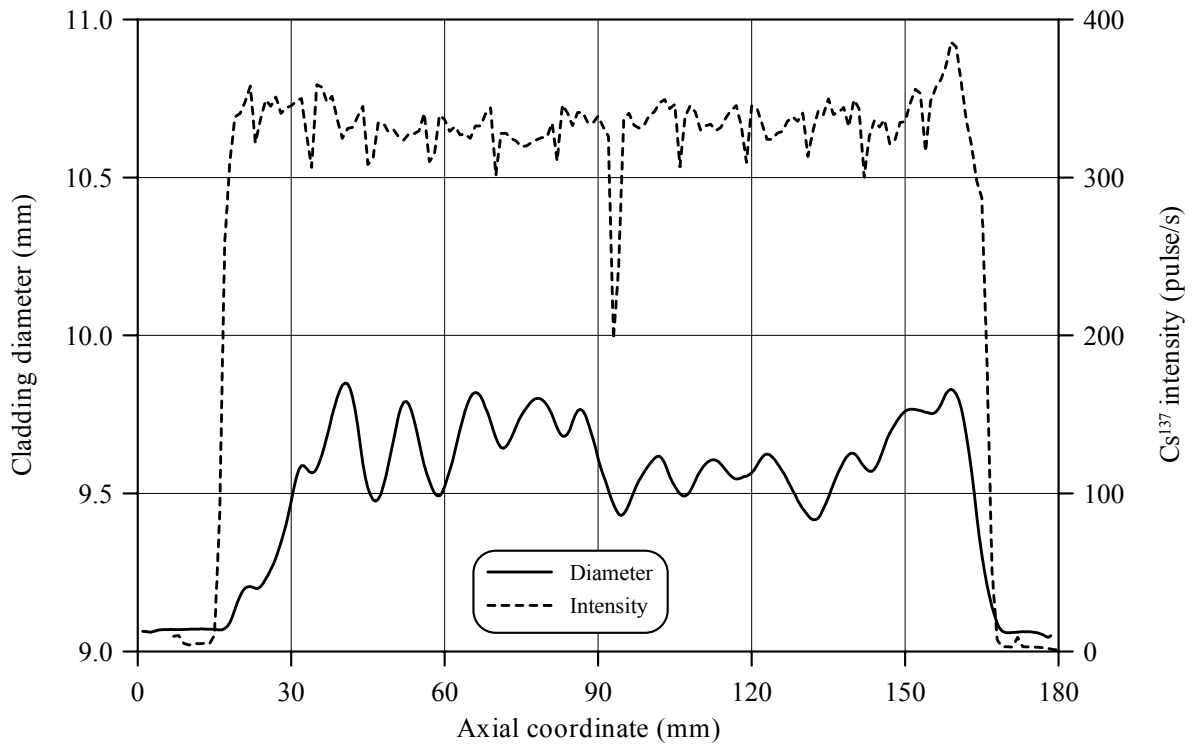


Fig.E-11.10. Cladding measured average diameter and γ -scanning results for fuel rod # RT11

RT11**Table E-11.4. The PIE results for fuel rod # RT11**

| Parameter | | Value |
|-----------|--|-------|
| 1. | Cladding outer diameter (mm): | |
| 1.1. | Maximum diameter of the bidimensional data sample in "fuel rod length - azimuthal angle" coordinates (mm) | 10.02 |
| 1.2. | Averaged azimuthal diameter and maximum diameter along the length selected from the sample of averaged azimuthal diameter (mm) | 9.85 |
| 1.3. | Averaged diameter of the bidimensional data sample in "fuel rod length - azimuthal angle" coordinates (mm) | 9.58 |
| 2. | Cladding maximum residual hoop strain (%) | 8.20 |
| 3. | Fuel pellet conditional diameter (mm) in cross-section*: at 157 mm elevation | 8.31 |
| 4. | ZrO ₂ outer thickness (μm) in cross-section: at 157 mm elevation | 4 |
| 5. | ZrO ₂ inner thickness (μm) in cross-section: at 157 mm elevation | 0 |
| 6. | Parameters characterizing FGR: | |
| 6.1. | Gas composition (% by volume): | |
| | He | - |
| | N ₂ | - |
| | O ₂ | - |
| | Ar | - |
| | CO ₂ | - |
| | Kr | - |
| | Xe | - |
| 6.2. | Free gas volume (cm ³) | - |
| 6.3. | Gas volume under normal conditions (cm ³) | - |
| 6.4. | Gas pressure under normal conditions (MPa) | - |

* Reference value determined by the processing of fuel cross-section photographs

Table E-11.5. Organized BGR test results for fuel rod # RT11

| Parameter | Unit | Value | | |
|--|---------------------|----------|------------|---------|
| | | Measured | Calculated | |
| | | | FRAP-T6 | RAPTA-5 |
| 1. Fuel burnup | MW d/kg U | 47.2 | 47.2 | 47.2 |
| 2. Initial gas pressure | MPa | 2.0 | 2.0 | 2.0 |
| 3. Energy deposition | cal/g fuel | 236.5 | 236.5 | 236.5 |
| 4. Peak fuel enthalpy* | cal/g fuel | - | 188.4 | 186.7 |
| 5. Fuel maximum temperature | K | - | 2782 | 2774 |
| 6. Maximum temperature of cladding outer surface | K | - | 1306 | 1333 |
| 7. Cladding burst | Failed, Unfailed | Failed | Failed | Failed |
| 8. Cladding residual hoop strain** | | | | |
| - average | % | 5.45 | 3.68 | 5.76 |
| - maximum | % | 8.20 | 22.90 | 5.76 |

* Average value of peak fuel enthalpy 187.5 cal/g fuel

** Average value along the fuel stack length

Appendix E-12
Individual Characteristics of Fuel Rod # RT12
after the BGR Test

RT12

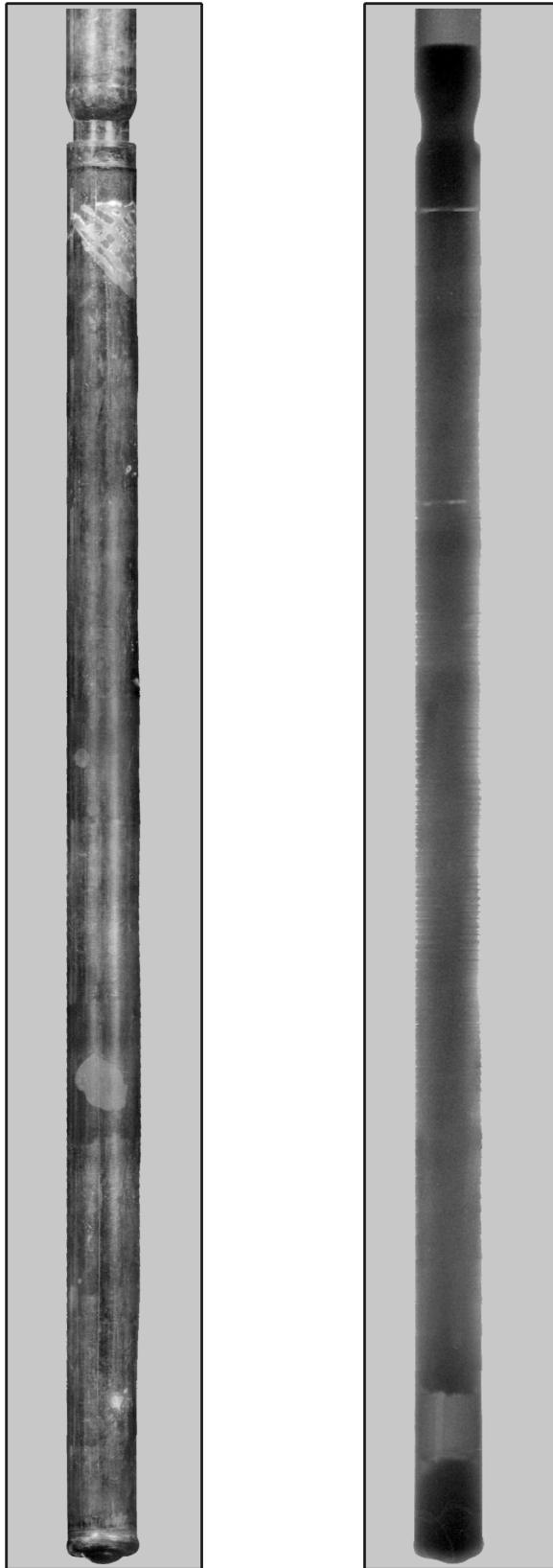


Fig.E-12.1. Appearance of unfailed fuel rod # RT12 after the BGR test (photographs and X-ray photograph)

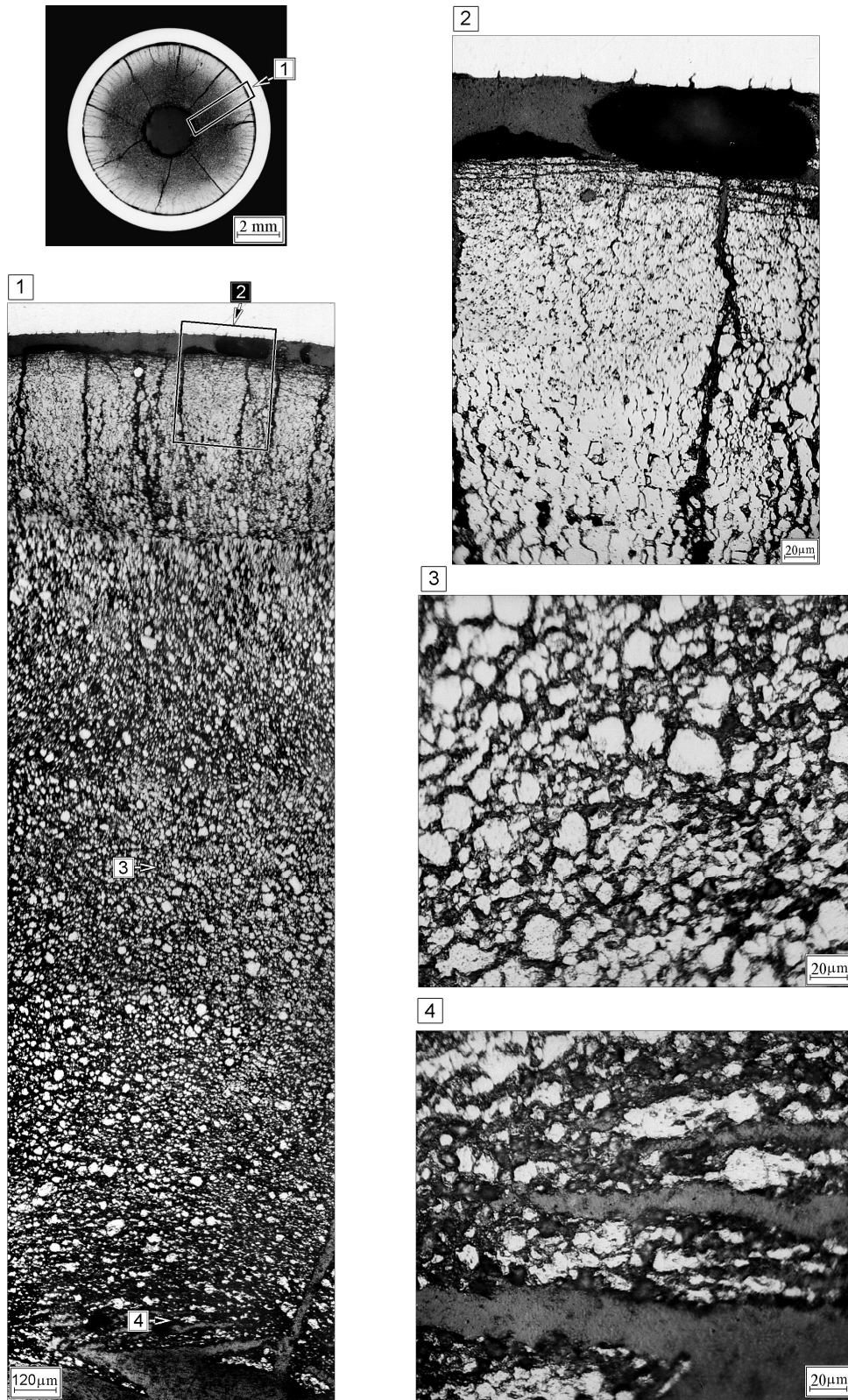


Fig.E-12.2. Cross-section and fuel microstructure of fuel rod # RT12 at 54 mm elevation (from low cap)

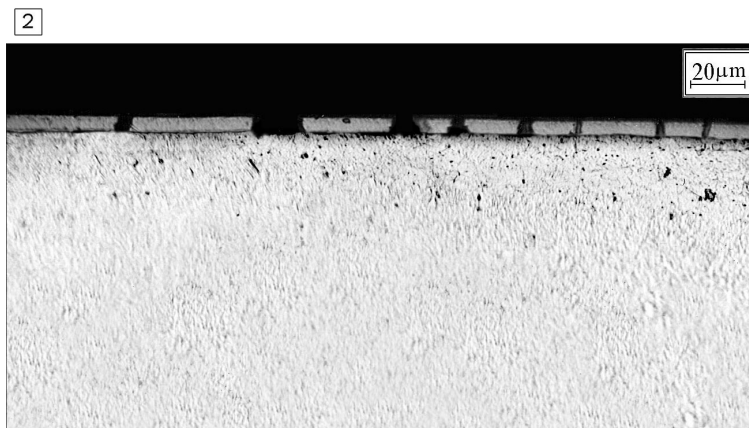
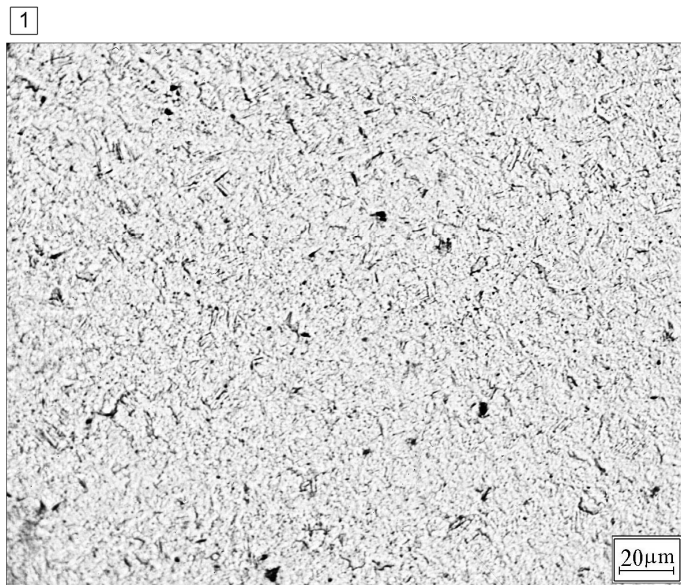
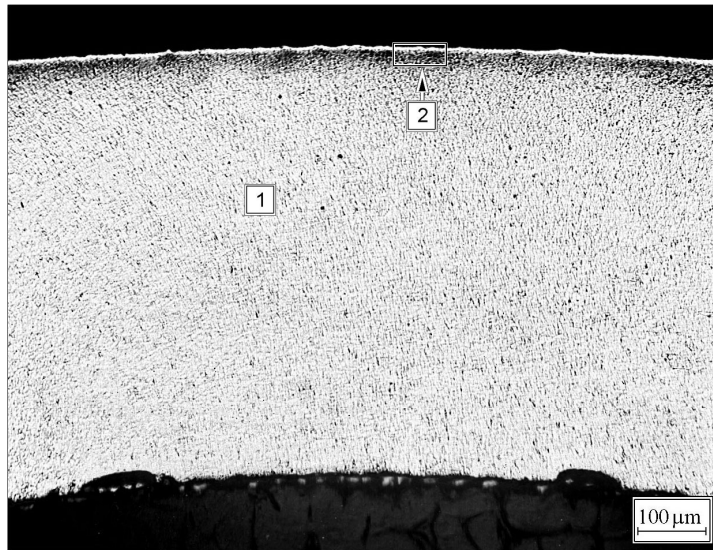


Fig.E-12.3. Cladding microstructure of fuel rod # RT12 at 54 mm elevation (from low cap)

Table E-12.1. Time dependent energy characteristics of fuel rod # RT12

| Time (s) | Relative reactor power (current/maximum value) (per-unit) | Cumulative number of fissions in fuel rod (fiss) x10 ⁻¹⁴ | Power of fuel rod ¹⁾²⁾ (kW) | Energy deposition | | Fuel enthalpy ³⁾ | |
|----------|---|---|--|-------------------|------------|-----------------------------|---------|
| | | | | (cal/g fuel) | (J/g fuel) | FRAP-T6 | RAPTA-5 |
| 0.000 | 0.00E+00 | 0.000 | 0.000 | 0.000 | 0.000 | 0.000 | 0.000 |
| 0.001 | 2.98E-03 | 0.039 | 21.69 | 0.042 | 0.177 | 0.671 | 0.010 |
| 0.002 | 1.23E-02 | 0.208 | 89.58 | 0.225 | 0.941 | 0.671 | 0.048 |
| 0.003 | 4.92E-02 | 0.882 | 357.9 | 0.951 | 3.983 | 0.671 | 0.221 |
| 0.004 | 1.95E-01 | 3.617 | 1420 | 3.901 | 16.33 | 1.238 | 0.983 |
| 0.005 | 6.03E-01 | 13.21 | 4386 | 14.24 | 59.60 | 4.254 | 3.962 |
| 0.006 | 9.97E-01 | 34.62 | 7246 | 37.34 | 156.3 | 14.601 | 14.236 |
| 0.007 | 7.64E-01 | 58.23 | 5558 | 62.78 | 262.8 | 36.948 | 36.820 |
| 0.008 | 3.89E-01 | 72.66 | 2829 | 78.35 | 328.0 | 61.565 | 61.560 |
| 0.009 | 1.92E-01 | 79.71 | 1397 | 85.97 | 359.9 | 76.845 | 76.530 |
| 0.010 | 1.09E-01 | 83.35 | 791.2 | 89.94 | 376.6 | 84.231 | 83.649 |
| 0.012 | 6.29E-02 | 87.45 | 457.6 | 94.31 | 394.8 | 90.308 | 89.170 |
| 0.014 | 5.87E-02 | 90.53 | 426.7 | 97.58 | 408.6 | 93.524 | 92.025 |
| 0.016 | 6.41E-02 | 93.60 | 466.8 | 101.0 | 422.7 | 96.353 | 94.690 |
| 0.018 | 6.96E-02 | 97.03 | 506.3 | 104.7 | 438.2 | 99.400 | 97.679 |
| 0.020 | 6.95E-02 | 100.6 | 505.4 | 108.5 | 454.3 | 102.696 | 100.975 |
| 0.022 | 6.41E-02 | 104.0 | 466.1 | 112.2 | 469.8 | 106.008 | 104.271 |
| 0.024 | 5.57E-02 | 107.1 | 405.1 | 115.5 | 483.6 | 109.043 | 107.294 |
| 0.026 | 4.72E-02 | 109.9 | 342.9 | 118.4 | 495.6 | 111.652 | 109.884 |
| 0.028 | 3.99E-02 | 112.0 | 290.2 | 120.8 | 505.6 | 113.817 | 112.022 |
| 0.030 | 3.49E-02 | 114.0 | 253.8 | 122.8 | 514.1 | 115.607 | 113.796 |
| 0.050 | 3.13E-02 | 130.1 | 227.8 | 140.2 | 587.1 | 126.792 | 127.562 |
| 0.070 | 2.54E-02 | 144.4 | 184.9 | 155.7 | 652.0 | 138.170 | 139.931 |
| 0.090 | 1.83E-02 | 155.5 | 133.2 | 167.8 | 702.6 | 146.854 | 149.141 |
| 0.110 | 8.26E-03 | 162.4 | 60.22 | 175.1 | 732.9 | 152.608 | 153.953 |
| 0.130 | 3.11E-03 | 165.0 | 22.83 | 177.8 | 744.6 | 154.473 | 154.893 |
| 0.150 | 1.52E-03 | 166.0 | 11.21 | 179.1 | 749.8 | 154.714 | 154.282 |
| 0.200 | 4.74E-04 | 167.1 | 3.632 | 180.3 | 754.7 | 153.881 | 151.725 |
| 1.000 | 7.48E-05 | 169.6 | 0.667 | 183.4 | 767.8 | 135.980 | 128.738 |
| 10.00 | 8.71E-06 | 175.4 | 0.089 | 191.3 | 800.7 | 60.607 | 30.472 |
| 100.0 | 1.76E-07 | 177.8 | 0.003 | 196.3 | 821.7 | 10.376 | 5.051 |
| 1000 | 6.91E-13 | 177.9 | 1.59E-04 | 198.1 | 829.2 | 0.000 | 0.000 |

¹⁾ Average values determined in accordance with results of RRC KI and VNIIEF calculations

²⁾ Maximum power value is 7270.5 kW (t=0.00606 s)

³⁾ Average radial value

RT12

Table E-12.2. Radial energy characteristics of fuel rod # RT12*

| Parameters | Coordinates of fuel radial layers (mm) | | | |
|---|--|--------------------------|--------------------------|--------------------------|
| | 1 layer (1.250-2.834) | 2 layer (2.834-3.452) | 3 layer (3.452-3.722) | 4 layer (3.722-3.808) |
| Number of fissions $\times 10^{-14}$ (fiss) | 7.961 | 5.152 | 3.130 | 1.569 |
| Fission density $\times 10^{-13}$ (fiss/g fuel) | 2.528 | 2.723 | 3.318 | 4.974 |
| Power ** (kW) | 3243 | 2102 | 1281 | 644.7 |
| Energy deposition (cal/g fuel) | 176.7 | 190.7 | 233.0 | 350.4 |
| Energy deposition (J/g fuel) | 740.0 | 798.3 | 975.4 | 1467 |
| Energy deposition *** (per-unit) | 0.505 | 0.544 | 0.665 | 1.000 |

* Average values were determined in accordance with results of RRC KI and VNIIEF calculations

** The power for the entire length of each layer at time 0.00606 s

*** Energy deposition in current layer/energy deposition in 4th layer

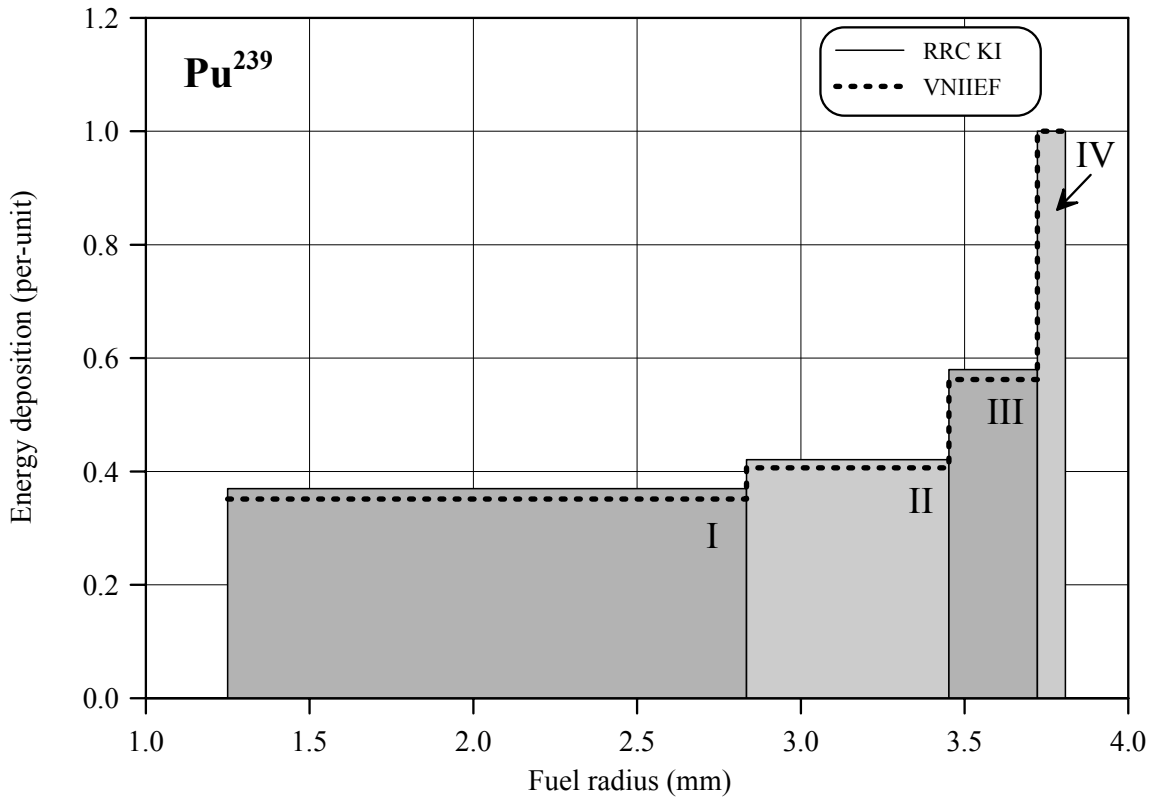
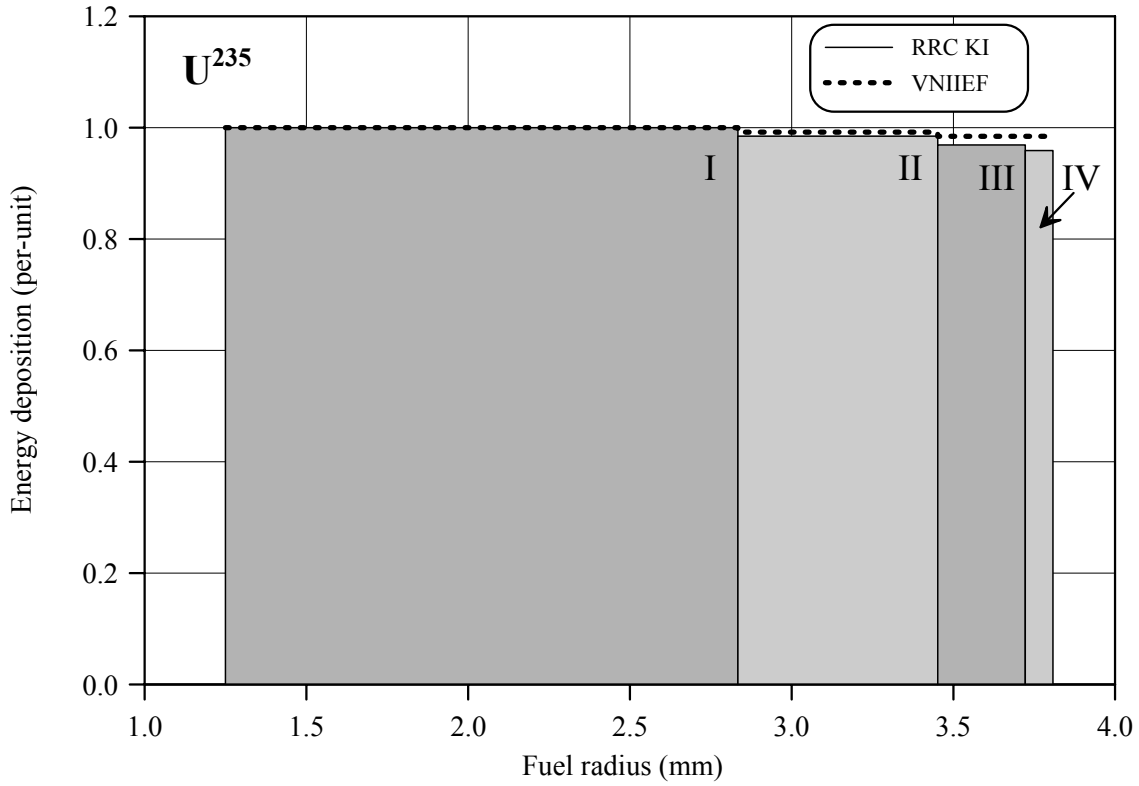


Fig.E-12.4. U²³⁵ and Pu²³⁹ radial distribution of energy deposition for fuel rod # RT12

RT12

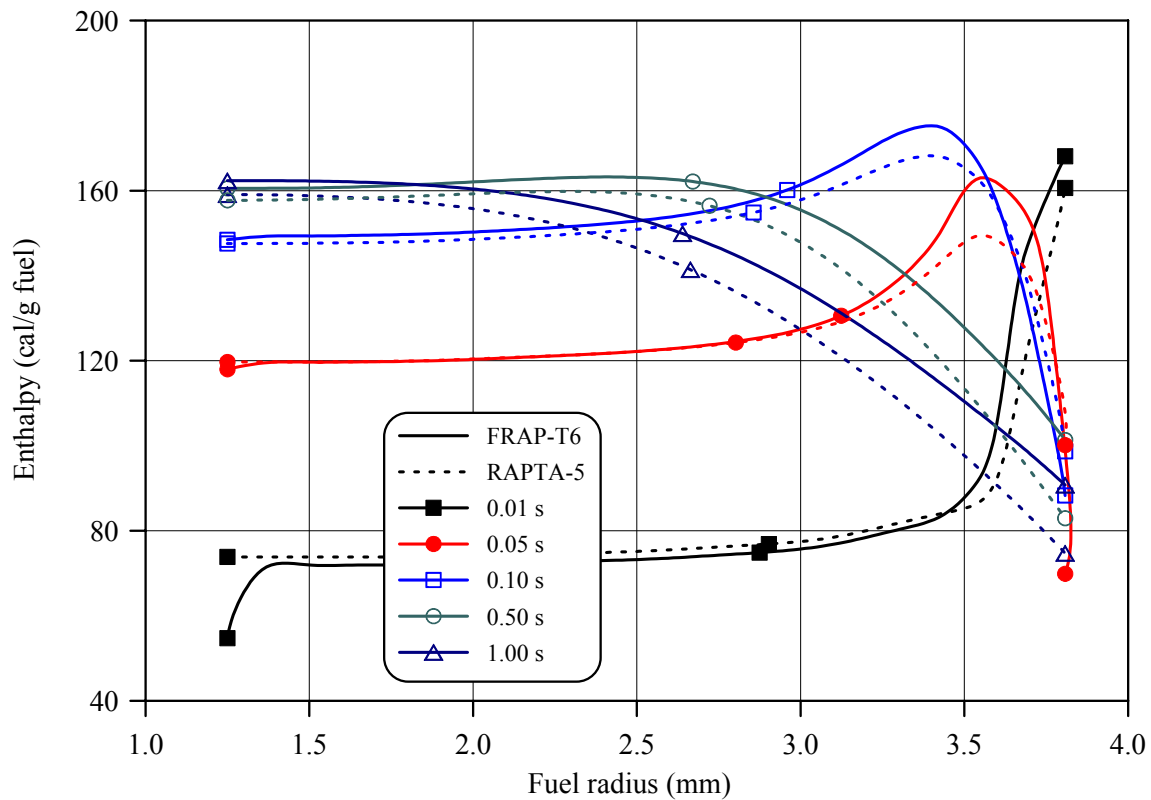
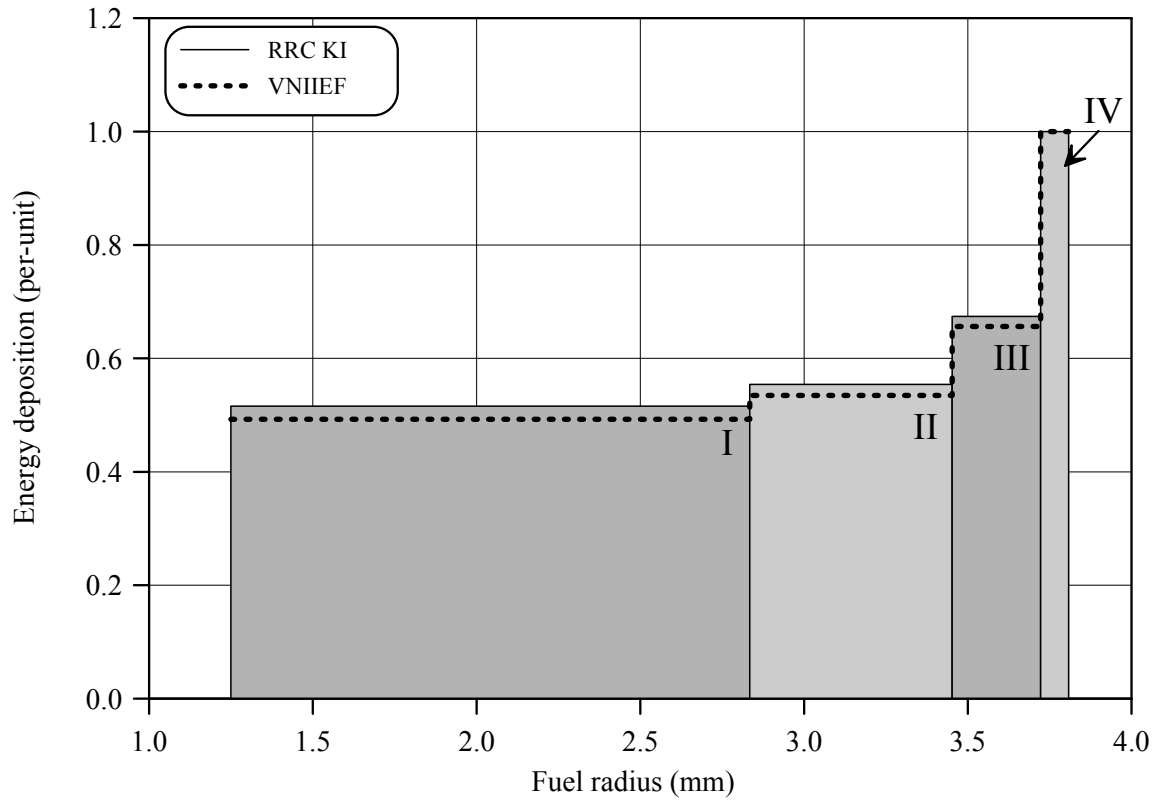


Fig.E-12.5. Radial distribution of energy deposition and fuel enthalpy for fuel rod # RT12

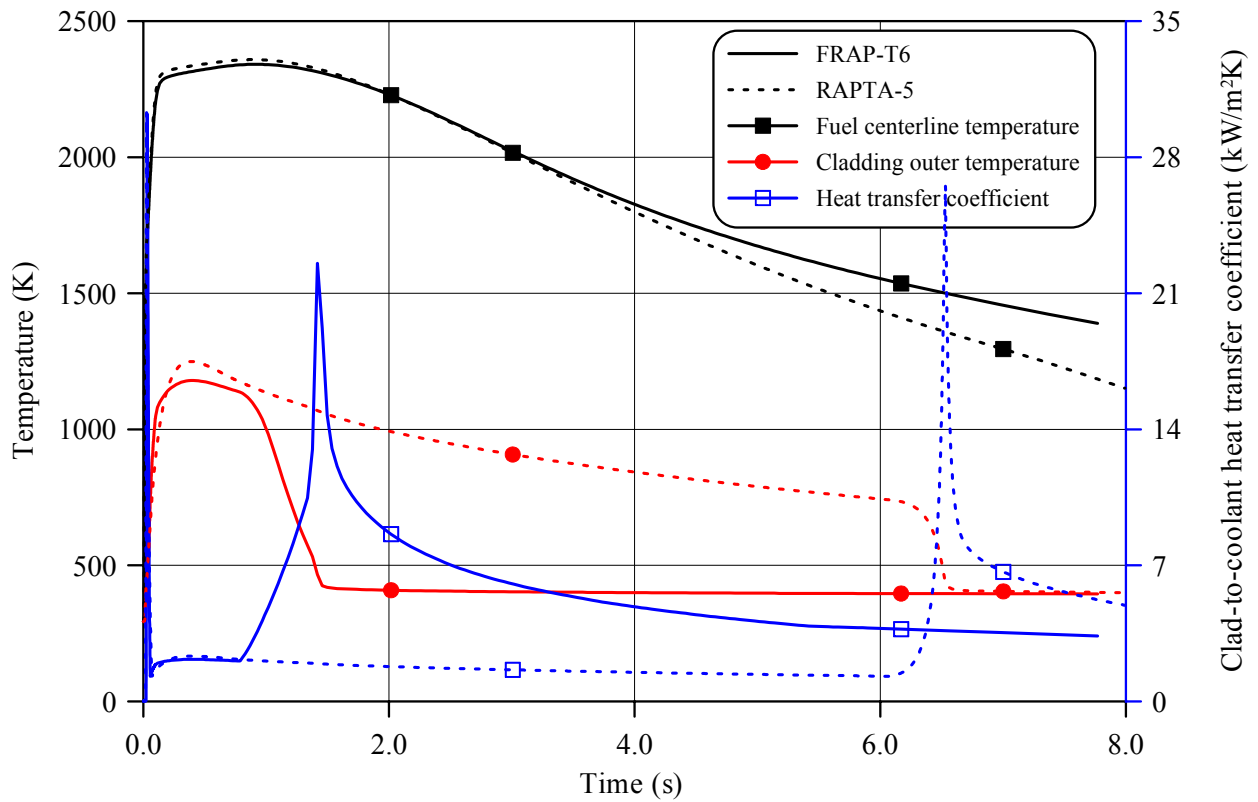
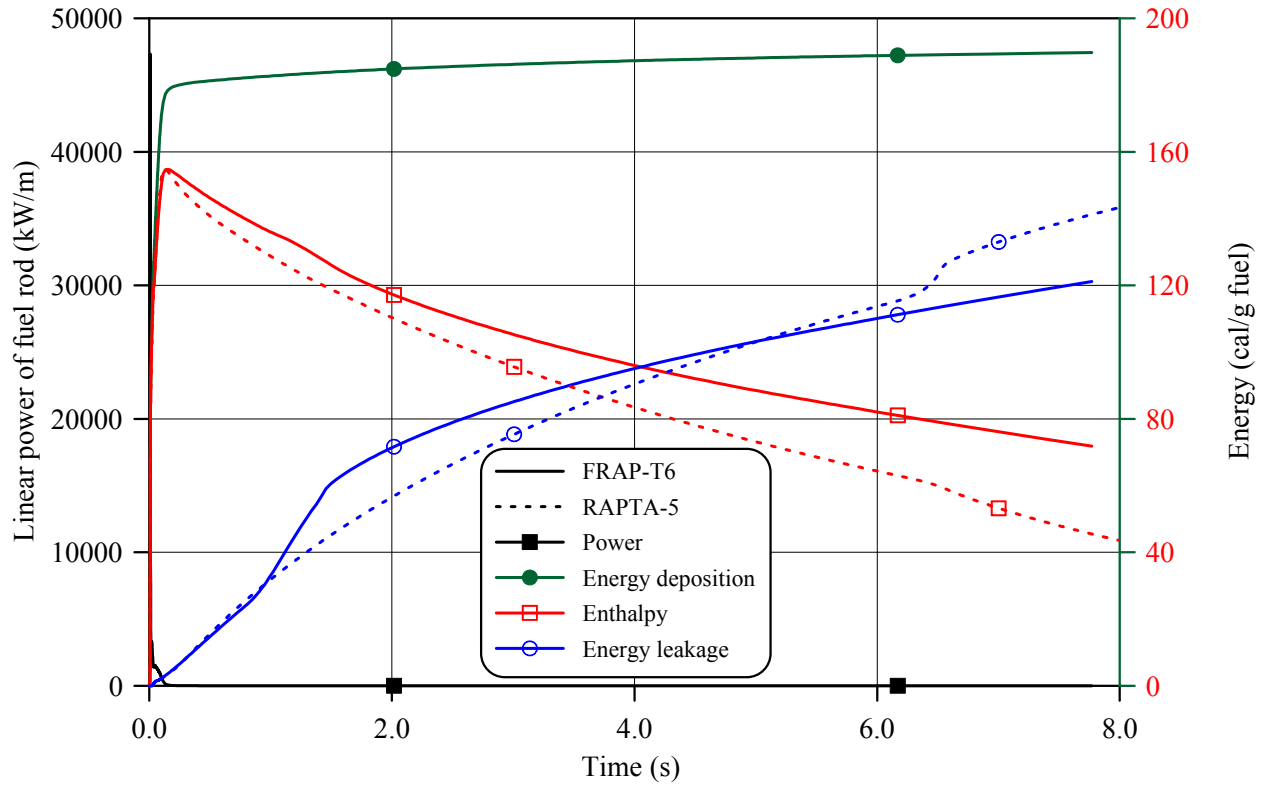


Fig.E-12.6. Thermal history of fuel rod # RT12 during the BIGH test in accordance with FRAP-T6/VVER and RAPTA-5 calculations

RT12

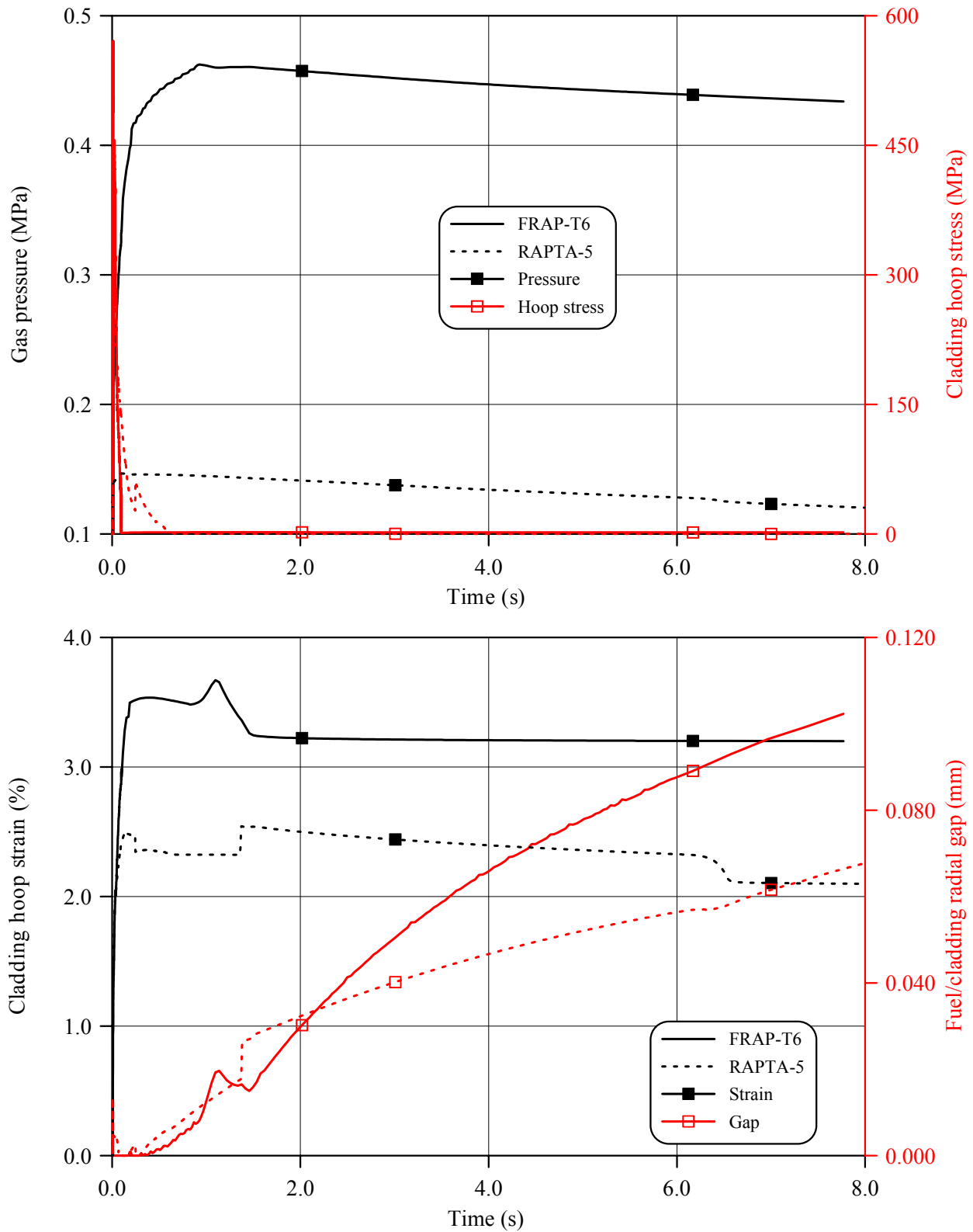


Fig.E-12.7. Mechanical behavior of fuel rod # RT12 during the BGR test in accordance with FRAP-T6/VVER and RAPTA-5 calculations

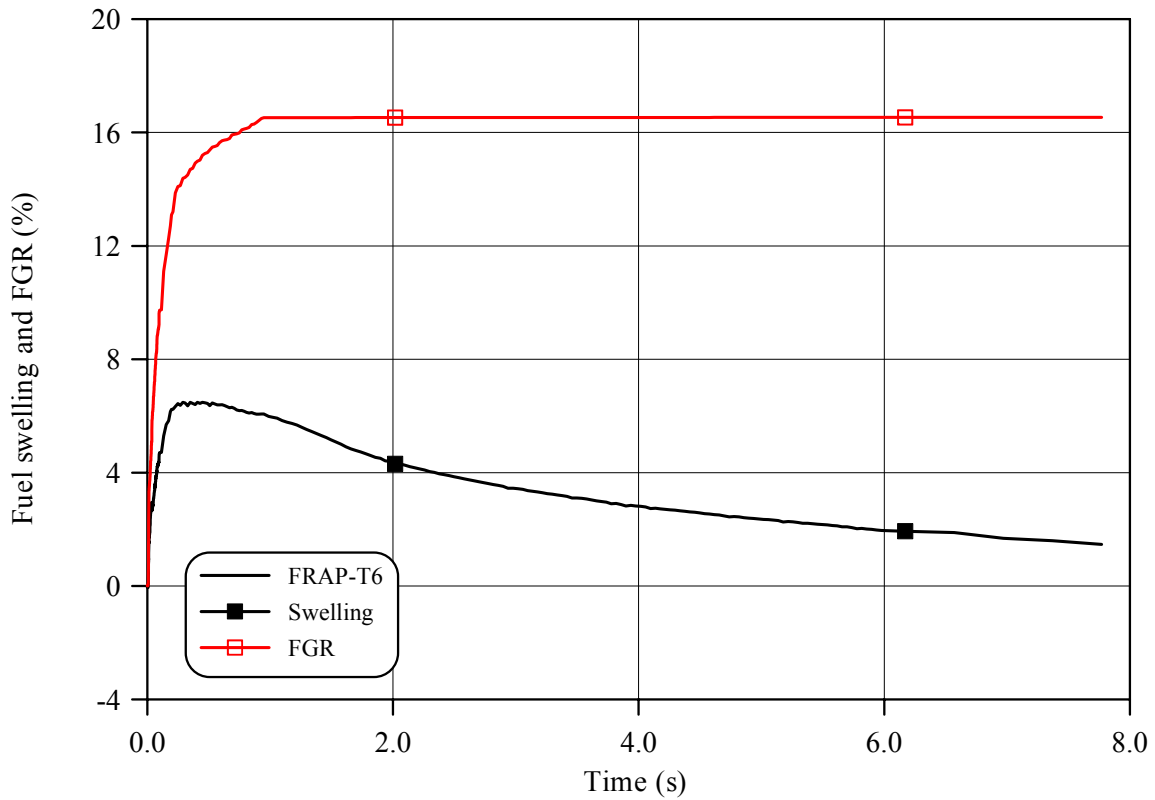
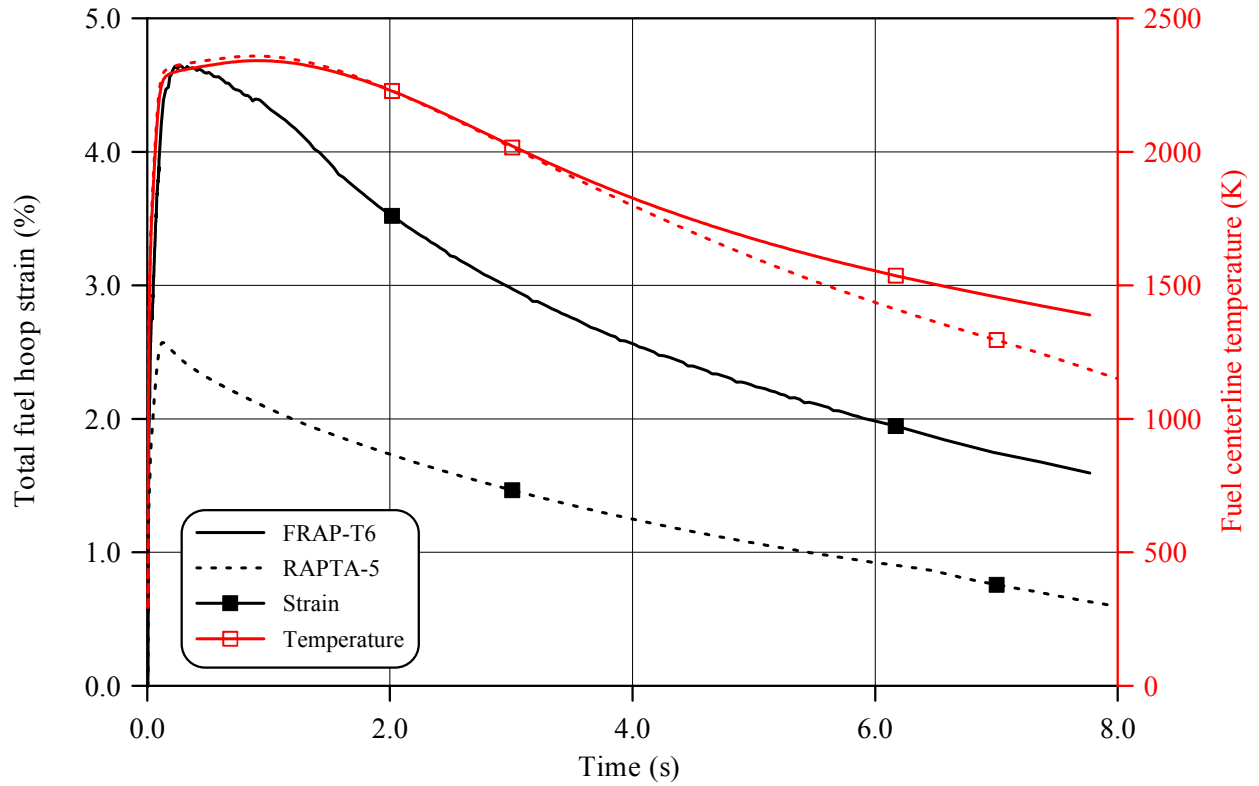


Fig.E-12.8. Fuel behavior during the BGR test of fuel rod # RT12 in accordance with FRAP-T6/VVER and RAPTA-5 calculations

RT12

Table E-12.3. Axial distribution of cladding average outer diameter in fuel rod # RT12*

| Axial coordinate (mm) | Cladding diameter (mm) | Axial coordinate (mm) | Cladding diameter (mm) | Axial coordinate (mm) | Cladding diameter (mm) | Axial coordinate (mm) | Cladding diameter (mm) |
|-----------------------|------------------------|-----------------------|------------------------|-----------------------|------------------------|-----------------------|------------------------|
| 24 | 9.263 | 62 | 9.520 | 100 | 9.487 | 138 | 9.390 |
| 26 | 9.313 | 64 | 9.513 | 102 | 9.457 | 140 | 9.400 |
| 28 | 9.370 | 66 | 9.480 | 104 | 9.490 | 142 | 9.387 |
| 30 | 9.430 | 68 | 9.447 | 106 | 9.517 | 144 | 9.330 |
| 32 | 9.447 | 70 | 9.443 | 108 | 9.490 | 146 | 9.287 |
| 34 | 9.473 | 72 | 9.490 | 110 | 9.450 | 148 | 9.297 |
| 36 | 9.537 | 74 | 9.513 | 112 | 9.430 | 150 | 9.360 |
| 38 | 9.570 | 76 | 9.510 | 114 | 9.433 | 152 | 9.423 |
| 40 | 9.567 | 78 | 9.480 | 116 | 9.453 | 154 | 9.470 |
| 42 | 9.530 | 80 | 9.470 | 118 | 9.470 | 156 | 9.470 |
| 44 | 9.500 | 82 | 9.517 | 120 | 9.480 | 158 | 9.450 |
| 46 | 9.483 | 84 | 9.563 | 122 | 9.480 | 160 | 9.420 |
| 48 | 9.507 | 86 | 9.573 | 124 | 9.463 | 162 | 9.420 |
| 50 | 9.547 | 88 | 9.563 | 126 | 9.473 | 164 | 9.420 |
| 52 | 9.570 | 90 | 9.550 | 128 | 9.480 | 166 | 9.400 |
| 54 | 9.573 | 92 | 9.567 | 130 | 9.483 | 168 | 9.370 |
| 56 | 9.553 | 94 | 9.593 | 132 | 9.463 | 170 | 9.320 |
| 58 | 9.510 | 96 | 9.580 | 134 | 9.430 | 172 | 9.240 |
| 60 | 9.527 | 98 | 9.533 | 136 | 9.380 | 174 | 9.167 |

* Measured value determined on the basis of profilometry data (16 azimuthal directions)

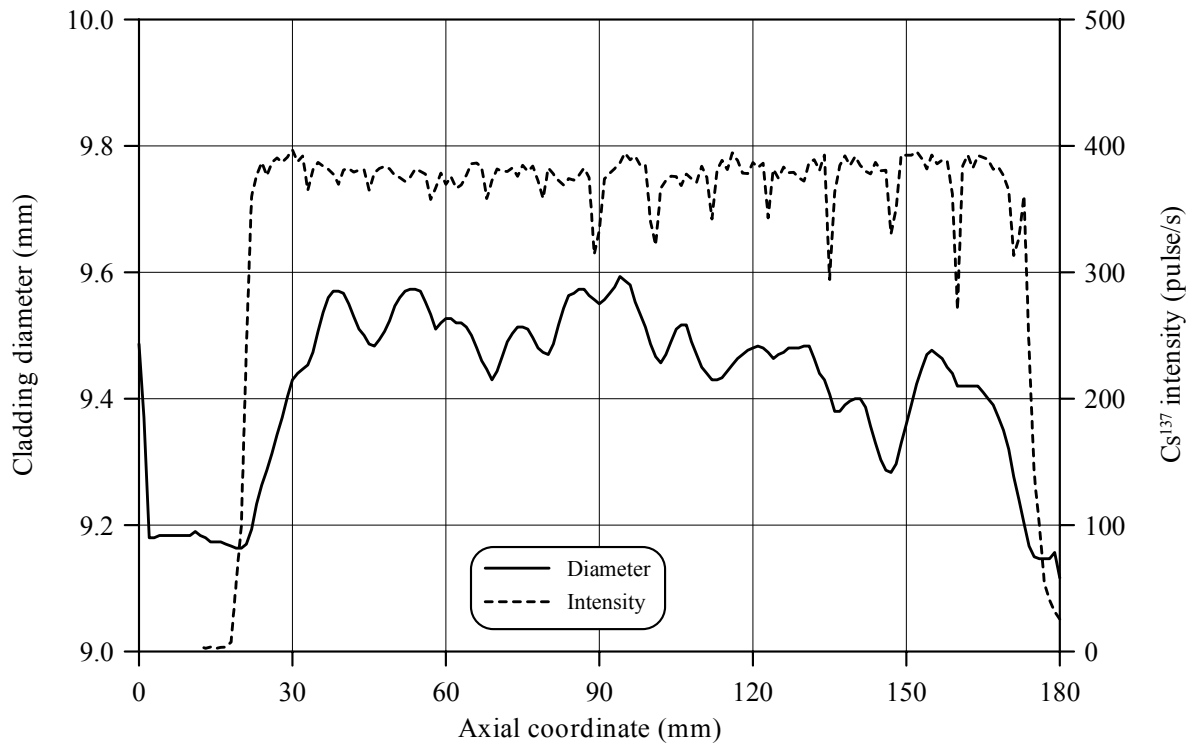


Fig.E-12.9. Cladding measured average diameter and γ -scanning results for fuel rod # RT12

Table E-12.4. The PIE results for fuel rod # RT12

| Parameter | | Value |
|-----------|--|-------|
| 1. | Cladding outer diameter (mm): | |
| 1.1. | Maximum diameter of the bidimensional data sample in "fuel rod length - azimuthal angle" coordinates (mm) | 9.60 |
| 1.2. | Averaged azimuthal diameter and maximum diameter along the length selected from the sample of averaged azimuthal diameter (mm) | 9.59 |
| 1.3. | Averaged diameter of the bidimensional data sample in "fuel rod length - azimuthal angle" coordinates (mm) | 9.46 |
| 2. | Cladding maximum residual hoop strain (%) | 5.78 |
| 3. | Fuel pellet conditional diameter (mm) in cross-section*: | |
| | at 54 mm elevation | 8.05 |
| 4. | ZrO ₂ outer thickness (μm) in cross-section: | |
| | at 54 mm elevation | 3–5 |
| 5. | ZrO ₂ inner thickness (μm) in cross-section: | |
| | at 54 mm elevation | 0 |
| 6. | Parameters characterizing FGR: | |
| 6.1. | Gas composition (% by volume): | |
| | He | 35.13 |
| | N ₂ | 0.58 |
| | O ₂ | 0.08 |
| | Ar | 0.030 |
| | CO ₂ | 0.100 |
| | Kr | 5.78 |
| | Xe | 58.30 |
| 6.2. | Free gas volume (cm ³) | 6.6 |
| 6.3. | Gas volume under normal conditions (cm ³) | 32.7 |
| 6.4. | Gas pressure under normal conditions (MPa) | 0.50 |
| 6.5. | FGR (%) | 22.70 |

* Reference value determined by the processing of fuel cross-section photographs

RT12

Table E-12.5. Organized BGR test results for fuel rod # RT12

| Parameter | | Unit | Value | | |
|-----------|---|---------------------|----------|------------|---------|
| | | | Measured | Calculated | |
| | | | | FRAP-T6 | RAPTA-5 |
| 1. | Fuel burnup | MW d/kg U | 47.4 | 47.4 | 47.4 |
| 2. | Initial gas pressure | MPa | 0.1 | 0.1 | 0.1 |
| 3. | Energy deposition | cal/g fuel | 198.1 | 198.1 | 198.1 |
| 4. | Peak fuel enthalpy* | cal/g fuel | - | 154.7 | 154.9 |
| 5. | Fuel maximum temperature | K | - | 2472 | 2466 |
| 6. | Maximum temperature of cladding outer surface | K | - | 1180 | 1249 |
| 7. | Cladding burst | Failed, Unfailed | Unfailed | -** | -** |
| 8. | Cladding residual hoop strain | | | | |
| | - average*** | % | 4.35 | 3.11 | 2.54 |
| | - maximum | % | 5.78 | 3.11 | 2.54 |

* Average value of peak fuel enthalpy 154.8 cal/g fuel

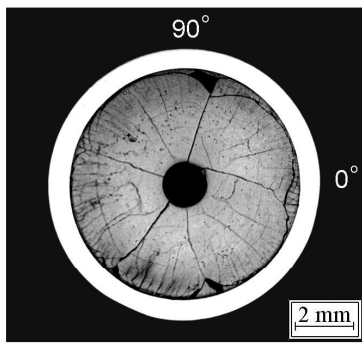
** This parameter was not calculated

*** Average value along the fuel stack length

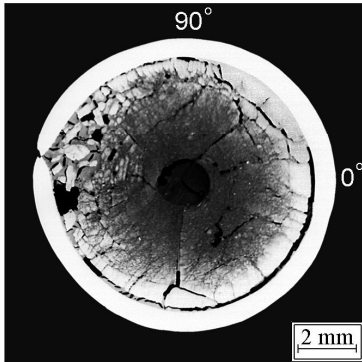
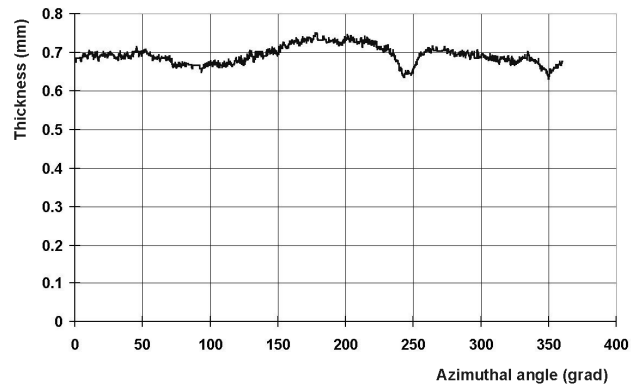
Appendix E-13

Azimuthal Distribution of Cladding Thickness for Fuel Rods

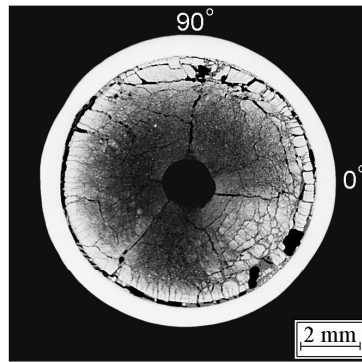
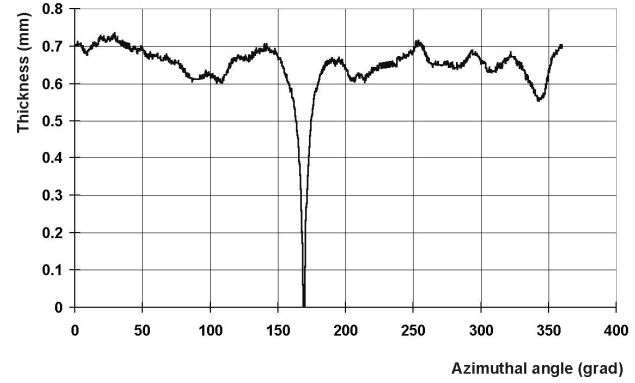
RT7-12



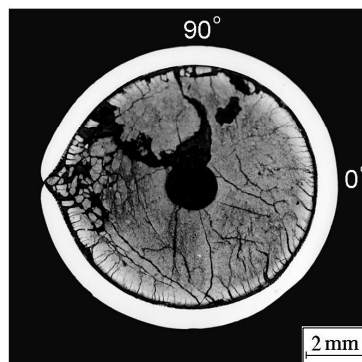
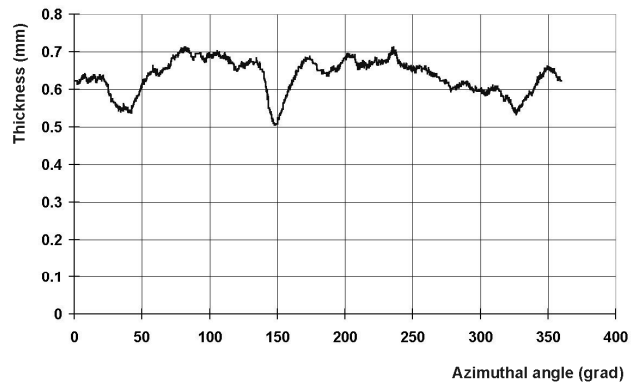
#RT7, elevation 107 mm



#RT8, elevation 53 mm



#RT8, elevation 97 mm



#RT8, elevation 133 mm

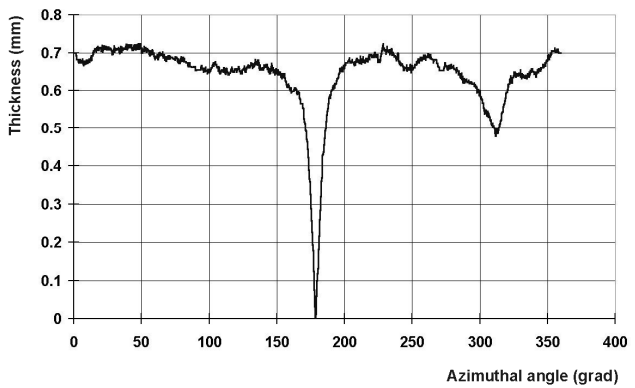
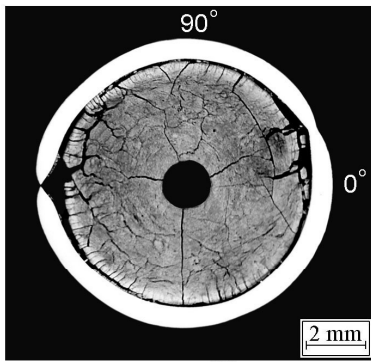
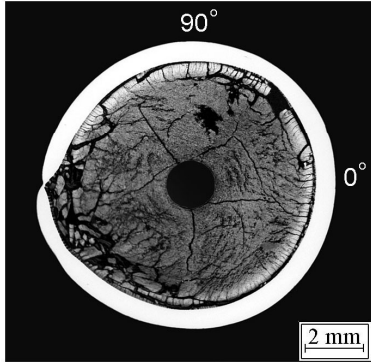
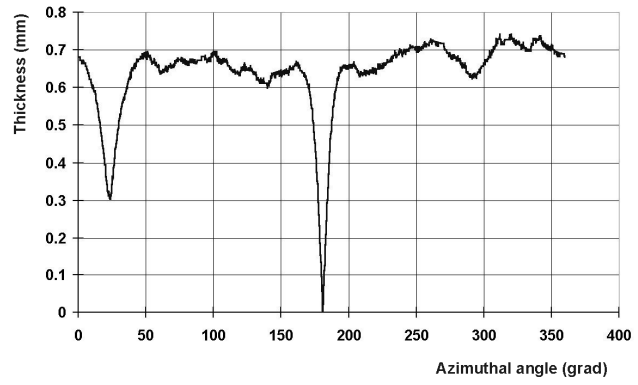


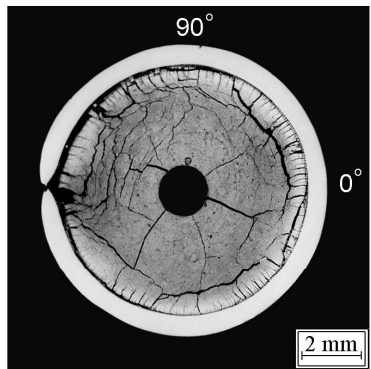
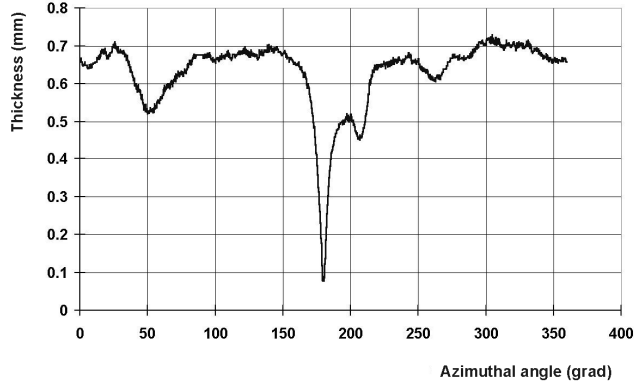
Fig.E-13.1. Cross-section and azimuthal distribution of cladding thickness in fuel rods ## RT7, 8 after the BGR tests



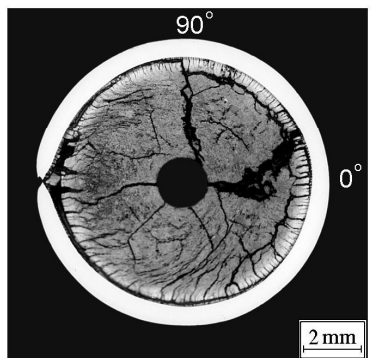
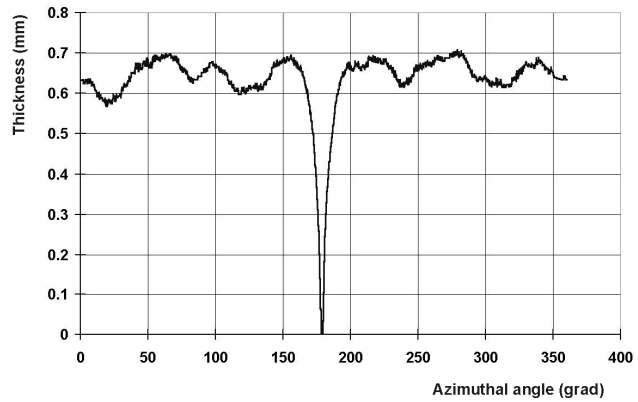
elevation 69 mm



elevation 88 mm



elevation 110 mm



elevation 144 mm

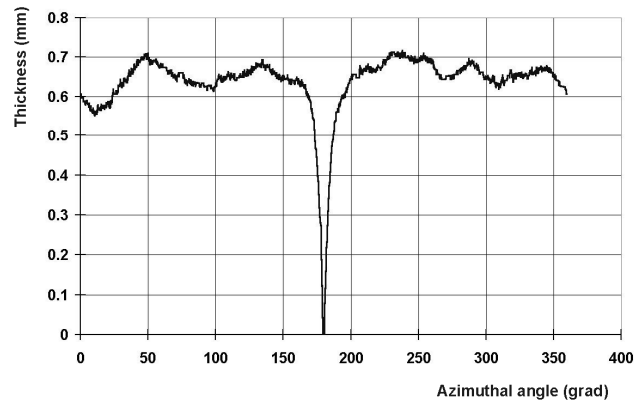
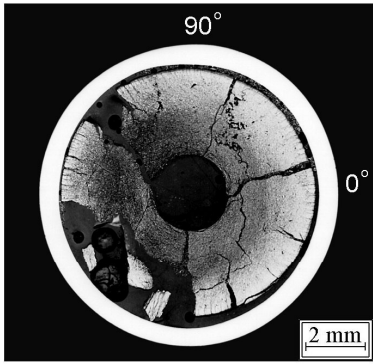
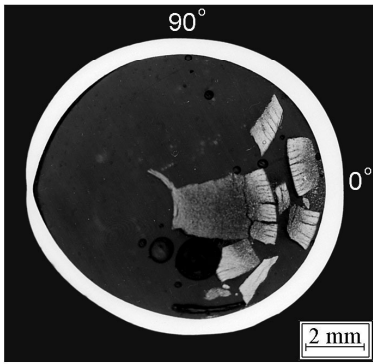
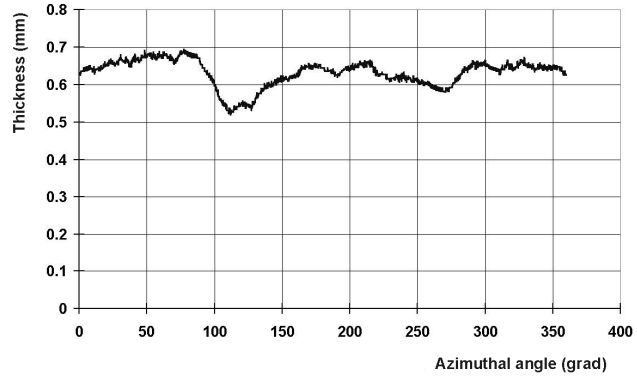


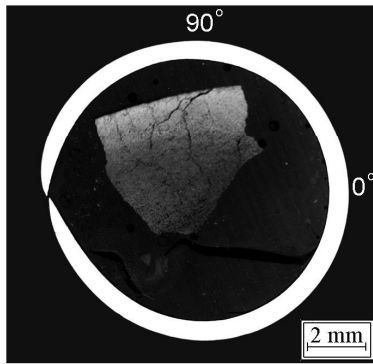
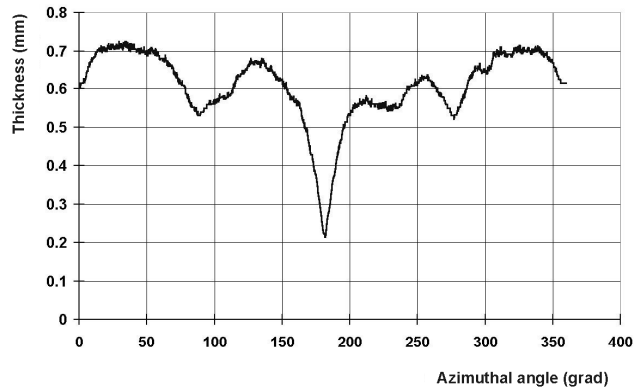
Fig.E-13.2. Cross-section and azimuthal distribution of cladding thickness in fuel rod # RT9 for different elevations after the BGR tests



elevation 33 mm



elevation 45 mm



elevation 60 mm

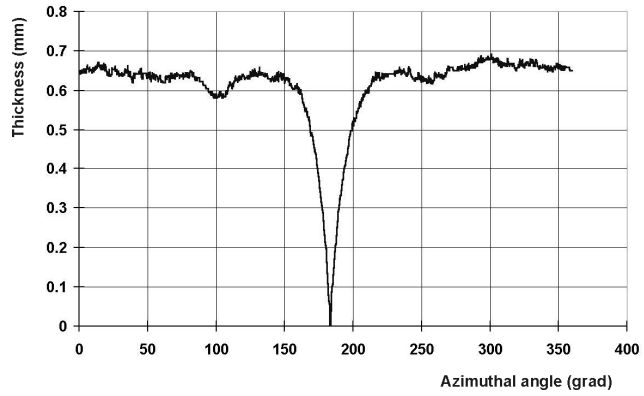
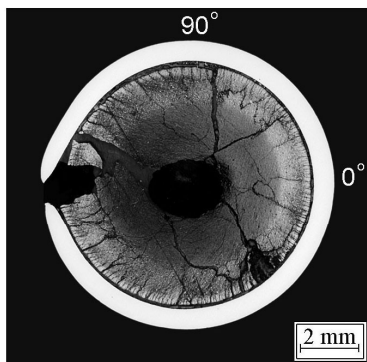
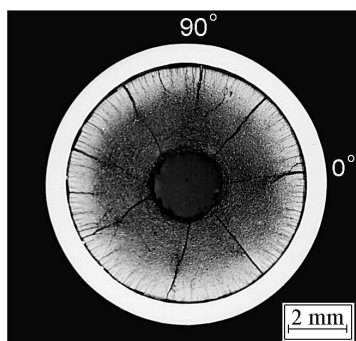
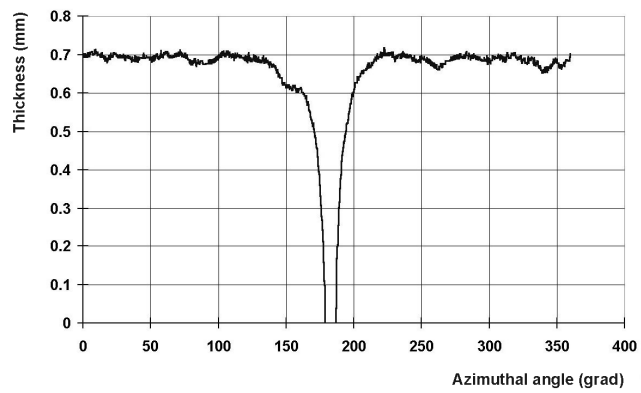


Fig.E-13.3. Cross-section and azimuthal distribution of cladding thickness in fuel rod # RT10 for different elevations after the BGR tests



#RT11, elevation 157 mm



#RT12, elevation 54 mm

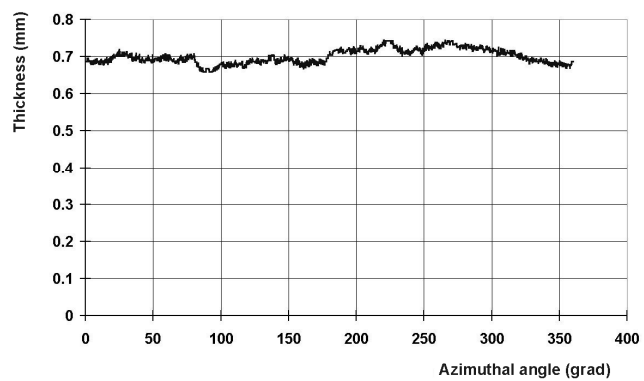


Fig.E-13.4. Cross-section and azimuthal distribution of cladding thickness in fuel rods ## RT11, 12 after the BGR tests

BIBLIOGRAPHIC DATA SHEET

(See instructions on the reverse)

NUREG/IA-0213, Vol. 2
IRSN/DPAM 2005-275
NSI RRC KI3230

2. TITLE AND SUBTITLE

Experimental Study of Narrow Pulse Effects on the Behavior of High Burnup Fuel Rods with Zr-1%Nb Cladding and UO₂ Fuel (VVER Type) under Reactivity-Initiated Accident Conditions: Test Conditions and Results

3. DATE REPORT PUBLISHED

| | |
|-------|------|
| MONTH | YEAR |
| March | 2006 |

4. FIN OR GRANT NUMBER

Y6723

5. AUTHOR(S)

L. Yegorova, K. Lioutov, N. Jouravkova
O. Nechaeva, A. Salatov
V. Smirnov, A. Goryachev
V. Ustinenko, I. Smirnov

6. TYPE OF REPORT

International Agreement

7. PERIOD COVERED (Inclusive Dates)

8. PERFORMING ORGANIZATION - NAME AND ADDRESS (If NRC, provide Division, Office or Region, U.S. Nuclear Regulatory Commission, and mailing address; if contractor, provide name and mailing address.)

Nuclear Safety Institute of Russian Research Centre "Kurchatov Institute" Moscow, Russian Federation
A.A. Bochvar All-Russian Research Institute of Inorganic Materials Moscow, Russian Federation
State Research Centre "Research Institute of Atomic Reactors" Dimitrovgrad, Russian Federation
Russian Federal Nuclear Centre "All-Russian Research Institute of Experimental Physics" Sarov, Russian Federation

9. SPONSORING ORGANIZATION - NAME AND ADDRESS (If NRC, type "Same as above"; if contractor, provide NRC Division, Office or Region, U.S. Nuclear Regulatory Commission, and mailing address.)

Division of Systems Analysis and Regulatory Effectiveness
Office of Nuclear Regulatory Research
U.S. Nuclear Regulatory Commission
Washington, DC 20555-0001

10. SUPPLEMENTARY NOTES

11. ABSTRACT (200 words or less)

This report contains a detailed description of calculation and test results obtained in the fast-pulse graphite-reactor (BGR) tests of twelve fuel rods refabricated from the VVER-440 and VVER-1000 high burnup fuel elements (50 - 60 MWd/kgU).

12. KEY WORDS/DESCRIPTORS (List words or phrases that will assist researchers in locating the report.)

BIGR
Cladding
E110
Kurchatov Institute
Nuclear Fuel
Reactivity-Initiated Accident
Russian
Zirconium

13. AVAILABILITY STATEMENT

unlimited

14. SECURITY CLASSIFICATION

(This Page)

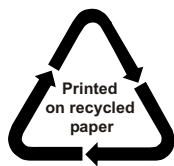
unclassified

(This Report)

unclassified

15. NUMBER OF PAGES

16. PRICE



Federal Recycling Program